AN ABSTRACT OF THE THESIS OF

Athena Erin Lieuallen for the degree of Master of Science in Geology
presented on September 10, 2010.
Title: Meeting of the Magmas: the Evolutionary History of the Kalama Eruptive Period, Mount St. Helens, Washington

Abstract approved:

_____

Frank J. Tepley III

Comprehension of eruptive histories is critical in understanding the evolution of magmatic systems at arc volcanoes and may supply evidence to the petrogenesis of intermediate and evolved magmas. Within the 300 ka eruptive history of Mount St. Helens, Washington, the Kalama Eruptive Period, 1479- ~1750 CE was bracketed by interludes of quiescence (Hoblitt *et al*., 1980) and thus likely represents an entire eruptive cycle within a span of 300 years. Study of the magmatic evolution during this short time period provides key information regarding inputs and the plumbing system of Mount St. Helens. This research aims to enhance comprehension of processes leading to the petrogenesis of intermediate magmas by providing whole rock and phase geochemical data of an eruptive cycle, thereby providing constraints on the magmatic evolution of the Kalama Eruptive Period.

The eruptive sequence is divided into early, middle and late subperiods. The early Kalama began with two dacitic plinian eruptions and continued with smaller eruptions of dacite domes (64.4-66.5 wt% SiO_2) that included quenched mafic inclusions (53.7-57.7 wt% SiO_2). The middle Kalama signified the onset of basaltic andesite and andesite eruptions ranging

between 55.5-58.5 wt % SiO_2. Subsequently, summit domes that began as felsic andesite (61-62.5 wt% SiO_2) and transitioned to dacite (62.5-64.6 wt% SiO_2) dominated the late Kalama. Previous work on Kalama-aged rocks suggests magma mixing is an integral process in their production. Compositions and textures of crystal phases, in addition to the presence of xenocrysts in middle and late Kalama rocks, confirm mechanical mixing of magmas likely produced many of the sampled compositions.

New petrographic observations were integrated with new whole rock and phase EMP and LA-ICP-MS data and the known stratigraphy in order to constrain the magmatic and crustal components active during the Kalama Eruptive Period. New findings include:

1. Two populations of quenched mafic inclusions, one olivine-rich and one olivine-poor, are identified from the early Kalama based on mineralogy, textures, and major and trace element chemistry. Major element modeling shows crustal anatexis of plutonic inclusions found in early Kalama dacites could produce the felsic magma source of the olivine-poor population. The olivine-rich population incorporated cumulate material.

2. Four distinct lava populations erupted during the early part of the middle Kalama (X lavas), including two found exclusively in lahar deposits: M-type lahars are the most mafic, B-type lahars are more mixed, the Two Finger Flow was previously grouped with other middle Kalama-age lavas, and the X lava (*in situ*) has unique geochemical and textural character. X tephras likely correlate with the lavas.

3. There were at least three mafic source contributions at Mount St. Helens during the eruptive period: the parent to the X deposits, the cumulate material in the olivine-rich QMIs, and the calc-alkaline parent to the MKLV and SDO.

The magma reservoir at Mount St. Helens has been modeled as a single, elongate chamber (Pallister *et al.*, 1992). Multiple coeval basaltic or basaltic andesite parents fluxing into the magmatic system beneath the volcano could indicate a more complex magma chamber structure.

Meeting of the Magmas: the Evolutionary History of the Kalama Eruptive Period, Mount St. Helens, Washington

by
Athena Erin Lieuallen

A THESIS

submitted to

Oregon State University

in partial fulfillment of
the requirements for the
degree of

Master of Science

Presented September 10, 2010
Commencement June 2011

Master of Science thesis of Athena Erin Lieuallen presented on September 10, 2010.

APPROVED:

Major Professor, representing Geology

Chair of the Department of Geosciences

Dean of the Graduate School

I understand that my thesis will become part of the permanent collection of Oregon State University libraries. My signature below authorizes release of my thesis to any reader upon request.

Athena Erin Lieuallen, Author

ACKNOWLEDGEMENTS

I would like to thank everyone who has helped make this research possible and who helped me see it through. I would like to express sincere appreciation for my major adviser, Frank, for his continued years of advice, encouragement, patience, education, field work, bloodshed, and hours of undivided attention.

Thank you to Mike Clynne for guidance and detailed revisions, which helped me become a better writer, and for sharing his knowledge of petrology, Mount St. Helens and the best outcrops. Thank you also to Ed Wolfe and Joel Robinson for their assistance with field work, and Rick Conrey and Laureen Wagner at Washington State University for teaching me about sample preparation.

I would also like to thank Adam Kent for being an integral part in my coming to Oregon State University for graduate school, and Anita Grunder for teaching me most of what I know about petrology and modeling, and that "there are all types of learning going on, including outside the classroom." My gratitude also goes to Dave Graham for serving on my committee, to all other faculty who had a part in shaping my education, and to the Department of Geosciences staff Melinda and Stacey, who have been consistently supportive in my graduate career.

I wish to thank my colleagues Alison Koleszar, Allison Weinsteiger, Ashley Bromley, Ashley Hatfield, Justin Milliard, Manggon Abot, Mark Ford, and Matt Loewen, and my other fellow graduate students for their insight, for relevant and irrelevant conversations and for helping me learn how to "do science."

Appreciation also goes to the Geological Society of America for providing partial funding of the project.

Lastly, I want to especially thank my husband, Rocco, for his infinite emotional and intellectual support from the beginning. Not only has he made my education priority and made many sacrifices along the way, he has repeatedly read this text and served as the most proficient thesaurus one could ask for. Thank you also to thank the rest of my family: my parents, Jane and Mike, and my in-laws, Rosemarie and Peyton and Gwen, all without whom graduate school would have been impossible. I would like to thank Leo, Beeker, and Mehitabel for all their support and years of fur therapy, all my siblings, and Angie, Bethany and Tara, who have all lent emotional support throughout my quest.

TABLE OF CONTENTS

TABLE OF CONTENTS (Continued)

Page

LIST OF FIGURES

LIST OF FIGURES (Continued)

Figure Page

LIST OF FIGURES (Continued)

Figure Page

LIST OF FIGURES (Continued)

LIST OF FIGURES (Continued)

LIST OF FIGURES (Continued)

Figure Page

LIST OF TABLES

LIST OF APPENDICES

LIST OF APPENDIX TABLES

Meeting of the Magmas: the Evolutionary History of the Kalama Eruptive Period, Mount St. Helens, Washington

Chapter 1: Introduction

There is little dispute that basalts are mantle-derived magmas (Hildreth & Moorbath, 1988; Rollinson, 1993; Winter, 2001; Yoder Jr., 1976), but the petrogenesis of intermediate and silicic magmas is a more complex subject (Annen *et al.*, 2006; Gill, 1981). Numerous hypotheses explain the compositional diversity among andesites and dacites derived by one or a combination of the following processes: crustal melting, fractional crystallization of primitive basaltic magmas, assimilation of country rock, and mixing between mafic and felsic magma compositions (Annen *et al.*, 2006; Bowen, 1928; Clynne, 1999; Eichelberger, 1981; Gardner *et al.*, 1995B; Hildreth & Moorbath, 1988; Leeman *et al.*, 1990; McBirney, 1978, 1980; Smith & Leeman, 1987, 1993). Despite these assessments, there are still considerable questions as to where and how intermediate magmas derive their geochemical characteristics (*e.g.* Annen *et al.*, 2006). Generalized competing hypotheses include:

1) Intermediate magma production occurs in deep crustal, water-rich hot zones (Annen *et al.*, 2006; Hildreth & Moorbath, 1988), and
2) Intermediate magmas are produced in the middle and upper crust and glean their geochemical characteristics from the melts from which they are mixed or crystallized (Annen *et al.*, 2006 and references therein).

A comprehensive understanding of intermediate magma production can be aided by thorough investigation of a particular magmatic system, including constraining the compositions and interactions of the components, to pinpoint

the combination of the aforementioned processes that lead to the petrogenesis of its volcanic rocks.

Comprehension of eruptive histories is critical in understanding the evolution of magmatic systems at arc volcanoes and may supply evidence of the processes that lead to petrogenesis of intermediate and evolved magmas. Linking compositional characteristics and textures to petrogenetic processes may accomplish this goal. The rock history of the Cascade arc provides excellent opportunity to explore the temporal progression of volcanism at a convergent margin with the goal of understanding the production of intermediate magmas. Mount St. Helens, with its easy accessibility, long history and frequency of eruption is an ideal location to synthesize observations of recent eruptions with investigations of older volcanics. The Kalama Eruptive Period of Mount St. Helens, 1479 - ~1750 CE (common era), was bracketed by interludes of quiescence (Hoblitt *et al*., 1980) and thus likely represents an entire eruptive cycle within a span of 300 years. Hopson & Melson (1990) define an eruptive cycle in which an episode of eruptions progress in eruptive style, mineralogy, and magmatic composition, and is then followed by a period of repose. Figure 1 is a photo of the pre-1980 form of Mount St. Helens in which the dark lava flows and nearly all the material above them are deposits of the Kalama Eruptive Period. Study of the magmatic evolution during this short time period provides key information regarding inputs and the plumbing system of Mount St. Helens. This research aims to enhance comprehension of the processes leading to the petrogenesis of intermediate magmas by providing whole rock and phase geochemical data of an eruptive cycle, thereby providing constraints on the magmatic evolution of the Kalama Eruptive Period.

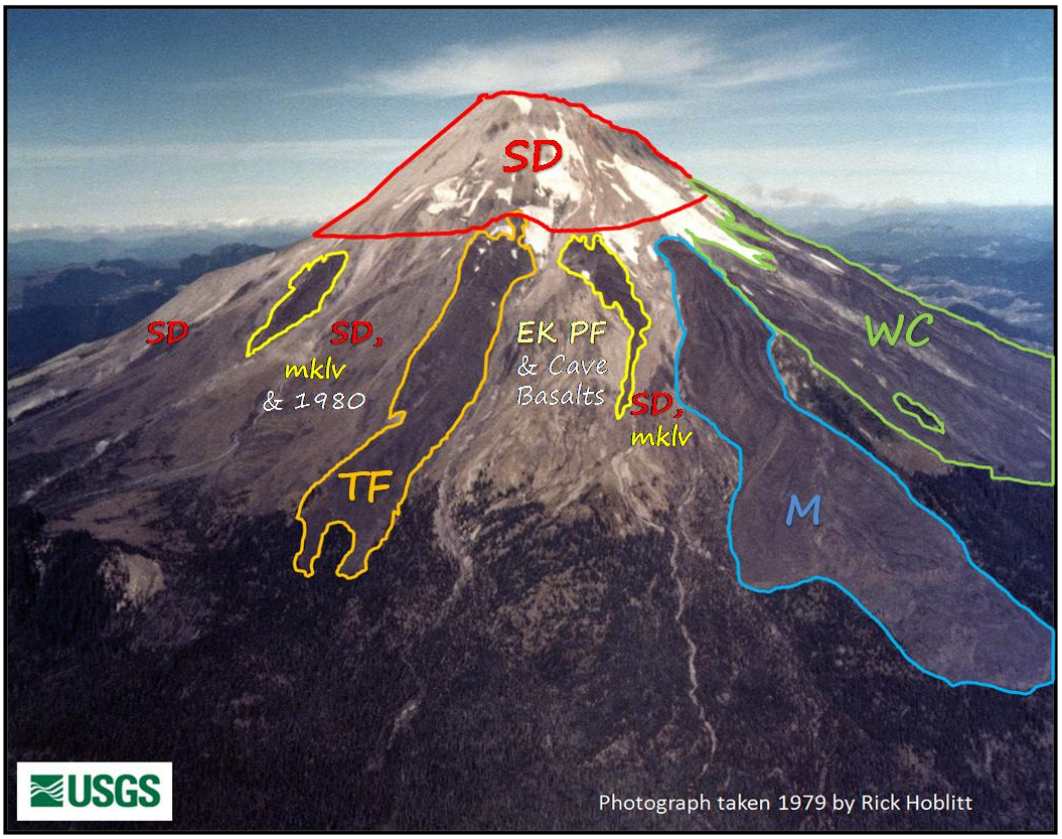

Figure 1. Pre-1980 form of Mount St. Helens. Lavas of the Kalama age are outlined and labeled: M=Mitten Flow, WC=Worm Complex flows (andesite), TF=Two Finger Flow (basaltic andesite),SD=Summit Dome (andesite and dacite), occurs in pyroclastic flows and lahars on the flanks MKLV=Middle Kalama-age lava, EKPF= Early Kalama pyroclastic flows. Flows in yellow with no labels are unnamed. Kalama-age lahars, pyroclastic flows and tephras are also seen in the image intermingled with deposits from other eruptive periods.

Chapter 2: Geologic Setting

2.1 The Cascade Volcanic Arc

The west coast of North America has been the site of plate convergence for the last 150 Ma where the Farallon plate has been subducting beneath the North American plate (Atwater, 1970; Riddihough, 1984) (Figure 2.1). When the Farallon plate was consumed at the southern end of the subduction zone about 30 Ma, the San Andreas Fault began propagating northward (Atwater, 1970). About 20 Ma the Juan de Fuca plate broke from the Farallon plate. Later, around 6.5 Ma, convergence rates ranged from 6 – 7 cm/yr, with the slower rates on the north end where the youngest crust was subducting (Riddihough, 1984). Subsequently, about 3.5 - 4 Ma, the Explorer plate broke away from the Juan de Fuca as a sub-plate on the north end of the arc coinciding with a reduction in convergence velocities to 3 - 4.5 cm/yr (Guffanti & Weaver, 1988; Riddihough, 1984). Today the Juan de Fuca, a remnant of the Farallon plate, continues to subduct beneath the North American plate at about the same rate (Guffanti & Weaver, 1988; Riddihough 1984) with convergence in the direction of N50°E (Guffanti & Weaver, 1988; Weaver & Malone 1987). Conversely, the Explorer plate near Vancouver Island appears to rotate about a pole rather than subduct (Guffanti & Weaver, 1988). The Gorda plate to the south also continues to subduct, likely at different geometries (Guffanti & Weaver, 1988).

The Cascade volcanic arc began to form about 40-35 Ma when subduction instigated volcanism resulting in the Western Cascades (Priest, 1990; Taylor, 1990). Figure 2.1 illustrates the relationship between the subducting plates and Cascade volcanic arc. Elevations of the pre-Quaternary

basement rocks currently range from 1200-2000 m (Hildreth, 2007). Volcanism of the central Cascade arc (in Oregon) has narrowed in the last 35 Ma, due to slab dip steepening at depths greater than 100 km (Priest, 1990). Meanwhile, the volcanic front has shifted eastward likely due to decreasing slab dip angle at shallow depths (Priest, 1990). Wells (1990) attributed the eastward volcanic front migration to westward clockwise rotation of the sub-arc crust. The resulting Quaternary High Cascades span 1250 km from British Columbia to northern California and the range varies in width between 25 – 100+ km (Hildreth, 2007). Volcanism began to migrate westward at the south end of the arc around 16 Ma (Christiansen & McKee, 1978; Guffanti & Weaver, 1988).

The Cascade arc is often divided into four or five segments based on such factors as vent distribution, geochemistry, or tectonic setting. Guffanti & Weaver (1988) divided the arc into five segments based on vent distribution and seismicity: (1) Garibaldi Volcanic Belt, (2) Rainier to Hood Segment, (3) Oregon segment, (4) Shasta Segment, and (5) Lassen Segment (Figure 2.2a). They considered the High Lava Plains as a sixth segment. Four segments identified by Schmidt *et al.* (2007) were divided by primitive basalt type, along with Sr and Nd isotope signatures: (1) North Segment from Mt. Meager to Glacier Peak, (2) Columbia Segment from Mt. Rainier to Mt. Jefferson, (3) Central Segment from the Three Sisters to Medicine Lake, and (4) South Segment from Mt. Shasta to Lassen Peak. Sherrod & Smith (1990) discussed arc segments in terms of Quaternary extrusion rates (Table 2.1), and also noted the arc is segmented by eruption styles, and changes that occur at different latitudes than the rate changes.

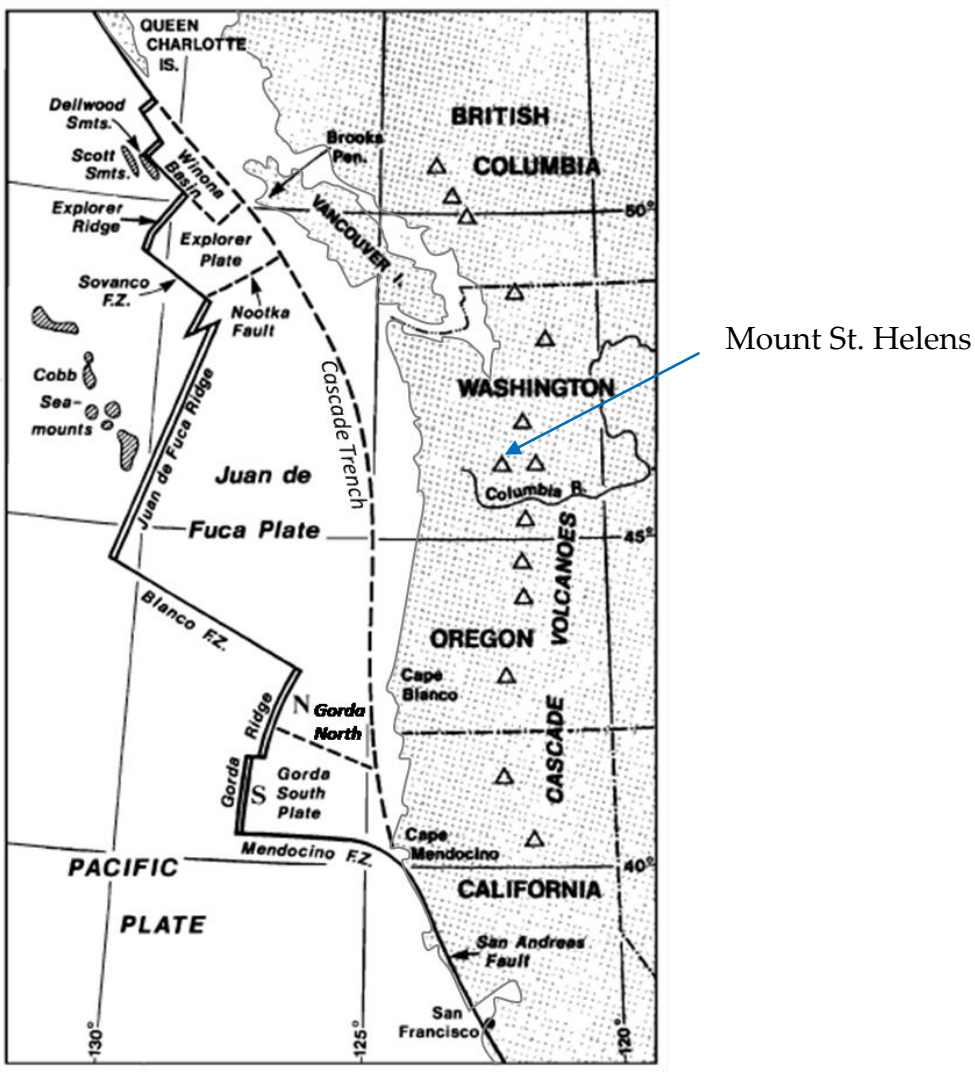

Figure 2.1 Regional tectonic setting of the Cascade Range. After Riddihough (1984).

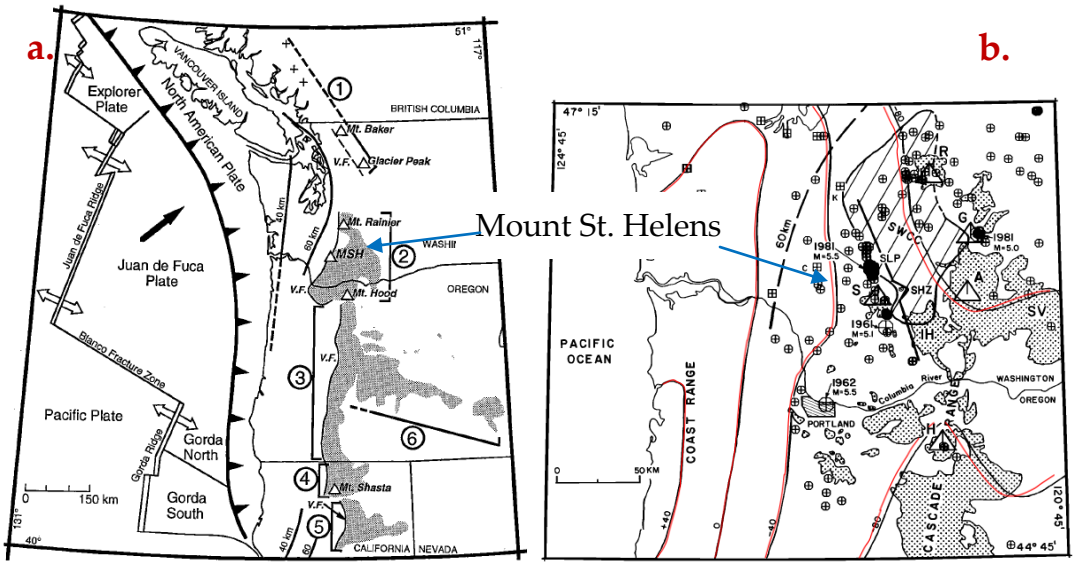

Figure 2.2 a. Regional tectonic and segmentation map From Smith & Leeman (1993) with tectonic features from Riddihough (1984), stippled vents < 5 Ma from Guffanti & Weaver (1988), and seismicity depth contours from Weaver & Baker (1988). V.F. = volcanic front. b. Regional gravity map After Weaver & Malone (1987). Red lines are Bouguer gravity contours (values in milli-Gals). Area of slanted lines indicates the Southern Washington Cascade Conductor (SWCC) from Stanley *et al*. (1987).

Table 2.1 Cascade Extrusion Rates for the Last 2 Ma by Arc Segment from Sherrod & Smith (1990)

Segment	**Extrusion Rate ($km^3/km/my$)**
North of Mount Rainer	0.21
Southern Washington – Mount Hood	1.6 - 2.9
Central and Southern Oregon	3 – 6
Northern California	3.2

The Cascades Arc is unusual due to its sections that contain concentrations of both numerous mafic vents such as those near Lassen Peak and in the Portland Basin (Hildreth, 2007) and high volume centers such as Mounts Rainier, St. Helens, and Shasta that occur significantly trenchward of

the arc axis (Hildreth, 2007). There are 148 known Quaternary vents in the geographic forearc in the southern Washington section of the arc, including Mount St. Helens (Hildreth, 2007). The arc in this section extends 160 km between Mount St. Helens and Simcoe Volcanic Field (Figure 2.3) and contrasts with the Garibaldi Volcanic Belt (GVB), which comprises almost no off-axis vents. The GVB also comprises dacite to rhyodacite whereas the Mount Rainier to Mount Hood segment is significantly more mafic. Over the past 4 Ma volcanism in the southern Washington section of the arc has become less alkalic (Leeman *et al.*, 1990). The locus of volcanism has locally shifted westward from Simcoe Mountain Volcanic Field to Mount Adams and Indian Heaven Volcanic Field, and within the last 40 ka, has been concentrated to its present day focus at Mount St. Helens (Leeman *et al.*, 1990) (Figure 2.3).

The north and south ends of the Cascade arc contrast in a number of ways. The southern Washington Cascade Range, where Mount St. Helens lies, is a transition zone, which is a region that displays volcanic, tectonic, and structural characteristics from both ends of the arc. Today the northern end of the arc experiences compressional stresses (Weaver & Malone, 1987) and exhibits virtually no evidence of rotation (Wells, 1990). This may restrict the concentration of volcanism to a few intermediate and silicic centers (Weaver & Malone, 1987). The southern end undergoes extensional processes and more significant clockwise rotation (Weaver & Malone, 1987; Wells, 1990), resulting in some of the erupted volume south of Mount Hood spread around scores of basaltic vents in addition to composite cones (Weaver & Malone, 1987). The volcanic cover in the transition zone is similar to the ubiquitous basaltic vents of the Oregon Cascades, with Simcoe Mountain and Indian Heaven Volcanic Fields, while the stratovolcanoes have similar morphology to volcanoes of the

north such as Mount Baker and Mount Garibaldi. Wells (1990) also noted the transition area is laden with folds and faults in the Eocene to Miocene volcanics and sedimentary deposits, possibly indicating it is a pivot area for arc block rotation.

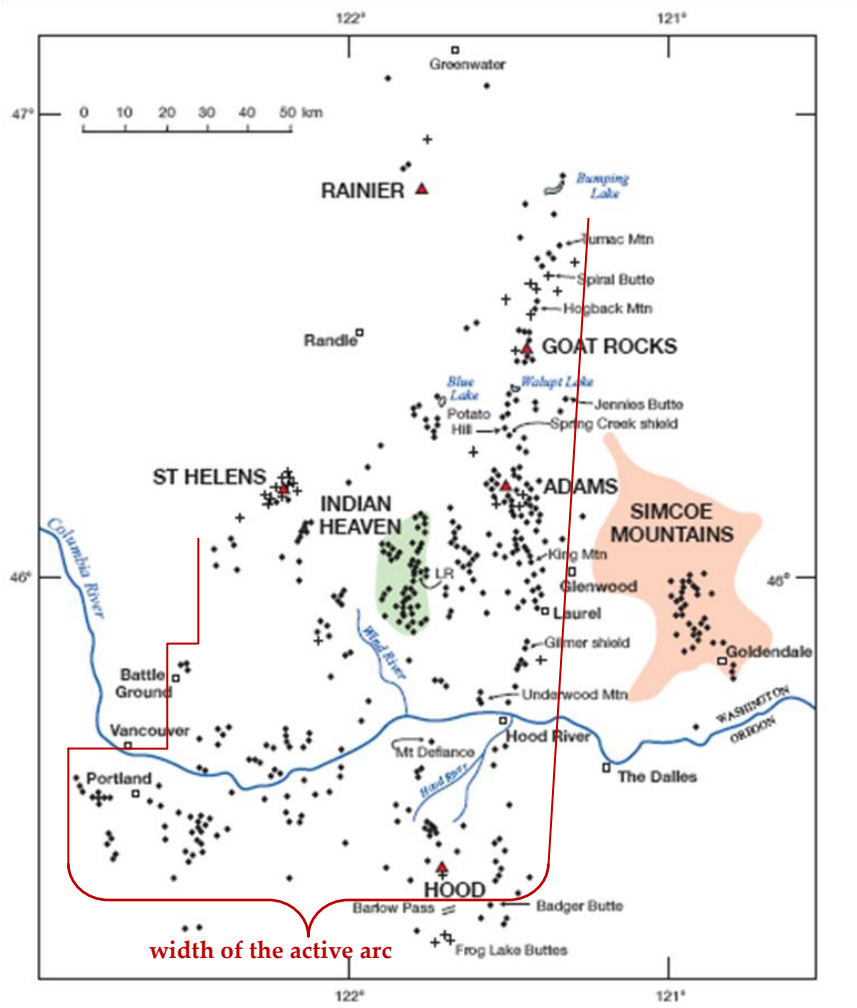

Figure 2.3 Regional volcanic setting of Quaternary vents after Hildreth (2007). The width of the active arc is outlined in red. Simcoe Mountain (4.5-0.6 Ma) and Indian Heaven (<1 Ma) Volcanic Fields are shaded to show full extent of older vents. Vents represented by: dots = basalt-basaltic andesite, + = dacite-rhyolite. ▲ = composite cones.

Differences between north and south of the transition zone are not limited to volcanism and structure; gravity and heat flow vary markedly (Weaver & Malone, 1987). Mount St. Helens lies within a low Bouguer gravity saddle that bisects a gradient from west to east (Thiruvathukal *et al*., 1970; Weaver & Malone, 1987) (Figure 2.2b). The area of low gravity is broad north of Mount Adams but narrows south of Mount Hood as it intersects the Basin and Range low (Thiruvathukal *et al*., 1970; Weaver & Malone, 1987). Heat flow values in the southern Washington Cascades are also transitional. Values range between 70-90 m W m^{-2} whereas those south of Mount Hood are ~100 m W m^{-2} and those north of Glacier Peak range between 40-60 m W m^{-2} (Blackwell *et al*., 1990a,b; Weaver & Malone, 1987).

The transition zone itself is also unique. A high conductivity anomaly in the area outlined by Mounts Adams, St. Helens, and Rainier contrasts with the flat lying conductivity structures south of Mount Hood (Stanley *et al*., 1990; Weaver & Malone, 1987). Additionally, a significant portion of the seismicity in the three sections of the Cascades from Canada to Oregon occurs in the transition zone, especially within the St. Helens seismic zone (SHZ) (Weaver & Malone, 1987).

Conrey *et al.* (1997 and references therein) contend central Oregon was the origination site of an intra-arc propagating rift system reaching northward into southern Washington around 7-8 Ma. The rift produced high degrees of partial melt as it passed through the arc, resulting in eruptions of a diverse suite of magmas, including MORB-like low-K tholeiites, and ash flow tuffs. After rifting passed through sections of Oregon, lower degrees of partial melt produced additional calc-alkaline and OIB-type basalts. The depleted Boring Volcanics in the Portland Basin at the northern tip of the rift were likely

produced from lower degrees of partial melt of a refractory source since the most active part of the rift had not yet reached that far north. The variety of erupted compositions, including high-K tholeiites and ash flow tuffs, indicates a heterogeneous mantle source (Conrey *et al*, 1997). Conrey *et al.* (1997) suggest Mount Adams is the current rift tip due to the abundance of surrounding low-K tholeiites.

2.2 Local Tectonic Setting of Mount St. Helens

Weaver *et al.* (1987) identified two distinct fault zones beneath Mount St. Helens. Like Mt. Hood to the south, Mount St. Helens appears to lay over a zone of crustal extension that trends NW (Leeman *et al.*, 1990; Weaver *et al.*, 1987; Williams *et al.*, 1982). The SHZ is a shallow N-NW striking dextral fault system (Figure 2.4). The fault strike shifts slightly from N to N-NW at Mount St. Helens (Weaver *et al.*, 1987). The right lateral displacement causes local extension between the offset fault segments (similar to a leaky transform fault). An older, perpendicular set of fractures related to a second fault system is deeper at 9-20 km and strikes NE (Weaver *et al.*, 1987). Mount St. Helens' location is due to the unique intersection of the SHZ with the older, deep fractures.

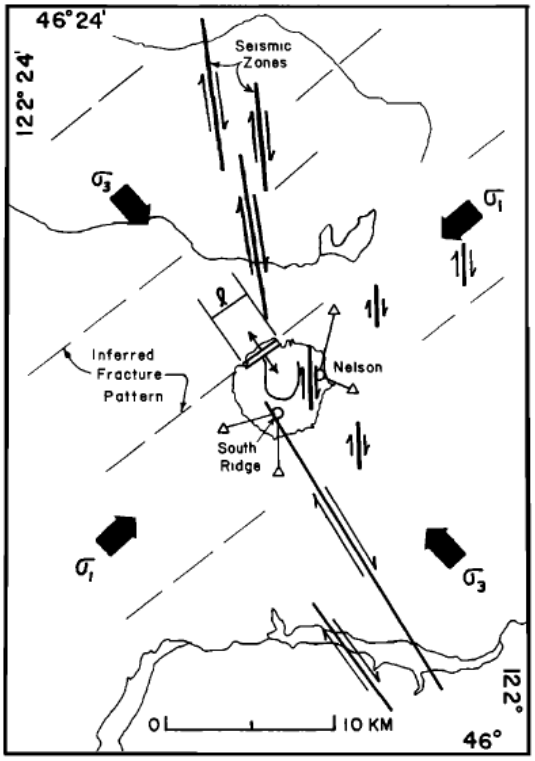

Figure 2.4 After Weaver *et al.* (1987). Local tectonic setting of Mount St. Helens where a prior set of deep NE-SW trending fractures intersects a NNW-SSE trending dextral fault of the St. Helens seismic zone. Crustal spreading at the intersection allows a pathway for magma ascent.

2.3 Eruptive History of Mount. St. Helens

Mount St. Helens, pre-1980 elevation 2950 m, has been the most active of the Cascade volcanoes over the past 4 ka. It has erupted at least 75 ± 15 km^3 of magma (Hildreth, 2007), and the main edifice comprises approximately 25 km^3 (Hildreth, 2007). The volcano's stratigraphy allows insight into its cyclic behavior of Plinian eruptions, dome growth and collapse, and lava flows. Mount St. Helens' history dates back 300 ka and is divided into four eruptive stages. The following brief eruptive history is summarized from Crandell (1987) as modified by Clynne *et al*. (2008) and Mullineaux (1996). The eruptive chronology is illustrated in Figure 2.5.

Mount St. Helens Eruption Chronology

Age	Stage	Period	Ash Set	Erupted products
(CE)				
Present	Spirit Lake Stage	Modern Period	1980	Lava dome, cryptodome
1980				
1857		Goat Rocks Period	T	Goat Rocks lava dome, Floating Island
1800				
1620		Kalama Period	Z	Summit Dome
1505			X	Xb, Xs, Xm, Xh
1479			W	Wn, Wa, Wb, Wc, We, Wd
Age (ka)				
		Sugar Bowl Period	D	Dacite domes, lateral blast
2		Castle Creek Period	B	Basalt lavas, dacite lava dome, pyroclastic flows, andesite flows
		Pine Creek Period	P	Lahars, pyroclastic flows, lava domes
3				Pm, Ps, Pu, Py
		Smith Creek Period	Y	Lava domes, pyrolcastic flows
4				Yn, Ye
11	Swift Creek Stage		J	Crescent and Cedar Flat fans
13			S	Swift Creek fan
17	Cougar Stage		K	Swift Creek lava flow
				White Pumice, 2 Pumice PF,
23			M	Debris avalanche, lava domes
35	Ape Canyon Stage		C	Lava domes, lahars
				Ash, lava domes
125		Butte Camp Dome		Butte Camp Dome
250		Goat Dome		Goat Mountain Dome
300				Unnamed ash

Figure 2.5 Eruptive chronology for the Kalama Period after Clynne *et al.* (2005). Note change in scale from ka to CE during the Spirit Lake Stage.

The oldest eruptive stage is Ape Canyon (300 – 35 ka), characterized by two distinct dome building periods west of the modern crater. The younger period produced the C tephra set, and some altered rocks show there was an active hydrothermal system during this stage.

The Ape Canyon Stage was succeeded by a dormant period of about 12 ky, followed by the Cougar Stage from 23-17 ka. The nearby Spirit Lake Pluton was emplaced shortly after the onset of the Cougar Stage at 21 ka (Evarts *et al.*, 1987; Weaver & Malone, 1987). During the Cougar Stage, a large debris avalanche on the south flank of the volcano originated near Butte Camp and deposited debris 180-275 m thick, followed by a Plinian eruption and pyroclastic flows that deposited ~90 m of dacitic pumiceous pyroclastic flow deposits on top of the avalanche deposits. Tephra sets M and K were subsequently deposited, followed by Mount St. Helens' largest lava flow, the Swift Creek Flow, also on the south flank.

A 4 ky interval separated the Cougar Stage from the Swift Creek Stage (13 – 11 ka), which was characterized by large fans of lahar and pyroclastic flow deposits from dome collapse on the south and west flanks. Tephra sets S and J and a cluster of domes added significant material to the edifice. The eruption of the J tephra was followed by 7000 years of dormancy.

The most recent eruptive stage, Spirit Lake, is the best characterized eruptive chronology because of the good exposure of erupted products and the capability of tree ring dating in the later part. Beginning about 3.9 ka, the Spirit Lake Stage is further divided into seven eruptive periods: Smith Creek, Pine Creek, Castle Creek, Sugar Bowl, Kalama, Goat Rocks, and the Modern Period (1980-2008 CE). Smith Creek Period produced mostly ash comprising the Y ash set, which included Yb and Yd (3.90 - 3.85 ka), Yn, Ye, and Yf (3.5 -

3.3 ka), and Yo and Yu (3.3 - 2.9 ka) ash layers. The Smith Creek Period eruption that produced the Yn was likely the largest in Mount St. Helens' history. After ~400 years of inactivity, the Pine Creek Period (2.9 - 2.55 ka) produced ash set P and pyroclastic flows, as well as lava dome eruptions that lead to debris avalanche deposits up to 180 m thick on the south flank. Following the Pine Creek Period, intermediate and mafic lavas were abundant during the Castle Creek Period (2.55 - 1.895 ka). Specifically, andesite lava flows erupted from 2.55 – 2.5 ka and at 2.2 ka, followed by dacite flows and domes. Three basalt flows erupted between 2.0 – 1.895 ka, the last of which is the Cave Basalt. Tephra set B was erupted during the Castle Creek Period.

After about 700 years of inactivity, the volcano briefly reawakened about 1.2 – 1.15 ka (850 to 900 CE) during the Sugar Bowl Period. The small amount of erupted material included lava dome eruptions, a small lateral blast, and ash layer D. Another nearly 500 years of inactivity passed before the Kalama Period (1479 - ~1750 CE). A detailed history of the Kalama Period follows. The last eruptive period before the Modern Period was Goat Rocks, which began with a pyroclastic eruption in 1800 CE that produced ash layer T. Other eruptions included the Floating Island Andesite Flow in 1801 CE and Goat Rocks Dome, and subsequent block and ash flows and lahars as late as 1857 CE.

The Modern Eruptive Period of Mount St. Helens began March 27, 1980 with a phreatic, ash eruption, followed by many others including the catastrophic Plinian eruption of May 18, 1980 (Hoblitt *et al.*, 1980). Erupted products include dacitic tephra, lava dome and cryptodome, pyroclastic flows, and lahars (Hoblitt *et al.*, 1980). Dome-forming eruptions continued until 1986, followed by ~18 years of quiescence. The latest eruption, 2004 – 2008,

ensued with a dacite lava dome consisting of at least 8 spines (Pallister *et al.*, 2008).

The segment of the Cascade arc from Mount Rainier to Mount Hood is predominantly basalt to andesite, but Mount St. Helens eruptions are dominated by dacite, lesser andesite, and rare basalt (Hildreth, 2007). Mount St. Helens is not the only silicic vent in this section. Evolved magmas are concentrated along a locus of dacite to rhyolite vents reaching from Goat Rocks northeast to Spiral Butte and at Mount Adams (Hildreth, 2007) (Figure 2.3). In contrast to the rest of the Cascades (with the exception of Lassen Volcanic Center), Mount St. Helens rocks contain quartz and biotite phenocrysts in earlier (pre-Kalama) erupted products (Hildreth, 2007). Despite this, Gardner *et al.* (1995a) suggest the basaltic input at Mount St. Helens has increased over the past 4 ka. Evidence for this change includes decreasing water content and increasing temperatures of the lavas, as well as the increased presence of hybrid lavas and tephras, such as andesites. Both petrologic and seismic work shows that the current reservoir depth since 1980 is ~7-13 km (Pallister *et al.*, 1992; Scandone & Malone, 1985).

2.4 History of the Kalama Eruptive Period

Mount St. Helens has been studied extensively since the catastrophic 1980 eruption. United States Geological Survey (USGS) mapping of tephra deposits by Mullineaux (1986) and flows by Crandell (1987) were combined with dating of Kalama-age deposits by Yamaguchi & Hoblitt (1995) as a basis for the following description of the eruptive history. Ongoing mapping and petrography were essential in refining the report.

The Kalama Eruptive Period lasted about 300 years and is divided into three sub-periods: early (1479-~1500 CE), middle (1505-1570 CE) and late (1620-1750 CE). Ash deposits accompanied each sub-period, although those from the beginning of the period were significantly more voluminous. A generalized stratigraphic column is illustrated in Figure 2.6. All SiO_2 values are in wt %. Rocks erupted during each sub-period of the Kalama Period carried gabbro or gabbronorite xenoliths (50.3-54.1 % SiO_2), some of which may be ~23 million years old (Kent *et al*., 2007). Other inclusions may be cumulates, evidenced by plagioclase-rich, layered textures.

The early Kalama was characterized by explosive eruptions of homogenous dacites. The eruptive sequence began in 1479 CE, after a 600-700 year dormant interval, with a large, explosive dacitic eruption producing Wn tephra (dense rock equivalent (DRE) 2 km^3). Wn tephra deposits are pumiceous bombs and lapilli of 66.6-67.9 % SiO_2. Subsequent ash and lapilli layers Wa and Wb of the same composition erupted within the next two-three years. This was followed in 1482 CE by a pyroclastic eruption with We air fall deposit (DRE 0.4 km^3), that was slightly more mafic (66.2-67.1 % SiO_2) than Wn. Wa and Wb were likely associated with dome growth as abundant dacitic lithics are in We, but none in Wn (Clynne, personal communication, 2010). A final early Kalama 66.0 % SiO_2 ash and lapilli, Wd, erupted either before or coeval with dacite blocks in pyroclastic flows (EKPF). The eruptions were amphibole-orthopyroxene dacites with dominant SiO_2 concentration of 64.8-68.6 % (Pallister *et al*., 1992; Yamaguchi & Hoblitt, 1995; Clynne *et al*., 2005; Clynne, written communication, 2008).

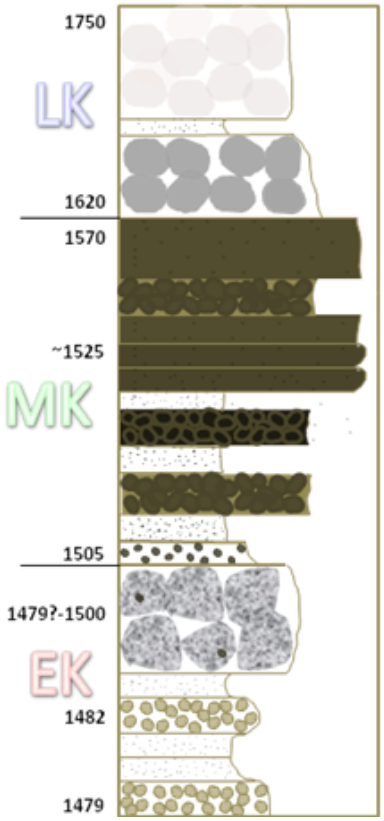

Age (CE)	Lithology	Description	Mineralogy	SiO_2 (wt %)	Samples
1750	Pl Inc in LK	gabbroic inclusions in late Kalama age rocks	cpx=opx>amphibole	51.1-54.0	06A, 12B
LK	SDY	dacite summit dome	opx>amphibole	61.1-63.4	4, 6B, 28, 13
	Z	dacite, ash, not necessarily between SDO & SDY	opx>±cpx±amphibole		
1620	SDO	andesite summit dome	cpx=opx>amphibole>olivine	60.3-61.0	5, 11, 12A
1570	Pl Inc in MK	gabbroic inclusion in middle Kalama age rocks	cpx=opx>amphibole	53.7	08B
	MKLV + PF	andesite lava & pyroclastic flows includes Mitten (M), western flank (WF), & Worm Complex (WC) lavas and Breadcrust Andesite Pyroclastic Flow	opx>cpx>>olivine	56.6-57.5	08A, 16, 3
~1525	MKLV-TF	basaltic andesite, Two Finger Flow, lava	olivine, opx, cpx	56.5-57.0	10
	X Lava Flow	andesite lava, near Windy Ridge	cpx>opx>olivine	59.6-61.2	30
MK	Xh	ash	opx>olivine>cpx		
	X lahar	basaltic andesite lava in lahar, M-type	olivine>cpx>opx>amphibole	55.8-56.3	1, 7
	Xm	basaltic andesite, ash	olivine>cpx>opx	54.7-55.3	
	X lahar	andesite lava in lahar or pf, B-type	olivine>cpx>opx>amphibole	58.2-59.3	2, 9
	Xs	andesite, ash	olivine>cpx>opx>amphibole	59.8	
1505	Xb	andesite, tephra - scoria lapilli	olivine>cpx>opx>amphibole	58.0-59.3	32
	QMI	basaltic andesite quenched inclusions, olivine-rich	amphibole>olivine>cpx>opx	53.7	19
1479?-1500	QMI	andesite quenched inclusions, olivine-poor	amphibole>opx>>±olivine>cpx	56.4-57.7	20, 22
	Pl Inc in EK	gabbroic inclusion in early Kalama age rocks	cpx=opx>amphibole>±olivine	53.2	18A
EK	EKPF	dacite, pyroclastic flows and lahars	opx>amphibole>cpx	64.8-68.6	14, 15, 17, 8B, 21, 23, 24
	Wd	dacite, ash, lapilli	opx>amphibole	66.0	
1482	We	dacite, tephra - lapilli and ash, pumice, dome lithics	opx>amphibole	66.2-67.1	27
	Wb	dacite, ash, lapilli	opx>amphibole	66.6	
	Wa	dacite, ash, lapilli	opx>amphibole	66.6	
1479	Wn	dacite, tephra - pumiceous, lapilli and bombs	opx>amphibole	66.6-67.9	31

Figure 2.6 Generalized stratigraphic column for the Kalama Eruptive Period with data from this study and Clynne *et al.* (2005). Exact stratigraphic placements of Z ash, Breadcrust Pyroclastic Flow, X lahars and ashes, and EKPFs are not well constrained. The Breadcrust Pyroclastic Flow erupted coeval with MKPF, but exact order is unknown. W ashes may have erupted coeval with EKPFs. The order of QMIs and plutonic inclusions listed in EKPFs is not indicative of erupted order

Quenched mafic inclusions (QMI) are found in the early Kalama pyroclastic flow dacites, but have not been previously analyzed. QMIs are rare in Wn and We tephras, where they are generally stretched and inflated (Clynne, personal communication, 2010). Some QMIs are olivine-rich (53.3-54.8 % SiO_2), with abundant clinopyroxene. Present in approximately equal amounts are olivine-poor (57.2-58.9 % SiO_2) orthopyroxene-bearing inclusions. However, virtually all QMIs are dominated by amphibole.

Around 1505 CE, andesitic pyroclastic and lava flows began erupting with the olivine-bearing X tephra set (Pallister *et al*., 1992). Xb was the first of the tephras to erupt and was the only one of the set containing scoria lapilli (Mullineaux**,** 1996). At 58.0-59.3 % SiO_2, Xb is compositionally similar to some lavas from X lahars and pyroclastic flows at 58.2–59.3 % SiO_2. Xs tephra exists only as ash at 59.8 % SiO_2 and may be coeval with these flows. The most mafic of the X tephras, Xm (54.7-55.3 % SiO_2), erupted subsequent to Xs. Basaltic andesite lavas (55.8-56.3 % SiO_2) found in lahar deposits probably correlate with the tephra (which is slightly higher in silica because whole rock analyses are mostly glass). There are no known analyses of the last erupted X tephra, Xh, which was not widely distributed. The X Lava Flow erupted on the eastern flank of the volcano near Windy Ridge. It has less olivine than the previous X deposits and is slightly more evolved (59.6-61.2 % SiO_2). It is unclear whether there were two flows or two lobes from the same flow.

Later middle Kalama lava (MKLV) and pyroclastic flows, dominated by orthopyroxene-clinopyroxene-andesite composition, erupted for ~25 years during the middle Kalama (Clynne, written communication, 2008; Pallister *et al*., 1992). The Two Finger Flow is the most mafic and the only olivine rich MKLV; it probably erupted first. Analyses range 56.5-58.0 % SiO_2, but most are ~57.0 % SiO_2. The Breadcrust Andesite Pyroclastic Flow (57.6-58.2 % SiO_2)

was intercalated with the MKLV. The middle Kalama eruption ended with other lava flows, including unnamed western and eastern flank flows of 58.1-59.3 % SiO_2. The Worm Complex, a network of intricately intertwined andesites (57.0-58.7 % SiO_2), was formed during this time. The Mitten Flow is a part of this complex.

The Kalama Period culminated with nearly 100 years of dome growth, during which the lavas transitioned from andesite back to dacite. The dome growth is divided into early (SDO) and late (SDY) summit domes on the basis of lithology. SDO is pumiceous to subpumiceous amphibole-clinopyroxene-orthopyroxene andesite with about 61-62.5% SiO_2, is porphyritic, and extremely crystal rich (Clynne, written communication, 2008). SDY deposits have a higher abundance of amphibole and SiO_2 at 62.5-64.6 % and appear to be denser than SDO. The clinopyroxene-amphibole-orthopyroxene dacite generally has a pinkish hue and is prismatically jointed. The late Kalama produced ash set Z, a low-volume layer which was likely the result of a dome collapse. It is not clear when the Z ash was produced. Previously, Yamaguchi and Hoblitt (1995) divided the late Kalama into three subphases: lower late Kalama (lithic dacite), the middle late Kalama (dacite pumice), and the upper late Kalama (lithic dacite).

2.5 Comparisons of Kalama Period with Other Eruptive Periods

Similar to some other periods like Smith Creek, eruptions were voluminous during the Kalama Period when Mount St. Helens attained its pre-1980 form (Clynne *et al.*, 2005). Other eruptive periods in Mount St. Helens' history, such as Castle Creek and Goat Rocks, have similar magmatic sequences (Smith & Leeman, 1987, 1993), although compositional ranges vary. The volcano erupted a wide range of compositions from basalt to dacite

during the Castle Creek period, but only high silica andesite (61-62 % SiO_2) to dacite during the Goat Rocks Period (1800 – 1857 CE). Eruptive periods tend to begin more silicic and erupt hydrous Fe-Mg phases while becoming progressively more mafic, and erupt anhydrous phases throughout its course (Carey *et al.*, 1995).

2.6 Previous Work on Kalama Period Rocks

Much of the previous work on Kalama Period rocks focused on two major lines of inquiry: petrogenesis and equilibration of the dacitic component (Gardner *et al.*, 1995a, b; Smith & Leeman, 1987) and models of magma mixing to explain the cyclic progression of felsic-intermediate-felsic eruptions (Gardner *et al.*, 1995a,b; Pallister *et al.*, 1992; Smith & Leeman, 1987; Smith & Leeman, 1993). Smith and Leeman (1987) found that dacites at Mount St. Helens have lower abundances of several incompatible trace elements compared to associated basalts, which precludes fractional crystallization as the dominant process of petrogenesis. Through geochemical analysis and numerical modeling of trace elements, Smith & Leeman (1987) concluded the dacite component at Mount St. Helens is likely generated from partial melting of an amphibolite facies lower crust. Alternately, Smith & Leeman's (1987) interpretation that the variance in trace element ratios in dacites of the Kalama Period and other eruptive periods within the last 40,000 years could be explained by either partial melting of a spatially heterogeneous source region with incompatible trace element abundances that are mid ocean ridge-like (MORB-like), or by open-system processes that introduce other magmas. Leeman *et al.* (1990) suggest the enrichment in hygromagmatic elements of Mount St. Helens rocks is due to the presence of subducted sediments and dehydration fluids. Conversely, Defant & Drummond (1993) completed trace

element modeling of the Juan de Fuca Ridge to demonstrate partial melting of a MORB, the down going slab, as the potential petrogenesis of the Mount St. Helens dacites.

Additional work on Kalama Period dacites includes investigation of the Wn dacitic reservoir conditions. Gardner *et al.*, (1995a) experimentally constrained the magma water content to (molar fraction of H_2O in fluid phase) 0.4-0.5, equilibrium temperature of 848 ±5 °C, and total pressure of 2.5-3.5 kbar. While both calc-alkaline and tholeiitic basalts are present at Mount St. Helens (Gardner *et al.*, 1995; Smith & Leeman, 1993) it is unclear whether there is any tholeiitic input during the Kalama Period. Gardner *et al.* (1995b) propose these middle and late Kalama products demonstrate a tholeiitic mafic component whereas rocks from the early Kalama have a calc-alkaline signature.

Most of the rocks erupted during the Kalama Period have been hypothesized to be a result of magma mixing events (Gardner *et al.,* 1995a; Gardner *et al.,* 1995b; Pallister *et al.*, 1992; Smith & Leeman, 1987; Smith & Leeman, 1993), but the source and composition of each end member is unclear. Banded pumices, sieve textures in plagioclase, resorption of olivine and plagioclase, and disequilibrium rims of pyroxenes and amphibole in W and X tephra sets (Pallister *et al.*, 1992), along with the presence of QMIs in lavas are evidence for mixing processes. The presence of QMIs has not been included in previous geochemical studies of Kalama-age rocks of Mount St. Helens. Such QMIs serve as macroscopic evidence for magma mixing or mingling. Pallister *et al.* (1992) concluded there is a simple two end member mixing scenario between Wn dacite and a north flank-like basalt, which erupted during the Castle Creek period, to produce the X intermediates. They also recognized that the rest of the middle Kalama likely required other basaltic

mixing end members, but did not speculate on compositions or origins other than to discuss reasons why fractionation of accessory minerals like apatite and zircon could not cause the high field strength element (HFSE) depletion at constant SiO_2, as seen in the progression from X rocks to MKLV.

More recent research done by Carroll (2009), concurred with the conclusion of Pallister *et al.*,(1992). Carroll (2009) used a Castle Creek basalt to model that an ocean island-like (OIB-like) basalt (enriched in HFSE and some large ion lithophile elements (LILE)) is indeed a likely end member for the X, but one with lower HREE than known Mount St. Helens basalt compositions. Carroll's models did not offer unique mixing components for MKLV and X products. She did, however, propose there were two dacitic components for the X, based on amphibole compositions, a possibility that will be discussed below. Her assumption was that compositional differences between the X tephra and middle Kalama lavas and pyroclastic flow were minimal, an interpretation based only on one X tephra sample and not lava and lahars. While data from this study does not contradict these previous interpretations, major and trace element data from additional samples provide a more extensive view of compositions that erupted during the middle Kalama and provide further constraints on the mixing end members. Moreover, the Pallister *et al.* (1992) proposal that the later part of the middle Kalama involved additional, poorly constrained end members has not been addressed until now.

Previous magma mixing models do not adequately explain existing major and trace element patterns relative to the dacite-andesite-basaltic andesite-dacite progression of erupted products, nor do they consider the xenoliths and QMIs as potential components of the system. These two types

of inclusions were included in the study to quantify their contribution to the system.

Chapter 3: Research Objectives

This research serves to clarify the petrogenetic history of the Kalama Eruptive Period. Understanding a system as a whole requires its dissection into components. Petrography and geochemistry of a suite of 32 rocks were analyzed to determine the temporal progression of events in the system. Whole rock trace elements were analyzed in addition to major elements. Because trace elements in igneous rocks are more sensitive to some system perturbations than major elements, they can provide details of petrological processes often not otherwise discernable. Analysis of individual phases in the rocks allows tracking of the system's evolution. Phenocryst trace element signatures can be used to distinguish xenocrystic material from parent magmas.

This study attempts to both improve existing models of mixing relationships and to determine if other petrologic processes contributed to the formation of rocks of the Kalama age. As it is expected that magma mixing did play an important role, constraining the end members will further define magmatic contributions at Mount St. Helens. To understand their interactions, I conducted a mass balance calculation for the individual lithologies which allowed it by identifying the crystal cargo and melt each magma contributed to the system. A systematic petrological and geochemical integration, along with observations and modeling scenarios, permits construction of a mixing model that reflects the observed compositions of Kalama-age rocks. Below is a research objective matrix describing the

questions intended to be answered by this study, the hypotheses tested, and the expected outcomes were the hypotheses true. Answering the questions posited below will lead to a model of the petrogenesis of rocks erupted during the Kalama Period.

Table 3.1 Research Objective Matrix

Research Objectives	Hypotheses	Expected Outcomes
Do the early, middle and late Kalama rocks result primarily from mixed magmas? A. Can the felsic component(s) be constrained? B. Can the mafic component(s) be constrained? C. What proportion of crystals and liquid did each component contribute? (Mass balance)	1. Early Kalama rocks are a mixture between a dacite & a mafic magma. 2. Middle Kalama rocks are a mixture between a dacite & 1 or more mafic magmas. 3. Late Kalama rocks are a mixture between a dacite & a mafic magma.	Whole rock geochemistries of a two-component mixture would produce linear trends on variation diagrams, disequilibrium textures would be apparent, and crystal populations would be mixed.
Are other petrologic processes identifiable? Did partial melting or assimilation of the xenolith sources contribute to the geochemical signature of any Kalama-age rocks?	Fractional crystallization and/or assimilation of wall rock also contributed to geochemical signatures and textures found in Kalama-age rocks.	Whole rock major and trace elements will show fractionation trends and modeling will show assimilation was likely. Disaggregated crystals from wall rock may be observed.
Are the QMI related to the middle Kalama rocks?	The QMI found in early Kalama rocks comprise a magma end member of the middle Kalama mixed magmas.	Whole rock geochemistry will show resemblance between middle Kalama rocks and QMIs. Crystal populations will be shared. Disequilibrium textures & compositions will point to mixing.
What is the source or liquid line of descent of the QMIs?	1. QMIs are fractionates of basalt. 2. QMIs are from a mixed magma.	Major and trace element modeling will show potential sources for the QMIs.
How are the early and late Kalama dacites related? Do they have the same felsic and/or mafic end members?	Early and late Kalama dacites have: 1. same felsic, but different mafic end members. 2. same mafic, but different felsic end members. 3. no end members in common	Whole rock and phase trace element geochemistry will show similarities between magmas if they share end members.

Chapter 4: Methods

4.1 Sample Collection

A suite of 29 rock samples, four of which were inclusions and four others that contained inclusions, was collected in September 2007 from known Kalama-age localities on the flanks of Mount St. Helens. Sites were selected with the guidance of Michael Clynne and Edward Wolfe of the USGS who are undertaking an extensive mapping project at Mount St. Helens and who shared details of stratigraphy and geochemical analysis of other eruptive periods. Lithologies collected include tephras and pyroclastic flow deposits with QMIs from the early Kalama, tephra and lavas from in situ flows and lahar deposits from the middle Kalama, and summit dome from the late Kalama, as well as plutonic inclusions from each of the three stages. Samples and lithologies are listed in Table 4.1, and locations are plotted on Figure 4.1.

Table 4.1 Lithologies and Locations of Kalama-age Samples for this Study. PF= pyroclastic flow. All EKPF are found in pyroclastic flows. BCD=Butte Camp Dome. All other lithology abbreviations as in text.

Sample & Sub-period		Lithology	Description	Location	Latitude N	Longitude W	Uncertainty (ft)
01	MK	X lava	In lahar, M-type	8123 Rd, Kalama R. drainage	46.1481	-122.2702	± 37
02	MK	X lava	In lahar, B-type	8123 Rd, Kalama R. drainage	46.1475	-122.2694	± 31
03	MK	PF	Breadcrust Andesite PF	8123 Rd, ~2miles from 02	46.1591	-122.2626	± 86
04	LK	SDY	SDY in lahar	8123 Rd, Kalama R. drainage	46.1661	-122.2601	± 24
05	LK	SDO	SDO in lahar	8123 Rd, Kalama R. drainage	46.1664	-122.2602	± 19
06A	LK	Pl Incl	Gabbro xenolith	8123 Rd, Kalama R. drainage	46.1664	-122.2605	appr by map
06B	LK	SDY	SDY - host to 06A	8123 Rd, Kalama R. drainage	46.1664	-122.2605	appr by map
07	MK	X lava	In lahar, M-type	June Lake Trailhead	46.1344	-122.1586	± 39
08A	MK	WC lava	Andesite lava flow	June Lake, slot canyon	46.1504	-122.1606	± 17
08B	MK	Pl Incl	Gabbro xenolith	June Lake, slot canyon	46.1504	-122.1606	± 17
09	MK	X lava	In lahar or PF, B-type	Red Rock Tr, SDY channel	46.1727	-122.2192	± 16
10	MK	TF lava	Block lava flow	Loowit Tr	46.1721	-122.2170	appr by aerial
11	LK	SDO	SDO in PF	Loowit Tr, between MK lobes	46.1839	-122.2242	appr by aerial
12A	LK	SDO	PF, host to 12B	Loowit Tr, between MK lobes	46.1839	-122.2242	appr by aerial
12B	LK	Pl Incl	Gabbro xenolith	Loowit Tr, between MK lobes	46.1839	-122.2242	appr by aerial
13	LK	SDY	PF or Lahar	1980 Lahar	46.1821	-122.2226	appr by aerial
14	EK	PF	Dense, lithic-rich PF	EK PF Quarry, Kalama R.	46.1364	-122.3229	appr by map
15	EK	PF	PF, pumice	EKPF Quarry, Kalama R.	46.1364	-122.3229	appr by map
16	MK	WF lava	Andesite lava flow	Toward Butte Camp Canyon	46.1669	-122.2446	± 37
17	EK	PF	Block from dome	Up canyon from 16	46.1678	-122.2421	± 49
18A	EK	Pl Incl	Gabbro xenolith	BCD drainage	46.169	-122.2433	appr by map
18B	EK	PF	Dacite host to 18A	BCD drainage	46.169	-122.2433	appr by map
19	EK	QMI	Vesicular rim	BCD drainage	46.1700	-122.2424	appr by map
20	EK	QMI	Crenulated margin	BCD drainage	46.1700	-122.2424	appr by map
21	EK	PF	Dacite host to 20	BCD drainage	46.1715	-122.2410	appr by map
22	EK	QMI	Fingers into host	BCD drainage	46.1725	-122.2403	appr by map
23	EK	Pl Incl	Slide=Inclusion Bulk rock=dacite PF host	BCD drainage	46.1733	-122.2396	appr by map
24	EK	PF	Slide=Inclusion Bulk rock=dacite PF host	BCD drainage	46.1733	-122.2396	appr by map
27	EK	We tephra	Pumice	Upper Pine Creek	46.1700	-122.1321	± 27
28	LK	SDY	Prismatic block from lahar	Pine Creek	46.1679	-122.1281	± 25
30	MK	X Lava	Dark, blocky flow	Windy Ridge	46.2181	-122.1535	± 13
31	EK	Wn tephra	Light gray pumice blocks	Windy Ridge	46.2339	-122.1527	± 13
32	MK	Xb tephra	Dark brown-gray, lapilli	Windy Ridge	46.2339	-122.1527	± 13

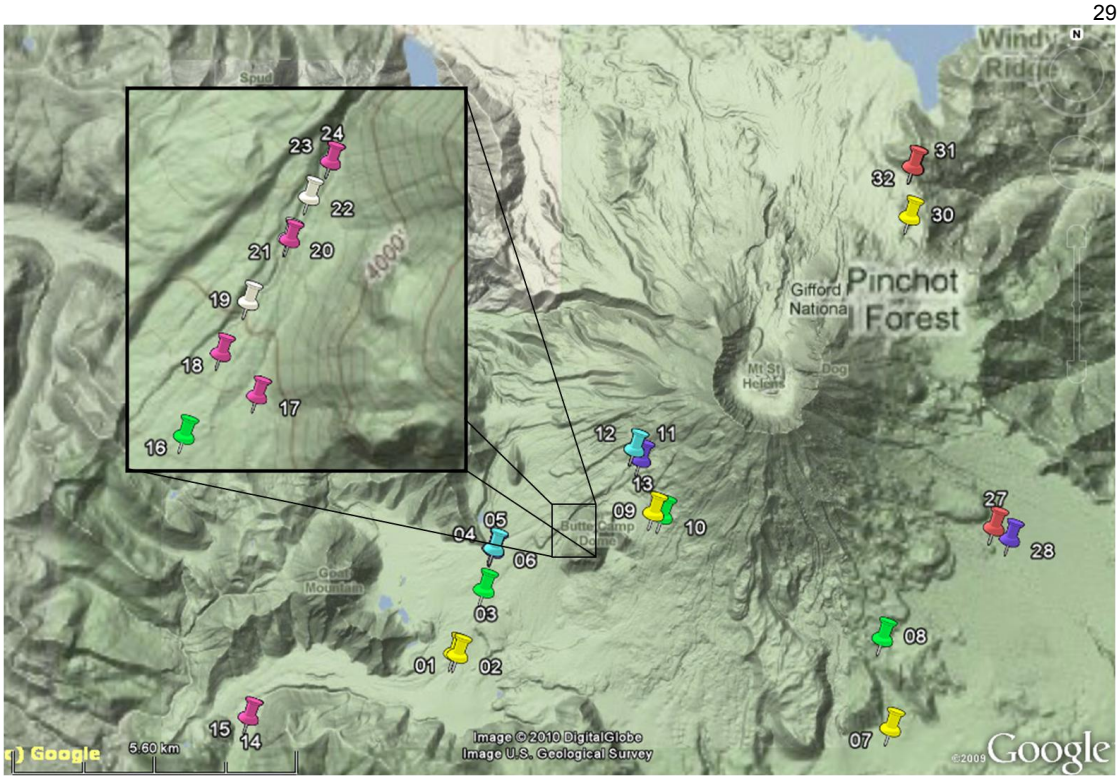

Figure 4.1 Map of Mount St. Helens area and sample locations. Pins color indicates sub-period of lithology: Red-W tephra, Pink-EKPF, White-QMI, Yellow-X deposits, Green-MKLV, Aqua-SDO, Purple-SDY. Inset is of Butte Camp Dome drainage.

4.2 Analytical Techniques

4.2.1 Petrography

A billet measuring 4 x 2.5 x 1 cm was cut from each of 29 samples and sent to Vancouver Petrographics in British Columbia, Canada, to be made into polished thin sections for petrography, electron microprobe analysis (EMPA), and laser ablation inductively coupled plasma mass spectrometry (LA-ICP-MS). Mineralogy and phase textures were examined in 29 thin sections at Oregon State University using a petrographic microscope, and descriptions are presented in Chapter 5.2. Photomicrographs of selected slide sections were taken using a Nikon digital camera (DXM1200) and ACT-1 image

software in the VIPER (Volcanology, Igneous Petrology, Economic Research) Laboratory at Oregon State University.

4.2.2 Whole Rock X-ray Fluorescence and Inductively Coupled-Mass Spectrometry

Thirty-two whole rock samples were prepared simultaneously for major element and trace element analysis by X-Ray Fluorescence (XRF) and trace element analysis by ICP-MS beginning at Oregon State University using an aluminum oxide-plated chipper. The remaining sample preparation was completed at Washington State University where the analyses were conducted. To ensure sample homogeneity, phaneritic sample chips (from the gabbroic inclusions) were separated through a Rock Lab rotary splitter for one minute while other samples were coned and quartered. The standard Washington State University single bead low-dilution fusion technique, detailed in Johnson *et al.* (1999), was subsequently applied to all samples. Twenty-eight g of chips were ground in a tungsten carbide swing mill for two minutes and 3.5 g combined with 7 g of dilithium tetraborate ($Li_2B_4O_7$) to aid in fusion. The mixture was poured into graphite crucibles and baked in a muffle furnace at 1000°C for five minutes. The cooled beads were reground in the swing mill for 35 seconds and the XRF beads were then refused for an additional five minutes. The final preparation comprised engraving labels, grinding off the excess carbon with 600 silicon carbide grit sandpaper, finishing with alcohol on a glass plate, and cleaning (Johnson *et al.*, 1999). ICP-MS powders were not refused, but rather forwarded to Washington State University staff for acid dissolution using the method described in Knaack *et al.* (1994).

XRF analysis of 10 major and minor elements and 18 trace elements was conducted using a ThermoARL Advant'XP+ sequential X-ray fluorescence spectrometer at the geoanalytical lab at Washington State University. The lab uses a Rhodium target run at 50 kV and 50 mA with full vacuum and a 25 mm mask. Results are listed in Table A.1. Twenty-seven trace elements were measured by ICP-MS using a Hewlett-Packard 4500+ quadrupole mass spectrometer following methods described in Knaack *et al*. (1994). Results and are listed in Table A.2. Internal standard beads BCR-P and GSP-1 are run between every 28 unknowns for precision. Accuracy is determined by use of one Brazilian quartz and nine USGS standards (listed in Table 4.2) run as unknowns. Additionally, results of known samples are compared with those analyzed in other labs.

Table 4.2 Washington State University Accuracy Standards Used for XRF

BCR-1	AGV-1	GSP-1	G-2	PCC-1
BIR-1	DNC-1	W-2	STM-1	QTZ

4.2.3 Electron Microprobe Analysis

Polished thin sections were carbon coated and analyzed on the Cameca SX-100 Electron Microprobe at Oregon State University, which employs 5 wavelength dispersive spectrometers (WDS) and one energy dispersive spectrometer (EDS). Minerals analyzed included olivine, spinel, plagioclase, orthopyroxene, and clinopyroxene, as well as groundmass glass, using a 15 keV accelerating voltage and 30 nA current. Counting times ranged from 10-60 seconds depending on the sensitivity of the spectrometer crystal and detection limits. Raw data was corrected using a stoichiometric PAP correction model detailed by Pouchou and Pichoir (1984). High resolution

photomicrographs were taken of samples using the system's high speed back scattered electron (BSE) imaging system and Cameca Peak Site software. The number of samples and types of analyses are summarized in Table (4.3).

Table 4.3 Mineral and Glass EMPA

Phase	**Crystal Sizes (mm)**	**Analysis Type**	**# of Samples**
Plagioclase Phenocrysts	0.1-2	Spot, Transect	15
Plagioclase Microphenocrysts	0.01-0.08	Spot	15
Pyroxene	0.1-2	Spot, Transect	4
Olivine	0.1-1.2	Spot, Transect	9
Spinel	0.05-0.02	Spot	4
Groundmass Glass	n/a	Spot	10

The EMP was calibrated using a variety of different standards, depending on phase analyzed and required sensitivity. Well-characterized mineral and glass standards were then analyzed as unknown samples to determine accuracy and precision. Representative plagioclase analysis calibrations and standards are summarized in Table 4.4.

Table 4.4 Standards for EMPA Calibration

EMP Plagioclase Analytical Precision and Accuracy

	Standard LABR	Overall Mean	n=	1 Stand Dev %	Accuracy %
SiO_2	51.25	51.06	13	0.38	0.36
Al_2O_3	30.91	30.95	13	0.20	0.12
FeO	0.49	0.42	13	6.05	13.37
CaO	13.64	13.58	13	0.40	0.47
Na_2O	3.45	3.43	13	0.75	0.60
MgO	0.14	0.14	13	2.25	0.37
P_2O_5	0.01	0.02	10	48.46	69.30
TiO_2	0.05	0.04	13	20.96	25.38
K_2O	0.18	0.11	13	6.80	36.57
MnO		0.02	11	78.59	
Cr_2O_3		0.00	8	3356.94	
SrO		0.07	3	15.77	
Total		99.79		0.23	

EMP Olivine Analytical Precision and Accuracy

	Standard Fo83	Mean n=16	1 Stand Dev %	Accuracy %
SiO_2	38.95	39.00	0.43	0.14
Al_2O_3		0.01	92.67	
Na_2O		0.00	204.61	
MgO	43.58	43.44	0.44	0.32
K_2O		0.00	480.29	
CaO		0.02	191.43	
MnO	0.3	0.29	10.04	2.81
FeO	16.62	16.63	1.73	0.07
NiO		0.02	318.20	
Cr_2O_3	0.02	0.02	83.25	4.81
TiO_2		0.02	153.98	

Table 4.4 (Continued)

EMP Spinel Analytical Precision and Accuracy

	Standard CROM	Mean n=4	1 Stand Dev %	Accuracy %
SiO_2		0.02	68.32	
Al_2O_3	9.92	9.95	0.25	0.31
FeO	13.04	12.88	0.94	1.24
NiO		0.16	23.39	
Na_2O		0.00	221.53	
MgO	15.20	15.35	0.18	0.96
CaO	0.12	0.00	232.41	100.58
TiO_2		0.11	7.09	
Cr_2O_3	60.50	60.10	0.18	0.65
MnO	0.11	0.15	9.58	36.93
ZnO		0.02	354.43	
Vr_2O_3		0.09	31.45	
CuO		0.00	1508.65	
CoO		0.02	146.42	

	Standard GAHN	Mean n=4	1 Stand Dev %	Accuracy %
SiO_2		0.01	105.32	
Al_2O_3	55.32	55.19	0.33	0.24
FeO	1.97	1.92	3.29	2.34
NiO		-0.01	208.39	
Na_2O		1.28	3.53	
MgO		0.02	31.36	
CaO		0.00	1528.73	
TiO_2		-0.01	136.98	
Cr_2O_3	0.38	0.00	27738.54	100.01
MnO		0.33	9.86	
ZnO	42.50	42.99	0.70	1.15
Vr_2O_3		-0.01	-287.85	
CuO		0.03	231.48	
CoO		0.01	383.76	

Table 4.4 (Continued)

EMP Pyroxene Analytical Precision and Accuracy

	Standard KAUG	Mean n=6	1 Stand Dev %	Accuracy %
SiO2	50.73	50.76	0.42	0.06
Al2O3	8.73	8.57	0.46	1.80
K2O	0	0.01	99.07	
NiO		0.03	67.52	
FeO	6.45	6.95	2.24	7.75
MnO	0.13	0.15	23.33	14.60
Na2O	1.27	1.29	1.17	1.65
MgO	16.65	16.67	0.47	0.09
TiO2	0.74	0.77	0.48	3.70
CaO	15.82	14.75	0.25	6.74
Cr2O3		0.16	5.99	
Total		100.11	0.30	

EMP Glass Analytical Precision and Accuracy

	Standard RHYO	Mean n=3	1 Stand Dev %	Accuracy %
SiO_2	76.71	76.63	0.44	0.10
Al_2O_3	12.06	12.55	0.54	4.04
P_2O_5	0.01	0.01	158.28	16.00
S		0.00	105.43	
Cl		0.11	2.80	
F		0.00	131.63	
K_2O	4.89	5.00	0.85	2.29
CaO	0.5	0.44	2.82	12.61
MnO	0.03	0.00	1254.54	111.22
Cr_2O_3		-0.02	51.88	
FeO	1.28	1.20	4.09	6.17
NiO		-0.01	587.75	
Na_2O	3.75	3.76	1.81	0.21
MgO	0.1	0.03	14.59	67.10
TiO_2	0.12	0.08	5.69	29.36
Total		99.84	0.37	

4.2.4 Laser Ablation-Inductively Coupled-Mass Spectrometry

LA-ICP-MS of individual plagioclase and pyroxene crystals was conducted at the W.M. Keck Collaboratory for Plasma Spectrometry at Oregon State University. A DUV 193 nm ArF Excimer laser on a VG Elemental ExCell quadrupole ICP-MS, with He as the transfer gas, used a 50 μm diameter laser spot and 40 s dwell time for analysis. NIST-612 glass served as calibration standard, while ^{43}Ca was used as an internal standard in combination with measured CaO wt % from EMPA. A summary of the analytical technique is described in Kent *et al.* (2004). Relative errors in concentrations calculated from the external standard deviation from multiple analyses typically correlate positively with $(C_i^{1/2})/C_i$, where C_i is the concentration of element i (Kent *et al.,* 2004). Error for measurements was generally < 8%, except for V (10 %), Dy (11 %), and Ta (18 %). Standards and errors are listed in Table 4.5. Measurements and uncertainties are shown in Appendices B and C.

Table 4.5 Analytical Precision for LA-ICP-MS. Accepted values for calibration and secondary standards for La-ICP-MS from Kent *et al.,* (2004).

Calibration Standard		Secondary Standard			
Isotope	**NIST-612 Accepted (ug/g)**	**BHVO-2G Accepted (ug/g)**	**Mean n=6 (ug/g)**	**1 Stand Dev %**	**Accuracy %**
7Li	42				
26Mg	77				
29Si	336107.0				
43Ca	85048.6	81475.1	81475.1	0.00	0.00
45Sc	41	33	30.9	3.28	6.34
47Ti	44	16300	17034	2.30	4.50
51V	39	308	339.9	3.40	10.35
52Cr	36				
55Mn	38				
57Fe	51				
65Cu	37				
85Rb	31.4	9.2	9.9	6.03	7.28
86Sr	78.4	396	422.0	4.09	6.58
88Sr	78.4				
89Y	38	26	25.1	7.86	3.45
90Zr	38	170	161.5	5.75	5.00
93Nb	40	18.3	18.4	2.82	0.58
137Ba	39.7	131	136.1	6.02	3.92
138Ba	39.7	131	140.1	3.33	6.93
139La	35.8	15.2	15.0	2.95	1.38
140Ce	38.7	37.6	39.7	4.25	5.52
141Pr	37.2	5.4	5.2	6.12	3.24
146Nd	35.9	24.5	24.1	7.75	1.51
147Sm	38.1	6.1	6.0	10.14	0.89
153Eu	35	2.1	2.1	4.80	0.69
157Gd	36.7	6.2	6.4	6.18	3.94
163Dy	36	5.3	4.7	9.26	10.93
166Er	38	2.6	2.4	10.90	4.87
172Yb	39.2	2.0	1.9	13.47	5.63
Ta		1.2	1.4	16.81	18.26
208Pb	38.6	1.7	1.8	9.67	7.81
Th		1.2	1.2	10.04	2.37
U		0.4	0.4	22.99	4.28

Chapter 5: Results

Results from this study will be described according to analytical technique from larger scale (hand sample) to the smaller scale (phase geochemistry) and generally in eruptive sequence. Petrographic descriptions of the general characteristics of rocks of the Kalama age are followed by detailed reports of each lithology and finally by summaries of the key features of each subperiod. Whole rock major and trace element geochemistry data are presented and summarized, as are major and trace element phase geochemistry data.

5.1 Hand Sample

Kalama-age volcanics are porphyritic, and except for the tephras, have either cryptocrystalline or microcrystalline groundmass. Many have seriate texture as well. Tephras generally have glassy groundmass with sparse phenocrysts. Early Kalama rocks are found either as tephra or pyroclastic flow deposits. Pyroclastic flow deposits, primarily found in drainages, consist of light to medium gray lithic-rich blocks. They are porphyritic with abundant plagioclase and amphibole. Early Kalama tephras Wn and We are light gray-tan and contain plagioclase, orthopyroxene and rare amphibole.

Three QMIs were analyzed for this study. QMI 19 is a dark, fine-grained, vesicular, irregularly-shaped mass with rounded edges. Adjacent disaggregated smaller globules (Figure 5.1) are found near the inclusion in the host rock. Vesicles are especially prevalent at the margin with the host rock and are visible in hand sample. QMI 20 has the largest (among the three QMI) contrast in color with the host dacite and is distinguished by well-defined cuspate margins (Figure 5.2). It is ~15% vesicular, and the bubbles are more

evenly dispersed than QMI 19, although a small degree of coalescence is visible. QMI 22 is also fine grained with an irregular shape that appears to finger into the host rock (Figure 5.3). Some crenulated margins are also visible as in QMI 20.

Middle Kalama samples were taken from tephra, pyroclastic flow and lahar deposits, and lavas. Middle Kalama Xb tephra is banded brown, dark brown and gray in color and contains prismatically jointed lapilli up to 5 cm in diameter. The lapilli contain glomerocrysts of olivine, plagioclase and pyroxene. X andesite and basaltic andesite lavas, in addition to the Breadcrust Andesite Pyroclastic Flow, are dark gray-black with olivine, pyroxene and sparse plagioclase phenocrysts. Late Kalama summit dome samples were collected from lahar and pyroclastic flow deposits. SDO and SDY are very similar in appearance. Both rocks are light gray prismatically jointed blocks, but SDY is especially crystal rich and fine grained. It usually has a pinkish hue and is more strongly prismatically jointed than SDO. Plutonic inclusions found in all sub-periods of Kalama-age rocks are holocrystalline and phaneritic with large plagioclase and pyroxene (Figure 5.4). Some contain olivine.

Figure 5.1 QMI 19 is the darker rock hosted in EKPF. Darker patch is wet rock to show detail. Note vesicles at the host-inclusion interface. Fe staining is alteration from handling. Also note small, dark globules near larger ones.

Figure 5.2 QMI 20 in EKPF 21. Note cuspate margins, and small disaggregated globules near larger ones.

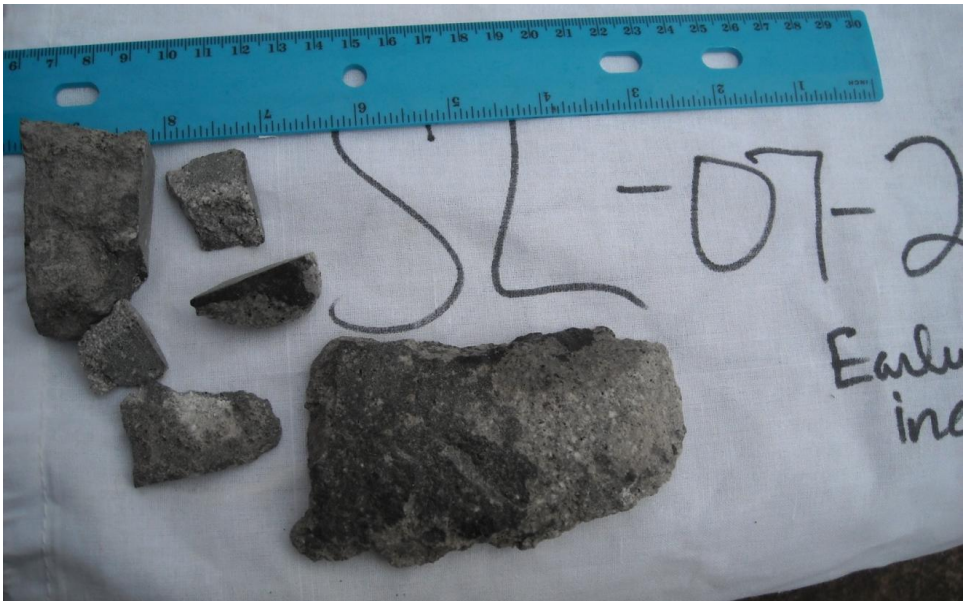

Figure 5.3 QMI 22 in early Kalama dacite. Note the finger –like projection of the mafic magma into the dacite.

Figure 5.4 Plutonic inclusion in EKPF.

5.2 Petrography

Kalama-age rocks vary in crystallinity from glass rich W set tephra (<30 % crystalline) to plagioclase-phyric SDY (> 80 % crystalline). Figure 5.5 shows representative examples of each lithology. Grains are euhedral through anhedral and range in size from 10s of microns to millimeters. Disequilibrium textures, such as resorption and rim overgrowths, are common in many phenocrysts in all sub-periods of Kalama-age rocks. Groundmass glass generally shows flow laminations around phenocrysts and vesicles.

Plagioclase is the dominant phenocryst and microlite phase in all samples and is present in a wide range of sizes (from 0.01 mm to 2.5 mm), textures and compositions. Feldspar textures include compositional zoning, sieving, skeletal structures, spongy or patchy cores, reaction rims, embayments, shattered crystals, and core overgrowths. Middle Kalama lavas and pyroclastic flow deposits especially contain numerous grains of plagioclase that have such disequilibrium textures. Oscillatory zoning is most prevalent, but normal zoning is common; reverse zoning is present, but rare. Plagioclase in many lithologies shows signs of dissolution between grains and along cracks that may have crenulated and embayed edges.

Orthopyroxene is also abundant in phenocryst (up to 1 mm) and microlite form. Clinopyroxene (up to 2 mm) is evident in fewer samples, predominantly in middle Kalama pyroclastic flows, lavas and tephra, and frequently in glomerocrysts. Wn tephra also contains small grains of clinopyroxene. Many pyroxenes have amphibole overgrowth rims and some have a spongy texture.

Figure 5.5 Representative photomicrographs of Kalama-age rocks. a. Wn 27. b. We 31. c. Plutonic inclusion 18B hosted by EKPF 18A. d. EKPF 14. e. Xb tephra 32. f. X Lava Flow 30. g. X lahar 02. h. X lahar 07. i. MKLV Two Finger Flow 10. j. MKLV Worm Complex lava 8A. k. MKLV western flank lava 16. l. Breadcrust Andesite Pyroclastic Flow 03. m. SDO 11. n. SDY 28. o. Plutonic inclusion in EKPF 24. p. Plutonic inclusion 8B in MKLV 8A.

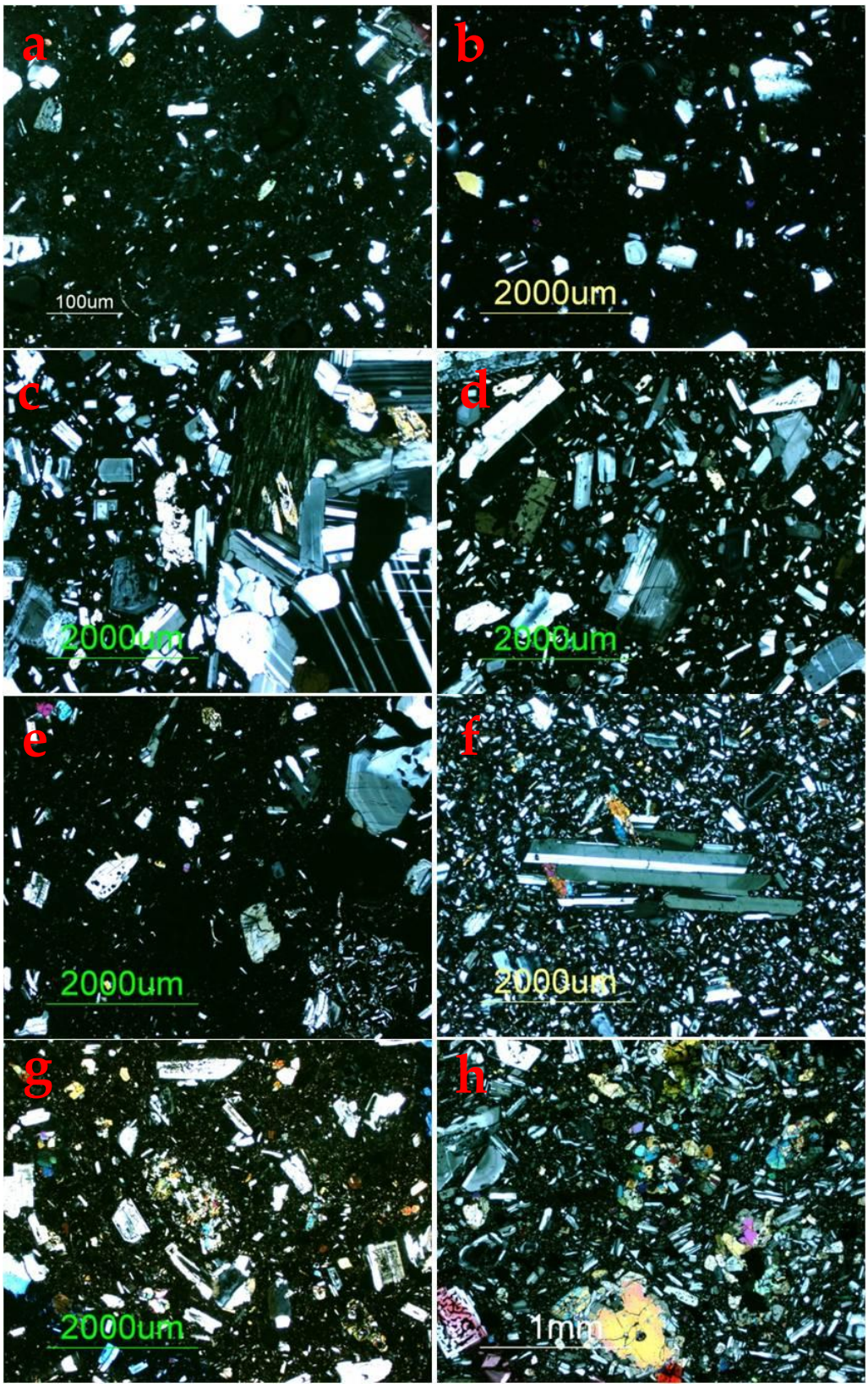
a
100um
b
2000um
c
2000um
d
2000um
e
2000um
f
2000um
g
2000um
h
1mm

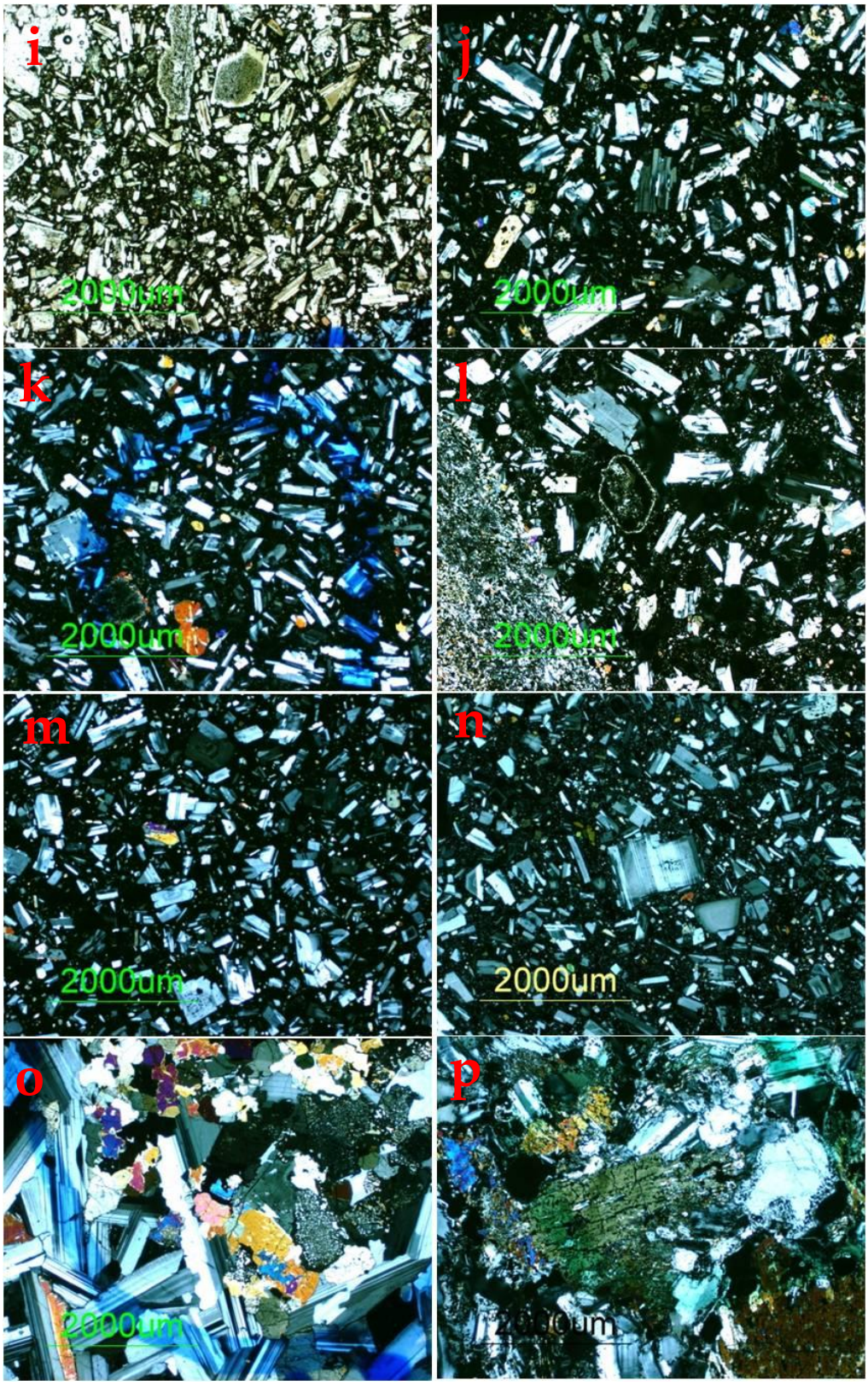

Figure 5.5 (Continued)

Amphibole crystals (up to 2 mm) are also common in all sub-periods, but are especially prevalent in QMIs. Amphibole has a variety of rim compositions, often present in the same thin section (Figure 5.6). Reaction rims on amphibole are often absent, most notably in the early Kalama tephras. Otherwise amphibole textures include thin to heavy opacite and breakdown rims comprising plagioclase, pyroxene and Fe oxides.

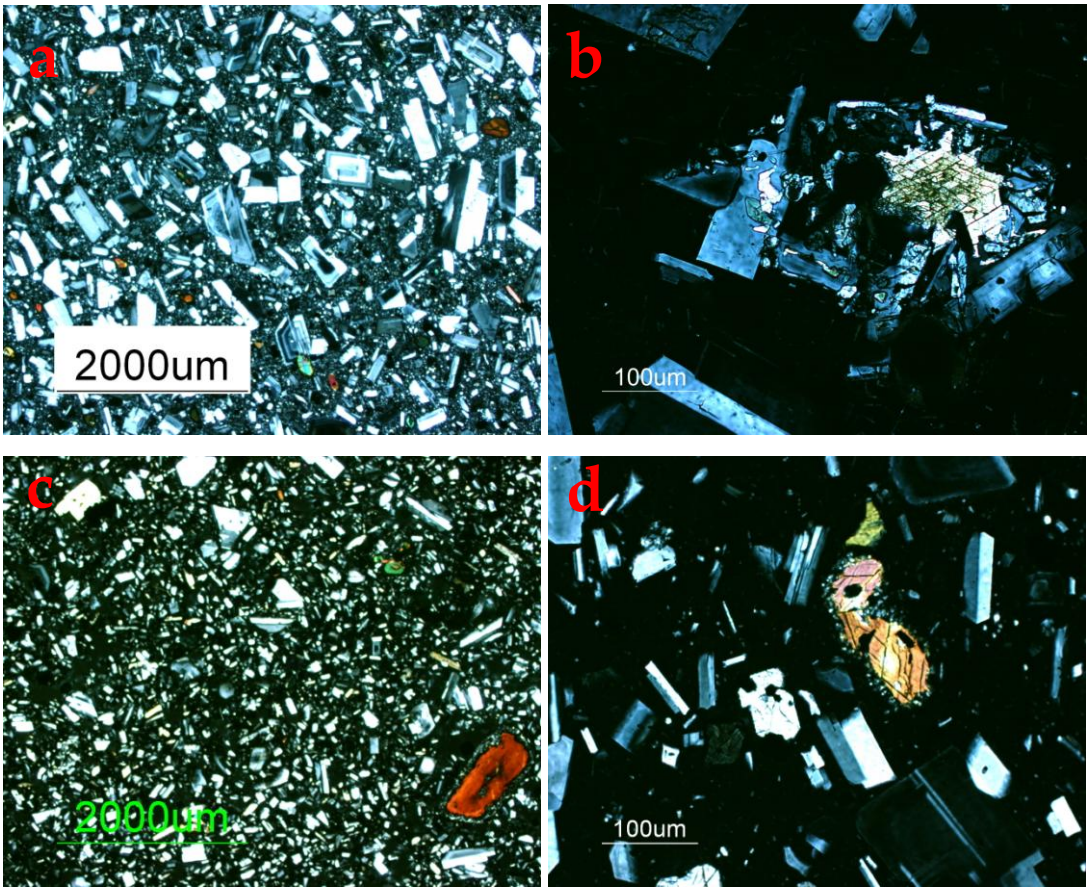

Figure 5.6 Amphibole textures present in Kalama-age rocks. a. SDY 28 amphibole with opacite rims. b. EKPF 14, breakdown/reaction rim of mostly plagioclase+Fe oxides around amphibole. c. X lava 30 amphibole with reaction rim. d. EKPF 14, thin reaction rim around amphibole.

Olivine (up to 2.1 mm) occurs primarily in middle Kalama rocks and plutonic inclusions, but is rare in early Kalama pyroclastic flows and late

Kalama Summit Dome. Many examples in middle Kalama rocks exhibit moderate to heavy resorption and reactions rims. BSE images of olivine show compositional variation between core and rims, as well as reaction rims along boundaries touching groundmass glass (Figure 5.7).

Figure 5.7 Backscatter electron (BSE) images of representative middle Kalama olivine textures. Bright areas in the BSE images represent higher mean atomic numbers, whereas darker areas represent lower mean atomic numbers. a. 10 crystal 7 (Fo_{63}) bordered by pyroxene overgrowth rim. b. Breadcrust Pyroclastic Flow 03 crystal 2 (Fo_{67}) with pyroxene overgrowth rim. c. X Lahar 01 crystal 7 (core Fo_{74}, rim Fo_{63}) with pyroxene reaction rim and embayments. d. X Lahar 02 crystal 1 (Fo_{73}) skeletal texture of olivine with Fe-Ti oxides (white). e. X Lahar 02 crystals 7 and 8 with large embayments. d. X Lahar 02 crystal 5 (Fo_{75-79}) skeletal olivine. e. X Lahar 01 X lahar crystal 10 (Fo_{75-79}) with reaction and diffusion rim. f. X Lahar 01 crystal 10 with relatively clean rim and diffusion profile.

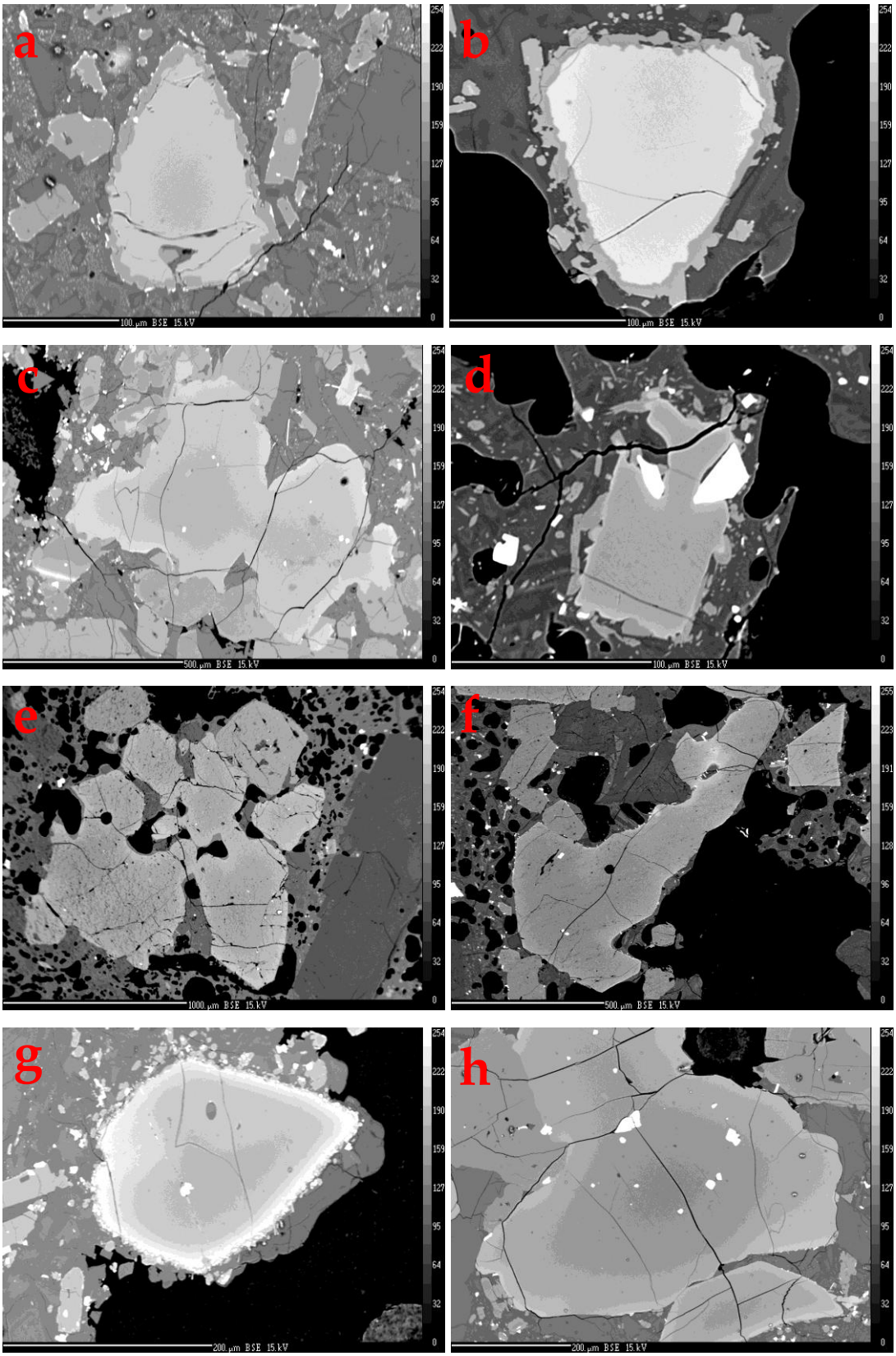
a
b
c
d
e
f
g
h
100 µm BSE 15 kV
500 µm BSE 15 kV
1000 µm BSE 15 kV
200 µm BSE 15 kV

5.2.1 Plutonic Inclusions

Most plutonic inclusions in Kalama-age rocks show signs of disequilibrium. Plagioclase is the dominant grain. Many grains display warped and bent albite twinning (Figure 5.8). Glass inclusions are common at crystal boundaries. Orthopyroxene and clinopyroxene are also present in all plutonic inclusions. Many pyroxenes show well-developed exsolution lamellae, which resembles granophyric textures. Much of the pyroxene is reacting to amphibole. Olivine is also abundant in some samples. Olivines are anhedral to subhedral, some with rim overgrowths. In some inclusions, the pyroxene and olivine do not form 120° boundaries, but rather are smaller anhedral grains that appear to have formed in pockets in between much larger plagioclase grains (Figure 5.9).

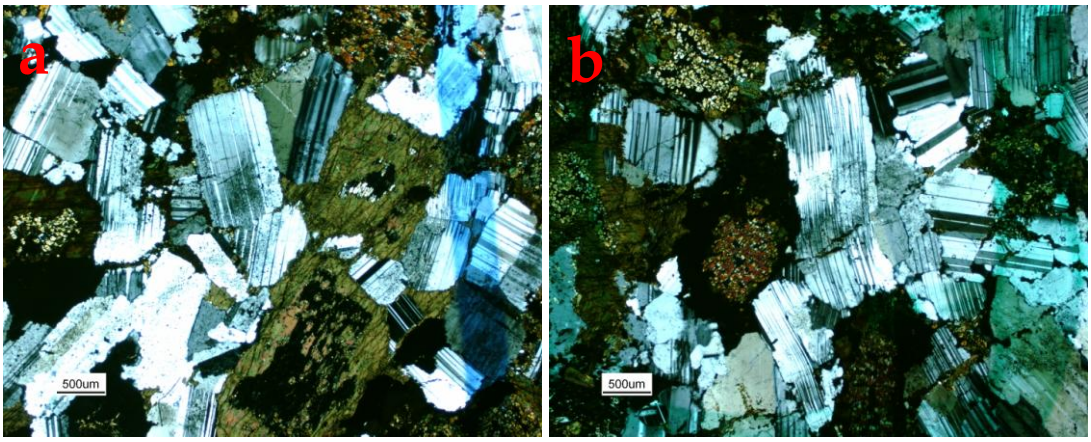

Figure 5.8 Photomicrographs of plutonic inclusions in (no whole rock chemistry done) in EKPF 23. a. Pyroxenes are reacting to amphibole, and plagioclase shows signs of melting at edges. b. Plagioclase in center displays bent albite twinning, indicative of heating or other stress. Blue and green streaks are artificial marks on thin section.

Figure 5.9 Photomicrographs of plutonic inclusion (no whole rock chemistry done) hosted by EKPF 24. The intersection of large plagioclase grains creates pockets of pyroxenes and olivine. Note the lamellae in pyroxenes.

5.2.2 Rocks of the Early Kalama Age

The early Kalama Period is dominated by porphyritic rocks with groundmass crystallinity ranging from mostly glassy to microcrystalline (plagioclase, orthopyroxene, and Fe oxides) with some glass. As in all Kalama-age rocks, plagioclase is the dominant phenocryst phase (An_{29-69}). Plagioclase phenocrysts with heavily sieved cores are largely absent from the W tephra but present in a small amount in the pyroclastic flows. Medium (0.5-1 mm) to large (1-1.5 mm) grains have varying textures including clear surfaces, sieved zones, complex and oscillatory zoning, and skeletal textures in cores and rims. Many grains are broken. Microphenocrysts are abundant in the pyroclastic flows, and less abundant in the tephras.

Orthopyroxene is the second most dominant phase in early Kalama rocks. It commonly occurs as phenocrysts, in glomerocrysts with plagioclase, and less often with other mafic phenocrysts. Amphibole is present in lesser amounts than orthopyroxene in all samples. Grains are small-medium (0.1-0.5 mm). Rims are not reacted in the pumice samples, but are a mix of those with no reaction rims and those with thick breakdown rims (no opacite) in the

pyroclastic flows. Clinopyroxene is rare in most samples, but as abundant as orthopyroxene in Wn tephra 31 and EKPF 15. Both samples also contain rare olivine, as does We pumice (Carroll, 2009). Clinopyroxenes are small (0.1-0.2 mm), reacted and present with oxides.

Wn 27 and We 31 pumice are estimated 20-30% vesicular. The groundmass consists of brown globules of glass, euhedral oxides and rare microphenocrysts. Glomerocrysts of plagioclase, orthopyroxene, clinopyroxene, amphibole and oxides are present in We 27, but not Wn 31. Plagioclase occurs as small microphenocrysts (An_{36-62}), medium (0.5-1 mm) (An_{29-69}) and large (1-2+ mm) (An_{37-64}) grains that display complex zoning patterns and agglutinations of 2 or more sutured grains. A few phenocrysts have sieve zones, but most are smooth with a little interior glass, patch cores or skeletal textures.

More crystalline than the tephra deposits, early Kalama pyroclastic flows (14, 15, 17, 18B, and 21) have abundant plagioclase microlites, microphenocrysts, phenocrysts, and 5-10% vesicles. EKPF 15 is less crystal-rich than the others. Groundmass comprises plagioclase needles, orthopyroxene and glass. At least one EKPF, sample 14, displays two glass populations within the same thin section (Figure 5.10), with one glass population more crystalline than the other. There is a very pale brown glass that appears smooth and has sparse microlites. The other population is darker brown and appears more mottled, due to more abundant microlites. These microlites are oriented subparallel to one another. Glasses are banded in a single direction, although they slightly intermingle at contacts. Amphibole phenocrysts with both clear and reacted rims are present in each glass type.

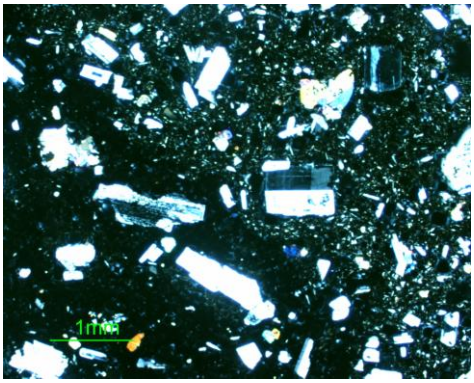

Figure 5.10 Photomicrograph of X lahar 02 (B-type) lava clast at 20x magnification. Sample shows there are two distinct types of groundmass, one being more crystalline than the other.

There are at least two plagioclase phenocryst populations in early Kalama pyroclastic flows. Large (1-2 mm) phenocrysts with heavily and coarsely sieved cores and clear, normally zoned rims comprise one population (Figure 5.11). The term population L is herein used to describe phenocrysts with this texture and general composition (An_{41-82}), but does not necessarily indicate genetic relation. The other phenocryst population has complex zoning and may be agglutinations of several plagioclases with continuously zoned rims (1-2 mm) (An_{39-57}). Some medium to large grains (0.5-0.9 mm) (An_{31-64}) display skeletal textures, and many have rounded and/or sieved edges. Some of these are rare, reversely zoned sodic phenocrysts (An_{31-44}) (Figure 5.12). Other plagioclase includes microphenocrysts (0.2-0.5 mm) (An_{39-64}), that are tabular or lath-shaped, and microlites (<0.2 mm) (An_{35-48}). Phenocryst An contents in Wn, We and EKPFs overlap, but Wn pumice 31 has the lowest An content, and EKPF 14 has the highest (Figure 5.13). Rare mafic minerals occur in glomerocrysts, similar to the microxenocrysts described by Dungan & Davidson (2004), with varying combinations of plagioclase, orthopyroxene, clinopyroxene, amphibole, olivine and oxides (Figure 5.14). Rare olivines are present in some samples (14, 15, 17).

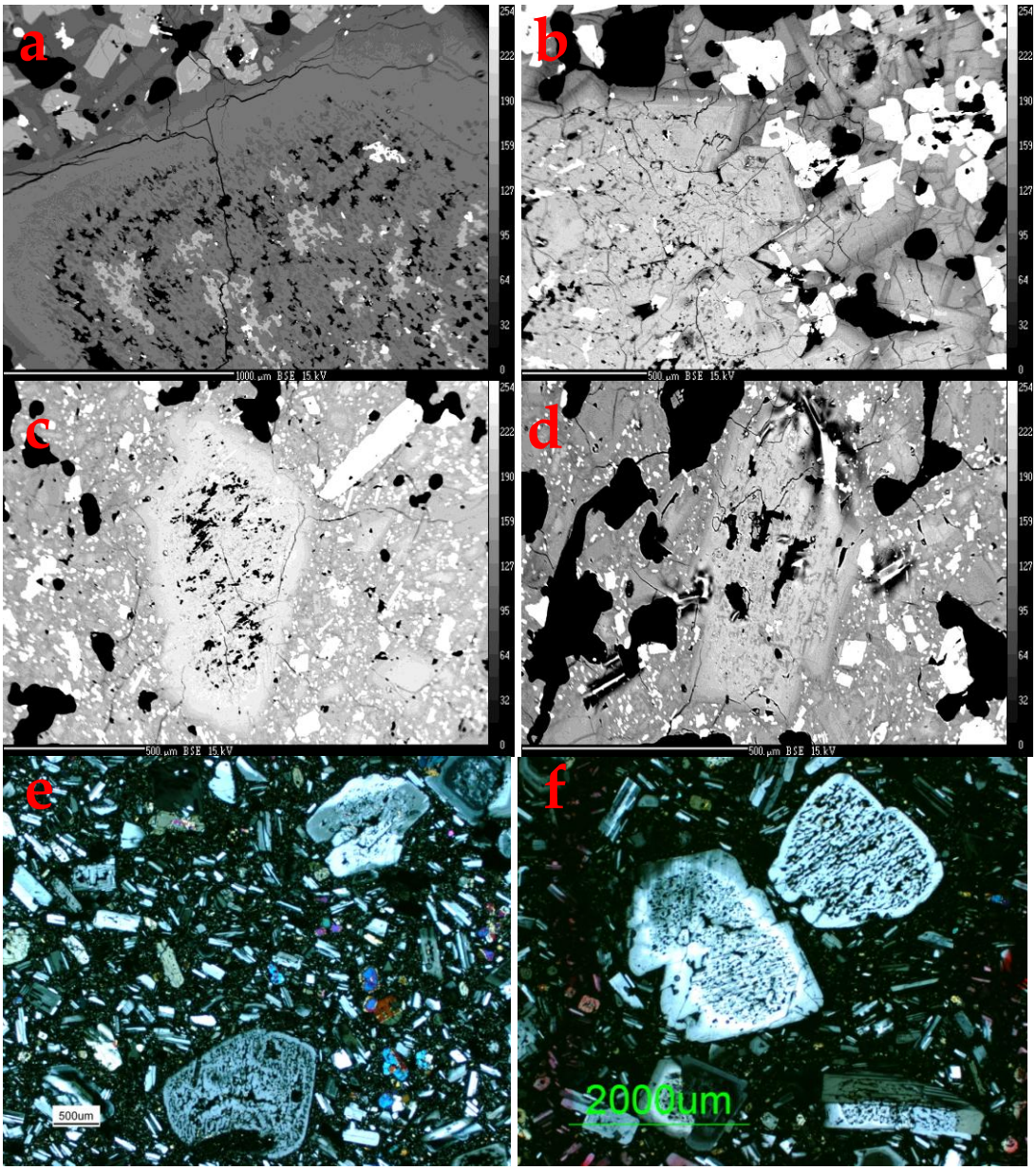

Figure 5.11 a-d. BSE images of population L plagioclase: large grains with coarsely sieved cores and clear rims. Grains first appear in Kalama-age rocks in EKPF. The above grains are from: QMI 19 a. crystal 1 and b. crystal 17. c. X Lava Flow plagioclase crystal 1 and d. Crystal 2. e-f. Photomicrographs of population L plagioclase from e. 07 M-type X Lahar and f. 07 crystal 1.

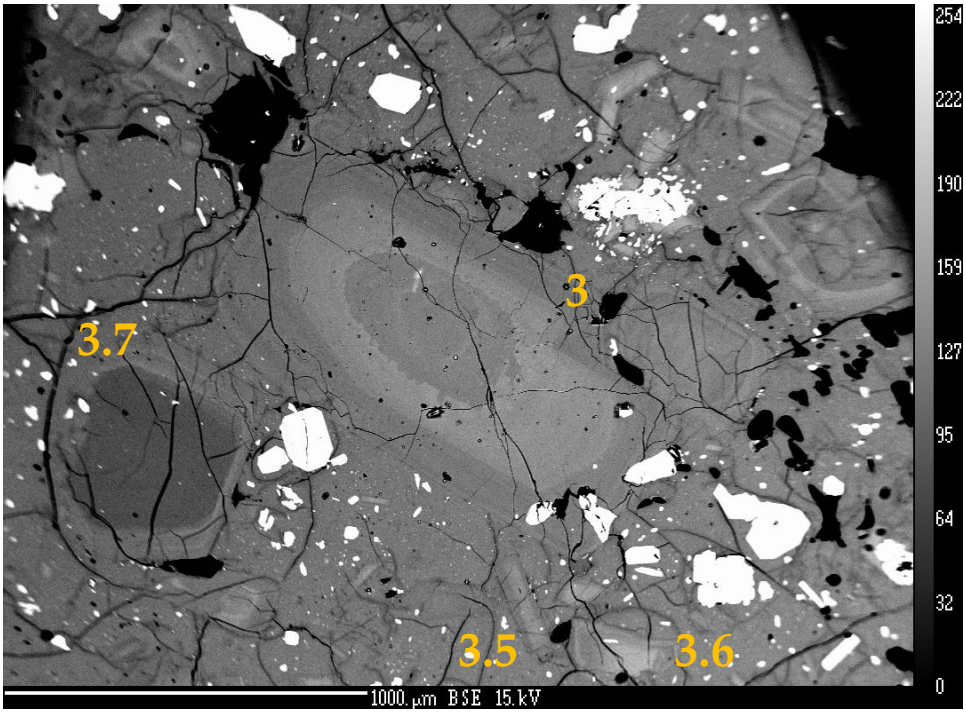

Figure 5.12 BSE image of EKPF 14 plagioclases 3, 3.5, 3.6, and 3.7. Note the sodic core, indicated by the dark shading and oscillatory zoning of crystal 3.7.

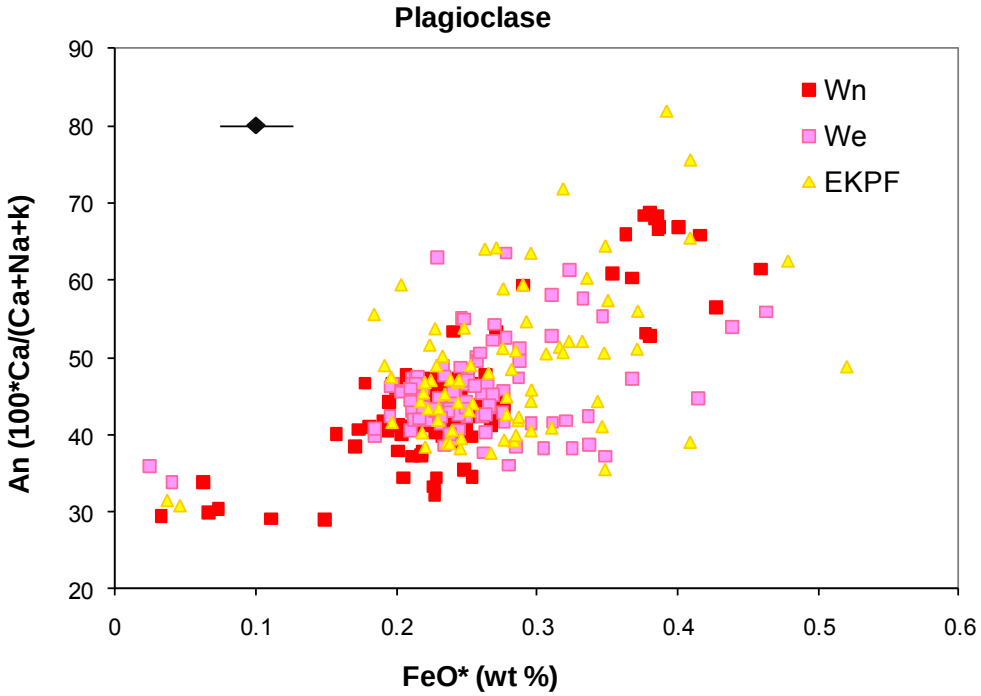

Figure 5.13 An content vs. FeO* (wt %) of early Kalama plagiolcase phenocrysts. An is molar (100*Ca/(Ca+Na+K)), and errors are smaller than symbols. Representative 1 s error shown for FeO.

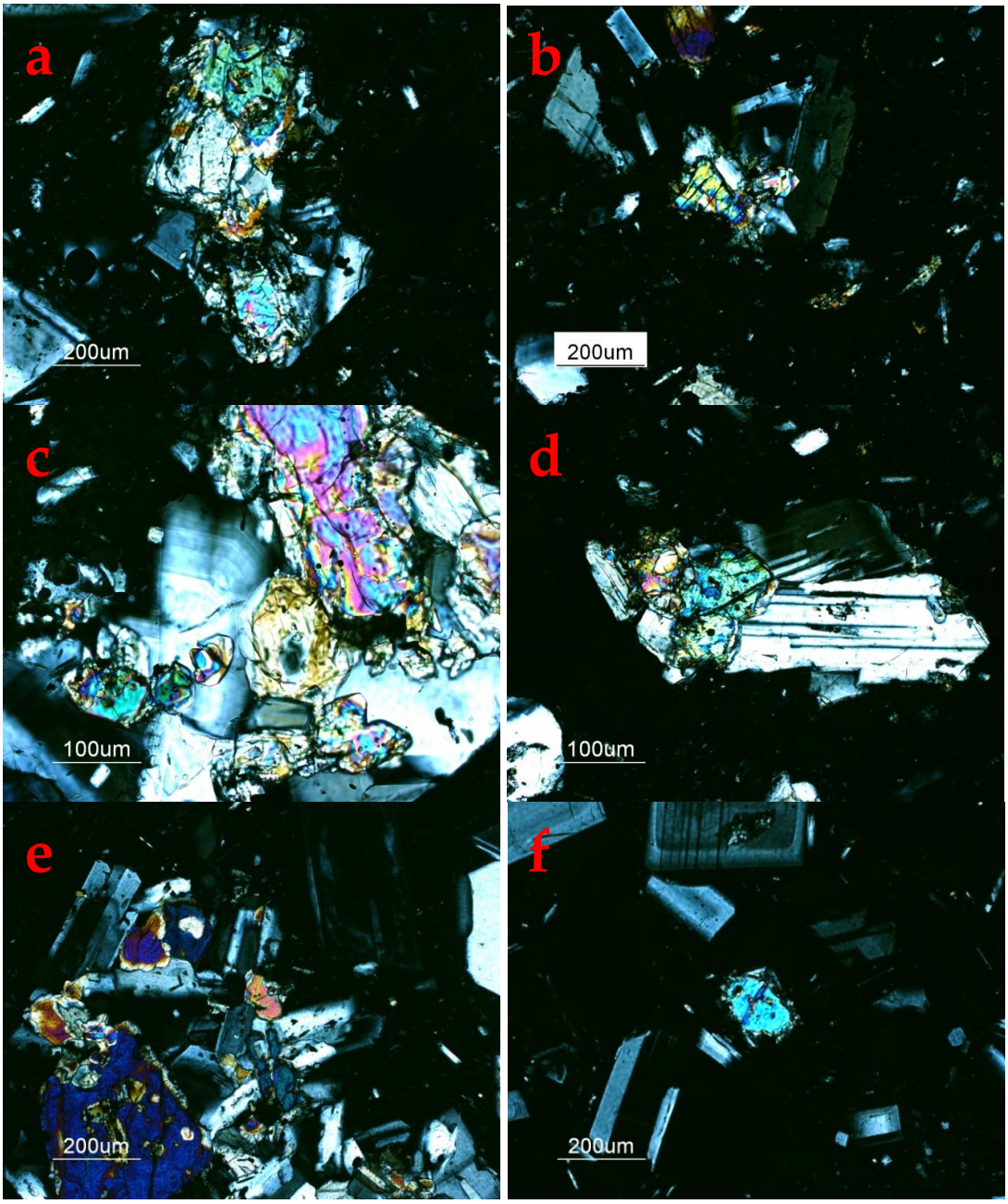

Figure 5.14 Photomicrographs in cross polarized transmitted light of olivine and plagioclase grains in EKPFs 15 (a-d) and 17 (e-f). Note the glomerocrystic nature of mafic minerals.

The term enclave encompasses a range of compositions and textures of inclusions, from granitic porphyries to ultramafic xenoliths, and may or may not be similar in composition and character to the host rock (Wiebe *et al.*, 2007). However, enclaves are generally blocks or blobs of mafic rock

encompassed by a more evolved rock, and are usually a result of magma mixing or mingling. From the investigation of textures, margins, associated structures, and host rock, details can be inferred about the conditions in the chamber, such as temperature, crystallinity, melt viscosity, crystallization mechanisms, or about conditions that relate to eruption, such as ascent rates or volatile contents (Bacon, 1986; Browne *et al.*, 2006; Clynne, 1999; Coombs *et al.*, 2002; Martin *et al.*, 2006;). In this study, the term quenched mafic inclusion (QMI) is used instead of enclave since those in rocks of the Kalama age have quenched textures.

Three QMIs found in EKPF were analyzed for this study, and fall within the range of compositions and textures and have comparable mineralogy to those identified by Clynne (written communication, 2009). There are two populations of QMIs based on mineralogy, mineral textures, and geochemistry. Both are dominated by plagioclase and amphibole, but an olivine-rich population contains abundant large (0.5-2 mm) olivine (Fo_{65-86}) (Figure 5.15). Most of the olivines, which are generally grouped in glomerocrysts with other mafic minerals, have embayed edges and contain Cr spinel and Fe-Ti oxides. Some have pyroxene overgrowths.

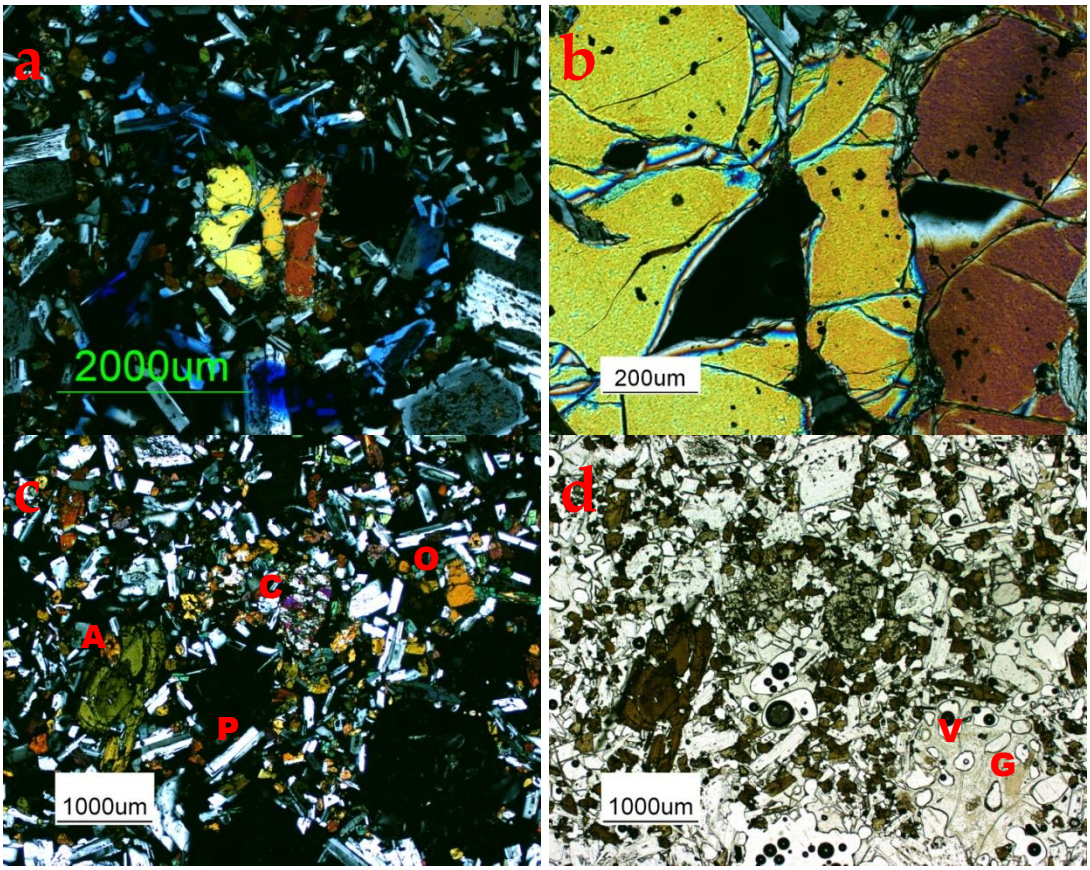

Figure 5.15 Photomicrographs with cross-polarized transmitted light (except d which is plain polarized light) from QMI 19. a. 2x magnification of resorbed olivine grains in groundmass of plagioclase, amphibole, and glass. b. 10x magnification of the same olivines showing detail of Cr spinel inclusions. c and d. 2x magnification showing large, zoned amphibole (A), clinopyroxene (C), olivine (O), plagioclase (P), glass (G), and vesicles (V).

Plagioclase in the olivine-rich group occurs as 1) 0.1-0.6 mm (An_{27-76}) groundmass laths with normal zoning, 2) 0.4 -0.9 mm (An_{47-66}) tabular phenocrysts with coarsely sieved or patchy cores and clear or rounded rims, and 3) as population L (1-2 mm) (An_{34-87})phenocrysts (Figure 5.16). Many of the groundmass laths also have a distinct calcic zone that truncates the normal zoning pattern (Figure 5.16c). Rims generally have the lowest An contents (< An_{40}). Xenocrystic plagioclase and pyroxene inclusions are also present in

the QMI (Figures 5.16b and 5.17). Amphibole are typically small (0.1-0.5 mm), stubby medium-dark brown (in both plain and cross polarized light) grains. Larger (0.5-1 mm), euhedral grains are less common. The olivine-rich QMIs also contain abundant clinopyroxene. One population of clinopyroxene consists of relatively large (0.4-1 mm) phenocrysts that have a distinctive texture of multiple, sometimes offset twins, referred to here as polysynthetic twinning (Figures 5.15c, 5.16b, and 5.19). Orthopyroxene is sparse, and some have amphibole overgrowths (Figure 5.16a). There is little glass in the olivine-rich QMIs and very few microlites. Vesicularity is between 5-10%, and vesicles have a diktytaxitic texture. They are both round and irregular, and evidence that smaller bubbles coalesced to form larger ones is obvious. The thin section from sample QMI 19 has a faint appearance of a seam of coalesced bubbles, which may be similar to segregation vesicles described by Bacon (1986).

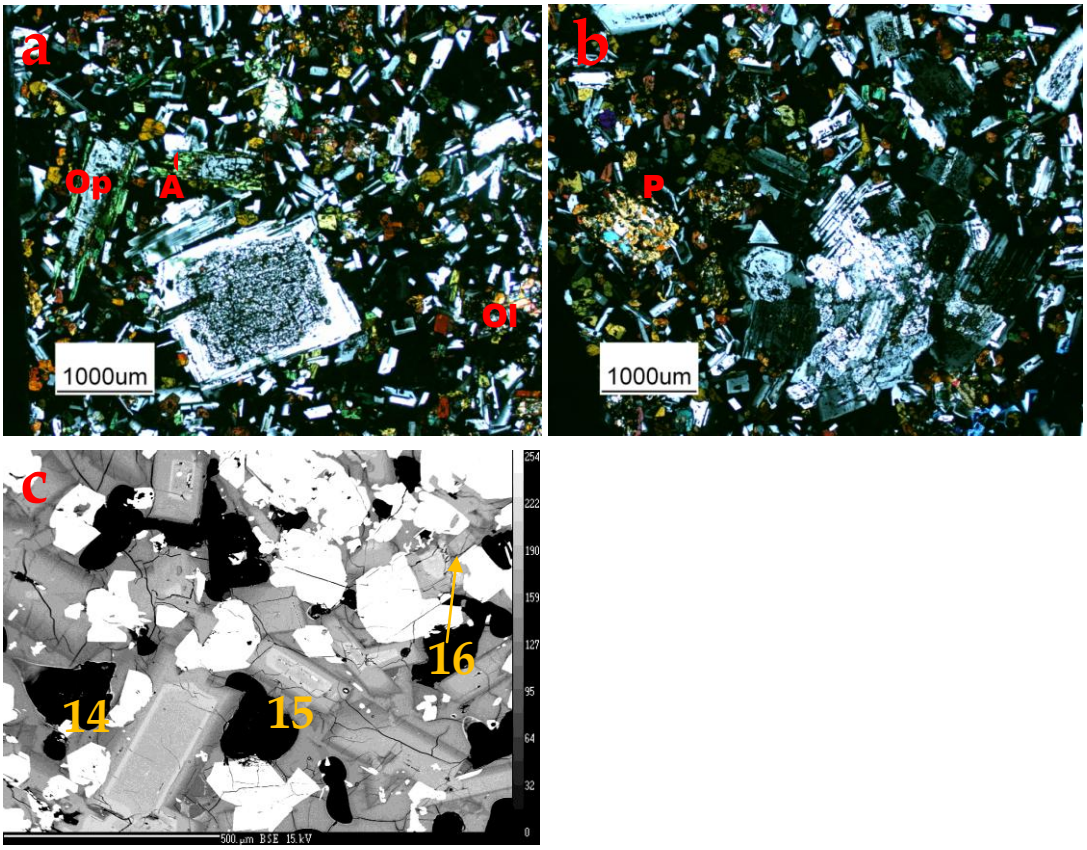

Figure 5.16 a-c. Photomicrographs in cross-polarized transmitted light of QMI 19. a. Orthopyroxene (Op) grains display amphibole (A) overgrowth rims. A tabular population L plagioclase core is also prominent. A small olivine is labeled Ol. b. Xenocrystic plagioclase and pyroxene are present in QMI 19. A polysynthetically twinned clinopyroxene is marked (P). c. BSE image of QMI 19 plagioclases 14, 15 and 16. A calcic zone indicated by a bright white strip with several crystals interrupts the normal zoning pattern.

A more felsic, olivine-poor population of QMI has smaller phenocrysts on average, and is finer grained. Phenocrysts include sparse orthopyroxene, clinopyroxene, and olivine (Figure 5.17). QMI 20 completely lacks olivine while QMI 22 contains sparse, heavily resorbed olivine either overgrown by or present in glomerocrysts with pyroxene (Figure 5.18). Polysynthetically twinned clinopyroxene are rare in this population. Orthopyroxene is present in a range of sizes (0.2-2 mm). Plagioclase occurs in three populations: (1) population L, which is sparse (< 1%) in this group of QMIs, (2) the dominant

population of medium-large phenocrysts (0.3-1 mm) (An_{42-68}) with finely sieved zones and rounded edges or coarsely sieved cores and normally zoned rims, and (3) small (0.05-0.4 mm) lath-shaped or acicular groundmass grains (An_{41-65}). As with the olivine-rich QMI population, phenocrysts are found as discrete grains and in glomerocrysts. The amphibole in the olivine-poor QMIs 20 and 22 are mostly acicular prisms, but also occur as large (0.6-1 mm), euhedral grains. Most of the larger grains have obvious zoning. Small (0.2 mm), euhedral amphibole are also ubiquitous in the groundmass. This QMI population is more vesicular (~15-20%) than the first, and vesicles are more evenly distributed. There is a small degree of coalescence. Sample 22 has a few large (1.5-2 mm) round vesicles that have phenocrysts protruding into them. The host to QMI 20 has glomerocrysts of clinopyroxene and plagioclase, large amphibole reacted to plagioclase and pyroxene, and is ~25% vesicular.

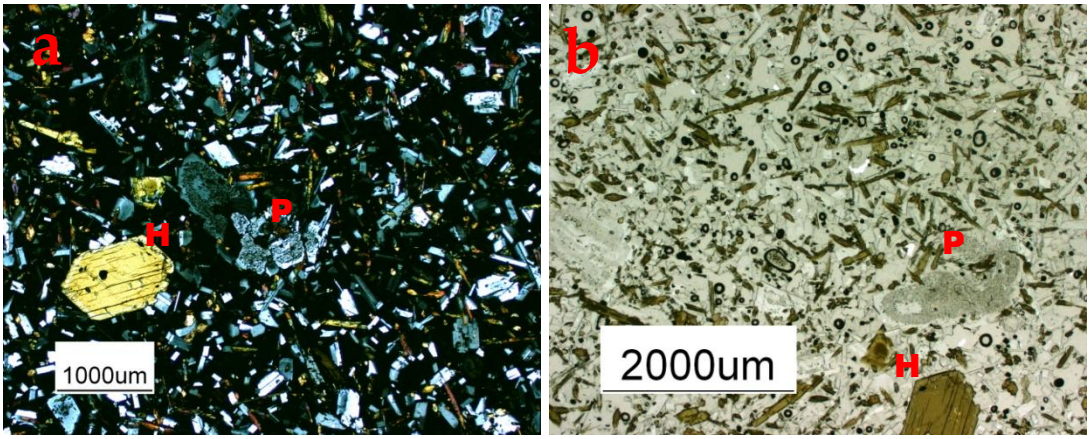

Figure 5.17 Photomicrographs of QMI-20 in a. cross-polarized transmitted light and b. plain-polarized transmitted light. A large, euhedral amphibole (H) and sieved plagioclase (P) glomerocryst are prominent. Note the acicular, prismatic morphology of most plagioclase and amphibole.

At least one early Kalama pyroclastic flow sample, EKPF 17, contains a small inclusion with the same texture (acicular plagioclase randomly oriented + amphibole) seen in the olivine-poor population of QMI. The olivine-rich population contains a larger proportion of population L plagioclase (8-10%) and glomerocrysts of mafic minerals (8-10 %) than the olivine-poor population, which contains <1% of each.

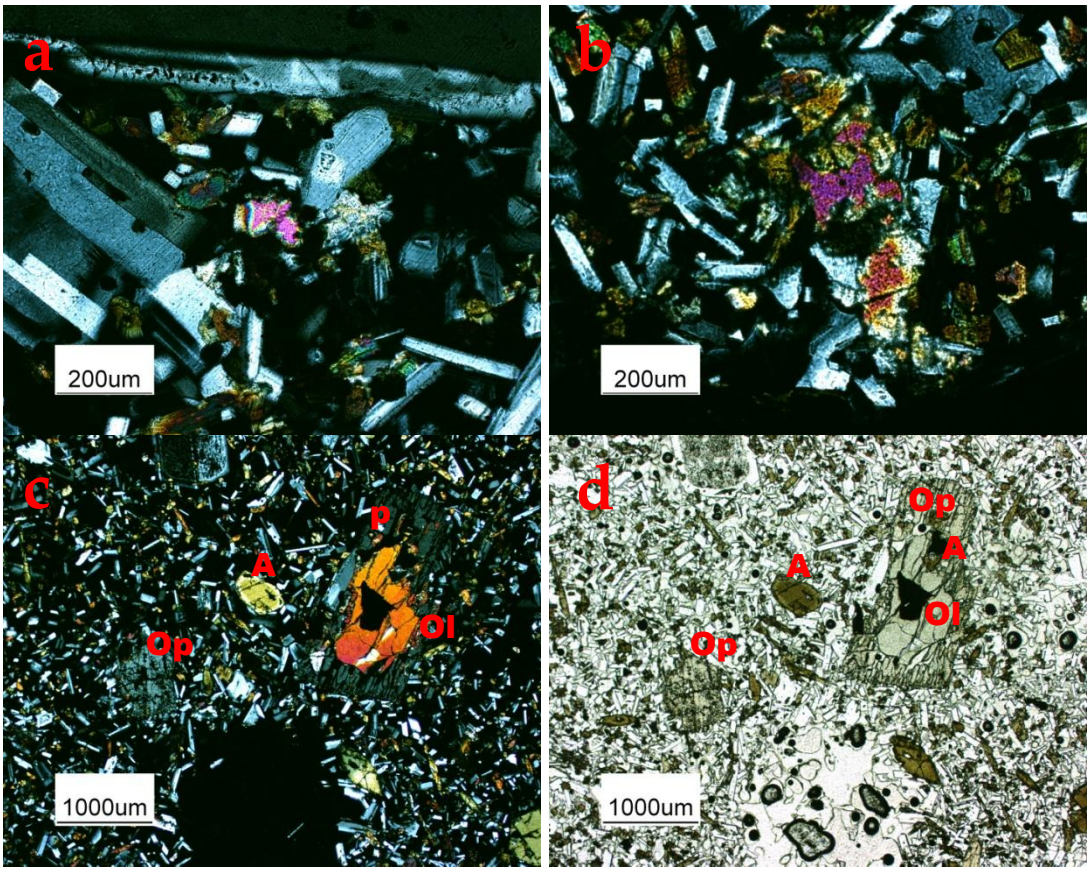

Figure 5.18 Photomicrographs of QMI 22 with cross-polarized transmitted light (d. is plain polarized light). a and b. 100x magnification. Olivine, pyroxene, and plagioclase glomerocrysts. c and d. 20x. Olivine (Ol) with orthopyroxene (Op) overgrowth. Also labeled are vesicles (V), and amphibole (A).

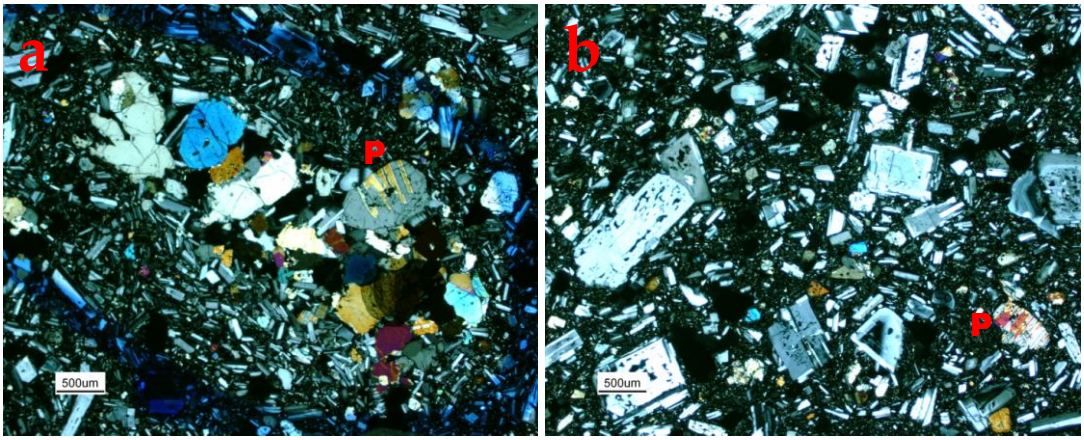

Figure 5.19 Photomicrographs of M-type X Lahars a. 01 and b. 07. Polysynthetically twinned clinopyroxene are marked with a P. a. Glomerocrysts of mafic minerals are common in M-type X lahars. B. Vesicles have a dictytaxitic texture also noted in QMI 19.

5.2.3 Rocks of the Middle Kalama Age

During the early part of the middle Kalama Period, lavas, tephras and pyroclastic flows erupted. Some lavas were reworked into lahars subsequent to eruptions, and the lavas from those lahars are termed X lahars for simplicity here. X lahars and pyroclastic flow deposits 01, 02, 07, and 09 and Xb tephra 32 samples are porphyritic and range from an estimated 8-20 % vesicular. All X deposits have plagioclase >> clinopyroxene ≥ orthopyroxene > olivine and abundant glass. Most have abundant Fe oxides. Middle Kalama tephras, lavas, lahars, and pyroclastic flows have more advanced disequilibrium textures than early Kalama rocks.

Plagioclase in X deposits varies in size and texture, including: microlites; small (0.1-0.4 mm), tabular and lath-shaped grains that are mostly free of disequilibrium textures; medium sized (0.5-1 mm) grains with coarsely sieved cores (smaller version of populations L) and clear, normal or oscillatory zoned rims; and medium-large sized (0.5-2 mm) phenocrysts with patchy cores and skeletal textures. Clinopyroxene is abundant, and some grains have

the distinctive polysynthetically twinned texture. Two populations of olivine occur in X deposits. Large, reacted olivines occur in glomerocrysts. Smaller olivine (0.1-0.2 mm) not found in glomerocrysts are either euhedral or have skeletal textures. Amphibole is very rare in X samples. Those in Xb scoria are mostly or completely reacted (Figure 5.6). Crystals, especially plagioclase, show signs of fragmentation.

Glomerocrysts, like those seen in early Kalama pyroclastic flow deposits, are also prevalent in the X tephra and lahars (Figure 5.19). The glomerocrysts include varying assemblages of plagioclase, clinopyroxene, orthopyroxene, olivine and Fe oxides. They are distinguished from the rest of the rock by the larger grain sizes and the lack of glass. The olivine (0.4-1 mm) and clinopyroxene in the glomerocrysts are reacted and embayed.

There appear to be at least three populations of X lavas, two found in lahar or pyroclastic flow deposits, and the other is found in situ near Windy Ridge. X lahars 01 and 07 have seriate texture and are more crystal rich than 02 and 09, which are strictly porphyritic. There are at least two populations of groundmass glass, and sample 02 contains both in the same thin section (Figures 5.10 and 5.20). The groundmass of 09 has a similar texture and appearance to the crystal-poor groundmass glass in 02, whereas the groundmass glass of 01 and 07 more closely resemble the crystallinity, color, and texture of the more crystalline groundmass in 02.

The group of X lahars 01 and 07 (M-type) that has the more crystalline groundmass is also distinguished from the other X lahars (B-type) by its differences in mineral modes. M-type lahars have a greater abundance of the population L plagioclase phenocrysts (5-10 %), whereas B-type have <1 % of these grains. Polysynthetically twinned clinopyroxene are also more abundant. Glomerocrysts in the M-type lahars have larger, more euhedral

grains of plagioclase, olivine, and pyroxene. Grains in B-type glomerocrysts have quenched textures. B-type lahars have smaller, more euhedral olivine and clinopyroxene and very elongate plagioclase. The Xb scoria is slightly less crystalline than the lavas but has a similar mineral assemblage to B-type X lahars. Two populations of olivine occur in X lahar deposits. Large olivine, (0.4-1 mm) are heavily reacted with large embayments around the edges and have Fo-rich cores (Fo_{75-80}). Smaller olivines (0.1-0.2 mm) are either euhedral or have skeletal textures and extend to slightly lower Fo compositions (Fo_{72-79}).

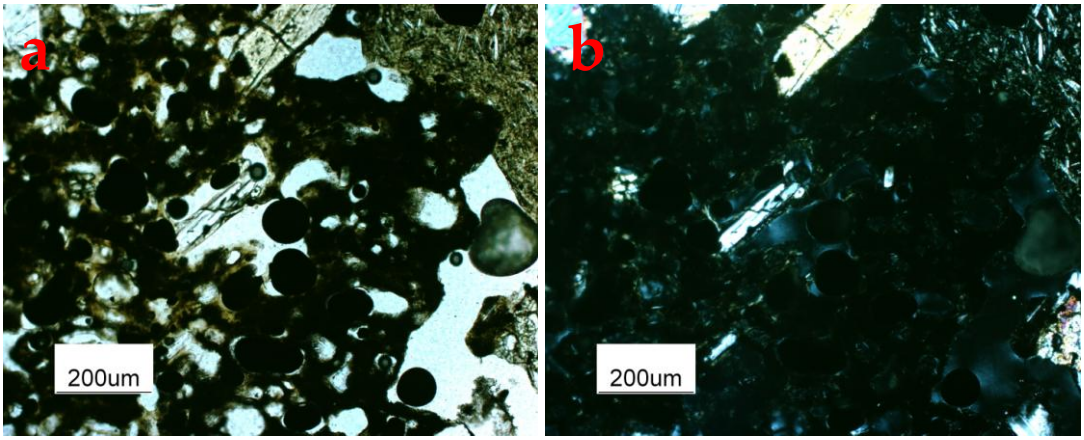

Figure 5.20 Photomicrographs of groundmass glass of B-type X Lahar 02 in a. Plain polarized light and b. Cross polarized light. Note the two types of groundmass glass: the microcrystalline type in the top right corner and the opaque, glassy type throughout the rest of the image. The microcrystalline groundmass is mostly found in M-type X Lahars, whereas the glassy groundmass is found predominantly in B-type X Lahars.

The X Lava Flow near Windy Ridge is crystal rich, dominated by plagioclase and clinopyroxene phenocrysts. The groundmass comprises plagioclase, orthopyroxene, and clinopyroxene, which are larger than microlites of other X deposits. The flow contains two distinct populations of plagioclase, one of which is the strongly reacted population L. Olivine occurs primarily as small (<0.2 mm) euhedral groundmass crystals, and is less

abundant in the lava flow (estimated 1-3 %) than in the Xb tephra and lahars. Amphibole is present with opacite rims of 25-50 μm. X Lava Flow contains clasts of xenocrystic material of large, sieved plagioclase and pyroxene grains. Figure 5.21 displays a photomicrograph of small grains that began to disaggregate from the xenocryst. The presence of nearly completely reacted minerals, such as plagioclase, clinopyroxene, and amphibole in the X Lava Flow is a unique feature among X deposits. This feature is also apparent in the middle Kalama Breadcrust Andesite Pyroclastic Flow (Figure 5.22).

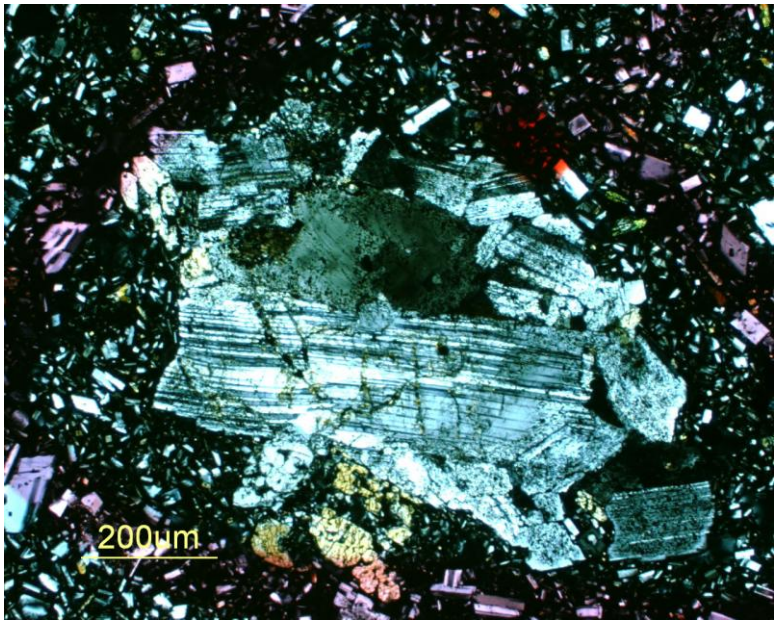

Figure 5.21 Photomicrograph of xenocrystic material in X Lava Flow 30. Plagioclase and pyroxene have begun to disaggregate from the rest of the xenocryst.

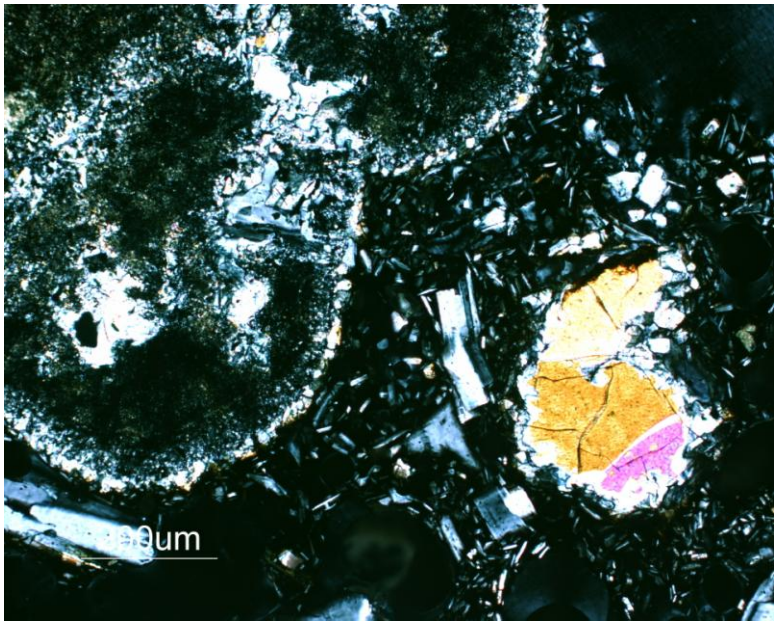

Figure 5.22 Photomicrograph of the middle Kalama Breadcrust Pyroclastic Flow 03. Phenocrysts that are nearly completely reacted such as the one on the top left are common in both this flow and the X Lava Flow 30.

Middle Kalama-age lavas (MKLV) and pyroclastic flow include the Two Finger Flow (10), Worm Complex lavas (08A), western flanks lavas (16), and the Breadcrust Andesite Pyroclastic Flow (03). The Two Finger Flow is grouped with the middle Kalama lavas, but textures and mineralogy are more similar to the X lahars, specifically the M-type. The flow has abundant glomerocrysts of plagioclase, orthopyroxene, clinopyroxene, olivine and Fe oxides, a feature which is not dominant in the other middle Kalama lavas. Also unlike other lavas, the Two Finger Flow is more crystal rich, has a more seriate texture, and has abundant olivine (estimated 5-6%). Worm Complex 08A and western flank lavas 16 are more strictly porphyritic, and bear little to no olivine. Some of the sparse olivines have pyroxene overgrowth rims (Figure 5.7). Phenocrysts are generally larger in Worm Complex lava 08A and western flank lava 16 than in the others. The Worm Complex lava 08A contains very large (up to 2mm) clinopyroxene grains with heavily reacted

cores that are also found in some X lahars (Figure 5.23). All middle Kalama andesites contain population L plagioclase phenocrysts, but MKLVs have significantly fewer than X deposits. Large, agglutinated plagioclase with patchy cores and finely sieved zones are also present. The Breadcrust Pyroclastic Flow 03 contains abundant olivine-bearing, heavily reacted glomerocrysts. The flow also contains relic mafic phenocrysts that are mostly reacted such as those found in the X Lava Flow. Orthopyroxene and clinopyroxene are both abundant.

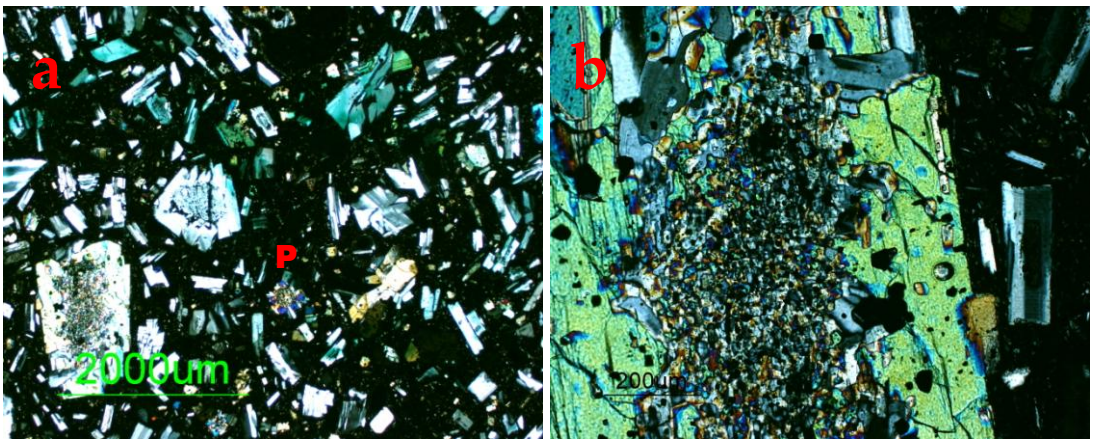

Figure 5.23 Photomicrograph of Worm Complex lava 08A under cross polarized light. a. Note the large, reacted clinopyroxene under scale bar and the polysynthetically twinned clinopyroxene near center (P). b. Close-up of large clinopyroxene as in a, under 100x magnification.

A rare olivine of Fo_{66} found in late Kalama andesite 13 bears a thin reaction rim (Figure 5.24). This particular olivine is on the low end of the Fo compositional range of cores analyzed from grains in volcanics (Fo_{57} in X lahar to Fo_{85} in QMI), but similar in range to some smaller olivines found in the Two Finger Flow 10 (Fo_{65}), Breadcrust Andesite Pyroclastic Flow 03 (Fo_{67}), and X lahar 01 (Fo_{57-80}). Rims of larger olivine found in X lahar 01 (M-type) and

Breadcrust Andesite 03 also bear comparable Fo content whereas gabbroic inclusions are significantly lower at Fo_{41-45}.

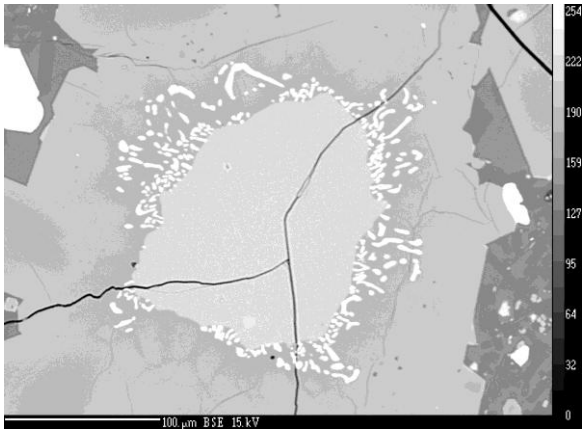

Figure 5.24 Backscattered electron image of olivine with Fe-Ti reaction rim in SDY 13.

5.2.4 Rocks of the Late Kalama Age

The two late Kalama lithologies, SDO and SDY, are similar in mineralogy and have seriate texture. Both are plagioclase-phyric and have notably fewer crystals with disequilibrium textures than early and middle Kalama rocks. Population L plagioclase phenocrysts are present in these rocks**.** Orthopyroxene is also abundant in both lithologies.

Oscillatory zoned plagioclase with clear rims is the dominant phase of SDO and SDY (An_{40-74}). Large complex, agglutinated grains are also present. Amphibole phenocrysts have a variety of rim textures: thin opacite rims, and both thick and thin plagioclase and oxide breakdown rims. Glomerocrysts of plagioclase, orthopyroxene, and clinopyroxene are sparse. Many of these glomerocrysts have a distinct rounded arrowhead shape, similar to those on the X lahars. Clinopyroxene and orthopyroxene occur as small, euhedral phenocrysts in SDO. Many orthopyroxene phenocrysts have breakdown rims

comprising plagioclase and Fe oxides. Others have reverse zoning patterns (Figure 5.25).

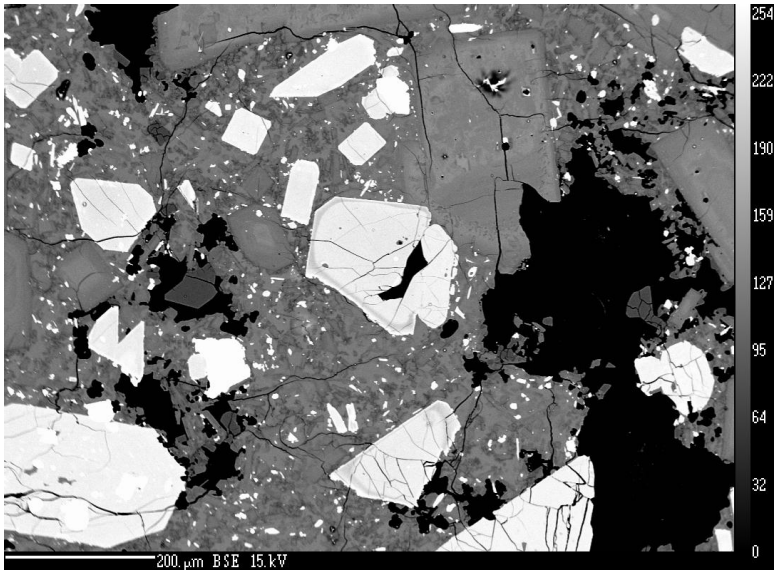

Figure 5.25 BSE image of reversely zoned orthopyroxene (opx 12) from late Kalama SDY 13.

5.2.5 Petrography Summary

Many of the relationships between the different magmatic components and their evolution throughout the Kalama Eruptive Period can be translated from petrographic observation. Some of the most important observations that will be used in a discussion of the evolution of the Kalama Period are gleaned from the preceding descriptions and summarized below.

Plutonic inclusions show signs of disequilibrium, including disaggregated crystal grains, bent and warped albite twinning in plagioclase, glassy inclusions at crystal edges, pyroxene exsolution lamellae, and overgrowth rims on mafic minerals (pyroxene jackets on olivine and amphibole rims on pyroxene). The early Kalama tephra eruptions are the most felsic and their mineral assemblages have fewer disequilibrium textures than later early Kalama and middle Kalama rocks. Early Kalama pyroclastic

flows contain population L plagioclase phenocrysts that are largely absent from tephras. Additionally, the pyroclastic flows contain somewhat smaller plagioclase phenocrysts with no disequilibrium textures. The early Kalama pyroclastic flows also include two populations of QMIs: (1) the olivine-rich group, which has very abundant population L plagioclase phenocrysts, polysynthetically twinned clinopyroxene, and glomerocrysts of olivine, clinopyroxene, and orthopyroxene, and (2) the olivine-poor group with sparse population L plagioclase and olivine, and few to no polysynthetically twinned clinopyroxene.

Middle Kalama X deposits have abundant glomerocrysts of olivine clinopyroxene, orthopyroxene, and plagioclase. There are three lava populations in X deposits: the X Lava Flow in situ near Windy Ridge, and two found reworked in lahars. The lahars may compositionally correlate with X tephras. The two types of lahars are distinguishable by groundmass texture and crystallinity, both of which are present in 02. M-type lahars have much more abundant population L plagioclase and olivine-clinopyroxene and orthopyroxene glomerocrysts. B-type lahars have less abundant population L plagioclase and glomerocrysts, but more abundant medium sized, clear plagioclase phenocrysts. The X Lava Flow has sparse olivine (1-3%) and also contains xenocrystic material. The Two Finger Flow has more abundant olivine at 5-6 %, and is mineralogically and texturally similar to the M-type lahars. Other MKLV have sparse olivine and polysynthetically twinned clinopyroxenes, along with very large pyroxene phenocrysts. The Breadcrust Andesite Pyroclastic Flow (MKPF) has moderately-abundant, heavily reacted olivine. The late Kalama summit dome rocks have similar glomerocrysts to the middle Kalama X lahars, but only SDO has olivine.

5.3 Whole Rock Chemistry

Whole rock major element data is both necessary for classification of materials involved in research and for first order determination of processes that lead to rock petrogenesis. Whole rock trace element data can then be used to further define the character of the rocks as well as provide information about the source and chemical evolution history of the magma (Gill, 1981).

5.3.1 Major Element Chemistry

Kalama-age rocks are medium K (Gill, 1981), subalkaline (Middlemost, 1975) (Figures 5.26 and 5.29), and all but some plutonic inclusions, which are low K and tholeiitic, plot in the calk-alkaline field defined by Miyashiro (1974) (Figure 5.27). Results are reported in Table A.1 and generally agree with published and other unpublished analyses of Kalama-age rocks (Carroll, 2009; Clynne, unpublished data; Crandell, 1987; Gardner *et al.*, 1995b; Halliday *et al.*, 1983; Hausback, 2000; Mullineaux, 1996; Pallister *et al.*, 1992; Pallister, 2008; Pallister, unpublished; Sisson, unpublished data; Smith, 1980, 1984; Smith & Leeman, 1982, 1987, 1993; Underwood, unpublished data; Verhoogen, 1937; Wolfe, unpublished data). Samples are therefore considered representative of the known array of Kalama-age rocks. Those analyzed for this study vary in SiO_2 content from 51.2-67.5 % with the most mafic samples being plutonic and QMIs (Figure 5.28). Magnesium numbers (Mg#), calculated by molar 100*Mg/(Mg+Fe), are between 39.7-57.4; X lava and QMI 19 are highest in the range. Early Kalama dacites are the most silica-rich rocks of the eruptive period with 64.4-66.1 % SiO_2, whereas late Kalama summit dome rocks are more mafic at 60.3-63.4 % SiO_2. Late Kalama SDO samples are andesitic in composition, whereas SDY sample are a mixture of felsic andesite and mafic dacite (after Le Bas *et al.*, 1986). Middle Kalama tephra, pyroclastic flows and

most lavas are andesite, but some lahars and the Two Finger Flow are basaltic andesite (after Le Bas *et al.*, 1986).

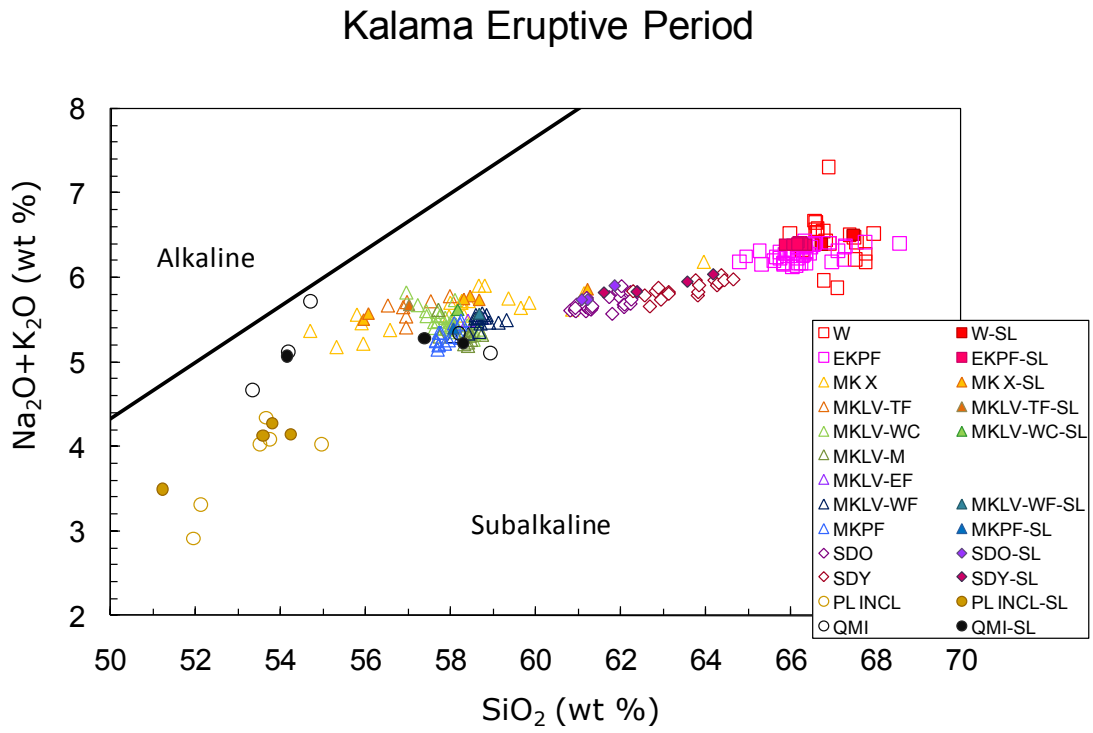

Figure 5.26 From Winter (2001) and Wilson (1989) after Middlemost (1975). Kalama-age rocks and plutonic inclusions are subalkaline. Data are normalized to 100 % anhydrous. Closed symbols with suffix SL from this study as in Table 5.1, and analyzed by XRF at Washington State University. Open symbols compiled from published and unpublished analyses by Clynne (written communication, 2009; Clynne, unpublished data; Crandell, 1987; Gardner *et al.*, 1995b; Halliday *et al.*, 1983; Hausback, 2000; Mullineaux, 1996; Pallister *et al.*, 1992; Pallister, 2008; Pallister, unpublished; Sisson, unpublished data; Smith, 1980, 1984; Smith & Leeman, 1982, 1987, 1993; Underwood, unpublished data; Verhoogen, 1937; Wolfe, unpublished data).

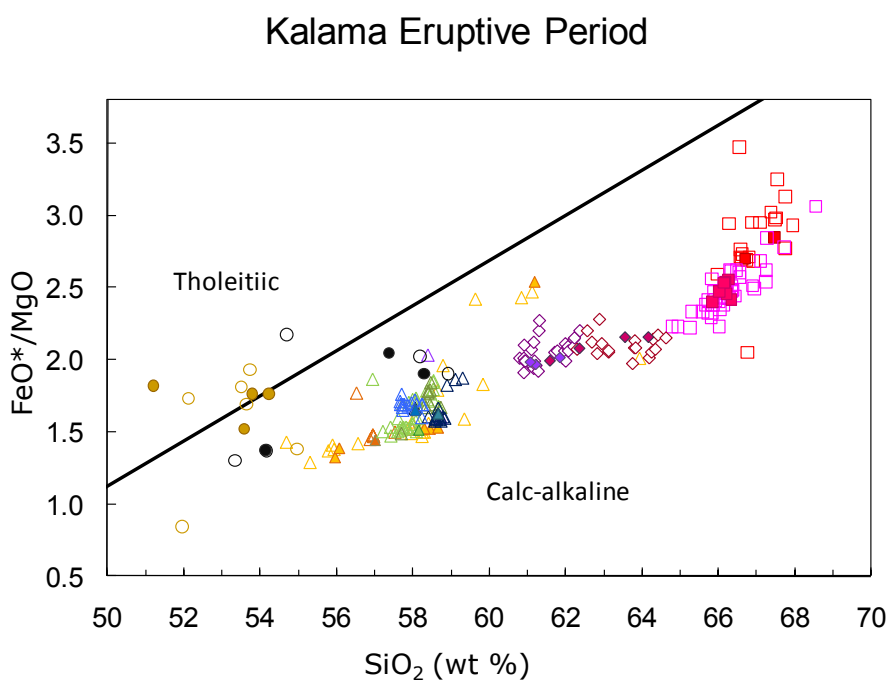

Figure 5.27 From Winter (2001) after Miyashiro (1974). Kalama-age rocks are calc-alkaline. Some plutonic inclusions are tholeiitic or transitional. Symbols as in 5.26.

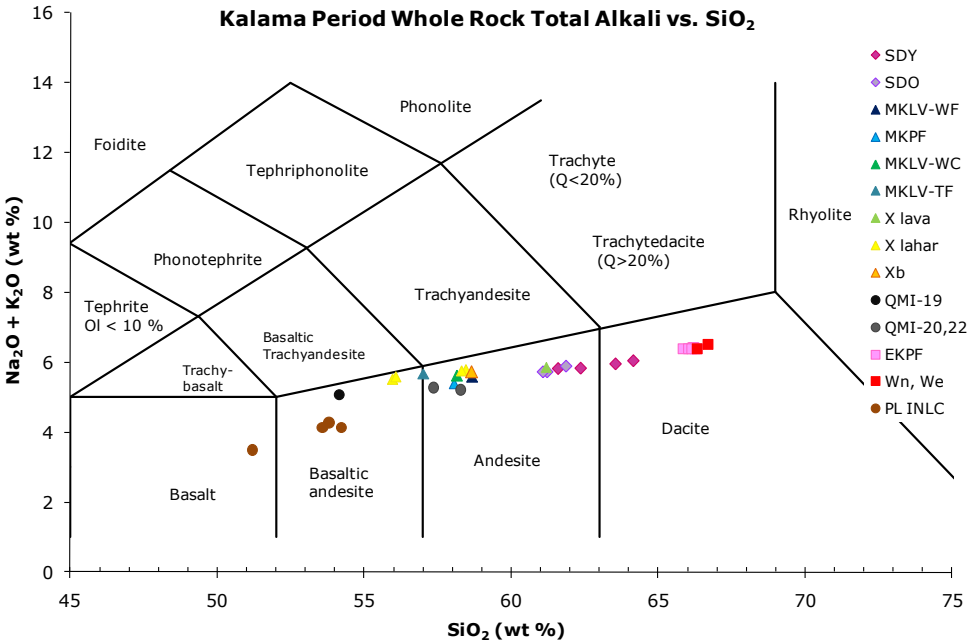

Figure 5.28 Total alkalis vs. SiO_2 after Le Bas *et al.* (1986) of Kalama-age rocks. Samples as in Table 5.1 and Figure 5.26, roughly in stratigraphic sequence. MKPF is Breadcrust Pyroclastic Flow. PL INCL encompasses all plutonic inclusions.

Figure 5.29 Whole rock major element geochemistry of Kalama-age rocks and inclusions. Data are normalized to 100 % anhydrous. Low, medium and high K series for andesites from Gill (1981). All Fe expressed as FeO*. Closed symbols from this study analyzed by XRF at Washington State University. Open symbols compiled by Clynne (written communication, 2009; Clynne, unpublished data; Crandell, 1987; Gardner *et al.*, 1995b; Halliday *et al.*, 1983; Hausback, 2000; Mullineaux, 1996; Pallister *et al.*, 1992; Pallister, 2008; Pallister, unpublished; Sisson, unpublished data; Smith, 1980, 1984; Smith & Leeman, 1982, 1987, 1993; Underwood, unpublished data; Verhoogen, 1937; Wolfe, unpublished data).

Kalama Eruptive Period

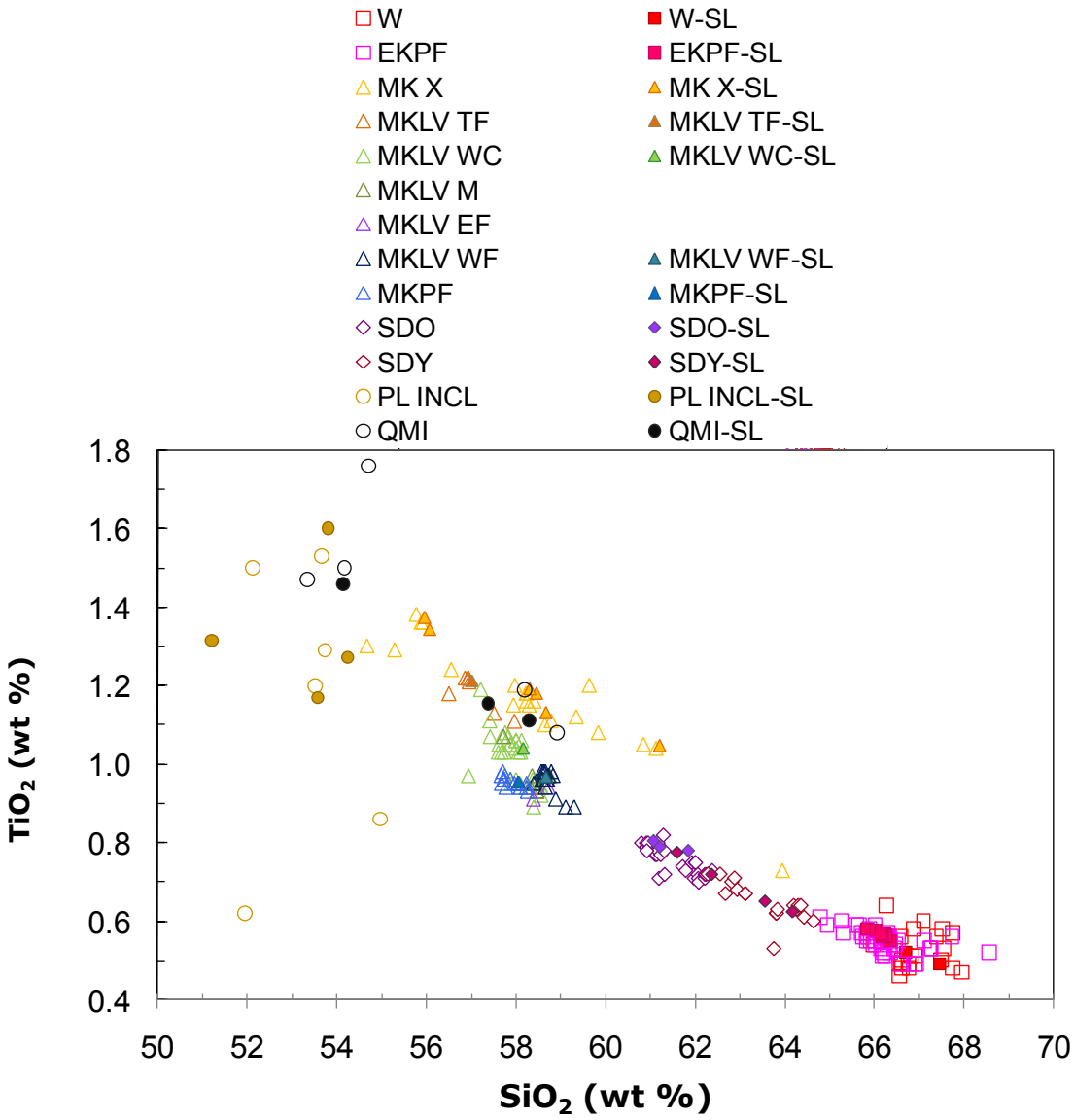

Kalama Eruptive Period

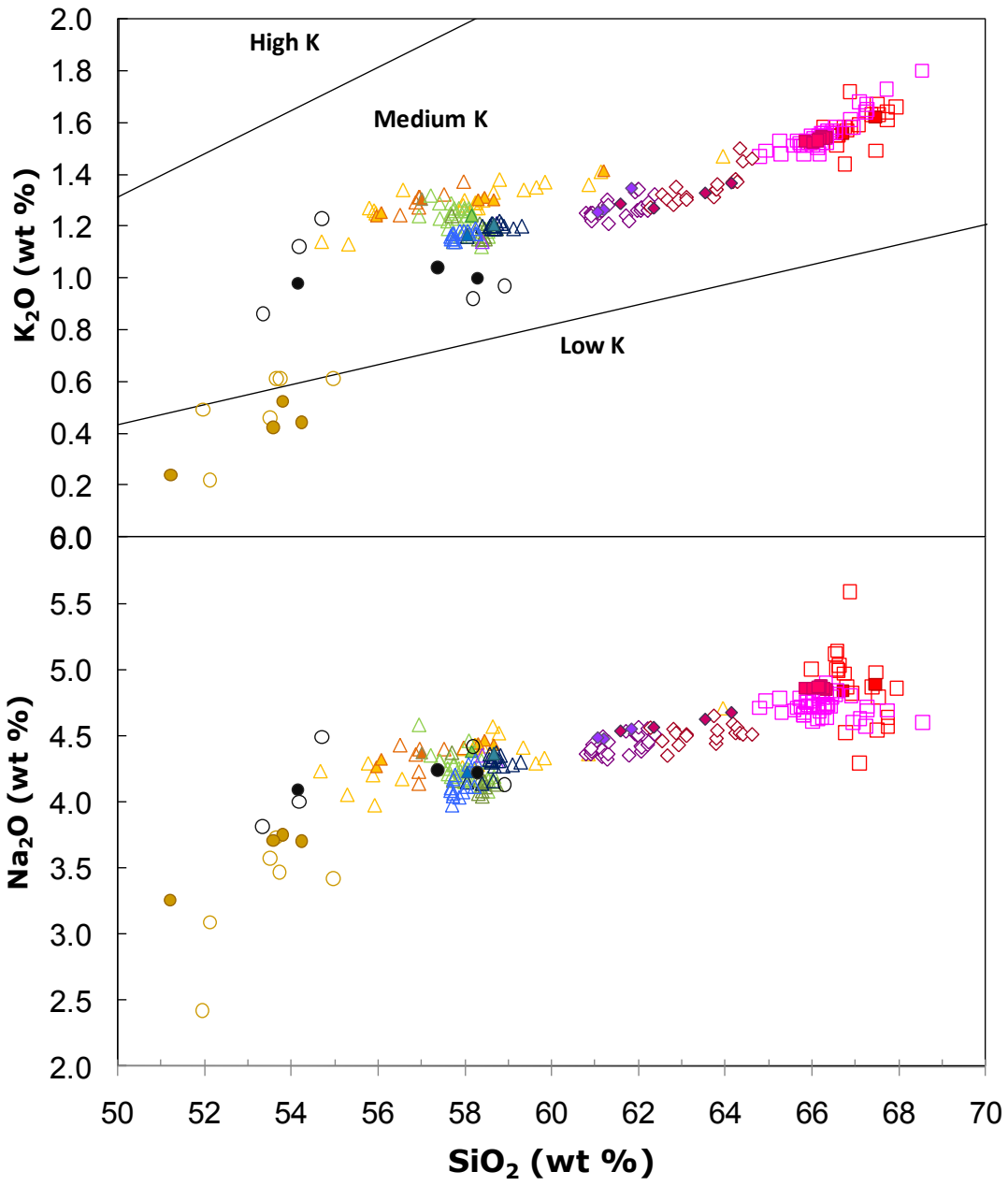

Figure 5.29 (Continued)

Kalama Eruptive Period

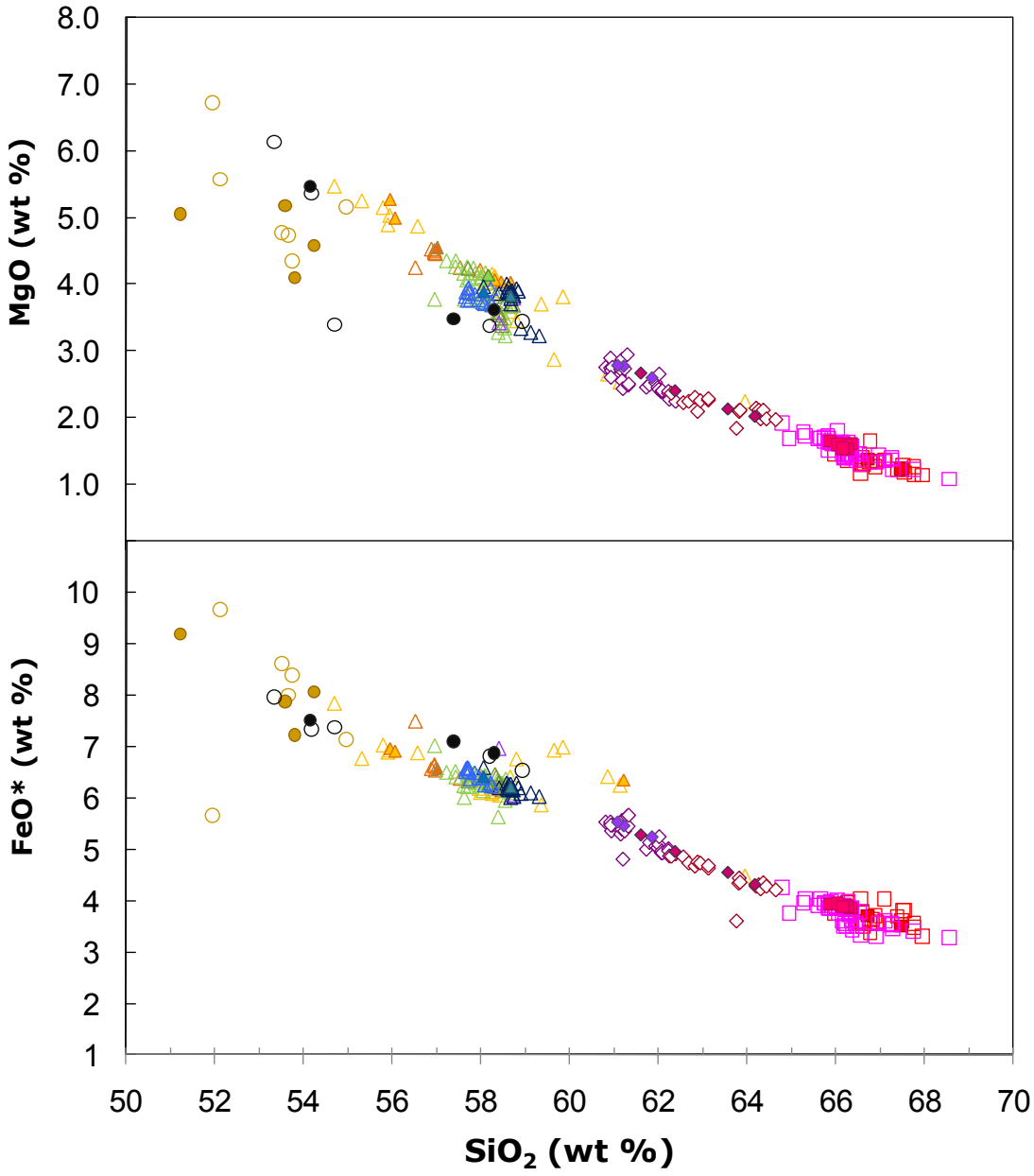

Figure 5.29 (Continued)

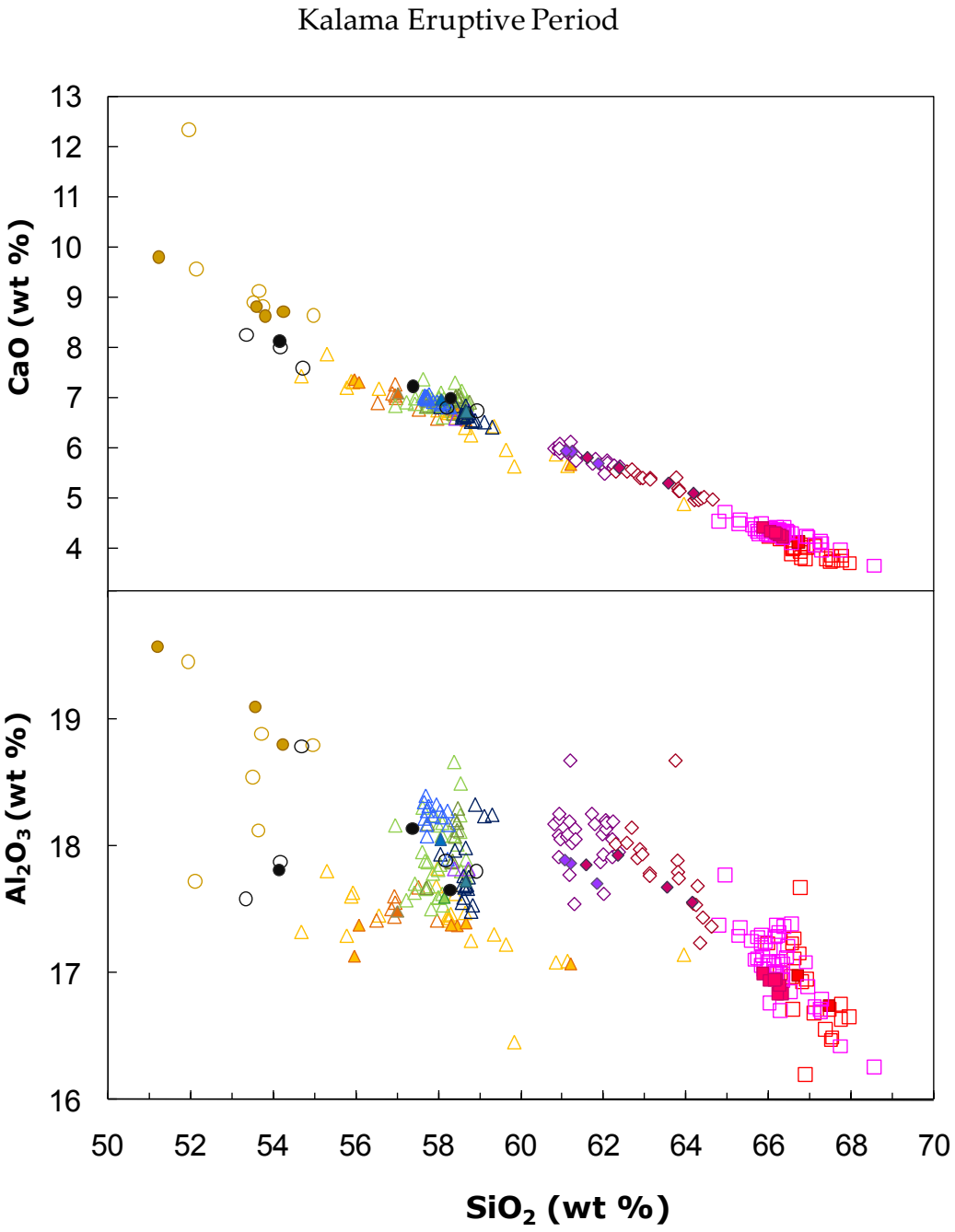

Figure 5.29 (Continued)

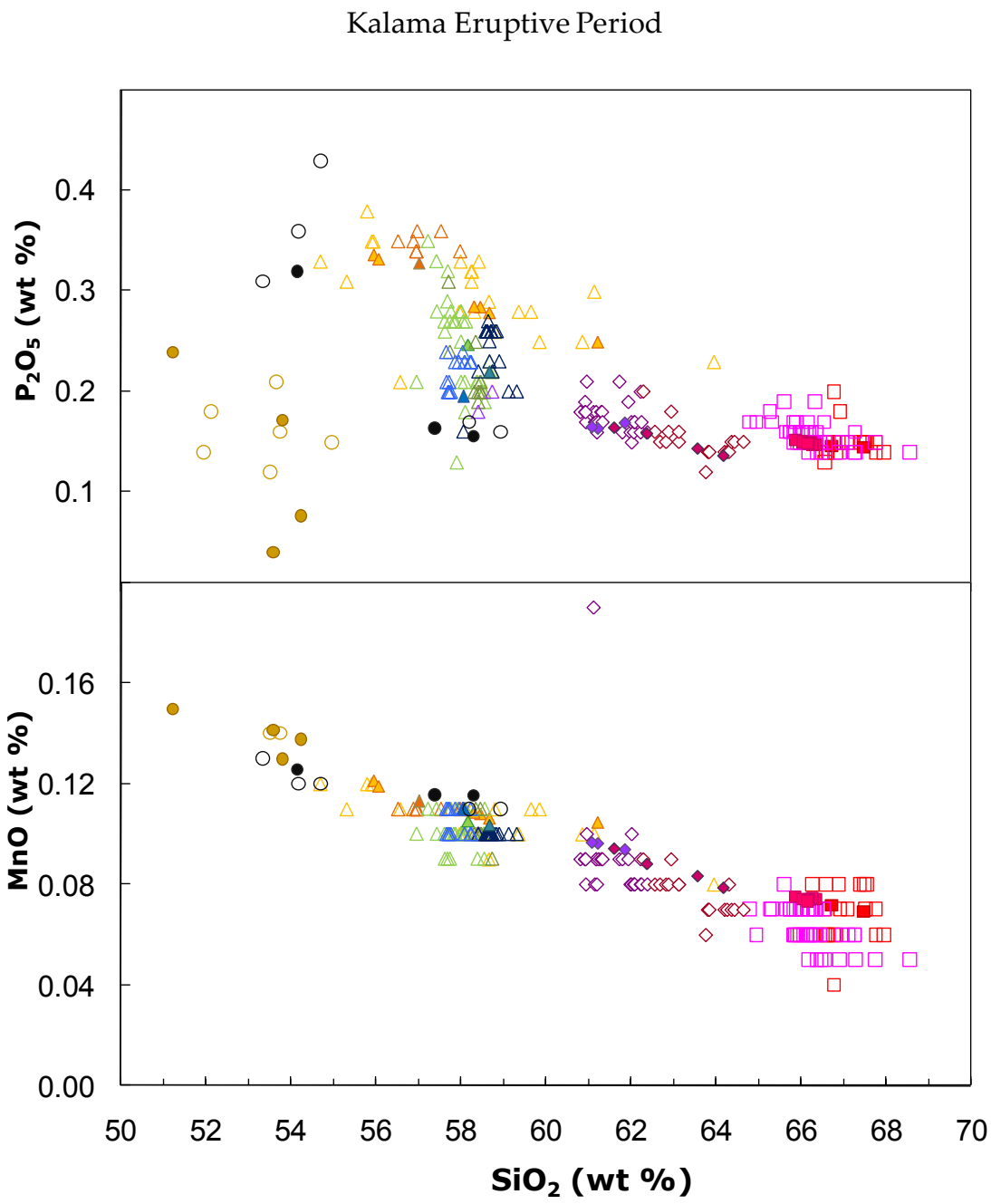

Figure 5.29 (Continued)

Most major elements correlate with SiO_2, positively or negatively, where R^2 values are 0.71-0.96 for all compiled Kalama-age data (Clynne, written communication, 2008). Some oxides such as Al_2O_3 and P_2O_5 show lower correlation with R^2 values of 0.40-0.48. Harker diagrams of major elements are presented in Figure 5.29. K_2O shows an increasing linear trend from plutonic inclusions on one end to early Kalama age rocks on the other. There is scatter in the middle Kalama range that may form a linear trend with the X lavas, lahars and tephra and the Two Finger Flow.

Major element data from this study plotted with other compiled data of Kalama-age rocks (Clynne, written communication, 2009; Clynne, unpublished data; Crandell, 1987; Gardner *et al.*, 1995b; Halliday *et al.*, 1983; Hausback, 2000; Mullineaux, 1996; Pallister *et al.*, 1992; Pallister, 2008; Pallister, unpublished; Sisson, unpublished data; Smith, 1980, 1984; Smith & Leeman, 1982, 1987, 1993; Underwood, unpublished data; Verhoogen, 1937; Wolfe, unpublished data) shows a distinctly linear trend on a Harker diagram with late Kalama summit domes in between Wn dacites and MKLV. X tephra, lahars and lava are offset from this primary trend in most elements, except for FeO* and CaO, which has a subtle offset. In contrast, Pallister *et al.* (1992) described major elements and several trace elements on SiO_2 variation diagrams as single linear trends (Figure 5.30).

The X Lava Flow is higher in SiO_2 than X tephra and lahars and plots near the late Kalama andesites. In some cases the lava acts as a transition from the other X rocks into the linear trend between early and late Kalama rocks and some plutonic inclusions. Examples of this are notable in MgO, K_2O, and Na_2O on SiO_2 Harker diagrams. TiO_2 of all X deposits remains offset from the main linear trend, while on an FeO* plot, only the X Lava Flow is offset higher than other Kalama rocks. Plutonic inclusions, particularly 18A, fall along a

linear trend with middle Kalama lavas and late Kalama intermediates opposite the early Kalama dacites in all major elements.

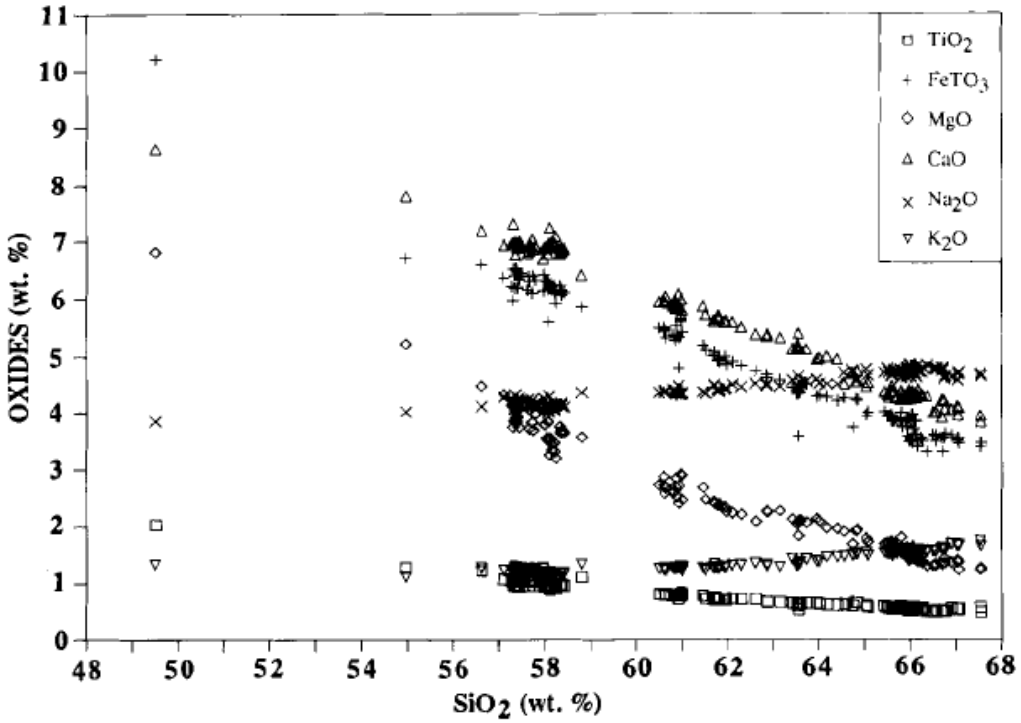

Figure 5.30 From Pallister *et al.* (1992). SiO_2 variation diagram for rocks of the Kalama eruptive period and for the north-flank basalt of Smith (1984). All Fe given as Fe_2O_3.

The two QMI populations are distinguishable by major elements, and QMI 19 typically lies at the most mafic end of the X segment. The more mafic olivine-rich population ranges between 53-54 % SiO_2. The olivine-poor QMI population is characterized by 56-58 % SiO_2 and lower concentrations of FeO*, MgO, CaO, TiO_2, and P_2O_5. M-type X lahars have lower SiO_2, ~56 %, and higher FeO*, MgO, CaO, TiO_2, and P_2O_5 than B-type lahars (~58 % SiO_2). Each lahar type produces a distinct trend on an Al_2O_3 vs. CaO diagram. The Xb tephra (58-59 % SiO_2) generally plots with the B-type lahars. The Two Finger Flow (57-58 % SiO_2) plots in between the two X lahar populations, and other

MKLV and the Breadcrust Pyroclastic Flow (57-59 % SiO_2) plot between the Two Finger Flow and X Lava Flow (60-61 % SiO_2). The late Kalama SDO may be divided by two groups with subtle chemical differences: (1) 60.8-61.3 % SiO_2 and (2) 61.7-62.3 % SiO_2. SDY also appears to have two groups (1) 62.3-62.9 % SiO_2 and (2) 63.5-64.6 % SiO_2. Each of the four summit dome groups are particularly evident on an FeO*/MgO vs. SiO_2 diagram.

5.3.2 Trace Element Chemistry

Trace element analyses by XRF are listed in Table A.2 and by ICP-MS in Table A.3. Elemental concentrations are normalized to primitive mantle values (Sun & McDonough, 1989) and displayed in Figures 5.31-5.34. Although some plutonic inclusions show positive Eu anomalies, rare earth element (REE) patterns are smooth for Kalama-age rocks. Light REE (LREE) show enrichment with respect to middle (MREE) and HREE abundances. There is significant variation in other trace elements such as Cs, Rb, and Pb.

Trace element patterns of inclusions and early, middle and late Kalama rocks display distinct differences. Strontium, Y, Sc, Co, V, U, and Th on SiO_2 variation diagrams were described by Pallister *et al.* (1992) as single linear trends. Cr, REE, and HFSE have counterclockwise loops with respect to stratigraphic sequence (Figure 5.35). Trace elements patterns from this study are in agreement with those from Pallister *et al.* (1992), except for U and Th, which have 2 intersecting linear trends (Figures 5.36 and 5.37). K_2O, Ba and Rb have less defined loop patterns in both studies.

84

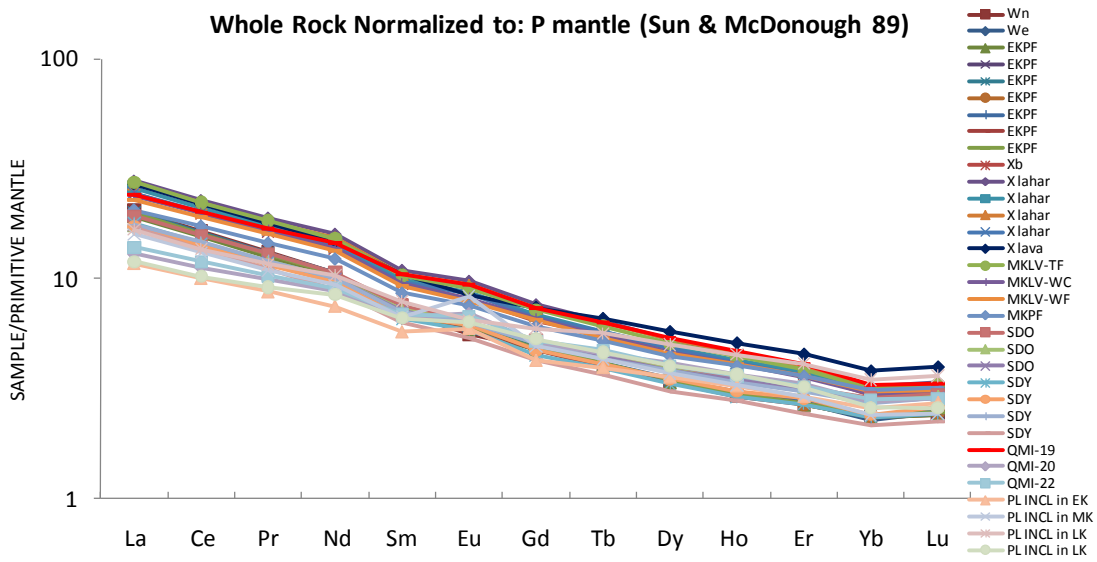

Figure 5.31 REE patterns for all Kalama-age rocks and inclusions from ICP-MS analysis. Concentrations are normalized to primitive mantle values from Sun & McDonough (1989).

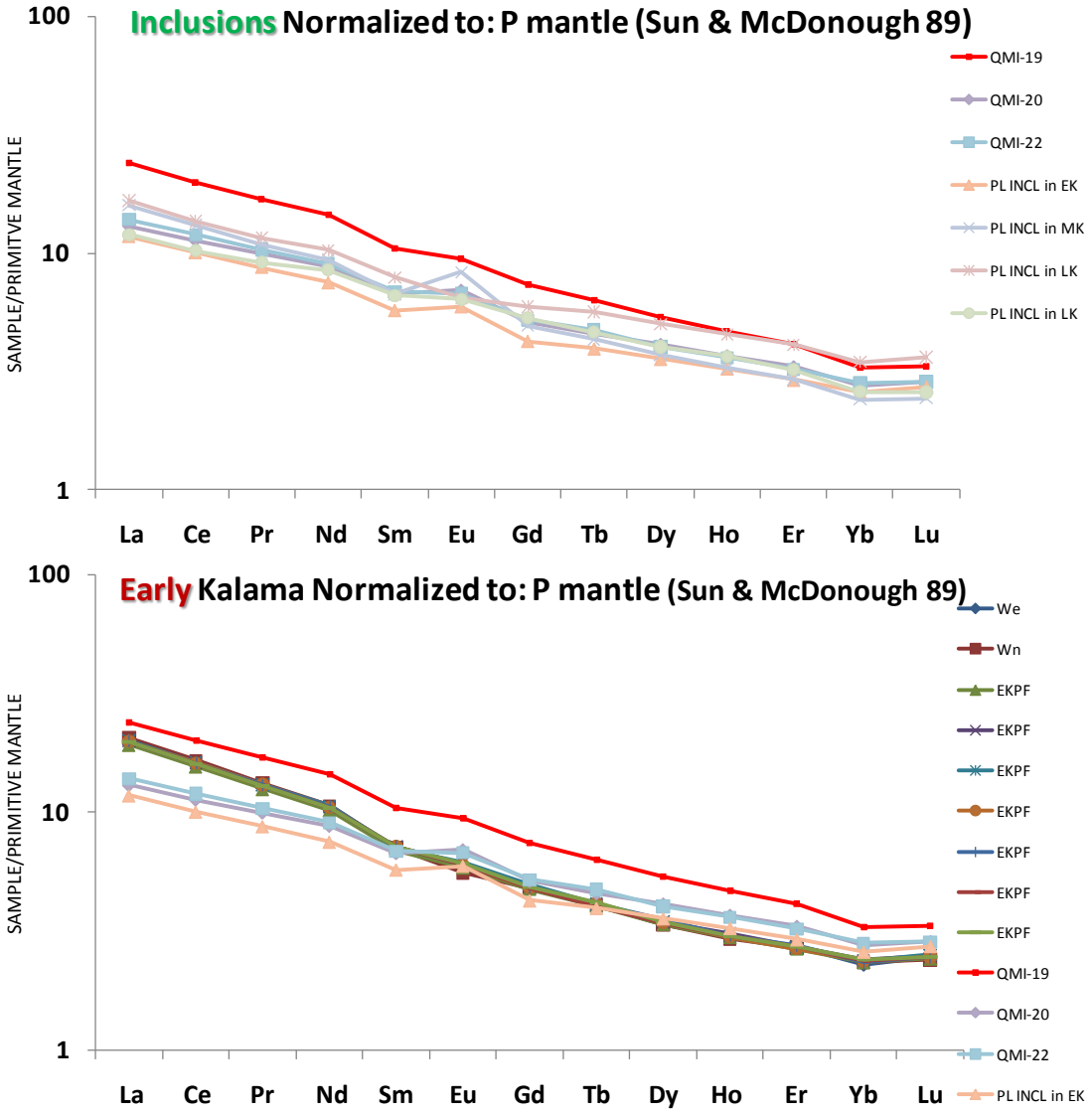

Figure 5.32 REE patterns for Kalama-age rocks and inclusions by groups from ICP-MS analysis. QMI-19 is shown on each diagram for reference. Concentrations are normalized to primitive mantle values from Sun & McDonough (1989).

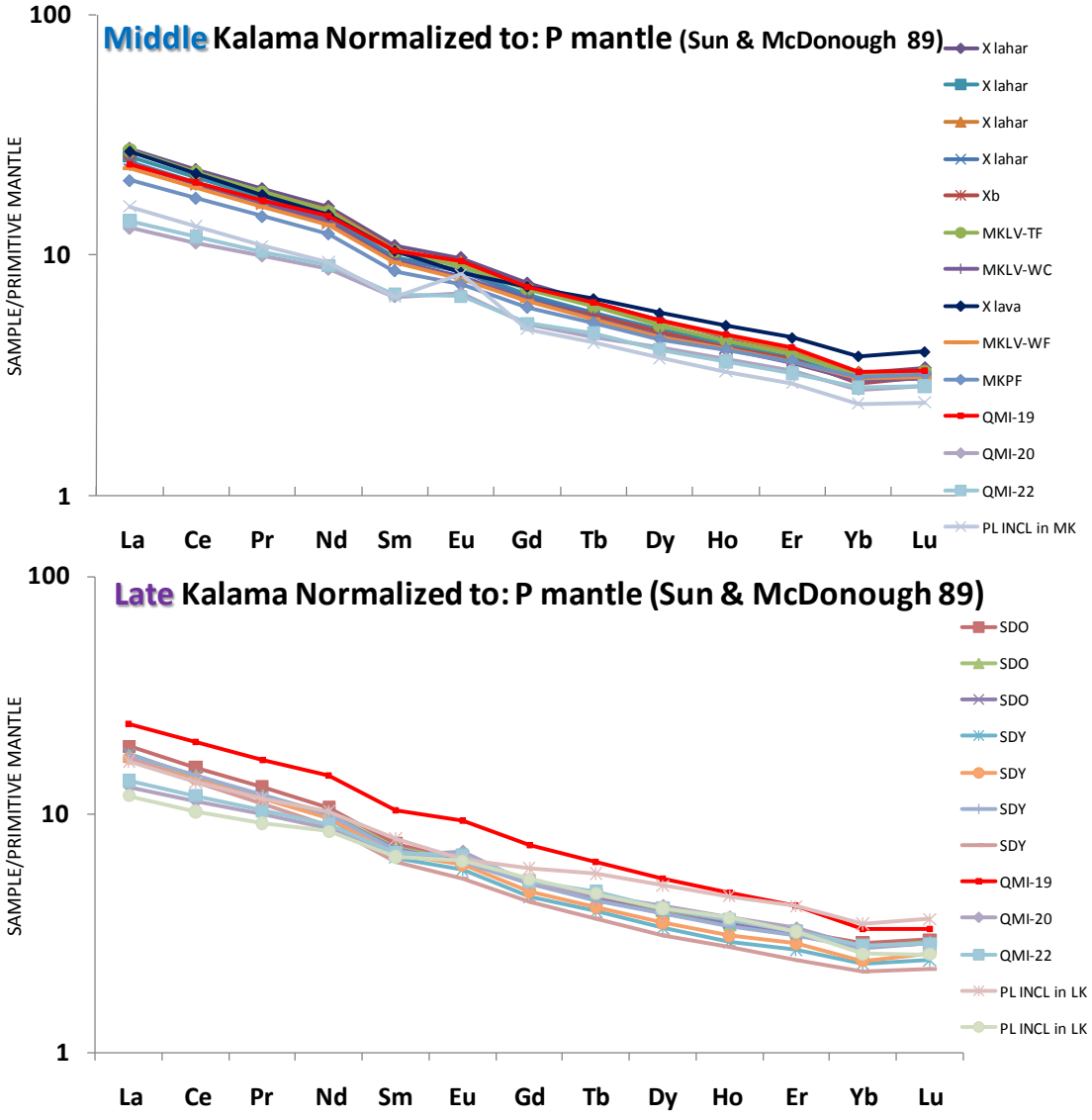

Figure 5.32 (Continued)

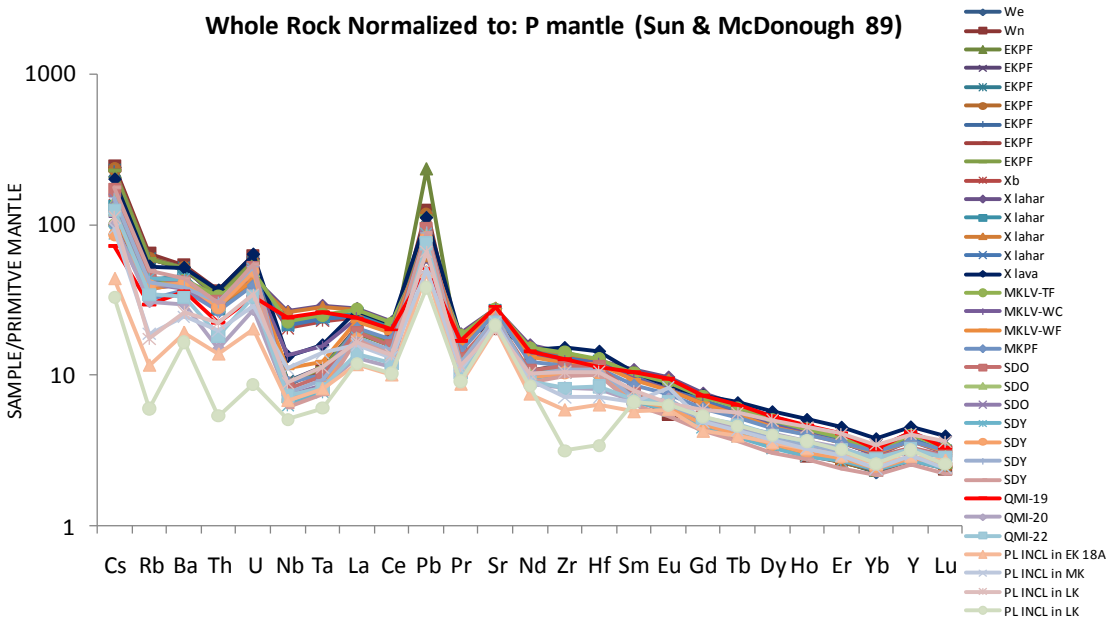

Figure 5.33 Spider diagram for all Kalama-age rocks and inclusions from ICP-MS analysis. Concentrations are normalized to primitive mantle values from Sun & McDonough (1989).

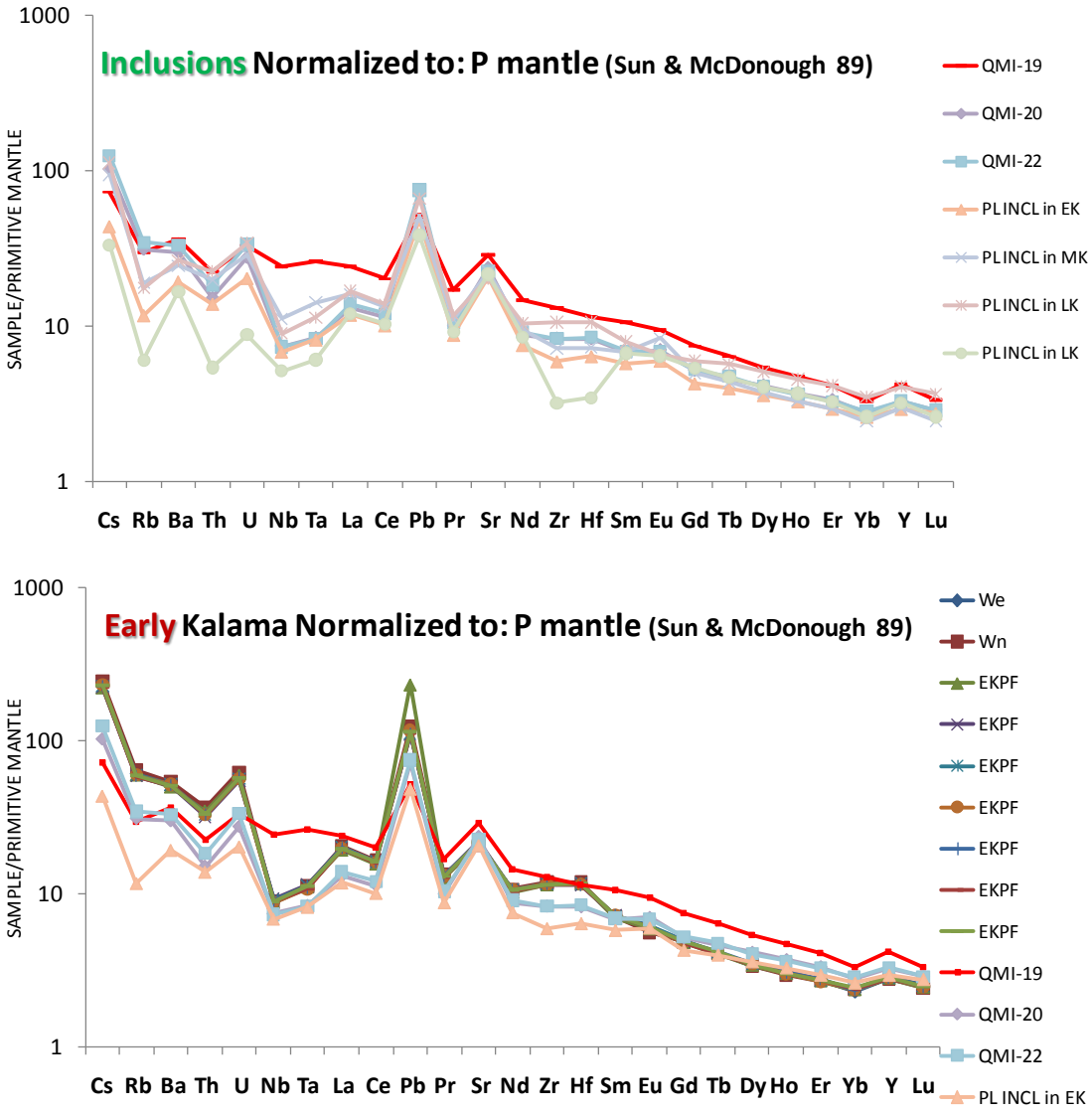

Figure 5.34 Spider diagrams for Kalama-age rocks and inclusions by groups from ICP-MS analysis. QMI-19 is shown on each diagram for reference. Concentrations are normalized to primitive mantle values from Sun & McDonough (1989).

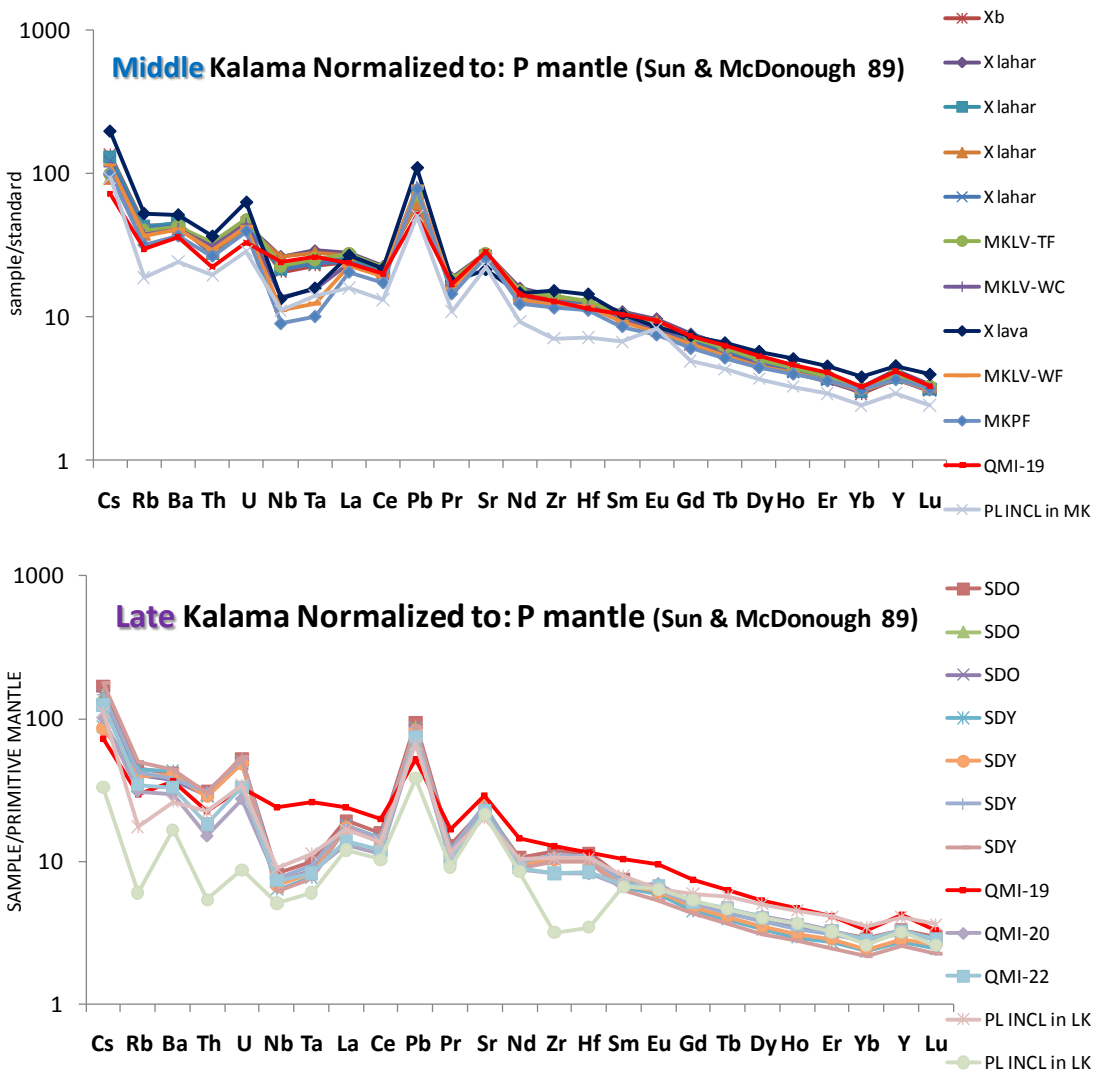

Figure 5.34 (Continued)

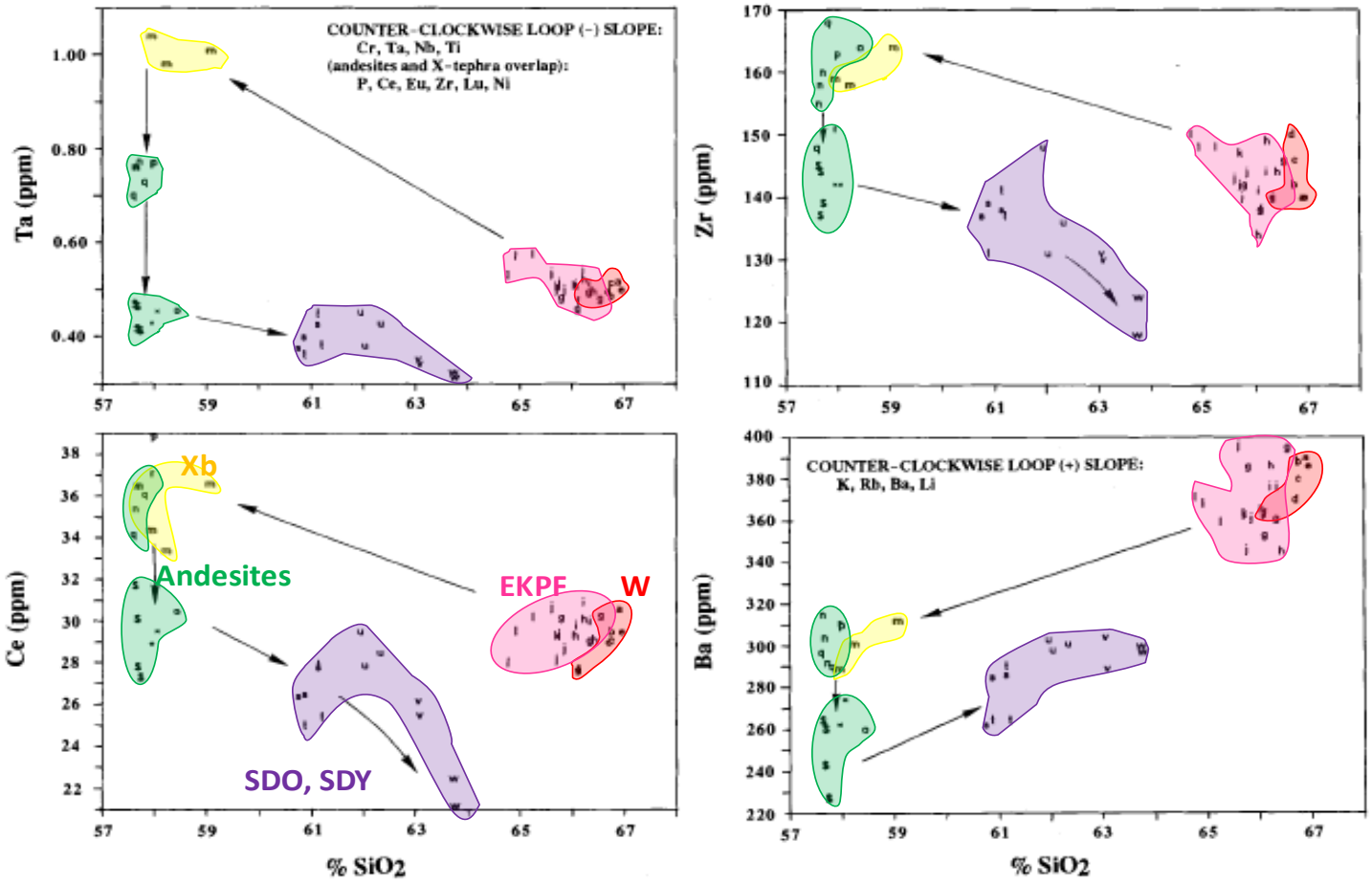

Figure 5.35 Modified from Pallister *et al.* (1992). SiO_2 variation diagrams showing trace element data from rocks of the Kalama Eruptive Period. Arrows indicate stratigraphic sequences and define counterclockwise loops with either negative slopes or positive slopes; elements are indicated for which similar loop patterns are seen. Fields are color coded: red=W, pink=pumice from EKPF, yellow=scoria from Xb, green=andesites, mostly MKLV-WC, purple=SDO and SDY.

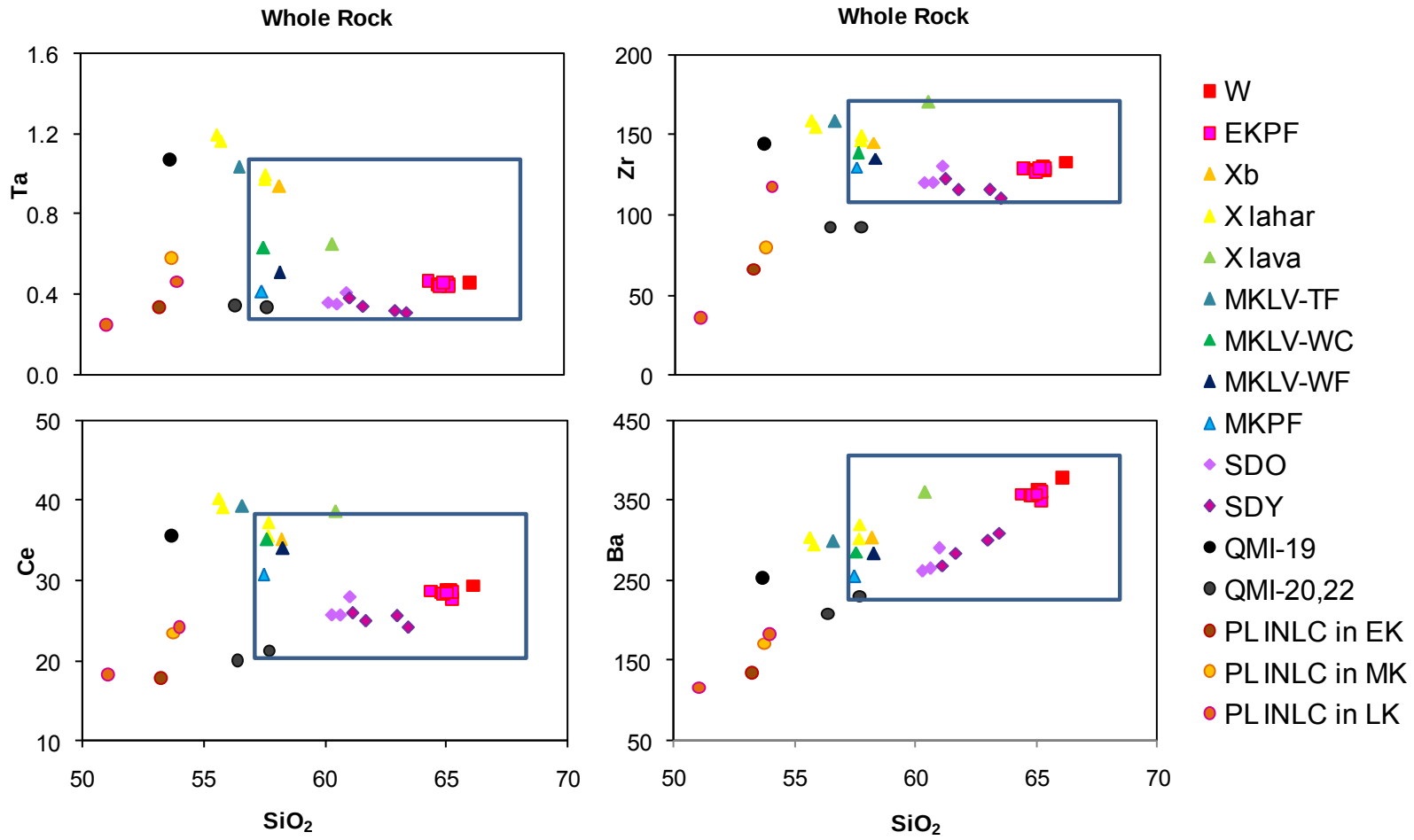

Figure 5.36 Selected trace element variation diagrams for comparison to data from Pallister *et al.* (1992), which fall within the blue boxes. Trace element concentrations in ppm. Range of compositions is increased with the addition of X lavas, Two Finger Flow, and plutonic and quenched mafic inclusions.

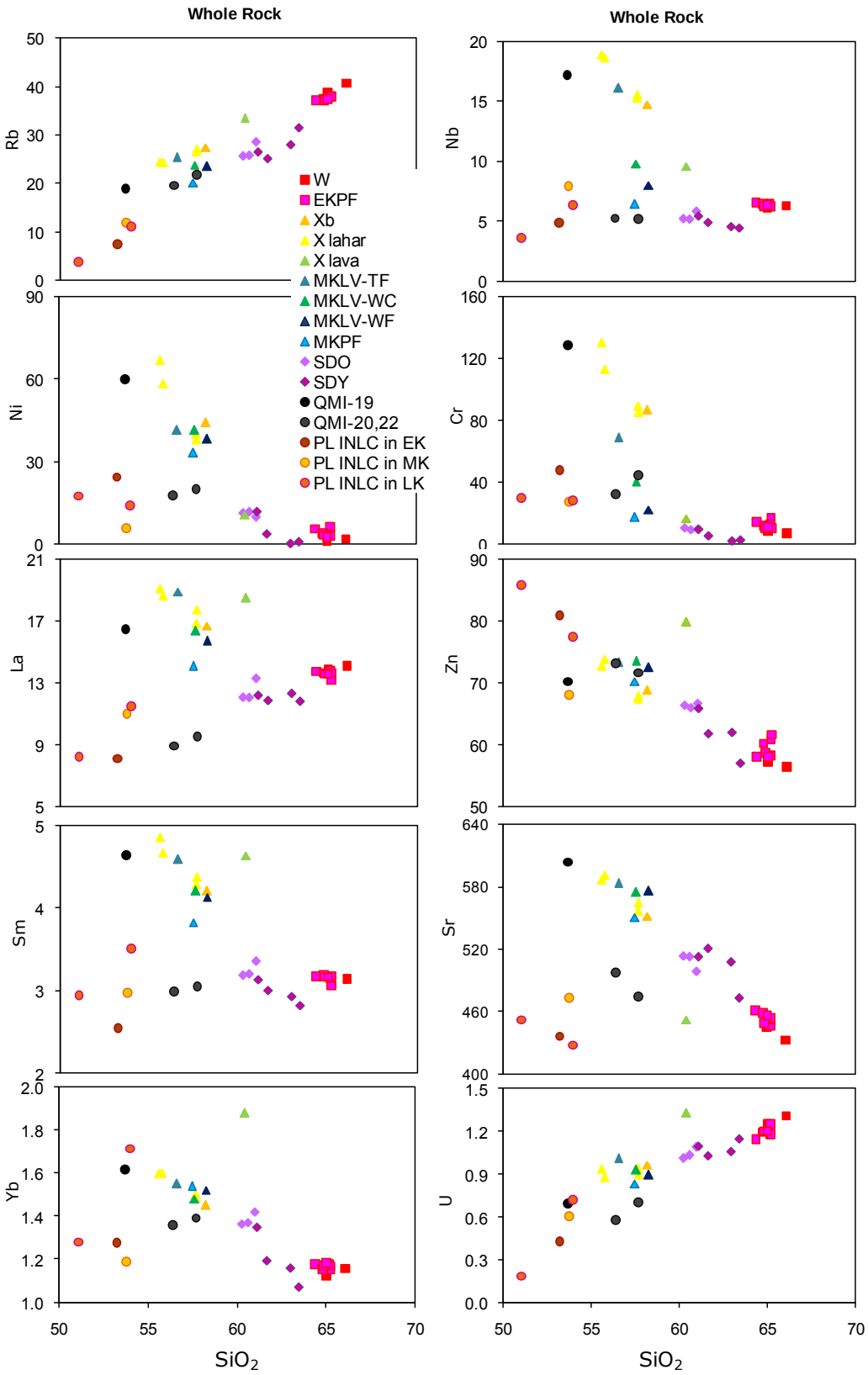

Figure 5.37 Representative whole rock trace element Harker diagrams analyzed by ICP-MS. Silica is not normalized to 100 % anhydrous.

Early Kalama rocks are enriched in Cs, Rb, Ba, U, and Th, but depleted in HREE relative to the other sub-periods, whereas middle Kalama rocks are characterized by enrichments in HFSE (Nb, Ta, Hf, Zr, and Ti) and REE. Middle Kalama X rocks imitate the pattern of QMI 19. Trace elements also serve to distinguish the two populations of QMI. Trace element patterns on spider diagrams are similar for the two populations, but the olivine-rich set is higher in nearly all concentrations (Figure 5.38). Strontium and transition metal concentrations of Ni and Cr are also higher in the olivine-rich QMI, but Zn, V and Sc are nearly identical. The most striking difference is the enrichment of Nb-Ta, LREE and MREE in QMI 19 set, whereas the other group displays a Nb-Ta trough.

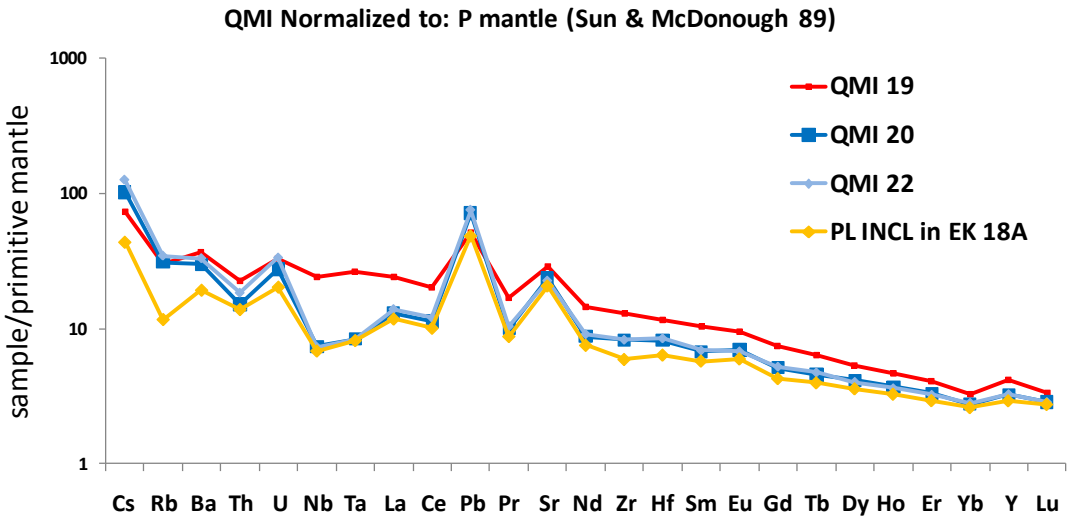

Figure 5.38 Spider diagram of QMIs and plutonic inclusion 18A (hosted by EKPF 18B). Concentrations are normalized to primitive mantle values of Sun & McDonough (1989). QMI 19 is from the olivine-rich population. QMIs 20 and 22 are from the olivine-poor population.

Trace elements are especially distinctive for the X Lava. Nearly all of them plot outside any Kalama trend, and X Lava is higher in HREE than all other Kalama rocks. The sample lacks the Nb-Ta enrichment of other X deposits. However, REE diagram show that the X Lava pattern mirrors that of the late Kalama andesites and dacites. This is also the case with early Kalama dacites, but there is a larger disparity between HREE. When normalized to primitive mantle values (Sun & McDonough, 1989), western flank and Worm Complex lavas have a similar pattern to X Lava, but with lower abundances. Additionally, the X Lava pattern is flatter than the MKLV lavas. Patterns for QMIs 20 and 22 are also flatter than the lavas and the plutonic inclusion 08B hosted by the Worm Complex andesite lava 08A.

Plutonic inclusion 28 hosted by late Kalama SDY shows significantly lower abundances of Th, Nb, Ta, Zr and Hf. Plutonic inclusion 18A anchors the mafic end of a linear trend on a Harker diagram, with QMIs 20 and 22 in between. Wn anchors the felsic end in all trace elements. The trend is less defined, or slightly curvilinear, in the HREE Tb-Lu, but still apparent. QMIs 20 and 22 show distinctly similar abundances and trends to plutonic inclusion 18A (Figure 5.38).

Late Kalama rocks have lower abundances of all trace elements. Late Kalama summit dome andesites and dacites fall along major element linear trends with early Kalama dacites, but small variations from this trend may be significant. This is true of most trace elements as well; at least two SDY samples have lower abundances in the following trace elements: Pb, Cs, Nb, Ta, Nd, Sm, Eu, Gd, Tb, Dy, Ho, Er, Tm, Yb, Lu, Hf, and Y. Each late Kalama sample plots lower in Nd. The late Kalama dacites also plot among or very close to the early Kalama dacites on ratio-element diagrams (Figure 5.39).

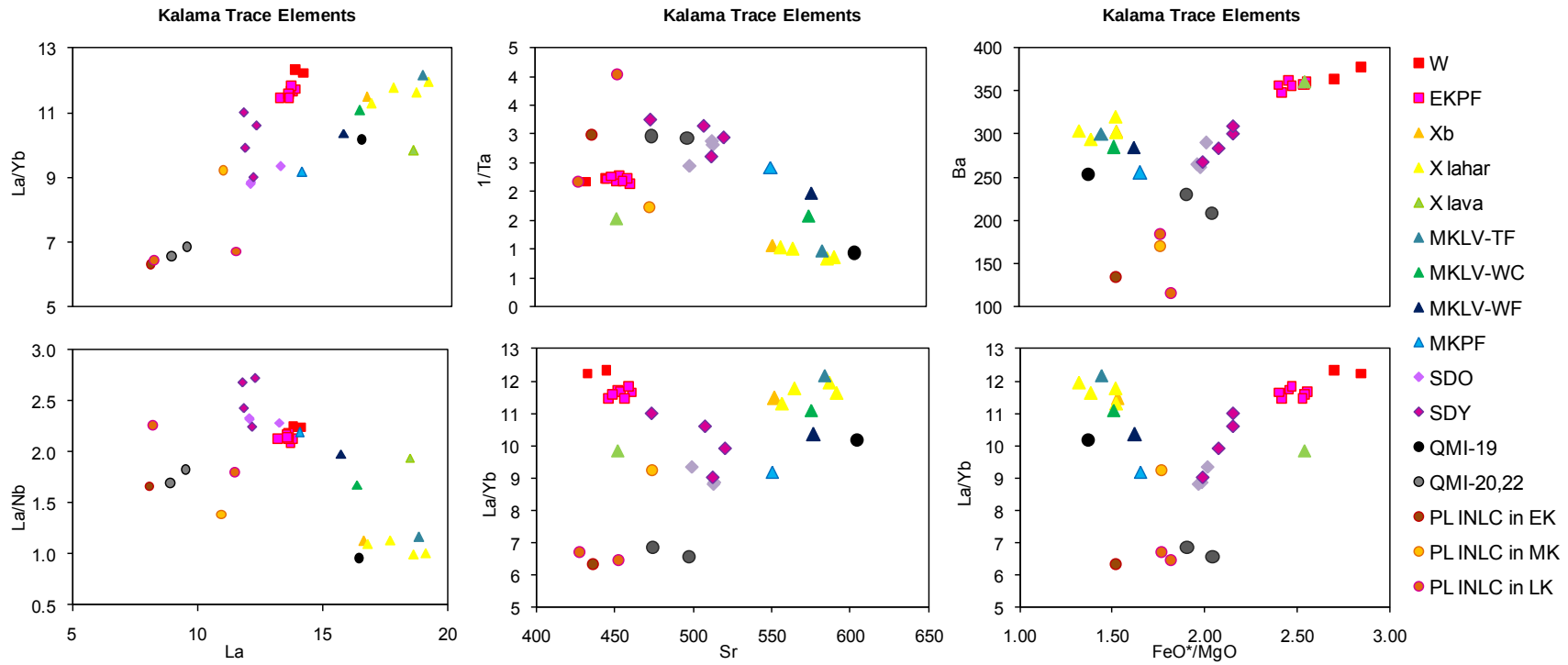

Figure 5.39 Representative trace element ratio Harker diagrams.

5.3.3 Whole Rock Chemistry Summary

Wn pumice is the most felsic and homogenous of all Kalama-age rocks. We pumice and EKPF become progressively more mafic and variable in composition. The two QMI populations are distinguished by both major and trace elements, with the olivine-rich population being more mafic and characterized by HFSE enrichment relative to other Kalama-age rocks. The Two Finger Flow and all X deposits except for the X Lava Flow also have a HFSE enrichment similar to that seen in the olivine-rich QMIs. X lahars and pyroclastic flows MKLV appear to be transitional in some major elements between X deposits and the apparent linear trend formed by early and late Kalama rocks and plutonic inclusions. M-type lahars are lower in SiO_2, and higher in FeO*, MgO, CaO, and TiO_2 than B-type lahars. The two types are also distinguishable by small trace element differences. Early and late Kalama dacites form similar major element trends and trace element patterns. Plutonic inclusions have variable compositions, but are consistently more mafic than Kalama-age rocks.

5.4 Phase Chemistry

Because bulk rock chemistry represents an aggregate of all the minerals, glass, and inclusions in a rock, individual phase chemistry is valuable for deciphering distinct inputs into a system. Olivine, spinel, pyroxene, plagioclase, and groundmass glass were analyzed for comparison between samples. If mechanical mixing occurred in Kalama magmas, a combination of crystals and liquid would have been exchanged between at least one magma source to the other, and potentially between them both.

Investigation of a range of crystal populations in representative samples could draw out connections between magmas.

Phase geochemistry may help clarify any relation between the plutonic inclusion and the QMI. If the plutonic inclusion crystallized from a magma of the same source as the QMIs and mixed with the dacitic reservoir, one might expect to see disaggregated crystals with geochemistry similar to that inclusion within the QMI. Alternately, if an inclusion is a xenolithic basement rock, trace elements of individual phases could be markedly different from those of the QMIs.

5.4.1 Plagioclase

Plagioclase crystallizes over a wide temperature-pressure regime and compositional range, making it valuable in tracking changes in a magma's history. Spots on plagioclase grains from all lithologies were analyzed by EMP for major and minor element chemistry. Microphenocrysts were also analyzed in samples with large enough grains to allow it; they typically had lower An (molar (100*Ca/(Ca+Na+K))) compositions than phenocrysts cores and mantles. Transects of either rims or core to rim were also conducted on 43 grains in 18 samples, and results from representative crystals are presented in Figure 5.40. Representative plagioclase analyses are listed in Table 5.1. Remaining transects and plagioclase analyses are presented in Table B.1 in Appendix B. All analyzed plagioclase points are plotted on An-Ab-Or ternary diagrams in Figure 5.41. An contents vary from $An_{23\text{-}87}$, although some microphenocrysts and rims were as low as $An_{20\text{-}29}$. These compositions form a solid solution series between bytownite and oligoclase (Deer *et al.*, 1963). Anorthite contents are displayed in histograms by lithology in Figure 5.42.

Table 5.1 Representative Plagioclase EMP Spots in wt %. Xtl = crytsal, MC = microphenocryst, T = transect

Sample	Lithology	Point	An	Or	Ab	Na_2O	MgO	SiO_2	Al_2O_3	FeO	CaO	P_2O_5	TiO_2	K_2O	Total
31 xtl 1	Wn	32 /1.	29.4	2.1	68.5	7.25	0.00	62.16	25.04	0.03	5.63	0.01	0.00	0.33	100.49
31 xtl 2	Wn	35 /2.	65.9	0.4	33.6	3.67	0.04	51.90	30.77	0.36	13.00	0.02	0.02	0.07	99.87
27 xtl 1	We	1 /5.	55.1	1.0	43.9	4.20	0.02	56.58	28.46	0.25	9.53	0.02	0.02	0.15	99.24
14 xtl 1 MC 2	EKPF	25 /1.	35.4	1.7	62.9	6.77	0.03	60.54	26.17	0.35	6.90	0.03	0.01	0.28	101.08
14 xtl 4	EKPF	33 /2.	81.9	0.3	17.9	1.95	0.01	47.61	33.93	0.39	16.21	0.00	0.01	0.05	100.17
32 xtl 4	Xb	26 /2.	80.7	0.3	18.9	2.05	0.07	48.26	33.11	0.50	15.82	0.01	0.04	0.06	99.99
32 xtl 4.1	Xb	27 /2.	40.9	1.5	57.7	6.23	0.01	59.12	26.76	0.28	7.98	0.01	0.01	0.24	100.66
07 xtl 1	X lahar	2 /1.	58.9	1.0	40.0	4.35	0.05	53.33	29.70	0.41	11.58	0.03	0.03	0.17	99.64
07 xtl 8 MC 2	X lahar	13 /2.	34.0	4.4	61.6	6.68	0.06	59.61	25.01	0.73	6.67	0.05	0.15	0.73	99.67
30 xtl 1	X lava	12 /1.	76.2	0.5	23.3	2.57	0.04	49.82	32.63	0.50	15.18	0.02	0.03	0.08	100.88
30 xtl 4	X lava	18 /6.	40.3	2.4	57.3	6.20	0.04	59.30	26.75	0.38	7.90	0.03	0.02	0.39	101.01
10 xtl 11.3	MKLV-TF	41 /2.	80.5	0.4	19.1	2.07	0.05	47.67	33.17	0.48	15.84	0.03	0.04	0.07	99.42
10 xtl 11.3	MLLV-TF	41/25.	36.8	3.6	59.6	6.47	0.06	58.55	25.51	0.76	7.22	0.03	0.13	0.59	99.33
08A xtl 1	MKLV-WC	28 /2.	46.9	1.7	49.5	5.39	0.09	56.43	27.53	0.63	9.63	0.02	0.10	0.29	100.11
08A xtl 3 T	MKLV-WC	38 /6.	85.4	1.3	43.0	4.74	0.08	54.93	29.00	0.64	11.11	0.02	0.07	0.21	100.85
03 xtl 10	MKPF	1 /1.	70.8	0.8	28.4	3.13	0.04	50.42	31.79	0.72	14.13	0.01	0.05	0.14	100.43
03 xtl 10 5	MKPF	1 /5.	47.8	2.0	50.2	5.32	0.60	56.84	26.85	1.25	9.17	0.03	0.08	0.33	100.48
03 xtl 14 MC 1	MKPF	26 /3.	23.7	1.8	47.2	5.10	0.07	55.78	27.62	0.83	9.96	0.03	0.10	0.29	99.78
05 xtl 1	SDO	34 /1.	75.8	0.4	23.9	2.62	0.03	48.75	32.46	0.40	15.06	0.02	0.02	0.06	99.47
05 xtl 5	SDO	39 /5.	46.5	1.3	52.3	5.61	0.05	56.31	26.79	0.52	9.02	0.02	0.05	0.21	98.58
11 xtl 1 T	SDO	5 /18.	45.0	1.4	53.6	5.88	0.05	57.76	27.24	0.43	8.94	0.04	0.04	0.24	100.62
13 xtl 1	SDY	1 /1.	53.7	1.0	45.3	4.95	0.04	54.94	28.73	0.46	10.63	0.00	0.03	0.17	99.99
28 xtl 10	SDY	31 /4.	67.1	0.5	32.5	3.58	0.03	51.34	31.05	0.32	13.39	0.01	0.02	0.08	99.81
19 xtl 3 rim	QMI-19	4 /5.	27.2	2.8	70.0	7.46	0.01	61.19	24.27	0.28	5.26	0.01	0.02	0.46	98.96
19 xtl 17	QMI-19	19 /2.	86.7	0.3	13.0	1.43	0.03	45.73	33.94	0.41	17.25	0.02	0.03	0.04	98.91
20 xtl 7	QMI-20	32/20.	61.9	0.7	37.5	4.17	0.03	53.10	30.25	0.40	12.45	0.03	0.03	0.11	100.57
20 xtl 7	QMI-20	32/25.	28.2	6.0	65.8	5.36	0.02	69.55	20.76	0.63	4.16	0.03	0.10	0.74	101.36
23 xtl 3	PLU INCL in EK	26 /2.	55.2	0.9	43.9	4.82	0.01	54.89	29.18	0.22	10.97	0.02	0.04	0.16	100.29
08B xtl 1	PLU INCL in MK	15 /1.	55.5	1.3	43.3	4.77	0.02	54.55	29.07	0.26	11.07	0.02	0.05	0.21	100.02
06A xtl 3 T	PLU INCL in LK	22 /2.	45.8	1.9	52.3	5.72	0.03	56.73	27.56	0.43	9.06	0.02	0.02	0.32	99.90
06A xtl 3 MC	PLU INCL in LK	23 /2.	20.2	9.7	70.1	7.56	0.00	62.63	23.28	0.52	3.94	0.03	0.05	1.60	99.62

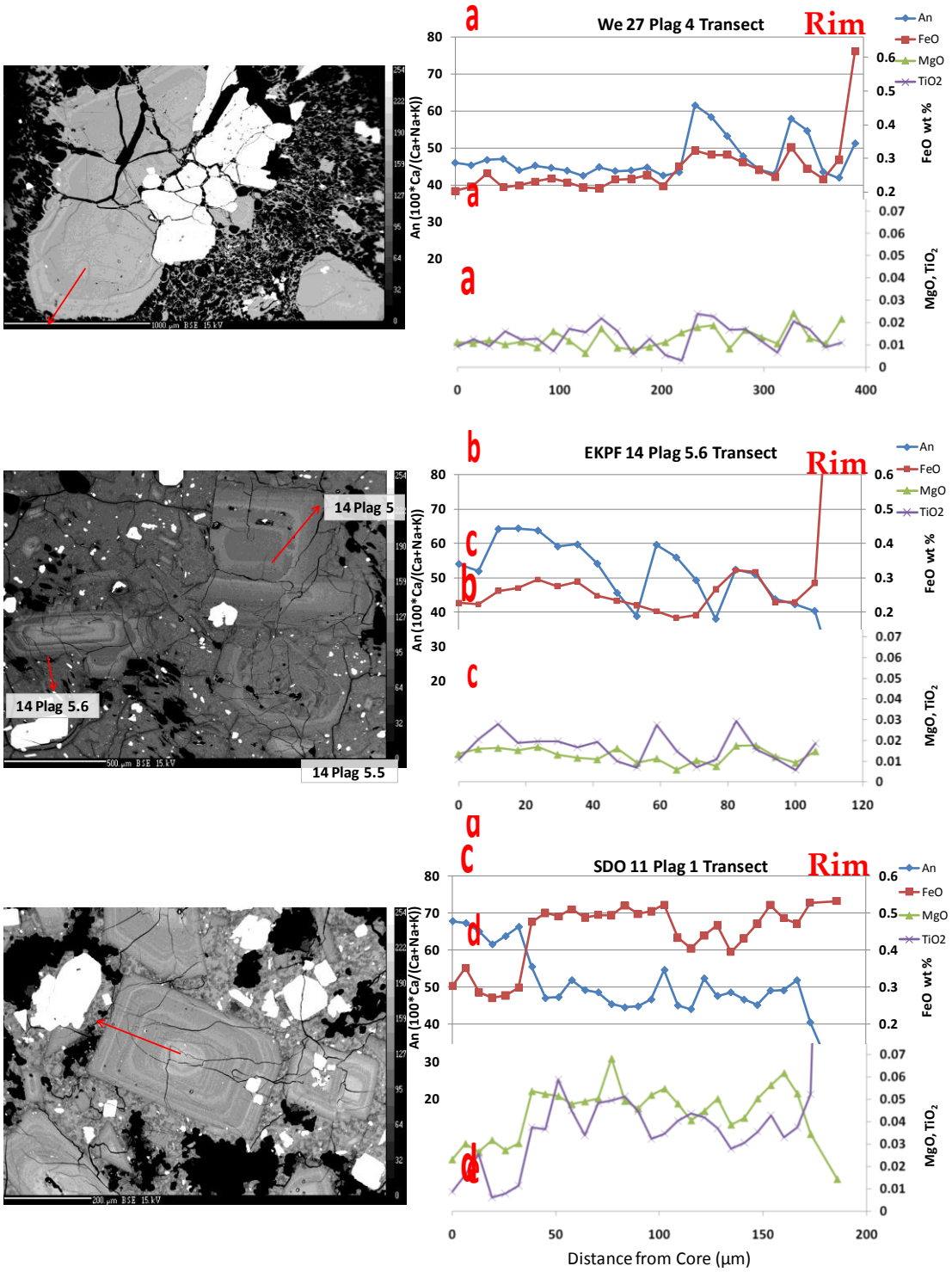

Figure 5.40 BSE images and transects from representative plagioclase grains. a. We 27 b. EKPF 14 c. SDO 11 d. SDO 11 e. QMI 20. The red line on the BSE image represents the transect, which starts near the core and progresses rimward. Normal, reverse, and oscillatory zoning are all present. Note change in vertical scale between FeO axis and MgO and TiO_2 axis.

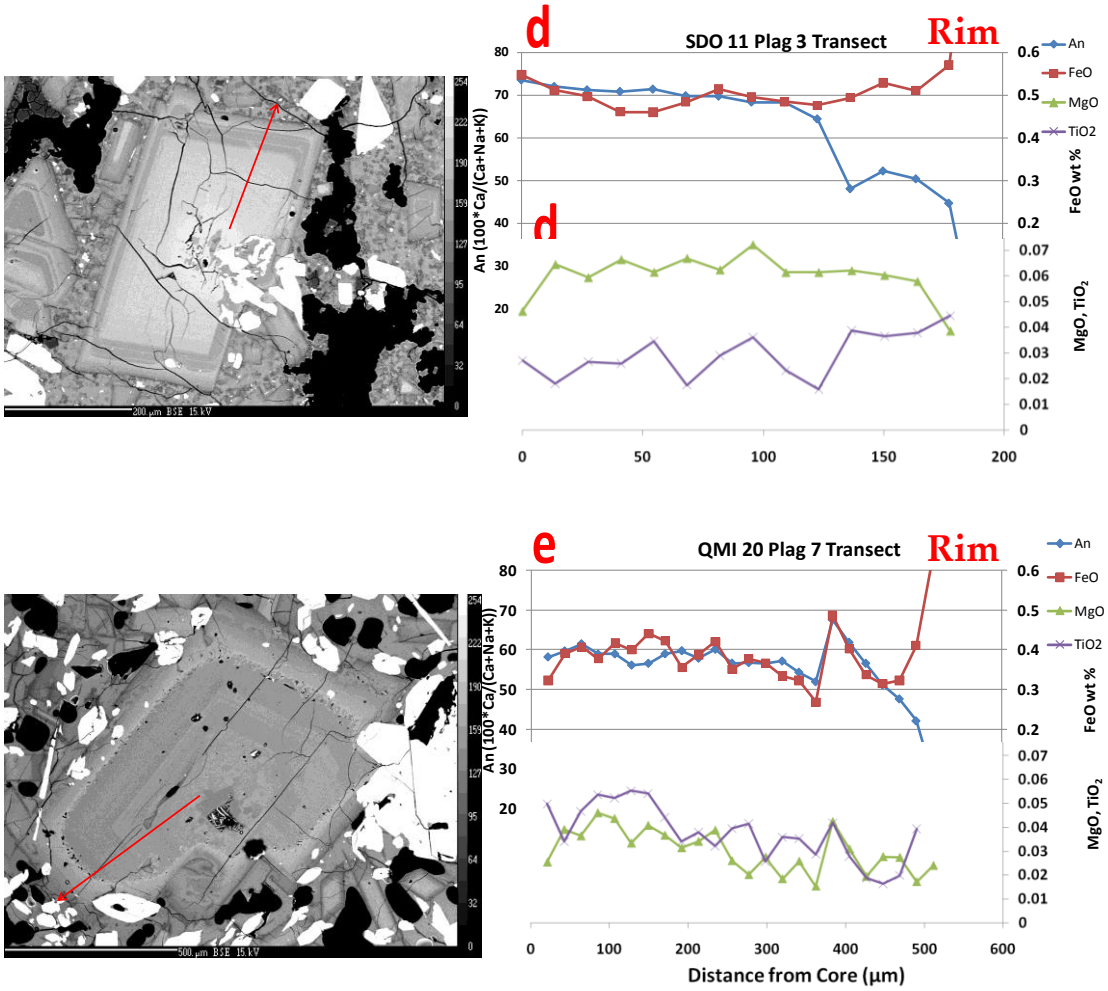

Figure 5.40 (Continued)

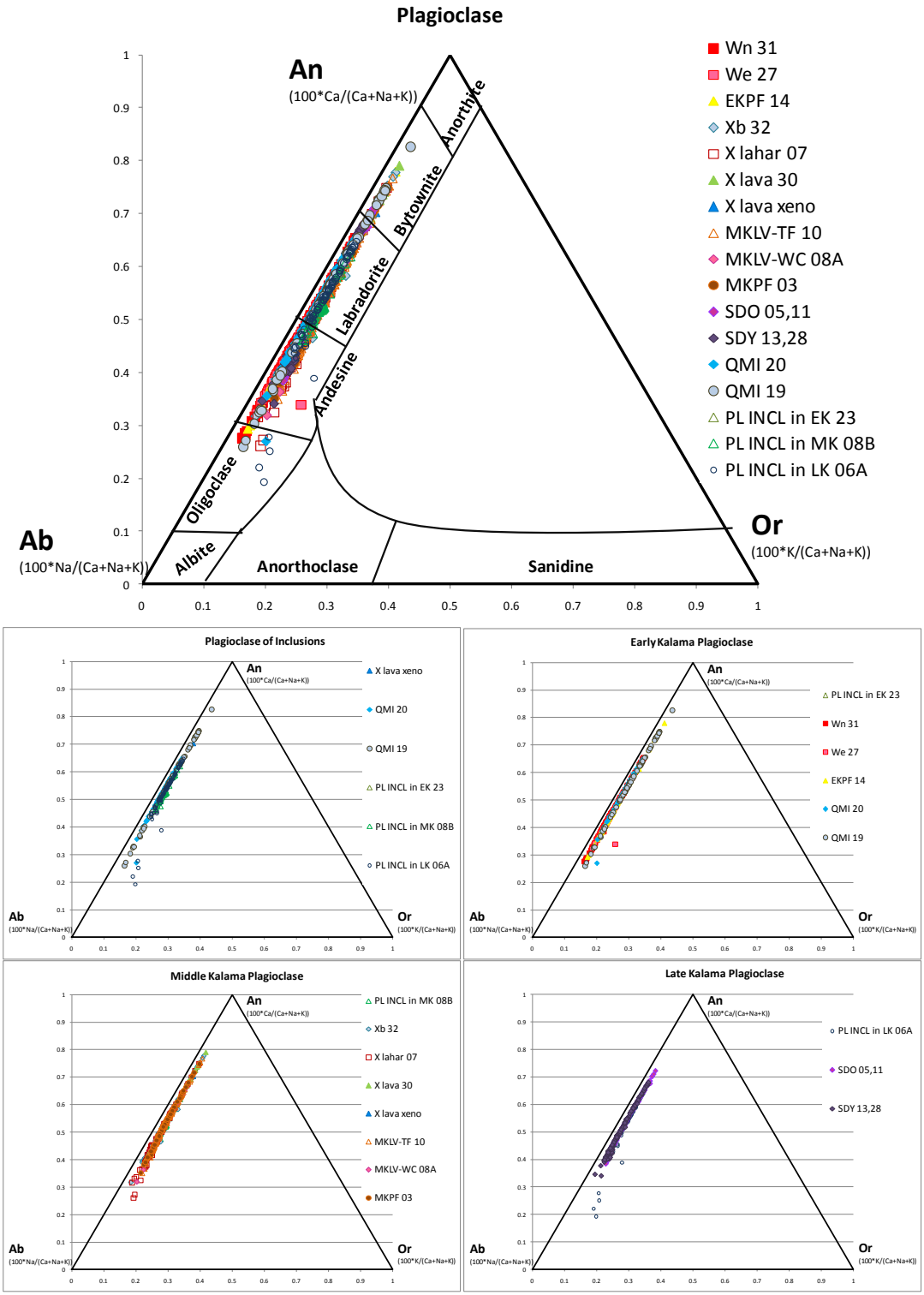

Figure 5.41 An-Ab-Or diagrams after Deer *et al.* (1963) of all 1462 plagioclase points from rocks of the Kalama age, then divided by subperiod.

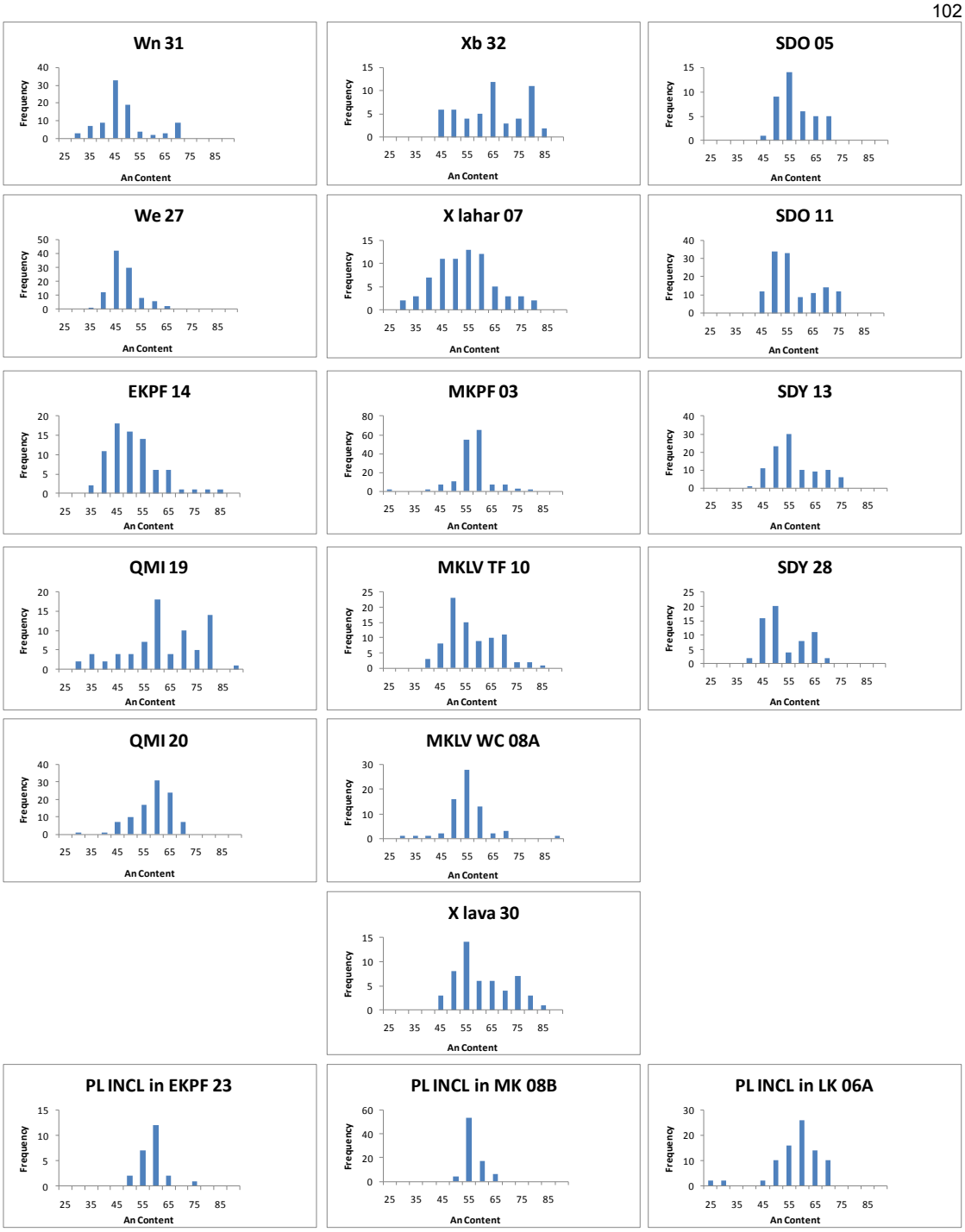

Figure 5.42 Histograms of plagioclase An contents from Kalama-age rocks by lithology and in columns by subperiod. Note that all spots and transects are included and no correction was made for oversampling of crystals with transects.

Anorthite-Ab-Or diagrams are useful for first order classification of plagioclase compositions, but few details of plagioclase compositional changes can be seen when only major components of the phase are considered. When major components can be compared with minor ones, small changes in magma chamber conditions may be discernable. Anorthite vs. MgO diagrams are used throughout the rest of this manuscript for this reason.

Microphenocrysts and phenocryst rims of late Kalama SDY and middle Kalama pyroclastic flows, generally comprise the lowest An contents, An_{20-29}. Rims from Wn pumice and QMI grains are also among the lowest, $<An_{30}$ (Figures 5.41, 5.42 and 5.43), while their cores are notably dissimilar. Among the highest An contents are the corroded cores of large population L phenocrysts from the Two Finger and Worm Complex flows, middle Kalama pyroclastic flow, X tephra and lava, QMI, and early Kalama pyroclastic flow ($>An_{70}$). Smaller, compositionally zoned grains (0.2-0.5 mm) with few to no disequilibrium textures from X tephra and lava, and QMI are also among the highest and lowest An contents measured (Figures 5.44 and 5.45).

The groundmass microphenocryst population in QMI 20 forms an arcuate trend from low MgO and An content to higher MgO and An content. The dominant phenocryst population in QMI 20 (patchy cores and sieve zone) does not follow such a discrete trend. Most are normally or oscillatory zoned and comprise the highest An content of QMI 20. There is very little overlap in plagioclase compositions between QMIs 19 and 20.

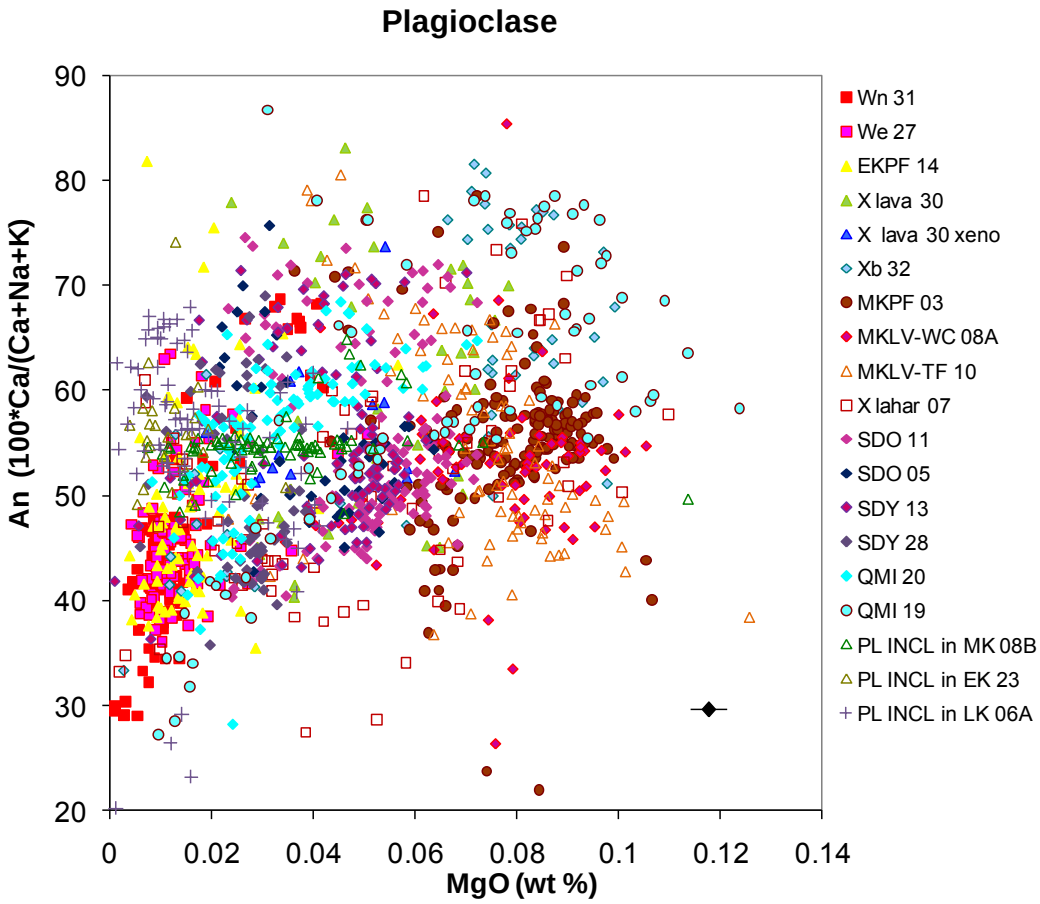

Figure 5.43 An content vs. MgO for all plagioclase in Kalama-age rocks from this study. X lava 30 xeno = xenocryst in X lava 30, MKPF = Breadcrust Pyroclastic Flow, xtl = crystal, mc = microphenocryst. Error for An is smaller than symbol. Representative 1 s error for MgO shown in top right corner.

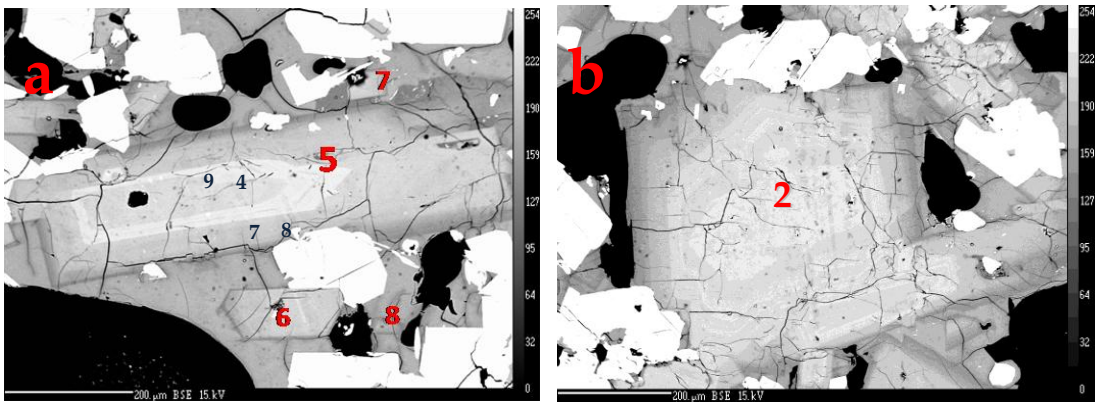

Figure 5.44 Backscattered electron images of plagioclase which contain zones among the highest and lowest An contents measured in Kalama plagioclase. a. QMI 19 crystals 5 through 8. Crystal 5 (An_{29-78}). b. Crystal 2 (An_{34-73}).

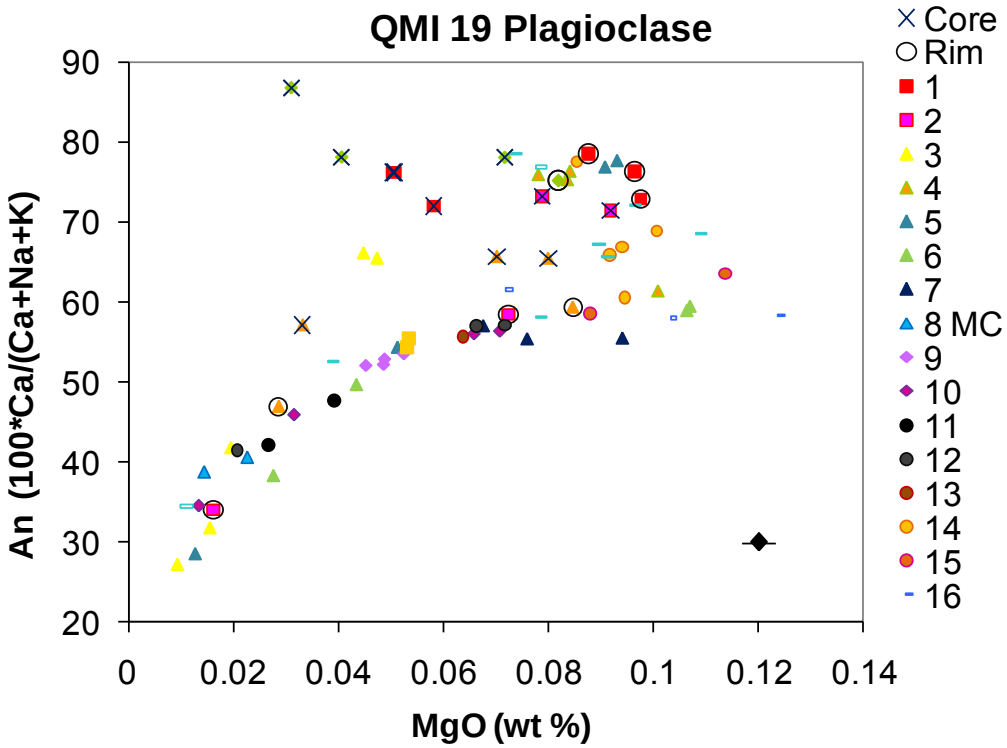

Figure 5.45 An content vs. MgO of QMI 19 plagioclase. Core and rim symbols are overlain onto some phenocryst symbols. Plagioclase 17 transect is of the rim. Representative 1 s error for MgO shown in bottom right corner.

QMI 19 plagioclase follow a few distinct geochemical trends. Cores from crystals 1 and 17 (Figure 5.11), population L phenocrysts, have anomalously high An contents. Figure 5.45 illustrates that rim MgO concentrations of such crystals cluster within a narrow range. The core from plagioclase 2, a moderately sized (0.4 mm) grain with no disequilibrium textures (Figure 5.44), also plots with the rim cluster. The rim spots from other phenocrysts follow the arcuate trend of decreasing MgO with decreasing An. Similarly, plagioclase 19 (<0.5 mm) core analyses increase in MgO outward from the core, while the rim displays the opposite behavior (Figure 5.46). Its core plots in proximity to other plutonic inclusion or xenocryst grains.

Plagioclase from M-type X Lahar 07 spans a wide compositional range (Figure 5.47). Figure 5.48 displays several phenocrysts that clearly have different crystallization histories. Reversely zoned sodic phenocrysts (crystal 1.4) are in close proximity to population L, and normally and oscillatory zoned (crystal 1.6) phenocrysts. Large (2+ mm) xenocrysts (crystals 3 and 4) plot in the same range as plagioclase grains from the plutonic inclusion in EKPF 23. The core of crystal 2 and most of crystal 4 plot just lower in An content and higher in MgO than the large xenocryst. Both of these crystals are large (1-2+ mm) and xenocrystic. A medium-size reversely-zoned sodic phenocryst with rounded edges has core compositions as low as An_{33} and rims as high as An_{67}. A group of points cluster along an increasing MgO, decreasing An path including crystals: 1, core of 1.3 core, mantle zone surrounding the sodic core of 1.4, rims of 8 and 1.6 and some microlites. These crystals fall along a vaguely linear (or curvilinear) trend with the patchy core and mantle of Wn crystal 2 at the high An end. Another group of points (crystal 1.5, rims of 1.4 and 4, core of 8, and core and mantle of 1.2 and 1.3) more loosely cluster between An_{50-80} with high MgO. There is very little overlap with the Two Finger Flow plagioclase.

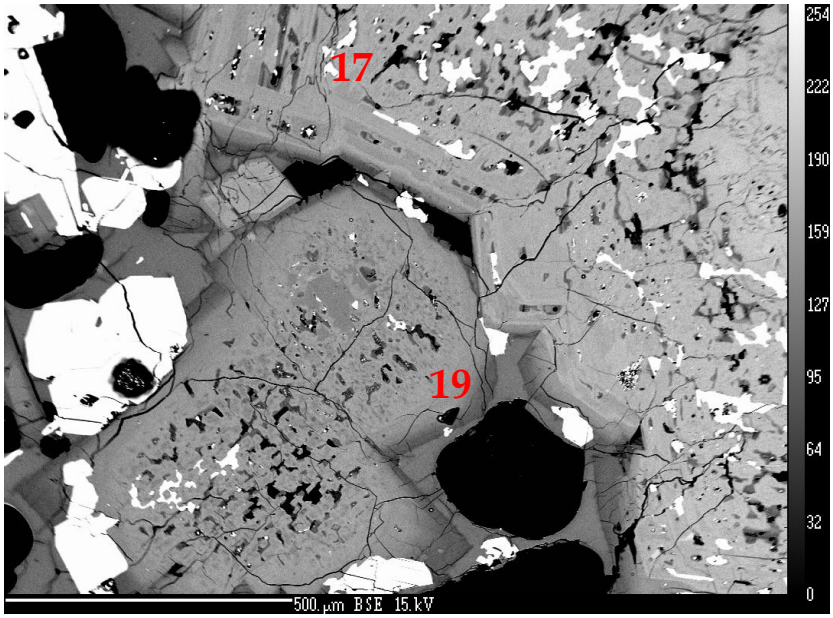

Figure 5.46 BSE image of QMI 19 plagioclase 19. Crystal 17 is also visible.

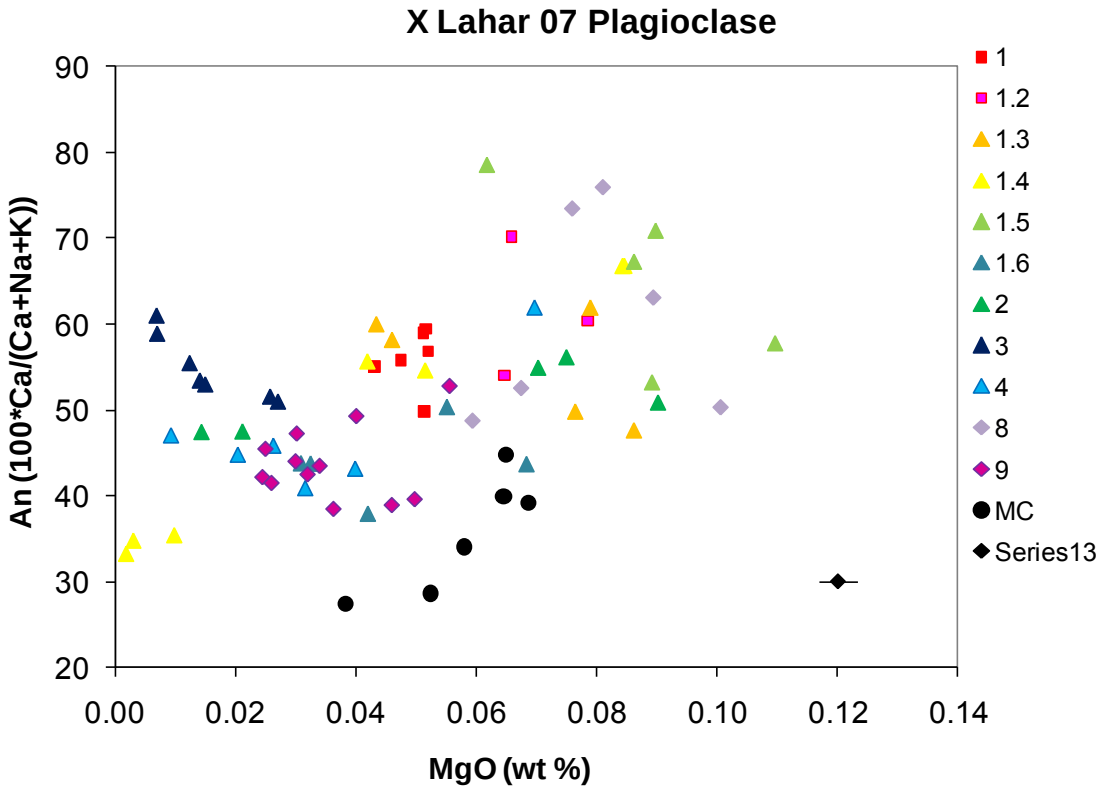

Figure 5.47 An content vs. MgO of M-type X lahar 07 plagioclase. Representative 1 s error for MgO shown in top right corner.

On an An content vs. MgO diagram, the Xb scoria 32 plagioclase appear to form a bimodal distribution (Figure 5.50). Population L phenocrysts (crystals 6 and 7) have high An content and high MgO, whereas smaller (~0.5 mm) grains with patchy zoning have low An content and MgO and have less well-developed, clear rims that surround the disequilibrium textures (Figures 5.48 and 5.49). Phenocryst 5 has compositions from both zones: low MgO and An content in the core and high MgO and An content in the rims. Plagioclase 5 also has a nearly identical texture and composition to X lahar plagioclase 2 (Figure 5.48d). Those with the highest An contents are generally, but not necessarily population L phenocrysts. Xb plagioclase (like those from QMI 19) are among the highest An and MgO compositions in Kalama-age rocks. In addition to plagioclase from M-type X lahar, there is some overlap with QMI 19 and early Kalama dacites.

X Lava Flow plagioclase are among the highest An contents in Kalama-age rocks (Figure 5.51), but have lower MgO, TiO_2 and FeO than Xb pumice, olivine-rich QMI, and Breadcrust Pyroclastic Flow phenocrysts. Compositions tend to straddle the Two Finger Flow on An vs. MgO diagrams, although a few rim compositions are comparable. Plagioclase 4 from the X Lava Flow 30 is comparable in MgO vs. An content to the sodic cores of plagioclase 12 and 14 of the Two Finger Flow; the size and textures of the crystals are roughly comparable (Figures 5.52 and 5.53). There is a paucity of crystals that are lower in both MgO and An content in the X Lava Flow and very little overlap with the middle Kalama pyroclastic flow, except a couple core and a few rim compositions.

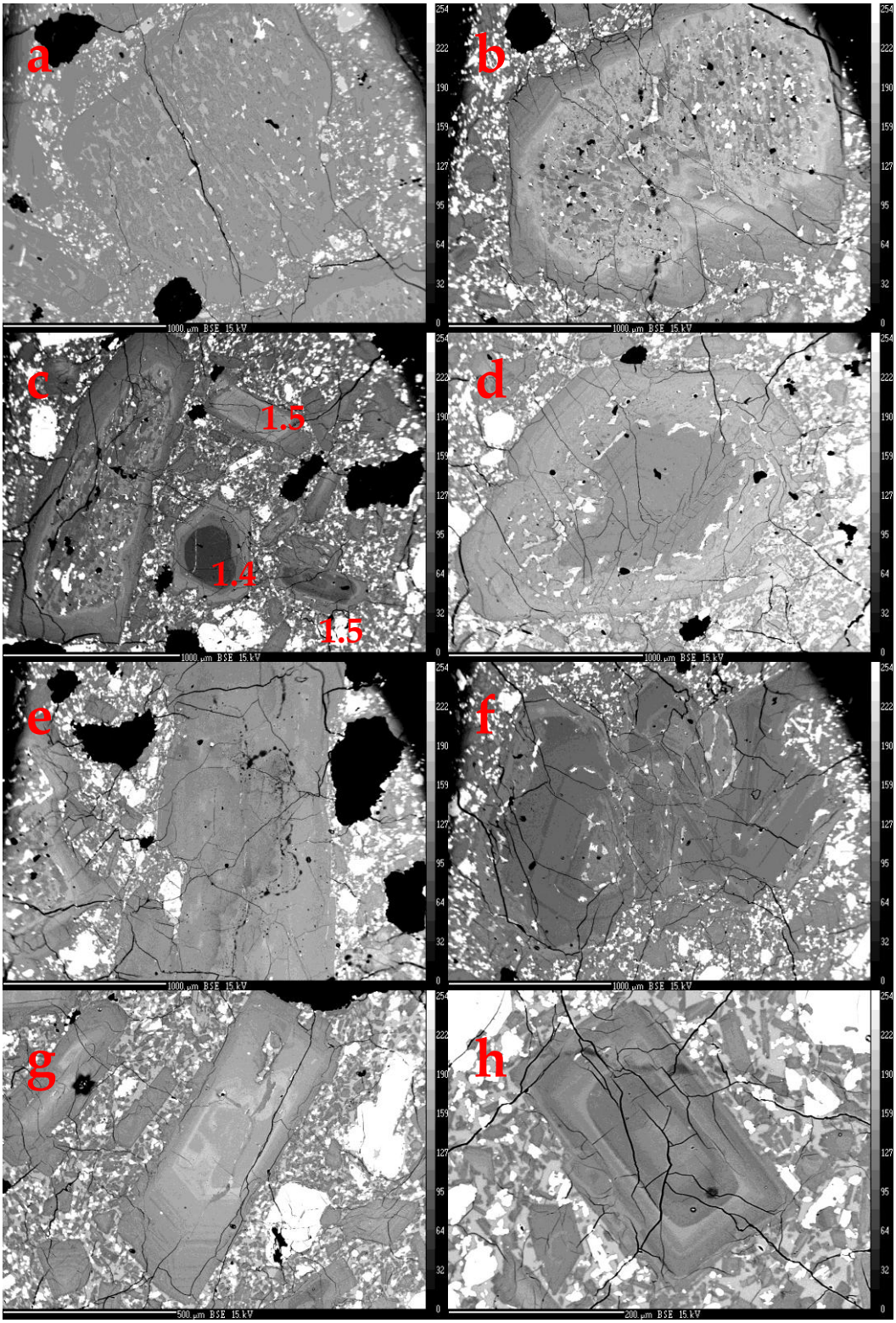

Figure 5.48 BSE image of M-type X lahar plagioclase a. 1 b. 1.2 c. 1.4, 1.5 and 1.6 d. 2 e. 3 f. 4 g. 8 h. 9

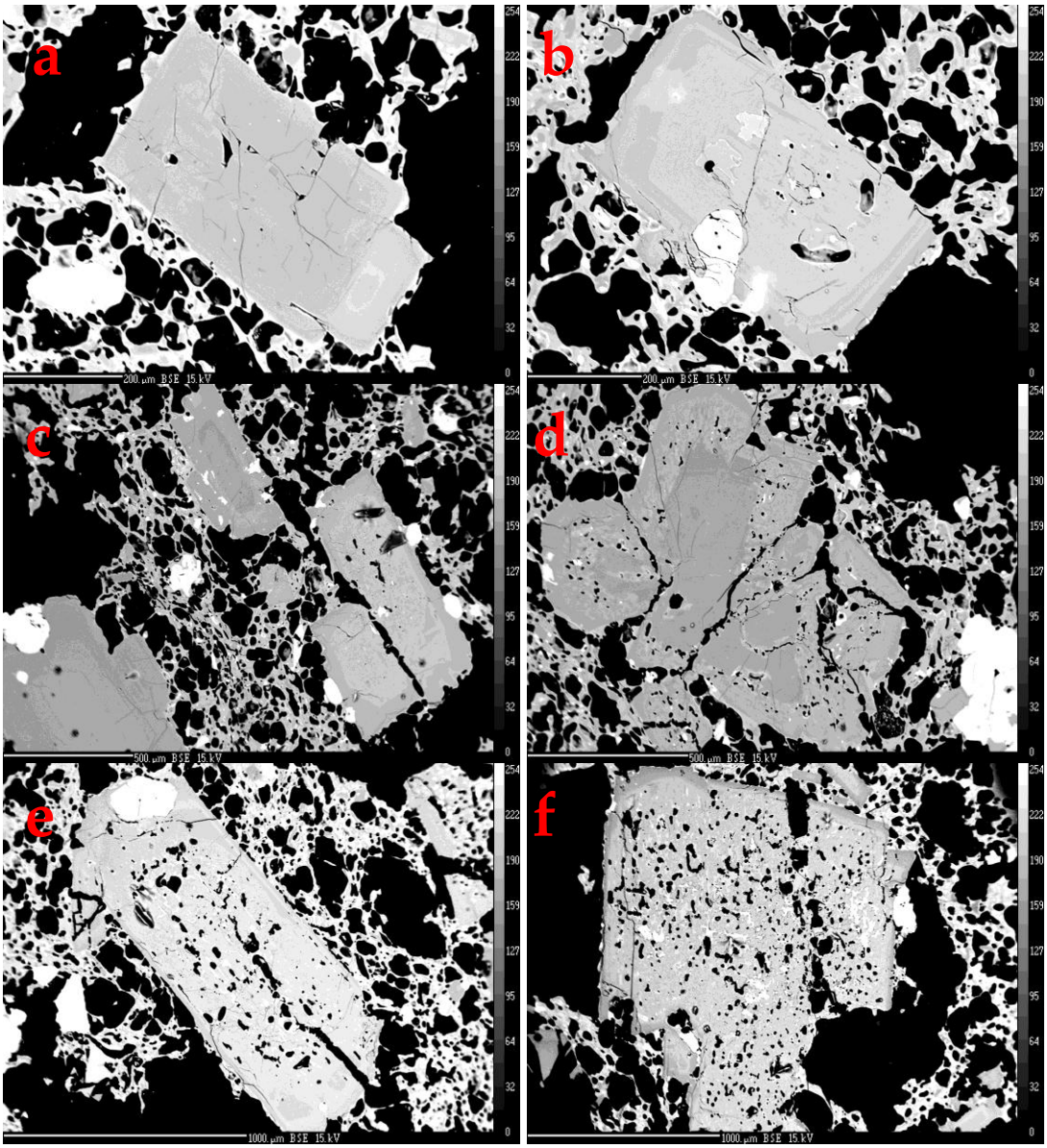

Figure 5.49 BSE images of Xb 32 scoria plagioclase. a. 1 b. 2 c. 4 d. 5 e. 6 f. 7.

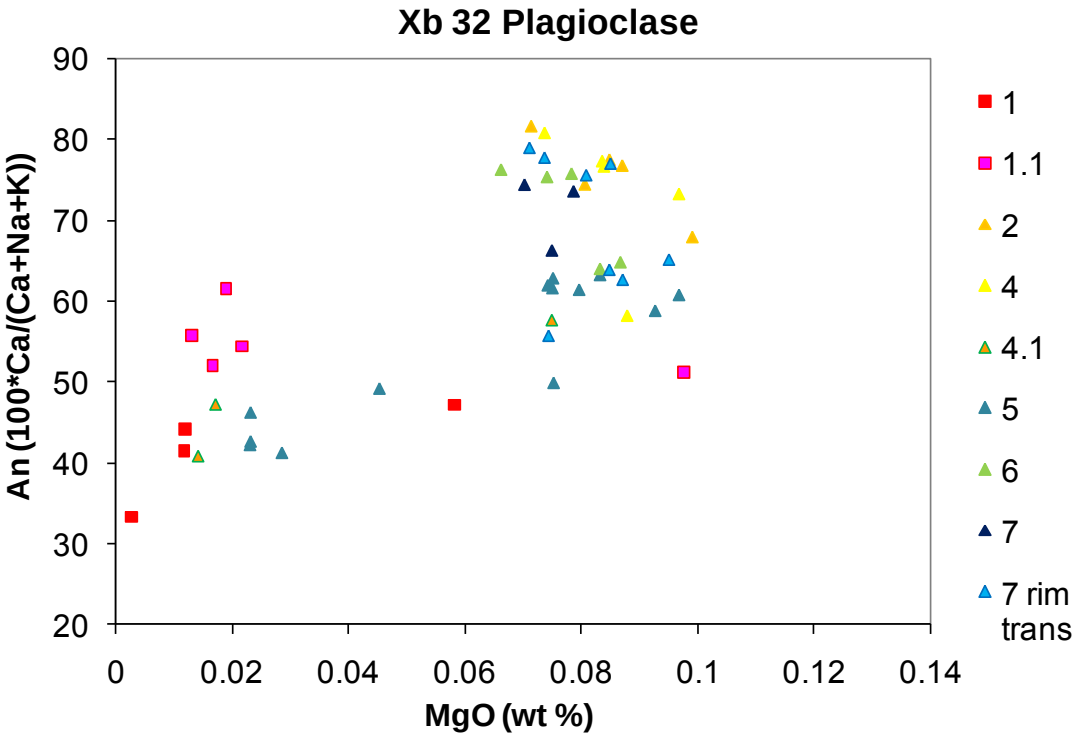

Figure 5.50 An content vs. MgO of Xb scoria 32 plagioclase.

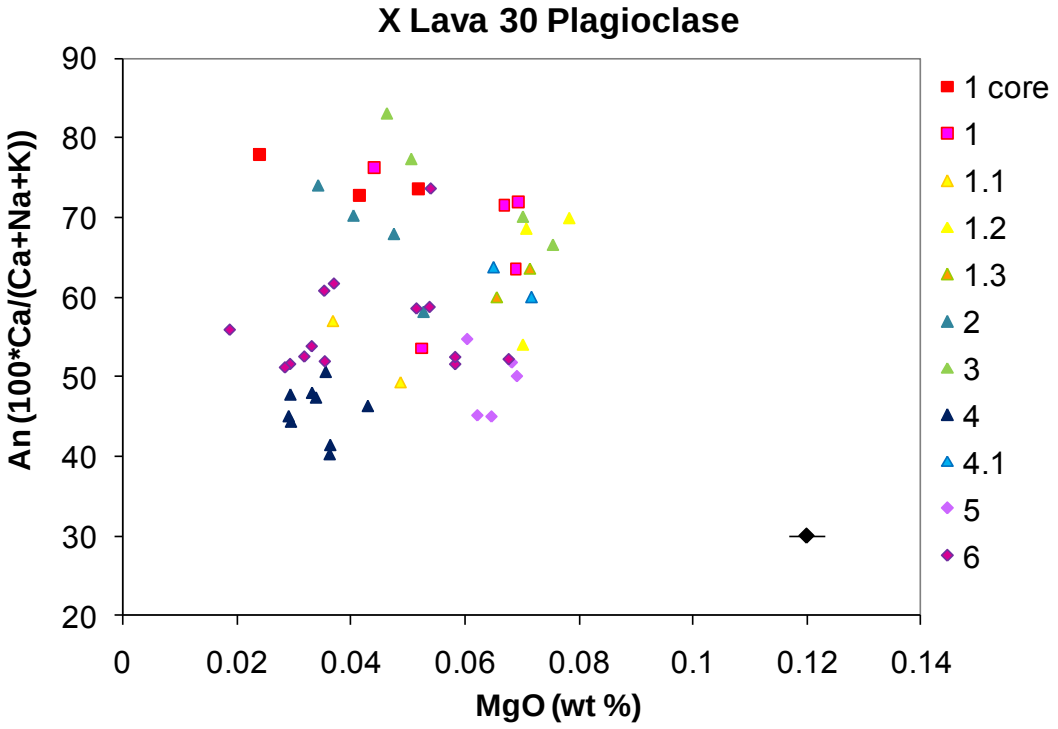

Figure 5.51 An content vs. MgO of X Lava 30 plagioclase. Representative 1 s error for MgO shown in bottom right corner.

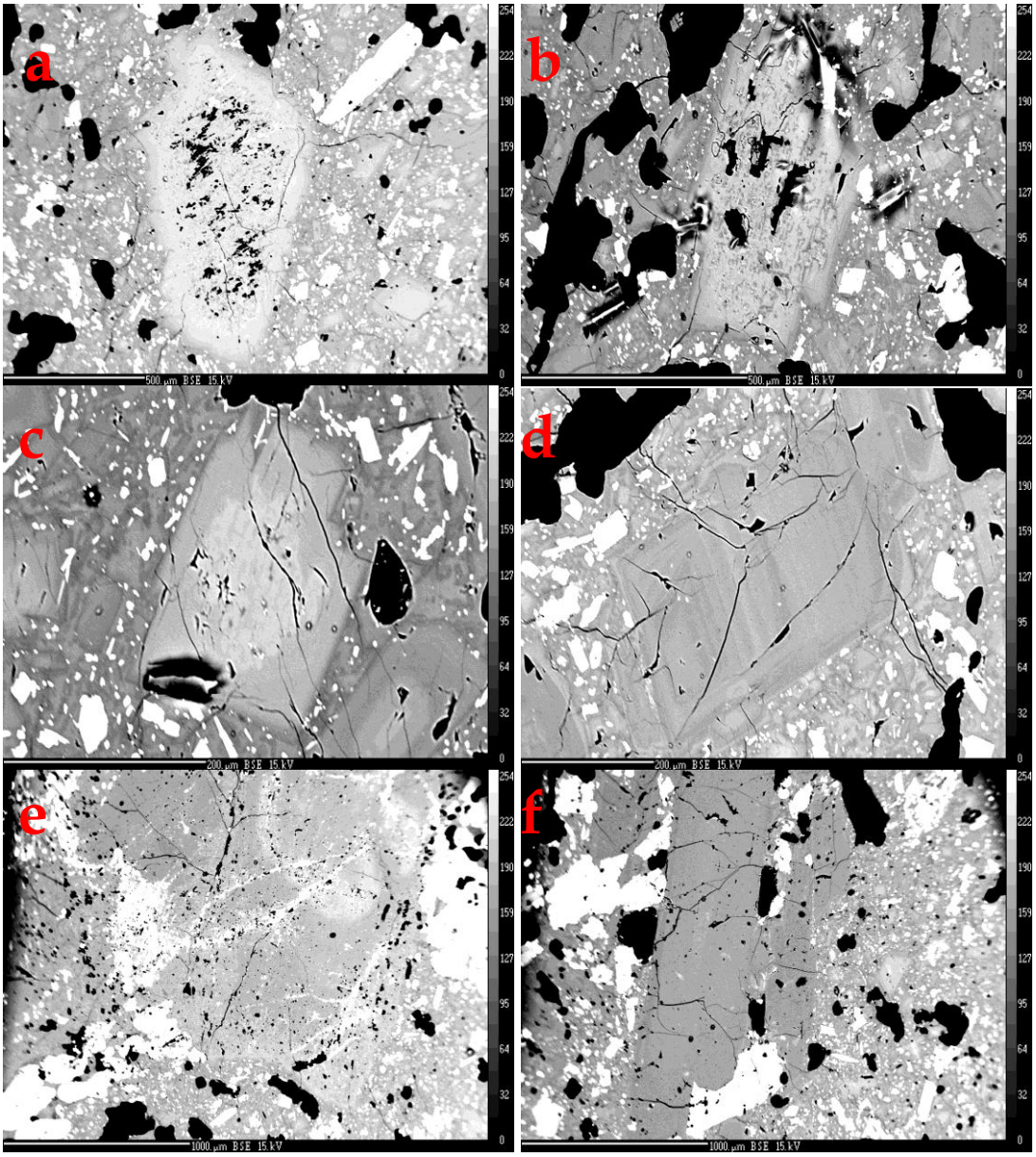

Figure 5.52 BSE images of X Lava 30 plagioclase a. 1 b. 2 c. 3 d. 4 e. 5 and f. 6.

There does not appear to be significant plagioclase variation in the Worm Complex lava. Most An contents measured hover between An_{43-68} with the cores in a more restricted range. Most compositions lie below (lower An content with increasing MgO) the QMI 19 microphenocryst trend, as do those of the Breadcrust Pyroclastic Flow 03. The pyroclastic flow (Figure 5.54) has

an even narrower range in terms of MgO, but a broader range in An content. The highest An contents (> An_{65}) in the pyroclastic flow are from population L (crystal 10) and from the patchy cores of large (1-2 mm) agglutinated, oscillatory zoned grains with 1-2 sieve zones (crystals 12, 14, and 15). Microphenocrysts from the pyroclastic flow have limited range in MgO (0.058-0.084 wt %) and An_{22-51}.

Plagioclase cores of early summit dome samples (late Kalama SDO) follow the same increasing An path as the Wn tephra sample in which An content increases more rapidly than MgO (Figure 5.55). The early and late (SDY) summit dome crystals overlap on An vs. MgO, but SDY is about 5% lower on average at An_{36-71}, whereas SDO's range is An_{41-76}. SDY plagioclase compositions also overlap with the sodic cores of Xb tephra grains (*i.e.* plagioclase 1, 1.1, and 4.1). Generally core and rim compositions of SDO and SDY are separated by a void on an An vs. MgO diagram, with cores being higher An and slightly lower MgO. Even though early Kalama dacite plagioclase, like the bulk rock compositions, tend to have a more restricted range than those in the late Kalama, SDY plagioclase falls within the same range as EKPF.

Eight plagioclase grains from three samples, SDY 13, Worm Complex lava 8A, and plutonic inclusion 8B hosted by that lava, were analyzed for trace elements using LA-ICP-MS (Table B.2). There is little variation between trace element patterns, which have the same shape in the three samples (Figure 5.56). The plutonic inclusion 08B shows the most variation, particularly in the LREE. The Worm Complex lava 8A has the smallest variation of the four samples. Pb, Y and the LREE have the widest range in values between samples. When normalized to primitive mantle values (Sun & McDonough, 1989) the SDY 13 plagioclase contained higher concentrations of

LREE than those of the Worm Complex lava, and overlaps the range of plutonic inclusion abundances.

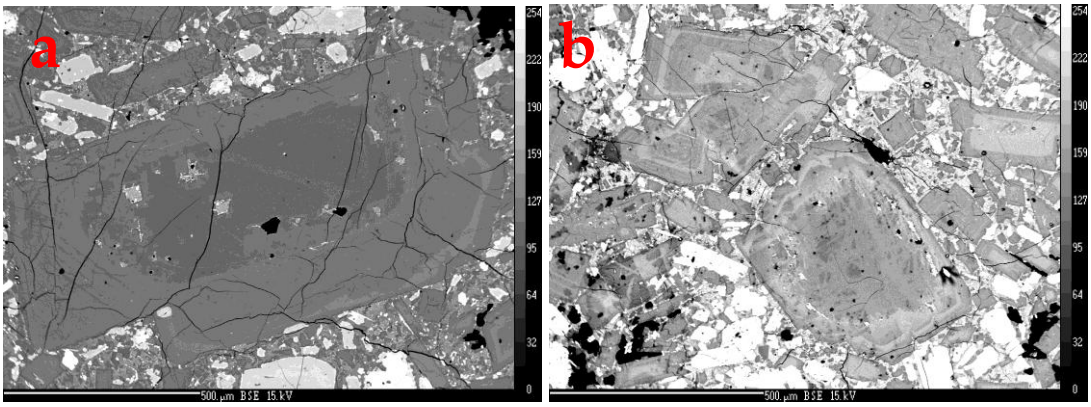

Figure 5.53 BSE images of MKLV-TF 10 plagioclase a. 12 and b. 14 and 15.

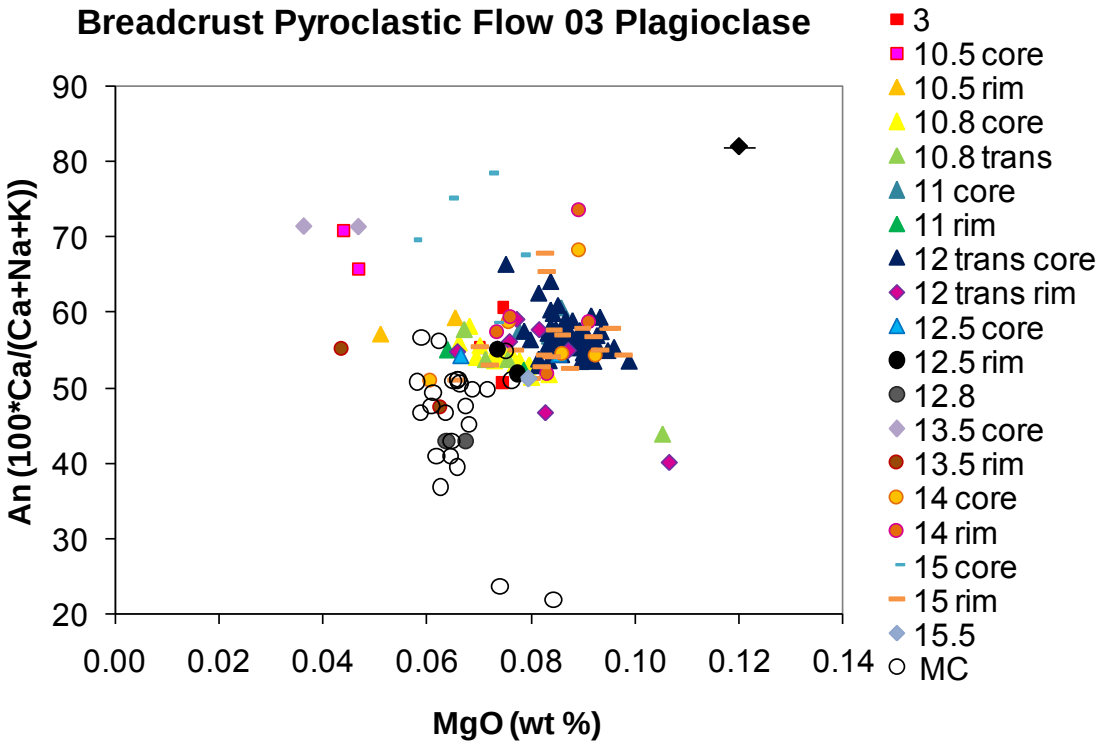

Figure 5.54 An content vs. MgO of Breadcrust Pyroclastic Flow (MKPF) 03 plagioclase. Representative 1 s error for MgO shown in top right corner.

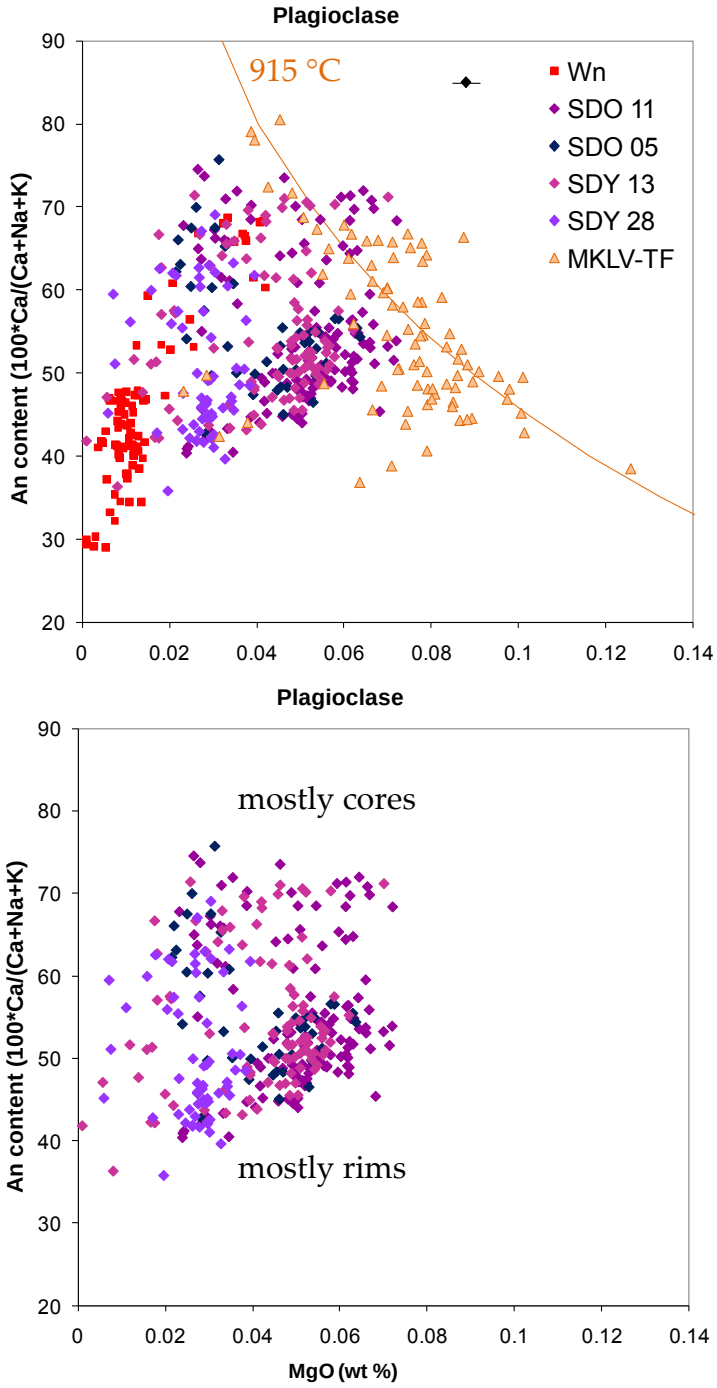

Figure 5.55 MgO vs. An content of SDO and SDY plagioclase compared to Wn and Two Finger Flow plagioclase. The line through the Two Finger Flow data represents experimentally derived adiabatic partioning concentration of MgO based on An content for beginning whole rock MgO measured for the flow. The temperature was adjusted to visually fit the data. The top group of SDO and SDY points are mostly from cores and the bottom group are mostly rims. Representative 1 s error for MgO shown in top right corner.

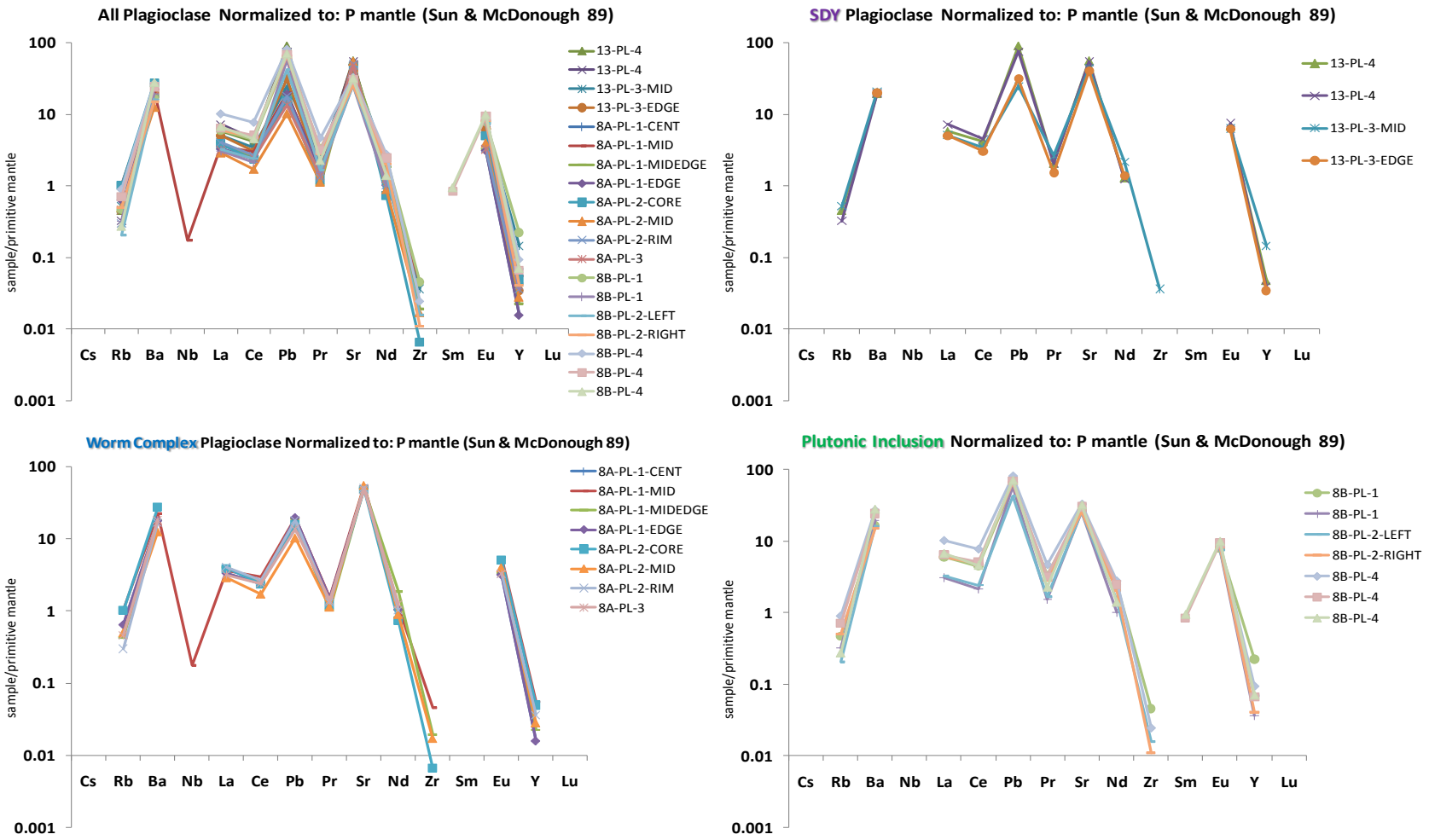

Figure 5.56 Spider diagrams of plagioclase from Worm Complex lava 08A, a plutonic inclusion 08B hosted by that lava and SDY normalized to primitive mantle values from Sun & McDonough (1989). Analyzed by LA-ICP-MS.

5.4.2 Pyroxene

Pyroxene crystals were measured in four samples (Worm Complex lava 08A, plutonic inclusion in that lava 08B, SDY 13, and plutonic inclusion in EKPF 23) for major and minor elements by EMPA (Tables 5.2, 5.3, C.1 and C.2 and Figure 5.57). Orthopyroxenes are categorized as enstatite (Morimoto, 1989), where compositions ranged between $Wo_2En_{56}Fs_{54}$ – $Wo_6En_{60}Fs_{40}$ and Mg#s 55-76. All clinopyroxenes plot as augite (Morimoto, 1989) with $Wo_{37}En_{46}Fs_{54}$-$Wo_{43}En_{43}Fs_{57}$, and Mg#s 64-82. Transects of four crystals from two samples were analyzed to determine compositional variations within single grains. Transects show normal compositional zoning, rim overgrowths, oscillatory zoning, and reverse zoning (Figure 5.58)

LA-ICP-MS was conducted on 17 pyroxene grains from the same three samples as plagioclase (SDY 13, Worm Complex lava 8A, and plutonic inclusion 8B hosted by that lava). The results are listed in Table C.3 and Figure 5.59. Clinopyroxene trace element patterns are similar for each sample and have between <1-2 orders of magnitude variation. MREE are slightly enriched compared to LREE and HREE. Nearly all clinopyroxene display a small, negative Eu anomaly. A unique clinopyroxene grain, CPX 5 from a middle Kalama Worm Complex lava, has lower concentrations in all REE and does not display a negative Eu anomaly like other clinopyroxenes. Higher degrees of variation exist in orthopyroxene trace element patterns, especially in the LREE, Rb and Ba. Orthopyroxene patterns are characterized by depletion in LREE and LILE compared to MREE and HREE in the two lavas analyzed, but the plutonic inclusion concentrations were higher in LILE, HFSE, and LREE. Orthopyroxenes also have an Yb enrichment relative to both primitive mantle and other REE, whereas clinopyroxenes have a

depletion relative other REE, but still enriched with respect to primitive mantle.

Pyroxene grains with high Cr_2O_3 (> 0.1 wt %) may have crystallized from basaltic magma (Carroll, 2009). Two large clinopyroxene crystals from Worm Complex lava 08A appear to contain zones in their cores that meet these criteria (Figures 5.60 and 5.61). Pyroxene 5 is part of a glomerocryst with other pyroxene and plagioclase. The sharp change in composition between zones could indicate it is antecrystic material that grew in a more mafic magma. Conversely, trace element patterns are nearly identical for LA-ICP-MS spots from the core and mantle of the crystal (Figure 5.62), but abundances normalized to primitive mantle are lower for the core. Whereas the core has a slight positive Eu anomaly, the mantle displays a slight negative one. Sr is higher in the core of pyroxene 5. The trace element pattern for pyroxene 10, a spot taken on the mantle, closely reflects the pattern of the mantle of pyroxene 5. Pyroxene 10 has less dramatic compositional changes, but does feature a heavily resorbed core, which also probably grew in a hotter magma.

Table 5.2 Orthopyroxene EMP Spots and Transects. T = transects.

Sample	Mg#	Wo	En	Fs
8A Px 1	72.57	4.08	69.62	26.31
8A Px 1	72.43	4.29	69.32	26.39
8A Px 3	74.88	3.05	72.60	24.35
8A Px 3	75.10	2.99	72.85	24.16
8A Px 3	75.18	2.98	72.94	24.08
8A Px 3	74.01	3.14	71.69	25.17
8A Px 4	75.27	3.06	72.97	23.97
8A Px 4	74.81	2.94	72.61	24.45
8A Px 4	74.65	2.98	72.43	24.60
8A Px 4	74.45	3.05	72.18	24.77
8A Px 4.6 T	73.95	4.06	70.94	25.00
8A Px 4.6 T	75.47	3.02	73.19	23.79
8A Px 4.6 T	75.50	3.01	73.22	23.76
8A Px 4.6 T	73.81	2.84	71.72	25.44
8A Px 4.6 T	75.19	3.13	72.84	24.03
8A Px 4.6 T	75.49	2.94	73.27	23.79
8A Px 4.6 T	75.69	2.99	73.43	23.59
8A Px 4.6 T	75.96	3.00	73.68	23.32
8A Px 4.6 T	75.24	2.89	73.07	24.04
8A Px 4.6 T	74.89	2.94	72.69	24.37
8A Px 4.6 T	75.24	2.91	73.06	24.04
8A Px 4.6 T	68.84	3.15	66.67	30.18
8A Px 9	75.12	3.02	72.85	24.13
8A Px 9	75.16	2.93	72.96	24.12
8A Px 9	74.92	3.57	72.24	24.19
8A Px 9.5	74.31	2.96	72.11	24.93
8A Px 9.5	74.54	2.94	72.35	24.71
8A Px 9.5	73.51	3.23	71.13	25.63

Sample	Mg#	Wo	En	Fs
13 Px 12	71.03	2.99	68.91	28.10
13 Px 12	71.84	3.02	69.67	27.31
13 Px 12	71.38	2.90	69.31	27.79
13 Px 12	73.06	2.79	71.02	26.19
13 Px 15	71.30	2.52	69.51	27.97
13 Px 15	68.98	2.26	67.42	30.32
13 Px 15	67.89	5.89	63.89	30.22
13 Px 15	70.28	2.59	68.46	28.95
13 Px 16 T	71.68	3.03	69.51	27.46
13 Px 16 T	72.17	3.20	69.86	26.94
13 Px 16 T	71.53	2.97	69.40	27.62
13 Px 16 T	71.43	2.94	69.33	27.73
13 Px 16 T	71.54	2.97	69.42	27.61
13 Px 16 T	71.36	3.05	69.18	27.76
13 Px 16 T	71.48	2.88	69.42	27.70
13 Px 16 T	70.33	2.78	68.38	28.84
13 Px 16 T	68.77	3.00	66.71	30.29
13 Px 16 T	68.38	2.60	66.60	30.80
13 Px 16 T	67.32	2.44	65.67	31.89
13 Px 16 T	67.30	2.39	65.69	31.92
13 Px 16 T	66.27	2.24	64.79	32.97
13 Px 17	69.80	2.60	67.99	29.42
13 Px 17	68.36	2.67	66.53	30.80
13 Px 17	64.32	6.16	60.35	33.48

Sample	Mg#	Wo	En	Fs
23 Px 1	57.87	2.10	56.65	41.25
23 Px 1	57.01	2.14	55.79	42.07
23 Px 2	57.25	2.25	55.96	41.79
23 Px 2	56.89	2.02	55.74	42.23
23 Px 2	54.95	2.28	53.70	44.02
23 Px 4	57.28	2.10	56.08	41.82
23 Px 4	57.25	2.02	56.09	41.89
8B Px 6	55.92	2.00	54.80	43.20
8B Px 6	55.53	3.31	53.69	43.00
8B Px 6	57.91	2.02	56.74	41.24
8B Px 6	59.86	3.42	57.81	38.77
8B Px 4	60.67	3.02	58.84	38.15
8B Px 4	60.46	3.31	58.45	38.24
8B Px 4	59.74	3.46	57.68	38.87
8B Px 4	60.19	3.21	58.26	38.54
8B Px 4	58.43	2.99	56.69	40.32
8B Px 3.5	59.27	2.26	57.93	39.81
8B Px 3.5	57.38	1.98	56.24	41.78
8B Px 3.5	56.44	2.48	55.04	42.47
8B Px 3	56.87	1.99	55.73	42.28
8B Px 3	57.76	2.39	56.38	41.23
8B Px 3	59.12	2.85	57.43	39.72
8B Px 2	55.69	2.26	54.43	43.31
8B Px 2	56.07	2.00	54.95	43.05
8B Px 2	58.83	3.28	56.91	39.82
8B Px 2	60.31	3.41	58.25	38.34

Table 5.3 Clinopyroxene EMP Spots and Transect (of 08A Px 5).

Sample	Mg#	Wo	En	Fs
8A Px 2	76.02	39.29	46.15	14.56
8A Px 2	75.59	38.66	46.37	14.97
8A Px 2	76.10	38.94	46.47	14.59
8A Px 2	75.83	39.58	45.81	14.60
8A Px 4.5	76.22	39.29	46.27	14.43
8A Px 4.5	76.69	38.24	47.36	14.40
8A Px 4.5	75.83	39.06	46.21	14.73
8A Px 5	81.70	42.80	46.73	10.47
8A Px 5	81.44	42.71	46.66	10.63
8A Px 5	81.30	42.78	46.52	10.70
8A Px 5	81.38	42.74	46.60	10.66
8A Px 5	81.53	42.96	46.51	10.54
8A Px 5	76.26	43.37	43.18	13.44
8A Px 5	78.54	42.35	45.27	12.37
8A Px 5	80.91	42.58	46.46	10.96
8A Px 5	81.42	42.60	46.74	10.66
8A Px 5	81.49	42.63	46.75	10.62
8A Px 5	81.75	42.84	46.73	10.43
8A Px 5	80.48	42.40	46.36	11.25
8A Px 5	79.51	42.58	45.65	11.77
8A Px 5	79.69	42.22	46.05	11.73
8A Px 5	78.60	41.94	45.64	12.43
8A Px 5	76.68	38.96	46.81	14.24
8A Px 5	76.50	38.04	47.40	14.56
8A Px 5	75.28	38.48	46.31	15.21
8A Px 5	74.77	38.31	46.12	15.57
8A Px 5	74.66	38.06	46.24	15.69

Sample	Mg#	Wo	En	Fs
8A Px 5	74.42	37.35	46.62	16.02
8A Px 5	74.98	37.61	46.78	15.61
8A Px 5	75.48	37.46	47.21	15.33
8A Px 5	75.17	38.20	46.45	15.35
8A Px 5	74.29	37.75	46.25	16.01
8A Px 5	73.70	37.10	46.35	16.54
8A Px 5	74.20	36.94	46.79	16.27
8A Px 5	76.09	38.18	47.04	14.78
8A Px 5	76.73	38.89	46.89	14.22
8A Px 5	75.77	38.14	46.87	14.99
8A Px 5	75.74	38.22	46.79	14.99
8A Px 5	75.02	37.27	47.06	15.67
8A Px 5	75.48	38.79	46.20	15.01
8A Px 6	73.05	36.61	46.31	17.09
8A Px 6	76.82	36.84	48.52	14.64
8A Px 6	75.34	38.12	46.62	15.26
8A Px 6	76.89	38.37	47.38	14.24
8A Px 7	75.94	38.39	46.79	14.83
8A Px 7	77.41	38.70	47.45	13.85
8A Px 7	75.21	38.59	46.19	15.23
8A Px 8	76.39	38.14	47.26	14.61
8A Px 10	74.13	37.35	46.44	16.21
8A Px 10	75.92	38.18	46.94	14.89
8A Px 10	75.60	37.99	46.88	15.13
8A Px 10	74.96	37.97	46.49	15.53
8A Px 10	74.86	37.88	46.51	15.62
8A Px 10	74.57	37.85	46.35	15.80

Sample	Mg#	Wo	En	Fs
8A Px 10	76.01	38.83	46.50	14.68
8A Px 10	75.15	38.98	45.86	15.16
8A Px 10	75.02	39.00	45.77	15.24
13 Px 13	73.64	39.91	44.25	15.84
13 Px 13	71.20	38.03	44.12	17.84
13 Px 14	74.28	39.67	44.81	15.52
13 Px 14	74.88	40.47	44.58	14.95
13 Px 14	74.80	40.09	44.82	15.10
13 Px 1	75.46	40.28	45.07	14.66
13 Px 1	74.51	39.26	45.26	15.48
13 Px 1	74.61	38.86	45.61	15.52
13 Px 1	74.62	39.95	44.81	15.24
8B Px 5	66.22	37.50	41.39	21.11
8B Px 5	66.39	37.99	41.17	20.84
8B Px 5	63.94	39.49	38.69	21.82
8B Px 4.5	67.04	39.59	40.50	19.91
8B Px 4.5	66.79	39.56	40.37	20.08
8B Px 4.5	65.48	38.72	40.12	21.16
8B Px 4.5	66.11	37.99	41.00	21.01
8B Px 3.6	66.15	38.99	40.36	20.65

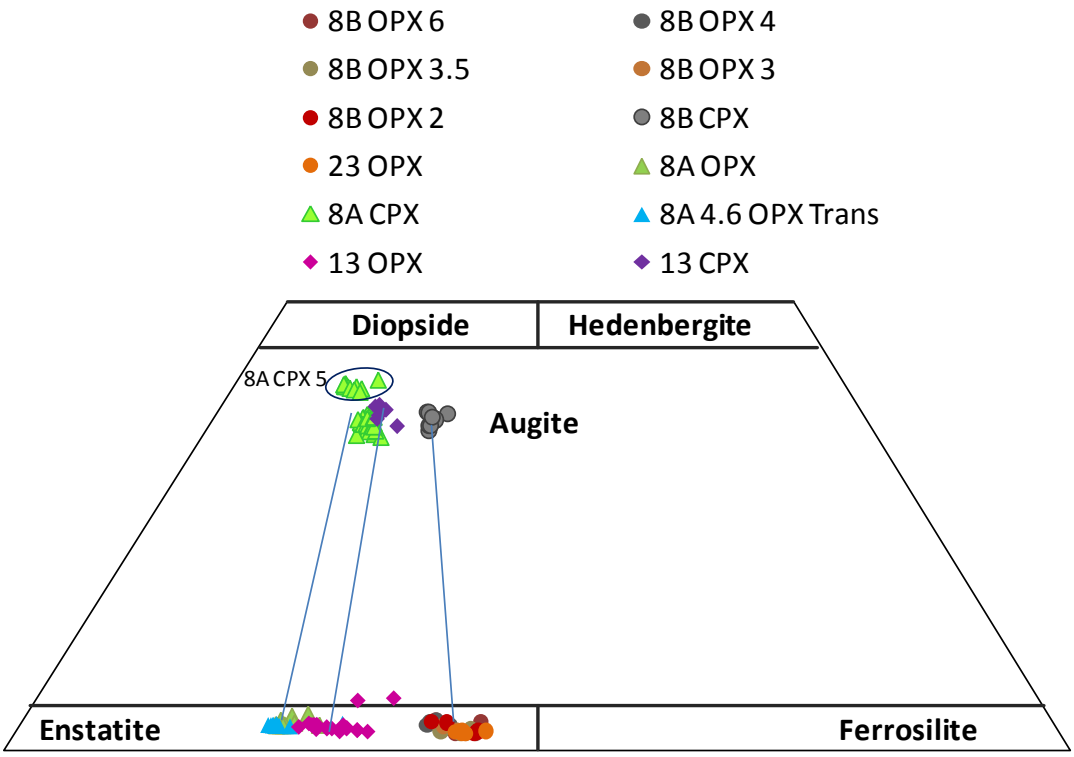

Figure 5.57 Pyroxene classification after Morimoto (1989). MKLV Worm Complex lava 08A, plutonic inclusion 08B in that lava, SDY 13, and an olivine-bearing plutonic inclusion hosted by EKPF 23. Tie lines connect orthopyroxene and clinopyroxene crystals from the same sample.

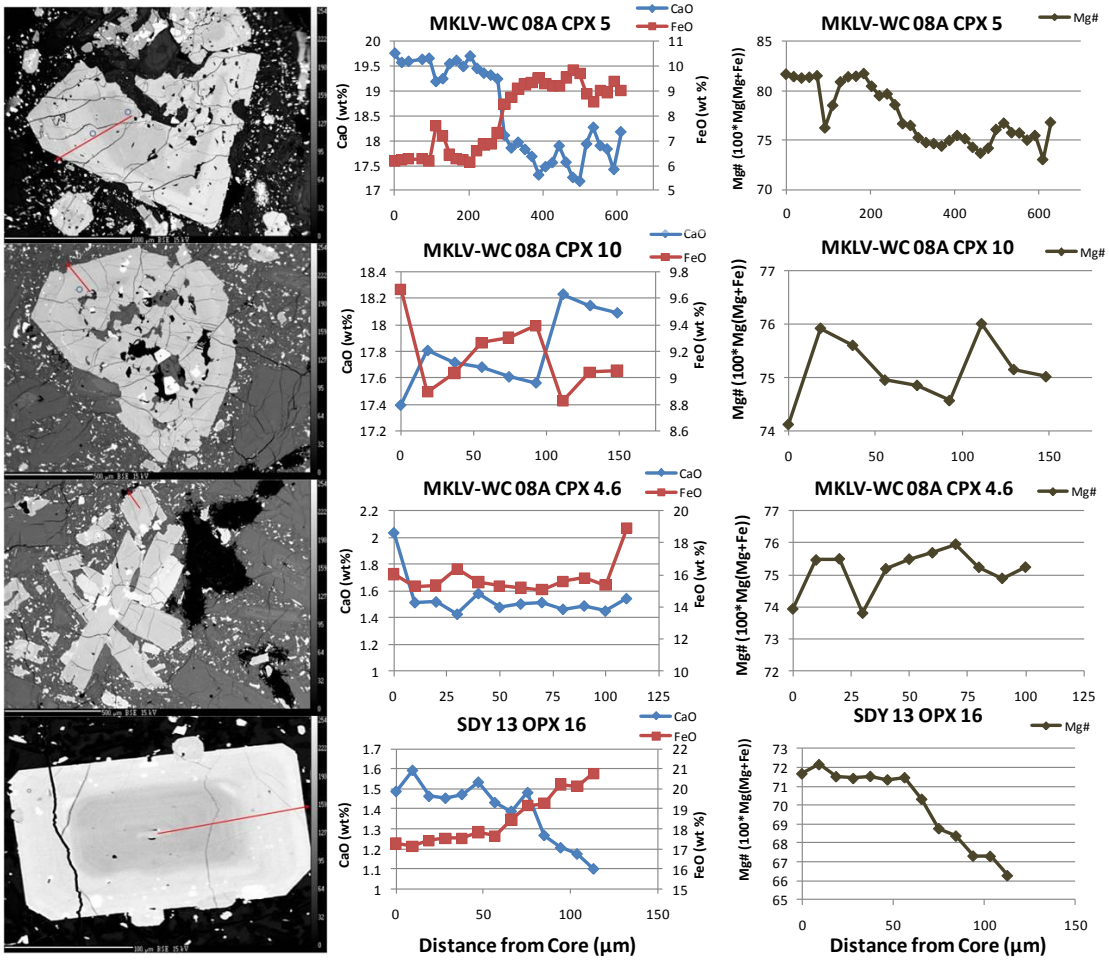

Figure 5.58 Transects of pyroxene crystals displaying various zoning patterns. The red line on BSE image indicates transect location. Note the variations in scale between diagrams.

Figure 5.59 Trace spider and REE spider diagrams for pyroxene in SDY 13, MKLV Worm Complex andesite 08A and its plutonic inclusion 08B. Clinopyroxene is generally enriched in trace elements while orthopyroxene is depleted. Analyzed by LA-ICP-MS.

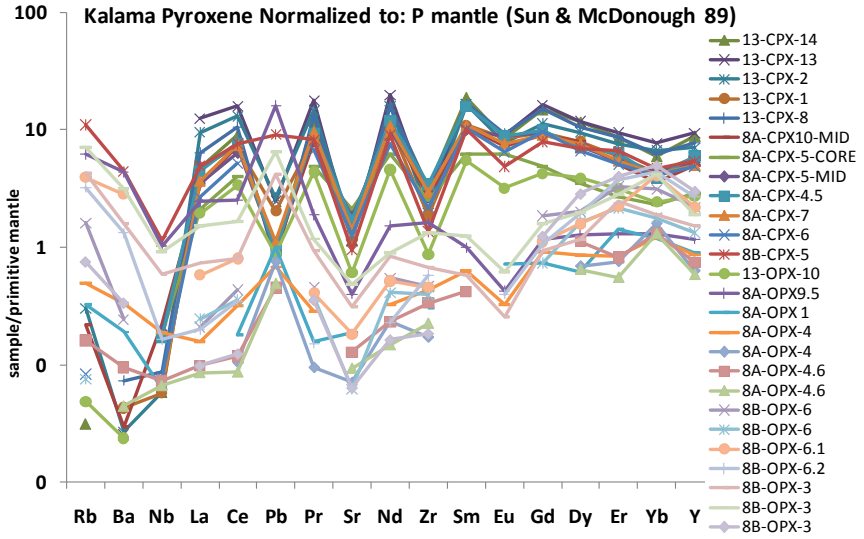
Kalama Pyroxene Normalized to: P mantle (Sun & McDonough 89)
sample/primitive mantle
100
10
1
0
Rb Ba Nb La Ce Pb Pr Sr Nd Zr Sm Eu Gd Dy Er Yb Y
13-CPX-14
13-CPX-13
13-CPX-2
13-CPX-1
13-CPX-8
8A-CPX10-MID
8A-CPX-5-CORE
8A-CPX-5-MID
8A-CPX-4.5
8A-CPX-7
8A-CPX-6
8B-CPX-5
13-OPX-10
8A-OPX9.5
8A-OPX 1
8A-OPX-4
8A-OPX-4
8A-OPX-4.6
8A-OPX-4.6
8B-OPX-6
8B-OPX-6
8B-OPX-6.1
8B-OPX-6.2
8B-OPX-3
8B-OPX-3
8B-OPX-3

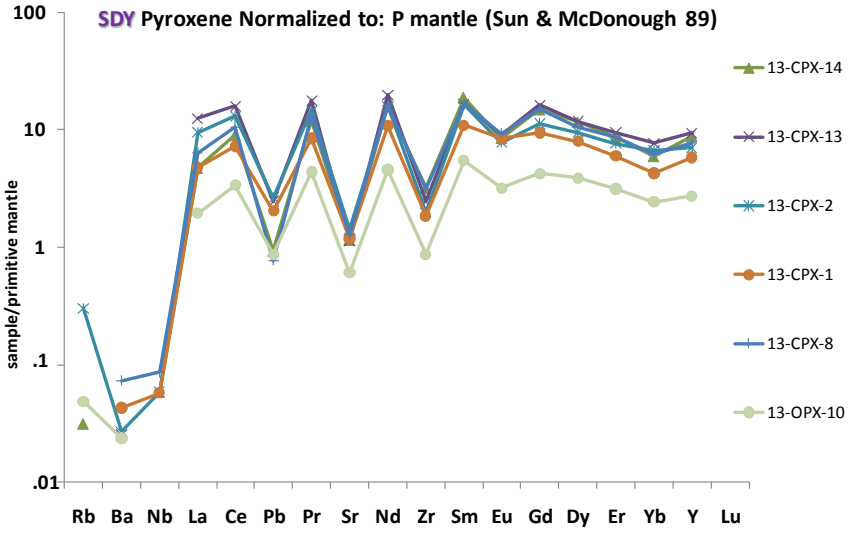
SDY Pyroxene Normalized to: P mantle (Sun & McDonough 89)
sample/primitive mantle
100
10
1
.1
.01
Rb Ba Nb La Ce Pb Pr Sr Nd Zr Sm Eu Gd Dy Er Yb Y Lu
13-CPX-14
13-CPX-13
13-CPX-2
13-CPX-1
13-CPX-8
13-OPX-10

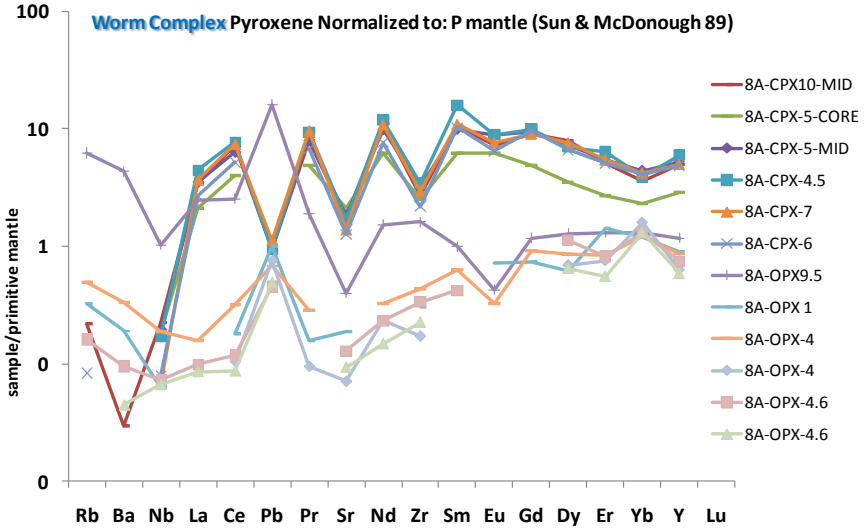
Worm Complex Pyroxene Normalized to: P mantle (Sun & McDonough 89)
sample/primitive mantle
100
10
1
0
Rb Ba Nb La Ce Pb Pr Sr Nd Zr Sm Eu Gd Dy Er Yb Y Lu
8A-CPX10-MID
8A-CPX-5-CORE
8A-CPX-5-MID
8A-CPX-4.5
8A-CPX-7
8A-CPX-6
8A-OPX9.5
8A-OPX 1
8A-OPX-4
8A-OPX-4
8A-OPX-4.6
8A-OPX-4.6

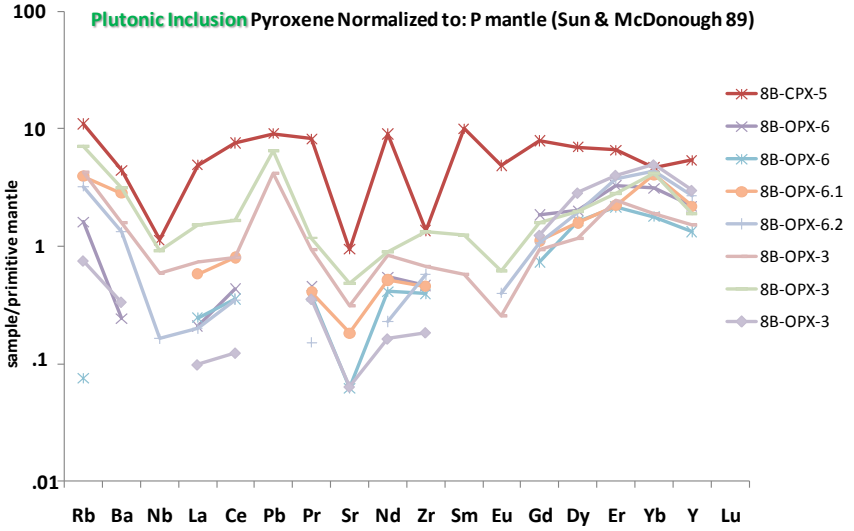
Plutonic Inclusion Pyroxene Normalized to: P mantle (Sun & McDonough 89)
sample/primitive mantle
100
10
1
.1
.01
Rb Ba Nb La Ce Pb Pr Sr Nd Zr Sm Eu Gd Dy Er Yb Y Lu
8B-CPX-5
8B-OPX-6
8B-OPX-6
8B-OPX-6.1
8B-OPX-6.2
8B-OPX-3
8B-OPX-3
8B-OPX-3

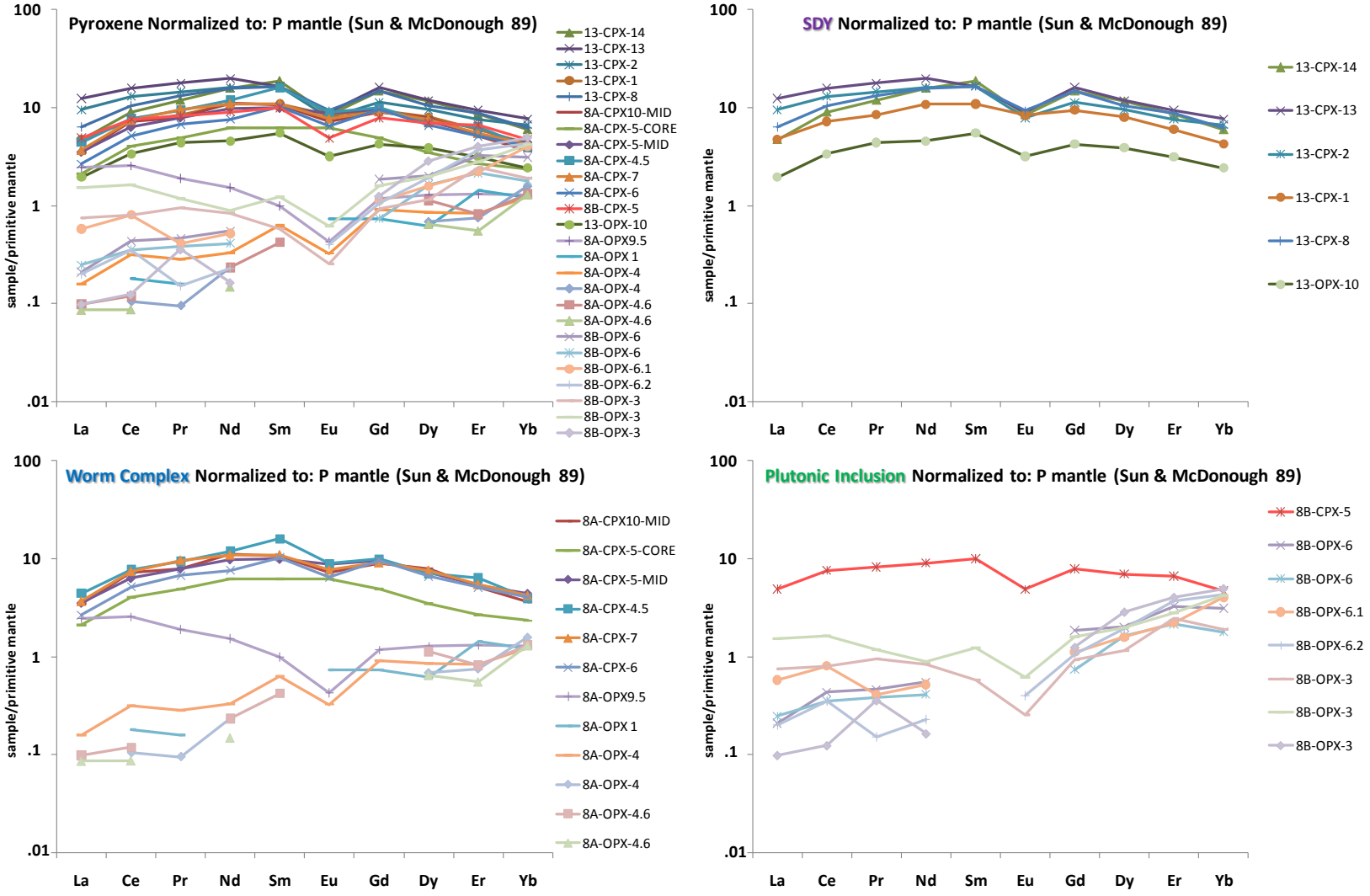

Figure 5.59 (Continued)

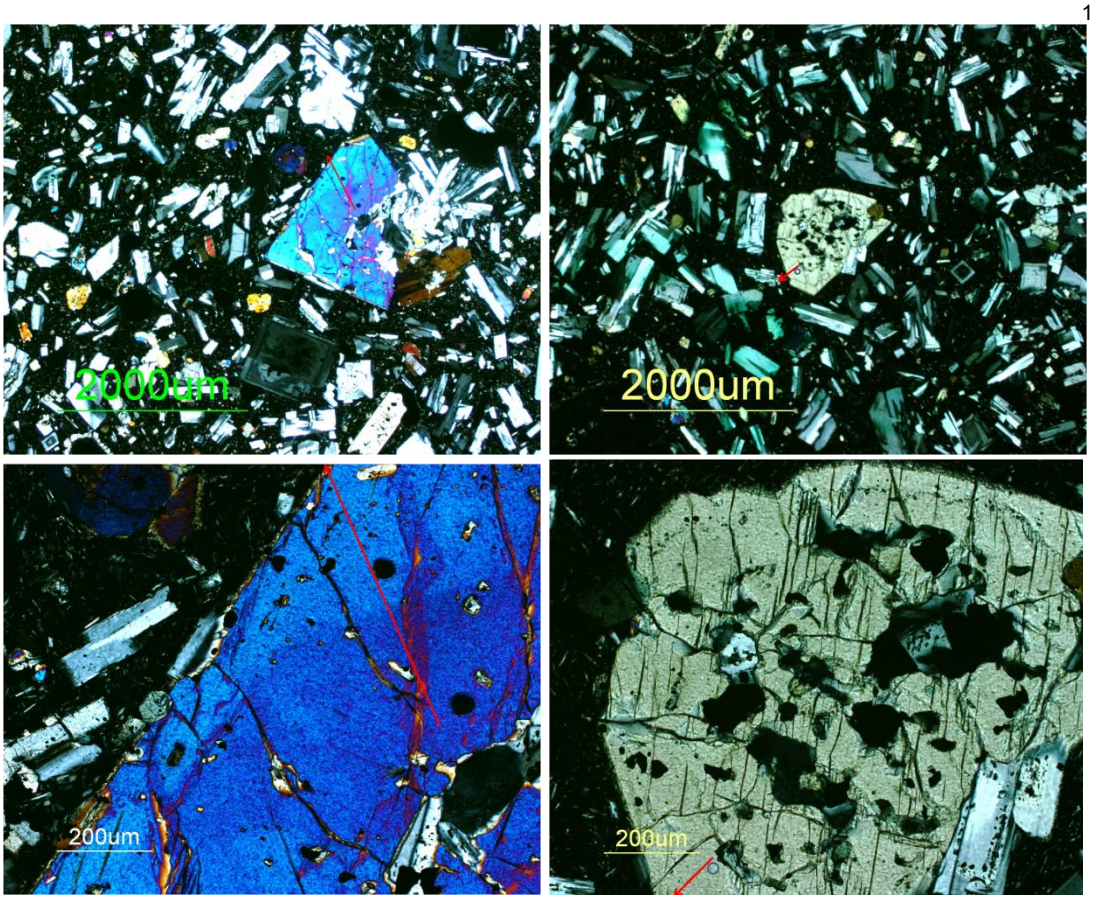

Figure 5.60 Photomicrographs of Worm Complex lava a. 8A cpx 5 and b. cpx 10. Red line represents core to rim transect. Black circles in a. and blue circle in b. represent laser spots.

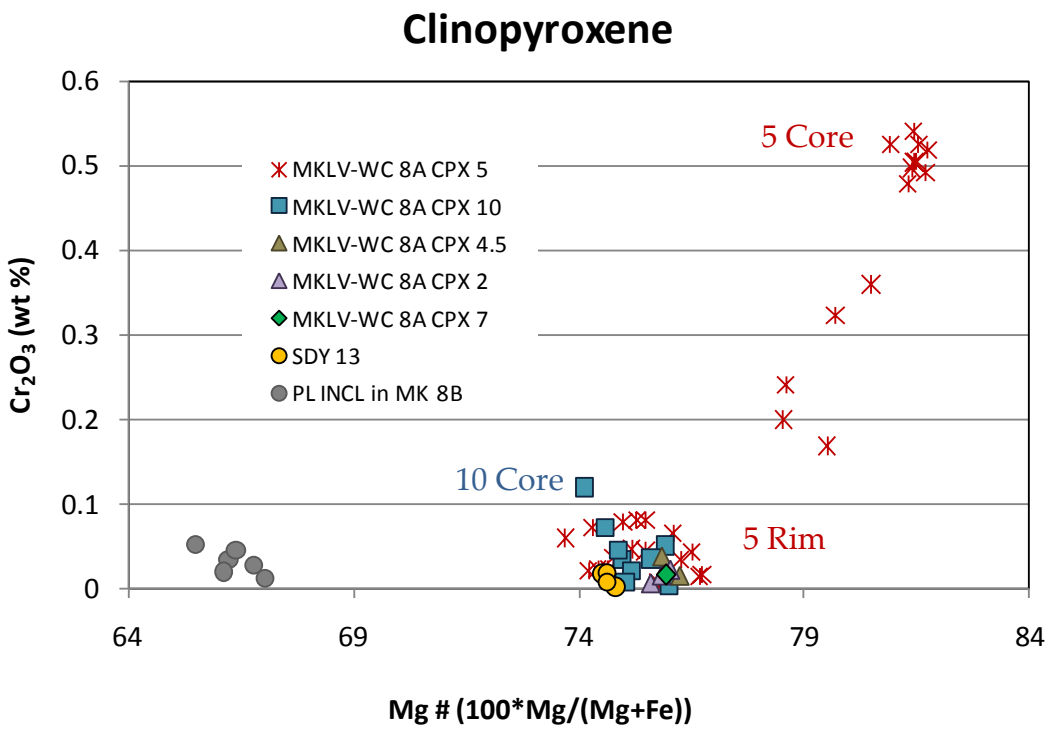

Figure 5.61 Clinopyroxene EMP data from Worm Complex lava 8A, plutonic inclusion in that lava 8B, and late Kalama SDY 13. Cores from two crystals from the Worm Complex lava appear to have grown in a basaltic magma, if using Cr_2O_3 > 0.1 wt % as an indicator.

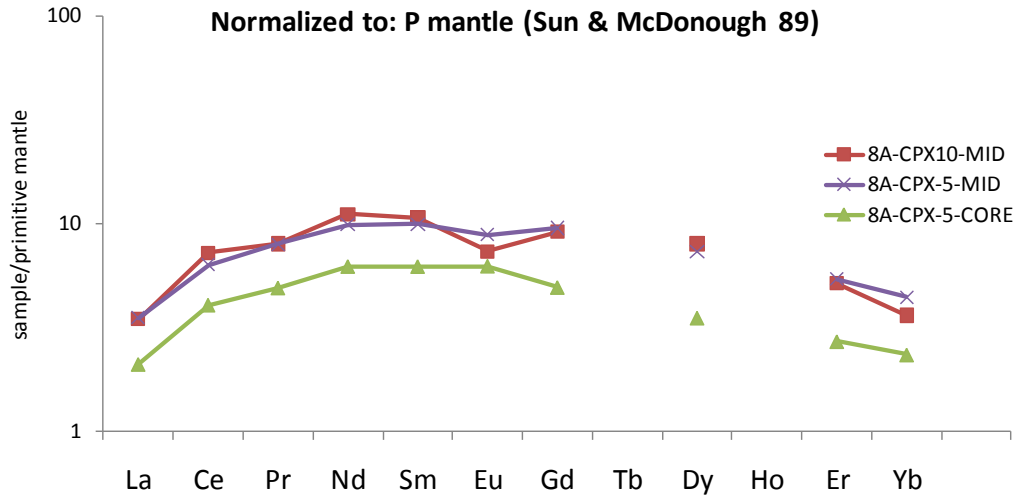

Figure 5.62 Spider diagram LA-ICP-MS spots of Work Complex lava 08A clinopyroxenes 5 and 10 which have cores that likely grew in a mafic magma, based on Cr_2O_3 > 0.1 wt %.. Values are normalized to primitive mantle values of Sun & McDonough (1989).

5.4.3 Olivine and Spinel

Olivine is a key phase in deciphering mixing relationships because forsterite only crystallizes from mafic magmas. Olivine core and rim spots and transects were measured in 9 samples and representative analyses are listed in Table D.1. Compositional range is Fo_{41-86} (100*Mg/(Fe+Mg)). The lowest Fo compositions come from gabbroic inclusions (Fo_{41-45}) in early Kalama pyroclastic flows and the highest from QMI 19 (Fo_{65-86}) (Figure 5.63). There are discrete differences between M-type and B-type X lahar olivines. Many M-type X lahar 01 olivines are nearly as Fo-rich (up to Fo_{84}) as those from QMI 19. B-type X lahar 02 (Fo_{67-84}) and 09 (Fo_{77-79}) compositions overlap each other and are less primitive than M-type olivines. Xb scoria olivines (Fo_{74-85}) generally overlap B-type lahar compositions, but one core analysis was as high as Fo_{85}. While several EMPA olivine transects showed no Fo content variation across the length of the crystal, others illustrate profiles with lower Fo compositions around the edges and may indicate either diffusion (Chakraborty, 1997; Costa & Dungan, 2005) or compositional zoning has occurred.

To assess the relative primitive nature of the magmas (Clynne, 1993; Clynne & Borg, 1997; Smith & Leeman, 2005), sixty olivine-spinel pairs were measured in 6 rocks (Table D.2 and Figure 5.64). Spinels trapped within olivine are compositionally heterogeneous and include a few ilmenite and titanomagnetite crystals. Spinel Cr# (100*Cr/(Cr+Al)) range is 22-62, and Mg# range is 6-48. Host olivines have a compositional range of Fo_{62-86}.

Olivine-hosted Cr spinel in olivine-bearing QMI population fall into two groups: one with lower Cr# and TiO_2, and higher Al_2O_3. There are 2 olivines that contain spinel from both groups. Chromian spinel crystallizes

early in a magma's history as a liquidus phase (Clynne, 1993; Luhr & Carmichael, 1985) and does not remain on the liquidus over a broad temperature range (Clynne & Borg, 1997 and references therein; Luhr & Carmichael, 1985). Although the host Fo contents generally overlap between the two groups, the higher Cr# group is slightly higher (Fo_{81-85} vs. Fo_{84-86}). Textural or other compositional differences are not discernable between the two groups, but core and rim compositions of the host olivine do vary (Figure 5.65).

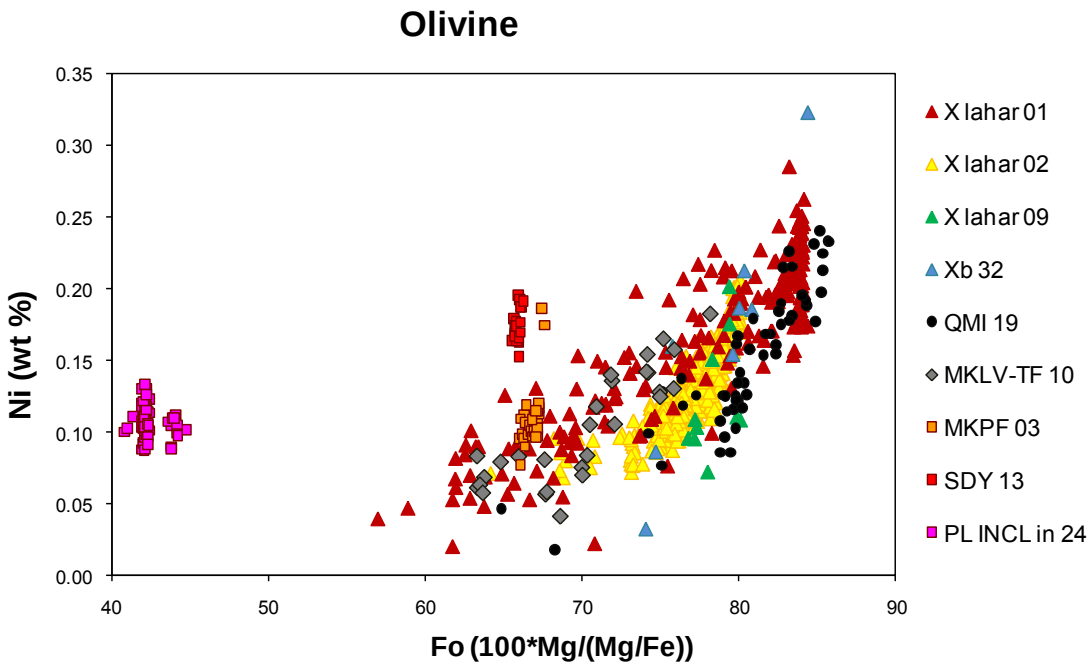

Figure 5.63 EMP spots and transects of olivine from various lithologies. Generalized vectors evidence for both magma mixing and fractional crystallization are from Straub *et al.* (2008).

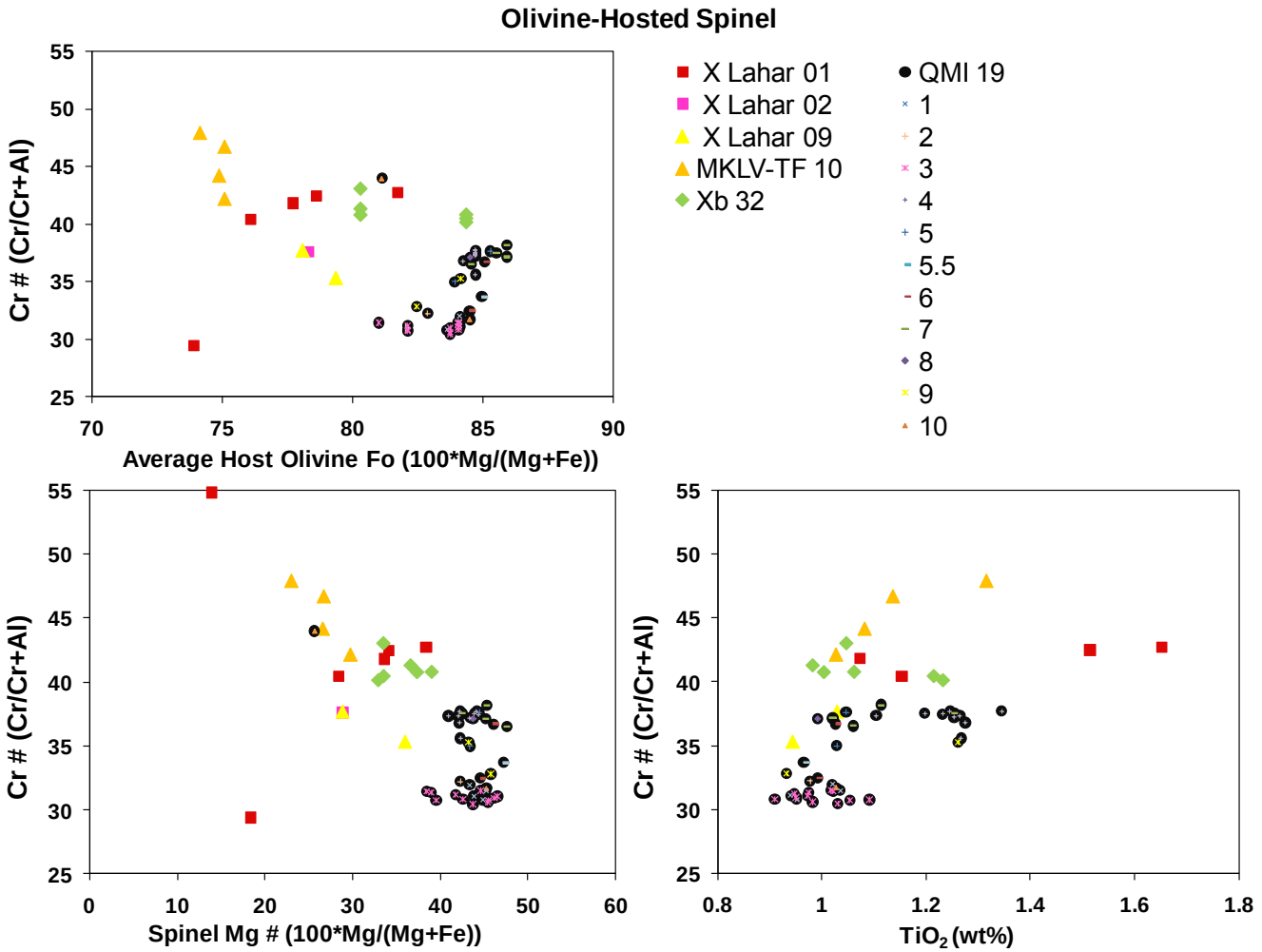

Figure 5.64 Olivine-hosted Cr spinel from QMI 19, X lahars, X tephra and the Two Finger flow. Spinel from individual olivine crystals are distinguished in QMI 19 by overlying symbols.

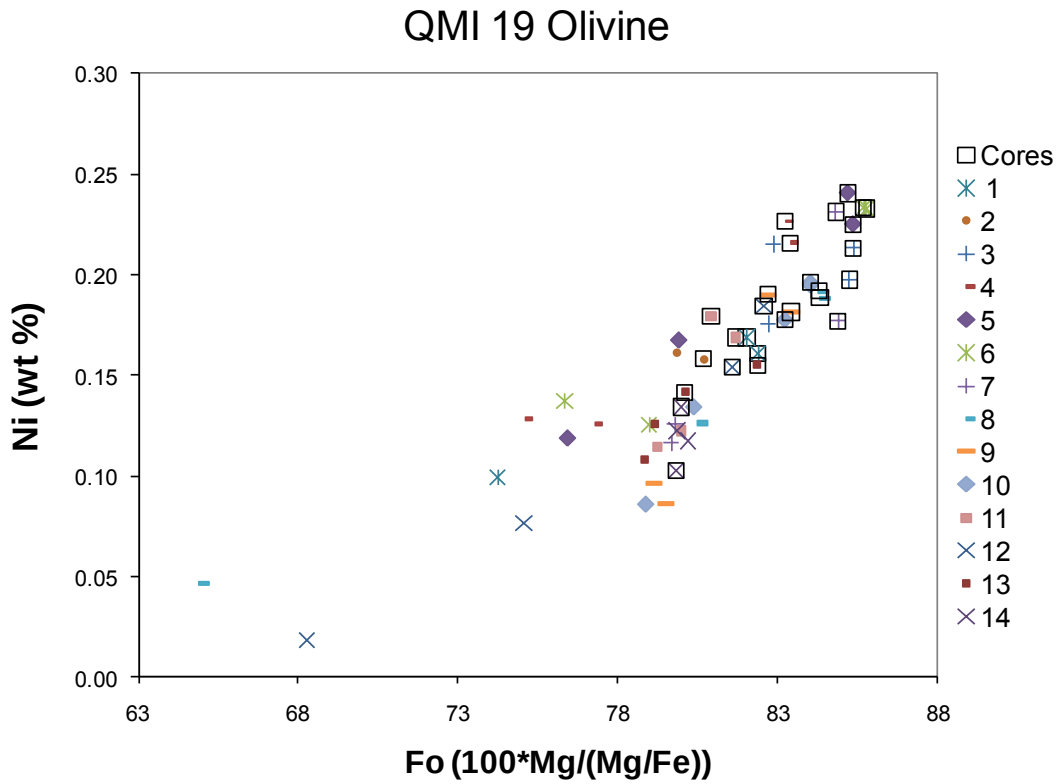

Figure 5.65 Detail of QMI 19 olivine Fo content vs. wt % Ni. Points encompassed by squares are olivine cores and all others are rim analyses. Crystals 1-3 as in Figure 5.15 a and b.

5.4.4 Groundmass Glass

EMPA was conducted on groundmass glass in 9 samples, which are summarized in Table D.3 and Figure 5.66. Representative Harker diagrams are presented in Figure 5.67. Analyses are listed in the Appendix. Of the groundmass glasses analyzed, X lahar 02 had the lowest SiO_2 content as well as the most variable range of 62.2 – 69.6 wt % SiO_2. QMI 19 had a particularly narrow range of 73.6-73.9 wt% SiO_2.

Table 5.4 Groundmass Glass EMPA of Representative Lithologies.

Sample	Lithology	Range SiO_2 wt%	Mean SiO_2 wt%	1 s	n=6
02	X Lahar	62.2-69.6	66.8	2.6	6
32	Xb	67.1-68.7	67.8	0.5	6
8A	MKLV-WC	71.8-73.0	72.8	0.6	5
19	QMI	73.6-73.9	73.7	0.1	5
31	Wn	74.8-75.5	75.2	0.4	5
13	SDY	75.5-77.7	76.7	0.8	5
11	SDO	75.0-77.9	76.9	0.8	25
14	EKPF	74.2-78.2	76.9	1.2	11
18	EKPF	76.7-77.2	76.9	0.3	3

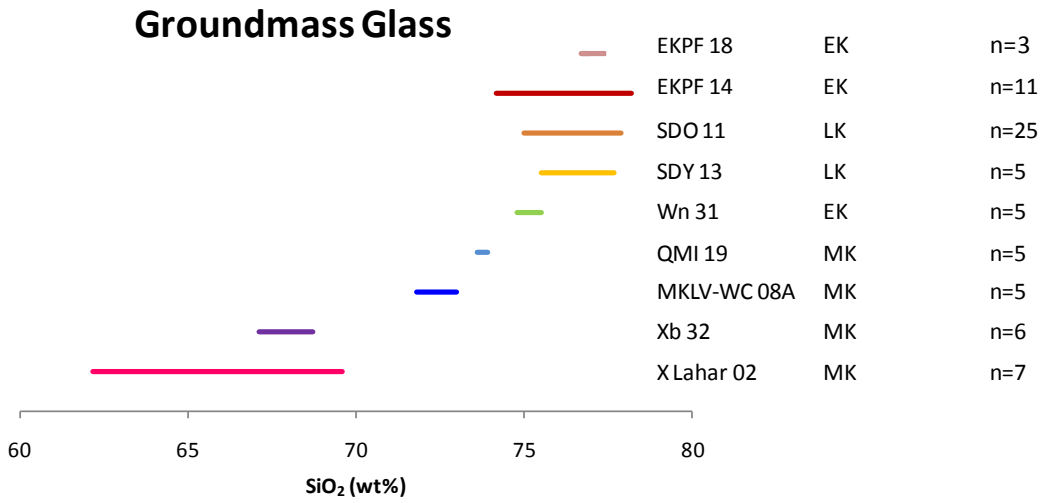

Figure 5.66 Groundmass glass range in SiO_2 (wt %). X Lahar 02 has the largest range and exhibits two types of groundmass in a single thin section (Figure 5.8.)

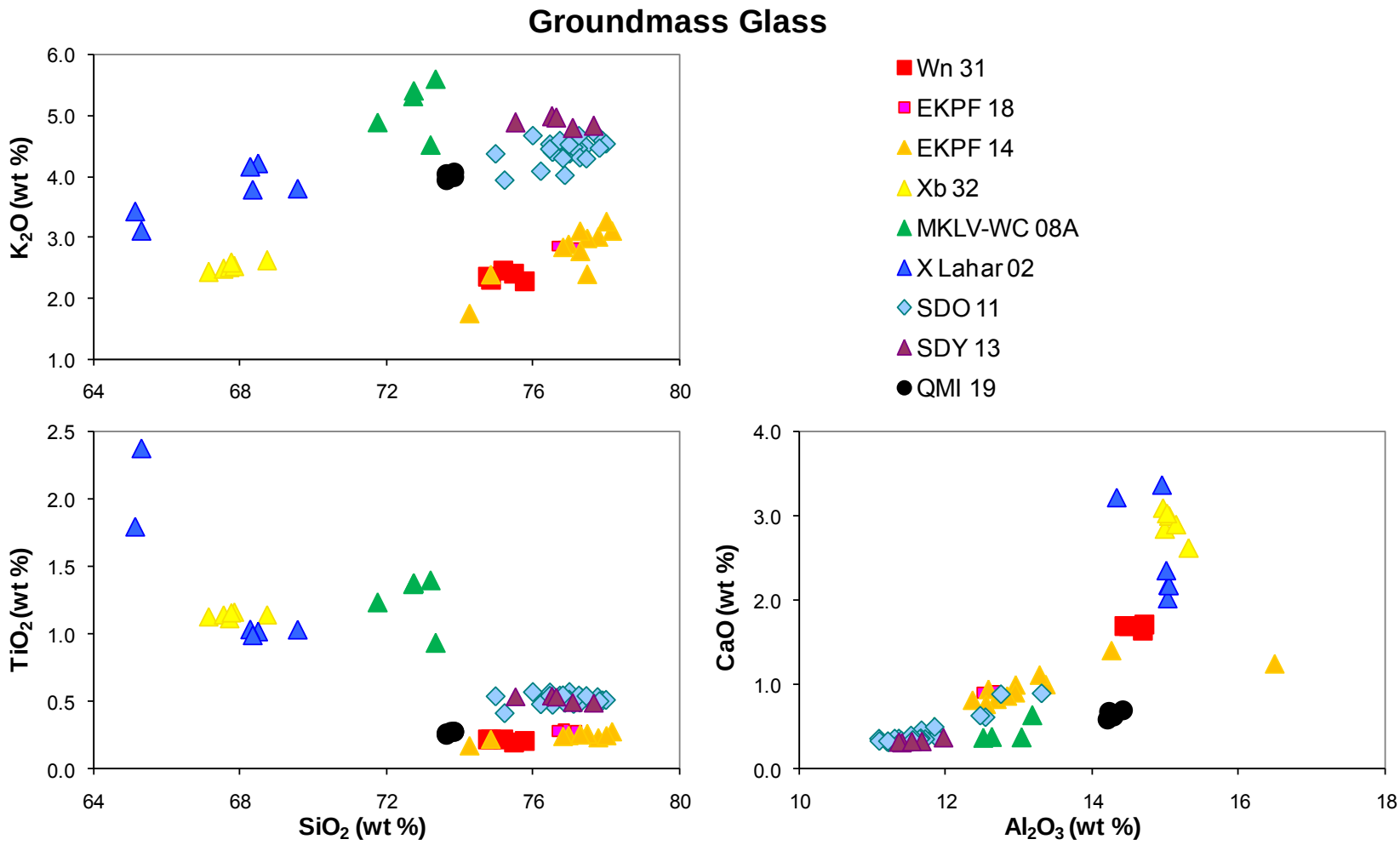

Figure 5.67 EMP groundmass glass spots of lithologies from the Kalama Period.

5.4.5 Phase Chemistry Summary

The heavily and coarsely sieved cores of population L plagioclase phenocrysts have high An cores and lower An clear rims that generally correlate with microphenocryst compositions within the same rock. These phenocrysts are found most prevalent in the olivine-rich QMIs and X deposits, but are also found in MKLV, SDO and SDY. There is little compositional overlap between the olivine-rich and olivine-poor QMIs. M-type X lahar 07 has a wide range of plagioclase compositions and zonation patterns. Large xenocrystic grains with comparable compositions to plutonic inclusion crystals plot near cores of sodic phenocrysts. Xb pumice and QMI 19 plagioclase generally have the highest An and MgO compositions, and X Lava Flow grains have high comparable An, but lower MgO. The middle Kalama Breadcrust Pyroclastic Flow 03 and Worm Complex lava 08A generally lie below the QMI and Xb 32 scoria populations. Plagioclase cores from SDO and SDY have higher An contents and form a curvilinear trend between W pumice 31 and the Two Finger Flow 10. A distinct dearth in compositions separates the cores from the lower An content rim trend.

QMI 19 has the most Fo-rich olivine, which also display prominent disequilibrium textures. M-type olivines are generally higher in Fo than B-type. Xb tephra olivine compositions correlate with B-type lahars save one Fo-rich core analysis. Plutonic inclusion olivines from EKPF are Fo-poor. Two populations of Cr spinel hosted by QMI 19 olivine are distinguished by Cr#, TiO_2, and Al_2O_3, but the host olivines do not show appreciable differences. At least two QMI 19 olivines contain spinel from each group. At least two clinopyroxene phenocrysts from Worm Complex lava 08a have high Cr chores, indicating they likely grew in a more mafic melt than the mantles

and rims. X lahar and EKPF 18 had the most variable glass compositions of those analyzed.

Chapter 6: Discussion

6.1 Statement of the Problem

Erupted tephras, pyroclastic flow and lahar deposits, and lavas of the Kalama Period are likely characterized, at least in some part, by magma mixing and mingling events (Carroll, 2009; Pallister *et al.*, 1992). However, the mafic end members are not well constrained, as no basalt erupted at Mount St. Helens could be the sole mafic component (Carroll, 2009; Pallister *et al.*, 1992). Evaluating QMIs from Kalama-age dacites and then plutonic inclusions may shed light on the magmatic inputs. The data gathered from this study allows some constraints on the mafic mixing end members and the role of assimilation of plutonic material into the magmatic system. This will, in turn, provide a better understanding of the felsic components and the degree of interaction with the mafic end members.

This chapter will describe the interpretations made from the petrography, chemistry and textural data for lithologies in eruptive sequence. This method is used so the progression of phase compositions and textures can be traced throughout the magmatic system during the Kalama Period. A discussion of the implications for the processes that lead to the magmatic evolution and how they are able to answer the research objectives will follow. The chapter will culminate with a proposed model of the magmatic evolution throughout the early and middle parts of the Kalama Eruptive Period.

6.2 Magma Evolutionary Processes

A leading aim of this research as outlined in the research objective matrix in Table 3.1 is to constrain the magmatic components involved in the Kalama eruptions. Constraining the evolutionary history of the components and the processes that generate the compositional changes is integral to this task. Magmatic systems can be open or closed to mass, volatiles, or heat fluctuations and can experience any combination of these factors along a continuum to change the conditions within the reservoir. The resulting changes affect the composition and textures of the erupted glasses and phenocrysts. Magma mixing is an open-system process, both physically and thermally, which encompasses both recharge and contamination by wall rock assimilation. Other mechanisms that change magma composition include closed system processes, such as decompression and convection due to heating (a thermally open-system process) (Ruprecht & Wörner, 2007). Several lines of evidence outlined below corroborate the argument for magma mixing as a dominant process during the early and middle Kalama. Additional evidence indicates that magmas experienced other evolutionary paths as well.

Magma mixing refers to the chemical mixing of more than one magma and involves chemical diffusion, whereas magma mingling is the physical interaction of two magmas that results in incomplete mixing (Bacon, 1986). Wide compositional variation in a suite of rocks can often be explained by mixing and mingling scenarios as a petrogenetic model for their formation. Evidence of magma mingling in the form of QMIs is apparent in hand sample in early Kalama-age rocks. If magma mixing were occurring during the Kalama Period, one would expect shared phenocryst populations, bulk rock

compositions intermediate between the parental magma compositions, and disequilibrium textures among phenocrysts if the magmas involved had distinctly different compositions and thermal properties. Previous work on Kalama-age rocks has described major and trace element chemistry, banded pumice, resorbed and skeletal textures of mafic phenocrysts, sieved and skeletal plagioclase textures, and reaction rims on amphibole and pyroxene as evidence for magma mixing (Carroll, 2009; Gardner *et al.*, 1995A, 1995B; Smith and Leeman, 1987, 1993; Pallister *et al.*, 1992). Observations from this study corroborate those accounts.

It is relevant to acknowledge recent research that investigates alternate explanations for the observed textures and compositions. Blundy *et al.* (2006) suggest that latent heat of crystallization produced from decompression (a closed system process) causes resorption and preservation of melt inclusions in plagioclase in a similar manner to mafic recharge (an open system process), resulting in textures such as sieved zones surrounded by a more An-rich zone. Their findings are based on calculated crystallinities and temperature increases up to 40 % and 100 °C, respectively, with decreasing pH_2O over a 230-0 MPa range, which they find consistent with data from both Shiveluch and Mount St Helens' 1980 and later eruptions. While the effects of latent heat cannot be ignored, neither can the prevalence of other evidence for magma mixing and mingling as dominant processes during the Kalama Period.

Phase chemistry is especially useful in delineating open vs. closed magmatic systems. Compositional zoning in plagioclase and other minerals is an important tool is deciphering magma chamber conditions and is helpful in constraining the magmatic inputs into the system. Anorthite vs. MgO diagrams of plagioclase analyses can be useful in distinguishing between open

and closed system processes. As a major element in the liquid, but a trace constituent in plagioclase, Mg substitutes primarily in the VIII-fold coordinated M-site, but can also partially substitute in the IV-coordinated T-site of plagioclase (Bindeman, 1998; Peters *et al.*, 1995). Peters *et al.*, (1995) conducted experimental fractional crystallization studies of anorthite to determine partition coefficients of Mg. They concluded that Mg is positively correlated with Na and that the activity coefficient for MgO increases with increasing liquid SiO_2, causing the D_{Mg} to also increase. Additionally, fO_2 had no affect on Mg partitioning since the valence does not change (Peters *et al.*, 1995; Ruprecht & Wörner, 2007)). One would then expect that as An content decreases with continued crystallization, MgO would increase since the SiO_2 content of the liquid increases. In a closed system, crystallizing plagioclase would lie along a curve of negative correlation of An with MgO (Figure 6.1). Points that fall in between the curvilinear trends probably represent crystal zones that grew in a mixed magma (Ginibre *et al.*, 2002; Ruprecht & Wörner, 2007). However, some scatter is expected; as An content may change from temperature changes (Blundy *et al.*, 2006), latent heat of crystallization could cause

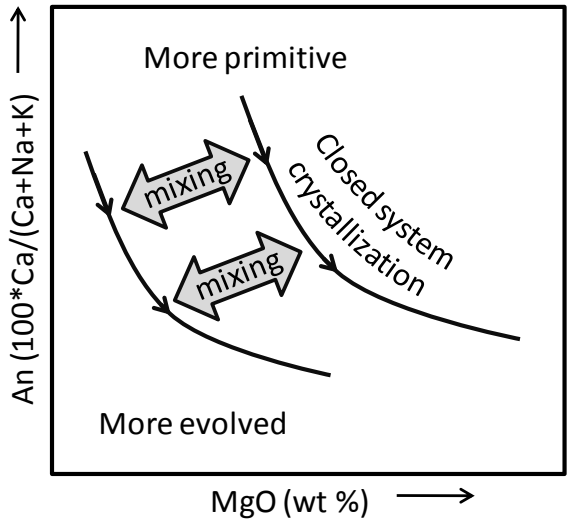

Figure 6.1 Schematic diagram of An content vs. MgO of plagioclase. As An content decreases, MgO partitioning into plagioclase increases. Lines represent trends, rather than partitioning concentration lines discussed in text.

sub-vertical trends. Conversely, cooling could cause lower An and lower MgO shifts in the curve. Higher pH2O will also increase An contents.

Harker diagrams of An vs. MgO, seen in Figure 6.2, bear lines of temperature-dependant equilibrium partitioning concentrations of MgO based on An contents. Each line is calculated for a given beginning bulk rock wt % MgO and An content using a linear regression calculation (Equation 6.1) that is consistent with experimental data (Bindeman *et al.*, 1998; Bédard, 2002; Tepley *et al.*, 2010).

Equation 6.1

$$RT \ln D_{Mg} = a X_{An} + b$$

Where $D = \frac{C^{xtl}_{Mg}}{C^{melt}_{Mg}}$

R = international gas constant, 8.314 J K^{-1} mol^{-1}

T = temperature, (K)

a = slope

b = y intercept

Temperature is adjusted in the equation until a best fit line is matched to the data. The curve shifts to the right and slightly up with increasing temperature. Therefore, if a magma experienced fractional crystallization while cooling, a trend might form similar to one of these lines, but would shift down in both An and MgO toward the bottom left corner of the diagram. The shift would likely be discernable, but not obvious as other factors might overprint the signature, such as pH2O or continuous change in liquid composition.

When all plagioclase data from this study are plotted on the diagram, considerable scatter is apparent (Figure 5.43). The overall trend of the data shows a rough positive correlation. Most plagioclase data plot between

QMI 19 (and Xb 32) and Wn 31 pumice. Grains from early Kalama dacites generally plot on the low MgO end of the scale, as do the plagioclase from the SDY samples, the last to erupt during the Kalama Period. QMI 19 and Xb 32 have the highest An content and MgO of any sample analyzed. Middle Kalama-age rocks, such as MKPF 03 and X lahar 07, also have the highest MgO, but do not bear remarkably high An contents.

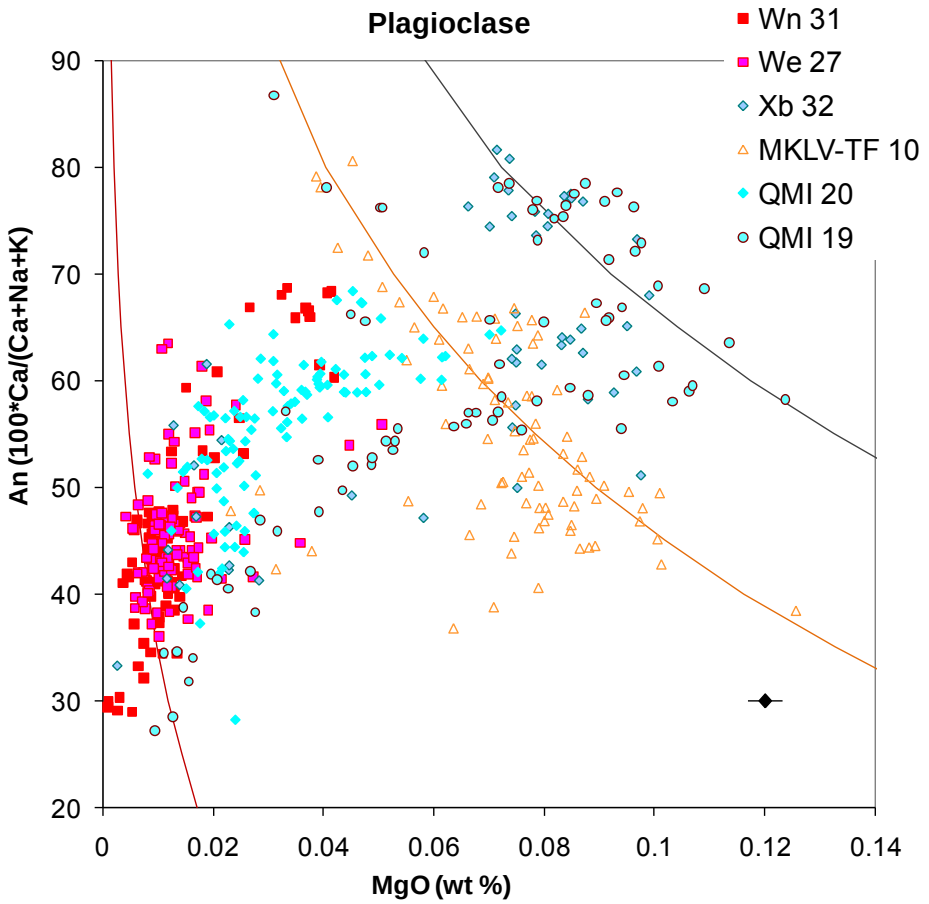

Figure 6.2 Selected plagioclase analyses for W tephras, Two Finger flow, X tephra, and QMI. Lines represent temperature-dependent partition concentrations of MgO as a function of An content for a given beginning whole rock MgO concentration for (left to right) Wn 31 tephra (600 °C), Two Finger Flow 10 (915 °C), and QMI 19 (1025 °C). Representative 1 s error for MgO shown in bottom right corner.

Despite the significant scatter and lack of obvious trends when plagioclase are plotted altogether, each sample has a distinct trend from which some mixing relationships may be inferred. Plagioclase data from QMI 20 on Figure 6.3 illustrate how An vs. MgO diagrams can reveal changes in the magma in which the crystal grew. Arrows on the diagram indicate progression from core to rim of the transect. Plagioclase 4 is a large (1.8 mm) grain with a sodic, coarsely sieved core that displays a horizontal trend, circled in red. The increase in An toward the outer edge of the core signals that the crystal experienced a change in magma reservoir conditions. The An spike could be either a result of the crystal moving into a hotter, more mafic melt or from crystallization in a mixed magma. The An-rich zone evolves to a normally zoned edge, which is represented on the diagram by a change in direction toward low MgO and An (the inferred felsic end member). The black and gray circles are microphenocrysts (<0.1 mm). Other crystals, such as plagioclase 3, display a similar pattern. The patterns from QMI 20 plagioclase likely indicate that most zones from the sampled grains grew in mixed magmas, which would also include a thermally and compositionally (both in terms of magmas and volatiles) heterogeneous magma chamber.

The An vs. MgO diagram is used throughout the Discussion section to illustrate the effects of open vs. closed system processes on plagioclase compositions, especially in relation to textures and crystal populations.

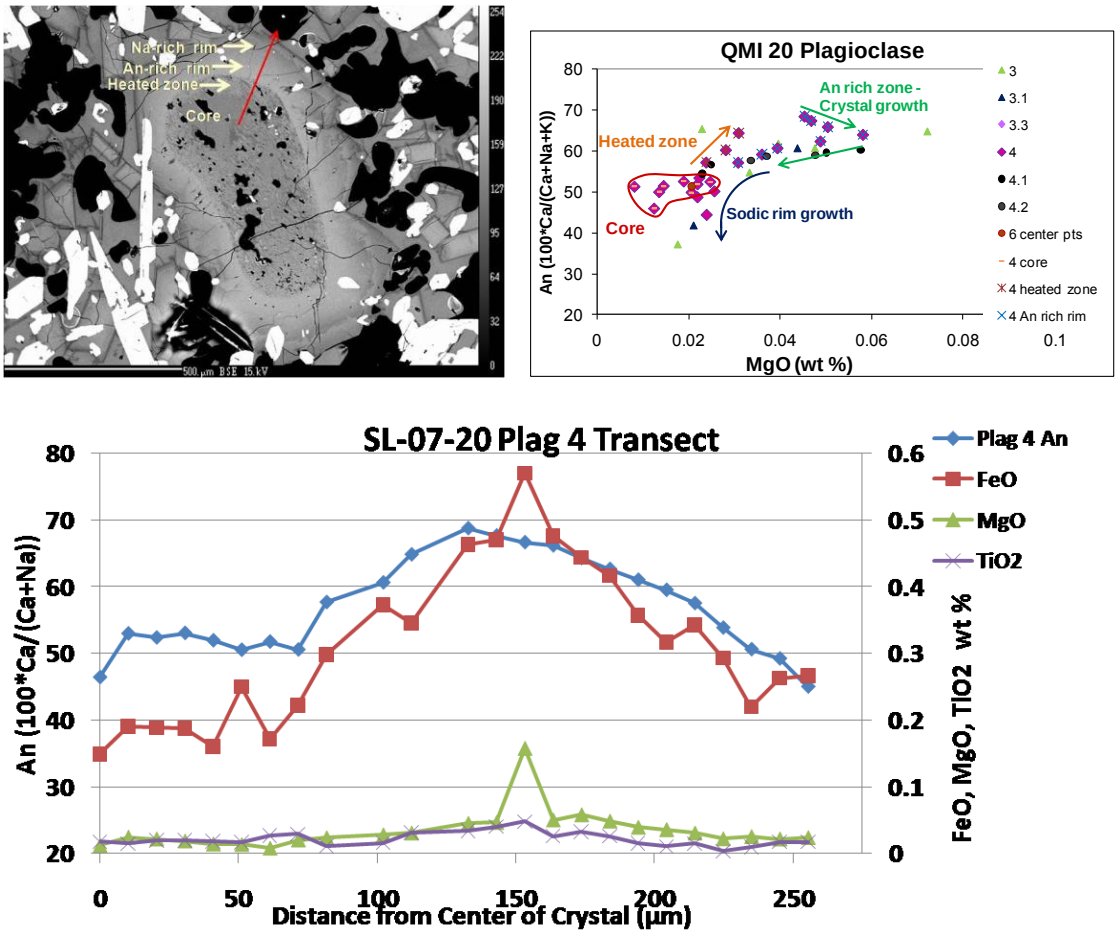

Figure 6.3 QMI 20 plagioclase 4 transect. a. Backscattered electron image showing transect location and the four zones annotated in B. b. EMPA analyses of plagioclase 4 and other nearby grains. Arrows indicate rimward progression from the core. Four distinct zones are annotated: core, heated zone which increases in An content, Fe and An-rich zone which is the light rim surrounding the core in the BSE, and the sodic rim which is normally zoned. c. An content, FeO*, MgO, and TiO2 along transect from core to rim of crystal.

6.2.1. Wn Pumice

The first eruption of the Kalama Period produced the most felsic and the most homogenous of the Kalama-age deposits. Wn pumices probably represent the closest composition to the felsic mixing end member erupted during the Kalama Period. Despite this, the presence of small, euhedral

clinopyroxene and relic olivine in Wn pumice 31 indicates at least a small amount of mafic input. There is relatively little evidence of cumulate or other plutonic material incorporated into the system. The compositions of plagioclase on An vs. MgO diagrams cluster in the low An and low MgO corner of the diagram. The cluster of sodic plagioclase grains could indicate crystallization on the closed-system (and felsic end member) end of the spectrum. Virtually all the high An points not within the cluster are from a single, large oscillatory zoned phenocryst, plagioclase 2 (Figures 6.4 and 6.5) that appears to have grown, at least partially, in a different magma. Plagioclase 2 represents the initiation of magma mixing prior to Kalama-age eruptions; the higher An contents indicate the magma in which it grew was any combination of more mafic, hotter, and different volatile content.

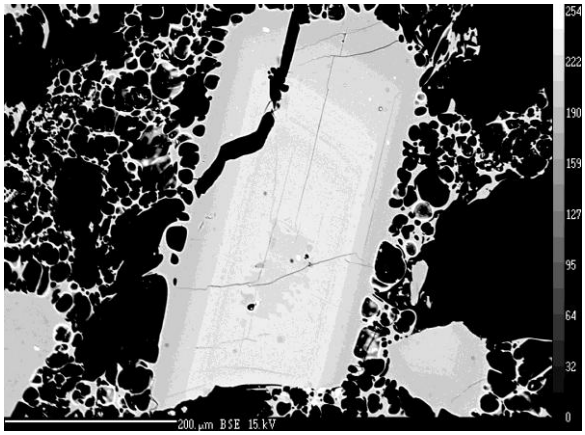

Figure 6.4 BSE image of Wn 31 plagioclase 2, which accounts for most high An points in that samples. The crystal is larger than most others in the sample.

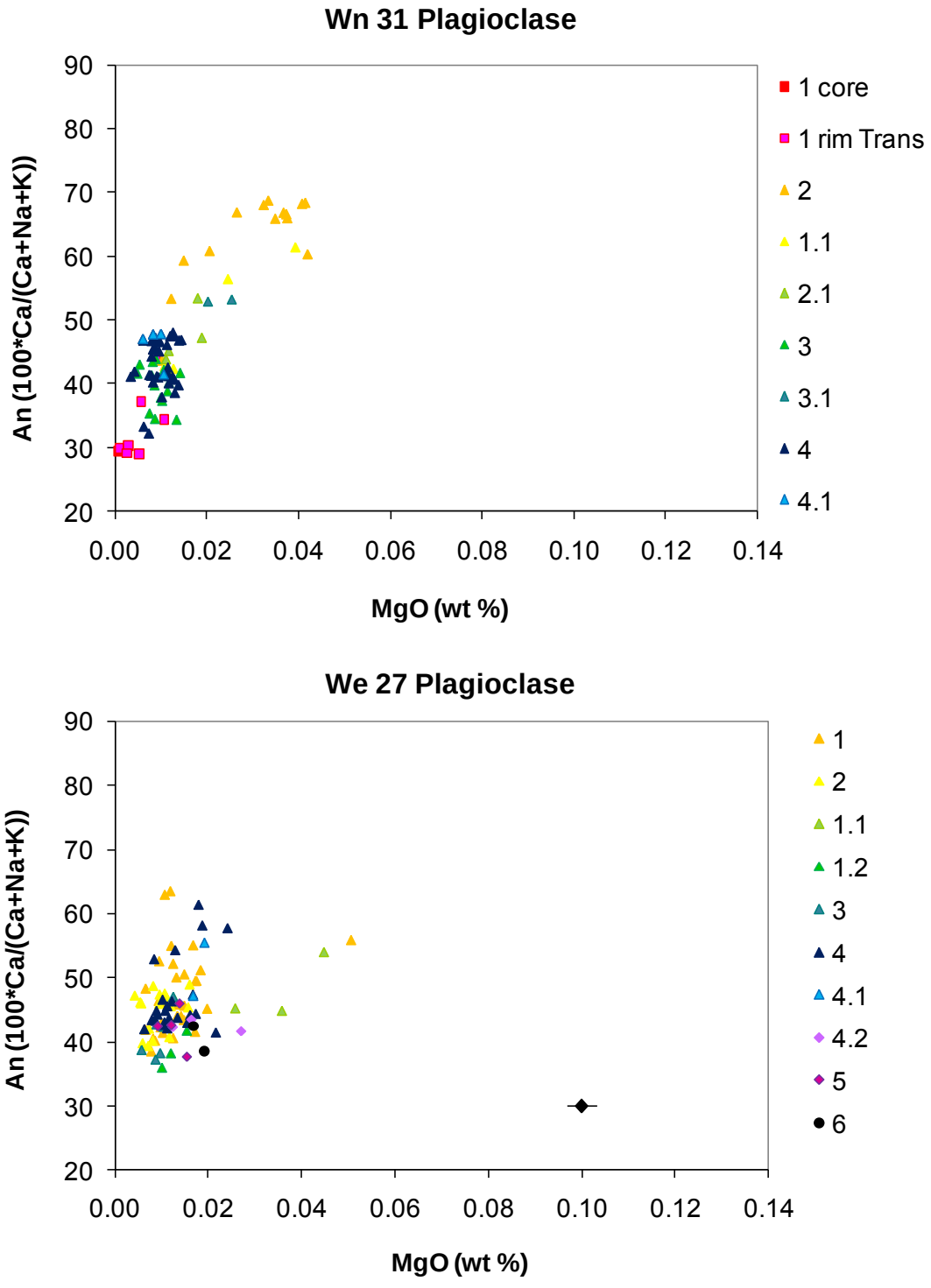

Figure 6.5 An vs. MgO diagram of EMPA of plagioclase from Wn 31 (top) and We 27 (bottom). Representative 1 s error for MgO shown in bottom right corner.

6.2.2. We Pumice

After the Wn pumice was deposited, another Plinian eruption produced the We pumice. We pumice shows an increase in mafic contribution with more phenocrysts with disequilibrium textures, lower SiO_2, higher TiO_2, MgO, CaO, and FeO*, as well as the rare presence of glomerocrysts of plagioclase, olivine, clinopyroxene and orthopyroxene. A mixing calculation between the bulk compositions of Wn dacite and QMI 19 basaltic andesite yields approximately a 5-9% mafic contribution, depending on the oxide. This estimate is in agreement with Carroll's (2009) calculations of X2 dacite plus an OIB-type basalt (with a similar composition to QMI 19). The X2 sample described in that study is nearly identical in composition and stratigraphic sequence to We pumice. Plagioclase analyses of We 27 pumice create a trend similar to Wn 31, but with higher An content and more scatter (Figure 6.5).

6.2.3. Early Kalama Pyroclastic Flow Deposits (EKPFs)

Following the large initial Plinian eruptions of the Kalama Period came a series of pyroclastic flows. The EKPFs are more variable in composition and have an even greater contribution of mafic magma than W dacites, evidenced by more calcic plagioclase phenocrysts, the presence of clinopyroxene and reversely zoned orthopyroxene, a greater amount of mafic glomerocrysts, and the presence of QMIs. Figure 6.6 illustrates the progressively higher degree of scatter in EKPF plagioclase. Two diverging trends emerge in this stage of the early Kalama (although barely discernable in We plagioclase); one trend has lower An/MgO and the other reaches to $>An_{70}$. The deviation indicates crystals are forming under two distinct sets of conditions. In addition to the abundant sodic plagioclase phenocrysts, EKPFs have population L plagioclase

with calcic cores. These large (1-2 mm), heavily and coarsely sieved grains have a size and texture unique from other phenocrysts in Kalama-age rocks. The coarsely and heavily corroded core is a texture similar to that described by Nelson & Montana (1992) resulting from decompression of andesites during high pressure piston cylinder experiments. Dungan & Davidson (2004) and Humphreys *et al.* (2006) also described similar textures in grains originating from cumulate material that experienced decompression and partial melting. Annen *et al.*, (2006) attribute such heavily corroded plagioclase grains to the entrainment of source material during rapid ascent of a H_2O-rich intermediate and evolved residual melts, which become superheated due to H_2O undersaturation at moderate to high pressures. Tsuchiyama (1985) noted a similar corroded texture from heating and mixing experiments, but the degree of the corrosion was not as extensive as those observed from population L plagioclase.

The combination of the texture and high An cores makes it possible that population L plagioclase are grains that disaggregated from cumulate material and were incorporated into the ascending magma. After the crystals were entrained into the Mount St. Helens magmatic system, crystallization continued to form rims free of heavy sieving and of similar compositions to groundmass microphenocrysts. Additionally, the mafic glomerocrysts that appear more commonly in EFPFs than in earlier erupted products are texturally and mineralogically similar to cumulate material of gabbroic xenoliths described by Costa *et al.* (2002) at Volcán San Pedro, Chile, and microxenoliths described by Dungan & Davidson (2004) at Tartara-San Pedro complex, Chile. The gabbroic xenoliths comprise anhedral, partially melted plagioclase and pyroxene, and the microxenoliths are similar to the

glomerocrysts in the X lahars, SDO and SDY with rounded edges (or distinct rounded arrowhead shape). The microxenoliths include partially melted mafic minerals, which are finer grained at the glass boundary.

The rocks from the first 10-11 years of the Kalama Period demonstrate a progressive increase in mafic contribution to the system, both from basaltic/basaltic andesite magma and from assimilation of cumulate crustal rocks. The increasing amount of calcic plagioclase and other mafic phenocrysts along with microxenoliths that include olivine and clinopyroxene, and finally the presence of QMIs support the interpretation.

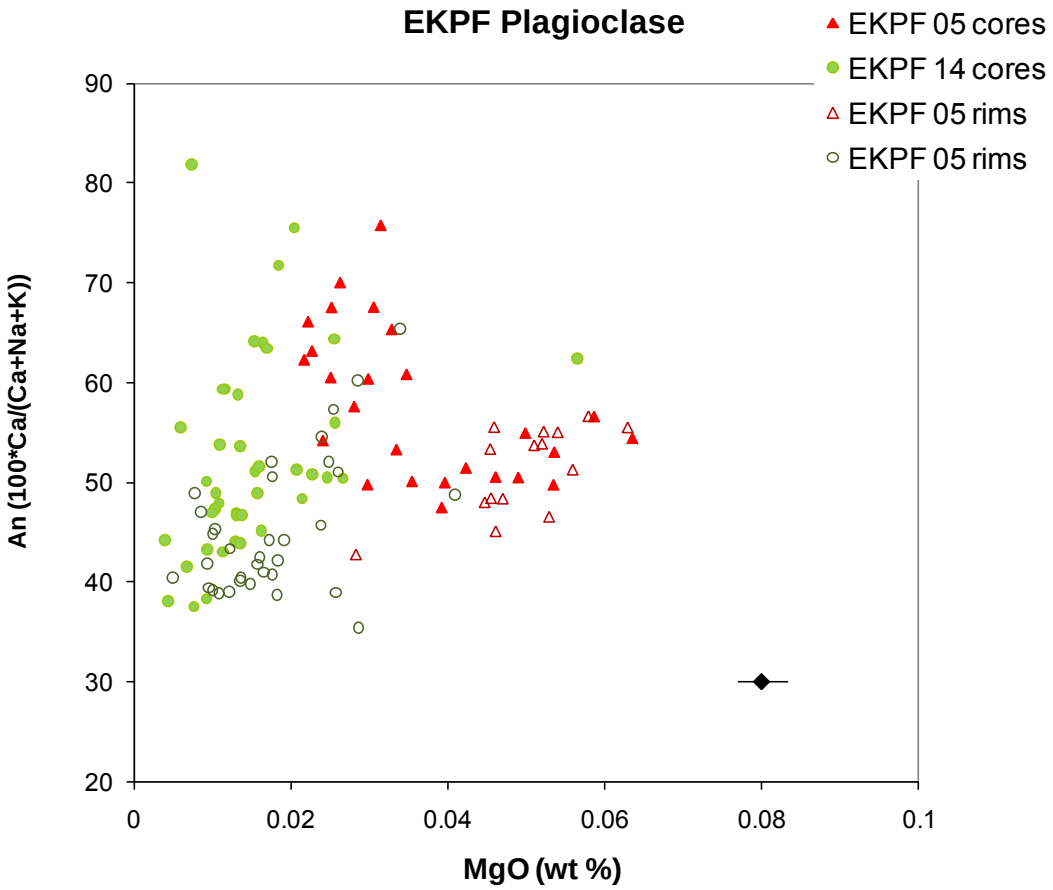

Figure 6.6 An vs. MgO diagram of EMPA of plagioclase from EKPFs. Representative 1 s error for MgO shown in bottom right corner.

6.2.4. Quenched Mafic Inclusions (QMIs)

Understanding the origin of QMI populations and their relationship to one another is important for deconvolving the history of the early and middle Kalama. This section will discuss the roles of magma mixing, fractional crystallization, vapor phase segregation, assimilation, and the potential for different sources in the petrogenesis of the QMIs.

The QMIs present in the EKPFs signify an increase in mafic contribution to the system because bulk rock analyses of both populations are lower in SiO_2 and have more mafic mineral assemblages than their host rocks. The hand sample observations that the QMIs: 1) have rounded and crenulated margins, 2) finger into the host dacites, and 3) are found in proximity to smaller mafic globules indicates these mafic magmas were mostly liquid at the time of interaction with the dacite (Figures 5.1, 5.2 and 5.3). As noted in the Results section, there are two distinct populations of QMI, and understanding the relationship between the two is important in order to constrain mixing end members. Therefore, it should be investigated whether QMI populations can be related by the evolution of the magmatic system.

Magma Mixing: One hypothesis for the origin of the QMIs is that the two groups have the same source, but the more evolved population is significantly more hybridized with the dacitic component. Simple major element mixing calculations between QMI 19 and Wn compositions (calculation as in Section 6.2.2) yielded mixed results. Most oxides, such as TiO_2, FeO*, CaO, MnO, Na_2O and K_2O had relatively reasonable fits of QMIs 20 and 22 on the mixing line when plotted on a SiO_2 diagram, but worse fits when plotted against MgO (Figures 6.7 and 6.8). Other oxides (Al_2O_3, Cr_2O_3,

P_2O_5) did not have a good fit with either abscissa. Mixing is probably occurring between the olivine-poor population and Wn, but is more complex than a simple two end member scenario.

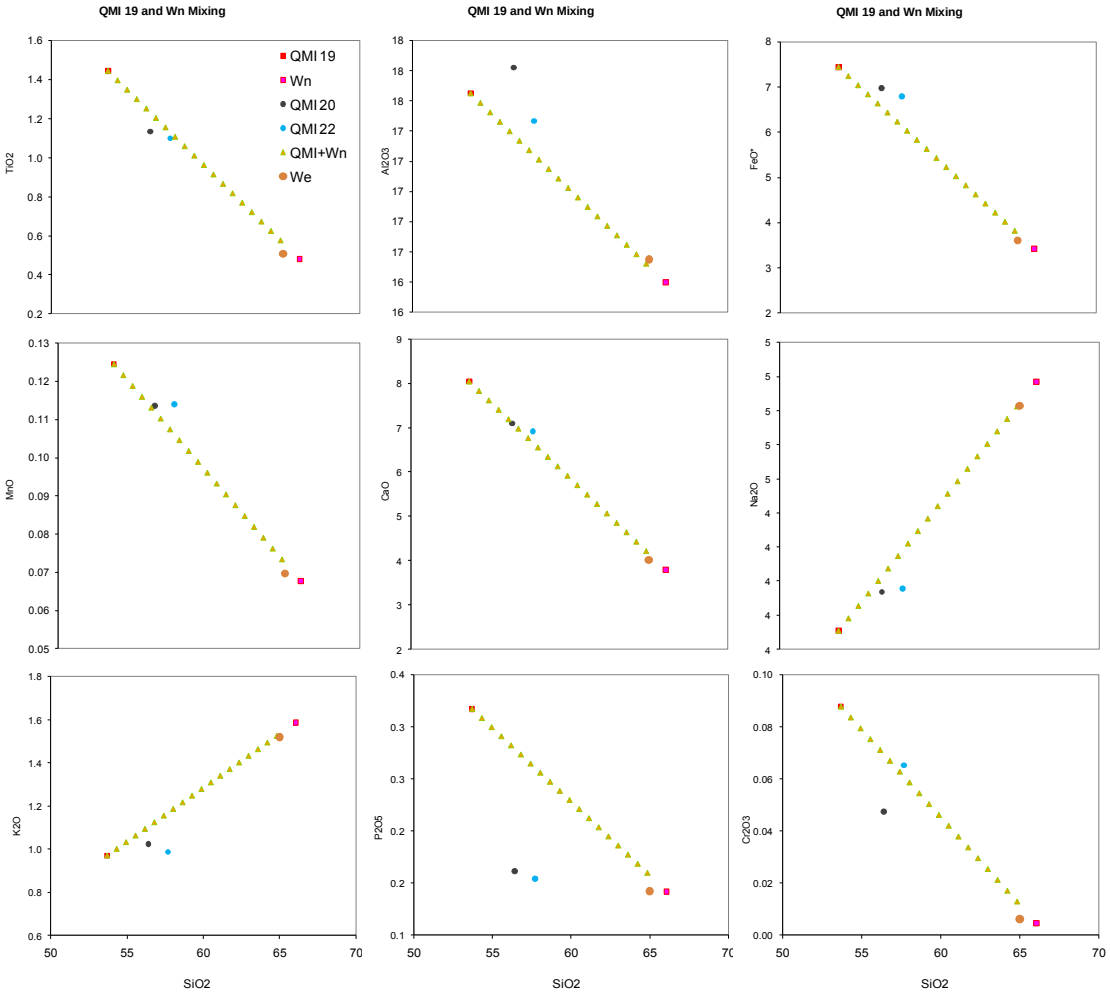

Figure 6.7 Calculated mixing trends between QMI 19 and Wn pumice 31 of oxides vs. SiO_2. The mixing calculation used was: $(F*Bulk_{Wn})+((1-F)*Bulk_{QMI19})$, where F = fraction of Wn. Note the location of We pumice with ~5-9% mafic contribution. The fit for QMIs 20 and 22 is variable.

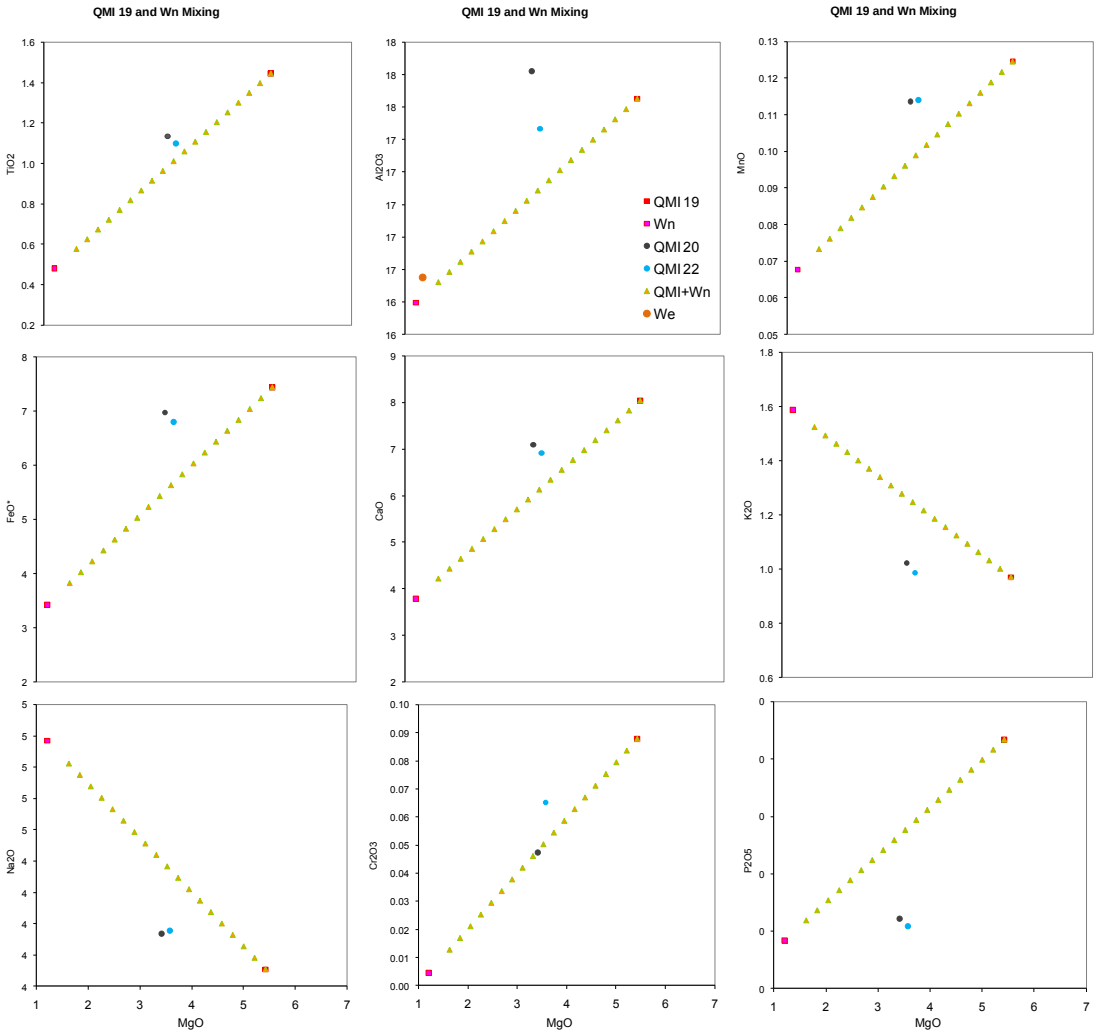

Figure 6.8 Calculated mixing trends between QMI 19 and Wn pumice 31 of major element oxides vs. MgO.

Plagioclase data suggest QMI 20 crystals grew in a mixture rather than a purely fractionated melt (Figure 6.9). There are no high Ca (> An_{68}) grains as there are in QMI 19. An content and MgO of QMI 20 appear to overlap with the W tephras and some EKPFs on the sodic end of the spectrum. The highest MgO concentrations in QMI 20 are from spots sampled in microphenocrysts or small phenocryst cores that are no higher in MgO than the Two Finger Flow

or X lava. That the magma was mixed is apparent because the arcuate trend that the data form spreads between the cluster of early Kalama dacites grains and the basaltic andesite plagioclase from the Two Finger Flow, QMI 19, and Xb tephra (Figure 6.2). However, most trace and some major elements of QMI 20 and 22 do not fall along mixing lines between Wn and QMI 19. If mixing were the dominant process in the petrogenesis of the olivine-poor QMI population, at least one other mixing end member would have been involved.

QMI 19 has also been mixed with the dacite component, but to a lesser extent and may have experienced some degree of fractionation. QMI 19, while consistently plotting at one extreme of the mixing spectrum, is not exactly at the end of a mixing line. For instance, trace element diagrams such as Zr, Nb, La, Ce, Pr, Nd, Sm, Eu, Gd, Tb, Dy, Tm, and Ta vs. SiO_2 show that QMI 19 plots slightly lower than the X lahar and tephra trend (Figure 5.37.). The Castle Creek basalt used in source component modeling of the Kalama Period by Carroll (2009) is higher in most of these trace elements, and therefore may be geochemically similar to the mixing end member. There are elements, however, where the OIB-like abundances are not a good fit: Ba, Ce, La, Ho, Dy, Tm, Lu, and Y. Simple mixing does not explain the formation of the two populations of QMIs. Phase chemistry supports this claim.

QMI 19 plagioclase have two distinct trends on An vs. MgO diagrams (Figure 5.45). Population L and other calcic grain cores form a curvilinear trend where An content and MgO are negatively correlated. That trend feeds into a cluster of other data that includes rims and mantles from both population L and other grains. The other distinct trend is also curvilinear, but convex in the opposite direction, and An content and MgO are positively

correlated. The trend comprises mostly rims and microphenocrysts that probably grew in a mixed magma (Ruprecht & Wörner, 2007).

The QMI 19 trends contrast with the QMI 20 trend which, although has a similar convex shape to the QMI 19 rim trend, only overlaps in the most sodic analyses (<An_{45}). The single QMI 20 trend shows significantly more scatter and plots in proximity to the plagioclase from plutonic inclusions (Figure 6.95). Pure mixing between the host dacite and QMI 19 to form QMI 20 is not plausible.

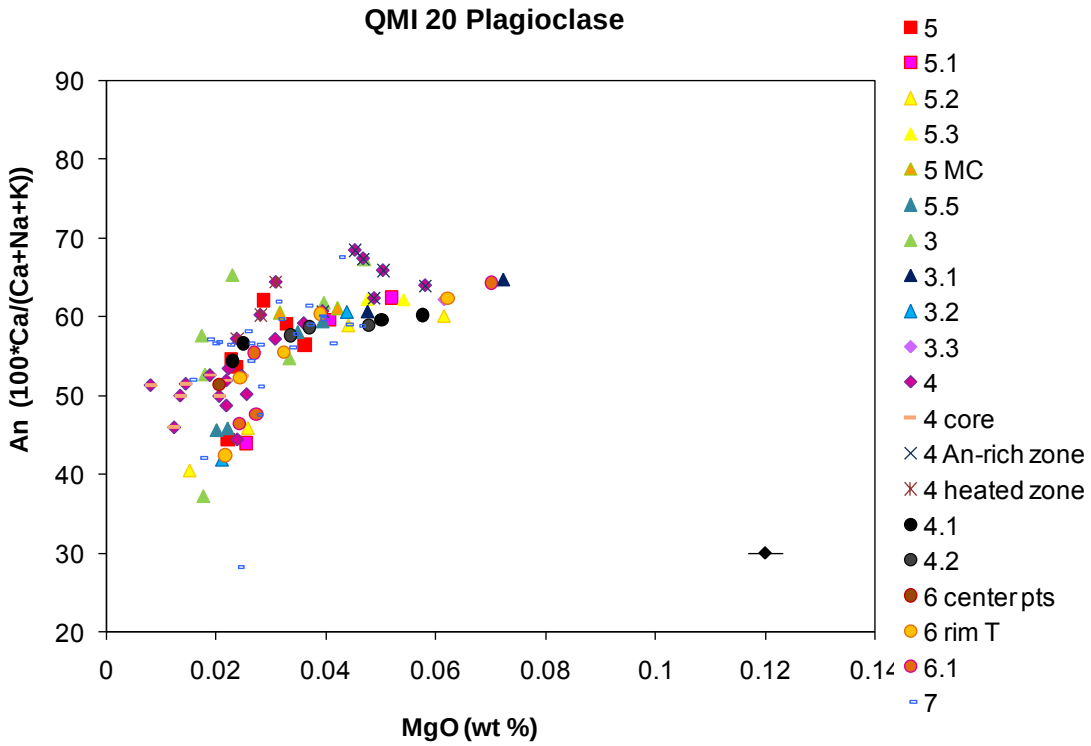

Figure 6.9 An content vs. MgO of QMI 20 plagioclase. MC= microphenocrysts, T = transect. Representative 1 s error for MgO shown in bottom right corner.

Fractional crystallization: Fractional crystallization modeling using MELTS (Asimow & Ghiorso, 1998; Ghiorso & Sack, 1995) for major elements and EC-RAxFC (Bohrson & Spera, 2007) for trace elements was conducted at 2

and 4 % water contents, at 2 and 3.5 kbar pressures to represent the modeled Mount St. Helens magma chamber conditions (Gardner et al., 1995A) and at QFM +2 (Figure 6.10). The composition of QMI 19 was used as the starting point at superliquidus temperature and allowed to run to complete crystallization. Major elements generally had a moderately good fit when plotted against SiO_2, with the exception of Al_2O_3 and CaO vs. Al_2O_3, but the only trace elements with realistic concentrations were Ni and Cr. Other trace elements were too incompatible to produce the lower concentrations seen in the olivine-poor group. Therefore, either some other process besides fractional crystallization is required to explain the link between the two populations, such as vapor or liquid transport, or they have different source melts.

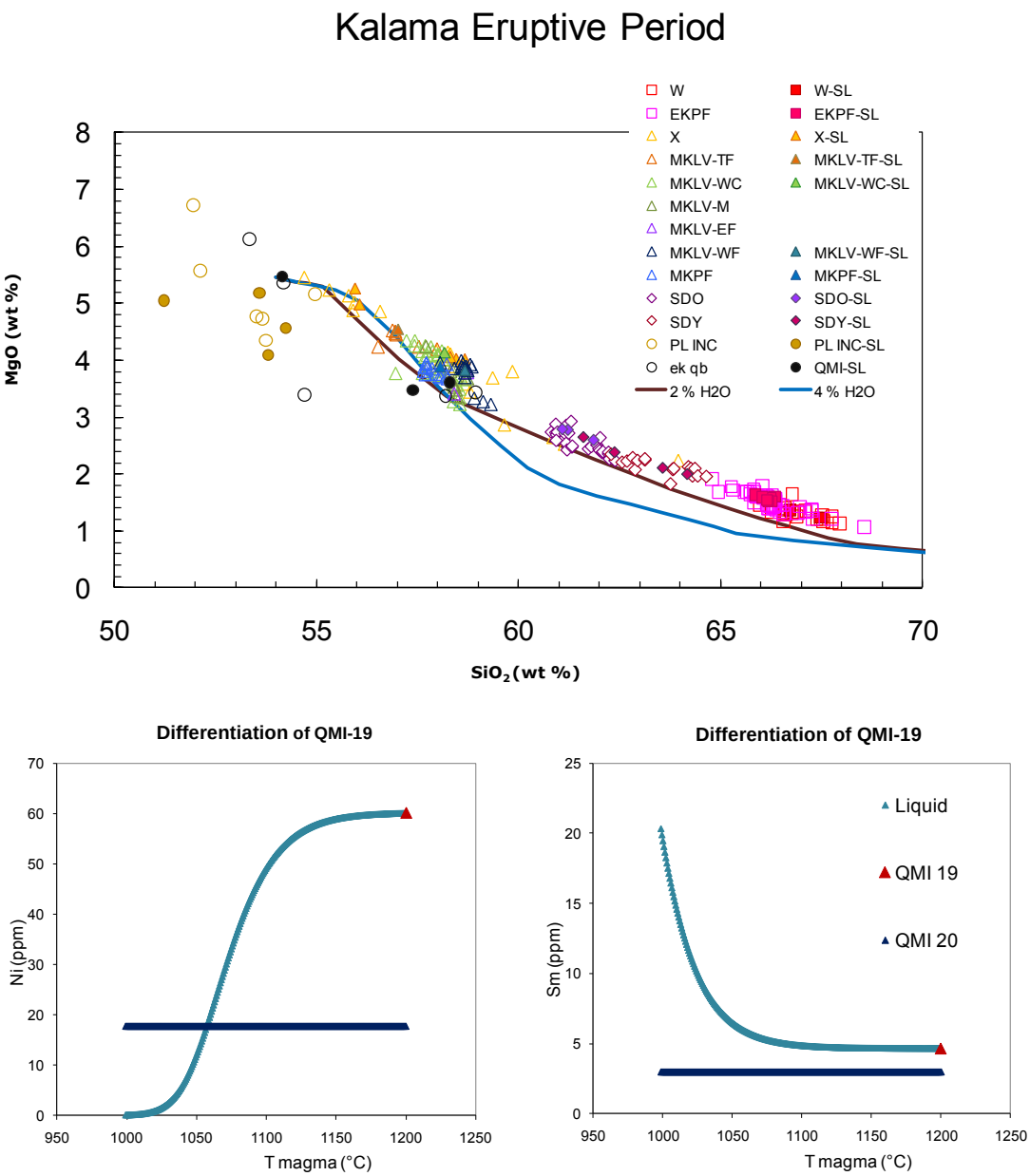

Figure 6.10 (Top) Representative results from MELTS modeling showing a good fit for differentiation of QMI 19 at 2 % and 4 % H_2O, 3.5 kbar, and QFM +2 for MgO. QMI 20 blue squares and purple diamonds show crystallization from QMI 20 starting composition to determine if QMI 22 could result. Symbols as in Figure 5. (Bottom) Representative results from EC-RAxFC modeling of a compatible trace element (Ni) and an incompatible trace element (Sm). Only Ni and Cr demonstrated feasible trace element concentrations. Trace element modeling results suggest QMI 20 did not form from differentiation of QMI 19.

Vapor Phase Segregation: Bacon (1986) describes the separation of a differentiated liquid from a crystallizing mafic inclusion into segregation vesicles through gas filter pressing as a process that moves the evolved liquid into the host magma. If the two QMI populations were formed by segregation through the method, also described by Anderson *et al.* (1984), one would expect that incompatible elements are concentrated in the one sample that was more liquid rich (or a more differentiated liquid), like QMIs 20 and 22. This could be difficult to discern since there is evidence that these two samples were hybridized with the host dacite significantly more than the olivine-rich QMI. The felsic influence could significantly override the trace element signature of the QMI. However, QMI 19 abundances are higher for all trace elements except some incompatible elements: K_2O, Cs, Rb, Pb, and U, and some compatible elements: Cu, Zn, V, and Sc. Moreover, trace element abundances are closer in compatible elements than they are for the other incompatible elements for the two populations. Because neither population has consistent incompatible element enrichment over the other, if gas filter pressing is involved in the inclusion formation, some other process must also be invoked. The overwhelming influence of the dacite could be the reason for the inconsistencies. If QMI 19 were from the residual liquid, it should be higher in virtually all incompatible elements.

Assimilation: Gabbroic inclusions found in deposits of all subperiods of the Kalama Period indicate assimilation of country rock could be important in the petrogenesis of the rocks. The following arguments will show that the olivine-rich QMI population descended from a mafic source and incorporated significant amounts of cumulate material while the olivine-poor population

likely originated from a more felsic magma and entrained plutonic material not necessarily of cumulate origin.

The phenocryst assemblage in the olivine-rich QMI group includes population L plagioclase, polysynthetically twinned clinopyroxene, significant amounts of olivine and clinopyroxene, and mafic glomerocrysts. These minerals and textures could all be indicative of a cumulate source. Additionally, the olivine-poor population has none of these groups in any significant amount. As previously mentioned, the population L phenocrysts have heavily and coarsely corroded cores which are consistent with textures from decompressed plagioclase in both natural and experimental systems (Costa *et al.*, 2002; Dungan & Davidson, 2004; Humphreys *et al.*, 2006; Nelson & Montana, 1992), indicating they were likely transported from deeper sources. Lastly, the unusually large size and high An cores also point to a cumulate origin.

Further indication of a cumulate source lies with the polysynthetically twinned clinopyroxenes, which have a unique texture that is not well understood. Because they are so distinctive, they may be used as tracer crystals throughout the magmatic system to help qualitatively estimate the contribution from its source. The texture of these pyroxenes is probably the result of either recrystallization of several smaller grains or deformation. A relatively similar, albeit not identical, texture was observed in clinopyroxene of experimentally shocked basaltic material, as well as Apollo 11 lunar rocks and Nevada Test Site basalts (Sclar, 1970). Raleigh & Talbot (1967) noted clinopyroxene polysynthetic twinning parallel to (100) (resembling plagioclase albite twinning in appearance) from mechanical strain and, to a lesser degree, basal twinning parallel to (001) in mafic and ultramafic rocks. The basal twins

were broader and discontinuous, a texture closer to that found in the polysynthetically twinned clinopyroxenes. It is more likely, however, that they are growth twins, which are broader, occur as one or two crystals, and for which the composition planes are stepped rather than continuous (Raleigh & Talbot, 1967). The polysynthetically twinned clinopyroxene of Kalama-age rocks are commonly found in mafic glomerocrysts with grain sizes significantly larger than the non-disequilibrium textured phenocrysts in the same sample. They are also found in or near plutonic xenocrysts in thin section. It is therefore possible the polysynthetically twinned texture results from the subsolidus recrystallization of pyroxene from cumulate material. If this hypothesis is correct, the gradual increase in the relative abundance of these pyroxenes, in addition to population L plagioclase, with the progression of eruptions should indicate a higher degree of incorporation of cumulate material into the Mount St. Helens magmatic system during the early and middle Kalama.

The assimilation of cumulate material is a commonly cited process for the Mount St. Helens system. Heliker (1995) described four populations of plutonic inclusions that account for ~3.1% by volume in Mount St. Helens lavas from 1980 through 1983. She noted that inclusions are abundant in lavas of the past 3000 ka. Compositions of plutonic inclusions hosted by Kalama-age rocks were consistent with those of Heliker's laminated gabbronorites, which were ~1 wt % lower in SiO_2. The laminated gabbronorites, the most common plutonic inclusion type at Mount St. Helens, contained veins of plagioclase and amphibole with lesser amounts of pyroxene, oxides, and interstitial glass. Amphibole norites, with a similar mode to the non-olivine

bearing QMI population, were found at Mount St. Helens, but the bulk compositions were notably dissimilar.

Heliker (1995) proposed a layered mafic pluton beneath the volcano as a source of the gabbros, but more recent Pb isotope and trace element studies argue that the origin of the inclusions are unrelated to recent magmatic system at Mount St. Helens (Kent *et al.*, 2008). However, the isotope study also found inclusion disaggregation contributed isotopically to the groundmass glass composition of the dacite dome in which they were encased; the glass lied along an apparent mixing line between the plutonic and volcanic rocks. It is reasonable that this would occur in Kalama-age rocks as well. The crenulated and embayed edges of plagioclase crystals and fragmentation of larger grains in some inclusions suggests they experienced partial melting, which could be indicative of a restite nature (Eichelberger, 1980).

The non-olivine bearing QMI population appears to have geochemical input from plutonic material similar to the inclusions found in Kalama-age rocks. Xenocrysts with bent albite twinning are found in this population and are indicative of heating or increased pressure regimes (Costa *et al.*, 2002). Besides falling on an apparent mixing line between plutonic inclusions and the early and late Kalama rocks in most major and trace elements variation diagrams (except TiO_2 and FeO*), QMIs 20 and 22 plot consistently with the plutonic inclusions in ratio-element and ratio-ratio diagrams (Figure 5.39). Plutonic inclusions from both the early (23) and middle Kalama (08B) display very similar REE patterns to QMIs 20 and 22, including slight positive Eu anomalies. A stronger positive anomaly occurs in the middle Kalama inclusion (08B), indicating, at least to a small degree, it is a plagioclase cumulate.

QMIs 20 and 22 contain crystals that likely originated from plutonic rocks. The plagioclase from the xenocrysts lacks the high An content (and MgO) that the population L plagioclase display, and there are few to no polysynthetically twinned clinopyroxene (Figure 6.11). The few olivines found in the studied samples are very heavily reacted, compared to the embayed and only moderately reacted olivine with spinel inclusions from the olivine-rich group. These xenocrysts, such as the one in Figure 5.18b, are larger than the associated phenocrysts, and contain sodic cores surrounded by zones of resorption or partial melting and an An-rich rim that is normally zoned. The petrographic and geochemical evidence suggest assimilation was important in the formation of both the olivine-poor QMI and olivine-rich QMI groups. The felsic source of the QMI could be a melt of plutonic material similar to the composition of plutonic inclusion 18A. MELTS (Asimow & Ghiorso, 1998; Ghiorso & Sack, 1995) was allowed to run the composition of this sample at a starting temperature of 600 °C and ending temperature of 1180 °C at 3.5 kbar and 4 wt % H_2O to determine if a melt from a plutonic inclusion found in an early Kalama sample could produce the olivine-poor compositions sampled. Most major elements produced a good fit for QMIs 20 and 22, with the exception of TiO_2 (Figure 6.12). Crustal anatexis of basement rock beneath Mount St. Helens could provide the felsic source of the olivine-poor QMI group.

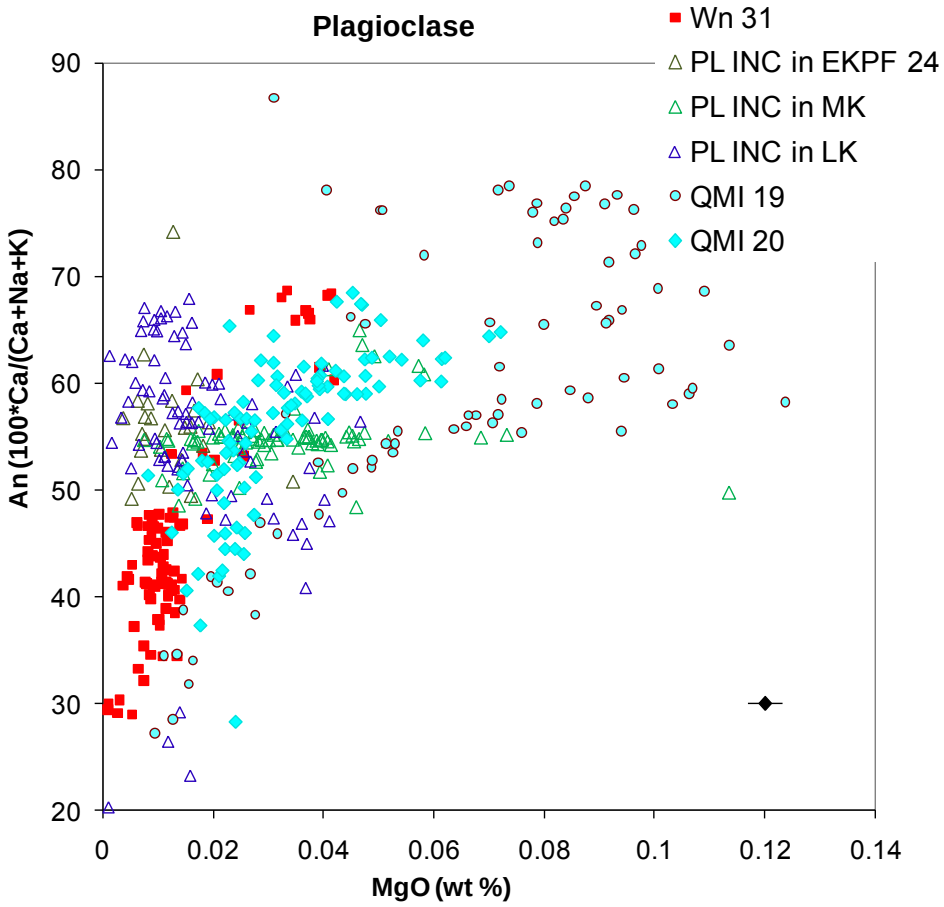

Figure 6.11 An content vs. MgO of plagioclase from selected lithologies to demonstrate the compositional similarities between QMI 20 and plutonic inclusions. Also note the lack of overlap in QMI 19 and QMI 20 grains. Representative 1 s error for MgO shown in bottom right corner.

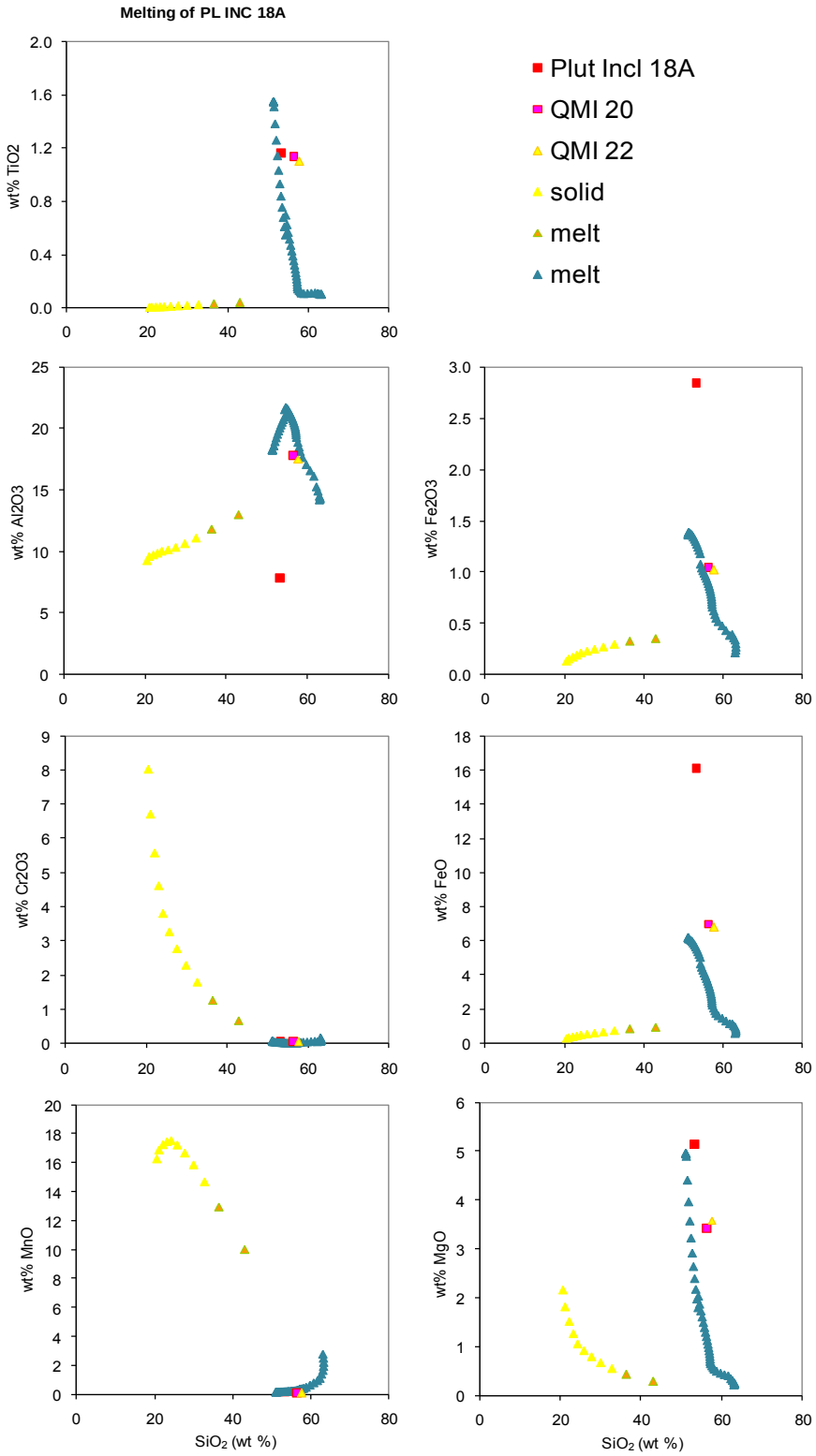

Figure 6.12 Harker diagrams of modeling results showing QMI 20 and 22 compositions could be produced from melting of plutonic inclusion 18A.

Different Sources: It is clear from the petrography, and whole rock and mineral chemistries that the two populations of QMIs have different sources and evolutionary histories. The compositions and textures of the entrained host rock material are also substantially different for the two populations, as are the phenocryst textures.

The differences in textures in the two QMI populations could indicate different temperature differentials between the andesite or basaltic andesite and their host dacite. The discrepancy in temperature could be the result of either different stages of equilibration being preserved or differences in magma temperature at the time of injection. The paucity of QMIs in the early Kalama dacites where both populations are found suggests the initial relative volume of mafic magma was not significant. Therefore, the injection of the basalt or basaltic andesite probably did not raise the dacite temperature significantly, so that a subsequent injection would not intrude into a much hotter melt. One would then expect that mafic magma temperature is probably a significant variable in explaining differences in crystal morphology.

Plagioclase and amphibole textures similar to those observed in the olivine-rich QMIs are described by Browne *et al.* (2006) from analogous enclaves, which are widely distributed throughout Unzen Volcano lavas. Browne *et al.*'s (2006) Equigranular population is similar to this olivine-rich QMI group in terms of plagioclase morphology, absence of a chilled or crenulated margin, and higher degree in uniformity of crystals size. Lofgren (1980) and Coombs *et al*. (2002) also describe similar textural results from basalt crystallization experiments with an undercooled ΔT of <40 °C. The ΔT equates to magmatic temperature differences between 10-45 °C. Textures

similar to those in the olivine-poor QMI group (abundant acicular amphibole and plagioclase with skeletal features) were observed by both Browne *et al.* (2006) in their Porphyritic enclaves and in the previously mentioned basalt crystallization experiments (Lofgren, 1980; Coombs *et al*., 2002) when undercooled conditions of ΔT were between 140 and 185 °C. A possible hypothesis for the temperature differentials could be the influence of two separate mafic magmas. The trace element chemistry of the olivine-rich group has an OIB-like signature, whereas the olivine-poor group has a calc-alkaline signature. These differences could reflect the origin of the mafic component.

The difference in amphibole and plagioclase morphologies between the two QMI populations is not necessarily a strong argument for separate sources. However, the distinctions in mineralogy and geochemistry do provide credence for the argument for different parents. In addition to the 2-5 wt % disparity in SiO_2, trace element chemistry more succinctly elucidates the genetic variation. The olivine-rich group's enrichment in Nb, Ta and other HFSEs that is lacking in the olivine-poor group (Figure 5.38) implies the potential for a different source. Niobium and Ta partition into amphibole, spinel and other Fe-Ti oxides (Rollinson, 1993; Ewart & Griffin, 1994), so the question arises whether the removal of olivine, and thereby, trapped spinel, could account for the change from enrichment to depletion. The very low modal percent of spinel in QMI 19 (<<1%), even with very high partition coefficients, would not reconcile the Nb-Ta concentrations. Lastly, the olivine-rich group consistently plots near the X lahars in ratio-element diagrams, whereas the olivine-poor group consistently plots with the plutonic inclusions (Figure 5.39).

Spinel and plagioclase data suggest there may have been two basaltic inputs in the olivine-rich QMI magma, which could account for some of the diversity. Potential explanations for the two clusters of QMI 19 spinel are:

1. Because Cr spinel crystallizes early in a magma's history as a liquidus phase (Clynne, 1993 and references therein; Clynne & Borg, 1997; Smith & Leeman, 2005), there could be two basaltic sources. In such a case, one might expect differences in whole rock and mafic phenocryst geochemistry.
2. The Cr# break between the two clusters is merely a coincidence, and the higher Cr # spinels are simply a more evolved set within a natural crystallization sequence, even though the Fo content of the host olivine are comparable or slightly higher for the more evolved group of spinel.
3. Variations in the melting source, fO_2, P, extent of fractional crystallization, or extent of partial melting are other factors that could affect the Cr # or TiO_2.

Because there are no discernable textural or compositional differences between the host olivines, if there are two distinct populations of spinel from separate basalts, the magmas would have interacted while still very hot and early in their crystallization history (before or during olivine crystallization). Trace element and isotopic work on the QMI mafic phases could clarify whether there is, in fact, more than one basaltic input.

The two populations of QMIs do not appear to be related by evolution of the magmatic system and therefore, probably do not have the same source. Phenocryst and xenolith textures and compositions suggest assimilation plays a significant role in the formation of the intruding mafic magmas. The olivine-poor QMI group may have incorporated plutonic country rock that is not necessarily of cumulate origin, whereas the parent to the olivine-rich

group probably entrained significant proportions of cumulate material, keeping the mafic character of the rock.

6.2.5. X Tephras, Lavas, and Lahars

Following the explosive eruptions of the early Kalama dacites, the middle Kalama saw a series of basaltic andesite and andesite tephras and lavas. There are four X lava populations, and those found reworked in lahar deposits *may* correlate to X tephras. The following section will discuss each population and the characteristics that make it a separate group.

The most mafic of the X deposits are the B-type lavas found in lahar deposits (X lahars 01 and 07). The B-type lavas may correlate to Xm tephra, which was erupted after Xs, but before Xh, and is the most mafic tephra for which there are analyses. Olivines from X lahar 07 are the most Fo-rich measured in the Kalama-age rocks, aside from those in QMI 19. B-type lavas have more population L phenocrysts, some of which have rim compositions similar to groundmass crystals in QMI 19.

M-type lavas (X lahars 02 and 09) are slightly more evolved than the B-type lavas and may correlate to Xb and Xs tephras, the first two to erupt during the middle Kalama. Whole rock major elements of M-type lavas correlate with those from Xb and Xs (Table 6.1). Trace elements for B-type lahars 01 and 07 are nearly identical, and are slightly offset from M-type lahars 02 and 09, which are also nearly identical to one another. Fewer population L plagioclase and polysynthetically twinned clinopyroxene were observed in the lahar samples. The olivines from X lahars 02 and 09 appear to form a discernibly different population from X lahar 07 olivines, which were less

Fo-rich than those from B-type lavas. However, rims from some X lahar 07 olivines did overlap in composition with cores of X lahars 02 and 09.

Table 6.1 Possible Correlations of X lavas and Tephras. Data from this study, Clynne (unpublished data, 2010), Hoblitt (unpublished data), Hoblitt *et al.* (1980), Mullineaux (1996), Pallister (unpublished data), and Smith & Leeman (1987, 1993). Tephras Xs, Xm, and Xh are deposits of only ash, which may preferentially fractionate out heavier minerals closer to the vent.

Lava	**SiO_2 (wt %)**	**Tephra**	**SiO_2 (wt %)**
B-type lahars	58.0 - 59.6	Xb	58.0 – 59.3
B-type lahars	58.0 - 59.6	Xs	59.8
M-type lahars	55.8 – 56.3	Xm	54.7 – 55.3
X lava (in situ)	59.6 – 61.2	Xh?	No analyses

Xb tephra includes plagioclase that appear to have grown in a dacite-rich melt as well as those that form a second trend on An vs. MgO diagrams along a higher temperature line (Figure 5.50). Plagioclase 1, 1.1, 4.1, and 5 have low An and MgO cores. Plagioclase 2, 4 and 6 grew in a more primitive magma (perhaps the hottest measured in this study), and each have a slight increase in An from the core inside of the oscillatory zoned rims. The overlap between the latter group and QMI 19 suggests they share the same basaltic source, which probably also sources other X deposits.

Evidence for magma mingling among the B-type lahars includes the presence of two distinct groundmass glass populations on a single thin section X lahar 02 (Figure 5.4). One glass population is significantly more crystalline than the other, and the compositions of the groundmass glasses vary between 65.15-69.23 wt % SiO_2, more than any other thin section analyzed for glass

(Figure 5.21). It is clear variable degrees of both magma mingling and mixing occurred to form the B-type lavas found in lahars.

The *in situ* X Lava Flow 30 located near Windy Ridge is grouped with the X deposits and shares geochemical characteristics with both X deposits and middle Kalama-age lavas. However, its mineralogic, geochemical and textural character suggest it may have a unique history from other X lavas. Trace elements of the X Lava Flow have not previously been published, and this study includes only one sample from the flow (Figures 5.34, 5.37 and 5.39). Therefore, only preliminary interpretations from whole rock data are attempted within the scope of this study. If other X lava samples plot within the vicinity of 30, two situations are possible: 1) There is a magmatic (or plutonic) input unique to this flow that is not seen elsewhere in the Kalama, or 2) The X Lava flow sampled is mapped as a Kalama-age lava, but is actually from a different eruptive period.

Whole rock major element chemistry of X lava 30 is more evolved than other X lavas (Figures 5.28 and 5.29), and trace elements are more akin to MKLV than X deposits (Figure 5.34). X lava 30 has significantly less olivine than other X deposits (like MKLV), although other thin sections collected outside of this study have slightly more than X lava 30. The paucity of plagioclase crystals lower in both MgO and An content (as seen in Xb 32 and X lahar 07) suggests either there was no crystal cargo from the dacitic end member or sodic plagioclase was resorbed during re-equilibration (Figure 5.51). However, plagioclase data show that X lahar 07 and X lava 30 have some overlap in compositions (especially on the high An end) on An content vs. FeO* and An content vs. TiO_2 (on the low An end) (Figure 6.13). There is

considerable overlap in the middle An contents on an An vs. MgO diagram (Figure 6.14).

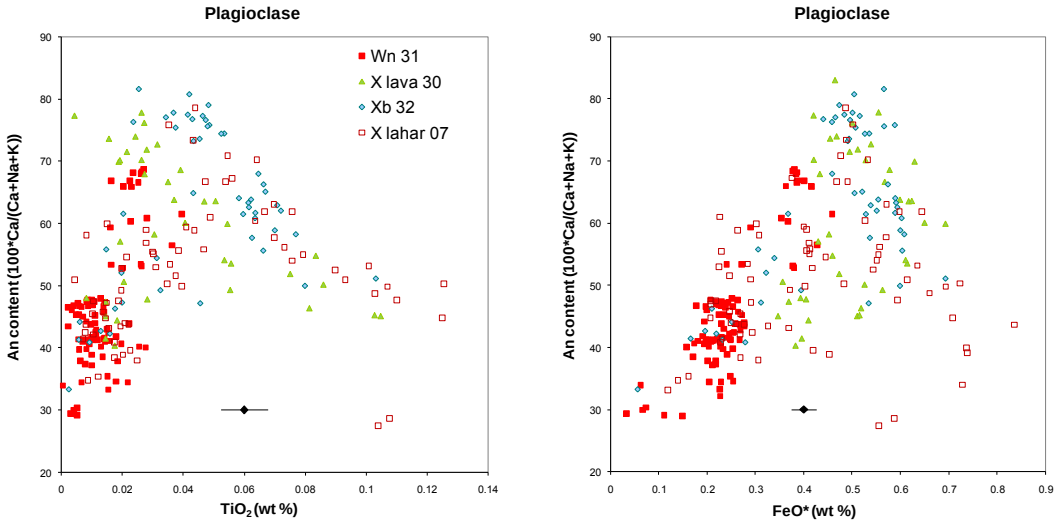

Figure 6.13 An vs. TiO2 and An vs. FeO* of plagioclase from selected early and middle Kalama rocks to show comparison of compositional overlap between X lava 30 and X lahar 07. Representative 1 s error shown in bottom center.

Another potential source for X rocks could originate from QMIs 20 and 22. X lava has more An-rich plagioclase, and the other plagioclase compositions rarely overlap (Figure 6.15). Core spots from grains 3.1 and 6.1, small grains (< 0.05 and 0.150 mm) from QMI 20, overlap with Xb 32 tephra. Plagioclase 6 from X lava 30 also overlaps, but this grain is a xenocryst and may indicate that both magmas entrained material from the same source. Assuming sampling bias is not a significant source of error, it is clear from plagioclase compositions that QMI 20 could not be the source for X lava 30.

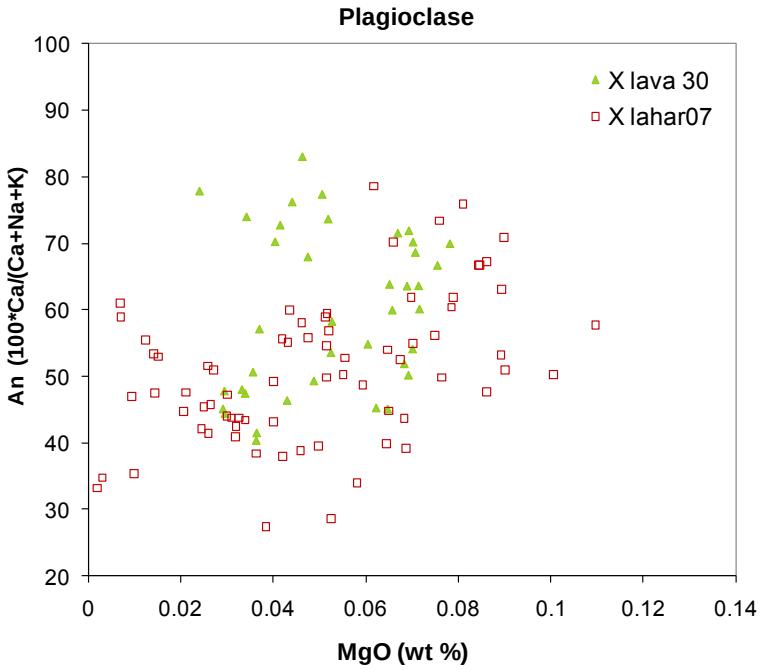

Figure 6.14 An content vs. MgO of plagioclase showing some compositional overlap in the middle An and MgO concentrations.

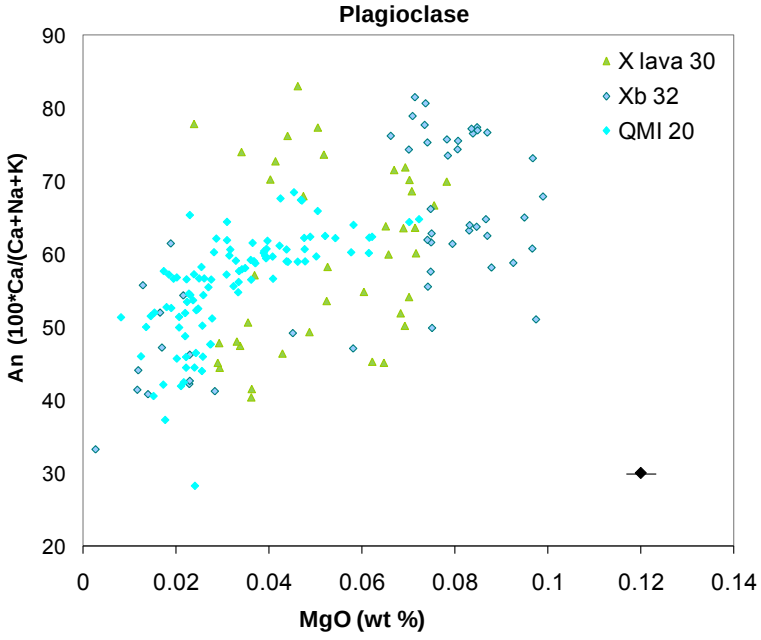

Figure 6.15 An content vs. MgO of plagioclase showing very little compositional overlap between X lava 30, QMI 20 and Xb 32. Representative 1 s error for MgO shown in bottom right corner.

The textures of X lava 30 tell a complex history. X lava 30 contains sparse olivine, but X lava *(in situ*) samples not analyzed in this study contain somewhat more. Most olivine shows signs of resorption, but at least one medium sized (0.8 mm) euhedral grain was observed with incipient reaction with the glass. Clinopyroxene textures are similar to olivine. Plagioclase textures range from heavily resorbed and sieved in medium to larger phenocrysts to euhedral microphenocrysts. Large xenocrysts are visible and show signs of advanced melting at crystal edges. This mix of textures is consistent with a system wavering in and out of chemical and thermal equilibrium, likely a result of advanced mixing and assimilation of crustal rock (Grove *et al.*, 1982).

The final of the four X lava populations is the Two Finger Flow. It has previously been grouped with MKLV, but demonstrates affinities with X deposits. The Two Finger Flow was probably the first lava eruption after the X lavas and lahars, estimated to have erupted between 1510 – 1535 CE (Clynne *et al.*, 2005). The paleomagnetic direction of the Two Finger Flow measured by Hagstrum *et al.*, (2002) closely matches that of a sample they called a mixed magma hot lahar. The lahar, located near the Two Finger Flow and described as a transitional flow, is probably an X lahar, but was grouped in with other middle Kalama lavas because it represented the first intermediate composition identified during the Kalama. Hagstrum *et al.* (2002) grouped the Two Finger Flow in with middle Kalama lavas, probably because X deposits were not widely identified or acknowledged as geochemically distinct. Regardless, the flow's paleomagnetic direction is similar to that of Worm Complex and other western flank andesites, but most closely corresponds to the hot lahar. If this

flow is the last one which displays the geochemical signature consistent with the X rocks, this may constrain the timing of magmatic interaction of its source material. Local paleomagnetic anomalies have been observed at Mount St. Helens, so these observations must be considered along with geochemical data from the rocks.

Geochemical data relate the Two Finger Flow to the X deposits. Bulk rock major elements portray the Two Finger Flow as a transitional composition between basaltic andesite X lahars and other middle Kalama intermediates (Figure 5.29). In all measured trace elements with SiO_2 on the abscissa, the Two Finger Flow plots among the X tephra and lahars, and higher than the middle Kalama lavas (Worm Complex, western flank) and pyroclastic flow, except for Cs and Pb, which are slightly lower (Figure 5.37). The Two Finger Flow also plots among X lahars and tephra on ratio-element and ratio-ratio trace element diagrams (Figure 5.39). A divergence between a dacite and late Kalama andesite trend and the middle Kalama plus QMI 19 trend is clear in fluid mobile elements such as Ba, U and Th. This pattern is even more evident in ratio-element diagrams La vs. La/Yb and La/Gd and Ho vs. Ce/Ho.

Olivines, which occur in the Two Finger Flow as glomerocrysts with plagioclase and pyroxene, are larger than other phenocrysts in the lava. The glomerocrysts could either be disaggregated crystals from a holocrystalline cumulate source or droplets of another magma (Bacon, 1986; Browne *et al.*, 2006). Regardless of their nature, olivine measured in the flow (Fo_{63-76}) crystallized along a relatively flat trend in which Ni is positively correlated with the Fo content of the olivine (Figure 5.63). However, the relatively flat, constant slope, compared to the trend of QMI 19 and X lahar 01, suggests

olivine from the Two Finger Flow crystallized almost entirely from mixed magmas, (Straub *et al.*, 2008). Olivine crystallizing in a closed system follows a steep, non-linear trend as Ni is heavily partitioned into olivine from a more mafic magma, as seen in the near vertical trend of X lahar 01 and the plutonic inclusion from EKPF 24 (Figure 5.63). Conversely, olivine crystallizing from mixed magmas are expected to follow a more shallow and straight magma mixing line (Straub *et al., 2008).*

The Two Finger Flow also shows a striking geochemical resemblance to the olivine-rich QMI population. The most An-rich zones from QMI 19 plagioclase lie along the same trend as the most An-rich zones of plagioclase from the Two Finger Flow on an An vs. MgO diagram. The highest An contents measured in the Two Finger Flow (i.e. plagioclase 11.3) are comparable to those from population L, but the grains are smaller (~ <0.5 mm) (Figure 6.16). The overlap between plagioclase crystallized from the two melts is also apparent in TiO_2 and FeO* data, but less well-defined (Figure 6.17). Considering the similarity in trace element concentrations between the two lavas, it is evident that QMI 19 and the Two Finger Flow share a basaltic source.

QMI 19 could be a modified mixing end member to the X deposits and Two Finger Flow. Bulk rock major and trace elements of X deposits show a discrete trend slightly offset from other Kalama rocks in most cases. The olivine-rich QMIs anchor the mafic end of these trends. Of particular note is the Nb-Ta and other HFSE enrichment in X deposits. As previously discussed, QMI 19 comprises plagioclase and olivine of similar composition to X tephra and lahars. Figure 5.63 shows that olivine from QMI 19 are more Fo-rich than X lahars, but that both of these types of deposits have fractionation

asymptote trends as described by Straub *et al,* (2008). The Two Finger Flow is consistently more evolved and primarily displays linear mixing trends between the QMI and an unidentified end member. The combination of these lines of evidence lead to the interpretation that the olivine-bearing QMI population could be a modified parent to X tephra and lahars.

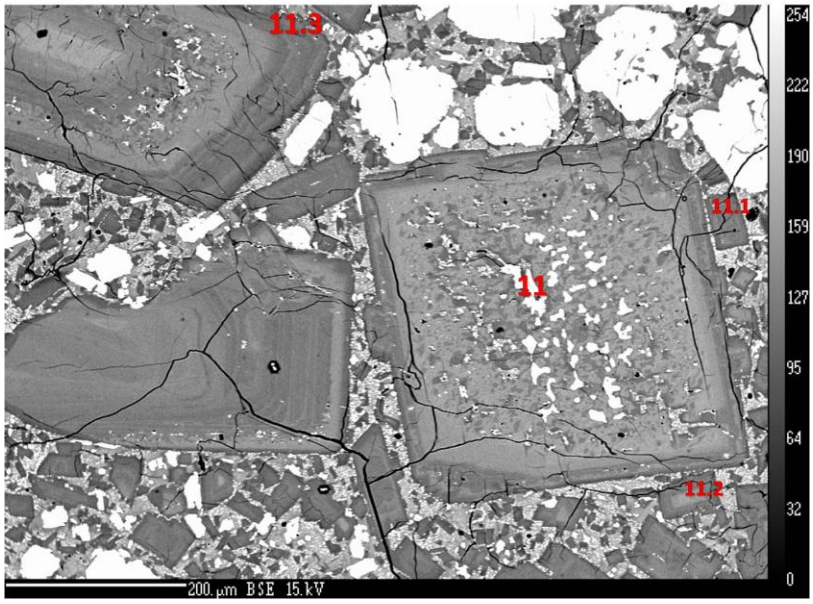

Figure 6.16 BSE image of Two Finger Flow 10 plagioclase 11, 11.3 and microphenocrysts 11.1 and 11.2.

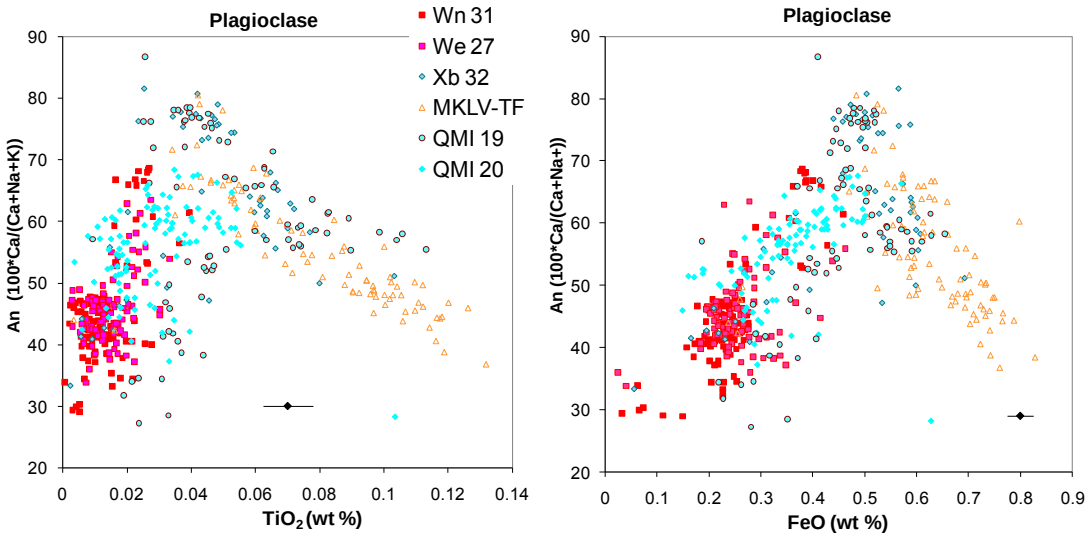

Figure 6.17 An content vs. TiO_2 and FeO* of selected lithologies. Representative 1 s error for MgO shown in bottom right corner.

Less convincing, but still viable, are geochemical and geophysical data (previously discussed paleomagnetic data) that relate the Two Finger Flow to other middle Kalama intermediate rocks. Whereas the Two Finger Flow trace elements show a Nb-Ta enrichment on a spider diagram like the X rocks, U, Th, and Cs, are higher than the QMI and closer to middle Kalama lava concentrations. Furthermore, sodic plagioclase from the Two Finger Flow overlap those of the Breadcrust Pyroclastic Flow 03 and Worm Complex lava 08A. Although Cr spinel were not observed in MKLVs, spinel from the Two Finger Flow are the most evolved (possibly decompressed) of those analyzed for this study.

X lavas and tephras erupted during the middle Kalama are distinct in many ways from the MKLVs: mineralogically, texturally, and chemically. X deposits also appear to have a genetic relationship to the olivine-rich QMI population found in EKPFs. The chemistry and petrographic descriptions of the olivine-rich QMI group may help constrain the evolution of the X magmatic sequence. M-type lahars (01 and 07) are nearly as primitive as QMI 19 (X lahar 01 is slightly higher in Cr and Ni), and they likely correspond to the Xm tephra. A mixture of ~25% Wn added to the bulk rock composition (liquid and crystal mixture) of X lahar 01 produces a composition close to Xb 32 tephra and B-type lahars (02 and 09). It was not possible within the scope of this study to quantitatively determine if 25% liquid and crystals from Wn occurs in Xb 32 and B-type lahars, but qualitative evidence shows significant mixing occurred to produce these lavas and tephra. The two glass populations in X lahar 02, and two apparent plagioclase populations (sodic plagioclase of An_{32-60} with low MgO and calcic plagioclase of An_{50-82} with

higher MgO) in Xb 32 suggest mixture with felsic magma. The opacite rims on amphiboles in the X samples also demonstrate disequilibrium conditions. The X tephras and lavas represent the first significant mafic input into the system during the Kalama Period. While many of these deposits have been recognized in previous work, X lava 30 and X lahars were either treated as a single composition (Xb), ignored, or not recognized. Subtle (and sometimes obvious) chemical and textural differences provide important information used to characterize the evolution of the system during the most dynamic period, the time between the early and middle Kalama.

6.2.6. Middle Kalama Lavas (MKLVs)

The middle Kalama continued with primarily effusive eruptions of lava flows and one known pyroclastic flow. The MKLVs appear to be transitional lavas on a continuum between the X and the other middle Kalama mafic end member. Major elements of the Worm Complex lavas plot between the X trend and other middle Kalama rocks, while the western flank lava (MKLV-WF) 16 and MKPF 03 consistently plot closer to the main dacite-plutonic inclusion trend. Mitten Flow measurements (not from this study) plot both among Worm Complex and MKPF deposits in K_2O, MgO, and TiO_2 (Figure 5.29). Other major elements such as Na_2O, CaO, and FeO* are too tight in range to discern differences between the lavas and pyroclastic flow and X deposits. Trace elements demonstrate the same trends with MKLV as transitional compositions between X deposits and the more silicic rocks (Figures 5.37 and 5.39).

Plagioclase data from MKPF 03 and the Worm Complex lava 08A suggest the magmas were well-mixed prior to eruption since most of the

compositions are neither on the high An, MgO nor low An, MgO ends of the spectrum (Figure 6.18). Pyroxene data also suggest chemical mixing occurred. Clinopyroxene grain 5 (and possibly 10) has a core that grew in a more Cr-rich basalt than the rim and mantle of the crystal (Figures 5.59, 5.60 and 5.61).

Investigation whether MKLV (i.e. Worm Complex and western flank) and MKPF 03 evolved from QMIs 20 and 22 is relevant. Trace element patterns of QMI 20 on spider diagrams are consistently lower than the MKLV and MKPF patterns and do not cross cut them (Figure 5.34). The greatest divergence is in the HFSEs Nb, Ta, Hf, and Zr, and in the LREEs La and Ce. It is possible the lavas and pyroclastic flow from later in the middle Kalama could have evolved from the same source as the olivine-poor QMI group. That is to say, it is plausible that MKLV has a significant chemical influence from plutonic rocks that lie beneath Mount St. Helens in addition to the other sources that fed the olivine-poor QMI population.

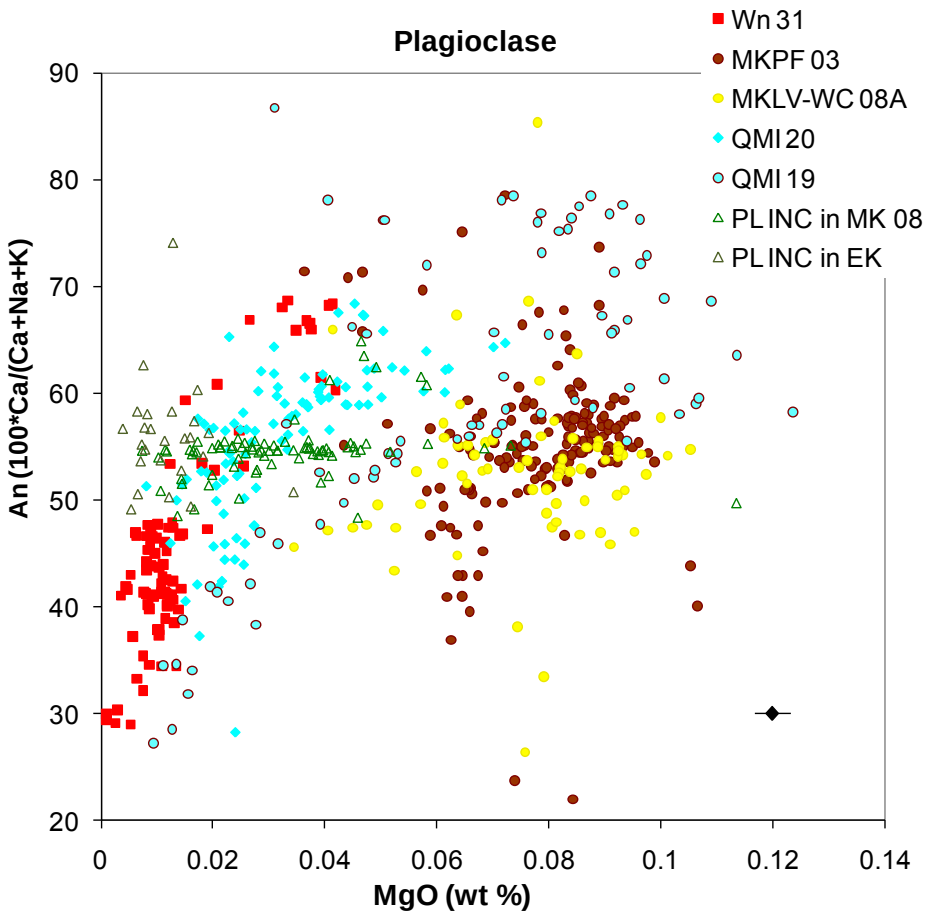

Figure 6.18 An content vs. MgO in plagioclase of selected lithologies. Note the location of the plutonic inclusions and QMI 20 in relation to MKPF 03 and MKLV-WC 08A. Representative 1 s error for MgO shown in bottom right corner.

6.3 Relationship Between Early and Late Kalama Dacites

The late Kalama saw eruptions of crystal-rich summit domes. The early summit domes (SDO) found in pyroclastic flow deposits are more vesicular than the later summit dome (SDY), indicating efficient degassing throughout the late Kalama. Because of this, the early Kalama deposits are significantly more pumiceous and vesicular than those from the late Kalama.

Although differences between the early and late Kalama do exist, they are not significant enough to conclude they have different mixing end members. However, because many trace element abundance in the last rocks to erupt during the Kalama Period (SDY) were lower than the early Kalama dacites abundances (Figure 5.37), there may be another component involved in the petrogenesis of the summit domes (SDO and SDY). The prevalence of plutonic inclusions and xenocrysts indicate the crustal anatexis may contribution chemically to the late Kalama-age rocks. Plagioclase data support this hypothesis. Crystals from late Kalama dacites form two trends, than follow the same paths, but are offset (Figure 6.19). The higher An/MgO trend consists primarily of core analyses, whereas the lower trend is made up of mostly rim analyses. There is some overlap with crystals from early Kalama dacites, but there is significant overlap between grains from QMI 20, plutonic inclusions and the cores from SDO and SDY. The compositions of the plagioclase cores correlate very closely with those from plutonic inclusions.

Early and late Kalama dacites demonstrate different degrees of mixing, assimilation and fractionation between the same end members. However, the late Kalama probably includes another component, or if the magma chamber were zoned, a different section was tapped.

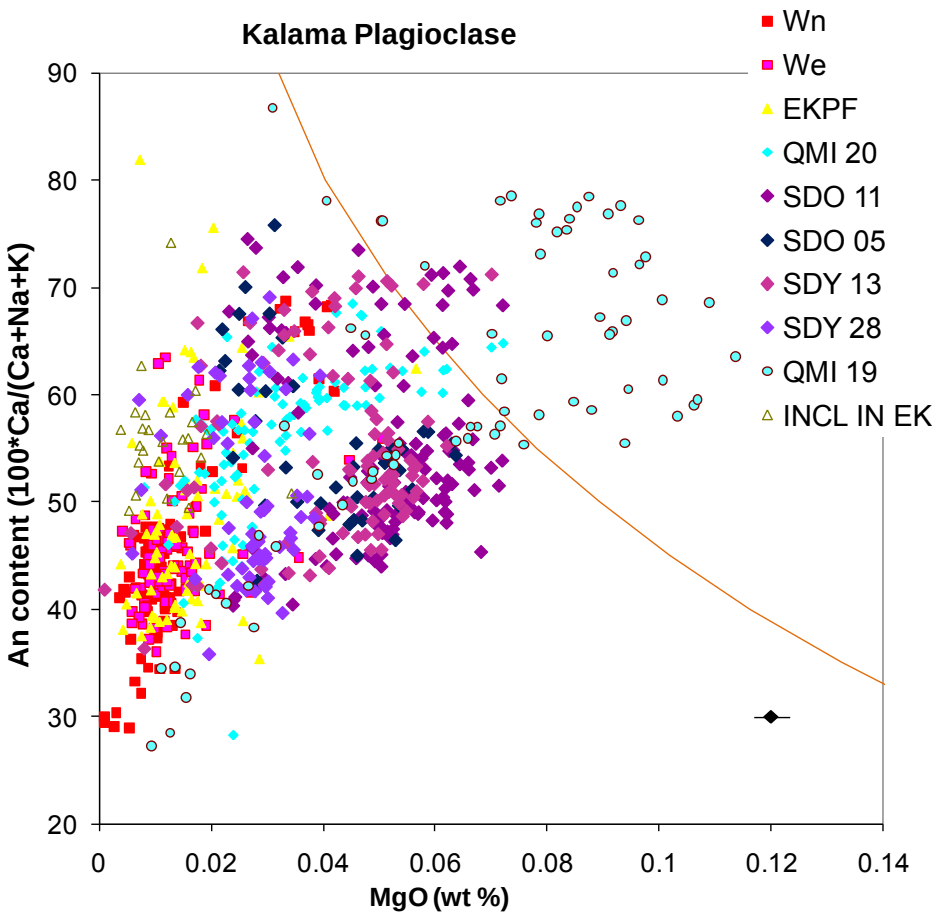

Figure 6.19 An vs. MgO of plagioclase from early and late Kalama rocks as well as QMIs. Plagioclase from the late Kalama show a higher An/MgO trend, which comprise predominantly core analyses and a lower An/MgO trend, which comprise mostly rims analyses. The line for Two Finger Flow data as in Figure 5.55. Representative 1 s error for MgO shown in bottom right corner.

6.4 Implications

New petrography, whole rock trace element and phase chemistry data have been combined with whole rock major element data to constrain magmatic components in the Mount St. Helens system during the Kalama Eruptive Period. Previous models of Kalama-age rocks have not considered the quenched mafic and plutonic inclusions, and it appears that assimilation of cumulate and crustal material is significant in the formation of both the

silicic and intermediate rocks (Figure 6.20). This was determined through the delineation of the two QMI groups and the relative contribution of xenocrystic material (both cumulate and non-cumulate in origin) to each. Additional constrains on the mafic mixing end member of the X deposits were provided from the olivine-rich QMI group.

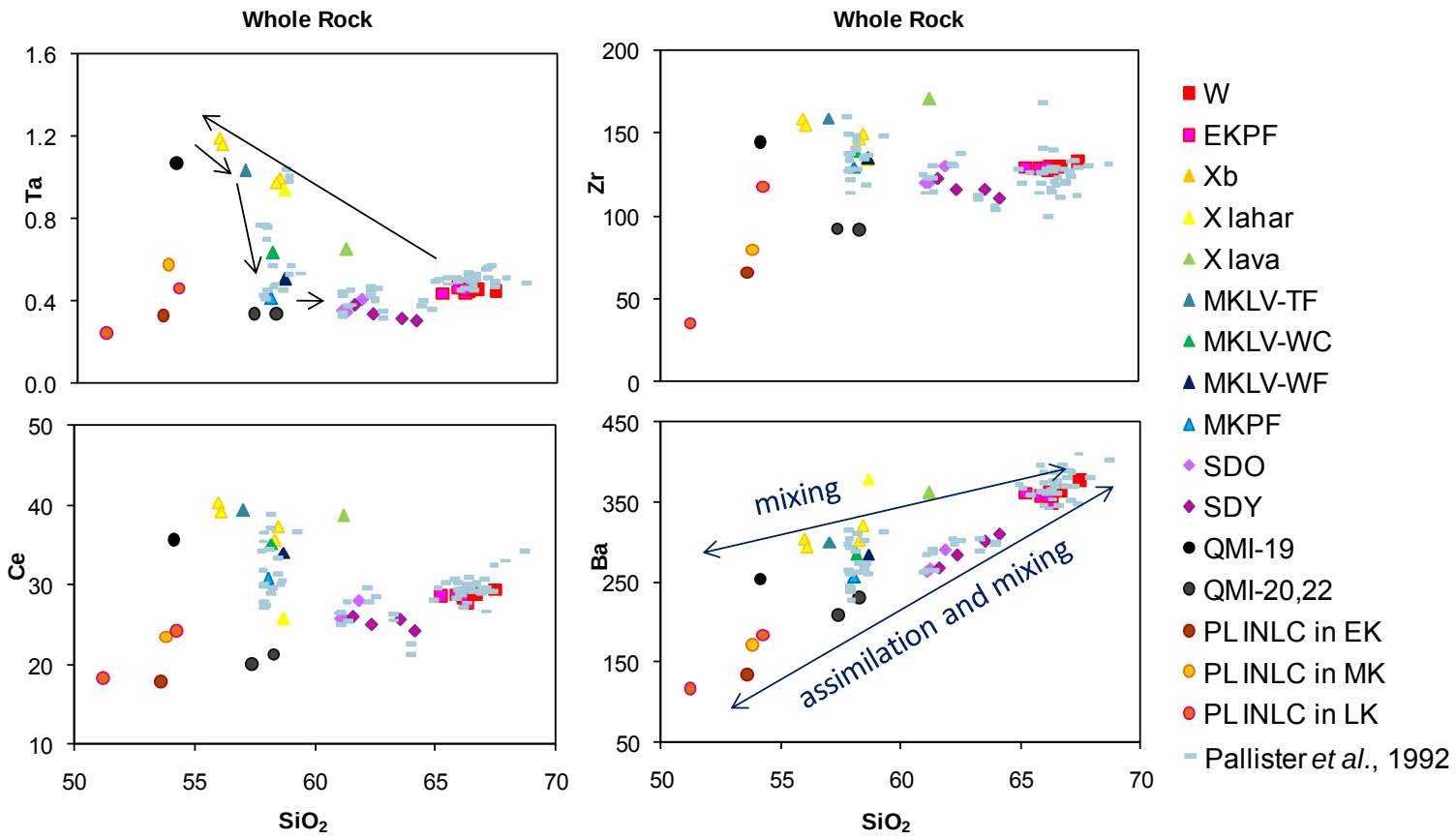

Figure 6.20 Whole rock trace element Harker diagrams. Pallister *et al.* (1992) data is plotted with data from this study to show both the overlap in compositions and the extended range of compositions included in the study. Black arrows on Ta graph represent stratigraphic sequence. The Ba graph notates the two generalized major mixing trends, the lower of which includes the olivine-poor QMI group as an intermediate composition between plutonic inclusions and Wn dacites. The blue arrow points left toward the parent of QMI 19.

6.5 Proposed Petrogenetic Model of the Kalama Eruptive Period

In conjunction with previous work on the rocks of the Kalama age, observations and interpretations of the textures and geochemical data gathered from this study are the basis for a proposed model for the evolution of the magmatic system. The model is illustrated in Figure 6.21. After several hundred years of repose, a felsic dacitic reservoir is intruded by a basalt with OIB-like chemistry, more primitive than QMI 19. Upon its ascent, the heat from basaltic magma begins to disaggregate the cumulate material. Basalt ponds at the base of the reservoir, but magmas begin to mix and mingle. The addition of the basalt leads to heating, inducing convection and overpressure within the chamber. The overpressure leads to eruption of the gas and H_2O-rich zone at the top of the chamber, which is also the most evolved and buoyant magma, Wn. After the large Plinian eruption, the pressure is relieved, and a dome begins to form. We, which is less gas and H_2O-rich than Wn, collects in the roof of the chamber. Continued interaction of the mafic magma leads to continued overpressure, which causes We to erupt with a slightly more mafic composition. The basalt begins to disrupt the interface between felsic & mafic magmas so that globules convect into the dacite magma space. This leads to the disaggregation of QMIs and to chemical mixing. Meanwhile, the olivine-poor QMI evolves by assimilating country rock by partial melting and incorporating plutonic material. Pyroclastic flows begin to erupt with QMIs in them. The early Kalama eruptions evacuate a significant amount of dacite from the chamber.

There is a short repose period, (~1-5 years) while the QMI 19 and X parent continues to mix with remaining dacite (25% dacite + 75 % basalt/basaltic andesite), but the magma reservoir remains heterogeneous.

Then the most buoyant magma of that mixture, Xb tephra, erupts followed by or coeval with B-type X lavas. The lavas likely erupted during a precipitous period, as the flows were carried away by lahars (and pyroclastic flows). Xs tephra erupts from the same zone after that, either from the same eruption or shortly thereafter. The more mafic zone of the chamber, which is scarcely mixed with the dacite, erupts Xm tephra and M-type X lavas. The lavas are also incorporated into lahar deposits and not preserved *in situ*. After degassing has depleted the reservoir of H_2O and other volatiles, the Two Finger Flow erupts on the south side of the volcano.

The remaining mafic magma evolves within the chamber, attempting to regain equilibrium. A second basalt or basaltic andesite intrusion occurs within the chamber, but with a more calc-alkaline composition. The reservoir composition transitions from the OIB-like character to that of the MKLV and MKPF. The small amount of remaining olivine and clinopyroxene is significantly reacted and resorbed. The X Lava Flow erupts, potentially along with Xh tephra. This is speculative, since there are no known chemical analyses of Xh ash. MKLV erupt on all sides of the volcano, with the majority of the volume in the Worm Complex flows on the southeast flank, relieving the pressure burden of the magma chamber.

As the chamber is degassed, a short repose period allows enough pressurization to erupt an andesitic dome. The dome is destroyed by subsequent pyroclastic flows, as dacite production continues, but with slightly different trace elements that early Kalama dacites. Finally, a large dome grows for approximately 100 years before the Kalama Period ceases with the dome in place.

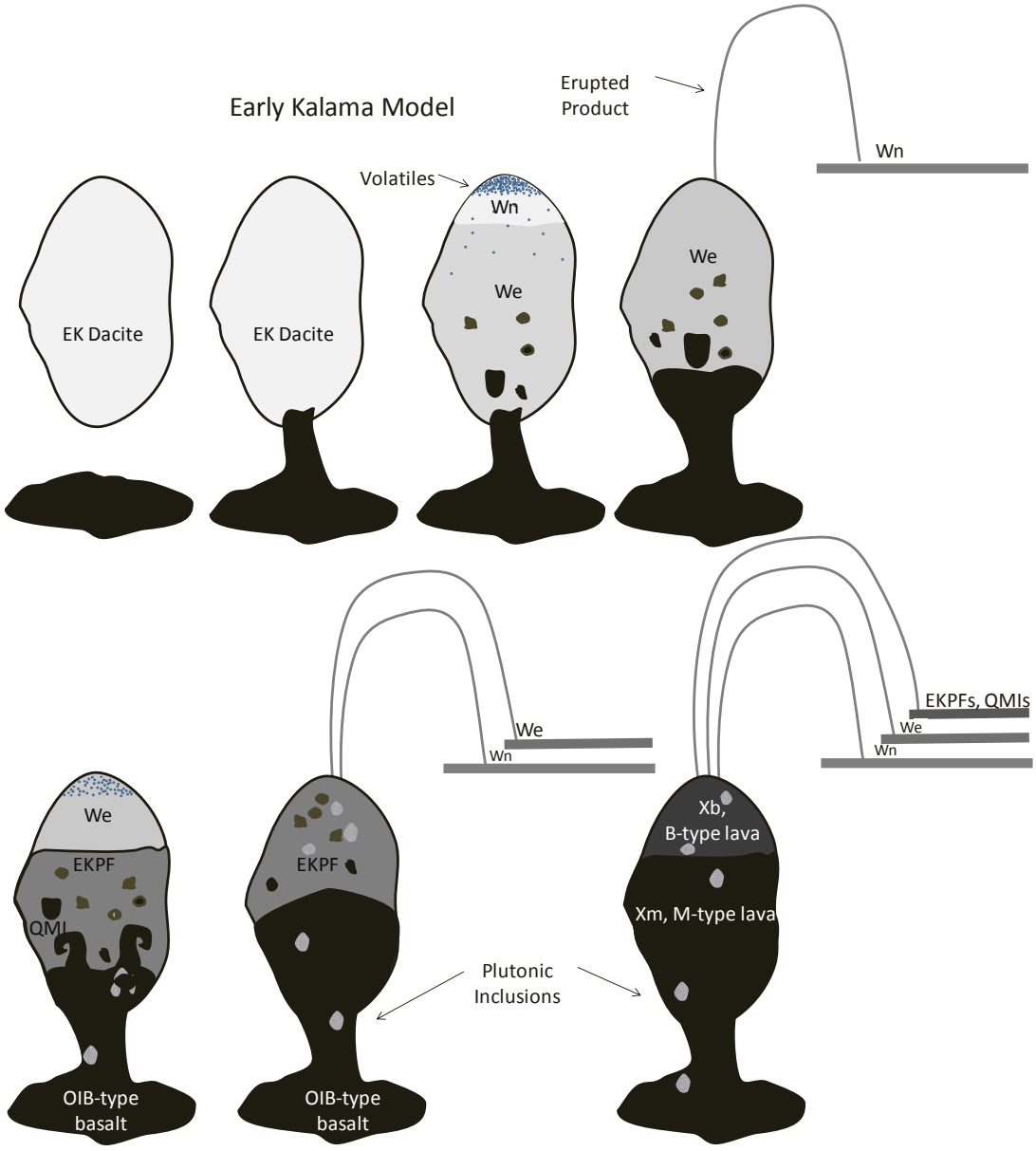

Figure 6.21 Proposed model for the petrogenetic evolution of the early and middle Kalama Periods. Each reservoir represents a successive period of time, beginning during the repose period and ending during the later part of the middle Kalama. Note the inclusion of the volatile-rich dacitic zone prior to the Wn and We eruptions, and the presence of plutonic inclusions.

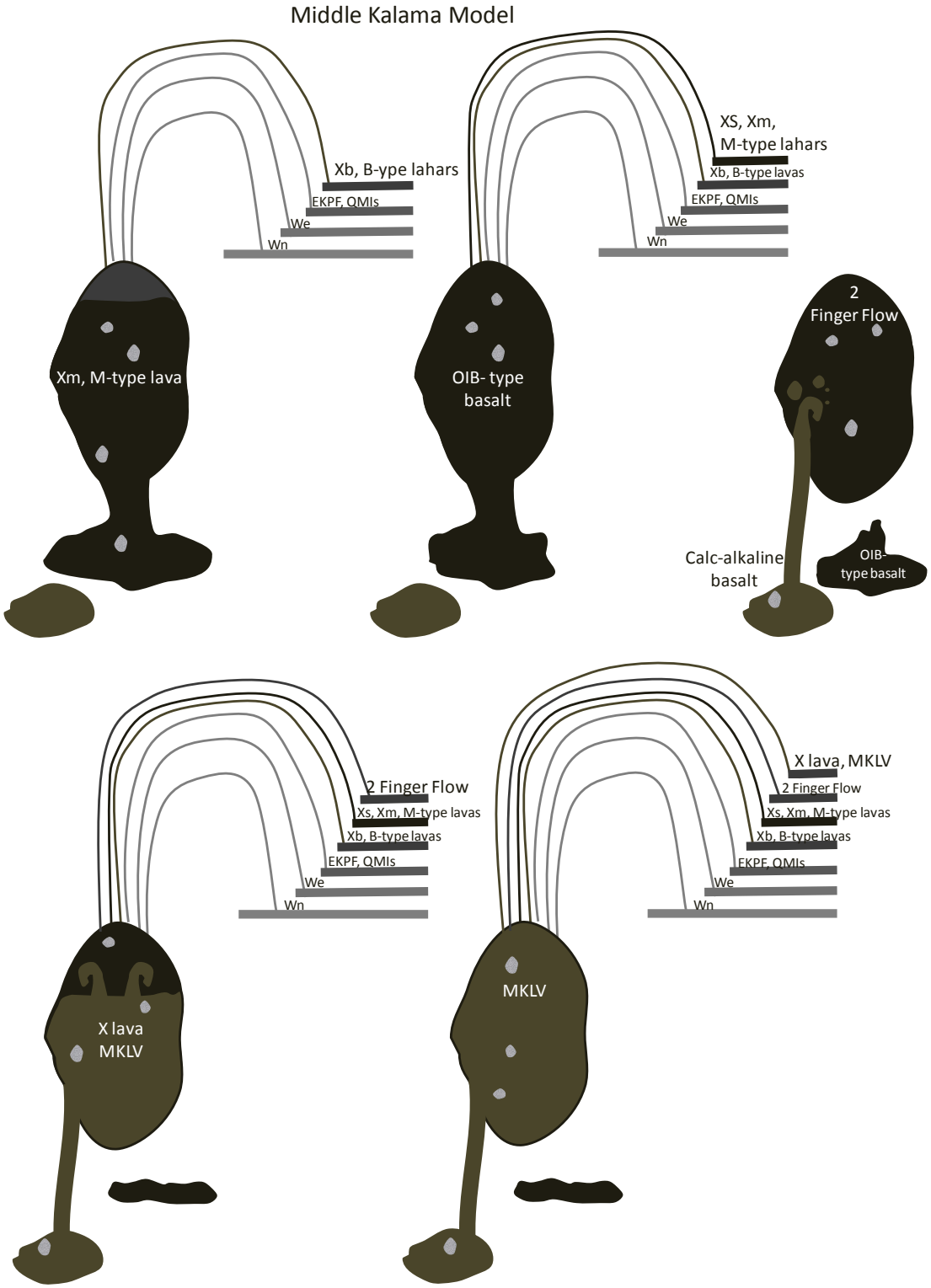

Figure 6.20 (Continued)

Chapter 7: Conclusion

Rocks from the Kalama Eruptive Period at Mount St. Helens provide a unique opportunity to investigate the magmatic inputs and interactions of an entire eruptive cycle that occurred within a 300 year time span. The rocks from the eruptive sequence of dacite, basaltic andesite, andesite and dacite, show evidence of various open and closed system evolutionary processes in their petrogenesis. New petrographic observations were integrated with new whole rock and phase EMP and LA-ICP-MS data and the known stratigraphy in order to constrain the magmatic and crustal components active during the Kalama Period.

There were at least three mafic source contributions at Mount St. Helens during the eruptive period. Two populations of QMI display distinct petrographic and geochemical character. Major element modeling shows crustal anatexis of plutonic inclusions found on EKPFS could produce the felsic magma source of the olivine-poor QMIs. This QMI group experienced more extensive hybridization between the dacite and the mafic end member. The mafic end member of the olivine-poor QMI population is not well-constrained, but could be the same calc-alkaline basalt seen later in the middle Kalama.

The early Kalama saw a progressive increase in the amount of mafic input that interacted with the dacitic host. An evolved daughter of one of the mafic parents was sampled in the olivine-rich QMI found in EKPF with an OIB-like geochemical signature. This parent also incorporated mafic cumulate material upon its ascent, evident from petrography and whole rock, olivine, and plagioclase chemistry. The olivine and pyroxene-rich cumulate material

experienced progressive disaggregation, leading to varying degrees of mingling and mixing with the felsic host magma. Minerals and glomerocrysts of cumulate origin were traced from the early Kalama in the olivine-rich QMIs through the X deposits. Their abundances waned during the later part of the middle Kalama and the early part of the late Kalama.

The Two Finger Flow has previously been mapped as a MKLV, but its petrographic, mineralogical and geochemical (and possibly paleomagnetic) signatures have closer affinities to X deposits than the MKLV. It was probably the last lava to erupt with the HFSE enrichment distinctive of the olivine-rich QMI group and X magma, signifying the end of the input of the OIB-like basalt. The X *in situ* lava, while grouped with X lavas, has a geochemical signature unique from other Kalama-age rocks. The trace element signatures suggest this andesite had a history unlike other middle Kalama-age lavas.

The third mafic source identified was first positively recognized in the middle Kalama, and is the calc-alkaline parent to the MKLV and SDO. It may have emerged as early as the EKPFs in the olivine-poor QMI group. Rocks analyzed with this calc-alkaline basalt as a mafic mixing end member harbor a trace element signature different from the olivine-rich QMI and X deposits, and the phase chemistry suggests it was well-mixed with the felsic host.

The magma reservoir at Mount St. Helens has sometimes been modeled as a single, elongate chamber (Pallister *et al.*, 1992). Multiple basaltic inputs have been recognized at the volcano, but not necessarily coeval with one another. If two different magmas with basaltic parents are represented in the QMIs during the early Kalama, the coexistence of multiple basalts in the plumbing system could indicate a more complex magma chamber structure.

Further work on Kalama-age rocks could include identification of significant events within the magma reservoir through correlation of crystal compositional changes. This could be accomplished by comparison of the plagioclase transects that were analyzed by EMPA. Additionally, isotopic work would allow quantification of the amount of crustal contamination in the system and fingerprinting of both the basaltic and felsic components in the mixed magmas.

Bibliography

Anderson Jr., A.T., Swihart, G.H., Artioli, G., Geiger, C.A., 1984, Segregation vesicles, gas filter-pressing, and igneous differentiation: The Journal of Geology, v. 92, p. 55-72.

Asimow, P.D., Ghiorso, M.S., 1998, Algorithmic modifications extending MELTS to calculate subsolidus phase relations: American Mineralogist, v. 83, p. 1127-1131

Atwater, T., December 1970, Implications of plate tectonics for the Cenozoic tectonic evolution of Western North America: Geological Society of America Bulletin, v. 81, p. 3513-3536.

Bacon, C.R., May 1986, Magmatic inclusions in silicic and intermediate volcanic rocks: Journal of Geophysical Research. v. 91, p. 6091-6112.

Bédard, J.H., 2006, Trace element partitioning in plagioclase feldspar: Geochimica et Cosmochimica Acta, v. 70, p. 3717-3742.

Bindeman, I.N., David, A.M., Drake, M.J., 1998, Ion microprobe study of plagioclase-basalt partition experiments at natural concentration levels of trace elements: Geochimica et Cosmochimica Acta, v. 62, p. 1175-1193.

Blackwell, D.D., Steele, J.L., Frohme, M.K., Murphy, C.F., Priest, G.R., Black, G.L., 1990a, Heat flow in the Oregon Cascade Range and its correlation with regional gravity, Curie point depths, and geology: Journal of Geophysical Research, v. 95, p. 19475-19493.

Blackwell, D.D., Steele, J.L., Kelley, S., Korosec, M.A., 1990b, Heat flow in the state of Washington and thermal conditions in the Cascade Range: Journal of Geophysical Research, v. 95, p. 19495-19516.

Blundy, J., Cashman, K., October 2005, Rapid decompression-driven crystallization recorded by melt inclusions from Mount St. Helens volcano: Geology, v. 33, no. 10, p. 793-796.

Browne, B. L., Eichelberger, J. C., Patino, L. C., Vogel, T. A.; Dehn, J., Uto, K., Hoshizumi, H., February 2006, Generation of porphyritic and equigranular mafic enclaves during magma recharge events at Unzen Volcano, Japan: Journal of Petrology, v. 47, no. 2, p. 301-328.

Bohrson, W.A., Spera, F. J., November 2007, Energy-constrained recharge, assimilation, and fractional crystallization (EC-RAxFC): a visual basic computer code for calculating trace element and isotope variations of open-system magmatic systems: Geochemistry, Geophysics, Geosystems, v. 8, no. 11, 11 p.

Bowen, N.L., 1928, The Evolution of the Igneous Rocks: Princeton, University Press, Princeton, 332 p.

Carey, S., Gardner, J., and Sigurdsson, H., 1995, The intensity and magnitude of Holocene plinian eruptions of Mount St. Helens volcano: Journal of Volcanology and Geothermal Research, v. 66, p. 185–202.

Carroll, K., 2009, Mixing Components and Dynamics of Kalama Period Intermediate Magmas at Mount St. Helens: Evidence from Mafic Phenocrysts, M.S. thesis, Portland State University, Oregon, 305 p.

Chakraborty, S. ,1997, Rates and mechanisms of Fe-Mg interdiffusion in olivine at 980°–1300°C, Journal of Geophysical Research, v. 102, no. B6, p. 12317-12331.

Christiansen, R.L., McKee, E.H., 1978, Late Cenozoic volcanic and tectonic evolution of the Great Basin and Columbia Intermontane regions: Geological Society of America Memoir, no. 152, p. 283-311.

Clynne, M. A., 1993, Mineralogic and geochemical constraints on the evolution and mantle sources of primitive tholeiitic and calk-alkaline lavas from the Lassen area, southernmost Cascade Range, California, Chapter 3 *in* Geologic studies of the Lassen volcanic center, Cascade Range, California. Ph.D. Thesis, University of California, Santa Cruz.

Clynne, M.A., January 1999, A complex magma mixing origin for rocks erupted in 1915, Lassen Peak, California: Journal of Petrology, v. 40, no. 1, p. 105-132.

Clynne, M. A., Borg, L.E., April 1997, Olivine and chromian spinel in primitive calc-alkaline and tholeiitic lavas from the southernmost Cascade Range, California; a reflection of relative fertility of the source: Canadian Mineralogist, v. 35, no. 2, p. 453-472.

Clynne, M.A., Ramsey, D.W., Wolfe, E.W., 2005, Pre-1980 eruptive history of Mount St. Helens, Washington. U.S. Geological Survey Fact sheet 2005-3045.

Conrey, R.M., Sherrod, D.R., Hooper, P.R., Swanson, D.A., 1997, Diverse primitive magmas in the Cascade arc, Northern Oregon and Southern Washington: Canadian Mineralogist, v. 35, p. 367-396.

Coombs, M.L., Eichelberger, J.C., Rutherford, M.J., January 2002, Experimental and textural constraints on mafic enclave formation in volcanic rocks: Journal of Volcanology and Geothermal Research, v. 119, no. 1-4, p. 125-144.

Cooper, K.M.; Reid, M.R., August 2003, Re-examination of crystal ages in recent Mount St. Helens lavas; implications for magma reservoir processes: Earth and Planetary Science Letters, v. 213, no. 1-2, p. 149-167.

Costa, F., Dungan, M., October 2005, Short time scales of magmatic assimilation from diffusion modeling of multiple elements in olivine: Geology, v. 33, p. 837-840.

Crandell, D.R., 1987, Deposits of pre-1980 pyroclastic flows and lahars from Mount St. Helens Volcano, Washington: U.S. Geological Survey Professional Paper 1444, 91p.

Deer, W.A., Howie, R.A., Zussman, J., 1963**,** An introduction to the rock-forming minerals: Prentice Hall, San Francisco, 696 p.

Defant, M.J., Drummond, M.S., 1990, Derivation of some modern arc magmas by melting of young subducted lithosphere: Nature, v. 347, p. 662-665.

Defant, M.J., Drummond, M.S., 1990, A model for trondhjemite-tonalite-dacite genesis and crustal growth via slab melting: Archean to modern comparisons: Journal of Geophysical Research, v. 95, p. 21,503-21,521.

Defant, M.J., Drummond, M.S., June 1993, Mount St. Helens: potential example of the partial melting of the subducted lithosphere in a volcanic arc: Geology, v. 21, p. 547-550.

Dungan, M.A., Davidson, J., 2004, Partial assimilative recycling of the mafic plutonic roots of arc volcanoes: An example from the Chilean Andes: Geology, v. 32, p. 773-776.

Eichelberger, J.C., 1981, Mechanism of magma mixing, Medicine Lake Highland Volcano, California: Guides to some volcanic terranes in Washington, Idaho, Oregon, and northern California. Johnston, D.A., Donnelly-Nolan, J., eds., U.S. Geological Survey circular, p. 183-189.

Ewart, A., Griffin, W.L., 1994, Application of proton-microprobe data to trace-element partitioning in volcanic rocks: Chemical Geology, v. 117, p. 251-284.

Gardner, J. E., Rutherford, M., Carey, S., 1995a, Experimental constraints on pre-eruptive water contents and changing magma storage prior to explosive eruptions of Mount St. Helens volcano: Bulletin of Volcanology, v. 57, p. 1-17.

Gardner, J.E., Carey, S., Rutherford, M.J., Sigurdsson, H., 1995b, Petrologic diversity in Mount ST. Helens dacites during the last 4,000: implications for magma mixing: Contributions in Mineralogy and Petrology, v. 119, p. 224-238.

Ghiorso, M. S., Sack, R. O., 1995, Chemical Mass Transfer in Magmatic Processes. IV. A Revised and Internally Consistent Thermodynamic Model for the Interpolation and Extrapolation of Liquid-Solid Equilibria in Magmatic Systems at Elevated Temperatures and Pressures: Contributions to Mineralogy and Petrology, v. 119, p. 197-212.

Gill, J., 1981, Orogenic Andesites and Plate Tectonics: Springer-Verlag, New York, 390 p.

Ginibre, C., Wörner, G., Kronz, A., 2002, Minor- and trace-element zoning in plagioclase: implications for magma chamber processes at Parinacota volcano, northern Chile: Contribution to Mineralogy and Petrology, v. 143, p. 300-315.

Guffanti, M., Weaver, C.S., June 1988, Distribution of Late Cenozoic volcanic vents in the Cascade Range: volcanic arc segmentation and regional tectonic considerations: Journal of Geophysical Research, v. 93, p. 6513-6529.

Hagstrum, J.T., Hoblitt, R.P., Gardner, C.A., Gray, T.E., 2002, Holocene geomagnetic secular variation recorded by volcanic deposits at Mount St. Helens, Washington: Bulletin of Volcanology, v. 63, p. 545-556.

Hausback, B.P., 2000, Geologic Investigations Series - U. S. Geological Survey Geologic map of the Sasquatch Steps area, north flank of Mount St. Helens, Washington.

Hart, S.R., Allègre, C.J., 1980, Trace element constraints on magma genesis, Chapter 4 *in* Hargraves, R.B., ed, Physics of Magmatic Processes.

Heliker, C., 1995, Inclusions in Mount St. Helens dacite erupted from 1980 through 1983: Journal of Volcanology and Geothermal Research, v. 66, p. 115-135.

Hildreth, W., 2007, Quaternary magmatism in the Cascades—Geologic Perspectives: U.S. Geological Survey Professional Paper 1744.

Hildreth, W., Moorbath, S., 1988, Crustal contributions to arc magmatism in the Andes of Central Chile: Contributions to Mineralogy and Petrology, v. 98, p. 455-489.

Hoblitt, R.P., Crandell, D. R., Mullineaux, D. R., 1980, Mount St. Helens eruptive behavior during the past 1,500 yr: Geology, v. 8, p. 555-559.

Hopson, C.A., Melson, W.G, September 1990, Compositional trends and eruptive cycles at Mount St. Helens: Geoscience Canada, v. 17, no. 3, pp. 131-141.

Humphreys, M.C.S., Blundy, J.D., Sparks, S.J., December 2006, Magma evolution and open-system processes at Shiveluch Volcano; insights from phenocryst zoning**:** Journal of Petrology, v. 47, n. 12, p. 2303-2334.

Iddings, J. P., 1909, Igneous Rocks: Composition, Texture and Classification, Volume 1: John Wiley and Sons, New York, 464 p.

Johnson, D.M., Hooper P.R., Conrey, R.M.,1999, XRF analysis of rocks and minerals for major and trace elements on a single low dilution Li-tetraborate fused bead**:** Advances in X-ray Analysis, v. 41, p. 843-867.

Kent, A.J.R., Rowe, M.C., Thornber, C.R., Pallister, J.S., 2008, Trace element and Pb-isotope composition of plagioclase from dome samples from the 2004–2005 eruption of Mount St. Helens, Washington, Chapter 35 *in* Sherrod, D.R., Scott, W.E., Stauffer, P.H., eds., A Volcano Rekindled: The Renewed Eruption of Mount St. Helens, 2004-2006: U.S. Geological Survey Professional Paper 1750.

Kent, A.J.R., Jacobsen, B., Peate, D.W., Waight, T.E., Baker, J.A., November 2004, Isotope dilution MC-ICP-MS rare earth element analysis of geochemical reference materials NIST SRM 610, NIST SRM 612, NIST SRM 614, BHVO-2G, BHVO-2, BCR-2G, JB-2, WS-E, W-2, AGV-1 and AGV-2: Geostandards and Geoanalytical Research, v. 28, no. 3, p. 417-429.

Kent, A.J.R., Stolper, E.M., Francis, D., Woodhead, J., Frei, R., and Eiler, J., 2004, Mantle heterogeneity during the formation of the North Atlantic Tertiary Province: Constraints from trace element and Sr-Nd-Os-O isotope systematics of Baffin Island picrites: Geochemistry Geophysics Geosystems, v. 5.

Knaack, C., Cornelius, S., Hooper, P.R., 1994, Trace element analysis of rocks and minerals by ICP-MS, Open File Report, Department of Geology, Washington State University.

Le Bas, M.J., Maitre, L.E., Streckeisen, B.Z., IUGS Subcommission on the Systematics of Igneous Rocks, 1986, A Chemical Classification of Volcanic Rocks Based on the Total Alkali-Silica Diagram: Journal of Petrology, v. 27, p. 745-750.

Leeman, W., D. Smith, W. Hildreth, Z. Palacz, and N. Rogers, 1990, Compositional Diversity of Late Cenozoic Basalts in a Transect Across the Southern Washington Cascades: Implications for Subduction Zone Magmatism: Journal of Geophysical. Research, v. 95, no. B12, p.19561-19582.

Lindsley, D. H., June 1983, Pyroxene thermometry: American Mineralogist, v. 68, no. 5-6, p. 477-493.

Luhr, J.F., Carmichael, I.S.E., 1985, Jorullo Volcano, Michoacán, Mexico (1759-1774): The earliest stages of fractionation in calc-alkaline magmas: Contributions to Mineralogy and Petrology, v. 90, p. 142-161.

Martin, V.M., Pyle, D.M., Holness, M.B., August 2006, The role of crystal frameworks in the preservation of enclaves during magma mixing: Earth and Planetary Science Letters, v. 248, p. 787-799.

McBirney, A. R., 1978, Volcanic evolution of the Cascade range: Annual Review of Earth and Planetary Sciences, v. 6, p. 437-456.

McBirney, A.R., May 1980, Mixing and unmixing of magmas: Journal of Volcanology and Geothermal Research, v. 7, no. 3-4, p. 357-371.

McDonough, W.F., Sun, S.S., 1995, The composition of the Earth, Chemical Geology, v. 120, 228 p.

Miyashiro, A., 1974, Volcanic rock series in island arcs and active continental margins: American Journal of Science, v. 274, p. 321-355.

Morimoto, N., chair, Subcommittee on Pyroxenes, 1989, Nomenclature of Pyroxenes: Canadian Mineralogist, v. 27, p. 143-156.

Mullineaux, D. R., 1996, Pre-1980 Tephra-fall deposits erupted from Mount St. Helens, Washington: U.S. Geological Survey Professional Paper 1563.

Mullineaux, D.R., Crandell, D.R., 1981, The eruptive history of Mount St. Helens: IN: Lipman, P.W., and Mullineaux, D.R., (eds.), 1981, The 1980

Eruptions of Mount St. Helens, Washington: U.S. Geological Survey Professional Paper 1250, 844 p.

Nelson, S.T., Montana, A., December 1992, Sieve-textured plagioclase in volcanic rocks produced by rapid decompression: American Mineralogist, v. 77, no 11-12, p. 1242-1249.

Pallister, J.S., Hoblitt, R.P., Crandell, D.R., Mullineaux, D.R., 1992, Mount St. Helens a decade after the 1980 eruptions: magmatic models, chemical cycles, and a revised hazards assessment: Bulletin of Volcanology, v. 54, p. 126-146.

Pallister, J.S., Thornber, C.R., Cashman, K.V., Clynne, M.A., Lowers, H.A., Mandeville, C.W., Brownfield, I.K., Meeker, G.P., 2008, Petrology of the 2004–2006 Mount St. Helens lava dome—implications for magmatic plumbing and eruption triggering, Chapter 30 *in* Sherrod, D.R., Scott, W.E., Stauffer, P.H., eds., A Volcano Rekindled: The Renewed Eruption of Mount St. Helens, 2004-2006: U.S. Geological Survey Professional Paper.

Peters, M.T., Shaffer, E.E., Burnett, D.S., Kim, S.S., July 1995, Magnesium and titanium partitioning between anorthite and Type B CAI liquid; dependence on oxygen fugacity and liquid composition: Geochimica et Cosmochimica Acta, v. 59, p. 2785-2796.

Pouchou, L. J., Pichoir, F., 1984, New model quantitative x-ray microanalysis, Application to the analysis of homogeneous samples: Research in Aerospace, v. 3, p. 13-38.

Priest, G.R., 1990, Volcanic and Tectonic Evolution of the Cascade Volcanic Arc, Central Oregon: Journal of Geophysical Research, v. 95, p. 19583-19599.

Raleigh, C.B., Talbot, J.L., 1967, Mechanical twinning in naturally and experimentally deformed diopside: American Journal of Science, v. 265, p. 151-165.

Riddihough, R., 1984, Recent movements of the Juan de Fuca plate system: Journal of Geophysical Research, v. 89, p. 6980–6994.

Rollinson, H., 1993, Using Geochemical Data: Evaluation, Presentation, Interpretation: Longman, Essex, 352 p.

Ruprecht, P., Wörner, G., 2007, Variable regimes in magma systems documented in plagioclase zoning patterns: El Misti stratovolcano and Andahua monogenetic cones: Journal of Volcanology and Geothermal Research, v. 165, no. 3-4, p. 142-162.

Scandone, R. and Malone, S. D., 1985, Magma supply, magma discharge and readjustment of the feeding system of Mount St. Helens during 1980: Journal of Volcanology and Geothermal Research, v. 11, p. 239-262.

Schmidt, M. E., Grander, A.L., Rowe, M.C., 2008, Segmentation of the Cascade Arc as indicated by Sr and Nd isotopic variation among diverse primitive basalts: Earth and Planetary Science Letters, v. 266, p. 166-181.

Smith, D.R., 1980, The mineralogy and phase chemistry of silicic tephras erupted from Mount St. Helens volcano, Washington, M.S. thesis, Rice University, Houston, Texas, 158 p.

Smith, D. R., 1984, The petrology and geochemistry of High Cascade volcanics in southern Washington: Mount St. Helens volcano and the Indian Heaven basalt field, Ph.D. dissertation, Rice University, Houston, Texas, 409 p.

Smith, D.R., Leeman, W.P., March 1982, Mineralogy and phase chemistry of Mount St. Helens tephra sets W and Y as keys to their identification: Quaternary Research, v. 17, no. 2, p. 211-217.

Smith, D.R., Leeman, W.P., September 1987, Petrogenesis of Mount St. Helens dacite magmas: Journal of Geophysical Research, v. 92, no. B 10, p. 10,313 – 10,334.

Smith, D.R., Leeman, W.P., 1993, The origin of Mount St. Helens andesites: Journal of Volcanology and Geothermal Research, v. 55, p. 271-303.

Smith, D.R., Leeman, W.P., 2005, Chromian spinel-olivine phase chemistry and the origin of the primitive basalts of the southern Washington Cascades: Journal of Volcanology and Geothermal Research, v. 140, p. 49-66.

Smith, R.L., Leudke, R.G., 1984, Potentially active volcanic lineaments and loci in western conterminous United States Studies in geophysics: United States: National Academy Press, Washington, DC.

Stanley, W.D., Mooney, W.D., Fuis, G.S., 1990, Deep crustal structure of the Cascade Range and surrounding regions from seismic refraction and magnetotelluric data: Journal of Geophysical Research, v. 95, p. 19419-19438.

Straub, S.M., LaGatta, A.B., Martin-Del Pozzo, A.L., Langmuir, C.H., March 2008, Evidence from high-Ni olivines for a hybridized peridotite/pyroxenite source for orogenic andesites from the central Mexican Volcanic Belt: Geochemistry, Geophysics, Geosystems, v. 9, n. 3, 33 p.

Sun, S.S., McDonough, W.F., 1989, Chemical and isotopic systematics of oceanic basalts: implications for mantle composition and processes in Saunders, A.D., Norry, M.J. Eds., Magmatism in Ocean Basins, Geological Society Special Publications, London, p. 313–345.

Tepley, F.J. III, Lundstrom, C.C., McDonough W.F., Thompson, A., 2010, Trace element partitioning between high An plagioclase and basaltic melt at 1 atmosphere pressure: Lithos, v. 118, no. 1-2, p. 82-94.

Thiruvathukal, J.V., Berg JR., J.W., Heinrichs, D.F., March 1970, Regional Gravity of Oregon: Geological Society of America Bulletin, v. 81, p. 725-738.

Tsuchiyama, A., 1985, Dissolution kinetics of plagioclase in the melt of the system diopside-albite-anorthite, and origin of dusty plagioclase in andesites: Contributions to Mineralogy and Petrology, v. 89, no. 1, p. 1-16.

Verhoogen, J., 1937, Mount Saint Helens, a recent Cascade volcano: University of California Publications in Geological Sciences, v. 24, p. 263-302.

Weaver, C. S., Grant, W. C., Shemeta, J. E., 1987, Local Crustal Extension at Mount St. Helens, Washington, Journal of Geophysical Research, v. 92 (B10), p. 10,170–10,178.

Weaver, C. S., Malone, S. D., 1987, Overview of the Tectonic Setting and Recent Studies of Eruptions of Mount St. Helens, Washington: Journal of Geophysical Research, v. 92 (B10), p. 10,149–10,154.

Wells, R.E., 1990, Paleomagnetic rotations and the Cenozoic tectonics of the Cascade arc, Washington, Oregon, and California: Journal of Geophysical Research, v. 95, 19409-19417.

Wiebe, R.A., Jellinek, M., Markley, M.J., Hawkins, D.P., Snyder, D., February 2007, Steep schlieren and associated enclaves in the Vinalhaven Granite, Maine; possible indicators for granite rheology: Contributions to Mineralogy and Petrology, v. 153, no. 2, p. 121-138.

Williams, D.L., Hull, D.A., Ackerman, H.D., Beeson, M.H. April 1982, The Mt. Hood region: volcanic history, structure, and geothermal energy potential: Journal of Geophysical Research, vol. 87, no. B4, p. 2767-2781.

Wilson, M., 1989, Igneous Petrogenesis: Unwin Hyman, Boston, 466 p.

Winter, J.D., 2001, An Introduction to Igneous and Metamorphic Petrology: Prentice Hall, New Jersey, 697p.

Yamaguchi, D.K., Hoblitt, R.P., September 1995, Tree-ring dating of pre-1980 volcanic flowage deposits at Mount St. Helens, Washington: Geological Society of America Bulletin, v. 107, no. 9, p. 1077–1093.

Yoder Jr., H.S., 1976, Generation of Basaltic Magma: National Academy of Sciences, Washington, D.C., 264 p.

APPENDICES

APPENDIX A: Whole Rock Chemistry

Table A.1 Major Element Chemistry of Kalama-age Rocks. Samples are arranged in roughly reverse stratigraphic sequence by group followed by inclusions. All data attained by XRF at Washington State University. All Fe expressed as FeO*. Mg # = molar Mg/(Mg+Fe*) x 100.

Sample	31	27	14	15	17	18B	21	23	24	19	20	22
	Wn	We	EKPF	EKPF	EKPF	EKPF	EKPF	EKPF	EKPF	QMI	QMI	QMI
SiO_2	66.08	65.01	65.21	64.37	65.15	65.23	64.78	64.86	65.02	53.68	56.39	57.69
TiO_2	0.48	0.51	0.54	0.57	0.56	0.55	0.57	0.55	0.56	1.45	1.13	1.10
Al_2O_3	16.39	16.55	16.55	16.61	16.56	16.63	16.62	16.61	16.65	17.65	17.82	17.47
FeO*	3.42	3.60	3.79	3.84	3.83	3.82	3.87	3.80	3.82	7.44	6.97	6.80
MgO	1.20	1.33	1.57	1.60	1.56	1.50	1.56	1.50	1.51	5.42	3.41	3.57
CaO	3.79	4.01	4.14	4.30	4.18	4.18	4.24	4.19	4.23	8.04	7.09	6.91
Na_2O	4.78	4.71	4.77	4.75	4.79	4.78	4.77	4.78	4.78	4.05	4.17	4.18
K_2O	1.59	1.52	1.51	1.49	1.52	1.52	1.49	1.51	1.50	0.97	1.02	0.99
P_2O5	0.14	0.14	0.14	0.15	0.15	0.14	0.15	0.15	0.15	0.32	0.16	0.15
MnO	0.07	0.07	0.07	0.07	0.07	0.07	0.07	0.07	0.07	0.12	0.11	0.11
Sum	97.95	97.45	98.31	97.75	98.37	98.44	98.11	98.00	98.29	99.15	98.29	98.97
FeO* / MgO	2.85	2.70	2.42	2.40	2.46	2.55	2.47	2.54	2.53	1.37	2.04	1.90
Mg #	38.52	39.77	42.46	42.62	42.07	41.12	41.91	41.25	41.35	56.52	46.61	48.38

Table A.1 (Continued)

Sample	32	01	02	07	09	30	10	08A	16	03
	Xb tephra	X lahar	X lahar	X lahar	X lahar	X lava	MKLV TF	MKLV WC	MKLV WF	MKPF
SiO_2	58.20	55.62	57.67	55.79	57.65	60.41	56.58	57.57	58.26	57.48
TiO_2	1.12	1.37	1.16	1.34	1.18	1.03	1.20	1.03	0.96	0.94
Al_2O_3	17.25	17.02	17.13	17.28	17.17	16.85	17.35	17.41	17.60	17.87
FeO*	6.09	6.92	6.04	6.87	6.11	6.25	6.50	6.18	6.16	6.34
MgO	3.99	5.24	3.98	4.96	4.02	2.46	4.51	4.09	3.80	3.84
CaO	6.48	7.31	6.59	7.26	6.68	5.57	7.03	6.80	6.67	6.88
Na_2O	4.40	4.24	4.41	4.30	4.39	4.39	4.34	4.33	4.33	4.18
K_2O	1.29	1.23	1.29	1.25	1.29	1.40	1.29	1.23	1.20	1.16
P_2O5	0.28	0.33	0.28	0.33	0.28	0.25	0.33	0.24	0.22	0.19
MnO	0.11	0.12	0.11	0.12	0.11	0.10	0.11	0.10	0.10	0.11
Sum	99.21	99.39	98.67	99.50	98.87	98.71	99.24	98.98	99.29	99.00
FeO* / MgO	1.53	1.32	1.52	1.39	1.52	2.54	1.44	1.51	1.62	1.65
Mg #	53.86	57.43	53.99	56.27	53.94	41.23	55.29	54.16	52.39	51.92

Table A.1 (Continued)

Sample	05	11	12A	04	06B	13	28	18A	08B	06A	12B
	SDO	SDO	SDO	SDY	SDY	SDY	SDY	Pl Inc in EK	Pl Inc in MK	Pl Inc in LK	Pl Inc in LK
SiO_2	61.01	60.62	60.28	61.11	62.98	61.66	63.45	53.23	53.75	53.99	51.06
TiO_2	0.77	0.78	0.79	0.77	0.64	0.71	0.62	1.16	1.60	1.27	1.31
Al_2O_3	17.46	17.69	17.65	17.71	17.51	17.72	17.36	18.97	20.07	18.71	19.51
FeO*	5.16	5.40	5.45	5.23	4.51	4.90	4.26	7.82	7.21	8.02	9.16
MgO	2.56	2.75	2.75	2.63	2.09	2.36	1.98	5.14	4.09	4.55	5.04
CaO	5.60	5.86	5.85	5.74	5.24	5.52	5.03	8.76	8.61	8.67	9.76
Na_2O	4.49	4.43	4.43	4.50	4.58	4.51	4.62	3.68	3.75	3.68	3.25
K_2O	1.33	1.25	1.24	1.27	1.31	1.25	1.35	0.42	0.52	0.44	0.24
P_2O5	0.17	0.16	0.16	0.16	0.14	0.16	0.13	0.04	0.17	0.08	0.24
MnO	0.09	0.10	0.10	0.09	0.08	0.09	0.08	0.14	0.13	0.14	0.15
Sum	98.64	99.04	98.69	99.23	99.10	98.88	98.89	99.36	99.91	99.55	99.71
FeO* / MgO	2.01	1.96	1.98	1.99	2.15	2.07	2.15	1.52	1.76	1.76	1.82
Mg #	46.96	47.58	47.37	47.27	45.32	46.22	45.31	53.99	50.29	50.27	49.51

Table A.2 Trace Element Chemistry of Kalama-age Rocks Analyzed by XRF. Concentrations are in ppm. Sum of major and trace elements in wt %.

Sample	31	27	14	15	17	18B	21	23	24	19	20	22
	Wn	We	EKPF	EKPF	EKPF	EKPF	EKPF	EKPF	EKPF	QMI	QMI	QMI
Ni	2	1	6	5	3	3	4	3	3	60	18	20
Cr	7	9	17	14	13	10	12	10	11	128	32	45
Sc	7	8	8	8	9	8	8	9	8	20	17	20
V	42	51	53	57	54	56	59	54	54	167	174	170
Ba	378	361	358	355	357	360	353	356	362	259	215	237
Rb	41	39	38	37	38	37	37	38	38	19	21	22
Sr	436	447	449	459	451	453	456	455	458	603	493	476
Zr	134	130	130	130	130	130	130	130	130	147	95	95
Y	13	13	13	14	13	13	13	13	13	19	15	15
Nb	6	6	6	6	5	6	6	5	6	16	5	5
Ga	19	20	18	18	19	18	20	20	19	21	20	20
Cu	25	14	17	18	21	17	28	22	34	29	46	38
Zn	56	57	61	58	58	62	60	59	58	70	73	72
Pb	8	7	15	7	7	8	7	8	7	3	5	3
La	12	12	10	12	14	15	12	9	11	18	10	7
Ce	26	28	28	24	29	26	31	25	26	34	13	16
Nd	13	15	15	13	15	13	15	13	15	21	9	12
Th	2	1	2	1	2	2	1	2	2	1	1	-1
U	1	2	1	1	0	2	1	1	1	0	1	2
sum trace	1227	1219	1244	1236	1238	1238	1252	1232	1254	1636	1261	1272
in %	0.12	0.12	0.12	0.12	0.12	0.12	0.13	0.12	0.13	0.16	0.13	0.13
sum m+tr	98.07	97.58	98.43	97.88	98.50	98.56	98.24	98.12	98.42	99.31	98.42	99.09

Table A.2 (Continued)

Sample	32	01	02	07	09	30	10	08A	16	03
	Xb tephra	X lahar	X lahar	X lahar	X lahar	X lava	MKLV TF	MKLV WC	MKLV WF	MKPF
Ni	44	67	38	58	40	11	42	46	38	33
Cr	87	130	86	113	89	16	69	40	22	17
Sc	14	19	16	18	16	14	17	17	17	17
V	125	151	129	147	129	106	145	148	149	154
Ba	310	296	306	297	305	364	306	295	286	253
Rb	28	24	27	25	27	34	26	24	24	20
Sr	551	580	551	589	556	452	589	577	571	547
Zr	149	160	151	159	151	176	162	144	138	130
Y	17	18	17	18	17	21	18	17	15	16
Nb	14	18	15	18	15	8	15	9	7	6
Ga	19	20	19	19	19	19	20	19	20	20
Cu	36	50	44	46	42	60	55	52	56	53
Zn	69	73	68	74	67	80	73	74	73	70
Pb	5	4	5	3	5	7	3	4	5	4
La	19	20	19	19	16	19	21	17	15	13
Ce	31	39	29	41	38	36	42	31	36	28
Nd	18	22	17	19	18	16	20	19	20	16
Th	2	1	1	1	1	2	1	1	1	1
U	0	1	1	3	1	1	1	1	2	0
sum trace	1536	1692	1536	1664	1552	1441	1626	1535	1494	1397
in %	0.15	0.17	0.15	0.17	0.16	0.14	0.16	0.15	0.15	0.14
sum m+tr	99.36	99.56	98.82	99.66	99.03	98.85	99.40	99.14	99.44	99.14

Table A.2 (Continued)

Sample	05	11	12A	04	06B	13	28	18A	08B	06A	12B
	SDO	SDO	SDO	SDY	SDY	SDY	SDY	Pl Inc in EK	Pl Inc in MK	Pl Inc in LK	Pl Inc in LK
Ni	10	12	11	0	4	12	1	24	6	14	17
Cr	9	9	10	2	5	9	2	47	27	28	30
Sc	13	13	14	10	11	12	11	27	22	27	29
V	105	110	114	86	97	108	88	247	222	232	439
Ba	287	272	273	298	283	282	314	139	181	191	123
Rb	29	26	27	29	25	26	32	8	12	12	4
Sr	496	514	512	507	520	516	480	430	475	426	451
Zr	133	124	124	118	118	126	115	69	85	124	36
Y	15	14	14	12	13	15	11	13	13	17	14
Nb	5	4	5	4	5	5	3	4	7	6	3
Ga	20	19	20	20	19	19	18	19	22	21	21
Cu	43	46	48	22	27	47	21	10	38	74	56
Zn	67	66	66	62	62	66	57	81	68	78	86
Pb	6	5	3	5	6	6	5	4	4	4	2
La	13	12	13	11	11	14	12	9	15	14	11
Ce	25	26	29	24	23	24	23	16	20	23	13
Nd	16	12	16	14	13	12	12	12	12	13	8
Th	1	0	1	1	1	1	1	0	1	2	-1
U	2	0	3	1	2	1	1	0	1	2	-1
sum trace	1292	1285	1302	1225	1241	1299	1207	1159	1230	1304	1341
in %	0.13	0.13	0.13	0.12	0.12	0.13	0.12	0.12	0.12	0.13	0.13
sum m+tr	98.77	99.16	98.82	99.22	99.01	99.36	99.01	99.47	100.03	99.68	99.84

Table A.3 Trace Element Chemistry of Kalama-age Rocks analyzed by ICP-MS. Concentrations are in ppm.

Sample	31	27	14	15	17	18B	21	23	24	19	20	22
	Wn	We	EKPF	EKPF	EKPF	EKPF	EKPF	EKPF	EKPF	QMI	QMI	QMI
La	14.12	13.83	13.20	13.72	13.81	13.63	13.65	13.56	13.58	16.46	8.92	9.53
Ce	29.34	28.88	27.64	28.67	28.76	28.55	28.44	28.33	28.47	35.57	20.03	21.25
Pr	3.67	3.61	3.45	3.61	3.61	3.60	3.59	3.56	3.56	4.67	2.75	2.86
Nd	14.43	14.20	13.78	14.20	14.40	14.25	14.35	14.12	14.19	19.64	11.86	12.27
Sm	3.14	3.16	3.07	3.17	3.15	3.18	3.19	3.16	3.17	4.64	2.98	3.05
Eu	0.94	0.96	0.98	1.03	1.03	1.01	1.01	1.00	1.02	1.59	1.17	1.14
Gd	2.87	2.92	2.84	2.90	2.97	2.86	2.89	2.84	2.88	4.40	3.06	3.11
Tb	0.44	0.44	0.44	0.44	0.44	0.44	0.45	0.43	0.45	0.68	0.49	0.51
Dy	2.48	2.49	2.49	2.55	2.56	2.54	2.60	2.51	2.55	3.95	3.04	2.97
Ho	0.48	0.49	0.49	0.51	0.50	0.49	0.50	0.49	0.49	0.77	0.61	0.59
Er	1.29	1.31	1.28	1.31	1.30	1.28	1.32	1.30	1.31	1.97	1.59	1.55
Tm	0.18	0.19	0.18	0.19	0.19	0.18	0.19	0.19	0.19	0.27	0.22	0.22
Yb	1.16	1.12	1.15	1.18	1.18	1.17	1.15	1.17	1.18	1.62	1.36	1.39
Lu	0.18	0.18	0.18	0.18	0.19	0.18	0.18	0.18	0.18	0.25	0.21	0.21
Th	3.11	2.97	2.95	2.71	2.81	2.78	2.79	2.84	2.82	1.90	1.28	1.56
Nb	6.31	6.16	6.21	6.58	6.50	6.26	6.44	6.26	6.35	17.20	5.26	5.22
Y	12.49	12.65	12.65	13.00	12.81	12.73	12.88	12.68	12.80	19.11	14.76	14.86
Hf	3.67	3.60	3.56	3.52	3.59	3.57	3.50	3.50	3.58	3.54	2.53	2.60
Ta	0.46	0.45	0.45	0.47	0.46	0.44	0.45	0.44	0.46	1.07	0.34	0.34
U	1.31	1.25	1.25	1.15	1.18	1.18	1.19	1.20	1.20	0.69	0.58	0.70
Pb	8.86	8.35	16.55	7.78	7.91	8.26	7.90	8.02	8.08	3.66	5.06	5.32
Rb	40.68	38.69	37.93	37.18	38.06	37.94	37.42	37.18	37.43	18.88	19.63	21.83
Cs	1.94	1.90	1.76	1.78	1.81	1.84	1.79	1.80	1.80	0.57	0.80	0.99
Sc	6.02	6.89	7.40	7.68	7.40	7.16	7.73	7.42	7.65	19.96	17.92	19.17
Ba	378	364	348	357	362	361	356	357	357	253	208	230
Sr	433	445	446	461	452	454	459	449	456	604	497	474
Zr	133	130	127	129	130	129	128	127	129	144	93	92

Table A.3 (Continued)

Sample	32	01	02	07	09	30	10	08A	16	03
	Xb tephra	X lahar	X lahar	X lahar	X lahar	X lava	MKLV TF	MKLV WC	MKLV WF	MKPF
La	16.66	19.10	17.71	18.62	16.82	18.50	18.86	16.38	15.74	14.09
Ce	35.17	40.27	37.27	39.14	35.59	38.70	39.36	35.10	33.98	30.72
Pr	4.53	5.21	4.79	5.01	4.58	4.92	5.06	4.56	4.40	4.00
Nd	18.55	21.60	19.77	20.88	18.92	19.93	20.64	18.75	18.05	16.65
Sm	4.21	4.85	4.38	4.67	4.29	4.63	4.60	4.21	4.13	3.82
Eu	1.36	1.64	1.45	1.57	1.43	1.42	1.52	1.36	1.33	1.26
Gd	3.84	4.55	4.08	4.40	4.01	4.41	4.31	3.91	3.86	3.61
Tb	0.61	0.69	0.63	0.68	0.62	0.71	0.66	0.60	0.58	0.56
Dy	3.53	3.94	3.60	3.88	3.54	4.24	3.75	3.41	3.38	3.29
Ho	0.68	0.75	0.70	0.76	0.68	0.84	0.72	0.67	0.67	0.66
Er	1.78	1.93	1.80	1.92	1.74	2.18	1.85	1.72	1.73	1.74
Tm	0.25	0.28	0.25	0.27	0.25	0.31	0.27	0.24	0.25	0.25
Yb	1.45	1.60	1.50	1.60	1.49	1.88	1.55	1.48	1.52	1.54
Lu	0.23	0.25	0.23	0.24	0.23	0.29	0.24	0.23	0.23	0.24
Th	2.48	2.35	2.35	2.45	2.45	3.12	2.84	2.63	2.51	2.26
Nb	14.72	18.93	15.57	18.67	15.28	9.54	16.16	9.77	7.96	6.43
Y	16.92	19.29	17.50	18.64	17.24	20.77	18.35	16.69	16.66	16.76
Hf	3.74	3.89	3.81	3.88	3.73	4.46	3.96	3.69	3.65	3.45
Ta	0.94	1.19	1.00	1.16	0.97	0.65	1.03	0.63	0.51	0.41
U	0.96	0.94	0.90	0.88	0.94	1.33	1.01	0.93	0.90	0.83
Pb	5.48	4.32	5.26	4.43	5.23	7.83	5.06	5.71	5.80	5.53
Rb	27.41	24.42	27.17	24.30	26.60	33.49	25.43	23.73	23.59	20.12
Cs	1.06	0.79	1.04	0.74	0.97	1.57	0.79	0.87	0.91	0.78
Sc	15.22	17.29	15.55	18.19	15.46	14.48	18.05	16.33	15.95	16.32
Ba	303	303	320	294	302	361	300	285	284	256
Sr	552	587	565	592	557	452	584	575	577	551
Zr	145	159	149	155	146	171	159	139	135	129

Table A.3 (Continued)

Sample	05	11	12A	13	04	06B	28	18A	08B	06A	12B
	SDO	SDO	SDO	SDY	SDY	SDY	SDY	Pl Inc in EK	Pl Inc in MK	Pl Inc in LK	Pl Inc in LK
La	13.26	12.05	12.06	12.17	12.29	11.83	11.78	8.08	10.96	11.48	8.23
Ce	27.93	25.67	25.69	25.99	25.64	25.02	24.23	17.84	23.39	24.22	18.23
Pr	3.59	3.30	3.29	3.32	3.26	3.20	3.05	2.41	3.02	3.21	2.53
Nd	14.49	13.68	13.60	13.54	13.00	13.03	12.10	10.16	12.65	13.98	11.49
Sm	3.35	3.20	3.19	3.14	2.93	3.00	2.81	2.55	2.98	3.51	2.95
Eu	1.07	1.07	1.05	1.06	0.99	1.03	0.90	1.00	1.40	1.09	1.07
Gd	3.13	3.04	3.07	3.05	2.69	2.83	2.56	2.54	2.94	3.54	3.18
Tb	0.50	0.48	0.48	0.47	0.42	0.44	0.39	0.43	0.47	0.61	0.50
Dy	2.93	2.85	2.82	2.81	2.45	2.58	2.28	2.63	2.74	3.71	2.97
Ho	0.58	0.57	0.57	0.55	0.48	0.51	0.46	0.53	0.54	0.74	0.60
Er	1.55	1.54	1.50	1.48	1.30	1.37	1.17	1.40	1.41	1.97	1.55
Tm	0.22	0.22	0.21	0.22	0.19	0.20	0.17	0.21	0.19	0.29	0.21
Yb	1.42	1.37	1.36	1.35	1.16	1.19	1.07	1.28	1.19	1.71	1.28
Lu	0.22	0.22	0.21	0.21	0.18	0.19	0.17	0.20	0.18	0.27	0.19
Th	2.61	2.49	2.46	2.60	2.46	2.42	2.58	1.18	1.68	1.90	0.46
Nb	5.82	5.17	5.21	5.42	4.52	4.88	4.40	4.86	7.91	6.36	3.64
Y	14.96	14.48	14.34	14.29	12.48	12.91	11.57	13.25	13.48	18.48	14.51
Hf	3.53	3.31	3.26	3.35	3.18	3.19	3.09	1.96	2.22	3.26	1.06
Ta	0.41	0.35	0.36	0.38	0.32	0.34	0.31	0.33	0.58	0.46	0.25
U	1.09	1.03	1.01	1.09	1.06	1.03	1.15	0.43	0.60	0.72	0.18
Pb	6.64	6.03	5.87	6.27	6.13	5.85	6.19	3.44	3.61	4.69	2.70
Rb	28.54	25.83	25.71	26.48	27.99	25.09	31.55	7.41	11.95	11.09	3.82
Cs	1.34	1.14	1.16	1.18	0.69	0.68	1.39	0.34	0.74	0.88	0.26
Sc	11.82	12.48	12.05	11.59	9.11	10.21	9.51	24.67	21.46	25.73	25.17
Ba	290	265	262	267	300	283	309	134	171	183	116
Sr	499	513	514	513	508	520	474	436	474	428	452
Zr	131	120	120	123	116	116	111	66	80	118	36

APPENDIX B: Plagioclase Data

Table B.1 Plagioclase EMP Spots and Transects in wt %. Xtl=crystal, T=transect, P=points, mc=microphenocrysts.

Sample	Lithology	An	Or	Ab	Na_2O	MgO	SiO_2	Al_2O_3	FeO	CaO	P_2O_5	TiO_2	K_2O	Total
31 Xtl 1	Wn	29.4	2.1	68.5	7.25	0.00	62.16	25.04	0.03	5.63	0.01	0.00	0.33	100.49
31 Xtl 1	Wn	33.9	1.7	64.4	6.83	0.00	60.88	25.72	0.06	6.51	0.02	0.00	0.28	100.32
31 Xtl 1 rim T	Wn	29.9	1.8	68.3	7.28	0.00	61.92	25.30	0.07	5.77	0.00	0.00	0.29	100.68
31 Xtl 1 rim T	Wn	30.3	1.8	67.9	7.19	0.00	61.48	25.27	0.07	5.81	0.01	0.01	0.29	100.13
31 Xtl 1 rim T	Wn	29.1	1.9	69.0	7.29	0.00	62.31	25.19	0.11	5.56	0.01	0.01	0.31	100.80
31 Xtl 1 rim T	Wn	29.0	1.7	69.3	7.40	0.01	61.82	25.03	0.15	5.60	0.00	-0.01	0.28	100.31
31 Xtl 1 rim T	Wn	37.2	1.4	61.4	6.60	0.01	59.65	26.15	0.21	7.22	0.02	0.01	0.23	100.10
31 Xtl 1 rim T	Wn	34.4	1.5	64.1	6.88	0.01	60.29	25.94	0.20	6.69	0.01	0.01	0.25	100.28
31 Xtl 1 rim T	Wn	43.8	1.2	55.0	5.94	0.01	57.96	27.43	0.23	8.57	0.01	0.01	0.19	100.36
31 Xtl 1.1	Wn	56.5	0.8	42.8	4.64	0.02	54.34	28.95	0.43	11.10	0.01	0.04	0.13	99.65
31 Xtl 1.1	Wn	61.5	0.6	37.9	4.12	0.04	52.76	29.92	0.46	12.07	0.01	0.04	0.10	99.51
31 Xtl 1.1	Wn	42.4	1.2	56.5	6.05	0.01	58.05	27.05	0.25	8.22	0.00	0.02	0.19	99.85
31 Xtl 1.1	Wn	42.8	1.2	56.0	6.04	0.01	57.83	27.10	0.27	8.36	0.02	0.01	0.20	99.86
31 Xtl 2	Wn	60.3	0.6	39.1	4.23	0.04	53.30	29.80	0.37	11.80	0.03	0.02	0.10	99.75
31 Xtl 2	Wn	65.9	0.4	33.6	3.67	0.04	51.90	30.77	0.36	13.00	0.02	0.02	0.07	99.87
31 Xtl 2	Wn	68.3	0.4	31.2	3.40	0.04	51.37	31.21	0.38	13.46	0.03	0.03	0.07	100.02
31 Xtl 2	Wn	68.2	0.4	31.4	3.42	0.04	51.48	31.17	0.39	13.43	0.01	0.02	0.07	100.03
31 Xtl 2	Wn	68.0	0.3	31.7	3.44	0.03	51.35	31.16	0.38	13.39	0.03	0.03	0.06	99.88
31 Xtl 2	Wn	66.6	0.4	33.0	3.61	0.04	51.89	30.80	0.39	13.17	0.01	0.03	0.07	99.99
31 Xtl 2	Wn	65.9	0.5	33.7	3.67	0.03	52.09	30.78	0.42	12.99	0.01	0.02	0.08	100.11
31 Xtl 2	Wn	66.8	0.4	32.8	3.58	0.04	51.78	31.08	0.40	13.18	0.01	0.02	0.07	100.18
31 Xtl 2	Wn	68.7	0.3	31.0	3.37	0.03	51.23	31.41	0.38	13.52	0.02	0.03	0.06	100.06
31 Xtl 2	Wn	66.9	0.5	32.7	3.54	0.03	51.96	30.90	0.39	13.12	0.02	0.02	0.08	100.06
31 Xtl 2	Wn	60.8	0.5	38.6	4.21	0.02	53.80	29.94	0.35	11.99	0.00	0.03	0.09	100.48
31 Xtl 2	Wn	59.3	0.6	40.1	4.35	0.02	53.78	29.80	0.29	11.65	0.01	0.02	0.10	100.00
31 Xtl 2	Wn	53.4	0.7	45.9	5.02	0.01	55.29	28.98	0.24	10.55	0.03	0.02	0.12	100.25
31 Xtl 2	Wn	43.7	1.1	55.2	5.97	0.01	58.33	27.12	0.27	8.55	0.02	0.01	0.18	100.49
31 Xtl 2.1	Wn	53.4	0.8	45.9	4.96	0.02	55.00	28.88	0.27	10.44	0.03	0.03	0.12	99.76
31 Xtl 2.1	Wn	47.3	1.0	51.8	5.61	0.02	56.88	27.96	0.24	9.26	0.02	0.01	0.16	100.20
31 Xtl 2.1	Wn	45.2	1.0	53.8	5.83	0.01	57.60	27.84	0.27	8.87	0.00	0.01	0.16	100.61
31 Xtl 2.1	Wn	43.9	1.0	55.0	5.94	0.01	58.28	27.28	0.28	8.58	0.02	0.01	0.17	100.59
31 Xtl 3	Wn	37.4	1.5	61.2	6.56	0.01	60.01	26.33	0.22	7.25	0.01	0.01	0.24	100.67
31 Xtl 3	Wn	34.4	1.5	64.1	6.82	0.01	60.67	25.88	0.23	6.63	0.02	0.02	0.24	100.52

Table B.1 (Continued)

Sample	Lithology	An	Or	Ab	Na_2O	MgO	SiO_2	Al_2O_3	FeO	CaO	P_2O_5	TiO_2	K_2O	Total
31 Xtl 3	Wn	34.5	1.4	64.1	6.92	0.01	60.62	26.09	0.25	6.75	0.02	0.02	0.23	100.95
31 Xtl 3	Wn	43.0	1.2	55.8	6.03	0.01	58.40	27.18	0.24	8.40	0.02	0.01	0.20	100.54
31 Xtl 3	Wn	35.4	1.5	63.2	6.74	0.01	60.58	26.23	0.25	6.83	0.01	0.02	0.24	100.91
31 Xtl 3	Wn	40.2	1.2	58.6	6.35	0.01	58.90	26.98	0.23	7.88	0.03	0.01	0.20	100.61
31 Xtl 3	Wn	41.3	1.2	57.5	6.19	0.01	58.61	27.04	0.25	8.03	0.02	0.01	0.20	100.37
31 Xtl 3	Wn	43.9	1.2	55.0	5.98	0.01	58.02	27.32	0.26	8.64	0.01	0.02	0.19	100.45
31 Xtl 3	Wn	41.6	1.3	57.2	6.23	0.00	58.63	27.03	0.24	8.20	0.02	0.01	0.21	100.58
31 Xtl 3	Wn	43.4	1.1	55.5	6.03	0.01	58.25	27.39	0.28	8.54	0.02	0.00	0.19	100.70
31 Xtl 3	Wn	37.8	1.4	60.8	6.52	0.01	59.74	26.41	0.22	7.34	0.01	0.02	0.23	100.51
31 Xtl 3	Wn	38.9	1.3	59.8	6.47	0.01	59.29	26.73	0.24	7.60	0.03	0.01	0.21	100.61
31 Xtl 3	Wn	39.8	1.2	59.0	6.43	0.01	59.01	26.68	0.25	7.84	0.02	0.01	0.21	100.47
31 Xtl 3	Wn	41.7	1.1	57.2	6.17	0.01	58.48	27.01	0.23	8.13	0.00	0.01	0.19	100.24
31 Xtl 3	Wn	42.1	1.3	56.6	6.10	0.01	58.07	27.25	0.25	8.21	0.01	0.01	0.21	100.16
31 Xtl 3.1	Wn	53.1	0.8	46.1	4.99	0.03	55.39	28.63	0.38	10.41	0.02	0.03	0.13	100.03
31 Xtl 3.1	Wn	52.8	0.8	46.4	5.03	0.02	55.06	28.39	0.38	10.35	0.03	0.02	0.13	99.44
31 Xtl 4	Wn	41.1	1.2	57.8	6.27	0.01	57.83	26.69	0.18	8.07	0.01	0.02	0.20	99.29
31 Xtl 4	Wn	41.3	1.2	57.4	6.23	0.01	58.33	26.90	0.20	8.11	0.01	0.01	0.21	100.00
31 Xtl 4	Wn	40.6	1.3	58.1	6.27	0.01	58.11	26.90	0.17	7.94	0.01	0.01	0.21	99.66
31 Xtl 4	Wn	41.1	1.2	57.7	6.20	0.01	58.24	26.80	0.20	7.98	0.01	0.01	0.19	99.68
31 Xtl 4	Wn	41.1	1.3	57.5	6.22	0.01	58.36	26.59	0.23	8.05	0.01	0.01	0.22	99.72
31 Xtl 4	Wn	40.9	1.4	57.7	6.20	0.01	58.25	26.52	0.21	7.97	0.00	0.01	0.23	99.43
31 Xtl 4	Wn	41.0	1.2	57.7	6.22	0.00	58.05	26.77	0.21	8.01	0.01	0.01	0.20	99.49
31 Xtl 4	Wn	41.8	1.2	57.0	6.15	0.00	58.03	26.86	0.19	8.16	0.03	0.02	0.20	99.63
31 Xtl 4	Wn	41.2	1.2	57.6	6.20	0.01	58.17	27.01	0.20	8.03	0.02	0.01	0.20	99.90
31 Xtl 4	Wn	41.2	1.3	57.4	6.25	0.01	58.17	27.03	0.21	8.11	-0.01	0.01	0.22	100.02
31 Xtl 4	Wn	40.6	1.2	58.2	6.28	0.01	58.33	26.95	0.19	7.93	0.02	0.02	0.20	99.96
31 Xtl 4	Wn	40.2	1.4	58.5	6.33	0.01	58.30	26.53	0.20	7.86	0.00	0.03	0.23	99.49
31 Xtl 4	Wn	38.5	1.4	60.1	6.54	0.01	59.03	26.57	0.17	7.58	0.01	0.01	0.23	100.18
31 Xtl 4	Wn	40.0	1.3	58.7	6.35	0.01	58.99	26.40	0.16	7.84	0.01	0.03	0.21	99.99
31 Xtl 4	Wn	46.0	1.0	52.9	5.73	0.01	57.17	27.55	0.20	9.01	0.00	0.00	0.17	99.87
31 Xtl 4	Wn	45.3	1.1	53.6	5.84	0.01	57.43	27.42	0.23	8.93	0.00	0.00	0.18	100.07
31 Xtl 4	Wn	44.2	1.2	54.6	5.91	0.01	57.97	27.35	0.19	8.65	0.01	0.01	0.19	100.29
31 Xtl 4	Wn	47.4	1.0	51.6	5.61	0.01	56.49	27.94	0.22	9.32	0.02	0.01	0.17	99.82

Table B.1 (Continued)

Sample	Lithology	An	Or	Ab	Na_2O	MgO	SiO_2	Al_2O_3	FeO	CaO	P_2O_5	TiO_2	K_2O	Total
31 Xtl 4	Wn	47.1	1.0	51.9	5.62	0.01	56.84	27.76	0.24	9.24	0.01	0.01	0.16	99.93
31 Xtl 4	Wn	47.9	1.0	51.1	5.53	0.01	57.11	28.05	0.25	9.39	0.01	0.01	0.17	100.53
31 Xtl 4	Wn	46.7	1.1	52.2	5.68	0.01	57.44	27.76	0.23	9.20	0.03	0.01	0.19	100.56
31 Xtl 4	Wn	45.3	1.1	53.6	5.80	0.01	57.96	27.37	0.22	8.88	0.01	0.01	0.18	100.44
31 Xtl 4	Wn	42.5	1.3	56.3	6.12	0.01	58.81	27.09	0.26	8.36	0.03	0.01	0.21	100.92
31 Xtl 4	Wn	39.7	1.4	58.9	6.38	0.01	59.17	26.75	0.23	7.78	0.01	0.01	0.23	100.62
31 Xtl 4	Wn	37.9	1.3	60.8	6.56	0.01	59.94	26.20	0.20	7.39	0.01	0.01	0.22	100.56
31 Xtl 4	Wn	33.2	1.7	65.1	7.01	0.01	61.15	25.49	0.23	6.48	0.01	0.02	0.28	100.70
31 Xtl 4	Wn	32.2	1.7	66.1	7.10	0.01	61.73	25.53	0.23	6.25	0.01	0.00	0.28	101.14
31 Xtl 4	Wn	46.6	1.0	52.4	5.60	0.01	57.37	27.72	0.20	9.01	0.01	0.01	0.17	100.14
31 Xtl 4	Wn	46.7	1.1	52.2	5.65	0.01	57.50	27.77	0.18	9.13	0.02	0.01	0.18	100.46
31 Xtl 4	Wn	47.4	1.0	51.6	5.59	0.01	57.37	27.94	0.23	9.28	0.02	0.01	0.17	100.66
31 Xtl 4	Wn	46.6	1.0	52.4	5.68	0.01	57.42	27.70	0.25	9.15	0.01	0.01	0.16	100.42
31 Xtl 4	Wn	46.5	1.1	52.4	5.66	0.01	57.23	27.73	0.24	9.07	0.02	0.00	0.19	100.14
31 Xtl 4	Wn	46.8	1.1	52.2	5.67	0.01	57.42	27.61	0.22	9.19	0.00	0.00	0.17	100.30
31 Xtl 4	Wn	45.0	1.2	53.8	5.81	0.01	57.68	27.52	0.25	8.79	0.02	0.01	0.19	100.26
31 Xtl 4	Wn	45.7	1.0	53.3	5.83	0.01	57.29	27.80	0.26	9.04	0.01	0.01	0.17	100.45
31 Xtl 4	Wn	41.3	1.1	57.5	6.18	0.01	58.57	26.90	0.25	8.03	0.01	0.01	0.19	100.20
31 Xtl 4	Wn	41.2	1.2	57.6	6.27	0.01	59.03	26.86	0.27	8.12	0.01	0.01	0.20	100.81
31 Xtl 4	Wn	40.3	2.1	57.6	5.75	0.08	63.19	26.63	0.42	7.29	-0.01	0.03	0.31	103.71
31 Xtl 4	Wn	46.9	1.0	52.0	5.62	0.01	57.00	27.99	0.22	9.18	0.02	0.01	0.17	100.27
31 Xtl 4	Wn	47.6	1.0	51.3	5.59	0.01	57.14	28.13	0.26	9.39	0.01	0.01	0.17	100.72
31 Xtl 4	Wn	41.4	1.3	57.3	6.23	0.01	58.82	27.13	0.22	8.14	0.03	0.01	0.21	100.86
31 Xtl 4	Wn	47.7	1.0	51.3	5.52	0.01	56.89	27.93	0.21	9.29	0.02	0.01	0.16	100.03
27 Xtl 1	We	63.5	0.6	35.9	3.91	0.01	52.75	30.41	0.28	12.50	0.02	0.03	0.09	100.05
27 Xtl 1	We	62.9	0.5	36.5	3.95	0.01	52.85	30.57	0.23	12.33	0.02	0.02	0.09	100.10
27 Xtl 1	We	52.6	0.8	46.6	5.08	0.01	55.68	28.66	0.28	10.39	0.01	0.02	0.14	100.27
27 Xtl 1	We	50.1	0.9	49.0	5.35	0.01	56.50	28.44	0.26	9.90	0.04	0.03	0.15	100.72
27 Xtl 1	We	55.1	1.0	43.9	4.20	0.02	56.58	28.46	0.25	9.53	0.02	0.02	0.15	99.24
27 Xtl 1	We	49.5	0.9	49.5	5.35	0.02	56.38	28.35	0.26	9.68	0.02	0.02	0.15	100.29
27 Xtl 1	We	51.2	0.9	47.9	5.17	0.02	56.01	28.27	0.29	10.00	0.01	0.02	0.15	99.98
27 Xtl 1	We	52.2	0.8	47.0	5.14	0.01	55.79	28.61	0.27	10.33	0.03	0.02	0.14	100.34
27 Xtl 1	We	45.7	1.1	53.2	5.75	0.01	57.48	27.58	0.28	8.94	0.00	0.03	0.18	100.30

Table B.1 (Continued)

Sample	Lithology	An	Or	Ab	Na_2O	MgO	SiO_2	Al_2O_3	FeO	CaO	P_2O_5	TiO_2	K_2O	Total
27 Xtl 1	We	50.6	0.9	48.5	5.29	0.01	56.61	28.48	0.26	9.97	0.02	0.02	0.15	100.86
27 Xtl 1	We	48.4	1.0	50.7	5.47	0.01	57.14	27.81	0.25	9.44	0.02	0.01	0.16	100.35
27 Xtl 1	We	46.3	1.1	52.7	5.68	0.01	57.32	27.76	0.26	9.03	0.03	0.02	0.18	100.32
27 Xtl 1	We	55.0	0.7	44.3	4.78	0.01	55.15	29.03	0.25	10.76	0.00	0.02	0.12	100.13
27 Xtl 1	We	49.6	0.9	49.5	5.37	0.02	56.56	28.08	0.29	9.72	0.02	0.01	0.15	100.22
27 Xtl 1	We	44.1	1.1	54.9	5.93	0.01	58.21	27.34	0.27	8.63	0.02	0.02	0.18	100.62
27 Xtl 1	We	43.5	1.2	55.4	6.02	0.02	58.07	27.34	0.22	8.54	0.02	0.02	0.19	100.44
27 Xtl 1	We	47.0	1.1	52.0	5.60	0.01	57.28	27.73	0.22	9.15	0.02	0.01	0.17	100.21
27 Xtl 1	We	45.9	1.1	53.0	5.75	0.01	57.66	27.47	0.24	9.00	0.00	0.01	0.18	100.35
27 Xtl 1	We	46.4	1.0	52.5	5.65	0.01	57.41	27.60	0.25	9.04	0.00	0.01	0.17	100.16
27 Xtl 1	We	44.1	1.1	54.7	5.90	0.01	58.55	27.61	0.22	8.60	0.01	0.01	0.19	101.10
27 Xtl 1	We	42.0	1.3	56.7	6.11	0.01	58.35	26.99	0.22	8.18	0.02	0.01	0.21	100.12
27 Xtl 1	We	41.5	1.3	57.2	6.15	0.01	58.58	26.98	0.23	8.07	0.02	0.01	0.21	100.27
27 Xtl 1	We	40.6	1.3	58.1	6.22	0.01	59.06	26.61	0.21	7.85	0.01	0.02	0.21	100.21
27 Xtl 1	We	42.4	1.3	56.4	6.05	0.01	58.10	26.78	0.25	8.23	0.01	0.01	0.21	99.65
27 Xtl 1	We	40.3	1.3	58.4	6.28	0.01	59.01	26.73	0.26	7.83	0.02	0.02	0.22	100.40
27 Xtl 1	We	45.2	1.2	53.6	5.83	0.02	57.55	27.50	0.26	8.90	0.03	0.01	0.20	100.31
27 Xtl 1	We	43.5	1.2	55.3	5.96	0.01	57.91	27.19	0.27	8.47	0.02	0.02	0.19	100.03
27 Xtl 1	We	40.7	1.3	58.1	6.25	0.01	58.65	26.62	0.24	7.91	0.01	0.01	0.21	99.91
27 Xtl 1	We	38.6	1.3	60.1	6.45	0.01	59.23	26.43	0.23	7.50	0.02	0.02	0.21	100.10
27 Xtl 1	We	43.0	1.2	55.8	5.98	0.01	58.33	27.05	0.23	8.35	0.03	0.02	0.19	100.20
27 Xtl 1	We	55.9	0.7	43.4	4.67	0.05	54.12	28.59	0.46	10.88	0.02	0.03	0.12	98.96
27 Xtl 1	We	41.6	1.3	57.0	6.15	0.02	58.27	26.82	0.28	8.12	0.01	0.02	0.21	99.90
27 Xtl 1.1	We	45.1	1.1	53.7	5.79	0.03	57.43	27.62	0.27	8.81	0.01	0.01	0.19	100.20
27 Xtl 1.1	We	44.8	1.1	54.1	5.80	0.04	58.10	27.01	0.42	8.69	0.03	0.03	0.18	100.29
27 Xtl 1.1	We	53.9	0.8	45.2	4.90	0.04	55.20	28.64	0.44	10.57	0.00	0.03	0.14	99.99
27 Xtl 1.1	We	35.6	8.0	56.4	4.18	0.12	68.72	21.29	0.88	4.77	0.02	0.11	0.90	101.05
27 Xtl 1.2	We	38.3	1.6	60.1	6.40	0.01	59.95	26.05	0.30	7.37	0.01	0.01	0.25	100.36
27 Xtl 1.2	We	36.0	1.7	62.3	6.59	0.01	60.64	25.87	0.28	6.90	0.03	0.01	0.27	100.61
27 Xtl 1.2	We	41.8	1.3	56.9	6.10	0.02	58.27	26.57	0.32	8.12	0.01	0.01	0.21	99.66
27 Xtl 2	We	47.2	1.0	51.8	5.60	0.01	56.99	27.83	0.21	9.23	0.01	0.00	0.16	100.06
27 Xtl 2	We	45.4	1.1	53.5	5.81	0.02	57.31	27.50	0.24	8.93	0.01	0.02	0.19	100.04
27 Xtl 2	We	47.2	1.0	51.7	5.62	0.00	56.88	28.03	0.21	9.29	0.00	0.01	0.17	100.22

Table B.1 (Continued)

Sample	Lithology	An	Or	Ab	Na_2O	MgO	SiO_2	Al_2O_3	FeO	CaO	P_2O_5	TiO_2	K_2O	Total
27 Xtl 2	We	49.0	1.0	50.1	5.18	0.02	57.38	28.21	0.23	9.18	0.02	0.01	0.15	100.38
27 Xtl 2	We	48.8	1.0	50.3	5.45	0.01	56.92	28.14	0.25	9.57	0.00	0.00	0.16	100.50
27 Xtl 2	We	46.5	1.0	52.4	5.67	0.01	57.36	27.80	0.20	9.11	0.02	0.02	0.17	100.41
27 Xtl 2	We	47.4	1.0	51.6	5.60	0.01	56.60	27.76	0.21	9.32	0.03	0.01	0.17	99.76
27 Xtl 2	We	47.6	1.0	51.4	5.53	0.01	57.22	27.91	0.23	9.25	0.02	0.01	0.16	100.38
27 Xtl 2	We	46.0	1.0	53.0	5.71	0.01	57.77	27.72	0.22	8.98	0.01	0.01	0.16	100.59
27 Xtl 2	We	45.9	1.0	53.1	5.72	0.01	57.64	27.75	0.22	8.95	0.00	0.01	0.16	100.46
27 Xtl 2	We	46.2	1.0	52.9	5.71	0.01	57.31	27.64	0.20	9.03	0.00	0.02	0.16	100.07
27 Xtl 2	We	39.7	1.4	58.9	6.39	0.01	59.16	26.69	0.18	7.81	0.02	0.01	0.23	100.50
27 Xtl 2	We	46.5	1.0	52.5	5.65	0.01	57.36	27.95	0.21	9.06	0.00	0.01	0.17	100.44
27 Xtl 2	We	45.6	1.2	53.2	5.36	0.01	58.84	27.50	0.20	8.31	0.01	0.01	0.19	100.44
27 Xtl 2	We	40.7	1.2	58.0	6.24	0.01	58.86	26.97	0.18	7.92	0.01	0.01	0.20	100.42
27 Xtl 2	We	42.0	1.2	56.7	6.15	0.01	58.20	27.21	0.22	8.24	0.01	0.02	0.20	100.25
27 Xtl 2	We	39.3	1.4	59.3	6.38	0.01	59.37	26.68	0.24	7.65	0.01	0.02	0.23	100.60
27 Xtl 2	We	40.1	1.2	58.7	6.34	0.01	58.87	26.98	0.24	7.85	0.00	0.01	0.20	100.49
27 Xtl 3	We	43.0	1.3	55.7	5.96	0.01	57.69	26.99	0.21	8.34	0.00	0.01	0.21	99.43
27 Xtl 3	We	47.0	1.0	51.9	5.62	0.01	57.24	27.62	0.25	9.22	0.03	0.01	0.17	100.18
27 Xtl 3	We	42.3	1.2	56.4	6.03	0.01	58.39	26.76	0.26	8.19	0.01	0.02	0.20	99.90
27 Xtl 3	We	42.7	1.2	56.1	6.05	0.01	57.96	27.20	0.23	8.33	0.01	0.01	0.20	99.99
27 Xtl 3	We	38.7	1.4	59.9	6.41	0.01	59.30	26.44	0.34	7.50	0.00	0.01	0.23	100.27
27 Xtl 3	We	38.2	1.3	60.5	6.47	0.01	59.30	26.18	0.33	7.39	0.02	0.02	0.22	100.00
27 Xtl 3	We	37.2	1.4	61.4	6.54	0.01	59.45	26.14	0.35	7.18	0.02	0.02	0.23	99.94
27 Xtl 4	We	45.5	1.1	53.4	5.73	0.01	57.27	27.52	0.20	8.83	0.02	0.01	0.17	99.78
27 Xtl 4	We	44.8	1.2	54.0	5.83	0.01	57.68	27.30	0.22	8.75	0.01	0.01	0.20	100.01
27 Xtl 4	We	46.3	1.1	52.6	5.67	0.01	57.20	27.70	0.26	9.01	0.01	0.01	0.18	100.06
27 Xtl 4	We	46.5	1.1	52.4	5.61	0.01	57.20	27.64	0.21	9.02	0.02	0.02	0.18	99.97
27 Xtl 4	We	43.5	1.1	55.4	5.94	0.01	58.15	27.35	0.22	8.45	0.03	0.01	0.18	100.36
27 Xtl 4	We	44.8	1.1	54.2	5.79	0.01	57.86	27.44	0.23	8.67	-0.01	0.01	0.17	100.24
27 Xtl 4	We	44.1	1.1	54.7	5.80	0.02	57.69	27.01	0.24	8.47	0.00	0.01	0.18	99.45
27 Xtl 4	We	43.3	1.2	55.5	5.74	0.01	58.58	27.22	0.23	8.11	0.01	0.02	0.19	100.12
27 Xtl 4	We	41.9	1.3	56.8	6.05	0.01	58.58	26.77	0.21	8.08	0.00	0.02	0.21	99.95
27 Xtl 4	We	44.3	1.2	54.5	5.85	0.02	58.13	27.22	0.21	8.60	0.02	0.02	0.19	100.27
27 Xtl 4	We	43.2	1.2	55.6	5.92	0.01	58.41	26.91	0.24	8.33	0.02	0.02	0.19	100.03

Table B.1 (Continued)

Sample	Lithology	An	Or	Ab	Na_2O	MgO	SiO_2	Al_2O_3	FeO	CaO	P_2O_5	TiO_2	K_2O	Total
27 Xtl 4	We	43.3	1.3	55.3	5.91	0.01	57.94	26.92	0.24	8.38	0.00	0.01	0.21	99.65
27 Xtl 4	We	44.2	1.2	54.6	5.87	0.01	57.50	27.28	0.25	8.60	0.02	0.01	0.20	99.74
27 Xtl 4	We	42.1	1.1	56.8	6.08	0.01	58.33	26.97	0.22	8.15	0.01	0.01	0.18	99.97
27 Xtl 4	We	42.9	1.2	55.9	5.96	0.02	58.11	26.80	0.28	8.28	0.03	0.00	0.19	99.66
27 Xtl 4	We	61.3	0.6	38.1	4.09	0.02	52.95	29.96	0.32	11.90	0.01	0.02	0.09	99.40
27 Xtl 4	We	58.1	0.7	41.2	4.45	0.02	54.27	29.40	0.31	11.35	0.00	0.02	0.11	99.99
27 Xtl 4	We	52.8	0.9	46.3	5.03	0.01	55.44	28.56	0.31	10.38	0.02	0.02	0.14	99.91
27 Xtl 4	We	47.3	1.0	51.7	5.58	0.02	56.89	27.76	0.29	9.25	0.01	0.02	0.17	100.03
27 Xtl 4	We	43.7	1.2	55.1	5.92	0.01	57.87	27.17	0.27	8.49	0.02	0.01	0.19	99.96
27 Xtl 4	We	42.6	1.2	56.2	6.04	0.01	58.22	27.08	0.24	8.27	0.01	0.01	0.19	100.09
27 Xtl 4	We	57.7	0.6	41.7	4.50	0.02	54.07	29.46	0.33	11.26	0.02	0.02	0.10	99.79
27 Xtl 4	We	54.2	0.8	44.9	4.83	0.01	55.56	29.08	0.27	10.56	0.03	0.02	0.14	100.51
27 Xtl 4	We	43.0	1.3	55.8	5.85	0.01	57.45	26.61	0.24	8.16	0.02	0.01	0.20	98.59
27 Xtl 4	We	41.4	1.2	57.4	6.02	0.02	58.80	26.85	0.30	7.86	0.01	0.01	0.19	100.08
27 Xtl 4.1	We	47.2	1.1	51.8	5.60	0.02	56.78	27.54	0.37	9.23	0.01	0.01	0.18	99.74
27 Xtl 4.1	We	55.4	0.7	43.9	4.72	0.02	54.79	29.14	0.35	10.76	0.01	0.02	0.12	99.93
27 Xtl 4.2	We	42.3	1.1	56.6	6.01	0.01	58.43	26.76	0.23	8.12	0.01	0.02	0.18	99.78
27 Xtl 4.2	We	43.5	1.2	55.4	5.92	0.02	57.92	27.18	0.25	8.40	0.01	0.02	0.19	99.90
27 Xtl 4.2	We	41.6	1.4	57.0	6.08	0.03	58.50	26.58	0.31	8.04	0.00	0.01	0.23	99.81
27 Xtl 5	We	42.6	1.1	56.3	6.00	0.01	58.22	26.74	0.26	8.21	0.01	0.01	0.18	99.72
27 Xtl 5	We	42.4	1.2	56.4	6.01	0.01	58.21	26.85	0.20	8.18	0.03	0.01	0.19	99.72
27 Xtl 5	We	46.0	1.1	52.9	5.62	0.01	57.07	27.49	0.21	8.83	0.02	0.02	0.18	99.45
27 Xtl 5	We	37.6	1.4	60.9	6.48	0.02	59.42	26.14	0.26	7.24	0.02	0.01	0.23	99.84
27 Xtl 6	We	33.8	1.6	64.6	6.80	0.00	60.40	25.57	0.04	6.44	0.02	0.01	0.26	99.53
27 Xtl 6	We	36.0	1.4	62.6	6.67	0.00	59.91	26.15	0.02	6.93	0.01	0.00	0.23	99.97
27 Xtl 6	We	42.4	1.2	56.3	6.00	0.02	58.19	26.79	0.34	8.17	0.01	0.02	0.20	99.73
27 Xtl 6	We	38.5	1.5	60.1	6.40	0.02	59.40	26.41	0.28	7.41	0.01	0.01	0.24	100.21
14 Xtl 1	EKPF	44.2	1.2	54.6	5.95	0.00	58.30	27.71	0.22	8.72	0.01	0.02	0.20	101.13
14 Xtl 1	EKPF	44.1	1.3	54.7	5.97	0.01	58.19	27.59	0.24	8.71	0.03	0.01	0.21	101.02
14 Xtl 1	EKPF	48.9	1.0	50.1	5.47	0.01	57.00	28.36	0.23	9.65	0.02	0.01	0.17	100.96
14 Xtl 1	EKPF	45.7	1.2	53.0	5.83	0.02	57.77	27.80	0.30	9.10	0.01	0.02	0.21	101.07
14 Xtl 1.5	EKPF	47.9	1.1	51.1	5.62	0.01	56.79	28.07	0.27	9.53	0.02	0.02	0.18	100.52
14 Xtl 1.5	EKPF	38.1	1.4	60.5	6.59	0.00	59.91	26.62	0.25	7.51	0.02	0.01	0.23	101.17

Table B.1 (Continued)

Sample	Lithology	An	Or	Ab	Na_2O	MgO	SiO_2	Al_2O_3	FeO	CaO	P_2O_5	TiO_2	K_2O	Total
14 Xtl 1.5	EKPF	39.0	1.4	59.5	6.47	0.01	59.53	26.65	0.28	7.68	0.01	0.02	0.24	100.94
14 Xtl 1 mc 1	EKPF	48.7	1.1	50.2	5.48	0.04	56.53	28.15	0.52	9.62	0.00	0.04	0.18	100.57
14 Xtl 1 mc 1	EKPF	41.0	1.5	57.6	6.32	0.02	59.36	26.89	0.35	8.13	0.02	0.02	0.24	101.38
14 Xtl 1 mc 2	EKPF	35.4	1.7	62.9	6.77	0.03	60.54	26.17	0.35	6.90	0.03	0.01	0.28	101.08
14 Xtl 1 mc 2	EKPF	40.4	1.6	58.0	6.28	0.01	59.49	26.84	0.30	7.92	0.04	0.01	0.26	101.14
14 Xtl 2	EKPF	47.4	1.4	51.3	5.65	0.01	56.90	27.89	0.20	9.44	0.02	0.02	0.23	100.37
14 Xtl 2	EKPF	46.9	1.3	51.8	5.67	0.01	57.75	28.01	0.22	9.30	0.01	0.01	0.21	101.21
14 Xtl 2	EKPF	41.5	1.6	56.9	6.15	0.01	58.76	27.04	0.20	8.11	0.00	0.01	0.26	100.53
14 Xtl 2	EKPF	45.3	1.2	53.5	5.84	0.01	57.28	27.51	0.22	8.95	0.01	0.01	0.20	100.05
14 Xtl 2	EKPF	57.3	0.8	41.9	4.58	0.03	54.93	29.61	0.35	11.32	0.04	0.03	0.13	101.03
14 Xtl 3	EKPF	50.1	1.0	48.9	5.37	0.01	56.14	28.17	0.23	9.95	0.03	0.02	0.17	100.10
14 Xtl 3	EKPF	46.7	1.1	52.2	5.71	0.01	57.18	27.74	0.22	9.23	0.01	0.01	0.18	100.33
14 Xtl 3	EKPF	51.1	0.9	48.0	5.26	0.02	56.01	28.45	0.28	10.13	0.01	0.02	0.15	100.36
14 Xtl 3	EKPF	50.8	0.9	48.3	5.28	0.02	55.86	28.38	0.28	10.04	0.02	0.02	0.15	100.08
14 Xtl 3	EKPF	40.5	1.4	58.2	6.37	0.00	58.55	26.81	0.24	8.03	0.01	0.01	0.23	100.23
14 Xtl 3	EKPF	38.9	1.6	59.6	6.40	0.01	59.52	26.25	0.24	7.55	0.02	0.00	0.25	100.25
14 Xtl 3 .5	EKPF	50.4	0.9	48.7	5.33	0.03	56.28	28.35	0.31	9.99	0.04	0.03	0.15	100.54
14 Xtl 3 .5	EKPF	64.4	1.1	34.6	2.99	0.03	57.37	29.02	0.35	10.09	0.04	0.04	0.14	100.08
14 Xtl 3 .6	EKPF	62.4	0.5	37.1	4.04	0.06	52.77	30.17	0.48	12.31	0.01	0.04	0.08	100.02
14 Xtl 3 .6	EKPF	51.2	0.9	47.8	5.21	0.02	55.69	28.62	0.32	10.10	0.01	0.01	0.15	100.14
14 Xtl 3 .6	EKPF	44.2	1.2	54.5	5.94	0.02	57.77	27.33	0.30	8.72	0.01	0.01	0.20	100.33
14 Xtl 3 .6	EKPF	52.0	0.9	47.1	5.14	0.02	55.38	28.54	0.33	10.28	0.02	0.03	0.15	99.95
14 Xtl 3 mc 1	EKPF	44.8	1.2	54.0	5.86	0.01	57.46	27.64	0.28	8.79	0.03	0.02	0.20	100.33
14 Xtl 3 .7	EKPF	31.4	1.8	66.8	7.19	0.00	61.09	25.38	0.04	6.12	0.02	0.00	0.30	100.17
14 Xtl 3 .7	EKPF	30.7	1.8	67.5	7.23	0.00	61.73	25.15	0.05	5.96	0.01	0.01	0.29	100.48
14 Xtl 3 .7	EKPF	42.5	1.3	56.2	6.13	0.02	58.61	27.14	0.28	8.39	0.00	0.01	0.21	100.79
14 Xtl 3. 7	EKPF	44.2	1.2	54.6	5.93	0.02	57.54	27.14	0.34	8.68	0.02	0.01	0.19	99.92
14 Xtl 4	EKPF	43.9	1.3	54.8	6.01	0.01	57.38	27.21	0.25	8.72	0.01	0.01	0.22	99.83
14 Xtl 4	EKPF	75.5	0.3	24.2	2.64	0.02	49.39	32.65	0.41	14.94	0.01	0.02	0.05	100.13
14 Xtl 4	EKPF	65.4	0.5	34.1	3.74	0.03	51.67	30.78	0.41	12.98	0.02	0.03	0.09	99.75
14 Xtl 4	EKPF	60.2	0.7	39.1	4.30	0.03	53.00	29.90	0.34	11.97	0.02	0.02	0.11	99.70
14 Xtl 4	EKPF	54.6	0.8	44.7	4.87	0.02	54.50	29.28	0.29	10.76	0.03	0.03	0.13	99.91
14 Xtl 4	EKPF	41.8	1.3	56.9	6.20	0.02	57.95	26.78	0.29	8.22	0.02	0.01	0.22	99.70

Table B.1 (Continued)

Sample	Lithology	An	Or	Ab	Na_2O	MgO	SiO_2	Al_2O_3	FeO	CaO	P_2O_5	TiO_2	K_2O	Total
14 Xtl 4	EKPF	40.8	1.5	57.7	6.30	0.02	58.16	26.77	0.31	8.05	0.01	0.02	0.24	99.88
14 Xtl 4	EKPF	71.8	0.4	27.8	3.07	0.02	50.30	32.14	0.32	14.31	0.01	0.01	0.07	100.25
14 Xtl 4	EKPF	81.9	0.3	17.9	1.95	0.01	47.61	33.93	0.39	16.21	0.00	0.01	0.05	100.17
14 Xtl 4 .6	EKPF	47.4	1.2	51.4	5.30	0.99	56.47	26.82	1.49	8.84	0.01	0.03	0.19	100.16
14 Xtl 4 .6	EKPF	38.9	1.5	59.6	6.30	0.03	58.45	26.20	0.41	7.45	0.03	0.03	0.24	99.18
14 Xtl 4 .8	EKPF	47.0	1.1	51.9	5.67	0.01	57.03	28.05	0.24	9.31	0.03	0.01	0.18	100.58
14 Xtl 4. 8	EKPF	39.4	1.4	59.2	6.41	0.01	59.31	26.88	0.25	7.72	0.01	0.01	0.23	100.84
14 Xtl 5	EKPF	46.7	1.1	52.2	5.67	0.01	56.82	27.67	0.24	9.20	0.02	0.01	0.18	99.84
14 Xtl 5	EKPF	47.0	1.0	52.0	5.68	0.01	56.27	27.70	0.24	9.27	0.01	0.01	0.16	99.35
14 Xtl 5	EKPF	48.9	0.9	50.2	5.50	0.02	56.10	28.09	0.25	9.69	0.02	0.02	0.16	99.90
14 Xtl 5	EKPF	55.9	0.8	43.3	4.75	0.03	53.93	29.32	0.37	11.11	0.02	0.03	0.13	99.70
14 Xtl 5	EKPF	50.5	0.9	48.6	5.33	0.02	55.26	28.29	0.35	10.02	0.03	0.01	0.15	99.46
14 Xtl 5	EKPF	48.4	1.1	50.6	5.54	0.02	55.84	27.95	0.28	9.59	0.03	0.02	0.18	99.49
14 Xtl 5	EKPF	38.8	1.3	59.9	6.51	0.02	58.71	26.31	0.24	7.62	0.02	0.02	0.22	99.74
14 Xtl 5	EKPF	42.2	1.1	56.7	6.12	0.02	57.99	26.96	0.29	8.24	0.02	0.02	0.18	99.83
14 Xtl 5	EKPF	40.2	1.3	58.5	6.34	0.01	58.34	26.68	0.22	7.88	0.00	0.01	0.21	99.71
14 Xtl 5.5	EKPF	43.3	1.2	55.5	5.99	0.01	57.97	26.92	0.22	8.45	0.01	0.01	0.20	99.78
14 Xtl 5.5	EKPF	43.0	1.2	55.8	6.04	0.01	58.41	27.09	0.25	8.42	0.02	0.01	0.19	100.43
14 Xtl 5.5	EKPF	51.0	0.9	48.1	5.21	0.03	55.76	28.39	0.37	10.00	0.03	0.02	0.14	99.97
14 Xtl 5.5	EKPF	39.2	1.5	59.3	6.36	0.01	59.09	26.52	0.28	7.62	0.01	0.02	0.24	100.15
14 Xtl 5.6	EKPF	53.6	0.8	45.6	4.99	0.01	54.82	29.06	0.23	10.63	0.01	0.01	0.13	99.92
14 Xtl 5.6	EKPF	51.5	0.8	47.6	5.21	0.02	55.39	28.55	0.22	10.20	0.03	0.02	0.14	99.80
14 Xtl 5.6	EKPF	64.0	0.5	35.6	3.89	0.02	52.20	30.84	0.26	12.64	0.00	0.03	0.08	100.00
14 Xtl 5.6	EKPF	64.1	0.5	35.4	3.88	0.02	52.32	30.91	0.27	12.74	0.02	0.02	0.08	100.28
14 Xtl 5.6	EKPF	63.4	0.6	36.0	3.94	0.02	52.67	30.60	0.30	12.55	0.03	0.02	0.09	100.22
14 Xtl 5.6	EKPF	58.8	0.6	40.6	4.46	0.01	53.65	29.87	0.28	11.69	0.02	0.02	0.10	100.10
14 Xtl 5.6	EKPF	59.3	0.7	40.0	4.38	0.01	53.57	29.98	0.29	11.76	0.01	0.02	0.12	100.13
14 Xtl 5.6	EKPF	53.7	0.8	45.4	4.93	0.01	55.15	29.09	0.25	10.55	0.03	0.02	0.14	100.18
14 Xtl 5.6	EKPF	45.2	1.1	53.7	5.85	0.02	57.22	27.69	0.23	8.90	0.02	0.01	0.18	100.17
14 Xtl 5.6	EKPF	38.3	1.4	60.3	6.48	0.01	59.31	26.47	0.22	7.45	0.01	0.01	0.23	100.23
14 Xtl 5.6	EKPF	59.3	0.6	40.1	4.37	0.01	53.79	29.97	0.20	11.71	0.01	0.03	0.10	100.19
14 Xtl 5.6	EKPF	55.5	0.9	43.6	4.77	0.01	54.26	29.28	0.18	10.97	0.02	0.01	0.14	99.65
14 Xtl 5.6	EKPF	48.9	0.9	50.2	5.44	0.01	56.18	28.15	0.19	9.58	0.03	0.01	0.15	99.76

Table B.1 (Continued)

Sample	Lithology	An	Or	Ab	Na_2O	MgO	SiO_2	Al_2O_3	FeO	CaO	P_2O_5	TiO_2	K_2O	Total
14 Xtl 5.6	EKPF	37.5	1.5	61.0	6.53	0.01	59.66	26.35	0.27	7.27	0.01	0.01	0.24	100.39
14 Xtl 5.6	EKPF	52.0	0.9	47.1	5.19	0.02	55.81	28.48	0.32	10.35	0.03	0.03	0.14	100.43
14 Xtl 5.6	EKPF	50.6	0.9	48.6	5.28	0.02	56.19	28.37	0.32	9.94	0.02	0.02	0.14	100.30
14 Xtl 5.6	EKPF	43.3	1.2	55.5	5.99	0.01	58.34	27.12	0.23	8.45	0.01	0.01	0.19	100.36
14 Xtl 5.6	EKPF	41.8	1.2	57.0	6.29	0.01	58.41	27.03	0.23	8.35	0.02	0.01	0.21	100.57
14 Xtl 5.6	EKPF	39.8	1.4	58.7	6.38	0.01	58.96	26.70	0.28	7.83	0.00	0.02	0.24	100.55
32 Xtl 1	Xb	33.3	1.7	65.0	6.85	0.00	61.36	25.74	0.06	6.35	0.02	0.00	0.28	100.70
32 Xtl 1	Xb	41.5	1.2	57.3	6.15	0.01	58.75	27.07	0.17	8.06	0.00	0.00	0.20	100.49
32 Xtl 1	Xb	44.1	1.4	54.5	5.83	0.01	58.13	27.29	0.25	8.55	0.00	0.01	0.22	100.29
32 Xtl 1	Xb	47.1	1.4	51.4	5.50	0.06	57.11	26.94	0.53	9.11	0.03	0.05	0.23	99.60
32 Xtl 1.1	Xb	55.8	0.8	43.4	4.70	0.01	55.10	29.32	0.31	10.93	0.04	0.01	0.13	100.60
32 Xtl 1.1	Xb	61.5	0.7	37.8	4.12	0.02	53.44	30.31	0.37	12.13	0.02	0.02	0.11	100.55
32 Xtl 1.1	Xb	54.4	0.8	44.8	4.86	0.02	55.42	29.03	0.34	10.67	0.03	0.03	0.13	100.52
32 Xtl 1.1	Xb	52.0	0.9	47.1	5.09	0.02	55.88	28.70	0.32	10.19	0.03	0.02	0.15	100.41
32 Xtl 1.1	Xb	51.1	1.4	47.5	5.03	0.10	56.36	27.61	0.69	9.80	0.01	0.10	0.23	99.94
32 Xtl 2	Xb	81.6	0.3	18.1	1.98	0.07	48.13	33.46	0.57	16.15	0.01	0.03	0.05	100.46
32 Xtl 2	Xb	74.4	0.6	25.0	2.71	0.08	50.01	32.12	0.54	14.59	0.01	0.05	0.09	100.20
32 Xtl 2	Xb	76.7	0.4	22.9	2.48	0.09	49.42	32.43	0.44	15.03	0.02	0.04	0.07	100.04
32 Xtl 2	Xb	68.0	0.6	31.4	3.44	0.10	51.73	30.82	0.46	13.47	0.01	0.06	0.11	100.20
32 Xtl 2	Xb	77.4	0.4	22.1	2.39	0.08	49.20	32.25	0.48	15.15	0.01	0.04	0.07	99.73
32 Xtl 4	Xb	73.2	0.5	26.3	2.85	0.10	50.43	31.75	0.49	14.36	0.03	0.04	0.08	100.14
32 Xtl 4	Xb	80.7	0.3	18.9	2.05	0.07	48.26	33.11	0.50	15.82	0.01	0.04	0.06	99.99
32 Xtl 4	Xb	76.6	0.4	23.0	2.50	0.08	49.45	32.49	0.50	15.07	0.02	0.05	0.07	100.28
32 Xtl 4	Xb	77.2	0.4	22.3	2.44	0.08	49.15	32.71	0.52	15.27	0.03	0.05	0.07	100.31
32 Xtl 4	Xb	58.2	1.0	40.8	4.38	0.09	53.68	29.06	0.61	11.31	0.02	0.08	0.16	99.38
32 Xtl 4.1	Xb	47.2	1.0	51.7	5.60	0.02	57.28	27.72	0.31	9.26	0.02	0.02	0.17	100.42
32 Xtl 4.1	Xb	40.9	1.5	57.7	6.23	0.01	59.12	26.76	0.28	7.98	0.01	0.01	0.24	100.66
32 Xtl 4.1	Xb	57.7	1.0	41.3	4.46	0.07	54.43	29.25	0.54	11.25	0.01	0.06	0.17	100.25
32 Xtl 5	Xb	46.3	1.3	52.4	5.67	0.02	57.37	27.50	0.21	9.05	0.02	0.02	0.22	100.09
32 Xtl 5	Xb	42.3	1.5	56.2	6.02	0.02	58.76	26.90	0.22	8.18	0.02	0.02	0.25	100.39
32 Xtl 5	Xb	42.7	1.4	55.9	5.99	0.02	58.56	26.93	0.20	8.27	0.01	0.01	0.23	100.22
32 Xtl 5	Xb	41.3	1.6	57.1	6.14	0.03	59.21	26.68	0.23	8.02	0.01	0.01	0.26	100.60
32 Xtl 5	Xb	61.7	0.8	37.5	4.04	0.08	53.89	29.87	0.59	12.02	0.03	0.06	0.13	100.75

Table B.1 (Continued)

Sample	Lithology	An	Or	Ab	Na_2O	MgO	SiO_2	Al_2O_3	FeO	CaO	P_2O_5	TiO_2	K_2O	Total
32 Xtl 5	Xb	54.0	2.1	43.9	4.54	0.26	56.13	27.00	1.08	10.09	0.06	0.20	0.33	99.69
32 Xtl 5	Xb	49.2	1.4	49.4	5.25	0.05	57.03	27.88	0.39	9.48	0.02	0.03	0.23	100.38
32 Xtl 5	Xb	63.3	0.8	35.9	3.90	0.08	52.76	29.90	0.59	12.44	0.02	0.06	0.13	99.90
32 Xtl 5	Xb	62.0	0.8	37.2	4.04	0.07	53.42	29.87	0.55	12.20	0.02	0.07	0.14	100.39
32 Xtl 5	Xb	62.9	0.8	36.3	3.95	0.08	53.29	30.29	0.54	12.37	0.02	0.07	0.13	100.79
32 Xtl 5	Xb	61.5	0.8	37.7	4.09	0.08	53.51	29.81	0.53	12.07	0.02	0.06	0.14	100.32
32 Xtl 5	Xb	60.8	0.8	38.4	4.15	0.10	53.54	29.63	0.60	11.90	0.02	0.06	0.13	100.14
32 Xtl 5	Xb	58.9	0.9	40.2	4.34	0.09	54.16	29.35	0.60	11.49	0.01	0.07	0.15	100.31
32 Xtl 5	Xb	49.9	1.2	48.8	5.26	0.08	56.49	27.90	0.60	9.74	0.04	0.08	0.20	100.41
32 Xtl 6	Xb	48.7	3.3	48.0	4.82	0.40	58.22	25.79	1.46	8.86	0.14	0.41	0.50	100.63
32 Xtl 6	Xb	75.4	0.5	24.1	2.63	0.07	49.89	32.20	0.51	14.87	0.02	0.04	0.08	100.33
32 Xtl 6	Xb	76.3	0.3	23.4	2.56	0.07	49.64	32.47	0.46	15.09	0.03	0.02	0.06	100.39
32 Xtl 6	Xb	64.8	0.6	34.6	3.76	0.09	52.68	30.48	0.50	12.76	0.02	0.04	0.09	100.43
32 Xtl 6	Xb	75.8	0.4	23.8	2.61	0.08	49.68	32.32	0.59	15.04	0.02	0.05	0.07	100.49
32 Xtl 6	Xb	64.0	0.8	35.2	3.84	0.08	52.83	30.36	0.59	12.66	0.00	0.06	0.13	100.57
32 Xtl 7	Xb	74.4	0.5	25.2	2.75	0.07	49.94	32.13	0.53	14.70	0.01	0.05	0.08	100.25
32 Xtl 7	Xb	66.2	0.8	32.9	3.61	0.07	52.54	30.94	0.57	13.13	0.02	0.07	0.14	101.10
32 Xtl 7	Xb	73.6	0.5	25.9	2.85	0.08	50.12	31.93	0.49	14.62	0.01	0.05	0.09	100.23
32 Xtl 7	Xb	61.1	2.5	36.4	3.71	0.50	54.56	27.39	1.75	11.28	0.25	0.39	0.39	100.24
32 Xtl 7 rim T	Xb	77.0	0.4	22.5	2.48	0.09	49.46	32.55	0.47	15.36	0.00	0.03	0.08	100.50
32 Xtl 7 rim T	Xb	77.8	0.3	21.9	2.40	0.07	49.08	32.76	0.50	15.41	0.01	0.04	0.06	100.33
32 Xtl 7 rim T	Xb	79.0	0.3	20.7	2.24	0.07	48.88	32.86	0.47	15.46	0.03	0.05	0.05	100.13
32 Xtl 7 rim T	Xb	75.6	0.5	23.9	2.61	0.08	49.79	32.56	0.57	14.90	0.01	0.05	0.08	100.66
32 Xtl 7 rim T	Xb	65.1	0.7	34.2	3.73	0.10	52.33	30.51	0.52	12.84	0.03	0.07	0.12	100.25
32 Xtl 7 rim T	Xb	63.8	0.8	35.4	3.85	0.08	52.87	30.24	0.55	12.57	0.02	0.06	0.13	100.39
32 Xtl 7 rim T	Xb	62.6	0.8	36.7	4.00	0.09	53.25	29.93	0.59	12.36	0.01	0.06	0.13	100.41
32 Xtl 7 rim T	Xb	55.6	1.0	43.4	4.70	0.07	54.82	28.78	0.60	10.89	0.02	0.07	0.17	100.14
07 Xtl 4	X Lahar	40.9	2.3	56.8	6.22	0.03	58.44	26.59	0.23	8.10	0.00	0.02	0.39	100.02
07 Xtl 4	X Lahar	44.7	1.6	53.7	5.88	0.02	57.16	27.39	0.21	8.87	0.01	0.01	0.27	99.81
07 Xtl 4	X Lahar	47.0	1.1	51.9	5.69	0.01	56.75	27.63	0.21	9.32	0.01	0.00	0.19	99.81
07 Xtl 4	X Lahar	45.8	1.5	52.7	5.78	0.03	57.03	27.65	0.25	9.08	0.02	0.01	0.25	100.08
07 Xtl 4	X Lahar	43.1	2.5	54.3	5.94	0.04	57.74	27.04	0.37	8.53	0.02	0.02	0.42	100.12
07 Xtl 4	X Lahar	61.9	1.2	36.9	4.05	0.07	52.78	30.01	0.60	12.29	0.02	0.07	0.21	100.08

Table B.1 (Continued)

Sample	Lithology	An	Or	Ab	Na_2O	MgO	SiO_2	Al_2O_3	FeO	CaO	P_2O_5	TiO_2	K_2O	Total
07 Xtl 1	X Lahar	58.9	1.0	40.0	4.35	0.05	53.33	29.70	0.41	11.58	0.03	0.03	0.17	99.64
07 Xtl 1	X Lahar	56.8	1.3	41.9	4.61	0.05	54.10	29.36	0.41	11.33	0.03	0.03	0.22	100.14
07 Xtl 1	X Lahar	59.4	1.0	39.6	4.35	0.05	53.43	29.86	0.40	11.81	0.00	0.04	0.16	100.10
07 Xtl 1	X Lahar	49.8	1.4	48.8	5.36	0.05	55.98	28.12	0.40	9.91	0.03	0.04	0.23	100.12
07 Xtl 1	X Lahar	55.8	1.2	43.0	4.71	0.05	54.14	29.19	0.41	11.07	0.04	0.05	0.20	99.85
07 Xtl 1	X Lahar	55.1	1.5	43.5	4.79	0.04	54.89	29.07	0.41	10.99	0.02	0.03	0.24	100.50
07 Xtl 1.3	X Lahar	59.9	0.9	39.1	4.30	0.04	53.36	30.11	0.30	11.90	0.02	0.01	0.16	100.20
07 Xtl 1.3	X Lahar	58.1	1.3	40.6	4.44	0.05	53.94	29.79	0.31	11.49	0.02	0.01	0.22	100.26
07 Xtl 1.3	X Lahar	61.8	1.1	37.1	4.06	0.08	52.81	29.97	0.64	12.26	0.01	0.08	0.18	100.09
07 Xtl 1.3	X Lahar	47.6	2.1	50.3	5.51	0.09	56.61	27.45	0.59	9.44	0.04	0.11	0.34	100.19
07 Xtl 1.3	X Lahar	49.8	2.1	48.1	5.27	0.08	55.77	27.77	0.69	9.88	0.03	0.11	0.35	99.95
07 Xtl 1.2	X Lahar	70.2	0.8	29.0	3.17	0.07	50.52	31.45	0.53	13.92	0.01	0.06	0.13	99.88
07 Xtl 1.2	X Lahar	60.4	1.0	38.6	4.26	0.08	53.09	29.69	0.53	12.07	0.01	0.06	0.18	99.98
07 Xtl 1.2	X Lahar	54.0	1.5	44.5	4.90	0.06	54.96	28.52	0.55	10.77	0.03	0.08	0.26	100.12
07 Xtl 1.4	X Lahar	33.2	2.2	64.7	7.04	0.00	60.19	25.60	0.12	6.54	0.02	0.00	0.36	99.88
07 Xtl 1.4	X Lahar	34.7	2.1	63.2	6.86	0.00	60.03	25.78	0.14	6.82	0.02	0.01	0.34	100.01
07 Xtl 1.4	X Lahar	35.3	2.4	62.2	6.84	0.01	59.64	25.94	0.16	7.03	0.01	0.01	0.40	100.04
07 Xtl 1.4	X Lahar	55.6	1.0	43.4	4.76	0.04	54.19	29.08	0.41	11.03	0.04	0.04	0.16	99.76
07 Xtl 1.4	X Lahar	54.5	1.1	44.4	4.85	0.05	54.58	28.87	0.45	10.79	0.05	0.02	0.18	99.84
07 Xtl 1.4	X Lahar	66.7	0.8	32.5	3.56	0.08	51.52	30.81	0.49	13.21	0.02	0.05	0.13	99.87
07 Xtl 1.4	X Lahar	66.7	0.8	32.5	3.55	0.08	51.20	30.89	0.47	13.16	0.03	0.05	0.13	99.56
07 Xtl 1.5	X Lahar	67.3	0.8	32.0	3.51	0.09	51.07	31.20	0.38	13.36	0.01	0.06	0.13	99.79
07 Xtl 1.5	X Lahar	70.9	0.7	28.4	3.12	0.09	50.41	31.63	0.48	14.08	0.02	0.05	0.12	100.00
07 Xtl 1.5	X Lahar	78.6	0.4	21.0	2.30	0.06	48.17	33.20	0.49	15.53	0.01	0.04	0.07	99.86
07 Xtl 1.5	X Lahar	57.7	1.6	40.6	4.49	0.11	52.89	29.39	0.57	11.55	0.04	0.07	0.27	99.40
07 Xtl 1.5	X Lahar	53.2	1.6	45.2	4.96	0.09	54.67	28.52	0.64	10.56	0.02	0.10	0.27	99.82
07 Xtl 1.6	X Lahar	43.7	1.7	54.5	5.94	0.03	57.55	27.00	0.28	8.62	0.03	0.02	0.29	99.76
07 Xtl 1.6	X Lahar	43.8	1.7	54.5	5.95	0.03	57.34	27.20	0.26	8.65	0.01	0.01	0.29	99.73
07 Xtl 1.6	X Lahar	38.0	2.2	59.8	6.56	0.04	59.24	25.98	0.31	7.54	0.02	0.02	0.37	100.09
07 Xtl 1.6	X Lahar	50.3	1.5	48.2	5.25	0.06	55.89	28.14	0.48	9.90	0.04	0.03	0.25	100.04
07 Xtl 1.6	X Lahar	43.7	3.3	53.0	5.79	0.07	57.25	26.54	0.84	8.63	0.03	0.14	0.55	99.84
07 Xtl 2	X Lahar	47.5	1.1	51.4	5.63	0.01	56.18	27.79	0.21	9.41	0.00	0.01	0.19	99.42
07 Xtl 2	X Lahar	47.5	1.2	51.3	5.60	0.02	56.35	27.79	0.22	9.39	0.01	0.02	0.20	99.59

Table B.1 (Continued)

Sample	Lithology	An	Or	Ab	Na_2O	MgO	SiO_2	Al_2O_3	FeO	CaO	P_2O_5	TiO_2	K_2O	Total
07 Xtl 2	X Lahar	55.0	1.4	43.6	4.76	0.07	54.37	28.70	0.55	10.86	0.02	0.08	0.23	99.64
07 Xtl 2	X Lahar	50.9	1.6	47.5	5.18	0.09	55.36	28.02	0.61	10.04	0.01	0.09	0.27	99.67
07 Xtl 2	X Lahar	56.2	1.5	42.3	4.63	0.07	54.14	28.96	0.56	11.12	0.01	0.07	0.24	99.81
07 Xtl 3	X Lahar	61.0	1.1	37.9	4.15	0.01	52.69	30.22	0.23	12.09	0.03	0.05	0.19	99.64
07 Xtl 3	X Lahar	55.4	1.4	43.2	4.73	0.01	54.39	29.14	0.23	10.99	0.01	0.03	0.23	99.77
07 Xtl 3	X Lahar	51.5	1.5	47.0	5.15	0.03	55.17	28.57	0.25	10.23	0.03	0.04	0.25	99.70
07 Xtl 3	X Lahar	58.9	1.3	39.8	4.36	0.01	53.37	29.83	0.26	11.67	0.03	0.04	0.21	99.79
07 Xtl 3	X Lahar	51.0	1.5	47.6	5.18	0.03	55.33	28.19	0.29	10.05	-0.01	0.00	0.24	99.31
07 Xtl 3	X Lahar	53.0	1.4	45.6	4.98	0.02	54.76	28.64	0.22	10.46	0.02	0.03	0.24	99.35
07 Xtl 3	X Lahar	53.4	1.5	45.1	4.93	0.01	54.87	28.64	0.28	10.57	-0.01	0.04	0.25	99.60
07 Xtl 9	X Lahar	47.2	1.8	51.0	5.51	0.03	56.25	27.59	0.29	9.23	0.03	0.01	0.29	99.23
07 Xtl 9	X Lahar	45.4	2.0	52.6	5.68	0.02	56.56	27.26	0.27	8.88	0.03	0.01	0.33	99.04
07 Xtl 9	X Lahar	42.1	2.3	55.6	6.05	0.02	57.55	26.74	0.27	8.30	0.03	0.01	0.38	99.36
07 Xtl 9	X Lahar	38.4	2.6	59.0	6.39	0.04	58.55	26.07	0.27	7.52	0.02	0.02	0.43	99.30
07 Xtl 9	X Lahar	44.0	2.3	53.8	5.86	0.03	57.27	26.87	0.25	8.68	0.01	0.02	0.38	99.37
07 Xtl 9	X Lahar	42.4	2.4	55.2	5.98	0.03	57.36	26.84	0.29	8.32	0.01	0.01	0.39	99.22
07 Xtl 9	X Lahar	41.4	2.4	56.1	6.10	0.03	57.83	26.61	0.23	8.15	0.01	0.01	0.40	99.37
07 Xtl 9	X Lahar	52.8	1.7	45.5	4.97	0.06	54.30	28.42	0.42	10.42	0.01	0.02	0.29	98.90
07 Xtl 9	X Lahar	49.2	1.9	48.8	5.29	0.04	55.46	28.01	0.37	9.65	0.03	0.02	0.32	99.18
07 Xtl 9	X Lahar	43.4	2.5	54.1	5.89	0.03	57.44	26.78	0.33	8.57	0.00	0.02	0.41	99.48
07 Xtl 9	X Lahar	39.5	3.0	57.5	6.29	0.05	58.38	26.15	0.42	7.83	0.02	0.02	0.50	99.66
07 Xtl 9	X Lahar	38.9	3.1	58.0	6.31	0.05	58.46	26.04	0.45	7.64	0.00	0.02	0.51	99.48
07 Xtl 8	X Lahar	75.9	0.4	23.7	2.57	0.08	49.04	32.50	0.50	14.89	0.02	0.04	0.07	99.70
07 Xtl 8	X Lahar	73.4	0.5	26.0	2.85	0.08	49.61	32.07	0.49	14.51	0.02	0.04	0.09	99.75
07 Xtl 8	X Lahar	63.0	1.0	36.0	3.92	0.09	52.30	30.00	0.57	12.42	0.01	0.07	0.16	99.53
07 Xtl 8	X Lahar	52.5	1.8	45.7	5.00	0.07	54.98	28.33	0.54	10.40	0.01	0.09	0.29	99.72
07 Xtl 8	X Lahar	50.3	1.7	48.0	5.24	0.10	55.55	27.81	0.72	9.94	0.05	0.13	0.29	99.82
07 Xtl 8	X Lahar	48.7	2.2	49.0	5.36	0.06	55.70	27.65	0.66	9.63	0.02	0.10	0.37	99.55
07 Xtl 8 mc 1	X Lahar	28.6	5.4	66.0	7.17	0.05	61.25	24.23	0.59	5.62	0.02	0.11	0.89	99.93
07 Xtl 8 mc 1	X Lahar	27.4	5.6	67.0	7.30	0.04	61.42	24.36	0.56	5.40	0.03	0.10	0.92	100.13
07 Xtl 8 mc 2	X Lahar	39.2	3.4	57.4	6.20	0.07	57.70	25.66	0.74	7.65	0.02	0.15	0.56	98.74
07 Xtl 8 mc 2	X Lahar	34.0	4.4	61.6	6.68	0.06	59.61	25.01	0.73	6.67	0.05	0.15	0.73	99.67
07 Xtl 8 mc 3	X Lahar	39.9	3.3	56.8	6.18	0.06	57.89	26.11	0.74	7.86	0.02	0.14	0.55	99.54

Table B.1 (Continued)

Sample	Lithology	An	Or	Ab	Na_2O	MgO	SiO_2	Al_2O_3	FeO	CaO	P_2O_5	TiO_2	K_2O	Total
07 Xtl 8 mc 3	X Lahar	44.8	2.5	52.7	5.76	0.06	56.47	27.09	0.71	8.86	0.03	0.12	0.42	99.54
30 Xtl 1 core	X lava	73.6	0.5	25.9	2.84	0.05	50.15	32.21	0.45	14.65	0.00	0.02	0.08	100.51
30 Xtl 1 core	X lava	77.8	0.4	21.8	2.39	0.02	49.30	32.95	0.56	15.48	0.00	0.03	0.06	100.79
30 Xtl 1 core	X lava	72.7	0.7	26.5	2.88	0.04	50.81	31.65	0.54	14.27	-0.01	0.03	0.12	100.37
30 Xtl 1	X lava	76.2	0.5	23.3	2.57	0.04	49.82	32.63	0.50	15.18	0.02	0.03	0.08	100.88
30 Xtl 1	X lava	71.5	0.5	28.0	3.05	0.07	50.71	31.75	0.50	14.12	0.02	0.02	0.08	100.33
30 Xtl 1	X lava	71.9	0.4	27.7	3.05	0.07	50.84	31.61	0.51	14.30	0.01	0.03	0.07	100.50
30 Xtl 1	X lava	63.5	0.7	35.8	3.94	0.07	53.11	30.27	0.62	12.66	0.02	0.05	0.11	100.86
30 Xtl 1	X lava	53.5	1.3	45.2	4.93	0.05	55.45	28.25	0.61	10.56	0.02	0.06	0.21	100.15
30 Xtl 1.1	X lava	57.1	0.9	42.0	4.56	0.04	54.61	29.59	0.43	11.22	0.02	0.02	0.15	100.68
30 Xtl 1.1	X lava	49.3	1.3	49.4	5.41	0.05	56.50	27.82	0.56	9.76	0.00	0.06	0.22	100.42
30 Xtl 1.2	X lava	68.6	0.6	30.8	3.40	0.07	51.74	31.22	0.58	13.68	0.00	0.04	0.10	100.82
30 Xtl 1.2	X lava	69.9	0.5	29.6	3.27	0.08	51.33	31.50	0.63	13.99	0.03	0.02	0.08	100.92
30 Xtl 1.2	X lava	54.1	1.3	44.7	4.89	0.07	55.63	28.60	0.61	10.72	0.03	0.05	0.21	100.84
30 Xtl 1.3	X lava	63.6	0.8	35.6	3.91	0.07	52.63	30.37	0.62	12.64	0.02	0.05	0.13	100.44
30 Xtl 1.3	X lava	59.9	1.0	39.1	4.27	0.07	53.40	29.58	0.69	11.83	0.01	0.05	0.16	100.09
30 Xtl 2	X lava	74.0	0.4	25.6	2.84	0.03	49.80	32.23	0.47	14.87	0.01	0.02	0.07	100.41
30 Xtl 2	X lava	70.2	0.6	29.2	3.21	0.04	50.87	31.74	0.42	13.95	0.02	0.03	0.10	100.38
30 Xtl 2	X lava	67.9	0.5	31.5	3.47	0.05	51.77	31.06	0.43	13.53	0.01	0.03	0.09	100.45
30 Xtl 2	X lava	58.2	1.0	40.8	4.47	0.05	54.21	29.55	0.45	11.53	0.03	0.03	0.16	100.49
30 Xtl 3	X lava	77.4	0.4	22.3	2.44	0.05	49.35	32.75	0.42	15.31	0.01	0.00	0.06	100.39
30 Xtl 3	X lava	83.0	0.2	16.7	1.83	0.05	47.92	33.92	0.46	16.46	0.04	0.00	0.04	100.80
30 Xtl 3	X lava	70.2	0.4	29.4	3.22	0.07	50.80	31.54	0.53	13.89	0.02	0.02	0.07	100.15
30 Xtl 3	X lava	66.7	0.6	32.7	3.61	0.08	52.05	30.80	0.57	13.29	0.01	0.04	0.10	100.54
30 Xtl 4	X lava	47.8	1.8	50.4	5.48	0.03	57.34	27.91	0.40	9.40	0.01	0.03	0.31	100.93
30 Xtl 4	X lava	50.6	1.5	47.9	5.24	0.04	56.47	28.11	0.36	10.02	0.01	0.02	0.25	100.55
30 Xtl 4	X lava	44.4	2.0	53.7	5.85	0.03	58.19	27.31	0.41	8.75	0.01	0.02	0.32	100.96
30 Xtl 4	X lava	45.1	1.9	53.1	5.82	0.03	57.83	27.48	0.35	8.94	0.01	0.01	0.31	100.80
30 Xtl 4	X lava	41.5	2.1	56.4	6.14	0.04	58.97	26.95	0.40	8.16	0.01	0.01	0.35	101.08
30 Xtl 4	X lava	40.3	2.4	57.3	6.20	0.04	59.30	26.75	0.38	7.90	0.03	0.02	0.39	101.01
30 Xtl 4	X lava	47.4	1.7	50.9	5.51	0.03	57.18	27.70	0.37	9.29	0.01	0.01	0.29	100.43
30 Xtl 4	X lava	48.0	1.7	50.3	5.51	0.03	57.06	27.98	0.39	9.50	0.01	0.01	0.28	100.79
30 Xtl 4	X lava	46.3	2.0	51.7	5.58	0.04	57.42	27.12	0.52	9.05	0.02	0.08	0.32	100.19

Table B.1 (Continued)

Sample	Lithology	An	Or	Ab	Na_2O	MgO	SiO_2	Al_2O_3	FeO	CaO	P_2O_5	TiO_2	K_2O	Total
30 Xtl 4.1	X lava	63.8	0.8	35.4	3.87	0.07	52.51	30.28	0.60	12.61	0.02	0.04	0.13	100.13
30 Xtl 4.1	X lava	60.1	0.9	39.0	4.25	0.07	53.58	29.84	0.65	11.86	0.01	0.04	0.15	100.46
30 Xtl 5	X lava	54.8	1.4	43.8	4.71	0.06	55.10	28.79	0.46	10.66	0.01	0.08	0.23	100.12
30 Xtl 5	X lava	51.9	1.5	46.7	5.06	0.07	55.95	27.96	0.47	10.17	0.00	0.08	0.25	100.01
30 Xtl 5	X lava	50.1	1.6	48.2	5.23	0.07	56.12	27.75	0.53	9.83	0.02	0.09	0.27	99.89
30 Xtl 5	X lava	45.1	1.9	53.0	5.78	0.06	57.68	27.13	0.51	8.88	0.00	0.10	0.32	100.52
30 Xtl 5	X lava	45.2	1.8	53.0	5.74	0.06	57.67	27.20	0.52	8.87	0.01	0.10	0.30	100.50
30 Xtl 6	X lava xeno	52.0	1.0	47.0	5.12	0.04	55.61	28.48	0.27	10.24	0.02	0.07	0.17	100.05
30 Xtl 6	X lava xeno	51.6	1.1	47.2	5.19	0.03	55.80	28.69	0.22	10.27	0.01	0.07	0.19	100.48
30 Xtl 6	X lava xeno	52.6	1.2	46.2	5.07	0.03	55.66	28.83	0.26	10.45	0.01	0.06	0.20	100.59
30 Xtl 6	X lava xeno	56.0	1.1	43.0	4.65	0.02	54.52	29.23	0.28	10.96	0.00	0.06	0.17	99.91
30 Xtl 6	X lava xeno	73.7	1.0	25.3	2.77	0.05	49.88	32.29	0.34	14.60	0.01	0.03	0.17	100.15
30 Xtl 6	X lava xeno	51.6	1.2	47.1	5.10	0.06	55.99	28.04	0.57	10.10	0.02	0.04	0.20	100.14
30 Xtl 6	X lava xeno	52.5	1.1	46.4	5.04	0.06	55.56	28.48	0.47	10.32	0.03	0.04	0.18	100.18
30 Xtl 6	X lava xeno	53.9	1.4	44.7	4.87	0.03	54.99	28.95	0.27	10.62	0.01	0.06	0.23	100.06
30 Xtl 6	X lava xeno	51.2	1.4	47.4	5.12	0.03	55.88	28.17	0.21	10.02	0.02	0.05	0.23	99.75
30 Xtl 6	X lava xeno	61.8	0.8	37.5	4.07	0.04	53.05	29.92	0.37	12.14	0.02	0.03	0.13	99.78
30 Xtl 6	X lava xeno	60.9	0.8	38.3	4.19	0.04	53.35	29.71	0.40	12.02	0.02	0.03	0.13	99.94
30 Xtl 6	X lava xeno	58.6	0.8	40.6	4.41	0.05	53.55	29.25	0.41	11.53	0.01	0.01	0.13	99.39
30 Xtl 6	X lava xeno	58.8	0.8	40.3	4.32	0.05	53.72	29.30	0.50	11.39	0.02	0.03	0.14	99.47
30 Xtl 6	X lava xeno	52.3	1.3	46.5	5.03	0.07	55.35	28.01	0.59	10.23	0.01	0.05	0.21	99.57
10 Xtl 10	MKLV-TF	59.7	1.3	39.0	4.28	0.07	52.76	29.62	0.55	11.84	0.01	0.06	0.21	99.40
10 Xtl 10	MKLV-TF	54.6	1.6	43.8	4.76	0.08	53.91	28.45	0.58	10.73	0.01	0.08	0.26	98.87
10 Xtl 10	MKLV-TF	65.1	0.9	34.0	3.70	0.08	51.44	30.32	0.47	12.84	0.01	0.05	0.15	99.07
10 Xtl 10	MKLV-TF	59.1	1.2	39.7	4.32	0.08	53.13	29.26	0.58	11.64	0.02	0.06	0.20	99.28
10 Xtl 10	MKLV-TF	53.1	1.6	45.3	4.96	0.08	54.70	28.24	0.60	10.54	0.02	0.07	0.27	99.48
10 Xtl 10	MKLV-TF	48.4	2.2	49.4	5.39	0.07	55.81	27.66	0.59	9.55	0.03	0.09	0.36	99.54
10 Xtl 10	MKLV-TF	66.8	0.9	32.4	3.56	0.07	51.29	30.52	0.63	13.29	0.02	0.05	0.15	99.57
10 Xtl 10	MKLV-TF	46.5	2.3	51.2	5.61	0.09	56.56	27.21	0.69	9.22	0.01	0.10	0.39	99.87
10 Xtl 1.1	MKLV-TF	45.9	2.4	51.7	5.63	0.08	56.62	27.00	0.74	9.04	0.02	0.13	0.39	99.65
10 Xtl 1.1	MKLV-TF	48.1	2.3	49.7	5.40	0.08	56.00	27.33	0.75	9.47	0.03	0.10	0.37	99.54
10 Xtl 1.1	MKLV-TF	38.8	3.1	58.1	6.32	0.07	58.28	25.71	0.74	7.63	0.00	0.12	0.51	99.39
10 Xtl 1.2	MKLV-TF	49.5	1.9	48.7	5.32	0.10	55.34	27.79	0.60	9.77	0.01	0.10	0.31	99.35

Table B.1 (Continued)

Sample	Lithology	An	Or	Ab	Na_2O	MgO	SiO_2	Al_2O_3	FeO	CaO	P_2O_5	TiO_2	K_2O	Total
10 Xtl 1.2	MKLV-TF	49.6	1.9	48.6	5.27	0.10	55.51	27.71	0.52	9.74	0.03	0.10	0.31	99.29
10 Xtl 1.2	MKLV-TF	66.3	0.9	32.7	3.57	0.09	51.27	30.61	0.54	13.08	0.02	0.05	0.15	99.37
10 Xtl 1.2	MKLV-TF	48.0	2.1	49.9	5.48	0.10	56.07	27.47	0.75	9.56	0.03	0.11	0.35	99.90
10 Xtl 1.2	MKLV-TF	46.8	2.0	51.1	5.50	0.10	56.07	27.05	0.72	9.11	0.04	0.12	0.33	99.05
10 Xtl 1 mc	MKLV-TF	38.4	3.5	58.1	6.21	0.13	57.86	25.67	0.83	7.44	0.05	0.14	0.57	98.89
10 Xtl 1 mc	MKLV-TF	50.2	2.1	47.7	5.20	0.08	55.36	27.65	0.92	9.89	0.02	0.11	0.35	99.58
10 Xtl 11	MKLV-TF	60.3	1.3	38.5	4.16	0.07	52.51	29.20	0.80	11.81	0.03	0.08	0.21	98.88
10 Xtl 11	MKLV-TF	59.5	1.5	39.0	4.22	0.06	52.86	29.16	0.57	11.65	0.03	0.07	0.24	98.85
10 Xtl 11	MKLV-TF	65.8	0.9	33.3	3.61	0.07	51.31	30.33	0.56	12.92	0.03	0.04	0.16	99.02
10 Xtl 11	MKLV-TF	47.4	2.0	50.5	5.46	0.08	56.11	27.17	0.68	9.28	0.02	0.10	0.33	99.24
10 Xtl 11	MKLV-TF	66.7	1.0	32.3	3.56	0.06	50.87	30.72	0.64	13.31	0.02	0.05	0.17	99.39
10 Xtl 11.1	MKLV-TF	46.2	2.4	51.4	5.62	0.08	56.21	26.93	0.73	9.13	0.02	0.11	0.40	99.25
10 Xtl 11.2	MKLV-TF	72.4	0.9	26.7	2.93	0.04	49.55	31.67	0.55	14.41	0.03	0.04	0.15	99.38
10 Xtl 11.2	MKLV-TF	71.7	1.0	27.3	2.97	0.05	49.61	31.46	0.52	14.14	0.03	0.03	0.17	98.99
10 Xtl 11.2	MKLV-TF	61.9	1.3	36.8	4.02	0.06	52.25	29.90	0.60	12.25	0.01	0.06	0.22	99.36
10 Xtl 11.2	MKLV-TF	48.7	2.2	49.1	5.34	0.06	55.54	27.44	0.68	9.59	0.02	0.10	0.37	99.13
10 Xtl 11 mc	MKLV-TF	44.3	2.6	53.1	5.77	0.09	56.82	26.65	0.77	8.70	0.02	0.12	0.43	99.37
10 Xtl 11 mc	MKLV-TF	45.5	2.5	51.9	5.69	0.07	56.89	26.96	0.77	9.03	0.03	0.11	0.42	99.96
10 Xtl 11.3	MKLV-TF	79.1	0.5	20.4	2.21	0.04	47.89	32.70	0.52	15.52	0.02	0.04	0.09	99.03
10 Xtl 11.3	MKLV-TF	80.5	0.4	19.1	2.07	0.05	47.67	33.17	0.48	15.84	0.03	0.04	0.07	99.42
10 Xtl 11.3	MKLV-TF	78.1	0.5	21.4	2.33	0.04	48.43	32.63	0.54	15.38	0.04	0.05	0.08	99.52
10 Xtl 11.3	MKLV-TF	68.8	0.8	30.4	3.31	0.05	50.67	30.97	0.50	13.55	0.04	0.06	0.14	99.28
10 Xtl 11.3	MKLV-TF	65.0	1.0	34.0	3.67	0.06	51.49	30.03	0.50	12.68	0.03	0.06	0.16	98.68
10 Xtl 11.3	MKLV-TF	60.2	1.2	38.7	4.19	0.07	52.83	29.49	0.61	11.80	0.03	0.07	0.19	99.29
10 Xtl 11.3	MKLV-TF	58.0	1.2	40.8	4.48	0.07	53.71	29.19	0.61	11.52	0.01	0.05	0.21	99.87
10 Xtl 11.3	MKLV-TF	56.0	1.6	42.5	4.54	0.08	53.62	28.50	0.70	10.82	0.04	0.09	0.25	98.63
10 Xtl 11.3	MKLV-TF	42.8	3.2	54.0	5.89	0.10	57.71	26.12	0.74	8.44	0.03	0.11	0.53	99.68
10 Xtl 11.3	MKLV-TF	55.9	1.7	42.3	4.62	0.06	54.17	28.56	0.68	11.05	0.00	0.10	0.29	99.53
10 Xtl 11.3	MKLV-TF	63.8	1.2	35.0	3.81	0.06	51.97	30.34	0.64	12.58	0.03	0.05	0.20	99.67
10 Xtl 11.3	MKLV-TF	58.2	1.4	40.4	4.43	0.07	53.18	28.91	0.66	11.55	0.03	0.07	0.24	99.15
10 Xtl 11.3	MKLV-TF	63.0	1.3	35.7	3.91	0.07	52.11	29.80	0.59	12.50	0.04	0.05	0.22	99.30
10 Xtl 11.3	MKLV-TF	67.3	0.9	31.8	3.44	0.05	50.89	30.75	0.57	13.21	0.01	0.04	0.15	99.12
10 Xtl 11.3	MKLV-TF	65.9	1.0	33.1	3.60	0.07	51.41	30.59	0.60	12.96	0.00	0.05	0.16	99.44

Table B.1 (Continued)

Sample	Lithology	An	Or	Ab	Na_2O	MgO	SiO_2	Al_2O_3	FeO	CaO	P_2O_5	TiO_2	K_2O	Total
10 Xtl 11.3	MKLV-TF	63.9	1.1	35.0	3.80	0.07	51.64	29.70	0.61	12.55	0.01	0.06	0.18	98.62
10 Xtl 11.3	MKLV-TF	54.7	1.6	43.7	4.76	0.08	54.42	28.36	0.71	10.80	0.02	0.07	0.26	99.50
10 Xtl 11.3	MKLV-TF	45.1	2.3	52.6	5.67	0.10	56.63	26.64	0.73	8.81	0.04	0.10	0.38	99.10
10 Xtl 11.3	MKLV-TF	51.7	1.7	46.6	5.13	0.09	55.24	28.07	0.70	10.28	0.02	0.07	0.29	99.88
10 Xtl 11.3	MKLV-TF	48.7	2.1	49.2	5.38	0.08	55.63	27.56	0.70	9.63	0.01	0.09	0.36	99.44
10 Xtl 11.3	MKLV-TF	50.5	2.0	47.5	5.14	0.07	54.77	27.46	0.72	9.88	0.03	0.09	0.32	98.49
10 Xtl 11.3	MKLV-TF	36.8	3.6	59.6	6.47	0.06	58.55	25.51	0.76	7.22	0.03	0.13	0.59	99.33
10 Xtl 12	MKLV-TF	44.0	1.9	54.1	5.88	0.04	56.25	27.14	0.24	8.67	0.00	0.00	0.32	98.54
10 Xtl 12	MKLV-TF	42.3	2.1	55.6	6.05	0.03	57.01	26.77	0.25	8.34	0.02	0.02	0.34	98.84
10 Xtl 12	MKLV-TF	54.5	1.6	43.9	4.75	0.08	54.03	28.31	0.60	10.66	0.03	0.08	0.26	98.80
10 Xtl 13 core	MKLV-TF	55.3	1.5	43.3	4.73	0.07	53.57	28.57	0.54	10.93	0.03	0.09	0.24	98.78
10 Xtl 13 core	MKLV-TF	54.5	1.6	43.8	4.75	0.07	53.87	28.53	0.57	10.69	0.02	0.06	0.27	98.83
10 Xtl 13.1	MKLV-TF	48.1	2.0	49.9	5.42	0.08	56.04	27.24	0.70	9.46	0.02	0.10	0.34	99.40
10 Xtl 13.1	MKLV-TF	53.5	1.7	44.8	4.87	0.08	54.54	28.33	0.63	10.51	0.02	0.08	0.28	99.32
10 Xtl 13.1	MKLV-TF	52.9	1.6	45.5	4.99	0.09	54.72	28.25	0.59	10.47	0.02	0.09	0.27	99.49
10 Xtl 13.1	MKLV-TF	64.2	1.1	34.7	3.74	0.08	51.69	29.90	0.63	12.54	0.02	0.05	0.18	98.83
10 Xtl 13.2	MKLV-TF	43.8	2.6	53.5	5.80	0.07	56.90	26.67	0.70	8.60	0.03	0.11	0.44	99.32
10 Xtl 13.2	MKLV-TF	44.5	2.5	52.9	5.77	0.09	56.83	26.80	0.72	8.77	0.02	0.12	0.42	99.53
10 Xtl 13.2	MKLV-TF	44.4	2.6	53.1	5.76	0.09	57.03	26.71	0.79	8.71	0.03	0.12	0.42	99.65
10 Xtl 14	MKLV-TF	49.7	1.3	49.0	5.38	0.03	55.55	28.21	0.26	9.89	0.01	0.09	0.22	99.65
10 Xtl 14	MKLV-TF	47.8	1.4	50.8	5.52	0.02	55.58	27.56	0.26	9.41	0.02	0.10	0.24	98.70
10 Xtl 14	MKLV-TF	58.5	1.3	40.2	4.38	0.08	52.88	29.10	0.62	11.56	0.02	0.06	0.22	98.92
10 Xtl 14	MKLV-TF	48.5	1.9	49.6	5.38	0.08	55.78	27.51	0.60	9.52	0.00	0.09	0.31	99.27
10 Xtl 14	MKLV-TF	63.5	1.1	35.5	3.83	0.08	51.57	29.70	0.66	12.39	0.02	0.05	0.18	98.48
10 Xtl 14	MKLV-TF	40.6	2.8	56.6	6.15	0.08	57.51	25.91	0.72	7.99	0.04	0.12	0.47	98.99
10 Xtl 14.1	MKLV-TF	66.0	0.9	33.1	3.62	0.07	51.07	30.61	0.61	13.04	0.01	0.05	0.15	99.22
10 Xtl 14.1	MKLV-TF	65.6	0.8	33.5	3.65	0.08	51.09	30.24	0.58	12.93	0.02	0.04	0.14	98.75
10 Xtl 14.1	MKLV-TF	46.8	2.4	50.8	5.55	0.08	55.42	27.09	0.67	9.26	0.02	0.11	0.39	98.59
10 Xtl 14.1	MKLV-TF	51.0	2.0	47.0	5.11	0.08	54.82	27.85	0.69	10.03	0.02	0.08	0.33	99.00
10 Xtl 14.2	MKLV-TF	48.9	2.1	49.0	5.37	0.09	55.43	27.60	0.70	9.71	0.04	0.10	0.34	99.38
10 Xtl 14.2	MKLV-TF	50.2	2.0	47.9	5.21	0.09	54.97	27.70	0.73	9.88	0.04	0.10	0.32	99.05
10 Xtl 14.2	MKLV-TF	50.4	2.1	47.5	5.17	0.07	54.71	27.64	0.73	9.92	0.03	0.09	0.34	98.72
10 Xtl 14.2	MKLV-TF	45.4	2.5	52.1	5.72	0.07	56.11	26.80	0.71	9.00	0.03	0.11	0.41	98.96

Table B.1 (Continued)

Sample	Lithology	An	Or	Ab	Na_2O	MgO	SiO_2	Al_2O_3	FeO	CaO	P_2O_5	TiO_2	K_2O	Total
10 Xtl 15	MKLV-TF	61.1	1.2	37.7	4.10	0.07	52.77	29.67	0.51	12.01	0.02	0.03	0.20	99.38
10 Xtl 15	MKLV-TF	67.8	0.9	31.3	3.40	0.06	51.11	31.01	0.57	13.35	0.01	0.06	0.15	99.73
10 Xtl 15	MKLV-TF	51.4	1.7	46.9	5.10	0.08	55.20	27.99	0.59	10.11	0.02	0.09	0.29	99.47
10 Xtl 15	MKLV-TF	49.7	1.7	48.6	5.26	0.09	55.30	27.25	0.65	9.74	0.03	0.11	0.29	98.72
10 Xtl 15	MKLV-TF	51.0	1.7	47.3	5.18	0.09	55.21	27.79	0.64	10.09	-0.01	0.10	0.29	99.39
10 Xtl 15	MKLV-TF	58.6	1.1	40.3	4.42	0.08	53.44	29.34	0.63	11.62	0.02	0.07	0.19	99.79
10 Xtl 15	MKLV-TF	48.2	2.1	49.7	5.42	0.09	55.81	27.19	0.67	9.52	0.04	0.10	0.35	99.18
08A Xtl 1 T	MKLV-WC	52.7	1.4	43.2	4.69	0.08	54.94	28.46	0.63	10.89	0.02	0.07	0.22	100.02
08A Xtl 1 T	MKLV-WC	54.2	1.5	45.8	5.04	0.09	55.18	28.19	0.59	10.48	0.02	0.08	0.25	99.91
08A Xtl 1 T	MKLV-WC	55.0	1.3	44.4	4.83	0.09	54.87	28.30	0.64	10.68	0.03	0.08	0.22	99.75
08A Xtl 1 T	MKLV-WC	55.5	1.3	43.7	4.76	0.09	54.97	28.60	0.59	10.84	0.00	0.07	0.22	100.14
08A Xtl 1 T	MKLV-WC	54.1	1.3	43.2	4.74	0.09	54.86	28.72	0.61	11.02	0.03	0.07	0.22	100.36
08A Xtl 1 T	MKLV-WC	49.9	1.4	44.5	4.87	0.09	55.06	28.56	0.62	10.69	0.03	0.08	0.23	100.24
08A Xtl 1	MKLV-WC	46.9	1.7	49.5	5.39	0.09	56.43	27.53	0.63	9.63	0.02	0.10	0.29	100.11
08A Xtl 1	MKLV-WC	52.4	1.9	51.1	5.56	0.10	56.91	27.24	0.60	9.23	0.03	0.13	0.32	100.13
08A Xtl 1.5	MKLV-WC	63.7	1.8	45.8	5.05	0.09	54.97	28.29	0.65	10.44	0.02	0.07	0.30	99.88
08A Xtl 1.5	MKLV-WC	52.2	1.1	35.2	3.93	0.06	52.36	30.70	0.46	12.88	0.02	0.03	0.19	100.64
08A Xtl 1.5	MKLV-WC	57.7	1.4	46.3	5.09	0.10	55.47	28.38	0.67	10.40	0.04	0.09	0.24	100.48
08A Xtl 1.5	MKLV-WC	50.4	1.4	40.9	4.51	0.09	53.84	29.04	0.62	11.50	0.03	0.07	0.23	99.94
08A Xtl 1.6	MKLV-WC	50.9	1.8	47.7	5.24	0.08	55.87	27.91	0.78	10.01	0.02	0.09	0.30	100.34
08A Xtl 1.6	MKLV-WC	54.1	1.6	47.5	5.20	0.10	55.79	28.08	0.67	10.11	0.03	0.08	0.27	100.33
08A Xtl 1.6	MKLV-WC	55.0	1.4	44.5	4.89	0.09	55.45	28.48	0.65	10.77	0.01	0.07	0.24	100.66
08A Xtl 1.6	MKLV-WC	45.8	1.4	43.5	4.74	0.09	54.83	28.78	0.67	10.84	0.01	0.08	0.24	100.28
08A Xtl 1.7	MKLV-WC	54.7	1.4	45.5	4.98	0.11	55.12	28.19	0.73	10.52	0.04	0.09	0.23	100.04
08A Xtl 1.7	MKLV-WC	54.3	1.3	44.0	4.83	0.10	54.73	28.46	0.69	10.88	0.03	0.07	0.22	100.04
08A Xtl 1.7	MKLV-WC	55.4	1.5	44.2	4.89	0.07	54.90	28.59	0.71	10.86	0.02	0.07	0.26	100.36
08A Xtl 1.8	MKLV-WC	38.1	1.4	43.2	4.77	0.07	54.39	28.77	0.70	11.06	0.01	0.06	0.23	100.09
08A Xtl 1.8	MKLV-WC	43.4	3.3	58.5	6.37	0.05	58.65	25.93	0.73	7.50	0.03	0.12	0.55	99.92
8A Xtl 6 rim T	MKLV-WC	55.1	0.9	28.9	3.18	0.06	50.65	31.46	0.61	13.98	0.02	0.04	0.16	100.17
8A Xtl 6 rim T	MKLV-WC	54.6	1.6	43.3	4.78	0.09	54.30	28.85	0.64	11.02	0.02	0.06	0.27	100.07
8A Xtl 6 rim T	MKLV-WC	26.4	1.4	44.0	4.87	0.08	54.72	28.73	0.66	10.93	0.03	0.07	0.23	100.36
8A Xtl 6 rim T	MKLV-WC	58.9	1.2	38.7	4.24	0.06	53.30	29.69	0.67	11.90	0.03	0.05	0.20	100.25
08A Xtl 6 mc	MKLV-WC	33.5	1.1	39.9	4.38	0.08	53.57	29.48	0.66	11.70	0.03	0.06	0.19	100.16

Table B.1 (Continued)

Sample	Lithology	An	Or	Ab	Na_2O	MgO	SiO_2	Al_2O_3	FeO	CaO	P_2O_5	TiO_2	K_2O	Total
08A Xtl 2	MKLV-WC	47.7	3.6	62.9	6.86	0.05	60.05	25.41	0.77	6.61	0.01	0.11	0.60	100.46
08A Xtl 2	MKLV-WC	47.4	1.9	50.5	5.55	0.08	56.35	27.54	0.53	9.49	0.04	0.11	0.32	100.03
08A Xtl 2	MKLV-WC	68.6	1.9	50.6	5.56	0.08	56.31	27.62	0.56	9.42	0.01	0.10	0.32	99.99
08A Xtl 2	MKLV-WC	67.3	1.0	30.4	3.37	0.06	51.02	31.59	0.52	13.74	0.02	0.05	0.17	100.55
08A Xtl 2	MKLV-WC	55.8	1.1	31.6	3.46	0.06	50.96	30.87	0.59	13.34	0.01	0.07	0.18	99.55
08A Xtl 2	MKLV-WC	53.8	1.4	42.8	4.69	0.09	54.40	28.97	0.57	11.08	0.02	0.10	0.23	100.17
08A Xtl 2	MKLV-WC	47.0	1.3	45.0	4.94	0.10	55.02	28.51	0.64	10.68	0.02	0.07	0.21	100.23
08A Xtl 2.5	MKLV-WC	52.7	2.0	51.0	5.58	0.07	56.44	27.42	0.70	9.30	0.04	0.08	0.33	99.97
08A Xtl 2.5	MKLV-WC	51.0	1.6	45.7	4.99	0.08	55.19	28.18	0.61	10.41	0.03	0.10	0.26	99.86
08A Xtl 2.5	MKLV-WC	47.9	1.7	47.3	5.19	0.08	55.86	27.97	0.63	10.10	0.03	0.10	0.28	100.26
08A Xtl 2.5	MKLV-WC	53.1	1.8	50.3	5.55	0.08	56.32	27.63	0.60	9.56	0.03	0.09	0.30	100.20
08A Xtl 2.5	MKLV-WC	46.7	1.4	45.5	5.01	0.09	55.67	28.43	0.66	10.56	0.02	0.07	0.24	100.82
08A Xtl 2.5	MKLV-WC	44.8	2.1	51.1	5.58	0.06	57.11	27.31	0.64	9.22	0.03	0.08	0.35	100.40
08A Xtl 3 T	MKLV-WC	52.6	2.3	52.9	5.82	0.06	57.41	27.01	0.69	8.91	0.04	0.08	0.38	100.42
08A Xtl 3 T	MKLV-WC	53.8	1.4	46.0	5.04	0.08	55.65	28.20	0.64	10.42	0.02	0.08	0.23	100.38
08A Xtl 3 T	MKLV-WC	49.6	1.3	44.9	4.88	0.08	55.53	28.33	0.61	10.59	0.01	0.07	0.22	100.32
08A Xtl 3 T	MKLV-WC	53.7	1.6	48.8	5.37	0.08	56.13	27.82	0.60	9.87	0.03	0.08	0.27	100.26
08A Xtl 3 T	MKLV-WC	55.7	1.3	45.0	4.96	0.08	55.53	28.38	0.66	10.69	0.04	0.08	0.22	100.64
08A Xtl 3 T	MKLV-WC	85.4	1.3	43.0	4.74	0.08	54.93	29.00	0.64	11.11	0.02	0.07	0.21	100.85
08A Xtl 3 P	MKLV-WC	57.4	1.2	43.6	4.78	0.08	55.33	28.66	0.65	10.96	0.03	0.06	0.20	100.85
08A Xtl 3 P	MKLV-WC	61.1	1.1	41.5	4.54	0.08	54.65	29.10	0.61	11.34	0.03	0.07	0.18	100.65
08A Xtl 3 P	MKLV-WC	57.2	1.2	37.6	4.15	0.06	53.33	29.79	0.66	12.20	0.02	0.06	0.20	100.50
08A Xtl 3 P	MKLV-WC	54.2	1.4	44.4	4.89	0.07	55.16	28.83	0.72	10.78	0.02	0.06	0.24	100.83
08A Xtl 3 P	MKLV-WC	51.5	1.8	46.7	5.12	0.07	55.85	28.20	0.74	10.22	0.03	0.08	0.29	100.59
08A Xtl 3 P	MKLV-WC	55.1	1.5	43.4	4.78	0.07	54.45	28.81	0.71	10.98	0.02	0.08	0.25	100.18
08A Xtl 3 P	MKLV-WC	55.9	1.3	42.7	4.67	0.08	54.69	28.80	0.71	11.07	0.02	0.09	0.22	100.39
08A Xtl 3 P	MKLV-WC	54.9	1.5	43.6	4.76	0.09	54.76	28.72	0.76	10.85	0.01	0.07	0.24	100.26
08A Xtl 3 P	MKLV-WC	49.6	2.1	48.3	5.27	0.05	56.13	27.95	0.39	9.79	0.03	0.01	0.35	99.97
08A Xtl 5	MKLV-WC	49.6	1.9	48.5	5.27	0.06	55.88	28.06	0.44	9.75	0.02	0.01	0.32	99.82
08A Xtl 5	MKLV-WC	47.4	2.0	50.7	5.51	0.05	56.56	27.71	0.29	9.32	0.02	0.01	0.32	99.80
08A Xtl 5	MKLV-WC	45.6	1.9	52.5	5.76	0.03	57.27	27.60	0.23	9.04	0.01	0.01	0.32	100.26
08A Xtl 5	MKLV-WC	47.1	1.9	50.9	5.57	0.04	56.82	27.95	0.27	9.32	0.01	0.01	0.32	100.38
08A Xtl 5	MKLV-WC	66.0	1.1	33.0	3.62	0.04	51.60	30.56	0.57	13.09	0.01	0.03	0.18	99.78

Table B.1 (Continued)

Sample	Lithology	An	Or	Ab	Na_2O	MgO	SiO_2	Al_2O_3	FeO	CaO	P_2O_5	TiO_2	K_2O	Total
08A Xtl 5	MKLV-WC	53.4	1.6	44.9	4.94	0.06	54.94	28.40	0.77	10.63	0.01	0.07	0.27	100.14
08A Xtl 5	MKLV-WC	47.4	2.0	50.5	5.49	0.05	56.35	27.13	0.79	9.32	0.04	0.10	0.34	99.63
08A Xtl 5	MKLV-WC	52.6	1.6	45.8	5.01	0.08	55.40	28.32	0.69	10.40	0.01	0.07	0.27	100.26
08A Xtl 5	MKLV-WC	52.9	1.6	45.5	5.00	0.07	55.14	28.38	0.70	10.53	0.00	0.07	0.27	100.16
08A Xtl 5 mc 1	MKLV-WC	53.1	1.5	45.5	4.96	0.07	55.03	28.49	0.61	10.49	0.04	0.08	0.25	100.06
08A Xtl 5 mc 1	MKLV-WC	52.2	1.6	46.2	4.95	0.08	55.02	28.09	0.66	10.12	0.00	0.08	0.26	99.26
08A Xtl 5 mc 1	MKLV-WC	50.9	1.6	47.6	5.18	0.09	54.98	27.68	0.72	10.03	0.02	0.08	0.26	99.05
08A Xtl 5 mc 1	MKLV-WC	52.9	1.5	45.6	4.97	0.09	55.03	28.45	0.71	10.44	0.04	0.07	0.25	100.07
08A Xtl 5 mc 2	MKLV-WC	55.6	1.5	42.9	4.69	0.07	54.10	28.88	0.67	10.99	0.02	0.06	0.25	99.75
08A Xtl 5 mc 2	MKLV-WC	48.7	1.8	49.5	5.36	0.08	56.20	27.74	0.71	9.55	0.02	0.08	0.30	100.05
03 Xtl 10	MKPF	70.8	0.8	28.4	3.13	0.04	50.42	31.79	0.72	14.13	0.01	0.05	0.14	100.43
03 Xtl 10	MKPF	65.8	1.3	32.9	3.67	0.05	52.09	30.10	0.71	13.27	0.01	0.06	0.22	100.18
03 Xtl 10	MKPF	59.3	1.2	39.5	4.29	0.07	53.23	29.33	0.74	11.67	0.02	0.05	0.20	99.65
03 Xtl 10	MKPF	57.1	1.3	41.6	4.55	0.05	54.19	29.05	0.67	11.32	0.02	0.05	0.21	100.16
03 Xtl 10 5	MKPF	47.8	2.0	50.2	5.32	0.60	56.84	26.85	1.25	9.17	0.03	0.08	0.33	100.48
03 Xtl 10.8 T	MKPF	53.6	1.3	45.1	4.90	0.08	55.43	28.42	0.60	10.54	0.02	0.06	0.22	100.26
03 Xtl 10.8 T	MKPF	55.5	1.2	43.3	4.72	0.09	54.85	28.69	0.62	10.94	0.02	0.06	0.20	100.21
03 Xtl 10.8 T	MKPF	54.3	1.3	44.4	4.82	0.07	55.51	28.57	0.66	10.66	0.02	0.07	0.21	100.68
03 Xtl 10.8 T	MKPF	52.9	1.3	45.8	4.99	0.08	55.92	28.16	0.62	10.43	0.02	0.06	0.22	100.51
03 Xtl 10.8 T	MKPF	53.0	1.3	45.7	4.98	0.08	55.70	28.13	0.64	10.47	0.02	0.07	0.22	100.34
03 Xtl 10.8 T	MKPF	51.8	1.4	46.9	5.09	0.08	55.87	28.14	0.63	10.17	0.02	0.08	0.23	100.35
03 Xtl 10.8 T	MKPF	53.6	1.4	45.1	4.87	0.07	54.76	27.97	0.61	10.48	0.02	0.06	0.22	99.10
03 Xtl 10.8 T	MKPF	53.9	1.4	47.2	5.14	0.07	56.08	28.13	0.63	10.13	0.02	0.07	0.23	100.53
03 Xtl 10.8 T	MKPF	51.4	1.2	43.7	4.76	0.08	54.97	28.74	0.58	10.83	0.03	0.06	0.20	100.26
03 Xtl 10.8 T	MKPF	55.0	1.4	45.4	4.94	0.08	55.88	28.21	0.60	10.48	0.02	0.06	0.23	100.51
03 Xtl 10.8 T	MKPF	53.2	1.4	44.6	4.89	0.08	55.70	28.70	0.54	10.71	0.01	0.06	0.23	100.93
03 Xtl 10.8 T	MKPF	54.0	1.3	43.1	4.69	0.07	55.22	28.92	0.61	10.93	0.03	0.06	0.22	100.76
03 Xtl 10.8 T	MKPF	55.6	1.3	42.8	4.67	0.07	55.15	29.13	0.61	11.05	0.01	0.05	0.21	100.97
03 Xtl 10.8 T	MKPF	55.9	1.2	40.7	4.47	0.07	54.50	29.24	0.64	11.56	0.03	0.05	0.20	100.79
03 Xtl 10.8 T	MKPF	58.1	1.4	44.9	4.91	0.07	55.65	28.44	0.65	10.63	0.02	0.06	0.24	100.66
03 Xtl 10.8 T	MKPF	53.7	1.3	41.1	4.46	0.08	54.55	29.26	0.63	11.32	0.02	0.06	0.21	100.60
03 Xtl 10.8 T	MKPF	57.7	1.3	42.6	4.65	0.07	54.83	28.89	0.66	11.11	0.02	0.05	0.21	100.50
03 Xtl 10.8 T	MKPF	53.7	1.5	44.8	4.90	0.07	55.67	28.31	0.74	10.63	0.02	0.07	0.25	100.67

Table B.1 (Continued)

Sample	Lithology	An	Or	Ab	Na_2O	MgO	SiO_2	Al_2O_3	FeO	CaO	P_2O_5	TiO_2	K_2O	Total
03 Xtl 10.8 T	MKPF	43.8	2.9	53.2	5.65	0.11	58.61	26.02	0.83	8.42	0.03	0.14	0.47	100.35
03 Xtl 10 mc 1	MKPF	56.7	1.3	42.0	4.63	0.06	54.64	28.76	0.72	11.30	0.02	0.05	0.22	100.43
03 Xtl 10 mc 1	MKPF	49.8	1.8	48.4	5.34	0.07	56.62	27.78	0.72	9.93	0.03	0.07	0.30	100.86
03 Xtl 10 mc 1	MKPF	41.0	2.5	56.6	6.20	0.06	59.00	26.25	0.70	8.12	0.16	0.08	0.41	101.02
03 Xtl 10 mc 1	MKPF	46.7	2.0	51.3	5.64	0.06	57.56	27.26	0.68	9.30	0.03	0.08	0.33	100.97
03 Xtl 10 mc 2	MKPF	54.9	1.5	43.6	4.77	0.08	55.27	28.34	0.83	10.87	0.02	0.08	0.25	100.49
03 Xtl 10 mc 2	MKPF	56.2	1.4	42.4	4.64	0.06	54.66	28.94	0.76	11.15	0.01	0.06	0.24	100.53
03 Xtl 10 mc 2	MKPF	51.1	1.8	47.1	5.15	0.07	56.60	27.91	0.81	10.11	0.04	0.08	0.29	101.06
03 Xtl 10 mc 2	MKPF	50.5	1.8	47.7	5.19	0.07	56.12	27.75	0.76	9.95	0.03	0.07	0.29	100.24
03 Xtl 11	MKPF	56.9	1.2	41.9	4.59	0.08	54.87	29.06	0.63	11.29	0.01	0.07	0.20	100.83
03 Xtl 11	MKPF	56.3	1.2	42.5	4.68	0.09	55.03	28.82	0.64	11.21	0.02	0.06	0.20	100.73
03 Xtl 11	MKPF	60.7	1.1	38.3	4.21	0.09	53.59	29.52	0.66	12.07	0.02	0.04	0.18	100.39
03 Xtl 11	MKPF	57.5	1.2	41.3	4.54	0.08	54.68	29.17	0.66	11.46	0.01	0.06	0.20	100.85
03 Xtl 11	MKPF	52.3	1.5	46.2	5.10	0.08	56.00	28.22	0.67	10.45	0.03	0.07	0.26	100.91
03 Xtl 11	MKPF	55.0	1.4	43.6	4.76	0.06	55.00	28.67	0.77	10.85	0.01	0.06	0.23	100.42
03 Xtl 12 T	MKPF	53.5	1.2	45.3	4.95	0.09	55.41	28.13	0.60	10.57	0.02	0.06	0.20	100.10
03 Xtl 12 T	MKPF	53.5	1.3	45.2	4.99	0.09	55.26	28.05	0.64	10.69	0.03	0.06	0.21	100.02
03 Xtl 12 T	MKPF	53.5	1.3	45.2	4.95	0.10	55.54	28.12	0.64	10.60	0.02	0.07	0.21	100.26
03 Xtl 12 T	MKPF	54.9	1.2	43.9	4.81	0.09	55.06	28.38	0.67	10.90	0.03	0.07	0.20	100.23
03 Xtl 12 T	MKPF	55.3	1.2	43.5	4.77	0.10	54.78	28.52	0.70	10.98	0.03	0.07	0.20	100.16
03 Xtl 12 T	MKPF	55.3	1.2	43.5	4.79	0.09	54.81	28.49	0.68	11.02	0.01	0.07	0.21	100.18
03 Xtl 12 T	MKPF	55.2	1.1	43.7	4.77	0.08	54.32	28.52	0.67	10.91	0.01	0.07	0.19	99.55
03 Xtl 12 T	MKPF	64.1	0.8	35.1	3.84	0.08	52.20	30.22	0.64	12.71	0.03	0.05	0.14	99.98
03 Xtl 12 T	MKPF	62.6	0.9	36.5	4.01	0.08	53.09	29.95	0.66	12.42	0.00	0.06	0.15	100.42
03 Xtl 12 T	MKPF	57.8	1.1	41.1	4.50	0.08	53.97	28.98	0.62	11.47	0.02	0.06	0.18	99.89
03 Xtl 12 T	MKPF	55.9	1.1	43.0	4.73	0.09	54.16	28.92	0.66	11.12	0.02	0.06	0.19	99.97
03 Xtl 12 T	MKPF	54.7	1.1	44.2	4.84	0.09	54.69	28.50	0.67	10.82	0.02	0.07	0.18	99.88
03 Xtl 12 T	MKPF	55.0	1.2	43.8	4.81	0.09	54.49	28.21	0.64	10.93	0.03	0.07	0.20	99.53
03 Xtl 12 T	MKPF	55.5	1.1	43.4	4.76	0.09	54.42	28.62	0.63	11.01	0.03	0.07	0.18	99.88
03 Xtl 12 T	MKPF	57.8	1.0	41.2	4.51	0.08	53.78	29.07	0.60	11.43	0.02	0.05	0.17	99.77
03 Xtl 12 T	MKPF	57.6	1.0	41.4	4.56	0.09	53.73	29.02	0.59	11.46	0.03	0.06	0.17	99.79
03 Xtl 12 T	MKPF	54.9	1.2	44.0	4.62	0.23	51.68	26.68	4.31	10.43	0.03	0.64	0.18	98.88
03 Xtl 12 T	MKPF	59.3	1.0	39.6	4.31	0.09	53.11	29.23	0.66	11.68	0.03	0.07	0.17	99.37

Table B.1 (Continued)

Sample	Lithology	An	Or	Ab	Na_2O	MgO	SiO_2	Al_2O_3	FeO	CaO	P_2O_5	TiO_2	K_2O	Total
03 Xtl 12 T	MKPF	53.6	1.2	45.2	4.94	0.08	54.77	28.22	0.64	10.58	0.03	0.07	0.20	99.52
03 Xtl 12 T	MKPF	58.0	1.0	41.0	4.46	0.09	53.53	29.12	0.61	11.42	0.02	0.06	0.17	99.48
03 Xtl 12 T	MKPF	58.9	1.0	40.1	4.37	0.09	53.30	29.28	0.66	11.61	0.01	0.06	0.17	99.54
03 Xtl 12 T	MKPF	55.9	1.1	43.0	4.69	0.09	53.96	28.76	0.60	11.06	0.01	0.06	0.18	99.41
03 Xtl 12 T	MKPF	57.2	1.0	41.8	4.58	0.09	54.03	29.13	0.61	11.35	0.02	0.06	0.17	100.05
03 Xtl 12 T	MKPF	59.5	0.9	39.5	4.33	0.09	53.41	29.30	0.66	11.81	0.01	0.07	0.16	99.84
03 Xtl 12 T	MKPF	56.9	1.1	42.0	4.56	0.09	54.05	29.11	0.66	11.17	0.00	0.06	0.18	99.91
03 Xtl 12 T	MKPF	53.6	1.2	45.2	4.91	0.09	54.72	27.98	0.60	10.52	0.02	0.07	0.19	99.11
03 Xtl 12 T	MKPF	54.6	1.2	44.2	4.83	0.09	54.70	28.65	0.64	10.80	0.02	0.08	0.19	100.01
03 Xtl 12 T	MKPF	54.4	1.2	44.5	4.88	0.09	54.81	28.65	0.61	10.79	0.02	0.07	0.19	100.14
03 Xtl 12 T	MKPF	60.3	1.0	38.7	4.26	0.08	53.26	29.59	0.64	12.00	0.01	0.05	0.16	100.05
03 Xtl 12 T	MKPF	55.6	1.1	43.3	4.74	0.08	54.62	28.72	0.63	11.02	0.01	0.06	0.18	100.05
03 Xtl 12 T	MKPF	53.8	1.2	45.0	4.94	0.08	55.29	28.44	0.63	10.67	0.04	0.07	0.19	100.41
03 Xtl 12 T	MKPF	56.2	1.1	42.7	4.66	0.09	54.47	28.75	0.66	11.10	0.04	0.06	0.19	100.02
03 Xtl 12 T	MKPF	56.5	1.0	42.4	4.63	0.09	54.20	28.97	0.63	11.16	0.02	0.06	0.17	99.94
03 Xtl 12 T	MKPF	56.7	1.1	42.2	4.61	0.09	54.11	28.71	0.62	11.22	0.03	0.07	0.19	99.69
03 Xtl 12 T	MKPF	58.1	1.1	40.9	4.51	0.09	53.95	29.24	0.65	11.60	0.02	0.07	0.18	100.33
03 Xtl 12 T	MKPF	57.2	1.1	41.7	4.53	0.08	53.80	28.99	0.59	11.24	0.03	0.06	0.17	99.51
03 Xtl 12 T	MKPF	59.9	1.0	39.1	4.36	0.08	53.38	29.27	0.35	12.08	0.01	0.01	0.17	99.72
03 Xtl 12 T	MKPF	57.0	1.1	41.8	4.65	0.09	54.36	28.88	0.41	11.46	0.01	0.04	0.19	100.10
03 Xtl 12 T	MKPF	57.4	1.0	41.6	4.56	0.09	53.71	29.05	0.66	11.40	0.03	0.06	0.16	99.72
03 Xtl 12 T	MKPF	54.6	1.2	44.2	4.84	0.08	54.81	28.53	0.63	10.85	0.02	0.07	0.20	100.04
03 Xtl 12 T	MKPF	55.9	1.1	43.0	4.67	0.08	54.28	28.64	0.57	10.99	0.03	0.06	0.19	99.53
03 Xtl 12 T	MKPF	56.4	1.1	42.6	4.67	0.08	53.72	28.64	0.64	11.18	0.02	0.06	0.18	99.19
03 Xtl 12 T	MKPF	57.7	1.1	41.2	4.49	0.08	53.52	28.88	0.64	11.37	0.02	0.06	0.17	99.24
03 Xtl 12 T	MKPF	57.2	1.1	41.7	4.57	0.09	54.22	28.55	0.65	11.35	0.01	0.06	0.18	99.73
03 Xtl 12 T	MKPF	59.1	1.1	39.8	4.34	0.09	54.27	28.98	0.63	11.64	0.01	0.05	0.18	100.17
03 Xtl 12 T	MKPF	60.9	1.0	38.1	4.18	0.09	53.36	29.47	0.65	12.09	0.00	0.05	0.17	100.04
03 Xtl 12 T	MKPF	56.9	1.1	41.9	4.55	0.09	54.80	28.88	0.68	11.18	0.03	0.06	0.19	100.47
03 Xtl 12 T	MKPF	57.5	1.1	41.4	4.52	0.08	54.32	28.66	0.64	11.37	0.01	0.06	0.19	99.86
03 Xtl 12 T	MKPF	52.9	1.4	45.7	4.97	0.08	55.36	28.25	0.56	10.41	0.01	0.06	0.23	99.93
03 Xtl 12 T	MKPF	56.7	1.2	42.0	4.55	0.08	54.16	28.72	0.58	11.11	0.02	0.05	0.20	99.51
03 Xtl 12 T	MKPF	66.4	0.8	32.8	3.62	0.08	52.03	30.60	0.63	13.28	0.02	0.04	0.14	100.46

Table B.1 (Continued)

Sample	Lithology	An	Or	Ab	Na_2O	MgO	SiO_2	Al_2O_3	FeO	CaO	P_2O_5	TiO_2	K_2O	Total
03 Xtl 12 T	MKPF	40.0	2.4	57.5	6.19	0.11	58.52	26.05	0.72	7.79	0.00	0.09	0.40	99.92
03 Xtl 12 T	MKPF	61.9	0.9	37.1	4.04	0.22	52.81	29.66	0.63	12.17	0.02	0.05	0.15	99.76
03 Xtl 12 T	MKPF	54.9	1.3	43.8	4.79	0.09	54.56	28.63	0.62	10.86	0.02	0.06	0.21	99.92
03 Xtl 12 T	MKPF	57.6	1.1	41.3	4.55	0.08	53.94	29.32	0.63	11.50	0.00	0.05	0.18	100.28
03 Xtl 12 T	MKPF	55.1	1.3	43.6	4.78	0.07	54.53	28.79	0.57	10.92	0.03	0.05	0.22	99.96
03 Xtl 12 T	MKPF	56.0	1.2	42.7	4.67	0.08	54.29	28.93	0.62	11.08	0.03	0.06	0.21	99.98
03 Xtl 12 T	MKPF	59.0	1.1	39.9	4.38	0.08	53.57	29.44	0.66	11.74	0.02	0.06	0.19	100.13
03 Xtl 12 T	MKPF	54.7	1.4	43.8	4.80	0.07	54.47	28.86	0.61	10.84	0.03	0.06	0.24	99.98
03 Xtl 12 T	MKPF	46.6	2.4	51.0	5.48	0.08	57.61	26.72	0.82	9.07	0.06	0.10	0.39	100.34
03 Xtl 12.5	MKPF	54.2	1.3	44.5	4.84	0.07	54.92	28.68	0.59	10.68	0.02	0.05	0.22	100.08
03 Xtl 12.5	MKPF	54.4	1.3	44.2	4.81	0.09	55.41	28.78	0.66	10.71	0.02	0.06	0.22	100.77
03 Xtl 12.5	MKPF	51.9	1.5	46.6	5.04	0.08	55.59	28.13	0.55	10.16	0.02	0.06	0.24	99.86
03 Xtl 12.5	MKPF	55.0	1.3	43.6	4.75	0.07	55.19	28.84	0.70	10.86	0.01	0.07	0.22	100.72
03 Xtl 12 mc 2	MKPF	45.2	2.1	52.7	5.77	0.07	57.57	26.95	0.71	8.95	0.13	0.08	0.35	100.60
03 Xtl 12 mc 2	MKPF	42.9	2.4	54.7	5.90	0.06	58.07	26.73	0.72	8.39	0.03	0.09	0.39	100.41
03 Xtl 12.8	MKPF	60.6	1.0	38.4	4.17	0.07	53.16	29.57	0.56	11.89	0.01	0.07	0.17	99.71
03 Xtl 12.8	MKPF	55.4	1.2	43.4	4.74	0.07	54.65	29.10	0.59	10.94	0.02	0.06	0.20	100.40
03 Xtl 12.8	MKPF	50.6	1.6	47.8	5.17	0.07	56.20	28.04	0.68	9.92	0.01	0.06	0.27	100.46
03 Xtl 12.8	MKPF	42.9	2.5	54.7	5.87	0.07	58.40	26.66	0.62	8.33	0.02	0.08	0.40	100.46
03 Xtl 12.8	MKPF	42.9	2.2	54.9	6.00	0.06	58.38	26.86	0.68	8.47	0.03	0.09	0.36	100.92
03 Xtl 13.5	MKPF	71.4	0.7	25.2	2.76	0.04	49.82	32.37	0.52	14.67	0.03	0.02	0.11	100.35
03 Xtl 13.5	MKPF	71.3	0.6	28.0	3.06	0.05	50.79	31.57	0.54	14.13	0.02	0.02	0.11	100.30
03 Xtl 13.5	MKPF	55.1	0.6	28.0	3.06	0.04	50.67	31.54	0.52	14.07	0.02	0.03	0.11	100.06
03 Xtl 13.5	MKPF	47.4	1.3	43.5	4.75	0.06	54.75	28.65	0.64	10.90	0.02	0.07	0.22	100.06
03 Xtl 13 mc 1	MKPF	51.0	1.9	50.7	5.45	0.07	56.57	27.06	0.73	9.22	0.04	0.08	0.32	99.56
03 Xtl 13 mc 1	MKPF	49.7	1.7	47.3	5.11	0.07	55.67	27.54	0.68	9.97	0.02	0.08	0.28	99.45
03 Xtl 13 mc 1	MKPF	46.7	1.8	48.4	5.26	0.06	56.43	27.44	0.67	9.78	0.03	0.08	0.30	100.06
03 Xtl 13 mc 1	MKPF	36.9	2.0	51.3	5.51	0.06	57.21	27.16	0.65	9.08	0.03	0.09	0.33	100.15
03 Xtl 13 mc 2	MKPF	50.8	3.1	60.1	6.40	0.06	59.55	25.50	0.65	7.11	0.02	0.08	0.50	99.87
03 Xtl 13 mc 2	MKPF	40.9	1.8	47.4	5.16	0.06	55.45	27.77	0.75	10.00	0.02	0.08	0.29	99.60
03 Xtl 13 mc 2	MKPF	47.6	2.6	56.6	6.09	0.06	58.35	26.14	0.73	7.97	0.02	0.09	0.42	99.88
03 Xtl 13 mc 2	MKPF	49.4	2.0	50.4	5.51	0.06	56.48	27.19	0.77	9.41	0.03	0.08	0.34	99.88
03 Xtl 13 mc 3	MKPF	39.5	1.8	48.9	5.30	0.07	56.16	27.48	0.76	9.68	0.04	0.08	0.29	99.89

Table B.1 (Continued)

Sample	Lithology	An	Or	Ab	Na_2O	MgO	SiO_2	Al_2O_3	FeO	CaO	P_2O_5	TiO_2	K_2O	Total
03 Xtl 15	MKPF	78.5	1.3	42.1	4.58	0.07	54.52	28.74	0.60	11.11	0.02	0.06	0.22	99.92
03 Xtl 15	MKPF	75.1	0.5	21.0	2.31	0.06	48.79	32.67	0.64	15.65	0.01	0.03	0.08	100.28
03 Xtl 15	MKPF	69.6	0.6	24.3	2.68	0.06	49.70	32.29	0.57	14.98	0.02	0.03	0.09	100.43
03 Xtl 15	MKPF	58.7	0.7	29.7	3.24	0.07	51.22	31.16	0.54	13.77	0.01	0.03	0.12	100.20
03 Xtl 15	MKPF	67.6	1.0	40.3	4.40	0.08	53.73	29.02	0.60	11.58	0.02	0.05	0.17	99.65
03 Xtl 15	MKPF	51.1	0.7	31.7	3.46	0.07	51.78	30.87	0.56	13.37	0.02	0.03	0.12	100.31
03 Xtl 15	MKPF	52.7	1.4	47.6	5.19	0.08	56.19	27.87	0.58	10.08	0.03	0.08	0.23	100.33
03 Xtl 15	MKPF	54.2	1.4	45.9	4.97	0.08	55.40	27.93	0.55	10.33	0.02	0.07	0.22	99.58
03 Xtl 15	MKPF	52.5	1.2	44.6	4.87	0.09	55.40	28.24	0.61	10.70	0.03	0.07	0.20	100.21
03 Xtl 15	MKPF	51.2	1.3	46.2	5.03	0.08	55.69	28.05	0.56	10.35	0.03	0.07	0.21	100.07
03 Xtl 15	MKPF	54.2	1.5	47.3	5.14	0.08	55.77	27.87	0.58	10.08	0.04	0.08	0.25	99.88
03 Xtl 15	MKPF	57.0	1.3	44.5	4.82	0.09	55.51	28.23	0.64	10.64	0.02	0.06	0.21	100.26
03 Xtl 15	MKPF	56.7	1.3	41.7	4.56	0.09	54.02	28.75	0.59	11.29	0.02	0.06	0.21	99.64
03 Xtl 15	MKPF	65.3	1.3	42.0	4.59	0.08	54.53	29.01	0.60	11.22	0.01	0.06	0.22	100.36
03 Xtl 15	MKPF	57.6	1.0	33.7	3.68	0.08	52.08	30.44	0.61	12.92	0.01	0.04	0.16	100.07
03 Xtl 15	MKPF	54.4	1.2	41.2	4.50	0.10	54.14	28.91	0.64	11.39	0.01	0.06	0.20	99.94
03 Xtl 15	MKPF	55.0	1.3	44.3	4.81	0.09	55.07	28.29	0.64	10.70	0.02	0.06	0.22	99.89
03 Xtl 15	MKPF	57.8	1.2	43.8	4.78	0.09	55.33	28.38	0.61	10.87	0.02	0.06	0.20	100.37
03 Xtl 15	MKPF	67.8	1.1	41.2	4.49	0.08	54.33	29.08	0.63	11.41	0.01	0.06	0.18	100.33
03 Xtl 15	MKPF	57.8	0.8	31.4	3.41	0.10	51.64	30.53	0.67	13.33	0.02	0.05	0.13	99.91
03 Xtl 15	MKPF	57.9	1.2	41.0	4.45	0.09	54.05	29.00	0.69	11.35	0.02	0.07	0.19	99.92
03 Xtl 15	MKPF	55.1	1.2	40.9	4.47	0.08	54.21	29.16	0.57	11.42	0.01	0.04	0.20	100.17
03 Xtl 15	MKPF	55.4	1.3	43.7	4.76	0.07	54.91	28.63	0.60	10.86	0.03	0.05	0.21	100.13
03 Xtl 15	MKPF	53.1	1.3	43.3	4.77	0.07	55.17	28.59	0.63	11.02	0.02	0.07	0.22	100.58
03 Xtl 15 mc 1	MKPF	47.6	1.5	45.4	4.96	0.07	55.29	28.18	0.70	10.48	0.02	0.06	0.25	100.03
03 Xtl 15 mc 2	MKPF	21.9	2.0	50.4	5.45	0.08	56.23	27.19	0.76	9.31	0.03	0.08	0.33	99.46
03 Xtl 15.5	MKPF	51.2	1.4	47.8	5.23	0.08	55.32	27.72	0.61	10.07	0.03	0.07	0.23	99.37
03 Xtl 14	MKPF	68.2	1.3	47.4	5.12	0.09	54.87	27.73	0.65	10.01	0.04	0.07	0.22	98.87
03 Xtl 14	MKPF	51.1	0.7	31.1	3.39	0.06	51.32	31.01	0.56	13.44	0.01	0.02	0.11	99.92
03 Xtl 14	MKPF	58.7	1.4	47.5	5.15	0.08	55.87	27.91	0.54	10.01	0.02	0.06	0.24	99.87
03 Xtl 14	MKPF	54.3	1.1	40.2	4.35	0.09	53.34	29.02	0.63	11.48	0.05	0.06	0.17	99.21
03 Xtl 14	MKPF	54.5	1.3	44.5	4.85	0.09	55.08	28.19	0.60	10.70	0.03	0.06	0.21	99.85
03 Xtl 14	MKPF	73.7	1.3	44.2	4.85	0.09	54.84	28.52	0.62	10.81	0.01	0.06	0.21	100.02

Table B.1 (Continued)

Sample	Lithology	An	Or	Ab	Na_2O	MgO	SiO_2	Al_2O_3	FeO	CaO	P_2O_5	TiO_2	K_2O	Total
03 Xtl 14	MKPF	57.4	0.6	25.8	2.84	0.07	49.94	31.63	0.64	14.67	0.02	0.03	0.10	99.95
03 Xtl 14	MKPF	58.8	1.1	41.4	4.53	0.09	54.22	29.10	0.60	11.35	0.01	0.07	0.19	100.17
03 Xtl 14	MKPF	51.9	1.1	40.1	4.38	0.08	54.25	29.23	0.67	11.63	0.02	0.05	0.18	100.51
03 Xtl 14	MKPF	59.3	1.4	46.7	5.03	0.08	55.36	27.89	0.61	10.10	0.03	0.06	0.24	99.38
03 Xtl 14 mc 1	MKPF	50.9	1.1	39.5	4.30	0.07	53.34	29.49	0.68	11.67	0.03	0.05	0.18	99.82
03 Xtl 14 mc 1	MKPF	51.0	1.7	47.4	5.16	0.08	55.49	27.77	0.77	10.02	0.02	0.08	0.27	99.65
03 Xtl 14 mc 1	MKPF	23.7	1.8	47.2	5.10	0.07	55.78	27.62	0.83	9.96	0.03	0.10	0.29	99.78
05 Xtl 1	SDO	75.8	0.4	23.9	2.62	0.03	48.75	32.46	0.40	15.06	0.02	0.02	0.06	99.47
05 Xtl 1	SDO	63.1	0.6	36.3	3.92	0.02	52.21	30.25	0.28	12.34	0.04	0.01	0.09	99.16
05 Xtl 1	SDO	62.2	0.6	37.1	4.02	0.02	52.59	29.97	0.23	12.21	0.03	0.01	0.10	99.18
05 Xtl 1	SDO	67.5	0.5	32.0	3.50	0.03	51.02	30.81	0.32	13.36	0.02	0.02	0.08	99.15
05 Xtl 1	SDO	70.0	0.4	29.6	3.24	0.03	50.51	31.29	0.41	13.87	0.03	0.02	0.07	99.45
05 Xtl 1	SDO	65.3	0.5	34.2	3.76	0.03	51.78	30.50	0.36	12.98	0.02	0.02	0.08	99.52
05 Xtl 1	SDO	60.8	0.6	38.6	4.23	0.03	52.95	29.83	0.33	12.07	0.03	0.01	0.11	99.58
05 Xtl 1	SDO	60.3	0.7	39.0	4.25	0.03	53.09	29.53	0.35	11.89	0.04	0.03	0.11	99.33
05 Xtl 1	SDO	49.9	1.2	48.9	5.30	0.04	56.00	27.37	0.39	9.78	0.02	0.03	0.20	99.14
05 Xtl 1	SDO	50.5	1.0	48.5	5.28	0.05	55.57	27.63	0.49	9.95	0.01	0.04	0.17	99.20
05 Xtl 1	SDO	51.4	1.1	47.5	5.16	0.04	55.24	27.80	0.46	10.09	0.03	0.02	0.18	99.07
05 Xtl 1	SDO	54.9	1.0	44.2	4.84	0.05	54.41	28.05	0.46	10.89	0.35	0.03	0.16	99.26
05 Xtl 1	SDO	54.4	0.9	44.7	4.83	0.06	54.56	28.31	0.52	10.63	0.02	0.04	0.15	99.13
05 Xtl 1	SDO	53.8	1.0	45.2	4.91	0.05	54.69	28.33	0.53	10.58	0.02	0.04	0.17	99.31
05 Xtl 1	SDO	45.0	1.2	53.7	5.79	0.05	57.15	26.72	0.43	8.78	0.03	0.04	0.20	99.19
05 Xtl 1	SDO	56.6	0.9	42.5	4.61	0.06	53.75	28.67	0.48	11.11	0.01	0.04	0.15	98.89
05 Xtl 1	SDO	48.3	1.3	50.4	5.47	0.05	56.28	27.32	0.54	9.47	0.00	0.05	0.21	99.39
05 Xtl 2	SDO	49.7	1.2	49.1	5.32	0.05	55.81	27.59	0.49	9.75	0.02	0.03	0.20	99.26
05 Xtl 2	SDO	50.4	1.1	48.5	5.25	0.05	55.52	27.67	0.45	9.87	0.03	0.04	0.18	99.07
05 Xtl 2	SDO	55.0	1.0	44.0	4.79	0.05	53.87	28.35	0.52	10.82	0.02	0.04	0.17	98.63
05 Xtl 2	SDO	51.2	1.0	47.8	5.20	0.06	55.27	27.80	0.52	10.09	0.03	0.05	0.17	99.20
05 Xtl 3	SDO	67.5	0.7	31.8	3.45	0.03	50.92	30.65	0.49	13.24	0.02	0.04	0.11	98.94
05 Xtl 3	SDO	66.1	0.7	33.3	3.62	0.02	51.47	30.53	0.49	13.01	0.02	0.02	0.11	99.30
05 Xtl 3	SDO	42.7	2.0	55.3	6.04	0.03	57.30	25.82	0.51	8.45	0.63	0.04	0.34	99.15
05 Xtl 4	SDO	54.1	1.0	44.9	4.89	0.02	54.52	28.57	0.26	10.67	0.02	0.02	0.16	99.14
05 Xtl 4	SDO	57.5	0.8	41.7	4.53	0.03	53.36	29.03	0.33	11.34	0.03	0.02	0.13	98.79

Table B.1 (Continued)

Sample	Lithology	An	Or	Ab	Na_2O	MgO	SiO_2	Al_2O_3	FeO	CaO	P_2O_5	TiO_2	K_2O	Total
05 Xtl 4	SDO	53.6	1.0	45.4	4.90	0.05	54.55	27.93	0.49	10.49	0.02	0.04	0.16	98.65
05 Xtl 4	SDO	55.4	0.9	43.6	4.75	0.06	54.24	28.46	0.57	10.92	0.03	0.04	0.15	99.22
05 Xtl 5	SDO	56.5	0.9	42.5	4.60	0.06	53.96	28.72	0.59	11.06	0.03	0.05	0.15	99.22
05 Xtl 5	SDO	53.0	1.0	46.0	4.97	0.05	55.01	28.20	0.57	10.34	0.02	0.05	0.17	99.38
05 Xtl 5	SDO	47.4	1.3	51.3	5.52	0.04	56.36	27.15	0.39	9.22	0.02	0.05	0.21	98.94
05 Xtl 5	SDO	48.3	1.2	50.4	5.46	0.05	56.12	27.26	0.40	9.47	0.01	0.03	0.20	98.98
05 Xtl 5	SDO	46.5	1.3	52.3	5.61	0.05	56.31	26.79	0.52	9.02	0.02	0.05	0.21	98.58
05 Xtl 6	SDO	53.2	0.9	45.9	4.95	0.03	54.66	28.27	0.33	10.39	0.03	0.01	0.15	98.82
05 Xtl 6	SDO	60.5	0.7	38.9	4.24	0.03	52.89	29.73	0.30	11.95	0.03	0.02	0.11	99.31
05 Xtl 6	SDO	55.5	0.9	43.6	4.77	0.05	54.04	28.50	0.49	10.98	0.01	0.03	0.15	99.02
05 Xtl 6	SDO	55.0	1.1	43.9	4.72	0.05	54.06	28.26	0.54	10.71	0.03	0.04	0.18	98.60
05 Xtl 7	SDO	50.0	1.2	48.8	5.25	0.04	55.31	27.87	0.49	9.74	0.02	0.04	0.19	99.02
05 Xtl 7	SDO	49.7	1.2	49.1	5.30	0.03	55.53	27.72	0.36	9.71	0.03	0.02	0.19	98.93
05 Xtl 7	SDO	53.3	1.1	45.7	4.94	0.05	54.59	28.21	0.52	10.42	0.02	0.04	0.17	99.00
05 Xtl 7	SDO	47.9	1.4	50.7	5.46	0.04	55.78	27.35	0.48	9.36	0.03	0.03	0.23	98.76
11 Xtl 2 T	SDO	56.4	1.0	42.6	4.69	0.06	54.05	28.98	0.57	11.25	0.02	0.05	0.17	99.86
11 Xtl 2 T	SDO	54.8	1.0	44.2	4.86	0.06	54.32	28.85	0.59	10.90	0.03	0.06	0.17	99.84
11 Xtl 2 T	SDO	53.2	1.2	45.6	4.99	0.07	54.89	28.45	0.61	10.54	0.02	0.06	0.20	99.83
11 Xtl 2 T	SDO	57.3	1.0	41.7	4.59	0.06	53.79	29.38	0.65	11.41	-0.01	0.06	0.17	100.11
11 Xtl 2 T	SDO	54.4	1.0	44.6	4.92	0.05	54.69	28.76	0.57	10.86	0.01	0.05	0.17	100.09
11 Xtl 2 T	SDO	56.2	1.0	42.8	4.73	0.06	54.20	29.06	0.58	11.26	0.01	0.05	0.17	100.12
11 Xtl 2 T	SDO	53.1	1.1	45.8	5.05	0.06	54.98	28.66	0.58	10.57	0.04	0.05	0.18	100.18
11 Xtl 2 T	SDO	51.1	1.2	47.7	5.23	0.07	55.54	28.16	0.52	10.14	0.02	0.05	0.20	99.93
11 Xtl 2 T	SDO	68.4	0.7	30.8	3.42	0.05	51.03	31.18	0.56	13.74	0.01	0.03	0.12	100.13
11 Xtl 2 T	SDO	54.8	1.3	43.9	4.85	0.06	54.53	28.88	0.61	10.94	0.01	0.06	0.22	100.16
11 Xtl 2 T	SDO	64.1	1.0	34.9	3.85	0.05	52.23	30.38	0.59	12.80	0.03	0.04	0.17	100.13
11 Xtl 2 T	SDO	71.9	0.6	27.5	3.06	0.04	50.06	31.75	0.63	14.47	0.03	0.04	0.11	100.17
11 Xtl 2 T	SDO	53.5	1.2	45.3	5.00	0.06	54.91	28.81	0.52	10.68	0.03	0.06	0.20	100.26
11 Xtl 2 T	SDO	53.7	1.0	45.3	4.97	0.07	54.89	28.52	0.54	10.65	0.03	0.05	0.17	99.90
11 Xtl 2 T	SDO	54.1	1.0	44.9	4.95	0.06	54.84	28.71	0.57	10.80	0.00	0.05	0.18	100.15
11 Xtl 2 T	SDO	54.8	1.1	44.2	4.87	0.06	54.85	28.80	0.53	10.93	0.02	0.06	0.18	100.29
11 Xtl 2 T	SDO	53.0	1.1	45.9	4.97	0.07	54.91	28.45	0.59	10.40	0.03	0.06	0.18	99.66
11 Xtl 2 T	SDO	53.9	1.1	45.0	4.93	0.07	55.01	28.68	0.59	10.67	0.02	0.05	0.19	100.21

Table B.1 (Continued)

Sample	Lithology	An	Or	Ab	Na_2O	MgO	SiO_2	Al_2O_3	FeO	CaO	P_2O_5	TiO_2	K_2O	Total
11 Xtl 2 T	SDO	68.4	0.7	30.8	3.39	0.05	51.21	31.33	0.60	13.64	0.01	0.03	0.12	100.39
11 Xtl 2 T	SDO	55.8	1.0	43.2	4.76	0.07	54.19	29.02	0.58	11.15	0.04	0.04	0.17	100.02
11 Xtl 2 T	SDO	70.9	1.2	28.0	3.08	0.40	50.51	29.79	1.35	14.12	0.11	0.26	0.20	99.80
11 Xtl 2 T	SDO	52.0	1.1	46.9	5.16	0.06	55.38	28.41	0.58	10.35	-0.01	0.06	0.18	100.18
11 Xtl 2 T	SDO	51.7	1.1	47.2	5.19	0.06	55.46	28.28	0.54	10.29	0.04	0.05	0.19	100.11
11 Xtl 2 T	SDO	54.4	1.0	44.7	4.83	0.06	54.60	28.76	0.60	10.64	0.01	0.05	0.16	99.70
11 Xtl 2 T	SDO	51.3	1.2	47.5	5.21	0.06	55.93	28.35	0.53	10.18	0.02	0.06	0.20	100.55
11 Xtl 2 T	SDO	47.9	1.3	50.8	5.57	0.05	56.69	27.73	0.51	9.51	0.00	0.04	0.22	100.34
11 Xtl 2 T	SDO	52.9	1.0	46.1	5.09	0.05	55.28	28.39	0.56	10.56	0.02	0.05	0.17	100.17
11 Xtl 2 T	SDO	44.0	1.5	54.5	5.98	0.05	57.63	27.26	0.46	8.73	0.02	0.04	0.24	100.41
11 Xtl 2 T	SDO	53.1	1.0	45.9	5.01	0.05	55.28	28.72	0.48	10.49	0.01	0.04	0.17	100.24
11 Xtl 2 T	SDO	49.9	1.1	49.0	5.35	0.04	56.23	27.92	0.43	9.87	0.02	0.03	0.18	100.09
11 Xtl 2 T	SDO	48.8	1.1	50.1	5.47	0.05	56.58	28.04	0.49	9.64	0.02	0.03	0.19	100.50
11 Xtl 2 T	SDO	55.4	0.9	43.6	4.80	0.06	54.49	29.12	0.49	11.04	0.01	0.03	0.16	100.20
11 Xtl 2 T	SDO	52.7	1.0	46.3	5.03	0.05	55.11	28.36	0.49	10.36	0.01	0.04	0.17	99.62
11 Xtl 2.4	SDO	50.2	1.0	48.8	5.33	0.06	56.21	27.86	0.51	9.92	0.02	0.04	0.17	100.12
11 Xtl 2.4	SDO	47.5	1.2	51.3	5.66	0.05	56.66	27.56	0.47	9.48	0.01	0.03	0.20	100.12
11 Xtl 2.4	SDO	49.6	1.2	49.2	5.43	0.06	56.21	28.01	0.44	9.90	0.02	0.03	0.20	100.29
11 Xtl 2.4	SDO	41.2	2.5	56.3	6.19	0.02	58.15	26.80	0.44	8.18	0.03	0.04	0.42	100.28
11 Xtl 2.4	SDO	40.9	2.6	56.5	6.23	0.02	58.40	26.78	0.46	8.17	0.02	0.04	0.44	100.56
11 Xtl 2.5	SDO	65.8	0.7	33.5	3.69	0.03	51.83	31.06	0.33	13.09	0.03	0.02	0.12	100.22
11 Xtl 2.5	SDO	58.3	0.9	40.7	4.50	0.04	53.63	29.51	0.43	11.65	0.02	0.04	0.16	99.96
11 Xtl 2.5	SDO	48.9	1.2	49.9	5.46	0.04	56.17	27.99	0.47	9.68	0.02	0.04	0.20	100.08
11 Xtl 2.5	SDO	49.4	1.6	49.0	5.36	0.04	55.98	27.99	0.53	9.76	0.03	0.04	0.26	99.99
11 Xtl 2 mc 1	SDO	49.2	1.5	49.2	5.38	0.05	56.27	28.00	0.59	9.74	0.03	0.05	0.25	100.36
11 Xtl 2 mc 1	SDO	60.8	0.8	38.4	4.22	0.05	53.13	29.97	0.56	12.09	0.01	0.03	0.13	100.19
11 Xtl 1 T	SDO	67.7	0.5	31.7	3.51	0.02	51.70	31.36	0.30	13.55	0.03	0.01	0.09	100.57
11 Xtl 1 T	SDO	67.2	0.6	32.2	3.54	0.03	51.44	31.23	0.35	13.37	0.02	0.02	0.10	100.10
11 Xtl 1 T	SDO	64.9	0.7	34.4	3.79	0.03	51.97	30.72	0.29	12.94	0.06	0.03	0.11	99.93
11 Xtl 1 T	SDO	61.5	0.7	37.8	4.17	0.03	53.14	30.51	0.27	12.28	0.03	0.01	0.12	100.56
11 Xtl 1 T	SDO	63.7	0.7	35.6	3.90	0.03	52.17	30.63	0.28	12.63	0.02	0.01	0.12	99.77
11 Xtl 1 T	SDO	66.2	0.6	33.2	3.67	0.03	51.90	31.21	0.30	13.26	0.00	0.01	0.10	100.49
11 Xtl 1 T	SDO	55.5	1.0	43.5	4.77	0.05	54.85	28.98	0.48	11.02	0.02	0.04	0.17	100.39

Table B.1 (Continued)

Sample	Lithology	An	Or	Ab	Na_2O	MgO	SiO_2	Al_2O_3	FeO	CaO	P_2O_5	TiO_2	K_2O	Total
11 Xtl 1 T	SDO	47.0	1.3	51.7	5.65	0.05	56.84	27.48	0.50	9.29	0.03	0.04	0.22	100.10
11 Xtl 1 T	SDO	47.3	1.2	51.5	5.61	0.05	56.52	27.49	0.49	9.31	0.01	0.06	0.20	99.74
11 Xtl 1 T	SDO	51.8	1.1	47.1	5.18	0.05	55.72	28.27	0.51	10.31	0.03	0.05	0.18	100.28
11 Xtl 1 T	SDO	49.2	1.2	49.6	5.48	0.05	56.38	27.81	0.49	9.83	0.07	0.03	0.20	100.35
11 Xtl 1 T	SDO	48.6	1.1	50.3	5.53	0.05	56.63	27.85	0.49	9.66	0.00	0.05	0.19	100.45
11 Xtl 1 T	SDO	45.4	1.8	52.9	5.87	0.07	57.33	27.39	0.49	9.11	0.02	0.05	0.30	100.62
11 Xtl 1 T	SDO	44.5	1.4	54.2	5.95	0.05	57.84	27.12	0.52	8.85	0.02	0.05	0.23	100.62
11 Xtl 1 T	SDO	44.8	1.4	53.8	5.93	0.05	57.83	27.19	0.50	8.93	0.05	0.04	0.24	100.75
11 Xtl 1 T	SDO	46.6	1.3	52.1	5.72	0.05	56.93	27.46	0.50	9.26	0.01	0.03	0.21	100.19
11 Xtl 1 T	SDO	54.6	1.0	44.4	4.91	0.05	55.03	28.82	0.52	10.91	0.02	0.03	0.17	100.47
11 Xtl 1 T	SDO	45.0	1.4	53.6	5.88	0.05	57.76	27.24	0.43	8.94	0.04	0.04	0.24	100.62
11 Xtl 1 T	SDO	44.0	1.5	54.5	5.98	0.04	57.58	27.18	0.40	8.75	0.01	0.04	0.25	100.23
11 Xtl 1 T	SDO	52.3	1.0	46.6	5.16	0.04	55.59	28.48	0.44	10.48	0.04	0.04	0.18	100.45
11 Xtl 1 T	SDO	47.6	1.2	51.2	5.64	0.05	56.85	27.80	0.47	9.49	0.02	0.04	0.21	100.57
11 Xtl 1 T	SDO	48.5	1.2	50.3	5.52	0.04	56.67	27.96	0.39	9.64	0.02	0.03	0.20	100.47
11 Xtl 1 T	SDO	46.6	1.2	52.2	5.71	0.04	57.08	27.59	0.43	9.24	0.02	0.03	0.20	100.35
11 Xtl 1 T	SDO	45.1	1.4	53.5	5.85	0.05	57.53	27.33	0.47	8.93	0.01	0.04	0.23	100.44
11 Xtl 1 T	SDO	49.0	1.0	49.9	5.50	0.06	56.08	28.04	0.52	9.78	0.01	0.04	0.18	100.20
11 Xtl 1 T	SDO	49.1	1.3	49.6	5.43	0.06	56.17	27.92	0.49	9.72	0.01	0.03	0.22	100.04
11 Xtl 1 T	SDO	51.8	1.1	47.1	5.15	0.05	55.20	28.39	0.47	10.26	0.03	0.04	0.17	99.77
11 Xtl 1 T	SDO	40.5	2.6	57.0	6.26	0.03	58.61	26.58	0.53	8.04	0.03	0.05	0.43	100.56
11 Xtl 1.1	SDO	47.1	1.2	51.7	5.74	0.05	56.94	27.93	0.43	9.47	0.01	0.04	0.19	100.80
11 Xtl 1.1	SDO	49.1	1.1	49.9	5.52	0.06	56.00	28.11	0.43	9.83	0.01	0.02	0.18	100.15
11 Xtl 1.1	SDO	45.7	2.0	52.3	5.77	0.03	57.28	27.77	0.46	9.14	0.02	0.04	0.34	100.85
11 Xtl 1.1	SDO	50.4	1.3	48.2	5.33	0.06	55.83	28.09	0.55	10.09	0.03	0.05	0.22	100.26
11 Xtl 1.2	SDO	70.9	0.6	28.5	3.14	0.03	50.74	31.90	0.36	14.16	0.03	0.03	0.10	100.48
11 Xtl 1.2	SDO	68.5	0.6	31.0	3.42	0.04	51.41	31.50	0.34	13.70	0.02	0.01	0.09	100.54
11 Xtl 1.2	SDO	61.1	0.7	38.2	4.24	0.03	53.53	30.17	0.33	12.26	0.01	0.02	0.12	100.71
11 Xtl 1.2	SDO	55.0	1.0	44.0	4.90	0.03	55.00	29.21	0.22	11.09	0.02	0.02	0.16	100.65
11 Xtl 1.2	SDO	53.9	0.9	45.2	5.01	0.05	55.20	28.68	0.47	10.81	-0.01	0.03	0.16	100.41
11 Xtl 1.2	SDO	48.9	1.2	49.9	5.51	0.06	56.50	27.75	0.50	9.77	0.03	0.04	0.19	100.35
11 Xtl 1.2	SDO	59.5	0.8	39.7	4.40	0.07	53.66	29.75	0.55	11.91	0.01	0.03	0.13	100.51
11 Xtl 1.3	SDO	48.4	1.3	50.3	5.50	0.05	56.50	27.92	0.52	9.57	0.02	0.05	0.22	100.36

Table B.1 (Continued)

Sample	Lithology	An	Or	Ab	Na_2O	MgO	SiO_2	Al_2O_3	FeO	CaO	P_2O_5	TiO_2	K_2O	Total
11 Xtl 1.3	SDO	48.9	1.5	49.6	5.50	0.06	56.27	28.20	0.54	9.80	0.01	0.04	0.25	100.69
11 Xtl 1.3	SDO	51.0	1.3	47.8	5.24	0.05	55.78	28.40	0.54	10.12	0.05	0.04	0.21	100.45
11 Xtl 1.3	SDO	43.3	2.3	54.4	5.96	0.03	57.48	27.24	0.50	8.60	0.01	0.04	0.39	100.27
11 Xtl 1.4	SDO	64.4	0.7	34.8	3.82	0.05	52.24	30.61	0.48	12.79	0.02	0.03	0.12	100.16
11 Xtl 1.4	SDO	48.2	1.2	50.6	5.54	0.05	56.39	27.96	0.51	9.53	0.02	0.05	0.20	100.25
11 Xtl 1.4	SDO	57.4	0.8	41.7	4.62	0.05	53.99	29.24	0.49	11.51	0.02	0.04	0.14	100.10
11 Xtl 1.4	SDO	64.7	0.6	34.6	3.79	0.06	52.20	30.59	0.55	12.82	0.02	0.03	0.10	100.17
11 Xtl 1.4	SDO	51.5	1.1	47.4	5.22	0.07	55.46	28.40	0.59	10.26	0.00	0.05	0.18	100.23
11 Xtl 1.4	SDO	41.9	2.7	55.4	6.01	0.03	58.28	26.88	0.54	8.22	0.03	0.05	0.44	100.47
11 Xtl 1 mc 1	SDO	42.9	2.6	54.6	6.00	0.03	57.34	27.18	0.63	8.52	0.03	0.05	0.43	100.21
11 Xtl 1 mc 1	SDO	40.4	2.7	56.9	6.29	0.02	58.49	26.87	0.59	8.07	0.02	0.05	0.46	100.87
11 Xtl 3	SDO	73.5	0.4	26.1	2.87	0.05	50.12	32.23	0.55	14.62	0.01	0.03	0.07	100.55
11 Xtl 3	SDO	71.9	0.4	27.6	3.03	0.06	50.52	31.83	0.51	14.27	0.00	0.02	0.07	100.31
11 Xtl 3	SDO	71.2	0.5	28.4	3.15	0.06	50.74	31.81	0.50	14.27	0.02	0.03	0.08	100.64
11 Xtl 3	SDO	70.8	0.4	28.9	3.16	0.07	51.00	31.60	0.46	14.05	0.02	0.03	0.06	100.44
11 Xtl 3	SDO	71.3	0.4	28.2	3.14	0.06	51.04	31.64	0.46	14.35	0.02	0.03	0.07	100.82
11 Xtl 3	SDO	69.8	0.3	29.9	3.31	0.07	51.09	31.54	0.48	13.98	0.01	0.02	0.06	100.56
11 Xtl 3	SDO	69.7	0.4	29.9	3.24	0.06	50.64	31.17	0.51	13.68	0.01	0.03	0.07	99.43
11 Xtl 3	SDO	68.3	0.4	31.3	3.44	0.07	51.76	31.28	0.50	13.61	0.02	0.04	0.07	100.78
11 Xtl 3	SDO	68.3	0.4	31.2	3.46	0.06	51.37	31.28	0.48	13.70	0.02	0.02	0.08	100.48
11 Xtl 3	SDO	64.4	0.6	35.0	3.89	0.06	52.58	30.52	0.48	12.94	0.03	0.02	0.10	100.60
11 Xtl 3	SDO	48.1	1.1	50.8	5.56	0.06	56.78	27.82	0.49	9.51	0.00	0.04	0.18	100.45
11 Xtl 3	SDO	52.2	1.0	46.8	5.16	0.06	55.89	28.46	0.53	10.42	0.00	0.04	0.17	100.73
11 Xtl 3	SDO	50.4	1.1	48.5	5.32	0.06	56.06	28.10	0.51	10.00	0.03	0.04	0.18	100.29
11 Xtl 3	SDO	44.7	2.0	53.3	5.81	0.04	57.57	27.19	0.57	8.83	0.02	0.04	0.34	100.42
11 Xtl 3.1	SDO	51.5	1.1	47.4	5.16	0.05	56.05	28.16	0.55	10.15	0.01	0.03	0.19	100.37
11 Xtl 3.1	SDO	50.2	1.1	48.7	5.33	0.06	56.37	28.16	0.57	9.93	0.02	0.06	0.18	100.67
11 Xtl 3.1	SDO	60.9	0.9	38.2	4.21	0.05	53.46	29.92	0.58	12.13	0.01	0.03	0.15	100.52
11 Xtl 3.1	SDO	50.0	1.2	48.8	5.33	0.06	56.07	28.16	0.56	9.89	0.02	0.04	0.19	100.32
11 Xtl 3.1	SDO	45.1	1.8	53.1	5.83	0.04	57.44	27.40	0.51	8.97	0.02	0.05	0.29	100.56
11 Xtl 4	SDO	73.7	0.4	25.9	2.86	0.03	50.24	32.48	0.50	14.68	0.03	0.02	0.06	100.90
11 Xtl 4	SDO	74.5	0.5	25.1	2.76	0.03	49.66	32.56	0.46	14.86	0.03	0.01	0.08	100.44
11 Xtl 4	SDO	50.0	1.1	48.9	5.45	0.04	56.33	28.07	0.50	10.07	0.02	0.03	0.18	100.69

Table B.1 (Continued)

Sample	Lithology	An	Or	Ab	Na_2O	MgO	SiO_2	Al_2O_3	FeO	CaO	P_2O_5	TiO_2	K_2O	Total
11 Xtl 4	SDO	70.2	0.7	29.1	3.20	0.04	50.87	31.78	0.47	13.94	0.02	0.03	0.12	100.47
11 Xtl 4	SDO	65.6	0.6	33.8	3.75	0.05	52.23	30.80	0.46	13.14	0.01	0.03	0.10	100.57
11 Xtl 4	SDO	48.8	1.2	50.1	5.53	0.05	56.47	28.03	0.50	9.75	0.01	0.05	0.19	100.59
11 Xtl 4	SDO	48.3	1.4	50.4	5.49	0.06	56.40	27.90	0.52	9.53	0.03	0.04	0.22	100.20
11 Xtl 4.1	SDO	47.8	1.8	50.4	5.54	0.05	56.39	27.76	0.63	9.51	0.02	0.05	0.29	100.24
11 Xtl 4.1	SDO	66.0	0.7	33.3	3.68	0.03	52.14	31.10	0.42	13.21	0.02	0.02	0.12	100.74
11 Xtl 4.2	SDO	70.1	0.5	29.5	3.27	0.05	51.19	31.53	0.41	14.06	0.02	0.01	0.08	100.62
11 Xtl 4.2	SDO	65.3	0.7	34.0	3.80	0.06	52.07	31.01	0.41	13.20	0.01	0.02	0.11	100.69
11 Xtl 4.2	SDO	63.6	0.6	35.8	3.85	0.06	51.96	30.14	0.43	12.37	0.02	0.02	0.10	98.95
13 Xtl 1	SDY	53.7	1.0	45.3	4.95	0.04	54.94	28.73	0.46	10.63	0.00	0.03	0.17	99.99
13 Xtl 1	SDY	66.7	0.7	32.7	3.56	0.02	52.19	30.97	0.34	13.16	0.01	0.01	0.11	100.38
13 Xtl 1	SDY	53.0	0.9	46.1	4.97	0.03	55.12	28.61	0.29	10.33	0.03	0.02	0.15	99.57
13 Xtl 1	SDY	52.4	1.0	46.6	5.09	0.05	55.30	28.24	0.48	10.37	0.02	0.03	0.17	99.76
13 Xtl 1	SDY	50.4	1.1	48.5	5.25	0.06	55.97	27.99	0.47	9.87	0.02	0.04	0.18	99.85
13 Xtl 1.5	SDY	69.0	0.5	30.5	3.31	0.04	50.95	31.25	0.51	13.52	0.03	0.03	0.08	99.74
13 Xtl 1.5	SDY	61.3	0.7	38.1	4.13	0.05	53.30	29.86	0.50	12.03	0.01	0.04	0.11	100.09
13 Xtl 1.5	SDY	43.3	2.0	54.6	5.95	0.03	57.71	26.94	0.47	8.55	0.02	0.03	0.33	100.04
13 Xtl 1.5	SDY	51.9	1.0	47.1	5.08	0.06	55.94	28.43	0.55	10.15	0.01	0.04	0.17	100.47
13 Xtl 1.6	SDY	71.2	0.4	28.4	3.10	0.07	50.96	31.62	0.50	14.02	0.01	0.03	0.07	100.36
13 Xtl 1.6	SDY	69.9	0.5	29.7	3.17	0.05	50.89	31.34	0.50	13.51	0.02	0.03	0.07	99.59
13 Xtl 1.6	SDY	50.0	1.4	48.7	5.28	0.05	56.15	28.12	0.51	9.81	0.01	0.04	0.22	100.23
13 Xtl 1.6	SDY	48.8	1.2	50.0	5.42	0.05	56.96	27.60	0.52	9.59	0.03	0.04	0.20	100.42
13 Xtl 1.7	SDY	58.5	0.8	40.7	4.47	0.05	53.80	29.04	0.59	11.61	0.01	0.05	0.14	99.80
13 Xtl 1.7	SDY	52.9	1.0	46.1	5.01	0.04	55.45	28.18	0.53	10.40	0.03	0.05	0.16	99.86
13 Xtl 1.7	SDY	51.6	1.0	47.4	5.17	0.05	55.80	28.16	0.46	10.21	0.02	0.04	0.17	100.07
13 Xtl 1.7	SDY	50.6	1.2	48.2	5.26	0.05	56.14	28.03	0.53	10.01	0.02	0.03	0.20	100.29
13 Xtl 1.8	SDY	65.5	0.4	34.1	3.72	0.03	52.45	30.52	0.33	12.93	0.00	0.02	0.06	100.07
13 Xtl 1.8	SDY	64.1	0.5	35.4	3.85	0.03	52.19	30.43	0.36	12.63	0.02	0.02	0.08	99.61
13 Xtl 1.8	SDY	57.0	0.6	42.3	4.63	0.02	54.54	29.40	0.28	11.28	0.03	0.01	0.11	100.29
13 Xtl 2	SDY	70.3	0.7	29.0	3.10	0.06	51.47	30.83	0.48	13.57	0.00	0.02	0.11	99.68
13 Xtl 2	SDY	71.0	0.5	28.5	3.10	0.05	50.53	31.29	0.44	13.98	0.01	0.03	0.08	99.51
13 Xtl 2	SDY	47.0	1.2	51.8	5.66	0.05	56.73	27.34	0.44	9.29	0.02	0.03	0.20	99.76
13 Xtl 2	SDY	52.4	1.0	46.5	5.06	0.06	55.31	28.29	0.53	10.31	0.02	0.04	0.17	99.78

Table B.1 (Continued)

Sample	Lithology	An	Or	Ab	Na_2O	MgO	SiO_2	Al_2O_3	FeO	CaO	P_2O_5	TiO_2	K_2O	Total
13 Xtl 2	SDY	50.6	1.0	48.5	5.27	0.05	55.34	28.12	0.48	9.95	0.01	0.03	0.16	99.45
13 Xtl 2.5	SDY	62.0	0.7	37.3	4.07	0.05	52.50	29.68	0.59	12.24	0.04	0.03	0.11	99.34
13 Xtl 2.5	SDY	61.5	0.9	37.7	4.15	0.04	52.88	29.88	0.55	12.24	0.01	0.04	0.15	99.93
13 Xtl 2.5	SDY	48.2	1.3	50.5	5.49	0.05	55.96	27.77	0.50	9.48	0.00	0.04	0.22	99.56
13 Xtl 2.5	SDY	44.9	2.0	53.1	5.79	0.04	57.14	27.13	0.51	8.85	0.02	0.05	0.33	99.86
13 Xtl 2.6	SDY	70.1	0.3	29.5	3.18	0.05	51.01	31.28	0.44	13.65	0.02	0.02	0.06	99.74
13 Xtl 2.6	SDY	70.6	0.4	29.0	3.13	0.05	50.81	31.42	0.43	13.76	0.04	0.03	0.07	99.74
13 Xtl 2.6	SDY	51.7	1.0	47.2	5.09	0.05	55.30	27.93	0.48	10.10	0.03	0.05	0.17	99.19
13 Xtl 2.6	SDY	47.1	1.6	51.3	5.53	0.04	56.80	27.27	0.51	9.17	0.01	0.04	0.26	99.63
13 Xtl 2.7	SDY	67.9	0.5	31.6	3.45	0.03	50.72	31.14	0.41	13.39	0.01	0.03	0.08	99.28
13 Xtl 2.7	SDY	63.7	0.7	35.6	3.85	0.04	52.02	30.52	0.42	12.50	0.02	0.03	0.12	99.56
13 Xtl 2.7	SDY	57.5	0.9	41.6	4.52	0.06	53.56	29.19	0.56	11.29	0.04	0.04	0.15	99.43
13 Xtl 2.7	SDY	43.7	2.3	54.0	5.89	0.03	57.40	27.07	0.45	8.63	0.03	0.04	0.38	99.92
13 Xtl 2 mc 1	SDY	42.2	2.6	55.2	5.96	0.02	58.15	26.72	0.47	8.26	0.02	0.04	0.43	100.08
13 Xtl 2 mc 1	SDY	45.6	2.1	52.2	5.64	0.02	57.20	27.45	0.37	8.93	0.01	0.03	0.35	100.04
13 Xtl 2.8	SDY	36.3	1.3	62.4	6.72	0.01	59.61	26.12	0.11	7.08	0.03	0.01	0.22	99.92
13 Xtl 2.8	SDY	51.0	0.7	48.2	5.21	0.02	55.57	28.57	0.26	9.98	0.01	0.03	0.12	99.81
13 Xtl 2.8	SDY	44.8	2.1	53.2	5.66	0.51	56.88	26.65	0.68	8.63	0.03	0.02	0.33	99.45
13 Xtl 2.8	SDY	51.3	0.8	47.9	5.22	0.02	55.63	28.51	0.26	10.11	0.01	0.02	0.13	99.95
13 Xtl 3	SDY	52.1	1.0	46.9	5.11	0.05	55.28	28.00	0.54	10.25	0.03	0.06	0.17	99.49
13 Xtl 3	SDY	55.7	0.9	43.4	4.71	0.05	54.59	28.64	0.52	10.93	0.02	0.04	0.14	99.69
13 Xtl 3	SDY	68.2	0.6	31.2	3.41	0.04	51.48	31.11	0.58	13.51	0.01	0.03	0.10	100.31
13 Xtl 3	SDY	54.5	1.0	44.5	4.82	0.05	54.85	28.44	0.51	10.71	0.03	0.05	0.16	99.69
13 Xtl 3	SDY	53.9	0.9	45.2	4.94	0.06	55.01	28.56	0.56	10.65	0.01	0.05	0.15	99.99
13 Xtl 3	SDY	51.8	1.0	47.2	5.16	0.05	55.67	28.07	0.50	10.23	0.02	0.05	0.17	99.94
13 Xtl 3	SDY	50.7	1.0	48.2	5.23	0.05	56.06	28.00	0.51	9.95	0.03	0.05	0.17	100.05
13 Xtl 3	SDY	49.2	1.1	49.7	5.41	0.05	56.01	27.70	0.53	9.67	0.03	0.06	0.18	99.68
13 Xtl 3	SDY	49.8	1.0	49.1	5.37	0.05	56.25	27.82	0.48	9.87	0.01	0.04	0.17	100.06
13 Xtl 3	SDY	48.6	1.1	50.3	5.50	0.05	56.44	27.62	0.48	9.62	0.00	0.04	0.18	99.95
13 Xtl 3	SDY	49.9	1.1	49.0	5.31	0.05	56.31	27.96	0.47	9.77	0.01	0.05	0.18	100.11
13 Xtl 3	SDY	45.5	1.3	53.2	5.78	0.05	57.23	27.35	0.51	8.94	0.03	0.06	0.21	100.17
13 Xtl 3	SDY	45.5	1.3	53.2	5.78	0.05	57.34	27.14	0.46	8.95	0.01	0.05	0.21	100.04
13 Xtl 3	SDY	51.5	1.0	47.5	5.17	0.05	55.89	28.22	0.49	10.15	0.03	0.05	0.16	100.22

Table B.1 (Continued)

Sample	Lithology	An	Or	Ab	Na_2O	MgO	SiO_2	Al_2O_3	FeO	CaO	P_2O_5	TiO_2	K_2O	Total
13 Xtl 3	SDY	49.5	1.0	49.4	5.42	0.05	56.19	27.79	0.45	9.83	0.01	0.03	0.17	99.95
13 Xtl 3	SDY	48.9	1.2	49.8	5.41	0.04	56.23	27.66	0.43	9.62	0.01	0.04	0.20	99.64
13 Xtl 3	SDY	48.3	1.2	50.6	5.54	0.04	56.54	27.54	0.38	9.57	0.00	0.03	0.19	99.91
13 Xtl 3	SDY	48.0	1.2	50.8	5.55	0.04	56.68	27.63	0.43	9.47	0.02	0.03	0.20	100.07
13 Xtl 3	SDY	46.7	1.2	52.1	5.66	0.05	57.03	27.34	0.39	9.18	0.03	0.02	0.20	99.90
13 Xtl 3	SDY	43.1	1.4	55.5	6.05	0.04	58.07	26.81	0.42	8.52	0.01	0.02	0.23	100.18
13 Xtl 3	SDY	53.0	1.0	46.0	5.02	0.04	55.30	28.43	0.48	10.48	0.02	0.04	0.17	100.03
13 Xtl 3	SDY	53.8	0.9	45.3	4.97	0.05	55.40	28.66	0.51	10.69	0.02	0.04	0.15	100.49
13 Xtl 3	SDY	50.1	1.0	48.9	5.33	0.05	56.08	28.13	0.48	9.89	0.02	0.04	0.17	100.20
13 Xtl 3	SDY	56.4	0.8	42.8	4.67	0.05	54.38	29.04	0.51	11.14	0.02	0.04	0.14	99.97
13 Xtl 3	SDY	50.9	0.9	48.2	5.24	0.05	56.03	28.08	0.49	10.02	0.00	0.05	0.15	100.13
13 Xtl 3	SDY	54.9	0.9	44.2	4.83	0.05	54.92	28.76	0.49	10.84	0.04	0.03	0.15	100.12
13 Xtl 3	SDY	53.3	0.9	45.8	5.03	0.05	55.54	28.72	0.47	10.60	0.02	0.04	0.15	100.61
13 Xtl 3	SDY	46.9	1.6	51.5	5.62	0.05	56.75	27.36	0.54	9.27	0.03	0.04	0.26	99.99
13 Xtl 3	SDY	64.7	0.7	34.6	3.78	0.05	51.90	30.48	0.57	12.76	0.02	0.04	0.11	99.71
13 Xtl 3	SDY	55.2	1.0	43.8	4.80	0.06	54.30	28.74	0.65	10.94	0.03	0.06	0.16	99.75
13 Xtl 3.5	SDY	57.5	0.6	42.0	4.59	0.02	53.69	29.44	0.32	11.40	0.01	0.03	0.09	99.65
13 Xtl 3.5	SDY	57.2	0.5	42.3	4.62	0.02	53.54	29.57	0.29	11.32	0.02	0.03	0.09	99.51
13 Xtl 3.5	SDY	71.4	0.4	28.2	3.06	0.03	50.22	31.81	0.40	14.01	0.02	0.01	0.06	99.66
13 Xtl 3.5	SDY	62.9	0.5	36.6	4.01	0.03	52.89	30.44	0.45	12.47	0.02	0.03	0.08	100.41
13 Xtl 3.6	SDY	62.7	0.5	36.9	4.03	0.02	53.40	30.65	0.34	12.40	0.01	0.01	0.08	100.94
13 Xtl 3.6	SDY	46.2	1.5	52.3	5.65	0.03	57.29	27.65	0.48	9.02	0.03	0.04	0.24	100.46
13 Xtl 3.6	SDY	42.3	2.1	55.6	6.01	0.03	57.89	26.83	0.49	8.27	0.01	0.04	0.35	99.96
13 Xtl 3 mc 1	SDY	44.3	2.7	53.1	5.79	0.02	57.39	27.02	0.60	8.74	0.05	0.05	0.44	100.15
13 Xtl 3 mc 1	SDY	42.1	2.9	55.0	5.98	0.02	58.14	26.86	0.55	8.29	0.01	0.04	0.47	100.39
13 Xtl 4	SDY	47.1	1.3	51.7	5.63	0.01	57.23	27.76	0.17	9.29	0.02	0.01	0.21	100.32
13 Xtl 4	SDY	47.1	1.4	51.6	5.59	0.00	56.92	27.85	0.18	9.24	0.00	0.00	0.22	100.01
13 Xtl 4	SDY	41.8	1.6	56.6	6.17	0.00	58.57	27.07	0.14	8.24	0.01	0.01	0.27	100.51
13 Xtl 4	SDY	51.6	1.3	47.1	5.15	0.01	55.70	28.52	0.23	10.23	0.01	0.01	0.22	100.09
13 Xtl 4	SDY	47.6	1.4	51.0	5.55	0.01	56.91	28.06	0.25	9.38	0.02	0.02	0.23	100.49
13 Xtl 4.5	SDY	54.2	1.0	44.7	4.89	0.05	55.04	28.67	0.45	10.73	0.00	0.04	0.17	100.04
13 Xtl 4.5	SDY	56.3	0.9	42.8	4.66	0.05	54.51	28.91	0.49	11.08	0.01	0.04	0.14	99.97
13 Xtl 4.5	SDY	43.8	1.5	54.7	5.93	0.04	57.61	27.07	0.54	8.59	0.00	0.04	0.24	100.12

Table B.1 (Continued)

Sample	Lithology	An	Or	Ab	Na_2O	MgO	SiO_2	Al_2O_3	FeO	CaO	P_2O_5	TiO_2	K_2O	Total
13 Xtl 4.5	SDY	53.1	1.0	46.0	5.02	0.06	55.44	28.34	0.52	10.49	0.02	0.04	0.16	100.12
13 Xtl 4.6	SDY	66.7	0.6	32.7	3.53	0.03	51.85	30.92	0.37	12.99	0.01	0.01	0.10	99.82
13 Xtl 4.6	SDY	57.7	0.8	41.5	4.51	0.05	54.25	29.28	0.51	11.34	0.01	0.04	0.13	100.12
13 Xtl 4.6	SDY	51.0	1.1	48.0	5.16	0.06	55.89	28.09	0.53	9.91	0.02	0.04	0.17	99.89
13 Xtl 4.6	SDY	52.5	1.1	46.4	5.03	0.05	55.74	28.44	0.52	10.28	0.02	0.04	0.18	100.31
13 Xtl 4 mc 1	SDY	69.6	0.5	29.9	3.29	0.04	51.33	31.55	0.55	13.84	0.02	0.02	0.08	100.76
13 Xtl 4 mc 1	SDY	49.8	1.4	48.9	5.30	0.04	56.27	27.89	0.54	9.75	0.02	0.04	0.22	100.07
13 Xtl 4.7	SDY	61.7	0.5	37.8	4.12	0.04	52.95	30.04	0.38	12.16	0.02	0.02	0.08	99.85
13 Xtl 4.7	SDY	65.9	0.4	33.7	3.69	0.03	51.79	30.97	0.37	13.03	0.01	0.02	0.06	100.06
13 Xtl 4.7	SDY	66.2	0.4	33.3	3.61	0.04	51.46	30.64	0.39	13.00	0.02	0.02	0.07	99.26
13 Xtl 4.7	SDY	53.3	0.9	45.8	4.99	0.06	55.08	28.67	0.53	10.52	0.01	0.04	0.16	100.06
28 Xtl 1	SDY	41.7	1.4	56.8	6.12	0.03	58.07	26.47	0.36	8.14	0.02	0.02	0.24	99.47
28 Xtl 1	SDY	39.6	1.5	58.9	6.34	0.03	58.08	26.08	0.35	7.70	0.01	0.01	0.24	98.86
28 Xtl 1	SDY	49.6	1.0	49.4	5.36	0.03	55.81	27.67	0.37	9.74	0.01	0.03	0.17	99.19
28 Xtl 1	SDY	49.9	1.0	49.1	5.34	0.03	55.80	27.65	0.37	9.83	0.01	0.03	0.16	99.27
28 Xtl 1	SDY	47.0	1.3	51.8	5.61	0.03	56.48	27.21	0.39	9.22	0.01	0.02	0.21	99.21
28 Xtl 1	SDY	45.9	1.2	53.0	5.75	0.03	56.77	27.16	0.43	9.00	0.00	0.03	0.19	99.37
28 Xtl 1	SDY	45.0	1.3	53.7	5.79	0.03	57.04	27.11	0.38	8.76	0.01	0.03	0.22	99.37
28 Xtl 1	SDY	49.2	1.0	49.8	5.37	0.03	56.01	27.88	0.37	9.61	0.03	0.02	0.17	99.51
28 Xtl 1	SDY	46.4	1.2	52.4	5.69	0.03	56.62	27.04	0.37	9.11	0.02	0.02	0.20	99.11
28 Xtl 1	SDY	43.2	1.4	55.4	6.02	0.02	57.63	26.74	0.35	8.48	0.00	0.03	0.23	99.52
28 Xtl 1	SDY	42.1	1.6	56.3	6.05	0.02	57.97	26.37	0.37	8.20	0.01	0.02	0.27	99.29
28 Xtl 1	SDY	41.6	1.5	56.9	6.09	0.03	57.75	26.47	0.36	8.07	0.01	0.02	0.25	99.05
28 Xtl 1	SDY	45.8	1.2	53.0	5.70	0.03	56.89	27.03	0.40	8.90	-0.01	0.02	0.20	99.20
28 Xtl 1	SDY	45.1	1.2	53.7	5.82	0.03	57.04	26.96	0.39	8.84	0.02	0.02	0.20	99.31
28 Xtl 1	SDY	47.1	1.2	51.7	5.58	0.03	56.32	27.39	0.39	9.20	0.02	0.01	0.20	99.15
28 Xtl 1	SDY	45.5	1.3	53.3	5.82	0.03	56.47	27.17	0.41	8.98	0.02	0.03	0.21	99.15
28 Xtl 2	SDY	43.7	1.3	54.9	5.97	0.03	57.12	27.02	0.38	8.60	0.01	0.03	0.22	99.40
28 Xtl 2	SDY	42.9	1.3	55.8	6.06	0.03	57.57	26.72	0.39	8.44	0.01	0.02	0.22	99.45
28 Xtl 2	SDY	44.4	1.3	54.3	5.92	0.03	57.08	27.05	0.39	8.77	0.02	0.02	0.21	99.53
28 Xtl 3	SDY	55.4	1.0	43.6	4.77	0.02	54.05	28.95	0.36	10.98	0.02	0.02	0.17	99.36
28 Xtl 3	SDY	42.8	2.9	54.4	5.93	0.02	56.99	26.87	0.42	8.44	0.05	0.03	0.47	99.23
28 Xtl 4	SDY	56.1	0.7	43.2	4.75	0.01	53.89	29.14	0.28	11.18	0.01	0.02	0.11	99.42

Table B.1 (Continued)

Sample	Lithology	An	Or	Ab	Na_2O	MgO	SiO_2	Al_2O_3	FeO	CaO	P_2O_5	TiO_2	K_2O	Total
28 Xtl 4	SDY	69.1	0.3	30.6	3.35	0.03	50.56	31.18	0.36	13.68	0.01	0.01	0.06	99.27
28 Xtl 4	SDY	62.1	0.6	37.3	4.08	0.03	52.37	30.04	0.34	12.31	0.01	0.02	0.10	99.35
28 Xtl 4	SDY	42.1	1.6	56.2	6.08	0.03	57.32	26.70	0.37	8.24	0.00	0.02	0.27	99.08
28 Xtl 5	SDY	62.0	0.6	37.4	4.08	0.02	52.29	30.01	0.29	12.25	0.02	0.02	0.10	99.10
28 Xtl 5	SDY	62.7	0.5	36.8	4.01	0.03	52.26	29.91	0.33	12.34	0.01	0.02	0.09	98.99
28 Xtl 5	SDY	57.4	0.7	41.9	4.60	0.03	53.58	29.17	0.36	11.40	0.03	0.02	0.11	99.31
28 Xtl 5	SDY	42.0	2.3	55.7	6.01	0.03	57.40	26.73	0.40	8.21	0.02	0.03	0.37	99.20
28 Xtl 6	SDY	61.8	0.6	37.7	4.13	0.04	52.82	29.96	0.34	12.27	0.02	0.02	0.10	99.71
28 Xtl 6	SDY	60.5	0.6	38.9	4.25	0.03	52.97	29.97	0.33	11.94	0.03	0.01	0.10	99.66
28 Xtl 6	SDY	48.5	1.1	50.4	5.50	0.04	55.85	27.56	0.43	9.60	0.02	0.03	0.18	99.21
28 Xtl 6	SDY	46.6	1.6	51.8	5.65	0.03	56.49	27.35	0.38	9.19	0.02	0.02	0.26	99.41
28 Xtl 6	SDY	35.7	3.6	60.7	6.67	0.02	59.34	25.64	0.39	7.11	0.01	0.03	0.60	99.81
28 Xtl 7	SDY	61.7	0.6	37.7	4.11	0.02	52.60	30.10	0.32	12.18	0.02	0.01	0.09	99.47
28 Xtl 7	SDY	45.1	0.9	53.9	5.87	0.01	56.91	27.62	0.16	8.88	0.01	0.00	0.15	99.61
28 Xtl 7	SDY	61.5	0.6	37.9	4.17	0.03	52.45	30.00	0.30	12.25	0.02	0.01	0.10	99.35
28 Xtl 7	SDY	44.7	2.3	53.0	5.76	0.03	57.12	27.19	0.37	8.80	0.02	0.02	0.38	99.71
28 Xtl 8	SDY	63.0	0.6	36.4	4.01	0.03	51.87	30.18	0.34	12.56	0.01	0.02	0.11	99.14
28 Xtl 8	SDY	62.5	0.7	36.7	4.04	0.02	52.29	30.27	0.39	12.45	0.02	0.03	0.12	99.63
28 Xtl 8	SDY	45.8	1.7	52.5	5.75	0.03	56.61	27.55	0.41	9.08	0.03	0.02	0.28	99.77
28 Xtl 9	SDY	63.2	1.0	35.8	3.91	0.03	52.19	30.30	0.44	12.52	0.01	0.02	0.16	99.61
28 Xtl 9	SDY	54.2	1.7	44.0	4.84	0.03	54.57	28.70	0.42	10.79	0.02	0.02	0.29	99.67
28 Xtl 10	SDY	59.9	0.5	39.5	4.32	0.02	53.03	29.85	0.24	11.86	0.03	0.02	0.09	99.44
28 Xtl 10	SDY	59.5	0.6	39.9	4.36	0.01	53.25	29.80	0.21	11.75	0.02	0.02	0.10	99.50
28 Xtl 10	SDY	51.1	0.8	48.1	5.26	0.01	55.26	28.41	0.20	10.10	0.01	0.02	0.13	99.44
28 Xtl 10	SDY	67.1	0.5	32.5	3.58	0.03	51.34	31.05	0.32	13.39	0.01	0.02	0.08	99.81
28 Xtl 10	SDY	60.4	0.5	39.1	4.28	0.03	53.05	29.96	0.33	11.97	0.02	0.02	0.09	99.78
28 Xtl 11	SDY	56.3	0.8	42.8	4.69	0.04	54.06	28.89	0.40	11.15	0.02	0.01	0.14	99.40
28 Xtl 11	SDY	46.7	1.2	52.1	5.67	0.03	56.26	27.32	0.40	9.20	0.02	0.02	0.20	99.15
28 Xtl 11	SDY	44.5	1.3	54.1	5.90	0.03	57.06	27.06	0.39	8.78	0.01	0.02	0.22	99.48
28 Xtl 11	SDY	41.0	1.9	57.1	6.20	0.03	57.71	26.40	0.36	8.05	0.02	0.03	0.31	99.14
28 Xtl 12	SDY	57.4	0.7	41.9	4.58	0.02	53.58	29.15	0.28	11.34	0.00	0.02	0.11	99.10
28 Xtl 12	SDY	55.9	0.8	43.3	4.75	0.02	54.14	29.04	0.27	11.11	0.01	0.01	0.14	99.53
28 Xtl 12	SDY	49.1	1.1	49.9	5.38	0.63	56.22	27.10	0.63	9.58	0.01	0.01	0.18	99.74

Table B.1 (Continued)

Sample	Lithology	An	Or	Ab	Na_2O	MgO	SiO_2	Al_2O_3	FeO	CaO	P_2O_5	TiO_2	K_2O	Total
28 Xtl 12	SDY	48.5	1.1	50.4	5.51	0.04	56.25	27.57	0.40	9.58	0.02	0.03	0.18	99.58
28 Xtl 12	SDY	50.5	1.0	48.4	5.26	0.04	55.40	27.87	0.42	9.93	0.02	0.02	0.17	99.14
28 Xtl 12	SDY	46.2	1.2	52.6	5.76	0.03	56.83	27.21	0.40	9.17	0.01	0.02	0.19	99.63
28 Xtl 12	SDY	44.6	1.3	54.1	5.90	0.03	57.31	26.88	0.38	8.80	0.02	0.02	0.21	99.56
28 Xtl 12	SDY	47.5	1.1	51.4	5.62	0.02	56.28	27.44	0.37	9.41	0.03	0.02	0.18	99.37
28 Xtl 12	SDY	50.4	1.0	48.5	5.35	0.04	55.46	28.00	0.41	10.06	0.00	0.02	0.18	99.51
28 Xtl 12	SDY	42.5	1.4	56.1	6.10	0.03	57.51	26.38	0.40	8.37	0.01	0.02	0.23	99.05
28 Xtl 12	SDY	41.8	1.6	56.6	6.19	0.03	57.83	26.65	0.39	8.29	0.03	0.03	0.26	99.70
20 Xtl 5	QMI	59.1	0.7	40.3	4.45	0.03	53.79	30.05	0.33	11.81	0.03	0.05	0.11	100.66
20 Xtl 5	QMI	56.5	0.7	42.8	4.74	0.04	54.57	29.37	0.33	11.29	0.01	0.04	0.12	100.51
20 Xtl 5	QMI	53.6	0.7	45.6	5.06	0.02	55.36	28.77	0.36	10.76	0.01	0.02	0.12	100.48
20 Xtl 5	QMI	62.1	0.7	37.2	4.10	0.03	52.81	30.56	0.41	12.40	0.03	0.05	0.12	100.51
20 Xtl 5	QMI	54.5	0.7	44.8	4.94	0.02	55.30	29.17	0.30	10.90	0.00	0.02	0.11	100.77
20 Xtl 5	QMI	44.4	1.1	54.4	5.99	0.02	57.83	27.57	0.29	8.85	0.00	0.01	0.19	100.76
20 Xtl 5.1	QMI	59.6	0.6	39.8	4.38	0.04	53.39	29.98	0.43	11.89	0.02	0.03	0.10	100.25
20 Xtl 5.1	QMI	62.4	0.5	37.1	4.07	0.05	52.63	30.46	0.44	12.40	0.01	0.03	0.08	100.17
20 Xtl 5.1	QMI	44.0	1.2	54.9	6.05	0.03	57.90	27.49	0.30	8.77	0.03	0.03	0.19	100.81
20 Xtl 5.2	QMI	58.9	0.6	40.5	4.49	0.04	53.92	29.84	0.37	11.82	0.01	0.03	0.10	100.63
20 Xtl 5.2	QMI	60.1	0.5	39.4	4.32	0.06	53.72	29.87	0.49	11.93	0.01	0.04	0.09	100.54
20 Xtl 5.2	QMI	45.9	1.1	52.9	5.80	0.03	57.32	27.68	0.27	9.11	0.03	0.03	0.19	100.45
20 Xtl 5.2	QMI	40.5	1.4	58.1	6.39	0.02	58.61	26.77	0.29	8.07	0.04	0.02	0.23	100.43
20 Xtl 5.3	QMI	62.2	0.5	37.3	4.10	0.05	52.69	30.18	0.44	12.38	0.02	0.03	0.09	99.98
20 Xtl 5.3	QMI	62.1	0.4	37.4	4.12	0.05	53.02	30.28	0.42	12.38	0.02	0.04	0.07	100.41
20 Xtl 5 mc	QMI	60.6	0.7	38.7	4.26	0.03	53.22	30.27	0.50	12.05	0.01	0.05	0.12	100.51
20 Xtl 5 mc	QMI	61.1	0.7	38.2	4.23	0.04	53.60	30.08	0.50	12.25	0.03	0.03	0.12	100.88
20 Xtl 5.5	QMI	58.0	0.6	41.4	4.58	0.03	54.12	29.63	0.37	11.64	0.01	0.03	0.10	100.52
20 Xtl 5.5	QMI	59.4	0.7	40.0	4.44	0.04	53.79	29.92	0.40	11.93	0.02	0.03	0.11	100.68
20 Xtl 5.5	QMI	45.9	1.0	53.1	5.84	0.02	57.35	27.65	0.31	9.13	0.02	0.01	0.17	100.50
20 Xtl 5.5	QMI	45.7	1.2	53.2	5.83	0.02	57.33	27.70	0.28	9.07	0.02	0.02	0.20	100.49
20 Xtl 3	QMI	52.7	0.8	46.5	5.17	0.02	55.47	29.06	0.26	10.60	0.02	0.02	0.14	100.77
20 Xtl 3	QMI	57.6	0.8	41.6	4.60	0.02	54.05	29.56	0.27	11.53	0.02	0.01	0.13	100.18
20 Xtl 3	QMI	65.3	0.5	34.2	3.79	0.02	52.34	31.01	0.41	13.08	0.02	0.03	0.08	100.77
20 Xtl 3	QMI	67.3	0.5	32.2	3.58	0.05	51.64	31.00	0.47	13.54	0.01	0.04	0.08	100.40

Table B.1 (Continued)

Sample	Lithology	An	Or	Ab	Na_2O	MgO	SiO_2	Al_2O_3	FeO	CaO	P_2O_5	TiO_2	K_2O	Total
20 Xtl 3	QMI	61.8	0.6	37.7	4.13	0.04	53.07	30.17	0.37	12.27	0.02	0.02	0.09	100.18
20 Xtl 3	QMI	54.7	0.7	44.5	4.91	0.03	54.88	29.23	0.33	10.92	0.04	0.02	0.12	100.48
20 Xtl 3	QMI	37.3	1.6	61.1	6.68	0.02	59.66	26.41	0.29	7.37	0.01	0.03	0.27	100.74
20 Xtl 3.1	QMI	64.7	0.5	34.8	3.84	0.07	52.12	30.51	0.50	12.93	0.03	0.05	0.08	100.14
20 Xtl 3.1	QMI	60.6	0.6	38.8	4.27	0.05	53.10	30.16	0.43	12.10	0.02	0.04	0.10	100.27
20 Xtl 3.2	QMI	60.6	0.5	38.9	4.30	0.04	53.25	30.05	0.48	12.14	0.00	0.05	0.09	100.40
20 Xtl 3.2	QMI	41.9	1.2	56.9	6.27	0.02	58.17	27.25	0.36	8.35	0.01	0.03	0.20	100.66
20 Xtl 3.3	QMI	62.2	0.6	37.2	4.12	0.06	52.98	30.17	0.50	12.46	0.02	0.03	0.09	100.44
20 Xtl 4	QMI	46.0	0.9	53.1	5.83	0.01	56.67	27.91	0.15	9.14	0.00	0.02	0.16	99.90
20 Xtl 4	QMI	52.5	0.9	46.6	5.13	0.02	55.21	28.70	0.19	10.46	0.03	0.02	0.14	99.89
20 Xtl 4	QMI	51.9	0.9	47.3	5.22	0.02	55.41	28.76	0.19	10.38	-0.01	0.02	0.14	100.14
20 Xtl 4	QMI	52.6	0.9	46.6	5.14	0.02	55.31	28.78	0.19	10.50	0.02	0.02	0.14	100.12
20 Xtl 4	QMI	51.5	0.9	47.7	5.27	0.01	55.56	28.67	0.16	10.29	0.02	0.02	0.15	100.15
20 Xtl 4	QMI	50.0	1.0	49.0	5.38	0.01	55.92	28.41	0.25	9.94	0.01	0.02	0.17	100.11
20 Xtl 4	QMI	51.3	0.8	47.9	5.26	0.01	55.55	28.47	0.17	10.21	0.01	0.03	0.14	99.84
20 Xtl 4	QMI	49.9	1.2	48.8	5.36	0.02	56.32	28.21	0.22	9.92	0.01	0.03	0.21	100.30
20 Xtl 4	QMI	57.2	0.8	42.0	4.63	0.02	54.09	29.64	0.30	11.41	0.01	0.01	0.14	100.25
20 Xtl 4	QMI	60.2	0.7	39.1	4.37	0.03	53.20	30.06	0.37	12.16	0.01	0.02	0.11	100.33
20 Xtl 4	QMI	64.4	0.7	35.0	3.85	0.03	52.04	30.78	0.35	12.83	0.03	0.03	0.11	100.05
20 Xtl 4	QMI	68.4	0.5	31.1	3.44	0.05	51.46	31.28	0.46	13.68	0.02	0.03	0.08	100.51
20 Xtl 4	QMI	67.4	0.4	32.2	3.53	0.05	51.45	31.11	0.47	13.36	0.00	0.04	0.07	100.08
20 Xtl 4	QMI	66.3	0.5	33.2	3.67	0.16	51.66	30.81	0.57	13.28	0.01	0.05	0.08	100.29
20 Xtl 4	QMI	65.9	0.4	33.7	3.71	0.05	51.95	30.85	0.48	13.11	0.01	0.03	0.07	100.25
20 Xtl 4	QMI	64.0	0.5	35.6	3.92	0.06	52.58	30.53	0.44	12.74	0.01	0.03	0.08	100.39
20 Xtl 4	QMI	62.3	0.5	37.2	4.09	0.05	52.81	30.32	0.42	12.39	0.03	0.03	0.08	100.21
20 Xtl 4	QMI	60.7	0.5	38.8	4.26	0.04	53.15	29.98	0.36	12.07	0.02	0.02	0.09	99.99
20 Xtl 4	QMI	59.2	0.6	40.3	4.40	0.04	53.48	29.80	0.32	11.69	0.02	0.01	0.09	99.85
20 Xtl 4	QMI	57.2	0.6	42.2	4.63	0.03	54.21	29.61	0.34	11.34	0.01	0.01	0.10	100.29
20 Xtl 4	QMI	53.4	0.7	45.8	5.05	0.02	54.94	28.99	0.29	10.66	0.01	0.00	0.13	100.09
20 Xtl 4	QMI	50.2	0.8	49.0	5.38	0.03	56.17	28.27	0.22	9.98	0.01	0.01	0.14	100.21
20 Xtl 4	QMI	48.7	1.0	50.3	5.51	0.02	56.99	28.36	0.26	9.66	0.02	0.02	0.16	101.00
20 Xtl 4	QMI	44.4	1.2	54.3	5.94	0.02	57.73	27.38	0.27	8.79	0.04	0.02	0.21	100.38
20 Xtl 4.1	QMI	59.6	0.6	39.8	4.40	0.05	53.23	29.89	0.46	11.93	0.03	0.05	0.10	100.13

Table B.1 (Continued)

Sample	Lithology	An	Or	Ab	Na_2O	MgO	SiO_2	Al_2O_3	FeO	CaO	P_2O_5	TiO_2	K_2O	Total
20 Xtl 4.1	QMI	60.2	0.6	39.2	4.31	0.06	53.53	29.98	0.49	11.99	0.01	0.03	0.10	100.49
20 Xtl 4.1	QMI	56.6	0.8	42.6	4.69	0.02	53.95	29.50	0.33	11.29	0.02	0.02	0.13	99.97
20 Xtl 4.1	QMI	54.4	0.8	44.8	4.93	0.02	54.59	29.19	0.35	10.83	0.03	0.02	0.14	100.11
20 Xtl 4.2	QMI	58.7	0.6	40.7	4.48	0.04	53.84	29.58	0.39	11.68	0.01	0.03	0.09	100.14
20 Xtl 4.2	QMI	59.0	0.6	40.5	4.43	0.05	53.52	29.76	0.43	11.69	0.03	0.03	0.10	100.03
20 Xtl 4.2	QMI	57.6	0.7	41.7	4.58	0.03	54.07	29.80	0.36	11.47	0.01	0.02	0.12	100.45
20 Xtl 6 core	QMI	51.4	0.9	47.8	5.25	0.02	55.66	28.66	0.27	10.22	0.02	0.02	0.14	100.26
20 Xtl 6 rim T	QMI	55.6	0.8	43.7	4.79	0.03	54.47	28.92	0.36	11.03	0.01	0.02	0.13	99.76
20 Xtl 6 rim T	QMI	62.3	0.4	37.2	4.07	0.06	52.63	30.07	0.46	12.34	-0.01	0.04	0.07	99.75
20 Xtl 6 rim T	QMI	60.4	0.5	39.1	4.33	0.04	53.28	29.92	0.37	12.09	0.02	0.01	0.08	100.13
20 Xtl 6 rim T	QMI	52.3	0.8	46.9	5.18	0.02	55.25	28.67	0.24	10.43	0.02	0.01	0.13	99.95
20 Xtl 6 rim T	QMI	42.4	1.3	56.3	6.17	0.02	58.05	27.36	0.29	8.41	0.00	0.01	0.21	100.52
20 Xtl 6.1	QMI	64.3	0.5	35.2	3.89	0.07	51.89	30.34	0.44	12.88	0.01	0.03	0.08	99.62
20 Xtl 6.1	QMI	55.4	0.7	43.9	4.84	0.03	54.39	29.21	0.31	11.05	0.01	0.01	0.12	99.97
20 Xtl 6.1	QMI	46.4	1.1	52.5	5.78	0.02	57.05	27.73	0.27	9.26	0.04	0.03	0.19	100.38
20 Xtl 6.1	QMI	47.6	1.1	51.3	5.62	0.03	56.55	28.01	0.33	9.43	0.01	0.02	0.18	100.18
20 Xtl 7	QMI	56.5	0.8	42.7	4.70	0.02	54.30	29.37	0.35	11.27	0.01	0.04	0.14	100.21
20 Xtl 7	QMI	58.2	0.8	41.0	4.53	0.03	53.66	29.67	0.32	11.63	0.01	0.05	0.13	100.02
20 Xtl 7	QMI	59.7	0.7	39.6	4.36	0.04	53.33	29.75	0.39	11.92	0.00	0.03	0.12	99.94
20 Xtl 7	QMI	61.5	0.6	37.9	4.20	0.04	53.02	30.14	0.41	12.35	0.01	0.05	0.11	100.33
20 Xtl 7	QMI	58.9	0.7	40.4	4.45	0.05	53.53	29.75	0.38	11.76	0.03	0.05	0.12	100.11
20 Xtl 7	QMI	59.0	0.7	40.3	4.46	0.04	53.64	29.67	0.42	11.81	0.02	0.05	0.12	100.24
20 Xtl 7	QMI	56.1	0.8	43.1	4.72	0.03	54.27	29.26	0.40	11.13	0.01	0.06	0.13	100.00
20 Xtl 7	QMI	56.6	0.8	42.6	4.69	0.04	54.12	29.36	0.44	11.27	0.02	0.05	0.14	100.14
20 Xtl 7	QMI	59.0	0.8	40.2	4.43	0.04	53.59	29.76	0.42	11.75	0.02	0.04	0.13	100.17
20 Xtl 7	QMI	59.8	0.7	39.6	4.32	0.03	53.05	30.00	0.36	11.81	0.02	0.03	0.11	99.74
20 Xtl 7	QMI	57.9	0.7	41.4	4.59	0.03	53.64	29.56	0.39	11.61	0.03	0.04	0.12	100.01
20 Xtl 7	QMI	60.1	0.7	39.2	4.32	0.04	53.17	29.96	0.42	11.99	0.02	0.03	0.11	100.06
20 Xtl 7	QMI	56.6	0.8	42.6	4.69	0.03	54.29	29.56	0.35	11.29	0.02	0.04	0.13	100.39
20 Xtl 7	QMI	56.8	0.7	42.6	4.68	0.02	54.15	29.39	0.38	11.30	0.02	0.04	0.11	100.10
20 Xtl 7	QMI	56.5	0.7	42.8	4.72	0.03	54.33	29.31	0.37	11.29	0.01	0.03	0.13	100.20
20 Xtl 7	QMI	57.2	0.7	42.2	4.66	0.02	53.85	29.39	0.33	11.42	0.04	0.04	0.11	99.87
20 Xtl 7	QMI	54.3	0.8	44.9	4.94	0.03	54.72	29.12	0.32	10.81	0.02	0.04	0.13	100.13

Table B.1 (Continued)

Sample	Lithology	An	Or	Ab	Na_2O	MgO	SiO_2	Al_2O_3	FeO	CaO	P_2O_5	TiO_2	K_2O	Total
20 Xtl 7	QMI	52.0	0.9	47.2	5.17	0.02	55.59	28.73	0.27	10.31	0.01	0.03	0.14	100.26
20 Xtl 7	QMI	67.6	0.4	32.0	3.52	0.04	51.35	31.18	0.49	13.44	0.02	0.04	0.07	100.14
20 Xtl 7	QMI	61.9	0.7	37.5	4.17	0.03	53.10	30.25	0.40	12.45	0.03	0.03	0.11	100.57
20 Xtl 7	QMI	56.6	0.7	42.7	4.70	0.02	54.33	29.46	0.34	11.29	0.03	0.02	0.12	100.31
20 Xtl 7	QMI	51.2	0.9	47.9	5.28	0.03	55.80	28.67	0.31	10.20	0.01	0.02	0.16	100.48
20 Xtl 7	QMI	47.6	1.0	51.3	5.60	0.03	56.12	27.52	0.32	9.40	0.01	0.02	0.17	99.19
20 Xtl 7	QMI	42.1	1.2	56.7	6.23	0.02	58.10	27.24	0.41	8.37	0.00	0.04	0.21	100.62
20 Xtl 7	QMI	28.2	6.0	65.8	5.36	0.02	69.55	20.76	0.63	4.16	0.03	0.10	0.74	101.36
19 Xtl 1	QMI	76.2	0.3	23.5	2.57	0.05	48.51	32.36	0.51	15.11	0.01	0.03	0.05	99.23
19 Xtl 1	QMI	76.2	0.4	23.4	2.58	0.05	48.41	32.31	0.52	15.21	0.02	0.03	0.07	99.20
19 Xtl 1	QMI	72.0	0.5	27.5	2.98	0.06	49.71	31.77	0.47	14.15	0.03	0.03	0.09	99.32
19 Xtl 1	QMI	72.9	0.5	26.6	2.90	0.10	49.38	31.77	0.45	14.37	0.02	0.05	0.08	99.13
19 Xtl 1	QMI	76.3	0.4	23.3	2.58	0.10	48.42	32.38	0.49	15.27	0.03	0.04	0.07	99.38
19 Xtl 1	QMI	78.5	0.4	21.1	2.33	0.09	47.98	32.65	0.48	15.65	0.02	0.04	0.06	99.34
19 Xtl 2 core	QMI	71.3	0.5	28.2	3.10	0.09	49.91	31.48	0.43	14.22	0.00	0.07	0.08	99.40
19 Xtl 2 core	QMI	73.1	0.5	26.4	2.90	0.08	49.24	31.90	0.44	14.55	0.03	0.05	0.08	99.28
19 Xtl 2 rim	QMI	58.5	0.9	40.6	4.39	0.07	52.96	29.33	0.53	11.43	0.02	0.06	0.15	98.97
19 Xtl 2 rim	QMI	34.0	2.0	64.0	6.85	0.02	59.45	25.38	0.26	6.59	0.02	0.02	0.32	98.91
19 Xtl 3 core	QMI	65.6	0.4	34.0	3.72	0.05	51.37	30.56	0.39	12.98	0.02	0.04	0.07	99.23
19 Xtl 3 core	QMI	66.2	0.5	33.3	3.63	0.04	50.89	30.41	0.46	13.05	0.02	0.03	0.08	98.64
19 Xtl 3 rim	QMI	41.8	1.5	56.7	6.15	0.02	57.25	26.70	0.31	8.22	0.02	0.03	0.24	98.95
19 Xtl 3 rim	QMI	31.8	2.3	65.9	7.08	0.02	60.33	25.29	0.23	6.18	0.01	0.02	0.38	99.59
19 Xtl 3 rim	QMI	27.2	2.8	70.0	7.46	0.01	61.19	24.27	0.28	5.26	0.01	0.02	0.46	98.96
19 Xtl 4	QMI	76.4	0.5	23.1	2.42	0.08	46.62	31.19	0.50	14.52	0.03	0.04	0.08	95.51
19 Xtl 4	QMI	75.4	0.5	24.2	2.64	0.08	48.54	31.97	0.50	14.86	-0.01	0.04	0.08	98.71
19 Xtl 4	QMI	76.0	0.5	23.5	2.56	0.08	48.62	32.40	0.47	14.96	0.01	0.05	0.08	99.23
19 Xtl 4	QMI	61.3	0.8	37.9	4.12	0.10	52.32	29.67	0.51	12.07	0.02	0.08	0.13	99.03
19 Xtl 5	QMI	77.6	0.5	21.9	2.40	0.09	48.50	32.46	0.48	15.37	0.03	0.04	0.08	99.44
19 Xtl 5	QMI	76.8	0.5	22.7	2.49	0.09	48.55	32.31	0.50	15.24	0.01	0.04	0.08	99.36
19 Xtl 5	QMI	54.3	1.1	44.7	4.80	0.05	54.06	28.51	0.45	10.56	0.03	0.05	0.17	98.67
19 Xtl 5	QMI	28.5	2.5	69.0	7.37	0.01	61.04	24.86	0.35	5.51	0.01	0.03	0.41	99.62
19 Xtl 6	QMI	59.0	0.9	40.2	4.34	0.11	53.31	29.13	0.57	11.55	0.01	0.07	0.14	99.24
19 Xtl 6	QMI	59.5	0.8	39.6	4.30	0.11	52.77	29.01	0.54	11.67	0.02	0.07	0.14	98.63

Table B.1 (Continued)

Sample	Lithology	An	Or	Ab	Na_2O	MgO	SiO_2	Al_2O_3	FeO	CaO	P_2O_5	TiO_2	K_2O	Total
19 Xtl 6	QMI	49.7	1.3	49.0	5.31	0.04	55.26	28.05	0.37	9.74	0.01	0.03	0.21	99.02
19 Xtl 6	QMI	38.3	2.3	59.5	6.35	0.03	58.43	26.01	0.37	7.40	0.02	0.04	0.37	99.04
19 Xtl 7	QMI	55.5	1.1	43.5	4.72	0.09	53.81	28.59	0.59	10.89	0.02	0.11	0.18	99.01
19 Xtl 7	QMI	55.4	1.1	43.6	4.76	0.08	53.79	28.57	0.56	10.95	0.03	0.09	0.18	99.01
19 Xtl 7	QMI	57.0	1.1	41.9	4.35	0.07	51.55	27.48	0.55	10.71	0.03	0.10	0.17	95.02
19 Xtl 8	QMI	40.5	1.7	57.8	6.25	0.02	57.74	26.54	0.34	7.92	0.04	0.04	0.27	99.16
19 Xtl 8	QMI	38.7	1.8	59.5	6.43	0.01	58.37	26.00	0.32	7.58	0.03	0.04	0.30	99.11
19 Xtl 9	QMI	52.0	1.2	46.9	5.08	0.05	55.05	28.33	0.43	10.20	0.02	0.04	0.19	99.39
19 Xtl 9	QMI	52.1	1.2	46.7	5.10	0.05	55.24	28.19	0.40	10.29	0.05	0.05	0.20	99.58
19 Xtl 9	QMI	52.8	1.1	46.1	5.02	0.05	54.75	28.35	0.45	10.41	0.04	0.05	0.18	99.33
19 Xtl 9	QMI	53.5	1.1	45.5	4.95	0.05	54.52	28.44	0.41	10.54	0.04	0.04	0.18	99.17
19 Xtl 10	QMI	56.0	1.1	43.0	4.72	0.07	54.15	28.88	0.54	11.11	0.04	0.07	0.18	99.76
19 Xtl 10	QMI	56.3	1.0	42.7	4.67	0.07	53.90	28.78	0.55	11.14	0.02	0.07	0.17	99.38
19 Xtl 10	QMI	45.9	1.4	52.8	5.78	0.03	56.54	27.33	0.39	9.10	0.00	0.03	0.23	99.45
19 Xtl 10	QMI	34.6	2.0	63.4	6.83	0.01	59.61	25.69	0.29	6.74	0.05	0.02	0.32	99.57
19 Xtl 11	QMI	42.2	1.7	56.1	6.11	0.03	57.69	26.80	0.29	8.30	0.05	0.03	0.28	99.60
19 Xtl 11	QMI	47.7	1.4	50.9	5.55	0.04	56.20	27.67	0.36	9.40	0.00	0.04	0.22	99.48
19 Xtl 12	QMI	57.1	1.0	41.9	4.58	0.07	53.79	29.04	0.59	11.27	0.01	0.07	0.16	99.60
19 Xtl 12	QMI	57.0	1.0	42.0	4.60	0.07	53.94	29.04	0.61	11.30	0.02	0.06	0.17	99.80
19 Xtl 12	QMI	41.4	1.7	56.9	6.16	0.02	57.82	26.50	0.41	8.11	0.02	0.03	0.28	99.36
19 Xtl 13	QMI	55.7	1.1	43.2	4.72	0.06	54.27	28.78	0.51	11.01	0.02	0.07	0.18	99.64
19 Xtl 14	QMI	66.9	0.8	32.3	3.55	0.09	50.99	30.64	0.41	13.28	0.01	0.05	0.14	99.16
19 Xtl 14	QMI	65.9	0.9	33.2	3.64	0.09	51.69	30.61	0.37	13.06	0.01	0.06	0.15	99.69
19 Xtl 14	QMI	68.8	0.8	30.4	3.35	0.10	50.84	31.06	0.47	13.73	0.02	0.06	0.13	99.80
19 Xtl 14	QMI	77.5	0.4	22.1	2.43	0.09	48.73	32.70	0.52	15.46	0.03	0.05	0.07	100.07
19 Xtl 14	QMI	60.5	0.9	38.6	4.23	0.09	52.86	29.70	0.57	11.99	0.02	0.09	0.15	99.70
19 Xtl 15	QMI	63.6	0.8	35.6	3.92	0.11	52.27	30.07	0.50	12.66	0.02	0.08	0.14	99.79
19 Xtl 15	QMI	58.6	1.0	40.4	4.42	0.09	53.33	29.22	0.58	11.60	0.02	0.08	0.16	99.52
19 Xtl 16	QMI	58.3	1.0	40.7	4.43	0.12	53.56	29.07	0.65	11.46	0.03	0.10	0.16	99.58
19 Xtl 16	QMI	58.0	1.0	41.0	4.47	0.10	53.38	29.07	0.63	11.45	0.04	0.11	0.17	99.42
19 Xtl 16	QMI	61.5	0.8	37.7	4.15	0.07	52.66	29.78	0.63	12.26	0.02	0.08	0.14	99.79
19 Xtl 17 T	QMI	78.5	0.4	21.1	2.32	0.07	48.21	32.78	0.49	15.59	0.03	0.04	0.06	99.61
19 Xtl 17 T	QMI	68.6	0.7	30.8	3.34	0.11	50.73	31.01	0.46	13.45	0.02	0.06	0.11	99.29

Table B.1 (Continued)

Sample	Lithology	An	Or	Ab	Na_2O	MgO	SiO_2	Al_2O_3	FeO	CaO	P_2O_5	TiO_2	K_2O	Total
19 Xtl 17 T	QMI	65.6	0.8	33.6	3.68	0.09	51.19	30.24	0.45	12.99	0.02	0.07	0.13	98.86
19 Xtl 17 T	QMI	67.2	0.7	32.0	3.52	0.09	50.85	30.68	0.46	13.36	0.02	0.05	0.12	99.16
19 Xtl 17 T	QMI	72.1	0.6	27.3	2.97	0.10	49.54	31.56	0.50	14.22	0.02	0.04	0.09	99.04
19 Xtl 17 T	QMI	76.9	0.5	22.6	2.47	0.08	48.18	32.37	0.47	15.17	0.04	0.04	0.08	98.95
19 Xtl 17 T	QMI	58.1	1.1	40.9	4.44	0.08	53.34	29.00	0.50	11.42	0.01	0.08	0.18	99.05
19 Xtl 17 T	QMI	52.6	1.1	46.3	5.00	0.04	54.48	28.18	0.39	10.25	0.01	0.04	0.18	98.60
19 Xtl 17 T	QMI	34.4	2.2	63.4	6.83	0.01	59.31	25.53	0.22	6.72	-0.01	0.03	0.36	99.03
19 Xtl 17 P	QMI	78.1	0.3	21.6	2.36	0.04	47.99	32.44	0.52	15.44	0.02	0.03	0.05	98.90
19 Xtl 17 P	QMI	86.7	0.3	13.0	1.43	0.03	45.73	33.94	0.41	17.25	0.02	0.03	0.04	98.91
19 Xtl 17 P	QMI	78.1	0.4	21.5	2.34	0.07	48.03	32.16	0.45	15.32	0.03	0.04	0.07	98.50
19 Xtl 17 P	QMI	75.2	0.5	24.3	2.66	0.08	48.94	31.83	0.45	14.87	0.02	0.05	0.08	98.99
19 Xtl 18	QMI	54.4	1.1	44.6	4.80	0.05	53.73	28.61	0.39	10.60	0.04	0.05	0.17	98.44
19 Xtl 18	QMI	55.5	1.1	43.5	4.73	0.05	53.86	28.86	0.44	10.93	0.05	0.05	0.18	99.15
19 Xtl 19	QMI	57.1	0.9	42.0	4.59	0.03	53.60	29.36	0.19	11.30	0.03	0.01	0.15	99.26
19 Xtl 19	QMI	65.7	0.7	33.7	3.66	0.07	51.23	30.38	0.51	12.93	0.03	0.06	0.11	99.00
19 Xtl 19	QMI	65.5	0.7	33.8	3.70	0.08	51.37	30.42	0.49	12.96	0.03	0.06	0.12	99.24
19 Xtl 19	QMI	59.3	1.0	39.7	4.31	0.08	52.88	29.29	0.54	11.67	0.02	0.07	0.16	99.04
19 Xtl 19	QMI	46.9	1.3	51.8	5.55	0.03	56.27	27.06	0.28	9.09	0.03	0.03	0.21	98.55
08B Xtl 1	PL INCL in MK	55.5	1.3	43.3	4.77	0.02	54.55	29.07	0.26	11.07	0.02	0.05	0.21	100.02
08B Xtl 1	PL INCL in MK	54.7	1.4	43.9	4.82	0.02	54.64	29.20	0.26	10.86	0.05	0.05	0.23	100.10
08B Xtl 1	PL INCL in MK	52.8	1.5	45.7	5.06	0.03	55.44	28.64	0.26	10.59	0.01	0.01	0.25	100.29
08B Xtl 1	PL INCL in MK	54.3	1.6	44.1	4.82	0.02	54.59	29.03	0.23	10.75	0.01	0.06	0.27	99.79
08B Xtl 1	PL INCL in MK	52.3	1.6	46.0	5.06	0.02	55.58	28.69	0.21	10.42	0.02	0.02	0.27	100.29
08B Xtl 1	PL INCL in MK	54.4	1.3	44.3	4.87	0.03	55.14	29.00	0.16	10.83	0.02	0.03	0.22	100.31
08B Xtl 1	PL INCL in MK	51.4	1.6	47.0	5.18	0.02	55.64	28.55	0.22	10.24	0.02	0.05	0.27	100.20
08B Xtl 2	PL INCL in MK	54.0	1.6	44.5	4.87	0.01	54.96	28.84	0.19	10.69	0.02	0.06	0.26	99.90
08B Xtl 2	PL INCL in MK	50.8	1.5	47.7	5.20	0.01	56.07	28.30	0.18	10.03	0.03	0.06	0.24	100.13
08B Xtl 2	PL INCL in MK	54.7	1.3	44.0	4.83	0.01	54.88	29.04	0.21	10.86	-0.01	0.03	0.21	100.08
08B Xtl 2	PL INCL in MK	48.5	1.8	49.7	5.47	0.01	56.64	27.93	0.20	9.64	0.02	0.02	0.30	100.22
08B Xtl 2	PL INCL in MK	49.1	1.7	49.2	5.41	0.02	56.30	28.12	0.16	9.77	0.02	0.01	0.29	100.11
08B Xtl 3	PL INCL in MK	54.6	1.4	44.0	4.86	0.01	54.72	29.21	0.17	10.92	0.02	0.04	0.24	100.18
08B Xtl 3	PL INCL in MK	54.6	1.4	44.1	4.87	0.01	55.27	28.96	0.18	10.90	0.02	0.04	0.23	100.49
08B Xtl 3	PL INCL in MK	52.0	1.6	46.5	5.10	0.01	55.81	28.55	0.18	10.33	0.01	0.03	0.26	100.30

Table B.1 (Continued)

Sample	Lithology	An	Or	Ab	Na_2O	MgO	SiO_2	Al_2O_3	FeO	CaO	P_2O_5	TiO_2	K_2O	Total
08B Xtl 3	PL INCL in MK	50.1	1.6	48.2	5.27	0.02	56.32	28.28	0.17	9.91	0.00	0.01	0.27	100.26
08B Xtl 3	PL INCL in MK	51.5	1.5	47.0	5.12	0.01	55.74	28.58	0.20	10.15	-0.01	0.03	0.25	100.07
08B Xtl 4	PL INCL in MK	48.3	1.9	49.8	5.42	0.05	56.07	27.35	0.83	9.53	0.02	0.07	0.32	99.65
08B Xtl 4	PL INCL in MK	57.6	1.7	40.7	4.37	0.03	54.77	28.71	0.69	11.17	0.02	0.06	0.28	100.11
08B Xtl 4	PL INCL in MK	55.0	1.5	43.5	4.75	0.05	54.37	28.66	0.39	10.87	0.00	0.02	0.24	99.34
08B Xtl 4	PL INCL in MK	55.3	1.4	43.3	4.73	0.05	54.68	28.86	0.37	10.93	0.02	0.03	0.23	99.89
08B Xtl 4	PL INCL in MK	54.5	1.4	44.1	4.80	0.05	54.47	28.78	0.34	10.73	0.05	0.03	0.24	99.47
08B Xtl 4	PL INCL in MK	55.3	1.4	43.4	4.75	0.06	54.65	28.70	0.32	10.95	0.03	0.02	0.23	99.71
08B Xtl 4	PL INCL in MK	60.8	1.1	38.1	4.15	0.06	53.34	29.95	0.35	11.98	0.01	0.05	0.19	100.06
08B Xtl 4	PL INCL in MK	54.7	1.7	43.6	4.76	0.05	54.89	28.82	0.28	10.81	0.04	0.05	0.28	99.97
08B Xtl 4	PL INCL in MK	54.6	1.7	43.7	4.76	0.04	54.76	28.90	0.26	10.76	0.03	0.04	0.29	99.84
08B Xtl 4	PL INCL in MK	54.6	1.8	43.6	4.76	0.03	54.80	28.82	0.15	10.79	0.04	0.04	0.29	99.73
08B Xtl 4	PL INCL in MK	54.2	1.7	44.1	4.82	0.04	54.78	28.86	0.21	10.72	0.03	0.05	0.28	99.78
08B Xtl 4	PL INCL in MK	54.9	1.9	43.2	4.69	0.07	54.40	28.61	0.34	10.77	0.03	0.06	0.32	99.28
08B Xtl 4	PL INCL in MK	54.6	1.9	43.5	4.72	0.03	54.53	29.04	0.18	10.73	0.01	0.04	0.31	99.60
08B Xtl 4	PL INCL in MK	54.9	1.8	43.2	4.75	0.04	54.59	29.09	0.21	10.93	0.03	0.05	0.30	99.99
08B Xtl 4	PL INCL in MK	55.1	1.9	43.0	4.65	0.07	54.19	28.73	0.51	10.78	0.03	0.40	0.31	99.67
08B Xtl 4	PL INCL in MK	54.9	2.1	43.0	4.68	0.04	54.34	28.95	0.20	10.84	0.01	0.05	0.35	99.45
08B Xtl 4	PL INCL in MK	54.8	2.1	43.1	4.69	0.04	54.70	28.98	0.23	10.80	0.01	0.05	0.34	99.83
08B Xtl 4	PL INCL in MK	54.6	2.1	43.3	4.73	0.04	54.71	28.85	0.22	10.79	0.03	0.06	0.34	99.76
08B Xtl 4	PL INCL in MK	54.5	2.1	43.4	4.74	0.05	54.44	28.82	0.29	10.77	0.02	0.06	0.34	99.53
08B Xtl 4	PL INCL in MK	64.9	1.3	33.7	3.68	0.05	51.91	30.90	0.29	12.83	0.00	0.05	0.22	99.94
08B Xtl 4	PL INCL in MK	54.7	2.1	43.3	4.71	0.04	54.24	28.91	0.24	10.77	0.02	0.06	0.34	99.33
08B Xtl 4	PL INCL in MK	54.7	1.9	43.4	4.73	0.03	54.50	28.91	0.21	10.77	0.01	0.05	0.32	99.53
08B Xtl 4	PL INCL in MK	54.9	1.9	43.2	4.71	0.04	54.54	28.72	0.23	10.82	0.01	0.05	0.31	99.44
08B Xtl 4	PL INCL in MK	54.3	2.0	43.7	4.73	0.04	54.51	28.98	0.23	10.65	0.01	0.05	0.33	99.52
08B Xtl 4	PL INCL in MK	54.8	1.9	43.3	4.71	0.04	54.37	28.84	0.22	10.80	0.02	0.05	0.32	99.35
08B Xtl 4	PL INCL in MK	54.6	1.8	43.6	4.76	0.03	54.53	28.94	0.23	10.79	0.00	0.05	0.29	99.62
08B Xtl 4	PL INCL in MK	54.9	1.8	43.3	4.72	0.04	54.61	28.90	0.27	10.83	0.03	0.06	0.29	99.75
08B Xtl 4	PL INCL in MK	49.7	2.9	47.5	5.07	0.11	56.34	27.57	0.50	9.61	0.02	0.04	0.46	99.73
08B Xtl 4	PL INCL in MK	53.9	1.7	44.4	4.83	0.04	54.90	28.73	0.26	10.61	0.02	0.05	0.28	99.72
08B Xtl 4	PL INCL in MK	54.2	1.8	44.1	4.84	0.04	54.52	28.83	0.29	10.77	0.01	0.02	0.30	99.61
08B Xtl 4	PL INCL in MK	61.6	1.5	37.0	4.05	0.06	52.97	30.11	0.37	12.19	0.01	0.03	0.24	100.04

Table B.1 (Continued)

Sample	Lithology	An	Or	Ab	Na_2O	MgO	SiO_2	Al_2O_3	FeO	CaO	P_2O_5	TiO_2	K_2O	Total
08B Xtl 4	PL INCL in MK	54.5	1.5	44.0	4.73	0.04	54.42	28.97	0.20	10.61	0.02	0.04	0.25	99.28
08B Xtl 4	PL INCL in MK	55.1	1.5	43.4	4.69	0.03	54.31	28.92	0.19	10.80	0.02	0.03	0.25	99.23
08B Xtl 4	PL INCL in MK	55.6	1.4	43.0	4.67	0.04	54.43	29.06	0.20	10.92	0.02	0.04	0.23	99.59
08B Xtl 4	PL INCL in MK	51.6	1.9	46.5	5.06	0.04	55.41	28.31	0.28	10.17	0.01	0.03	0.31	99.61
08B Xtl 4	PL INCL in MK	55.7	1.5	42.8	4.68	0.02	54.49	29.13	0.21	11.04	0.00	0.05	0.24	99.87
08B Xtl 4	PL INCL in MK	55.5	1.5	43.0	4.64	0.03	54.35	28.87	0.21	10.85	0.03	0.04	0.24	99.26
08B Xtl 4	PL INCL in MK	55.3	1.4	43.3	4.70	0.03	54.35	29.13	0.20	10.87	0.03	0.04	0.23	99.58
08B Xtl 4	PL INCL in MK	55.5	1.4	43.1	4.66	0.03	54.23	29.09	0.22	10.85	0.02	0.04	0.23	99.38
08B Xtl 4	PL INCL in MK	55.2	1.3	43.5	4.67	0.02	54.49	28.96	0.22	10.74	0.01	0.04	0.22	99.37
08B Xtl 4	PL INCL in MK	55.4	1.4	43.2	4.66	0.03	54.60	29.18	0.23	10.81	0.02	0.04	0.23	99.81
08B Xtl 4	PL INCL in MK	53.9	1.5	44.6	4.89	0.02	54.79	28.65	0.27	10.69	0.03	0.04	0.25	99.63
08B Xtl 4	PL INCL in MK	52.6	1.5	45.9	5.01	0.03	55.27	28.75	0.24	10.38	0.00	0.03	0.25	99.95
08B Xtl 4	PL INCL in MK	54.6	1.4	43.9	4.79	0.03	54.63	28.98	0.29	10.78	0.02	0.05	0.24	99.81
08B Xtl 4	PL INCL in MK	53.1	1.4	45.4	4.93	0.02	54.93	28.82	0.25	10.42	0.03	0.05	0.24	99.68
08B Xtl 4	PL INCL in MK	54.7	1.3	44.0	4.75	0.03	54.59	28.87	0.26	10.71	0.02	0.04	0.21	99.48
08B Xtl 4	PL INCL in MK	54.1	1.3	44.5	4.85	0.03	54.70	28.90	0.27	10.68	0.02	0.04	0.22	99.71
08B Xtl 4	PL INCL in MK	54.9	1.4	43.7	4.75	0.02	54.62	28.88	0.24	10.80	0.01	0.04	0.23	99.59
08B Xtl 4	PL INCL in MK	54.9	1.4	43.8	4.80	0.02	54.63	29.05	0.23	10.89	0.01	0.04	0.23	99.89
08B Xtl 4	PL INCL in MK	54.5	1.4	44.2	4.85	0.02	55.15	29.13	0.23	10.83	0.02	0.03	0.23	100.49
08B Xtl 4	PL INCL in MK	54.9	1.4	43.8	4.73	0.02	54.57	29.10	0.22	10.73	0.02	0.04	0.23	99.66
08B Xtl 4	PL INCL in MK	54.9	1.3	43.8	4.74	0.02	54.25	28.73	0.25	10.77	0.03	0.04	0.21	99.04
08B Xtl 4	PL INCL in MK	54.6	1.4	44.0	4.74	0.02	54.52	28.69	0.21	10.64	0.02	0.06	0.23	99.12
08B Xtl 4	PL INCL in MK	55.0	1.4	43.7	4.73	0.03	54.47	28.86	0.22	10.77	0.01	0.04	0.22	99.35
08B Xtl 4	PL INCL in MK	55.5	1.3	43.2	4.70	0.02	54.57	28.93	0.22	10.92	0.03	0.04	0.21	99.66
08B Xtl 4	PL INCL in MK	55.0	1.4	43.6	4.74	0.03	54.55	29.20	0.23	10.82	0.02	0.05	0.24	99.87
08B Xtl 4	PL INCL in MK	55.1	1.4	43.6	4.76	0.02	54.47	29.11	0.21	10.89	0.01	0.04	0.22	99.73
08B Xtl 4	PL INCL in MK	54.5	1.5	44.1	4.80	0.03	54.60	29.04	0.24	10.73	0.01	0.03	0.24	99.72
08B Xtl 4	PL INCL in MK	53.4	1.6	45.0	4.87	0.03	54.85	28.72	0.23	10.43	0.01	0.03	0.26	99.42
08B Xtl 4	PL INCL in MK	52.2	1.7	46.1	4.99	0.04	54.81	28.54	0.25	10.24	0.00	0.03	0.28	99.20
08B Xtl 4	PL INCL in MK	55.3	1.5	43.2	4.71	0.04	54.22	28.89	0.44	10.93	-0.01	0.03	0.25	99.51
08B Xtl 4	PL INCL in MK	62.5	1.0	36.5	3.93	0.05	51.89	29.96	0.57	12.18	0.00	0.02	0.17	98.77
08B Xtl 4	PL INCL in MK	63.5	1.1	35.3	3.86	0.05	52.00	30.40	0.57	12.56	0.01	0.04	0.19	99.68
08B Xtl 4	PL INCL in MK	61.3	1.3	37.4	4.04	0.04	53.14	29.90	0.62	11.99	0.00	0.05	0.22	100.00

Table B.1 (Continued)

Sample	Lithology	An	Or	Ab	Na_2O	MgO	SiO_2	Al_2O_3	FeO	CaO	P_2O_5	TiO_2	K_2O	Total
06A Xtl 1 T	PL INCL in LK	52.1	1.7	46.2	5.04	0.04	55.48	28.53	0.57	10.26	0.01	0.03	0.28	100.24
06A Xtl 1 T	PL INCL in LK	49.1	1.4	49.5	5.39	0.04	56.11	28.01	0.44	9.68	0.02	0.02	0.23	99.93
06A Xtl 1 T	PL INCL in LK	52.7	1.0	46.4	5.06	0.03	55.40	28.70	0.33	10.40	0.03	0.05	0.16	100.16
06A Xtl 1 T	PL INCL in LK	53.6	0.9	45.5	4.99	0.03	55.05	28.83	0.24	10.65	0.01	0.05	0.16	100.00
06A Xtl 1 T	PL INCL in LK	52.8	0.9	46.2	5.08	0.01	55.30	28.72	0.24	10.49	0.01	0.04	0.16	100.05
06A Xtl 1 T	PL INCL in LK	51.9	1.1	47.0	5.15	0.01	55.43	28.66	0.25	10.31	0.02	0.04	0.19	100.05
06A Xtl 1 T	PL INCL in LK	52.3	1.1	46.6	5.13	0.01	55.54	28.77	0.23	10.41	0.02	0.04	0.19	100.34
06A Xtl 1 T	PL INCL in LK	52.0	1.2	46.8	5.17	0.01	55.46	28.68	0.22	10.40	0.00	0.03	0.20	100.16
06A Xtl 1 T	PL INCL in LK	53.1	1.3	45.6	5.01	0.01	55.58	29.06	0.20	10.55	0.02	0.05	0.21	100.69
06A Xtl 1 T	PL INCL in LK	52.8	1.3	45.9	5.03	0.01	55.32	28.88	0.22	10.47	0.01	0.04	0.21	100.19
06A Xtl 1 T	PL INCL in LK	53.1	1.2	45.7	5.02	0.01	55.32	28.76	0.18	10.57	0.03	0.04	0.20	100.13
06A Xtl 1 T	PL INCL in LK	54.8	1.3	43.9	4.79	0.01	54.54	29.08	0.27	10.82	0.03	0.04	0.21	99.78
06A Xtl 1 T	PL INCL in LK	54.4	1.3	44.3	4.86	0.00	55.04	29.31	0.20	10.81	0.05	0.03	0.21	100.51
06A Xtl 1 T	PL INCL in LK	54.4	1.4	44.2	4.88	0.01	54.78	29.08	0.23	10.88	0.02	0.03	0.23	100.14
06A Xtl 1 T	PL INCL in LK	53.5	1.4	45.1	4.96	0.01	55.08	28.96	0.25	10.66	0.01	0.01	0.24	100.18
06A Xtl 1 T	PL INCL in LK	54.2	1.3	44.5	4.91	0.01	54.97	29.07	0.22	10.84	0.03	0.03	0.21	100.29
06A Xtl 1 T	PL INCL in LK	56.8	1.3	41.9	4.60	0.00	54.05	29.62	0.26	11.27	0.02	0.03	0.22	100.06
06A Xtl 1 T	PL INCL in LK	58.6	1.2	40.2	4.37	0.01	53.38	29.68	0.21	11.51	0.01	0.03	0.20	99.41
06A Xtl 1 T	PL INCL in LK	60.1	1.3	38.7	4.25	0.01	53.52	30.15	0.22	11.94	0.01	0.03	0.21	100.34
06A Xtl 1 T	PL INCL in LK	62.6	1.0	36.4	4.00	0.00	53.01	30.52	0.23	12.44	0.02	0.03	0.17	100.42
06A Xtl 1 T	PL INCL in LK	65.8	0.9	33.3	3.66	0.01	51.84	31.08	0.30	13.11	0.01	0.03	0.15	100.19
06A Xtl 1 T	PL INCL in LK	65.1	0.9	34.0	3.76	0.01	51.97	30.84	0.21	13.00	0.02	0.02	0.15	99.98
06A Xtl 1 T	PL INCL in LK	64.9	0.9	34.2	3.76	0.01	52.30	30.99	0.29	12.89	0.02	0.01	0.14	100.41
06A Xtl 1 T	PL INCL in LK	62.0	1.1	36.9	4.06	0.01	52.82	30.43	0.31	12.35	0.01	0.02	0.18	100.19
06A Xtl 1 T	PL INCL in LK	62.3	1.0	36.7	4.03	0.00	52.62	30.43	0.29	12.37	0.02	0.02	0.17	99.96
06A Xtl 1 T	PL INCL in LK	59.3	1.2	39.6	4.33	0.01	53.49	29.83	0.27	11.72	0.01	0.03	0.19	99.87
06A Xtl 1 T	PL INCL in LK	58.9	1.2	39.9	4.39	0.01	53.63	29.90	0.31	11.75	0.01	0.03	0.21	100.24
06A Xtl 1 T	PL INCL in LK	58.3	1.2	40.5	4.46	0.00	53.87	29.92	0.24	11.63	0.03	0.04	0.21	100.41
06A Xtl 1 T	PL INCL in LK	57.4	1.3	41.4	4.55	0.01	54.04	29.60	0.26	11.42	0.02	0.05	0.21	100.16
06A Xtl 1 T	PL INCL in LK	56.4	1.2	42.4	4.62	0.02	54.02	29.31	0.29	11.12	0.02	0.02	0.21	99.62
06A Xtl 1 T	PL INCL in LK	55.7	1.3	42.9	4.71	0.02	54.47	29.30	0.39	11.07	0.01	0.09	0.22	100.26
06A Xtl 1 T	PL INCL in LK	52.2	1.6	46.3	5.12	0.01	55.26	28.53	0.25	10.44	0.02	0.03	0.26	99.92
06A Xtl 1 T	PL INCL in LK	56.2	1.5	42.3	4.66	0.01	54.25	29.29	0.24	11.20	0.03	0.02	0.24	99.94

Table B.1 (Continued)

Sample	Lithology	An	Or	Ab	Na_2O	MgO	SiO_2	Al_2O_3	FeO	CaO	P_2O_5	TiO_2	K_2O	Total
06A Xtl 1 T	PL INCL in LK	57.2	1.3	41.5	4.53	0.01	54.07	29.61	0.25	11.29	0.01	0.03	0.21	100.01
06A Xtl 1 T	PL INCL in LK	59.4	1.1	39.5	4.35	0.01	53.55	29.89	0.24	11.82	0.02	0.03	0.19	100.08
06A Xtl 1 T	PL INCL in LK	62.2	1.0	36.9	4.02	0.01	52.82	30.35	0.25	12.28	0.04	0.02	0.16	99.94
06A Xtl 1 T	PL INCL in LK	60.5	1.1	38.4	4.24	0.01	53.18	30.03	0.27	12.08	0.01	0.02	0.18	100.02
06A Xtl 1 T	PL INCL in LK	65.7	0.9	33.4	3.69	0.02	52.01	31.14	0.27	13.11	0.04	0.02	0.15	100.43
06A Xtl 1 T	PL INCL in LK	67.1	0.9	32.0	3.52	0.01	51.54	31.40	0.26	13.35	0.05	0.02	0.15	100.29
06A Xtl 1 T	PL INCL in LK	67.9	0.9	31.2	3.44	0.02	51.30	31.37	0.27	13.54	0.02	0.02	0.14	100.12
06A Xtl 1 T	PL INCL in LK	66.7	0.8	32.4	3.58	0.01	51.69	31.22	0.26	13.34	0.01	0.02	0.14	100.29
06A Xtl 1 T	PL INCL in LK	64.9	0.9	34.2	3.75	0.01	52.11	30.77	0.25	12.90	0.03	0.02	0.16	100.01
06A Xtl 1 T	PL INCL in LK	66.3	0.8	32.9	3.63	0.01	51.62	31.23	0.26	13.26	0.01	0.03	0.14	100.19
06A Xtl 1 T	PL INCL in LK	66.0	0.8	33.2	3.67	0.01	51.91	31.08	0.26	13.18	0.03	0.02	0.14	100.30
06A Xtl 1 T	PL INCL in LK	64.4	1.0	34.6	3.79	0.01	52.20	30.96	0.23	12.78	0.02	0.02	0.16	100.19
06A Xtl 1 T	PL INCL in LK	64.8	0.8	34.4	3.79	0.01	52.19	31.04	0.28	12.91	0.01	0.03	0.13	100.40
06A Xtl 1 T	PL INCL in LK	66.1	0.8	33.1	3.62	0.01	51.73	31.11	0.25	13.11	0.03	0.02	0.14	100.01
06A Xtl 1 T	PL INCL in LK	60.1	1.0	38.9	4.28	0.02	53.30	30.03	0.22	11.96	0.02	0.03	0.17	100.03
06A Xtl 1 T	PL INCL in LK	58.2	1.1	40.7	4.47	0.02	53.86	29.62	0.22	11.56	0.03	0.04	0.18	99.99
06A Xtl 1 T	PL INCL in LK	57.1	1.1	41.7	4.56	0.02	54.20	29.54	0.20	11.31	0.02	0.04	0.19	100.08
06A Xtl 1 T	PL INCL in LK	56.4	1.2	42.4	4.67	0.02	54.20	29.43	0.24	11.24	0.04	0.03	0.20	100.05
06A Xtl 1 T	PL INCL in LK	58.5	1.0	40.5	4.41	0.02	53.83	29.75	0.19	11.53	0.02	0.01	0.17	99.93
06A Xtl 1 T	PL INCL in LK	59.9	1.0	39.1	4.29	0.02	53.46	30.05	0.19	11.91	0.01	0.04	0.17	100.13
06A Xtl 1 T	PL INCL in LK	57.1	0.9	42.0	4.63	0.02	54.27	29.41	0.22	11.40	0.00	0.03	0.16	100.14
06A Xtl 1 T	PL INCL in LK	55.1	1.0	43.9	4.81	0.02	54.64	29.05	0.26	10.91	0.02	0.03	0.17	99.91
06A Xtl 1 T	PL INCL in LK	55.5	2.0	46.9	5.13	0.03	55.50	28.17	0.37	10.12	0.03	0.02	0.34	99.70
06A Xtl 1 T	PL INCL in LK	40.8	7.5	51.7	5.65	0.04	58.34	25.74	0.50	8.07	0.00	0.06	1.25	99.64
06A Xtl 1 T	PL INCL in LK	56.8	1.4	41.8	4.40	0.04	53.15	29.19	0.60	10.83	0.06	0.02	0.23	98.52
06A Xtl 1 T	PL INCL in LK	47.3	1.9	50.8	5.42	0.03	55.74	27.49	0.61	9.15	0.05	0.00	0.31	98.80
06A Xtl 1 T	PL INCL in LK	59.7	1.0	39.3	4.33	0.03	53.55	29.63	0.36	11.92	0.01	0.01	0.17	100.02
06A Xtl 1 T	PL INCL in LK	49.2	1.4	49.4	5.41	0.03	56.09	27.87	0.33	9.75	0.02	0.03	0.24	99.78
06A Xtl 2	PL INCL in LK	49.5	1.1	49.4	5.43	0.02	56.11	28.28	0.20	9.84	0.02	0.02	0.19	100.10
06A Xtl 2	PL INCL in LK	50.4	1.1	48.4	5.33	0.02	55.89	28.25	0.15	10.04	0.01	0.04	0.19	99.91
06A Xtl 2	PL INCL in LK	49.4	1.1	49.5	5.42	0.02	56.17	28.04	0.22	9.80	0.01	0.02	0.18	99.88
06A Xtl 2	PL INCL in LK	44.9	2.6	52.5	5.72	0.04	57.36	27.03	0.49	8.86	0.02	0.04	0.42	99.98
06A Xtl 2 mc	PL INCL in LK	47.8	2.6	49.6	5.43	0.02	56.49	27.86	0.54	9.47	0.02	0.03	0.43	100.29

Table B.1 (Continued)

Sample	Lithology	An	Or	Ab	Na_2O	MgO	SiO_2	Al_2O_3	FeO	CaO	P_2O_5	TiO_2	K_2O	Total
06A Xtl 2 mc	PL INCL in LK	47.2	2.9	49.9	5.47	0.02	56.38	27.44	0.54	9.38	0.02	0.04	0.49	99.79
06A Xtl 3 T	PL INCL in LK	45.8	1.9	52.3	5.72	0.03	56.73	27.56	0.43	9.06	0.02	0.02	0.32	99.90
06A Xtl 3 T	PL INCL in LK	46.8	1.3	51.9	5.66	0.04	56.64	27.76	0.27	9.25	0.00	0.01	0.22	99.85
06A Xtl 3 T	PL INCL in LK	47.1	1.4	51.6	5.65	0.04	56.66	27.55	0.28	9.33	0.01	0.02	0.23	99.76
06A Xtl 3 T	PL INCL in LK	58.1	1.2	40.8	4.44	0.03	53.94	29.54	0.22	11.43	0.02	0.04	0.20	99.85
06A Xtl 3 T	PL INCL in LK	56.4	1.2	42.3	4.61	0.05	54.33	29.14	0.30	11.12	0.02	0.03	0.21	99.81
06A Xtl 3 T	PL INCL in LK	61.7	1.2	37.1	4.09	0.04	53.02	29.94	0.34	12.30	0.02	0.04	0.20	100.00
06A Xtl 3 T	PL INCL in LK	60.8	1.1	38.1	4.17	0.04	52.92	29.91	0.28	12.03	0.03	0.04	0.18	99.58
06A Xtl 3 T	PL INCL in LK	60.0	1.0	39.0	4.27	0.02	53.16	30.00	0.24	11.89	0.01	0.02	0.17	99.78
06A Xtl 3 T	PL INCL in LK	66.8	0.8	32.4	3.56	0.01	51.39	31.20	0.22	13.27	0.04	0.04	0.13	99.86
06A Xtl 3 T	PL INCL in LK	63.7	0.9	35.4	3.89	0.02	52.14	30.59	0.23	12.67	0.01	0.03	0.15	99.72
06A Xtl 3 T	PL INCL in LK	56.3	0.9	42.8	4.68	0.03	54.10	29.37	0.23	11.14	0.02	0.05	0.15	99.77
06A Xtl 3 T	PL INCL in LK	56.3	0.9	42.8	4.69	0.02	53.99	29.54	0.24	11.15	0.02	0.04	0.16	99.84
06A Xtl 3 T	PL INCL in LK	29.1	6.0	64.8	7.02	0.01	61.06	24.31	0.44	5.71	0.03	0.04	0.99	99.62
06A Xtl 3 T	PL INCL in LK	23.2	7.4	69.4	7.26	0.02	64.11	22.99	0.50	4.39	0.02	0.04	1.19	100.52
06A Xtl 3 mc	PL INCL in LK	26.4	7.6	66.1	7.09	0.01	61.58	23.95	0.65	5.12	0.02	0.06	1.24	99.71
06A Xtl 3 mc	PL INCL in LK	20.2	9.7	70.1	7.56	0.00	62.63	23.28	0.52	3.94	0.03	0.05	1.60	99.62
23 Xtl 1 T	PL INCL in EK	50.5	1.1	48.4	5.23	0.01	55.25	28.11	0.24	9.88	0.02	0.02	0.17	98.93
23 Xtl 1 T	PL INCL in EK	54.7	0.9	44.3	4.88	0.01	54.61	29.23	0.24	10.91	0.00	0.06	0.15	100.10
23 Xtl 1 T	PL INCL in EK	55.8	0.9	43.4	4.75	0.01	54.32	29.37	0.23	11.05	0.00	0.05	0.14	99.92
23 Xtl 1 T	PL INCL in EK	52.8	1.0	46.2	5.01	0.01	55.05	28.65	0.27	10.36	0.01	0.06	0.17	99.60
23 Xtl 1 T	PL INCL in EK	56.3	1.0	42.8	4.66	0.02	54.35	29.41	0.20	11.11	0.01	0.00	0.16	99.92
23 Xtl 1 T	PL INCL in EK	53.7	1.0	45.3	4.94	0.01	55.02	29.12	0.23	10.61	0.03	0.06	0.17	100.18
23 Xtl 1 T	PL INCL in EK	58.1	0.9	41.0	4.46	0.01	53.75	29.79	0.22	11.42	0.02	0.04	0.15	99.86
23 Xtl 1 T	PL INCL in EK	58.3	0.9	40.8	4.45	0.01	53.49	29.85	0.25	11.51	0.01	0.03	0.15	99.74
23 Xtl 1 T	PL INCL in EK	53.6	1.1	45.3	4.93	0.01	54.84	29.09	0.25	10.55	0.01	0.05	0.17	99.92
23 Xtl 1 T	PL INCL in EK	49.4	1.1	49.5	5.41	0.02	56.08	28.30	0.21	9.76	0.04	0.06	0.19	100.06
23 Xtl 1 T	PL INCL in EK	50.7	1.0	48.2	5.37	0.03	55.07	28.58	0.23	10.23	0.03	0.06	0.18	99.77
23 Xtl 1 T	PL INCL in EK	56.8	0.9	42.3	4.62	0.01	54.08	29.68	0.23	11.22	0.03	0.04	0.15	100.05
23 Xtl 1 T	PL INCL in EK	55.9	1.0	43.2	4.72	0.02	54.19	29.55	0.23	11.05	0.01	0.04	0.16	99.96
23 Xtl 1 T	PL INCL in EK	74.1	0.4	25.4	2.79	0.01	49.62	32.67	0.20	14.70	0.03	0.01	0.07	100.11
23 Xtl 1 T	PL INCL in EK	56.7	0.9	42.4	4.61	0.01	54.04	29.41	0.28	11.15	0.02	0.05	0.15	99.71
23 Xtl 1 T	PL INCL in EK	55.6	0.9	43.5	4.78	0.01	54.32	29.30	0.24	11.04	0.03	0.04	0.15	99.91

Table B.1 (Continued)

Sample	Lithology	An	Or	Ab	Na_2O	MgO	SiO_2	Al_2O_3	FeO	CaO	P_2O_5	TiO_2	K_2O	Total
23 Xtl 1 T	PL INCL in EK	58.3	0.8	40.9	4.47	0.01	53.60	30.05	0.25	11.53	0.00	0.03	0.13	100.09
23 Xtl 1 T	PL INCL in EK	54.1	0.8	45.1	4.94	0.02	54.55	29.37	0.21	10.73	0.03	0.04	0.14	100.02
23 Xtl 2	PL INCL in EK	60.3	0.7	39.0	4.23	0.02	53.29	30.12	0.76	11.87	0.02	0.10	0.12	100.53
23 Xtl 2	PL INCL in EK	57.4	0.8	41.8	4.60	0.02	54.10	29.90	0.32	11.42	0.02	0.03	0.13	100.54
23 Xtl 2	PL INCL in EK	50.3	1.0	48.7	5.36	0.01	56.08	28.72	0.21	10.00	0.02	0.02	0.17	100.58
23 Xtl 3	PL INCL in EK	62.6	0.8	36.6	3.96	0.01	52.34	29.96	0.44	12.29	0.01	0.05	0.13	99.18
23 Xtl 3	PL INCL in EK	55.2	0.9	43.9	4.82	0.01	54.89	29.18	0.22	10.97	0.02	0.04	0.16	100.29
23 Xtl 3	PL INCL in EK	56.7	0.8	42.5	4.64	0.00	54.34	29.47	0.25	11.20	0.02	0.06	0.14	100.12
23 Xtl 3	PL INCL in EK	49.1	1.0	49.9	5.50	0.01	56.39	28.34	0.20	9.79	0.02	0.02	0.17	100.43

Table B.2 Plagioclase LA-ICP-MS Spots in μg/g. CaO wt % from EMPA at laser spot location.

Sample	Lithology	Li	Mg	Si	Ca	Sc	Ti	V	Cr	Mn	Fe
8A-Plag-1-center	MKLV-WC	14.7	781	247088	76418	3.92	440	1.16	6.08	26.4	2952
8A-Plag-1-mid	MKLV-WC	15.8	886	261812	76311	3.58	561	1.60	7.41	28.9	3060
8A-Plag-1-midedge	MKLV-WC	15.5	833	254778	77902	4.13	496	1.38	9.83	26.8	2876
8A-Plag-1-edge	MKLV-WC	14.7	781	247088	76418	3.92	440	1.16	6.08	26.4	2952
8A-Plag-2-core	MKLV-WC	11.8	685	241963	67817	3.03	646	2.21	7.84	23.2	2600
8A-Plag-2-mid	MKLV-WC	12.6	648	236736	95363	2.94	430	1.23	10.57	38.0	2607
8A-Plag-2-rim	MKLV-WC	13.8	781	237205	76346	3.73	436	1.31	7.86	31.0	2809
8A-Plag-3	MKLV-WC	10.1	711	253381	70562	3.70	442	1.37	6.98	31.2	2797
8B-Plag-1	PL INCL in MK	11.3	104	233074	76851	3.21	262	2.83	9.63	25.2	1449
8B-Plag-1	PL INCL in MK	11.8	93	230103	76851	2.65	252	2.21	9.65	24.1	1397
8B-Plag-2-left	PL INCL in MK	9.3	100	210165	71541	2.80	329	3.43	9.80	27.4	1356
8B-Plag-2-right	PL INCL in MK	10.5	161	222661	71541	2.99	222	1.16	8.08	26.0	1241
8B-Plag-4	PL INCL in MK	13.5	347	268631	76830	2.95	142	1.17	10.54	28.0	1378
8B-Plag-4	PL INCL in MK	12.6	318	250493	76830	2.74	224	1.59	9.74	25.7	1502
8B-Plag-4	PL INCL in MK	12.9	171	267638	76830	3.66	220	2.75	9.48	22.3	1583
13-Plag-4	SDY	20.2	94	342394	58924	3.52	29		12.63	21.3	990
13-Plag-4	SDY	16.8	49	293605	65752	2.20	52	0.07	11.47	30.5	796
13-Plag-3-mid	SDY	17.8	461	276635	69683	4.60	358	0.70	12.63	27.8	2611
13-Plag-3-edge	SDY	15.8	364	276170	65752	3.10	183	0.27	8.78	22.3	2019

Table B.2 (Continued)

Sample	Cu	Rb	Sr	Sr	Y	Zr	Ba	Ba	La	Ce	Pr	Nd	Eu	Pb	CaO wt %
8A-Plag-1-center	5.71	0.41	1049	1049	0.07		123	119	2.28	4.22	0.41	1.40	0.53	1.38	10.7
8A-Plag-1-mid	9.26	0.65	1137	1148	0.25	0.51	157	163	2.48	5.31	0.42	1.51	0.93	1.40	10.7
8A-Plag-1-midedge	3.17	0.27	1065	1087	0.10	0.21	127	125	2.78	4.36	0.29	2.48	0.55	1.34	10.9
8A-Plag-1-edge	5.71	0.41	1049	1049	0.07		123	119	2.28	4.22	0.41	1.40	0.53	1.38	10.7
8A-Plag-2-core		0.64	1011	1023	0.22	0.07	191	186	2.66	4.16	0.34	0.98	0.85	1.12	9.5
8A-Plag-2-mid	1.37	0.31	1154	1169	0.13	0.19	87	84	1.97	3.02	0.31	1.20	0.66	0.72	11.1
8A-Plag-2-rim	9.14	0.19	1074	1058	0.16		117	117	2.78	4.68	0.36	1.39	0.55	1.28	10.7
8A-Plag-3	2.29	0.29	1011	1020			127	123	2.16	4.27	0.39	1.67	0.55	0.96	9.9
8B-Plag-1	0.87	0.30	569	567	1.02	0.51	117	120	4.08	7.92	0.91	3.32	1.33	4.40	10.8
8B-Plag-1	0.68	0.20	541	565	0.16		136	128	2.11	3.81	0.42	1.35	1.27	4.07	10.8
8B-Plag-2-left	0.88	0.13	544	548	0.31	0.18	113	113	2.23	4.30	0.46	2.03	1.27	2.99	10.0
8B-Plag-2-right	0.56	0.32	542	552	0.19	0.12	104	101	4.09	8.48	0.78	2.72	1.38	4.69	10.0
8B-Plag-4	2.62	0.57	686	698	0.43	0.28	187	177	6.94	13.63	1.29	3.75	1.54	5.69	10.8
8B-Plag-4	0.38	0.45	637	648	0.30		169	165	4.40	9.07	0.89	3.33	1.57	4.86	10.8
8B-Plag-4	0.47	0.17	678	684	0.32		196	189	4.66	8.17	0.63	1.90	1.68	5.03	10.8
13-Plag-4	4.33	0.29	1186	1173	0.22		136	146	3.96	7.38	0.57	1.76	1.16	6.44	8.2
13-Plag-4	0.98	0.21	1141	1137	0.18		137	143	4.96	7.98	0.57	1.69	1.27	5.34	9.2
13-Plag-3-mid	9.21	0.33	913	911	0.66	0.41	146	141	3.53	6.11	0.73	2.95	1.07	1.74	9.8
13-Plag-3-edge	2.66		850	849	0.16		139	145	3.45	5.40	0.42	1.90	1.04	2.23	9.2

APPENDIX C: Pyroxene Data

Table C.1 Orthopyroxene EMP Spots and Transects in wt %. T = transects.

Sample	Lithology	SiO_2	Al_2O_3	K_2O	NiO	FeO	MnO	Na_2O	MgO	TiO_2	CaO	Cr_2O_3	Total
8A Px 1	MKLV-WC	54.87	1.34	0.01	0.03	16.79	0.43	0.07	24.92	0.56	2.03	0.02	101.05
8A Px 1	MKLV-WC	54.39	1.30	0.03	0.02	17.06	0.38	0.08	25.14	0.56	2.16	0.02	101.14
8A Px 3	MKLV-WC	55.75	0.74	0.03	0.03	15.78	0.33	0.12	26.40	0.24	1.54	0.00	100.98
8A Px 3	MKLV-WC	55.71	0.60	0.02	0.03	15.70	0.39	0.11	26.56	0.24	1.52	0.01	100.90
8A Px 3	MKLV-WC	54.52	2.01	0.03	0.04	15.56	0.32	0.06	26.44	0.38	1.50	0.07	100.93
8A Px 3	MKLV-WC	54.27	1.80	0.03	0.03	16.10	0.41	0.06	25.73	0.40	1.57	0.03	100.41
8A Px 4	MKLV-WC	55.65	0.77	0.00	0.06	15.57	0.36	0.03	26.58	0.26	1.55	0.02	100.85
8A Px 4	MKLV-WC	55.39	1.01	0.00	0.06	15.73	0.39	0.03	26.20	0.31	1.48	0.01	100.61
8A Px 4	MKLV-WC	55.67	0.74	0.00	0.02	15.89	0.37	0.04	26.25	0.27	1.50	0.01	100.76
8A Px 4	MKLV-WC	54.62	1.54	0.01	0.03	15.83	0.37	0.04	25.89	0.39	1.52	0.01	100.25
8A Px 4.6 t	MKLV-WC	54.35	1.63	0.00	0.03	16.04	0.38	0.07	25.54	0.45	2.03	0.00	100.52
8A Px 4.6 t	MKLV-WC	55.50	0.79	0.03	0.02	15.29	0.36	0.07	26.38	0.26	1.51	0.01	100.22
8A Px 4.6 t	MKLV-WC	55.79	0.77	0.01	0.00	15.33	0.40	0.03	26.51	0.27	1.52	0.02	100.66
8A Px 4.6 t	MKLV-WC	55.06	0.93	0.01	0.00	16.38	0.43	0.05	25.90	0.33	1.43	0.02	100.53
8A Px 4.6 t	MKLV-WC	55.86	0.76	0.02	0.09	15.54	0.39	0.04	26.43	0.26	1.58	0.02	100.98
8A Px 4.6 t	MKLV-WC	55.50	0.66	0.00	0.05	15.31	0.41	0.04	26.46	0.24	1.48	0.01	100.15
8A Px 4.6 t	MKLV-WC	55.69	0.79	0.02	0.08	15.20	0.40	0.05	26.54	0.27	1.50	0.02	100.55
8A Px 4.6 t	MKLV-WC	55.69	0.62	0.02	0.05	15.07	0.31	0.04	26.70	0.23	1.51	0.00	100.23
8A Px 4.6 t	MKLV-WC	55.43	0.95	0.01	-0.02	15.60	0.36	0.04	26.59	0.30	1.46	0.01	100.75
8A Px 4.6 t	MKLV-WC	55.04	0.75	0.01	0.05	15.82	0.38	0.04	26.47	0.28	1.49	-0.01	100.32
8A Px 4.6 t	MKLV-WC	55.23	0.72	0.01	-0.01	15.37	0.41	0.04	26.21	0.27	1.45	0.00	99.71
8A Px 4.6 t	MKLV-WC	54.50	0.67	0.02	0.00	18.93	0.50	0.04	23.46	0.33	1.54	0.00	99.99
8A Px 9	MKLV-WC	55.73	0.72	0.03	0.02	15.40	0.42	0.04	26.08	0.28	1.50	0.00	100.23
8A Px 9	MKLV-WC	54.95	0.78	0.01	0.02	15.40	0.37	0.07	26.13	0.29	1.46	0.01	99.49
8A Px 9	MKLV-WC	54.95	0.96	0.02	0.04	15.32	0.33	0.06	25.66	0.34	1.77	0.00	99.45
8A Px 9.5	MKLV-WC	54.76	0.92	0.01	-0.01	16.01	0.34	0.04	25.98	0.32	1.48	0.02	99.89

Table C.1 (Continued)

Sample	Lithology	SiO_2	Al_2O_3	K_2O	NiO	FeO	MnO	Na_2O	MgO	TiO_2	CaO	Cr_2O_3	Total
8A Px 9.5	MKLV-WC	54.73	0.91	0.01	0.06	15.81	0.36	0.06	25.97	0.33	1.47	0.00	99.70
8A Px 9.5	MKLV-WC	54.05	1.94	0.02	0.02	16.17	0.41	0.06	25.18	0.43	1.59	0.01	99.89
13 Px 12	SDY	54.30	0.91	0.00	0.07	17.16	0.49	0.03	23.61	0.29	1.42	0.01	98.30
13 Px 12	SDY	54.12	0.94	0.02	0.04	17.12	0.45	0.03	24.51	0.27	1.48	0.00	98.99
13 Px 12	SDY	54.58	0.71	0.01	0.02	17.64	0.52	0.03	24.67	0.22	1.43	-0.01	99.83
13 Px 12	SDY	53.28	2.39	0.02	0.02	16.34	0.43	0.04	24.86	0.31	1.36	0.01	99.07
13 Px 15	SDY	54.72	0.64	0.00	0.02	17.69	0.48	0.00	24.66	0.17	1.24	0.01	99.63
13 Px 15	SDY	54.41	0.47	0.00	0.01	19.11	0.59	0.02	23.84	0.17	1.11	-0.01	99.74
13 Px 15	SDY	52.76	0.48	0.02	0.03	18.83	0.52	0.03	22.33	0.19	2.87	-0.01	98.07
13 Px 15	SDY	54.61	0.78	0.01	0.01	18.19	0.50	0.02	24.14	0.23	1.27	0.02	99.77
13 Px 16	SDY	54.41	1.49	-0.01	0.03	17.27	0.45	0.02	24.53	0.31	1.49	-0.01	99.99
13 Px 16	SDY	54.95	1.00	0.00	0.03	17.15	0.44	0.01	24.94	0.24	1.59	0.00	100.36
13 Px 16	SDY	54.02	1.81	0.03	0.03	17.42	0.51	0.03	24.55	0.33	1.46	0.00	100.19
13 Px 16	SDY	53.45	2.21	0.00	0.04	17.54	0.43	0.01	24.60	0.38	1.45	0.01	100.13
13 Px 16	SDY	53.83	1.97	0.01	0.03	17.54	0.43	0.02	24.74	0.34	1.47	0.02	100.41
13 Px 16	SDY	54.20	1.63	0.01	0.05	17.84	0.39	0.05	24.93	0.36	1.53	-0.01	100.98
13 Px 16	SDY	54.31	1.16	0.01	0.05	17.66	0.49	0.03	24.82	0.29	1.43	0.00	100.25
13 Px 16	SDY	54.29	1.08	-0.01	0.06	18.47	0.54	0.02	24.56	0.30	1.39	-0.01	100.70
13 Px 16	SDY	53.62	0.99	-0.01	-0.03	19.16	0.52	0.02	23.67	0.27	1.48	0.01	99.75
13 Px 16	SDY	53.87	0.81	0.01	0.01	19.28	0.57	0.02	23.38	0.23	1.27	0.00	99.43
13 Px 16	SDY	53.79	0.73	0.01	0.01	20.21	0.65	0.01	23.35	0.20	1.21	-0.02	100.18
13 Px 16	SDY	53.82	0.80	0.00	0.02	20.11	0.60	0.04	23.22	0.21	1.18	0.00	100.00
13 Px 16	SDY	54.00	0.42	0.01	0.01	20.77	0.68	0.05	22.89	0.16	1.10	0.02	100.11
13 Px 17	SDY	54.91	0.54	0.00	0.04	18.60	0.53	0.03	24.12	0.18	1.28	0.00	100.22
13 Px 17	SDY	54.30	0.46	0.01	-0.03	19.29	0.61	0.02	23.38	0.20	1.31	0.01	99.59
13 Px 17	SDY	51.58	0.44	0.02	0.00	20.76	0.75	0.04	21.00	0.18	2.98	0.00	97.75

Table C.1 (Continued)

Sample	Lithology	SiO_2	Al_2O_3	K_2O	NiO	FeO	MnO	Na_2O	MgO	TiO_2	CaO	Cr_2O_3	Total
23 Px 1	PL INC in EK	53.26	0.34	0.01	-0.01	25.30	0.67	0.01	19.49	0.07	1.00	0.02	100.19
23 Px 1	PL INC in EK	52.98	0.79	0.00	0.02	25.89	0.63	0.02	19.26	0.09	1.03	0.00	100.69
23 Px 2	PL INC in EK	53.51	0.25	0.01	-0.05	25.65	0.70	0.01	19.27	0.04	1.08	0.00	100.51
23 Px 2	PL INC in EK	53.42	0.34	0.02	0.05	26.01	0.69	0.01	19.26	0.05	0.97	0.01	100.83
23 Px 2	PL INC in EK	52.81	0.61	0.01	0.02	27.04	0.75	0.04	18.50	0.06	1.09	0.01	100.96
23 Px 4	PL INC in EK	52.86	0.75	0.00	-0.04	25.21	0.64	0.02	18.97	0.09	0.99	0.02	99.55
23 Px 4	PL INC in EK	52.83	0.69	0.02	0.04	25.42	0.62	0.01	19.10	0.10	0.96	0.01	99.81
8B Px 6	PL INC in MK	52.16	0.67	0.00	0.04	26.31	0.60	0.01	18.72	0.25	0.95	0.03	99.73
8B Px 6	PL INC in MK	51.75	0.73	0.00	0.02	25.86	0.50	0.03	18.11	0.31	1.55	0.00	98.86
8B Px 6	PL INC in MK	52.18	0.39	0.01	-0.01	25.52	0.46	0.00	19.70	0.13	0.97	0.02	99.36
8B Px 6	PL INC in MK	52.57	0.92	0.01	-0.05	23.85	0.53	0.04	19.95	0.30	1.64	0.03	99.84
8B Px 4	PL INC in MK	52.84	0.63	0.01	0.00	23.46	0.53	0.04	20.30	0.19	1.45	0.02	99.48
8B Px 4	PL INC in MK	52.39	0.76	0.00	-0.02	23.44	0.52	0.03	20.10	0.24	1.58	0.01	99.08
8B Px 4	PL INC in MK	52.11	0.88	0.00	0.08	23.84	0.59	0.04	19.85	0.27	1.66	0.00	99.30
8B Px 4	PL INC in MK	52.39	0.77	0.01	0.02	23.57	0.50	0.02	19.98	0.23	1.53	0.03	99.04
8B Px 4	PL INC in MK	52.51	0.71	0.02	-0.02	24.46	0.59	0.05	19.29	0.21	1.42	0.00	99.26
8B Px 3.5	PL INC in MK	52.51	0.51	-0.01	-0.01	24.36	0.64	0.01	19.89	0.13	1.08	0.00	99.12
8B Px 3.5	PL INC in MK	52.62	0.58	0.03	0.00	25.45	0.62	0.02	19.22	0.12	0.94	0.03	99.65
8B Px 3.5	PL INC in MK	52.59	0.56	-0.01	0.03	26.03	0.62	0.02	18.92	0.13	1.19	0.02	100.12
8B Px 3	PL INC in MK	52.26	0.53	0.00	-0.06	25.60	0.62	0.02	18.93	0.14	0.94	0.02	99.06
8B Px 3	PL INC in MK	52.33	0.50	0.01	0.04	25.24	0.56	0.03	19.36	0.15	1.14	0.02	99.38
8B Px 3	PL INC in MK	52.47	0.61	0.03	-0.03	24.47	0.58	0.02	19.85	0.20	1.37	0.01	99.61
8B Px 2	PL INC in MK	52.97	0.21	0.00	-0.02	26.61	0.65	0.03	18.76	0.09	1.08	0.01	100.42
8B Px 2	PL INC in MK	52.55	0.29	0.00	0.05	26.55	0.65	0.02	19.01	0.09	0.96	0.02	100.19
8B Px 2	PL INC in MK	52.33	0.85	0.00	0.04	24.44	0.44	0.03	19.59	0.26	1.57	0.00	99.55
8B Px 2	PL INC in MK	52.74	0.88	0.00	-0.03	23.70	0.52	0.03	20.20	0.29	1.65	0.03	100.03

Table C.2 Clinopyroxene EMP Spots in wt %. First column is sample # and grain #. Px = clinopyroxene

Sample	Lithology	SiO_2	Al_2O_3	K_2O	NiO	FeO	MnO	Na_2O	MgO	TiO_2	CaO	Cr_2O_3	Total
8A Px 2	MKLV-WC	52.16	2.55	0.03	0.02	8.70	0.25	0.42	15.47	0.75	18.33	0.02	98.70
8A Px 2	MKLV-WC	52.34	2.77	0.02	0.00	8.93	0.22	0.43	15.52	0.83	18.00	0.01	99.07
8A Px 2	MKLV-WC	52.29	2.53	0.01	-0.01	8.72	0.21	0.36	15.58	0.81	18.17	-0.01	98.67
8A Px 2	MKLV-WC	53.39	5.22	0.06	0.04	8.05	0.25	1.01	14.17	0.52	17.03	0.02	99.76
8A Px 4.5	MKLV-WC	51.89	2.69	0.01	-0.02	8.61	0.28	0.36	15.48	0.86	18.29	0.02	98.47
8A Px 4.5	MKLV-WC	53.05	1.78	0.01	0.01	8.75	0.27	0.35	16.14	0.59	18.14	-0.01	99.08
8A Px 4.5	MKLV-WC	52.09	2.67	0.04	0.01	8.83	0.22	0.37	15.53	0.82	18.27	0.04	98.90
8A Px 5	MKLV-WC	51.88	4.22	0.01	0.00	6.19	0.14	0.41	15.51	0.94	19.77	0.49	99.55
8A Px 5	MKLV-WC	50.88	4.40	0.03	0.00	6.24	0.18	0.41	15.37	1.00	19.58	0.50	98.59
8A Px 5	MKLV-WC	51.32	4.33	0.02	-0.01	6.28	0.16	0.41	15.32	0.97	19.60	0.48	98.89
8A Px 5	MKLV-WC	51.40	4.22	0.03	0.00	6.27	0.13	0.41	15.39	0.95	19.64	0.50	98.95
8A Px 5	MKLV-WC	51.70	4.25	0.02	0.06	6.18	0.15	0.41	15.30	0.96	19.66	0.53	99.20
8A Px 5	MKLV-WC	49.06	7.35	0.00	0.00	7.62	0.15	0.47	13.74	1.62	19.20	0.03	99.24
8A Px 5	MKLV-WC	50.49	5.51	0.00	0.03	7.21	0.15	0.49	14.79	1.24	19.25	0.20	99.36
8A Px 5	MKLV-WC	51.51	4.29	0.00	0.05	6.45	0.15	0.41	15.33	0.96	19.55	0.53	99.24
8A Px 5	MKLV-WC	51.30	4.22	0.04	0.03	6.29	0.12	0.43	15.47	0.96	19.62	0.54	99.03
8A Px 5	MKLV-WC	51.40	4.37	0.02	0.02	6.22	0.17	0.42	15.37	1.01	19.50	0.50	98.99
8A Px 5	MKLV-WC	51.11	4.23	0.02	0.06	6.15	0.18	0.40	15.45	0.94	19.71	0.52	98.76
8A Px 5	MKLV-WC	51.40	4.47	0.02	0.00	6.61	0.18	0.41	15.29	1.05	19.46	0.36	99.25
8A Px 5	MKLV-WC	50.35	5.20	0.01	0.01	6.85	0.12	0.40	14.92	1.30	19.36	0.17	98.70
8A Px 5	MKLV-WC	51.02	4.63	0.03	0.04	6.88	0.15	0.40	15.15	1.12	19.32	0.32	99.06
8A Px 5	MKLV-WC	51.19	4.31	0.01	0.01	7.31	0.13	0.41	15.06	1.10	19.25	0.24	99.02
8A Px 5	MKLV-WC	52.11	2.85	0.02	-0.02	8.48	0.20	0.42	15.64	0.93	18.12	0.01	98.79
8A Px 5	MKLV-WC	52.60	2.50	0.00	0.02	8.76	0.24	0.39	16.00	0.83	17.86	0.04	99.25
8A Px 5	MKLV-WC	51.89	2.92	0.01	-0.01	9.10	0.22	0.44	15.55	0.95	17.98	0.08	99.14
8A Px 5	MKLV-WC	51.64	2.83	0.02	0.01	9.28	0.24	0.48	15.43	0.97	17.83	0.04	98.78

Table C.2 (Continued)

Sample	Lithology	SiO_2	Al_2O_3	K_2O	NiO	FeO	MnO	Na_2O	MgO	TiO_2	CaO	Cr_2O_3	Total
8A Px 5	MKLV-WC	51.35	2.71	0.03	0.03	9.34	0.23	0.63	15.45	1.09	17.69	0.02	98.58
8A Px 5	MKLV-WC	51.60	2.80	0.02	0.04	9.52	0.28	0.47	15.54	1.03	17.32	0.02	98.65
8A Px 5	MKLV-WC	52.41	2.46	0.01	0.02	9.30	0.22	0.44	15.63	0.90	17.49	0.08	98.96
8A Px 5	MKLV-WC	52.76	2.16	0.01	0.03	9.21	0.24	0.43	15.91	0.85	17.57	0.08	99.26
8A Px 5	MKLV-WC	52.22	2.30	0.01	0.06	9.22	0.22	0.42	15.65	0.89	17.91	0.05	98.93
8A Px 5	MKLV-WC	51.91	2.61	0.01	0.02	9.55	0.22	0.40	15.48	1.11	17.58	0.07	98.96
8A Px 5	MKLV-WC	51.85	2.66	0.02	0.01	9.86	0.27	0.43	15.51	1.08	17.27	0.06	99.01
8A Px 5	MKLV-WC	51.71	2.44	0.04	-0.02	9.70	0.24	0.43	15.65	1.04	17.20	0.02	98.46
8A Px 5	MKLV-WC	52.41	2.50	0.04	0.01	8.90	0.26	0.48	15.89	0.75	17.94	0.07	99.25
8A Px 5	MKLV-WC	52.16	2.66	0.01	0.01	8.56	0.23	0.40	15.84	0.81	18.28	0.02	98.97
8A Px 5	MKLV-WC	52.20	2.58	0.02	0.06	9.02	0.18	0.37	15.81	0.82	17.91	0.01	98.98
8A Px 5	MKLV-WC	51.99	2.56	0.02	0.04	8.97	0.26	0.40	15.70	0.82	17.84	0.01	98.59
8A Px 5	MKLV-WC	51.36	3.10	0.04	-0.03	9.39	0.25	0.39	15.82	0.93	17.43	0.01	98.71
8A Px 5	MKLV-WC	52.16	2.91	0.03	0.03	9.01	0.27	0.39	15.57	0.66	18.19	0.04	99.25
8A Px 6	MKLV-WC	52.95	1.57	0.00	0.01	10.29	0.28	0.39	15.65	0.66	17.21	0.01	99.03
8A Px 6	MKLV-WC	52.72	1.87	-0.01	0.04	8.90	0.27	0.30	16.55	0.54	17.48	0.03	98.71
8A Px 6	MKLV-WC	50.92	2.93	0.01	0.06	9.07	0.28	0.39	15.55	0.89	17.70	0.03	97.83
8A Px 6	MKLV-WC	52.32	1.73	0.01	0.01	8.59	0.29	0.36	16.04	0.60	18.07	0.03	98.04
8A Px 7	MKLV-WC	52.13	2.60	0.01	0.01	8.85	0.25	0.41	15.67	0.84	17.90	0.02	98.69
8A Px 7	MKLV-WC	53.08	1.83	0.01	0.00	8.38	0.22	0.34	16.10	0.63	18.26	-0.01	98.85
8A Px 7	MKLV-WC	51.56	2.55	0.02	-0.01	9.10	0.17	0.45	15.48	0.79	18.00	-0.01	98.12
8A Px 8	MKLV-WC	52.58	1.81	0.03	-0.03	8.80	0.25	0.38	15.98	0.59	17.94	0.03	98.39
8A Px 10	MKLV-WC	52.31	2.12	0.02	0.00	9.67	0.22	0.46	15.54	0.82	17.40	0.12	98.68
8A Px 10	MKLV-WC	52.24	2.36	0.02	-0.01	8.89	0.27	0.39	15.73	0.78	17.81	0.05	98.54
8A Px 10	MKLV-WC	51.77	2.64	0.02	0.01	9.04	0.27	0.46	15.71	0.83	17.72	0.04	98.50
8A Px 10	MKLV-WC	51.88	2.46	0.02	0.06	9.27	0.27	0.41	15.56	0.93	17.68	0.04	98.57

Table C.2 (Continued)

Sample	Lithology	SiO_2	Al_2O_3	K_2O	NiO	FeO	MnO	Na_2O	MgO	TiO_2	CaO	Cr_2O_3	Total
8A Px 10	MKLV-WC	51.73	2.67	0.00	0.04	9.30	0.24	0.41	15.54	0.89	17.61	0.05	98.48
8A Px 10	MKLV-WC	51.52	2.45	0.03	0.01	9.40	0.27	0.51	15.46	0.89	17.56	0.07	98.16
8A Px 10	MKLV-WC	51.95	2.38	0.01	0.02	8.83	0.27	0.39	15.69	0.72	18.23	0.00	98.50
8A Px 10	MKLV-WC	51.09	3.11	0.01	0.07	9.04	0.25	0.38	15.34	0.88	18.14	0.02	98.32
8A Px 10	MKLV-WC	50.92	3.06	0.03	0.04	9.06	0.24	0.37	15.26	0.92	18.09	0.01	97.99
13 Px 13	SDY	52.62	1.15	0.01	0.02	9.48	0.33	0.32	14.86	0.28	18.65	-0.02	97.73
13 Px 13	SDY	52.67	1.53	0.14	-0.02	10.61	0.41	0.44	14.72	0.43	17.65	0.00	98.59
13 Px 14	SDY	52.50	1.17	0.00	0.01	9.30	0.27	0.32	15.07	0.39	18.56	-0.01	97.60
13 Px 14	SDY	52.27	1.50	0.01	-0.02	8.88	0.31	0.31	14.85	0.38	18.76	0.00	97.26
13 Px 14	SDY	51.83	2.13	0.00	0.00	8.99	0.23	0.33	14.98	0.52	18.64	0.00	97.66
13 Px 1	SDY	52.92	1.31	0.01	0.01	8.82	0.29	0.29	15.21	0.36	18.91	0.00	98.11
13 Px 1	SDY	52.81	0.97	-0.01	0.06	9.34	0.33	0.27	15.32	0.30	18.50	0.02	97.92
13 Px 1	SDY	51.22	2.41	0.00	0.03	9.26	0.28	0.31	15.26	0.58	18.09	0.02	97.47
13 Px 1	SDY	52.26	1.86	0.03	0.01	9.06	0.31	0.32	14.94	0.49	18.53	0.01	97.82
8B Px 5	Pl Incl in MK	51.68	1.60	0.01	0.00	12.61	0.30	0.20	13.87	0.47	17.48	0.03	98.25
8B Px 5	Pl Incl in MK	52.45	1.41	-0.01	0.00	12.42	0.33	0.26	13.77	0.36	17.67	0.05	98.72
8B Px 5	Pl Incl in MK	51.54	2.03	0.00	0.02	12.87	0.27	0.28	12.80	0.40	18.17	0.07	98.45
8B Px 4.5	Pl Incl in MK	53.46	0.63	0.00	-0.02	11.95	0.28	0.15	13.63	0.19	18.55	0.01	98.85
8B Px 4.5	Pl Incl in MK	52.86	0.63	0.00	-0.01	12.05	0.23	0.15	13.59	0.17	18.53	0.03	98.25
8B Px 4.5	Pl Incl in MK	52.72	1.45	0.01	-0.03	12.60	0.33	0.20	13.40	0.37	18.00	0.05	99.13
8B Px 4.5	Pl Incl in MK	51.92	1.81	0.00	0.03	12.52	0.27	0.21	13.70	0.38	17.67	0.02	98.52
8B Px 3.6	Pl Incl in MK	51.76	1.09	0.01	0.03	12.21	0.29	0.18	13.39	0.26	18.00	0.01	97.24

Table C.3 Pyroxene LA-ICP-MS Spots in µg/g.

Sample #	Lithology	Li	Mg	Si	Ca	Sc	Ti	V	Cr	Mn	Fe
8A-CPX10-mid	MKLV-WC	12.2	139394	208986	126617	91.2	5634	413	243.7	2033	46740
8A-CPX-5-core	MKLV-WC	5.7	126229	170051	140080	90.2	5891	278	1623.9	1031	26312
8A-CPX-5-mid	MKLV-WC	4.9	130470	188968	127659	101.0	6047	366	216.1	1732	39364
8A-CPX-4.5	MKLV-WC	17.1	131200	178320	130074	108.1	4907	269	84.2	1658	37621
8A-CPX-7	MKLV-WC	15.4	129963	179145	128631	94.8	4512	260	49.9	1670	37882
8A-CPX-6	MKLV-WC	16.4	132731	169142	126429	91.2	3535	192	42.2	1760	36681
8B-CPX-5	PL INCL in MK	15.1	111552	204939	125786	133.1	2879	773	101.4	2236	78245
13-CPX-14	SDY	17.5	115648	189093	131504	145.1	2091	149	10.2	2088	38230
13-CPX-13	SDY	13.8	119344	189963	132218	128.0	1881	118	8.9	2299	39043
13-CPX-2	SDY	31.1	119108	179775	128645	111.7	2125	140	13.9	2062	37375
13-CPX-1	SDY	7.6	122088	187461	129360	108.6	2150	142	17.2	2053	37425
13-CPX-8	SDY	14.5	115844	187767	129360	133.0	2770	185	16.2	2018	38437
8A-OPX9.5	MKLV-WC	13.3	233778	240579	10720	37.1	2352	90	48.9	3031	79133
8A-OPX 1	MKLV-WC	18.2	272391	281749	14506	42.0	3153	155	125.7	3482	91389
8A-OPX-4	MKLV-WC	8.5	200585	211386	10720	35.0	2194	87	33.0	2531	61002
8A-OPX-4	MKLV-WC	9.3	233797	238501	10720	29.7	1991	79	38.0	2733	69870
8A-OPX-4.6	MKLV-WC	9.7	229206	235494	10720	35.5	2353	102	53.1	2676	69390
8A-OPX-4.6	MKLV-WC	8.8	239043	240801	10649	30.4	1817	75	68.8	2680	69031
8B-OPX-6	PL INCL in MK	10.8	146353	217219	9148	61.8	2270	311	50.8	3634	148724
8B-OPX-6	PL INCL in MK	7.3	106058	150724	9148	42.3	1128	216	43.5	2375	100118
8B-OPX-6.1	PL INCL in MK	12.3	167561	246571	9148	69.2	2477	348	66.7	4248	172893
8B-OPX-6.2	PL INCL in MK	16.2	214259	310599	9148	78.7	4313	446	68.1	5607	223438
8B-OPX-3	PL INCL in MK	9.6	138052	193360	8219	52.5	1673	299	45.0	3401	128336
8B-OPX-3	PL INCL in MK	12.1	164841	235581	8219	57.4	1195	311	51.1	4363	154254
8B-OPX-3	PL INCL in MK	11.4	169315	249325	8219	57.7	1174	254	54.1	5029	206055
13-OPX-10	SDY	11.3	70822	110084	71469	56.6	1158	84	7.5	1215	22012

Table C.3 (Continued)

Sample #	Cu	Rb	Sr	Sr	Y	Zr	Nb	Ba	Ba	La	Ce	Nd	Sm	Eu
8A-CPX10-mid	6.48	0.14	37.7	35.9	22.5	30.0	0.16	0.21	0.25	2.37	12.8	15.0	4.72	1.23
8A-CPX-5-core	3.26		44.8	46.4	13.0	28.1	0.13		0.04	1.44	7.2	8.4	2.75	1.04
8A-CPX-5-mid	3.21		38.7	34.8	23.9	36.1	0.14		0.11	2.41	11.2	13.3	4.40	1.48
8A-CPX-4.5	20.95		35.9	32.4	27.2	38.4	0.12		0.13	3.05	13.7	16.1	7.07	1.50
8A-CPX-7	7.01		29.2	32.7	22.8	33.0	0.05		0.06	2.53	13.2	14.7	4.85	1.29
8A-CPX-6	9.75	0.05	26.8	26.9	22.3	24.4	0.06		0.04	1.83	9.2	10.3	4.56	1.09
8B-CPX-5	6.32	7.00	19.9	19.7	24.7	15.3	0.81	31.00	32.15	3.38	13.5	12.2	4.44	0.82
13-CPX-14	3.43	0.02	24.4	21.9	40.3	35.7	0.04		0.09	3.25	16.0	21.5	8.37	1.43
13-CPX-13	3.34		24.0	24.6	42.7	27.5		0.18	0.46	8.56	28.1	26.8	7.36	1.51
13-CPX-2	4.15	0.19	29.9	27.8	32.1	22.0	0.04	0.19	0.50	6.52	23.1	21.6	7.34	1.31
13-CPX-1	19.63		25.1	25.1	26.5	20.7	0.04	0.30	0.13	3.27	12.9	14.7	4.84	1.42
13-CPX-8	12.47		26.9	27.0	35.1	35.3	0.06	0.51	0.31	4.38	18.7	21.5	7.38	1.57
8A-OPX9.5	60.67	3.94	8.48	7.42	5.35	18.01	0.74	30.45	27.66	1.69	4.52	2.07	0.44	0.07
8A-OPX 1	12.98	0.21	3.96	2.41	4.09	3.39	0.04	1.33	1.12		0.32			0.12
8A-OPX-4	10.55	0.32		1.99	3.95	4.83	0.13	2.35	2.40	0.11	0.56	0.44	0.28	0.05
8A-OPX-4	8.36		1.50	0.45	2.87	1.93			0.11		0.19	0.32		
8A-OPX-4.6	8.36	0.10	2.71	1.21	3.40	3.75	0.05	0.66	0.63	0.07	0.21	0.32	0.19	
8A-OPX-4.6	8.03		1.98	0.86	2.67	2.53	0.05	0.31	0.35	0.06	0.15	0.20		
8B-OPX-6	2.87	1.02		0.47	9.95	5.21		1.70	2.55	0.14	0.77	0.74		
8B-OPX-6	1.69	0.05	1.31	0.71	6.07	4.43			0.25	0.17	0.63	0.56		
8B-OPX-6.1	4.97	2.51	3.86	1.86	10.02	5.13		19.85	17.35	0.40	1.42	0.70		
8B-OPX-6.2	6.30	2.05		0.63	12.16	6.49	0.12	9.26	9.06	0.14	0.62	0.31		0.07
8B-OPX-3	3.25	2.71	6.60	5.04	6.92	7.61	0.42	11.01	11.44	0.51	1.42	1.13	0.26	0.04
8B-OPX-3	5.50	4.48	10.24	10.11	8.61	14.83	0.65	21.85	22.23	1.05	2.92	1.21	0.55	0.10
8B-OPX-3	3.56	0.48	1.35	0.17	13.65	2.08		2.36	1.72	0.07	0.22	0.22		
13-OPX-10	1.77	0.03	12.86	13.34	12.45	9.73		0.17	0.10	1.34	6.01	6.17	2.44	0.54

Table C.3 (Continued)

Sample #	Pr	Gd	Dy	Er	Yb	Pb	CaO wt %
8A-CPX10-mid	2.20	5.40	5.85	2.46	1.78	0.07	17.72
8A-CPX-5-core	1.35	2.93	2.58	1.30	1.15		19.60
8A-CPX-5-mid	2.19	5.66	5.36	2.59	2.17		17.86
8A-CPX-4.5	2.59	5.91	5.17	3.05	1.93	0.07	18.20
8A-CPX-7	2.66	5.41	5.61	2.63	2.08	0.08	18.00
8A-CPX-6	1.86	5.70	4.89	2.46	2.00		17.69
8B-CPX-5	2.27	4.71	5.15	3.18	2.32	0.65	17.60
13-CPX-14	3.30	8.85	8.58	4.11	2.94	0.07	18.40
13-CPX-13	4.90	9.66	8.68	4.54	3.78	0.17	18.50
13-CPX-2	4.02	6.73	7.02	3.66	3.30	0.19	18.00
13-CPX-1	2.34	5.61	5.90	2.88	2.11	0.14	18.10
13-CPX-8	3.63	8.87	7.76	4.18	3.05	0.05	18.10
8A-OPX9.5	0.52	0.70	0.94	0.63	0.64	1.15	1.50
8A-OPX 1	0.04	0.44	0.46	0.68	0.59	0.07	2.03
8A-OPX-4	0.08	0.54	0.63	0.40	0.60	0.05	1.50
8A-OPX-4	0.03		0.51	0.36	0.78	0.05	1.50
8A-OPX-4.6			0.83	0.39	0.65	0.03	1.50
8A-OPX-4.6			0.48	0.27	0.64	0.03	1.49
8B-OPX-6	0.13	1.11	1.48	1.57	1.54		1.28
8B-OPX-6	0.10	0.44	1.21	1.04	0.88		1.28
8B-OPX-6.1	0.11	0.67	1.17	1.07	2.00		1.28
8B-OPX-6.2	0.04	0.63	1.42	1.79	2.13		1.28
8B-OPX-3	0.26	0.56	0.86	1.17	0.94	0.30	1.15
8B-OPX-3	0.33	0.94	1.46	1.35	2.08	0.46	1.15
8B-OPX-3	0.10	0.74	2.10	1.93	2.44		1.15
13-OPX-10	1.21	2.53	2.87	1.51	1.19	0.06	10.00

APPENDIX D: Olivine, Spinel and Glass Data

Table D.1 Olivine EMPA Spots and Transects in wt %. T = transects, P = points, glom = glomerocryst, spl = spinel, rx rim = reaction rim, Lg = large. Fo content is calculated as molar 100*Mg/(Mg+Fe).

Sample	Lithology	Fo	SiO_2	Al_2O_3	Na_2O	MgO	K_2O	CaO	MnO	FeO	NiO	Cr_2O_3	TiO_2	Total
32 xtl 1	Xb	80.32	39.05	0.04	0.00	41.69	0.00	0.16	0.27	18.21	0.21	0.03	0.01	99.66
32 xtl 1	Xb	80.00	38.76	0.03	0.01	41.71	0.00	0.14	0.23	18.58	0.19	0.03	0.01	99.69
32 xtl 1	Xb	80.79	39.06	0.04	0.00	42.27	0.00	0.14	0.21	17.91	0.19	0.03	0.00	99.85
32 xtl 2	Xb	84.36	39.40	0.04	-0.01	44.85	0.01	0.14	0.17	14.82	0.32	0.00	0.01	99.77
32 xtl 2	Xb	79.59	38.99	0.04	0.01	41.30	0.01	0.15	0.24	18.88	0.15	0.02	0.00	99.80
32 xtl 3	Xb	75.75	37.83	0.02	0.01	38.69	0.00	0.18	0.31	22.09	0.16	0.02	0.03	99.34
32 xtl 3	Xb	74.68	38.04	0.02	0.01	38.09	0.00	0.17	0.30	23.02	0.09	0.00	0.02	99.75
32 xtl 3	Xb	74.04	37.75	0.02	0.01	37.83	0.00	0.17	0.36	23.64	0.03	0.02	0.02	99.85
01 xtl 1 T	X lahar	62.56	35.13	0.03	0.02	29.87	0.01	0.21	0.50	31.86	0.12	-0.02	0.04	97.77
01 xtl 1 T	X lahar	66.60	35.80	0.02	0.00	32.52	0.01	0.18	0.41	29.07	0.11	0.02	0.02	98.14
01 xtl 1 T	X lahar	68.14	36.08	0.03	0.01	33.55	0.02	0.16	0.42	27.96	0.09	0.00	0.04	98.36
01 xtl 1 T	X lahar	68.74	36.22	0.02	0.01	33.99	0.02	0.14	0.37	27.55	0.07	0.03	0.02	98.43
01 xtl 1 T	X lahar	69.56	36.41	0.04	0.00	34.50	0.00	0.16	0.34	26.91	0.13	0.02	0.03	98.53
01 xtl 1 T	X lahar	69.30	36.25	0.03	0.01	34.34	0.02	0.19	0.34	27.11	0.11	0.00	0.01	98.40
01 xtl 1 T	X lahar	69.18	36.43	0.02	0.01	34.22	-0.01	0.22	0.37	27.18	0.14	-0.01	0.06	98.65
01 xtl 1 T	X lahar	68.55	36.39	0.02	0.00	34.09	0.00	0.19	0.39	27.87	0.13	0.02	0.00	99.10
01 xtl 1 T	X lahar	68.67	36.31	0.04	0.00	33.74	0.01	0.16	0.39	27.45	0.11	-0.01	0.02	98.22
01 xtl 1 T	X lahar	67.75	36.25	0.02	0.00	33.38	0.00	0.16	0.40	28.32	0.12	0.01	0.04	98.70
01 xtl 1 T	X lahar	66.63	36.25	0.01	0.02	32.55	0.02	0.19	0.44	29.06	0.07	0.00	0.01	98.61
01 xtl 1 T	X lahar	65.64	35.93	0.01	0.01	31.90	0.00	0.20	0.44	29.77	0.08	0.01	0.01	98.36
01 xtl 1 T	X lahar	61.89	35.37	0.02	0.01	29.59	0.01	0.23	0.50	32.48	0.09	0.00	0.01	98.29
01 xtl 1 T	X lahar	58.87	34.92	0.00	0.02	27.65	0.03	0.23	0.54	34.44	0.06	0.00	0.07	97.98
01 xtl 3 lg	X lahar	77.88	37.80	0.03	0.02	39.93	0.00	0.14	0.25	20.22	0.17	0.00	0.02	98.57
01 xtl 3 lg	X lahar	79.02	37.98	0.04	0.00	40.74	-0.01	0.15	0.26	19.28	0.21	0.03	0.01	98.70
01 xtl 3 lg	X lahar	64.86	36.19	0.03	0.00	31.37	0.01	0.21	0.48	30.30	0.09	0.00	0.05	98.73
01 xtl 4 P	X lahar	69.44	36.50	0.03	0.00	34.32	0.00	0.16	0.37	26.92	0.12	0.02	0.00	98.45
01 xtl 4 P	X lahar	69.19	36.46	0.02	0.02	34.01	-0.01	0.15	0.36	27.00	0.12	0.01	0.01	98.16
01 xtl 4 P	X lahar	56.95	34.84	0.03	0.01	26.33	0.02	0.21	0.57	35.47	0.05	-0.03	0.05	97.56
01 xtl 4 P	X lahar	61.93	35.41	0.02	0.02	29.49	0.00	0.21	0.48	32.32	0.08	0.02	0.00	98.07
01 xtl 6 P	X lahar	78.21	38.31	0.03	0.00	40.09	0.00	0.13	0.25	19.91	0.27	0.00	0.00	98.99
01 xtl 6 P	X lahar	79.10	38.19	0.04	-0.01	40.87	0.02	0.14	0.22	19.25	0.27	0.03	0.03	99.06

Table D.1 (Continued)

Sample	Lithology	Fo	SiO_2	Al_2O_3	Na_2O	MgO	K_2O	CaO	MnO	FeO	NiO	Cr_2O_3	TiO_2	Total
01 xtl 6 P	X lahar	70.39	51.95	0.79	0.06	24.13	0.00	2.03	0.38	18.10	0.00	0.00	0.52	97.95
01 xtl 6 P	X lahar	70.78	51.69	0.85	0.06	24.21	0.00	2.12	0.38	17.82	0.03	0.02	0.68	97.85
01 xtl 7 P	X lahar	74.40	37.54	0.04	0.03	37.69	0.00	0.16	0.28	23.12	0.14	0.00	-0.03	98.98
01 xtl 7 P	X lahar	73.64	37.38	0.02	0.01	37.05	0.00	0.17	0.30	23.65	0.12	0.01	0.00	98.70
01 xtl 7 P	X lahar	62.83	35.68	0.01	0.02	30.21	0.00	0.21	0.44	31.86	0.07	-0.03	0.03	98.50
01 xtl 7 P	X lahar	62.84	35.75	0.06	0.03	30.26	0.02	0.24	0.45	31.90	0.09	0.00	0.05	98.84
01 xtl 8 small	X lahar	70.95	37.02	0.02	0.01	35.32	0.01	0.17	0.36	25.78	0.19	0.02	-0.01	98.89
01 xtl 8 small	X lahar	71.41	36.86	0.02	0.02	35.75	0.01	0.22	0.34	25.51	0.14	-0.01	0.03	98.89
01 xtl 8 small	X lahar	65.75	36.07	0.03	0.01	32.15	0.03	0.20	0.43	29.86	0.12	0.00	0.06	98.97
01 xtl 8 small	X lahar	63.79	35.66	0.04	0.01	30.80	0.00	0.23	0.45	31.16	0.09	0.00	0.05	98.51
01 xtl 10 rx rim	X lahar	79.51	37.96	0.01	0.01	41.10	-0.01	0.15	0.25	18.88	0.17	0.01	0.05	98.58
01 xtl 10 rx rim	X lahar	78.25	37.81	0.03	0.01	40.12	0.02	0.11	0.27	19.88	0.13	0.01	0.04	98.43
01 xtl 10 rx rim	X lahar	73.72	37.10	0.02	0.01	37.42	0.00	0.14	0.33	23.78	0.12	0.01	0.06	99.00
01 xtl 10 rx rim	X lahar	65.22	36.02	0.03	0.01	31.46	0.02	0.18	0.46	29.91	0.07	0.02	0.01	98.19
01 xtl 11 small	X lahar	72.05	37.20	0.01	0.02	36.15	-0.02	0.17	0.35	25.00	0.16	0.01	0.00	99.05
01 xtl 11 small	X lahar	71.22	37.10	0.02	0.01	35.83	0.02	0.14	0.32	25.81	0.15	0.00	0.04	99.44
01 xtl 11 small	X lahar	61.91	35.50	0.03	0.01	29.58	-0.01	0.24	0.50	32.44	0.10	0.01	0.06	98.47
01 xtl 2, spl 3	X lahar	83.77	39.08	0.04	0.00	44.10	0.00	0.15	0.16	15.24	0.29	0.06	0.01	99.12
01 xtl 2, spl 3	X lahar	83.71	39.24	0.03	-0.01	44.26	-0.01	0.14	0.13	15.35	0.32	0.03	0.01	99.50
01 xtl 2, spl 4	X lahar	77.19	38.31	0.04	0.02	39.74	0.00	0.17	0.27	20.93	0.21	0.10	0.04	99.82
01 xtl 2, spl 4	X lahar	76.88	37.67	0.05	0.00	39.47	0.01	0.14	0.27	21.16	0.19	0.02	0.03	99.02
01 xtl 3, spl 5	X lahar	81.39	38.53	0.08	0.00	42.47	0.00	0.16	0.22	17.31	0.29	0.19	0.02	99.27
01 xtl 3, spl 5	X lahar	82.10	38.73	0.03	0.00	42.89	0.00	0.14	0.21	16.67	0.24	0.07	0.02	98.98
01 xtl 3, spl 6	X lahar	77.53	37.92	0.05	0.02	39.92	0.00	0.14	0.30	20.62	0.23	0.08	0.02	99.29
01 xtl 3, spl 6	X lahar	79.68	38.26	0.04	0.00	41.38	0.00	0.15	0.27	18.81	0.23	0.06	0.00	99.20
01 xtl 4, spl 7	X lahar	79.08	38.42	0.04	0.01	40.89	-0.01	0.14	0.31	19.29	0.23	0.04	0.01	99.39
01 xtl 4, spl 7	X lahar	76.38	37.81	0.04	0.00	38.91	0.00	0.17	0.39	21.45	0.21	0.16	0.01	99.15
01 xtl 5, spl 8	X lahar	63.74	35.65	0.00	0.00	31.00	0.00	0.20	0.52	31.44	0.06	0.07	0.09	99.05
01 xtl 5, spl 8	X lahar	61.72	34.55	0.07	0.00	29.30	0.00	0.24	0.57	32.40	0.03	0.01	0.38	97.55
01 xtl 6, spl 9	X lahar	75.46	37.69	0.03	0.03	38.37	0.00	0.15	0.41	22.24	0.10	0.01	0.02	99.05
01 xtl 6, spl 9	X lahar	75.82	37.57	0.02	0.02	38.75	0.00	0.17	0.29	22.03	0.15	-0.01	0.01	98.98
01 xtl 2 T	X lahar	61.75	35.71	0.02	0.01	29.53	0.02	0.22	0.65	32.61	0.07	-0.03	0.05	98.87

Table D.1 (Continued)

Sample	Lithology	Fo	SiO_2	Al_2O_3	Na_2O	MgO	K_2O	CaO	MnO	FeO	NiO	Cr_2O_3	TiO_2	Total
01 xtl 2 T	X lahar	68.85	37.18	0.02	0.02	33.97	0.00	0.19	0.54	27.39	0.12	-0.04	0.01	99.40
01 xtl 2 T	X lahar	71.50	37.39	0.04	0.00	35.55	0.01	0.17	0.43	25.26	0.15	0.02	0.01	99.02
01 xtl 2 T	X lahar	73.90	37.85	0.02	0.00	37.46	-0.01	0.15	0.33	23.58	0.16	0.04	0.02	99.61
01 xtl 2 T	X lahar	76.33	38.04	0.02	0.01	39.01	0.01	0.13	0.28	21.57	0.19	0.02	0.01	99.31
01 xtl 2 T	X lahar	77.39	38.88	0.03	0.01	40.46	-0.01	0.13	0.26	21.07	0.28	-0.04	0.03	101.10
01 xtl 2 T	X lahar	79.53	38.56	0.03	0.02	41.03	-0.01	0.13	0.23	18.83	0.27	0.00	0.02	99.11
01 xtl 2 T	X lahar	80.56	38.42	0.03	0.01	41.83	0.00	0.13	0.27	17.99	0.22	0.04	0.01	98.94
01 xtl 2 T	X lahar	81.58	39.01	0.03	0.01	42.35	0.00	0.14	0.28	17.04	0.21	0.04	0.02	99.12
01 xtl 2 T	X lahar	82.10	39.12	0.03	0.01	42.77	0.00	0.14	0.20	16.62	0.22	0.06	0.00	99.18
01 xtl 2 T	X lahar	82.30	39.14	0.02	0.01	42.97	0.01	0.15	0.23	16.47	0.25	0.01	0.01	99.27
01 xtl 2 T	X lahar	82.65	39.05	0.06	0.01	42.58	-0.01	0.17	0.17	15.94	0.25	0.01	0.02	98.26
01 xtl 2 T	X lahar	83.19	39.32	0.04	0.01	43.98	0.01	0.15	0.24	15.84	0.36	0.00	0.02	99.96
01 xtl 2 T	X lahar	83.08	39.08	0.04	0.00	43.84	0.00	0.16	0.27	15.91	0.25	0.09	0.00	99.66
01 xtl 2 T	X lahar	83.45	39.33	0.05	-0.01	43.81	0.00	0.16	0.19	15.49	0.26	0.01	0.02	99.32
01 xtl 2 T	X lahar	83.52	39.02	0.05	0.01	43.20	-0.01	0.15	0.15	15.20	0.20	0.06	0.03	98.04
01 xtl 2 T	X lahar	83.58	39.40	0.03	0.02	43.69	0.01	0.15	0.25	15.31	0.29	0.01	0.00	99.16
01 xtl 2 T	X lahar	83.44	39.18	0.03	0.02	43.86	0.01	0.13	0.24	15.51	0.20	0.01	0.01	99.19
01 xtl 2 T	X lahar	83.71	39.30	0.02	0.00	43.64	0.00	0.14	0.25	15.13	0.24	0.03	0.01	98.77
01 xtl 2 T	X lahar	83.64	39.32	0.03	0.01	43.61	0.01	0.14	0.16	15.20	0.23	0.02	0.02	98.76
01 xtl 2 T	X lahar	83.71	39.69	0.04	0.01	43.92	0.00	0.14	0.24	15.24	0.31	0.01	0.01	99.62
01 xtl 2 T	X lahar	83.59	39.70	0.04	0.02	43.98	-0.01	0.15	0.18	15.39	0.26	0.07	0.01	99.79
01 xtl 2 T	X lahar	83.88	39.72	0.03	0.02	43.93	0.01	0.15	0.14	15.05	0.27	0.09	0.01	99.43
01 xtl 2 T	X lahar	83.93	39.86	0.03	0.01	43.81	-0.01	0.16	0.28	14.95	0.26	0.08	0.01	99.43
01 xtl 2 T	X lahar	84.37	32.71	0.04	0.04	43.18	0.01	0.19	0.14	14.26	0.22	0.08	0.01	90.88
01 xtl 2 T	X lahar	83.83	39.72	0.02	0.01	43.96	0.01	0.15	0.16	15.12	0.24	0.11	0.01	99.50
01 xtl 2 T	X lahar	83.91	39.58	0.02	0.00	43.97	0.01	0.14	0.19	15.03	0.25	0.10	0.01	99.31
01 xtl 2 T	X lahar	83.84	39.98	0.03	0.00	44.17	0.01	0.15	0.14	15.18	0.31	0.04	0.01	100.00
01 xtl 2 T	X lahar	83.98	39.57	0.04	0.01	43.92	0.01	0.15	0.17	14.93	0.26	0.07	0.00	99.12
01 xtl 2 T	X lahar	84.13	39.87	0.05	0.00	43.99	-0.01	0.14	0.25	14.80	0.33	-0.01	0.00	99.41
01 xtl 2 T	X lahar	83.85	39.77	0.04	0.02	43.97	0.00	0.15	0.22	15.10	0.30	-0.02	0.01	99.54
01 xtl 2 T	X lahar	84.02	39.63	0.04	0.00	44.05	0.00	0.14	0.25	14.94	0.29	0.02	0.00	99.38
01 xtl 2 T	X lahar	83.96	39.77	0.04	0.00	44.00	0.00	0.14	0.12	14.98	0.22	0.06	0.00	99.33

Table D.1 (Continued)

Sample	Lithology	Fo	SiO_2	Al_2O_3	Na_2O	MgO	K_2O	CaO	MnO	FeO	NiO	Cr_2O_3	TiO_2	Total
01 xtl 2 T	X lahar	84.02	39.59	0.02	0.02	44.07	0.00	0.15	0.19	14.95	0.24	0.02	0.01	99.25
01 xtl 2 T	X lahar	84.07	39.86	0.03	0.01	44.14	0.00	0.14	0.26	14.91	0.29	0.04	0.01	99.69
01 xtl 2 T	X lahar	84.05	40.14	0.02	0.00	44.05	0.01	0.14	0.13	14.90	0.23	0.02	0.00	99.63
01 xtl 2 T	X lahar	84.10	39.74	0.03	0.01	44.16	0.01	0.15	0.17	14.88	0.31	0.02	0.02	99.49
01 xtl 2 T	X lahar	83.84	39.77	0.03	0.01	44.10	0.01	0.15	0.21	15.15	0.31	0.00	0.01	99.73
01 xtl 2 T	X lahar	83.97	39.60	0.04	-0.01	44.06	0.01	0.14	0.25	14.99	0.26	0.00	0.00	99.35
01 xtl 2 T	X lahar	84.06	39.86	0.04	0.01	43.87	0.00	0.14	0.23	14.83	0.29	0.00	0.02	99.28
01 xtl 2 T	X lahar	83.92	39.60	0.03	0.00	44.00	0.01	0.14	0.20	15.02	0.23	0.06	0.03	99.31
01 xtl 2 T	X lahar	83.89	39.65	0.03	0.02	43.95	0.00	0.14	0.16	15.05	0.25	0.03	0.01	99.27
01 xtl 2 T	X lahar	84.00	39.91	0.02	0.01	43.90	0.00	0.15	0.20	14.91	0.29	0.03	0.01	99.41
01 xtl 2 T	X lahar	83.73	39.34	0.04	0.01	43.94	0.01	0.15	0.19	15.21	0.29	0.02	0.02	99.21
01 xtl 2 T	X lahar	83.92	39.26	0.02	0.00	43.78	0.01	0.14	0.21	14.95	0.22	0.00	0.02	98.61
01 xtl 2 T	X lahar	83.67	39.59	0.02	0.00	43.82	0.00	0.14	0.28	15.24	0.29	0.03	0.02	99.45
01 xtl 2 T	X lahar	83.64	39.32	0.03	0.01	43.75	0.02	0.14	0.10	15.26	0.30	0.04	0.00	98.97
01 xtl 2 T	X lahar	83.54	39.46	0.02	0.01	43.68	0.00	0.14	0.17	15.34	0.29	0.02	0.01	99.14
01 xtl 2 T	X lahar	83.43	39.48	0.03	0.02	43.44	0.00	0.15	0.15	15.38	0.26	-0.02	0.00	98.90
01 xtl 2 T	X lahar	83.11	39.27	0.04	0.01	43.42	0.00	0.14	0.20	15.72	0.25	0.04	0.02	99.12
01 xtl 2 T	X lahar	83.00	39.35	0.04	-0.01	43.17	0.01	0.12	0.22	15.76	0.28	0.07	0.01	99.03
01 xtl 2 T	X lahar	82.59	38.94	0.03	0.01	43.07	-0.01	0.15	0.23	16.18	0.25	-0.05	0.01	98.87
01 xtl 2 T	X lahar	82.24	39.30	0.06	0.01	42.94	0.00	0.14	0.19	16.53	0.28	0.07	0.02	99.54
01 xtl 2 T	X lahar	82.32	39.10	0.04	0.01	42.71	0.00	0.14	0.19	16.35	0.28	0.01	0.02	98.85
01 xtl 2 T	X lahar	81.87	39.10	0.05	0.02	42.46	0.01	0.13	0.20	16.76	0.25	0.05	0.00	99.03
01 xtl 2 T	X lahar	81.53	39.05	0.04	0.01	42.50	0.00	0.14	0.22	17.16	0.19	-0.02	0.02	99.32
01 xtl 2 T	X lahar	81.20	39.02	0.02	0.02	42.06	0.00	0.13	0.29	17.35	0.25	0.08	0.01	99.23
01 xtl 2 T	X lahar	80.16	39.24	0.70	0.20	40.10	0.18	0.14	0.23	17.69	0.25	0.04	0.07	98.85
01 xtl 2 T	X lahar	80.58	38.98	0.03	0.01	41.50	0.00	0.14	0.20	17.83	0.21	0.03	0.00	98.93
01 xtl 2 T	X lahar	80.40	38.96	0.05	0.01	41.72	0.01	0.13	0.22	18.13	0.26	0.06	0.02	99.56
01 xtl 2 T	X lahar	80.43	38.93	0.01	0.01	41.53	-0.01	0.13	0.21	18.02	0.26	0.02	0.02	99.14
01 xtl 2 T	X lahar	79.98	38.60	0.01	0.01	41.56	0.01	0.13	0.28	18.55	0.25	-0.02	0.00	99.40
01 xtl 2 T	X lahar	79.82	38.43	0.01	0.01	41.38	0.00	0.14	0.23	18.65	0.20	0.00	0.02	99.06
01 xtl 2 T	X lahar	79.70	38.75	0.02	0.00	41.06	0.00	0.14	0.24	18.64	0.25	0.10	0.00	99.19
01 xtl 2 T	X lahar	79.45	38.55	0.01	0.01	40.85	0.00	0.14	0.32	18.83	0.23	-0.02	0.01	98.94

Table D.1 (Continued)

Sample	Lithology	Fo	SiO_2	Al_2O_3	Na_2O	MgO	K_2O	CaO	MnO	FeO	NiO	Cr_2O_3	TiO_2	Total
01 xtl 2 T	X lahar	78.99	38.77	0.02	-0.01	40.80	0.00	0.13	0.29	19.35	0.26	0.01	0.01	99.65
01 xtl 2 T	X lahar	78.44	38.59	0.03	0.00	40.43	0.00	0.14	0.31	19.81	0.29	0.01	0.02	99.62
01 xtl 2 T	X lahar	78.07	38.32	0.01	0.03	40.04	0.01	0.13	0.24	20.06	0.21	0.03	0.01	99.08
01 xtl 2 T	X lahar	77.52	38.20	0.03	0.01	39.88	0.00	0.13	0.34	20.62	0.26	0.06	0.01	99.52
01 xtl 2 T	X lahar	77.52	38.46	0.02	0.01	39.61	0.00	0.12	0.29	20.48	0.20	-0.03	0.00	99.19
01 xtl 2 T	X lahar	77.06	38.36	0.01	0.00	39.50	0.00	0.13	0.23	20.96	0.23	0.01	0.01	99.46
01 xtl 2 T	X lahar	76.46	38.14	0.04	0.03	39.20	0.00	0.13	0.26	21.51	0.18	0.00	0.01	99.51
01 xtl 2 T	X lahar	76.45	38.24	0.03	0.04	38.77	0.01	0.14	0.36	21.29	0.26	0.04	0.00	99.19
01 xtl 2 T	X lahar	75.53	38.10	0.04	0.02	38.50	0.00	0.15	0.28	22.23	0.24	-0.02	0.01	99.56
01 xtl 2 T	X lahar	75.35	37.98	0.03	0.01	38.15	0.01	0.14	0.29	22.25	0.18	0.03	0.00	99.08
01 xtl 2 T	X lahar	74.63	37.78	0.04	0.03	37.78	0.01	0.14	0.32	22.90	0.14	0.04	0.02	99.19
01 xtl 2 T	X lahar	73.46	38.17	0.06	0.03	36.89	0.01	0.20	0.26	23.75	0.19	0.02	0.03	99.59
01 xtl 2 T	X lahar	73.00	37.37	0.07	0.01	37.03	0.00	0.15	0.39	24.42	0.20	0.07	0.01	99.71
01 xtl 2 T	X lahar	72.69	37.68	0.13	0.03	36.17	0.01	0.19	0.34	24.23	0.19	0.05	0.02	99.03
01 xtl 2 T	X lahar	72.16	37.86	0.24	0.06	35.98	0.04	0.26	0.35	24.75	0.16	0.06	0.04	99.79
01 xtl 2 T	X lahar	71.48	37.02	0.15	0.01	35.73	0.02	0.18	0.34	25.41	0.19	0.02	0.03	99.08
01 xtl 2 T	X lahar	71.64	37.24	0.11	0.02	35.64	0.03	0.16	0.35	25.15	0.13	-0.01	0.01	98.85
01 xtl 2 T	X lahar	71.52	37.47	0.09	0.02	35.76	0.03	0.16	0.34	25.38	0.15	0.02	0.00	99.42
01 xtl 2 T	X lahar	70.84	37.02	0.03	0.02	35.27	0.00	0.18	0.36	25.88	0.16	-0.01	0.00	98.93
01 xtl 2 T	X lahar	69.74	36.87	0.02	0.01	34.67	0.00	0.18	0.36	26.82	0.20	-0.02	0.01	99.14
01 xtl 2 T	X lahar	67.95	36.72	0.09	0.02	33.36	0.01	0.21	0.49	28.04	0.14	-0.07	0.03	99.12
01 xtl 2 T	X lahar	65.32	36.45	0.09	0.02	31.29	0.00	0.34	0.41	29.61	0.11	-0.01	0.14	98.45
01 xtl 2 T	X lahar	63.40	36.08	0.07	0.01	30.24	0.01	0.41	0.55	31.12	0.11	0.02	0.32	98.92
01 xtl 2 T	X lahar	62.54	36.39	0.06	0.01	29.85	0.01	0.31	0.52	31.87	0.11	-0.01	0.17	99.30
01 xtl 2 T	X lahar	62.93	35.39	0.06	0.00	29.95	0.01	0.22	0.57	31.46	0.13	-0.05	0.45	98.24
01 xtl 2 T	X lahar	63.22	36.00	0.03	0.01	30.39	0.01	0.27	0.38	31.51	0.11	0.00	0.11	98.84
01 xtl 2 T 2	X lahar	65.08	36.51	0.03	0.01	31.73	0.02	0.23	0.63	30.34	0.16	-0.01	0.07	99.73
01 xtl 2 T 2	X lahar	67.12	36.63	0.06	0.01	33.07	0.00	0.18	0.44	28.88	0.09	-0.01	0.02	99.38
01 xtl 2 T 2	X lahar	67.06	35.09	0.19	0.01	33.60	0.00	0.16	0.44	29.42	0.17	0.09	0.36	99.52
01 xtl 2 T 2	X lahar	73.44	37.00	0.09	0.04	36.64	0.00	0.17	0.34	23.62	0.25	0.05	0.02	98.20
01 xtl 2 T 2	X lahar	79.41	38.55	0.04	0.02	41.00	0.01	0.15	0.22	18.95	0.19	-0.04	0.02	99.14
01 xtl 2 T 2	X lahar	81.72	39.01	0.06	0.02	42.48	0.01	0.15	0.24	16.94	0.25	0.04	0.02	99.21

Table D.1 (Continued)

Sample	Lithology	Fo	SiO_2	Al_2O_3	Na_2O	MgO	K_2O	CaO	MnO	FeO	NiO	Cr_2O_3	TiO_2	Total
01 xtl 2 T 2	X lahar	82.54	39.25	0.03	0.00	43.06	0.00	0.15	0.24	16.23	0.31	-0.01	0.02	99.29
01 xtl 2 T 2	X lahar	82.48	39.55	0.13	0.02	42.16	0.01	0.19	0.19	15.96	0.24	0.05	0.02	98.51
01 xtl 2 T 2	X lahar	82.92	39.24	0.04	0.02	43.36	-0.01	0.15	0.18	15.92	0.27	0.05	0.00	99.23
01 xtl 2 T 2	X lahar	83.36	39.33	0.03	0.01	43.49	0.00	0.15	0.23	15.47	0.29	0.01	0.01	99.03
01 xtl 2 T 2	X lahar	83.27	38.77	0.03	0.02	43.62	0.00	0.14	0.22	15.62	0.27	0.04	0.01	98.74
01 xtl 2 T 2	X lahar	83.14	39.21	0.05	0.01	43.61	0.00	0.14	0.20	15.77	0.26	0.00	0.02	99.27
01 xtl 2 T 2	X lahar	83.48	39.27	0.04	0.01	43.58	0.00	0.15	0.20	15.37	0.22	0.02	0.00	98.86
01 xtl 2 T 2	X lahar	83.65	39.34	0.04	0.00	43.70	0.00	0.14	0.23	15.22	0.26	0.03	0.01	98.98
01 xtl 2 T 2	X lahar	83.85	39.39	0.03	0.01	43.96	0.00	0.14	0.24	15.09	0.26	-0.02	0.01	99.12
01 xtl 2 T 2	X lahar	83.63	39.50	0.01	0.02	43.88	0.00	0.14	0.16	15.31	0.26	0.07	0.02	99.37
01 xtl 2 T 2	X lahar	83.74	39.55	0.04	0.00	43.74	0.01	0.14	0.18	15.14	0.27	0.01	0.00	99.09
01 xtl 2 T 2	X lahar	83.83	39.51	0.02	0.00	44.01	0.00	0.14	0.15	15.13	0.27	0.01	0.01	99.25
01 xtl 2 T 2	X lahar	83.77	39.31	0.02	0.01	43.96	-0.01	0.15	0.22	15.18	0.27	0.02	0.00	99.16
01 xtl 2 T 2	X lahar	83.94	39.29	0.04	0.02	43.84	-0.01	0.15	0.15	14.95	0.24	0.03	0.01	98.72
01 xtl 2 T 2	X lahar	83.84	39.21	0.06	0.02	43.93	-0.01	0.15	0.17	15.10	0.23	0.01	0.00	98.87
01 xtl 2 T 2	X lahar	83.90	39.23	0.05	0.02	43.79	0.00	0.14	0.18	14.98	0.23	0.01	0.01	98.64
01 xtl 2 T 2	X lahar	84.03	39.35	0.03	0.00	43.98	0.00	0.15	0.18	14.90	0.29	0.08	0.00	98.96
01 xtl 2 T 2	X lahar	83.80	39.62	0.02	0.01	44.06	0.01	0.14	0.12	15.19	0.30	0.02	0.01	99.49
01 xtl 2 T 2	X lahar	83.90	39.40	0.03	0.01	44.13	0.00	0.14	0.22	15.10	0.29	0.01	0.00	99.33
01 xtl 2 T 2	X lahar	83.97	39.22	0.02	0.00	44.18	0.02	0.13	0.21	15.03	0.30	0.03	0.02	99.17
01 xtl 2 T 2	X lahar	83.98	39.32	0.02	0.02	44.12	0.00	0.14	0.20	15.00	0.31	0.03	0.01	99.17
01 xtl 2 T 2	X lahar	84.10	39.35	0.02	-0.01	44.10	0.01	0.13	0.23	14.86	0.25	0.02	0.01	98.99
01 xtl 2 T 2	X lahar	83.94	39.59	0.02	0.00	44.11	0.00	0.14	0.15	15.04	0.26	-0.01	0.01	99.33
01 xtl 2 T 2	X lahar	83.95	39.74	0.05	0.00	44.12	0.00	0.14	0.23	15.03	0.30	0.03	0.01	99.67
01 xtl 2 T 2	X lahar	84.03	39.38	0.04	0.00	44.12	0.01	0.14	0.16	14.94	0.28	0.00	0.00	99.06
01 xtl 2 T 2	X lahar	84.05	39.16	0.03	0.02	43.87	0.00	0.15	0.16	14.84	0.26	-0.05	0.00	98.49
01 xtl 2 T 2	X lahar	84.06	39.15	0.03	0.01	44.12	0.00	0.14	0.22	14.91	0.28	0.03	0.02	98.90
01 xtl 2 T 2	X lahar	83.87	39.13	0.04	0.02	44.03	0.00	0.14	0.17	15.10	0.28	-0.01	0.02	98.94
01 xtl 2 T 2	X lahar	83.77	39.38	0.01	0.00	44.17	0.00	0.13	0.21	15.25	0.27	0.04	0.00	99.46
01 xtl 2 T 2	X lahar	83.99	39.13	0.03	0.01	43.99	-0.01	0.13	0.20	14.95	0.32	-0.03	0.02	98.77
01 xtl 2 T 2	X lahar	83.62	39.25	0.02	-0.01	43.69	0.00	0.15	0.22	15.25	0.22	0.05	0.03	98.88
01 xtl 2 T 2	X lahar	82.65	38.96	0.02	0.01	43.12	0.00	0.13	0.14	16.13	0.26	0.03	0.01	98.82

Table D.1 (Continued)

Sample	Lithology	Fo	SiO_2	Al_2O_3	Na_2O	MgO	K_2O	CaO	MnO	FeO	NiO	Cr_2O_3	TiO_2	Total
01 xtl 2 T 2	X lahar	82.04	38.89	0.02	0.00	42.59	0.00	0.13	0.24	16.62	0.22	-0.01	0.02	98.73
01 xtl 2 T 2	X lahar	81.26	38.65	0.02	0.00	42.54	-0.01	0.14	0.20	17.48	0.21	0.00	0.02	99.26
01 xtl 2 T 2	X lahar	81.01	38.39	0.01	0.00	42.10	-0.01	0.13	0.24	17.59	0.27	0.01	0.03	98.77
01 xtl 2 T 2	X lahar	80.12	38.57	0.02	0.00	41.50	0.00	0.14	0.25	18.36	0.24	0.01	0.01	99.10
01 xtl 2 T 2	X lahar	79.27	38.29	0.02	-0.01	41.16	0.02	0.14	0.26	19.19	0.19	0.00	0.01	99.28
01 xtl 2 T 2	X lahar	78.67	38.25	0.00	0.01	40.59	0.00	0.13	0.19	19.62	0.20	0.00	0.00	99.00
01 xtl 2 T 2	X lahar	77.57	38.24	0.01	0.00	39.93	0.01	0.14	0.34	20.59	0.21	-0.03	0.00	99.47
01 xtl 2 T 2	X lahar	76.79	38.16	0.00	0.00	39.29	0.00	0.14	0.27	21.17	0.18	-0.01	0.01	99.22
01 xtl 2 T 2	X lahar	76.29	37.79	0.02	0.01	38.72	0.00	0.15	0.32	21.45	0.18	-0.01	0.01	98.64
01 xtl 2 T 2	X lahar	75.31	37.61	0.04	0.01	38.36	0.00	0.13	0.29	22.42	0.20	-0.04	0.01	99.07
01 xtl 2 T 2	X lahar	74.05	37.43	0.01	0.01	37.57	-0.01	0.13	0.32	23.47	0.17	-0.01	0.01	99.12
01 xtl 2 T 2	X lahar	73.05	37.34	0.01	0.02	36.98	-0.01	0.14	0.30	24.31	0.18	0.01	0.01	99.30
01 xtl 2 T 2	X lahar	72.04	37.15	0.01	0.03	36.32	0.01	0.13	0.37	25.12	0.17	0.06	0.02	99.39
01 xtl 2 T 2	X lahar	71.26	37.31	0.05	0.01	35.71	0.01	0.16	0.37	25.67	0.15	-0.03	0.01	99.45
01 xtl 2 T 2	X lahar	70.69	37.02	0.03	0.02	35.32	0.01	0.17	0.32	26.11	0.15	0.00	0.03	99.18
01 xtl 2 T 2	X lahar	69.65	36.37	0.08	0.03	33.82	0.01	0.23	0.34	26.27	0.17	0.01	0.03	97.35
01 xtl 2 T 2	X lahar	69.69	36.87	0.06	0.02	34.48	0.01	0.25	0.49	26.72	0.12	0.10	0.03	99.15
02 xtl 2 T	X lahar	68.97	39.46	1.67	0.81	32.99	0.08	0.51	0.40	26.45	0.10	0.02	0.26	102.77
02 xtl 2 T	X lahar	74.73	38.06	-0.07	-0.03	38.70	0.02	0.17	0.33	23.33	0.11	0.02	0.04	100.76
02 xtl 2 T	X lahar	75.13	38.16	-0.09	-0.04	38.98	0.02	0.15	0.32	23.00	0.14	0.02	-0.02	100.79
02 xtl 2 T	X lahar	75.62	38.26	-0.08	-0.04	39.18	0.01	0.17	0.33	22.52	0.11	0.01	-0.02	100.60
02 xtl 2 T	X lahar	75.91	38.21	-0.07	-0.04	39.69	0.01	0.18	0.33	22.46	0.15	0.03	-0.02	101.08
02 xtl 2 T	X lahar	76.61	38.48	-0.09	-0.03	40.14	0.00	0.17	0.28	21.84	0.13	0.01	0.01	101.07
02 xtl 2 T	X lahar	77.09	38.32	-0.07	-0.02	40.47	0.00	0.16	0.29	21.44	0.16	0.01	-0.01	100.85
02 xtl 2 T	X lahar	77.04	37.74	0.24	-0.01	39.38	0.03	0.19	0.26	20.92	0.13	0.00	0.01	98.90
02 xtl 2 T	X lahar	77.93	38.91	-0.07	-0.04	41.21	0.01	0.18	0.27	20.80	0.15	0.01	-0.03	101.53
02 xtl 2 T	X lahar	77.89	38.46	-0.08	-0.03	41.01	0.02	0.18	0.29	20.75	0.18	0.03	0.00	100.92
02 xtl 2 T	X lahar	77.99	38.43	-0.08	-0.04	40.88	0.02	0.16	0.28	20.57	0.15	0.02	0.02	100.53
02 xtl 2 T	X lahar	77.90	38.40	-0.07	-0.03	40.79	0.01	0.17	0.27	20.63	0.16	0.02	-0.01	100.45
02 xtl 2 T	X lahar	78.06	38.41	-0.07	-0.03	40.94	0.02	0.17	0.27	20.51	0.15	0.01	0.02	100.49
02 xtl 2 T	X lahar	77.88	38.40	-0.07	-0.05	41.09	0.03	0.18	0.27	20.80	0.17	0.01	0.02	100.98
02 xtl 2 T	X lahar	78.18	38.46	-0.07	-0.02	41.05	0.01	0.17	0.28	20.43	0.14	0.03	0.01	100.58

Table D.1 (Continued)

Sample	Lithology	Fo	SiO_2	Al_2O_3	Na_2O	MgO	K_2O	CaO	MnO	FeO	NiO	Cr_2O_3	TiO_2	Total
02 xtl 2 T	X lahar	78.02	38.45	-0.09	-0.03	40.98	0.01	0.19	0.28	20.58	0.17	0.00	0.05	100.71
02 xtl 2 T	X lahar	78.44	38.42	-0.08	-0.04	41.10	0.02	0.18	0.28	20.14	0.16	0.01	0.01	100.33
02 xtl 2 T	X lahar	78.52	38.43	-0.08	-0.04	41.08	0.01	0.18	0.27	20.04	0.15	0.01	0.06	100.22
02 xtl 2 T	X lahar	78.19	38.42	-0.07	-0.03	41.02	0.02	0.18	0.27	20.39	0.17	0.02	0.04	100.54
02 xtl 2 T	X lahar	78.16	38.26	-0.08	-0.03	40.74	0.01	0.20	0.28	20.29	0.14	0.01	0.05	99.98
02 xtl 2 T	X lahar	77.84	38.41	-0.06	-0.03	40.63	0.01	0.19	0.28	20.62	0.18	0.02	0.03	100.37
02 xtl 2 T	X lahar	77.39	38.31	-0.07	-0.02	40.40	0.01	0.17	0.29	21.04	0.14	0.01	0.02	100.40
02 xtl 2 T	X lahar	75.50	37.96	-0.07	-0.04	39.20	0.02	0.19	0.29	22.67	0.13	0.02	-0.02	100.46
02 xtl 1 T	X lahar	69.75	36.72	-0.07	-0.05	35.22	0.02	0.18	0.41	27.23	0.12	0.02	0.11	100.04
02 xtl 1 T	X lahar	73.35	37.59	-0.09	-0.03	38.05	0.00	0.15	0.34	24.64	0.11	0.01	-0.03	100.89
02 xtl 1 T	X lahar	73.08	36.67	-0.08	-0.04	37.18	0.00	0.16	0.35	24.41	0.10	0.03	0.00	98.91
02 xtl 1 T	X lahar	73.28	37.41	-0.09	-0.03	37.83	0.00	0.15	0.36	24.59	0.11	0.00	0.03	100.49
02 xtl 1 T	X lahar	73.15	37.48	-0.09	-0.04	37.78	0.00	0.15	0.37	24.71	0.09	0.02	0.00	100.60
02 xtl 1 T	X lahar	73.34	37.45	-0.08	-0.03	37.83	-0.01	0.15	0.38	24.52	0.12	0.01	0.04	100.51
02 xtl 1 T	X lahar	73.13	37.43	-0.08	-0.04	37.76	0.01	0.15	0.34	24.73	0.10	0.01	0.04	100.57
02 xtl 1 T	X lahar	73.19	37.76	-0.08	-0.04	37.79	0.02	0.16	0.34	24.68	0.12	0.02	0.00	100.87
02 xtl 1 T	X lahar	73.36	37.51	-0.09	-0.03	37.87	0.00	0.14	0.34	24.52	0.11	0.01	0.04	100.54
02 xtl 1 T	X lahar	73.14	37.45	-0.08	-0.04	37.84	0.00	0.13	0.37	24.77	0.11	0.00	0.07	100.74
02 xtl 1 T	X lahar	72.56	37.13	-0.09	-0.04	37.29	0.01	0.15	0.36	25.14	0.13	0.03	0.04	100.27
02 xtl 1 T	X lahar	70.71	37.01	-0.09	-0.04	36.19	0.02	0.16	0.38	26.72	0.12	0.02	0.10	100.73
02 xtl 1 T	X lahar	68.23	36.65	-0.08	-0.03	34.43	0.02	0.15	0.45	28.58	0.12	0.01	0.12	100.52
02 xtl 1 T	X lahar	68.66	37.10	0.28	0.09	34.24	0.08	0.18	0.39	27.86	0.11	0.03	0.28	100.64
02 xtl 1 T	X lahar	72.41	37.14	-0.07	-0.03	37.47	0.02	0.15	0.35	25.45	0.12	0.01	0.26	100.97
02 xtl 1 T	X lahar	73.23	36.86	-0.08	-0.05	37.56	0.01	0.15	0.36	24.47	0.10	0.01	0.20	99.73
02 xtl 1 T	X lahar	73.26	37.51	-0.08	-0.05	38.02	0.01	0.15	0.35	24.73	0.10	0.00	0.13	101.01
02 xtl 1 T	X lahar	73.86	36.60	-0.05	-0.04	38.22	0.03	0.16	0.36	24.11	0.10	0.01	0.13	99.71
02 xtl 1 T	X lahar	73.14	37.68	-0.07	-0.04	37.79	0.02	0.15	0.35	24.74	0.12	0.00	0.10	100.94
02 xtl 1 T	X lahar	70.83	37.27	-0.08	-0.04	36.08	0.01	0.17	0.37	26.49	0.11	0.00	0.06	100.56
02 xtl 3 T	X lahar	68.82	36.77	-0.06	-0.04	34.53	0.02	0.19	0.44	27.88	0.09	0.01	0.04	99.97
02 xtl 3 T	X lahar	74.54	37.86	-0.08	-0.04	38.47	0.02	0.16	0.32	23.42	0.12	0.03	-0.02	100.39
02 xtl 3 T	X lahar	75.22	37.74	-0.08	-0.03	38.79	0.02	0.18	0.34	22.78	0.14	0.02	-0.01	100.01
02 xtl 3 T	X lahar	75.19	37.67	-0.08	-0.04	38.92	0.01	0.16	0.31	22.89	0.12	0.02	0.01	100.11

Table D.1 (Continued)

Sample	Lithology	Fo	SiO_2	Al_2O_3	Na_2O	MgO	K_2O	CaO	MnO	FeO	NiO	Cr_2O_3	TiO_2	Total
02 xtl 3 T	X lahar	75.62	37.43	-0.08	-0.05	39.23	0.01	0.17	0.32	22.55	0.12	0.02	-0.03	99.85
02 xtl 3 T	X lahar	75.89	37.91	-0.08	-0.03	39.36	0.00	0.16	0.31	22.29	0.16	0.02	0.03	100.25
02 xtl 3 T	X lahar	76.16	37.92	-0.08	-0.02	39.22	0.01	0.18	0.31	21.88	0.12	0.01	0.03	99.68
02 xtl 3 T	X lahar	76.11	37.93	-0.08	-0.06	39.65	0.02	0.16	0.30	22.18	0.16	0.02	0.03	100.45
02 xtl 3 T	X lahar	76.43	37.74	-0.07	-0.05	39.65	0.00	0.15	0.30	21.80	0.15	0.02	0.00	99.80
02 xtl 3 T	X lahar	76.49	37.92	-0.09	-0.05	39.90	0.00	0.17	0.28	21.87	0.14	0.03	0.06	100.37
02 xtl 3 T	X lahar	76.43	37.96	-0.09	-0.04	40.06	-0.01	0.17	0.28	22.02	0.17	0.02	0.03	100.71
02 xtl 3 T	X lahar	76.43	37.80	-0.08	-0.05	39.98	0.00	0.17	0.31	21.98	0.17	0.01	-0.03	100.42
02 xtl 3 T	X lahar	76.27	37.73	-0.08	-0.05	39.75	0.02	0.16	0.30	22.04	0.14	0.01	0.04	100.19
02 xtl 3 T	X lahar	76.16	37.84	-0.08	-0.04	39.72	0.00	0.16	0.29	22.16	0.13	0.01	0.01	100.33
02 xtl 3 T	X lahar	75.69	37.69	-0.08	-0.05	39.50	0.00	0.16	0.31	22.61	0.15	0.00	0.05	100.47
02 xtl 3 T	X lahar	75.49	37.51	-0.08	-0.05	39.23	0.01	0.18	0.31	22.71	0.13	0.02	-0.01	100.10
02 xtl 3 T	X lahar	75.34	37.73	-0.07	-0.05	39.10	0.00	0.18	0.32	22.81	0.14	0.02	0.02	100.31
02 xtl 4 T	X lahar	70.54	36.01	0.96	-0.03	34.20	0.02	0.16	0.37	25.46	0.10	0.02	0.09	97.37
02 xtl 4 T	X lahar	74.78	37.40	-0.08	-0.03	38.74	0.02	0.16	0.35	23.29	0.12	0.03	0.05	100.16
02 xtl 4 T	X lahar	75.01	37.71	-0.08	-0.04	38.75	0.01	0.16	0.32	23.02	0.11	0.01	0.05	100.14
02 xtl 4 T	X lahar	75.07	37.65	-0.08	-0.04	38.74	0.01	0.16	0.32	22.94	0.14	0.01	0.04	100.01
02 xtl 4 T	X lahar	75.04	37.74	-0.08	-0.05	38.97	0.01	0.16	0.31	23.11	0.13	0.02	-0.01	100.46
02 xtl 4 T	X lahar	75.17	37.64	-0.09	-0.04	39.12	0.01	0.17	0.30	23.04	0.14	0.02	0.01	100.45
02 xtl 4 T	X lahar	75.79	37.49	-0.08	-0.03	39.42	0.00	0.16	0.31	22.44	0.15	0.02	0.00	100.00
02 xtl 4 T	X lahar	75.66	37.93	-0.07	-0.05	39.41	0.02	0.16	0.31	22.59	0.15	0.02	0.02	100.62
02 xtl 4 T	X lahar	76.00	37.78	-0.08	-0.04	39.52	0.01	0.17	0.31	22.25	0.14	0.01	0.00	100.20
02 xtl 4 T	X lahar	75.87	37.73	-0.08	-0.04	39.34	0.01	0.17	0.29	22.30	0.14	0.02	0.05	100.06
02 xtl 4 T	X lahar	76.02	37.74	-0.07	-0.05	39.53	0.01	0.15	0.29	22.23	0.14	0.01	-0.01	100.09
02 xtl 4 T	X lahar	76.18	37.78	-0.07	-0.03	39.63	0.00	0.17	0.29	22.09	0.15	0.00	-0.03	100.11
02 xtl 4 T	X lahar	76.32	37.59	-0.08	-0.05	39.67	0.01	0.16	0.30	21.95	0.13	0.02	0.02	99.85
02 xtl 4 T	X lahar	76.25	37.71	-0.08	-0.04	39.73	0.00	0.16	0.29	22.06	0.17	0.01	0.01	100.14
02 xtl 4 T	X lahar	76.46	38.02	-0.08	-0.03	40.02	0.00	0.15	0.30	21.96	0.16	0.01	-0.02	100.61
02 xtl 4 T	X lahar	76.26	37.94	-0.08	-0.04	39.81	0.02	0.16	0.28	22.09	0.16	0.03	0.02	100.52
02 xtl 4 T	X lahar	76.47	38.06	-0.08	-0.04	39.93	0.00	0.15	0.31	21.90	0.15	0.00	0.05	100.55
02 xtl 4 T	X lahar	76.31	37.88	-0.08	-0.03	39.74	0.03	0.15	0.31	21.99	0.16	0.01	0.02	100.29
02 xtl 4 T	X lahar	75.96	37.87	-0.07	-0.03	39.10	-0.01	0.17	0.30	22.05	0.14	0.01	-0.02	99.63

Table D.1 (Continued)

Sample	Lithology	Fo	SiO_2	Al_2O_3	Na_2O	MgO	K_2O	CaO	MnO	FeO	NiO	Cr_2O_3	TiO_2	Total
02 xtl 4 T	X lahar	75.72	36.86	-0.07	-0.04	38.51	0.01	0.18	0.27	22.01	0.14	0.01	-0.01	98.00
02 xtl 4 T	X lahar	75.52	37.75	-0.08	-0.04	39.16	0.00	0.15	0.31	22.63	0.14	0.02	0.01	100.16
02 xtl 4 T	X lahar	75.46	38.26	-0.07	-0.04	39.40	0.02	0.17	0.31	22.84	0.14	0.01	0.04	101.20
02 xtl 4 T	X lahar	75.30	37.73	-0.08	-0.03	38.78	0.02	0.15	0.33	22.67	0.12	0.02	0.02	99.84
02 xtl 4 T	X lahar	73.02	37.15	-0.08	-0.05	37.56	0.01	0.16	0.32	24.74	0.12	0.01	0.03	100.11
02 xtl 4 T	X lahar	64.22	38.75	1.96	0.63	28.51	0.54	0.43	0.46	28.31	0.09	0.02	0.15	99.85
02 xtl 5 T	X lahar	74.84	38.20	-0.07	-0.04	38.32	0.00	0.17	0.31	22.96	0.11	0.01	0.03	100.11
02 xtl 5 T	X lahar	76.39	37.92	-0.08	-0.04	39.99	0.02	0.16	0.30	22.04	0.17	0.01	0.00	100.61
02 xtl 5 T	X lahar	77.46	38.12	-0.08	-0.06	40.60	0.02	0.15	0.29	21.06	0.16	0.00	0.01	100.41
02 xtl 5 T	X lahar	77.98	38.06	-0.08	-0.04	41.09	-0.02	0.17	0.29	20.69	0.16	0.02	0.04	100.52
02 xtl 5 T	X lahar	78.59	38.03	-0.06	-0.05	41.24	-0.01	0.16	0.29	20.03	0.18	0.01	0.04	99.98
02 xtl 5 T	X lahar	78.71	38.15	-0.08	-0.04	41.60	0.00	0.16	0.27	20.06	0.17	0.02	-0.02	100.42
02 xtl 5 T	X lahar	78.95	38.32	-0.08	-0.04	41.59	-0.02	0.17	0.29	19.76	0.19	0.02	-0.04	100.34
02 xtl 5 T	X lahar	79.08	38.27	-0.08	-0.05	41.75	0.00	0.14	0.28	19.69	0.20	0.02	-0.03	100.35
02 xtl 5 T	X lahar	79.27	38.44	-0.08	-0.04	42.03	0.01	0.15	0.27	19.59	0.20	0.02	-0.02	100.70
02 xtl 5 T	X lahar	79.23	38.07	-0.09	-0.04	41.82	0.00	0.15	0.24	19.55	0.20	0.00	0.02	100.06
02 xtl 5 T	X lahar	79.36	38.26	-0.07	-0.03	41.84	-0.01	0.15	0.26	19.40	0.19	0.03	0.00	100.14
02 xtl 5 T	X lahar	79.18	38.19	-0.08	-0.04	41.60	-0.01	0.16	0.26	19.50	0.23	0.02	0.00	99.96
02 xtl 5 T	X lahar	78.82	38.10	-0.08	-0.04	41.38	0.00	0.15	0.25	19.82	0.22	0.01	-0.04	99.93
02 xtl 5 T	X lahar	78.26	38.06	-0.09	-0.05	40.91	0.01	0.16	0.26	20.25	0.18	0.01	-0.05	99.84
02 xtl 5 T	X lahar	77.19	37.95	-0.08	-0.05	40.46	0.00	0.15	0.30	21.32	0.14	0.01	0.03	100.37
02 xtl 5 T	X lahar	76.73	37.48	-0.08	-0.05	40.22	0.00	0.17	0.29	21.75	0.17	0.01	-0.02	100.10
02 xtl 5 T	X lahar	76.89	37.90	-0.08	-0.05	40.29	0.03	0.17	0.31	21.59	0.15	0.01	-0.02	100.44
02 xtl 5 T	X lahar	76.59	37.59	-0.08	-0.04	40.25	0.01	0.14	0.31	21.93	0.14	0.02	-0.02	100.39
02 xtl 5 T	X lahar	76.86	37.99	-0.08	-0.04	40.31	0.02	0.17	0.28	21.63	0.16	0.01	0.01	100.58
02 xtl 5 T	X lahar	77.23	38.10	-0.08	-0.06	40.41	0.01	0.15	0.30	21.24	0.16	0.02	0.14	100.54
02 xtl 5 T	X lahar	77.72	38.19	-0.08	-0.04	40.73	0.00	0.16	0.27	20.81	0.17	0.01	-0.03	100.34
02 xtl 5 T	X lahar	77.82	37.06	-0.04	-0.03	40.55	0.01	0.16	0.27	20.61	0.20	0.03	0.01	98.90
02 xtl 5 T	X lahar	77.85	37.98	-0.09	-0.03	40.85	0.00	0.16	0.28	20.72	0.19	0.02	0.03	100.24
02 xtl 5 T	X lahar	78.25	38.01	-0.08	-0.04	41.31	-0.01	0.16	0.28	20.47	0.16	0.02	0.00	100.43
02 xtl 5 T	X lahar	78.47	37.56	0.10	-0.04	41.37	0.00	0.15	0.26	20.23	0.16	0.01	-0.02	99.86
02 xtl 5 T	X lahar	78.61	38.15	-0.08	-0.04	41.38	0.00	0.17	0.28	20.07	0.21	0.02	0.01	100.30

Table D.1 (Continued)

Sample	Lithology	Fo	SiO_2	Al_2O_3	Na_2O	MgO	K_2O	CaO	MnO	FeO	NiO	Cr_2O_3	TiO_2	Total
02 xtl 5 T	X lahar	78.59	38.05	-0.09	-0.03	41.47	0.01	0.15	0.25	20.14	0.20	0.02	-0.01	100.29
02 xtl 5 T	X lahar	78.68	38.26	-0.08	-0.05	41.43	0.00	0.15	0.27	20.01	0.21	0.01	0.02	100.37
02 xtl 5 T	X lahar	78.83	38.35	-0.08	-0.03	41.53	0.01	0.15	0.26	19.88	0.20	0.02	-0.02	100.40
02 xtl 5 T	X lahar	78.93	38.35	-0.08	-0.05	41.60	0.01	0.15	0.26	19.79	0.21	0.01	0.03	100.43
02 xtl 5 T	X lahar	78.78	38.20	-0.08	-0.05	41.50	0.02	0.16	0.30	19.92	0.18	0.00	0.03	100.31
02 xtl 5 T	X lahar	78.77	38.42	-0.08	-0.03	41.73	0.03	0.16	0.26	20.04	0.20	0.02	-0.01	100.85
02 xtl 5 T	X lahar	78.83	38.28	-0.07	-0.04	41.69	0.00	0.15	0.25	19.95	0.21	0.03	0.02	100.59
02 xtl 5 T	X lahar	78.81	37.87	-0.08	-0.05	41.63	0.00	0.16	0.28	19.96	0.18	0.02	-0.02	100.09
02 xtl 5 T	X lahar	78.87	38.36	-0.07	-0.04	41.62	0.00	0.16	0.28	19.87	0.20	0.01	-0.01	100.51
02 xtl 5 T	X lahar	78.72	38.19	-0.07	-0.05	41.52	0.01	0.15	0.26	20.01	0.18	0.02	-0.04	100.33
02 xtl 5 T	X lahar	78.56	38.24	-0.06	-0.03	41.41	0.01	0.15	0.28	20.15	0.20	0.03	0.02	100.48
02 xtl 5 T	X lahar	78.35	38.43	-0.07	-0.03	41.40	0.00	0.17	0.28	20.39	0.20	0.01	0.03	100.90
02 xtl 5 T	X lahar	78.07	38.22	-0.07	-0.05	41.10	0.01	0.17	0.28	20.58	0.18	0.03	0.02	100.59
02 xtl 5 T	X lahar	77.66	38.24	-0.07	-0.04	40.99	0.00	0.17	0.29	21.02	0.17	0.02	-0.05	100.89
02 xtl 5 T	X lahar	77.42	38.18	-0.08	-0.04	40.62	0.01	0.16	0.30	21.12	0.20	0.00	0.02	100.61
02 xtl 5 T	X lahar	77.24	37.93	-0.08	-0.04	40.49	0.00	0.15	0.31	21.27	0.19	0.01	-0.04	100.35
02 xtl 5 T	X lahar	77.25	38.02	-0.07	-0.04	40.52	0.02	0.16	0.30	21.27	0.16	0.00	0.00	100.45
02 xtl 5 T	X lahar	76.88	37.84	0.10	-0.04	39.41	0.02	0.15	0.27	21.12	0.16	0.02	0.00	99.10
02 xtl 5 T	X lahar	77.48	38.00	-0.08	-0.05	40.69	-0.01	0.16	0.28	21.08	0.15	0.02	-0.03	100.38
02 xtl 5 T	X lahar	77.71	38.07	-0.07	-0.05	40.86	0.01	0.16	0.29	20.89	0.19	0.01	0.03	100.52
02 xtl 5 T	X lahar	77.65	38.20	-0.09	-0.04	40.86	0.02	0.15	0.28	20.96	0.17	0.02	0.01	100.67
02 xtl 5 T	X lahar	78.01	38.11	-0.08	-0.04	40.94	0.01	0.15	0.28	20.58	0.20	0.03	-0.01	100.30
02 xtl 5 T	X lahar	77.59	38.16	-0.07	-0.03	40.75	0.01	0.17	0.26	20.98	0.19	0.01	0.01	100.53
02 xtl 5 T	X lahar	77.61	38.08	-0.07	-0.04	40.76	-0.01	0.15	0.28	20.96	0.16	0.02	-0.05	100.42
02 xtl 5 T	X lahar	77.28	37.77	-0.08	-0.03	40.56	0.01	0.16	0.26	21.25	0.18	0.02	0.02	100.24
02 xtl 5 T	X lahar	77.65	37.72	-0.08	-0.02	40.78	-0.01	0.17	0.28	20.93	0.17	0.01	-0.01	100.05
02 xtl 5 T	X lahar	77.77	38.19	-0.07	-0.06	40.83	0.01	0.16	0.25	20.80	0.18	0.02	-0.04	100.43
02 xtl 5 T	X lahar	77.81	38.15	-0.08	-0.04	40.89	0.00	0.16	0.29	20.78	0.20	0.04	0.02	100.54
02 xtl 5 T	X lahar	77.68	38.08	-0.07	-0.04	40.81	0.00	0.16	0.30	20.90	0.16	0.02	0.03	100.46
02 xtl 5 T	X lahar	77.57	38.19	-0.08	-0.04	40.87	0.02	0.17	0.29	21.06	0.19	0.02	-0.01	100.80
02 xtl 5 T	X lahar	77.54	37.75	-0.08	-0.05	40.96	0.00	0.16	0.28	21.15	0.16	0.01	0.01	100.48
02 xtl 5 T	X lahar	77.53	37.78	-0.08	-0.04	40.71	0.01	0.16	0.28	21.03	0.20	0.03	-0.05	100.22

Table D.1 (Continued)

Sample	Lithology	Fo	SiO_2	Al_2O_3	Na_2O	MgO	K_2O	CaO	MnO	FeO	NiO	Cr_2O_3	TiO_2	Total
02 xtl 5 T	X lahar	77.25	37.57	-0.08	-0.03	40.59	0.01	0.16	0.28	21.31	0.19	0.01	0.03	100.15
02 xtl 5 T	X lahar	76.99	37.66	-0.08	-0.03	40.27	0.01	0.16	0.28	21.46	0.16	0.02	0.00	100.01
02 xtl 5 T	X lahar	76.52	37.91	-0.08	-0.04	40.07	0.02	0.16	0.30	21.92	0.16	0.02	-0.01	100.56
02 xtl 5 T	X lahar	76.32	37.90	-0.08	-0.03	39.82	-0.01	0.15	0.31	22.02	0.16	0.03	-0.02	100.40
02 xtl 5 T	X lahar	75.96	37.87	-0.08	-0.05	39.80	0.00	0.17	0.30	22.45	0.16	0.05	-0.01	100.79
02 xtl 5 T	X lahar	75.75	37.69	-0.07	-0.03	39.53	0.00	0.15	0.30	22.55	0.11	0.00	0.00	100.33
02 xtl 5 T	X lahar	75.66	37.94	-0.08	-0.03	39.55	-0.01	0.17	0.33	22.68	0.16	0.02	0.00	100.85
02 xtl 5 T	X lahar	75.71	37.80	-0.09	-0.04	39.50	-0.01	0.15	0.27	22.59	0.12	0.02	0.06	100.51
02 xtl 5 T	X lahar	75.49	37.34	-0.06	-0.04	39.11	0.02	0.15	0.32	22.63	0.15	0.03	-0.02	99.75
02 xtl 5 T	X lahar	75.65	37.84	-0.07	-0.06	39.46	0.00	0.15	0.29	22.64	0.16	0.01	0.01	100.55
02 xtl 5 T	X lahar	75.69	37.46	-0.08	-0.05	39.58	-0.01	0.15	0.32	22.66	0.15	0.01	-0.02	100.35
02 xtl 5 T	X lahar	75.79	37.90	-0.09	-0.04	39.49	0.00	0.16	0.33	22.48	0.13	0.02	-0.02	100.52
02 xtl 5 T	X lahar	75.75	37.33	-0.09	-0.04	39.46	0.01	0.16	0.33	22.52	0.14	0.01	0.02	99.99
02 xtl 5 T	X lahar	75.47	37.75	-0.08	-0.02	39.45	0.02	0.14	0.32	22.86	0.15	0.02	0.01	100.73
02 xtl 5 T	X lahar	75.38	37.66	-0.08	-0.05	39.29	0.02	0.14	0.29	22.88	0.15	0.00	0.01	100.43
02 xtl 5 T	X lahar	75.37	37.78	-0.08	-0.04	39.33	0.01	0.15	0.34	22.91	0.15	0.02	0.00	100.69
02 xtl 5 T	X lahar	75.35	37.11	-0.07	-0.04	39.14	0.01	0.14	0.30	22.82	0.14	0.01	-0.02	99.68
02 xtl 5 T	X lahar	74.93	37.91	-0.08	-0.03	39.01	0.01	0.16	0.34	23.27	0.13	0.02	0.00	100.86
02 xtl 5 T	X lahar	75.25	37.32	-0.08	-0.05	39.11	0.01	0.14	0.30	22.93	0.15	0.01	0.04	100.01
02 xtl 5 T	X lahar	75.16	37.47	0.57	-0.04	38.77	0.02	0.16	0.31	22.84	0.14	0.01	0.04	100.33
02 xtl 5 T	X lahar	75.49	37.74	-0.08	-0.04	39.42	-0.01	0.14	0.31	22.81	0.13	0.01	-0.02	100.56
02 xtl 5 T	X lahar	75.86	37.79	-0.06	-0.05	39.53	0.01	0.14	0.31	22.42	0.14	0.02	0.03	100.40
02 xtl 5 T	X lahar	75.89	38.03	-0.07	-0.04	39.70	0.02	0.15	0.30	22.48	0.16	0.02	0.03	100.89
02 xtl 5 T	X lahar	75.94	37.51	-0.08	-0.04	39.74	0.01	0.15	0.30	22.45	0.15	0.01	0.01	100.33
02 xtl 5 T	X lahar	76.15	37.64	-0.09	-0.04	39.88	0.02	0.15	0.29	22.26	0.16	0.02	-0.04	100.42
02 xtl 5 T	X lahar	75.98	37.81	-0.08	-0.04	39.82	0.02	0.16	0.28	22.45	0.14	0.04	0.00	100.71
02 xtl 5 T	X lahar	76.36	38.00	-0.08	-0.04	40.02	0.01	0.17	0.32	22.09	0.18	0.02	0.05	100.84
02 xtl 5 T	X lahar	76.61	37.92	-0.08	-0.04	40.06	0.01	0.16	0.28	21.80	0.19	0.00	0.07	100.50
02 xtl 5 T	X lahar	76.61	37.83	-0.07	-0.04	40.20	0.00	0.16	0.29	21.88	0.16	0.03	0.01	100.57
02 xtl 5 T	X lahar	76.82	37.76	-0.07	-0.04	40.03	-0.01	0.15	0.29	21.53	0.15	0.01	0.00	99.92
02 xtl 5 T	X lahar	77.02	37.79	-0.09	-0.04	40.38	0.01	0.16	0.30	21.48	0.14	0.02	0.03	100.30
02 xtl 5 T	X lahar	77.34	37.82	-0.07	-0.05	40.49	-0.01	0.15	0.27	21.15	0.14	0.02	0.00	100.05

Table D.1 (Continued)

Sample	Lithology	Fo	SiO_2	Al_2O_3	Na_2O	MgO	K_2O	CaO	MnO	FeO	NiO	Cr_2O_3	TiO_2	Total
02 xtl 5 T	X lahar	77.43	37.98	-0.08	-0.04	40.64	0.02	0.15	0.29	21.12	0.15	0.02	0.05	100.43
02 xtl 5 T	X lahar	77.46	38.02	-0.09	-0.04	40.62	0.01	0.17	0.28	21.07	0.17	0.00	0.00	100.35
02 xtl 5 T	X lahar	77.52	38.17	-0.08	-0.03	40.64	0.00	0.14	0.26	21.00	0.17	0.01	-0.03	100.40
02 xtl 5 T	X lahar	77.59	38.09	-0.08	-0.04	40.69	0.00	0.16	0.27	20.96	0.16	0.01	0.04	100.37
02 xtl 5 T	X lahar	77.60	37.85	-0.08	-0.04	40.69	0.01	0.16	0.28	20.94	0.17	0.02	0.02	100.15
02 xtl 5 T	X lahar	77.76	38.29	-0.08	-0.04	40.79	0.00	0.15	0.28	20.80	0.17	0.02	0.02	100.52
02 xtl 5 T	X lahar	77.52	38.32	-0.08	-0.04	40.95	0.01	0.15	0.28	21.17	0.21	0.02	-0.01	101.10
02 xtl 5 T	X lahar	77.48	38.09	-0.08	-0.04	40.76	0.01	0.15	0.27	21.11	0.18	0.03	0.05	100.65
02 xtl 5 T	X lahar	77.70	38.14	-0.07	-0.04	40.85	0.02	0.16	0.27	20.90	0.19	0.01	0.00	100.54
02 xtl 5 T	X lahar	77.06	38.06	-0.08	-0.04	40.37	-0.01	0.15	0.30	21.42	0.17	0.02	0.04	100.54
02 xtl 5 T	X lahar	76.01	36.91	-0.01	-0.05	38.62	0.00	0.16	0.29	21.73	0.16	0.01	0.02	97.90
02 xtl 5 T	X lahar	74.77	37.33	-0.08	-0.03	38.78	0.01	0.16	0.30	23.33	0.15	0.01	0.05	100.12
02 xtl 6 T	X lahar	76.73	38.09	-0.07	-0.04	39.97	0.01	0.16	0.29	21.60	0.15	0.02	0.02	100.32
02 xtl 6 T	X lahar	77.19	37.25	-0.06	-0.03	38.95	0.01	0.16	0.28	20.52	0.16	0.02	-0.02	97.36
02 xtl 6 T	X lahar	77.92	38.25	-0.07	-0.03	40.76	0.01	0.16	0.30	20.59	0.17	0.00	-0.01	100.24
02 xtl 6 T	X lahar	78.24	38.07	0.52	-0.02	40.99	0.01	0.18	0.28	20.33	0.16	0.02	0.01	100.58
02 xtl 6 T	X lahar	78.20	38.35	-0.07	-0.05	41.00	0.00	0.16	0.29	20.37	0.21	0.02	0.01	100.41
02 xtl 6 T	X lahar	78.15	38.37	-0.08	-0.03	41.28	0.00	0.16	0.26	20.57	0.18	0.02	0.00	100.83
02 xtl 6 T	X lahar	78.66	37.92	-0.06	-0.02	40.75	0.01	0.16	0.27	19.71	0.17	0.02	-0.03	99.01
02 xtl 6 T	X lahar	78.64	38.44	-0.08	-0.05	41.47	0.01	0.16	0.26	20.08	0.17	0.03	0.05	100.66
02 xtl 6 T	X lahar	78.81	38.23	-0.07	-0.04	41.68	0.01	0.16	0.27	19.98	0.20	0.00	0.00	100.53
02 xtl 6 T	X lahar	78.84	38.37	-0.07	-0.03	41.70	0.00	0.15	0.28	19.95	0.17	0.01	0.00	100.65
02 xtl 6 T	X lahar	78.95	38.40	-0.05	-0.04	41.74	0.01	0.16	0.27	19.84	0.18	0.03	0.04	100.66
02 xtl 6 T	X lahar	79.21	38.47	-0.06	-0.03	41.93	0.01	0.15	0.25	19.61	0.21	0.03	-0.01	100.66
02 xtl 6 T	X lahar	79.20	38.37	-0.07	-0.03	41.84	0.00	0.16	0.26	19.59	0.20	0.02	0.01	100.44
02 xtl 6 T	X lahar	79.12	38.63	0.02	-0.02	41.74	0.00	0.19	0.26	19.64	0.20	0.03	-0.01	100.71
02 xtl 6 T	X lahar	79.31	38.38	-0.07	-0.04	41.94	0.00	0.16	0.24	19.51	0.21	0.02	-0.05	100.48
02 xtl 6 T	X lahar	79.34	38.39	-0.06	-0.04	41.96	0.00	0.15	0.25	19.48	0.20	0.02	-0.02	100.45
02 xtl 6 T	X lahar	79.28	38.21	-0.07	-0.04	42.19	0.01	0.14	0.25	19.66	0.23	0.03	-0.03	100.71
02 xtl 6 T	X lahar	79.43	38.53	-0.06	-0.03	42.12	0.00	0.15	0.23	19.45	0.20	0.01	-0.01	100.69
02 xtl 6 T	X lahar	79.57	38.47	-0.07	-0.02	42.06	0.00	0.16	0.24	19.25	0.25	0.03	0.04	100.51
02 xtl 6 T	X lahar	79.47	38.52	-0.06	-0.04	42.06	0.00	0.16	0.24	19.37	0.23	0.03	-0.02	100.61

Table D.1 (Continued)

Sample	Lithology	Fo	SiO_2	Al_2O_3	Na_2O	MgO	K_2O	CaO	MnO	FeO	NiO	Cr_2O_3	TiO_2	Total
02 xtl 6 T	X lahar	79.42	38.39	-0.08	-0.04	42.08	0.02	0.17	0.25	19.44	0.22	0.00	-0.03	100.57
02 xtl 6 T	X lahar	79.55	38.42	-0.05	-0.04	42.12	0.01	0.17	0.22	19.30	0.22	0.03	-0.04	100.48
02 xtl 6 T	X lahar	79.42	38.38	-0.07	-0.03	42.16	0.01	0.16	0.25	19.48	0.24	0.01	0.00	100.68
02 xtl 6 T	X lahar	79.66	38.48	-0.07	-0.03	42.06	-0.01	0.15	0.25	19.14	0.26	0.04	0.03	100.42
02 xtl 6 T	X lahar	79.34	38.45	-0.07	-0.04	42.20	0.00	0.16	0.24	19.59	0.22	0.03	-0.02	100.88
02 xtl 6 T	X lahar	79.71	38.58	-0.07	-0.05	42.17	0.00	0.16	0.24	19.13	0.22	0.02	-0.02	100.54
02 xtl 6 T	X lahar	79.58	38.46	-0.07	-0.04	42.27	-0.01	0.15	0.25	19.34	0.25	0.04	0.07	100.82
02 xtl 6 T	X lahar	79.73	38.34	-0.07	-0.05	42.18	0.00	0.16	0.27	19.12	0.22	0.02	0.05	100.37
02 xtl 6 T	X lahar	79.64	38.17	-0.08	-0.04	42.25	0.01	0.15	0.25	19.26	0.21	0.02	-0.03	100.33
02 xtl 6 T	X lahar	79.63	38.59	-0.08	-0.03	42.16	-0.01	0.15	0.26	19.22	0.21	0.02	0.03	100.65
02 xtl 6 T	X lahar	79.67	38.58	-0.07	-0.04	42.28	0.00	0.14	0.26	19.23	0.21	0.03	0.01	100.74
02 xtl 6 T	X lahar	79.43	38.51	-0.06	-0.04	42.21	0.00	0.17	0.25	19.48	0.23	0.04	0.01	100.90
02 xtl 6 T	X lahar	79.60	38.57	-0.08	-0.04	42.15	0.00	0.17	0.24	19.26	0.21	0.02	-0.01	100.62
02 xtl 6 T	X lahar	79.75	38.61	-0.07	-0.04	42.22	0.01	0.17	0.26	19.11	0.23	0.01	0.04	100.66
02 xtl 6 T	X lahar	79.57	38.55	-0.08	-0.04	42.23	0.01	0.16	0.26	19.32	0.22	0.03	0.01	100.79
02 xtl 6 T	X lahar	79.65	38.41	-0.08	-0.04	42.21	0.02	0.16	0.27	19.22	0.24	0.02	0.02	100.55
02 xtl 6 T	X lahar	79.61	38.47	-0.07	-0.04	42.26	0.01	0.16	0.26	19.29	0.22	0.03	0.00	100.70
02 xtl 6 T	X lahar	79.65	38.51	-0.09	-0.04	41.97	0.00	0.17	0.27	19.12	0.21	0.02	0.02	100.28
02 xtl 6 T	X lahar	79.58	38.58	-0.08	-0.03	42.10	0.00	0.16	0.24	19.26	0.20	0.02	-0.02	100.56
02 xtl 6 T	X lahar	79.29	38.58	-0.08	-0.03	42.26	0.00	0.16	0.26	19.68	0.20	0.02	0.00	101.14
02 xtl 6 T	X lahar	79.62	38.54	-0.08	-0.05	42.25	0.00	0.15	0.24	19.28	0.20	0.01	0.02	100.69
02 xtl 6 T	X lahar	79.58	38.40	-0.08	-0.04	42.00	0.01	0.15	0.25	19.21	0.22	0.03	0.02	100.30
02 xtl 6 T	X lahar	79.33	38.56	-0.08	-0.03	41.89	0.00	0.16	0.23	19.46	0.20	0.02	0.02	100.53
02 xtl 6 T	X lahar	79.39	38.39	-0.07	-0.03	41.80	0.00	0.16	0.23	19.35	0.21	0.02	-0.01	100.16
02 xtl 6 T	X lahar	79.29	38.40	-0.08	-0.04	42.02	0.02	0.16	0.24	19.56	0.20	0.04	0.00	100.63
02 xtl 6 T	X lahar	79.40	38.11	-0.07	-0.04	42.18	0.01	0.17	0.26	19.51	0.17	0.02	-0.03	100.42
02 xtl 6 T	X lahar	79.28	38.24	-0.07	-0.05	41.99	0.01	0.16	0.24	19.57	0.21	0.03	-0.01	100.44
02 xtl 6 T	X lahar	79.00	38.64	-0.08	-0.04	41.99	0.00	0.16	0.24	19.90	0.20	0.01	0.01	101.16
02 xtl 6 T	X lahar	78.95	38.48	-0.08	-0.04	41.68	0.00	0.14	0.28	19.81	0.18	0.01	0.00	100.58
02 xtl 6 T	X lahar	79.08	38.33	-0.08	-0.04	41.58	0.01	0.16	0.28	19.61	0.19	0.02	-0.02	100.17
02 xtl 6 T	X lahar	78.93	38.40	-0.07	-0.02	41.82	0.00	0.15	0.28	19.90	0.17	0.02	0.00	100.74
02 xtl 6 T	X lahar	78.90	38.40	-0.09	-0.04	41.80	0.00	0.16	0.28	19.93	0.17	0.02	-0.02	100.76

Table D.1 (Continued)

Sample	Lithology	Fo	SiO_2	Al_2O_3	Na_2O	MgO	K_2O	CaO	MnO	FeO	NiO	Cr_2O_3	TiO_2	Total
02 xtl 6 T	X lahar	78.86	38.45	-0.08	-0.04	41.70	0.00	0.16	0.29	19.93	0.17	0.03	0.02	100.73
02 xtl 6 T	X lahar	78.69	38.41	-0.08	-0.05	41.75	0.01	0.15	0.27	20.15	0.17	0.02	0.09	101.01
02 xtl 6 T	X lahar	78.69	38.33	-0.09	-0.03	41.46	0.00	0.17	0.25	20.02	0.18	0.00	0.01	100.43
02 xtl 6 T	X lahar	78.48	38.28	-0.08	-0.03	41.42	0.01	0.17	0.28	20.25	0.18	0.02	-0.01	100.62
02 xtl 6 T	X lahar	78.30	38.21	-0.08	-0.04	41.47	0.00	0.16	0.28	20.49	0.16	0.02	-0.01	100.78
02 xtl 6 T	X lahar	78.16	38.34	-0.08	-0.04	41.25	0.00	0.16	0.28	20.55	0.15	0.03	-0.04	100.76
02 xtl 6 T	X lahar	77.98	38.24	-0.08	-0.03	41.05	0.00	0.16	0.28	20.66	0.16	0.01	0.00	100.56
02 xtl 6 T	X lahar	77.67	38.26	-0.07	-0.04	40.84	0.01	0.17	0.29	20.94	0.16	0.01	0.03	100.70
02 xtl 6 T	X lahar	77.30	37.84	-0.08	-0.04	40.55	0.00	0.15	0.29	21.23	0.21	0.01	0.02	100.30
02 xtl 6 T	X lahar	76.97	38.08	-0.09	-0.05	40.30	0.00	0.15	0.28	21.49	0.16	0.02	0.05	100.53
02 xtl 6 T	X lahar	75.96	37.86	-0.08	-0.03	39.49	0.00	0.15	0.32	22.28	0.18	0.03	0.04	100.35
02 xtl 6 T	X lahar	75.85	37.84	-0.08	-0.05	39.34	0.02	0.14	0.32	22.33	0.14	0.03	-0.01	100.15
02 xtl 6 T	X lahar	74.90	37.63	-0.09	-0.04	38.77	0.02	0.14	0.34	23.16	0.15	0.02	0.01	100.22
02 xtl 6 T	X lahar	73.27	37.41	-0.08	-0.04	37.66	0.02	0.15	0.37	24.49	0.14	0.02	0.07	100.34
02 xtl 6 T	X lahar	68.60	36.83	-0.07	-0.04	34.54	0.02	0.16	0.42	28.19	0.09	0.02	0.05	100.32
02 xtl 7 T	X lahar	74.46	37.40	-0.08	-0.05	38.21	0.02	0.21	0.33	23.36	0.15	0.01	0.02	99.70
02 xtl 7 T	X lahar	74.92	37.50	-0.08	-0.03	38.72	0.01	0.17	0.35	23.10	0.12	0.02	0.01	100.00
02 xtl 7 T	X lahar	75.57	37.67	-0.08	-0.03	39.19	0.01	0.16	0.31	22.58	0.14	0.00	-0.02	100.07
02 xtl 7 T	X lahar	76.71	37.61	-0.08	-0.03	39.41	0.01	0.15	0.26	21.33	0.14	0.00	-0.01	98.92
02 xtl 7 T	X lahar	76.82	37.77	-0.08	-0.03	39.96	0.00	0.16	0.28	21.50	0.18	0.01	-0.01	99.86
02 xtl 7 T	X lahar	77.18	37.89	-0.06	-0.03	40.28	0.00	0.15	0.30	21.23	0.19	0.02	-0.01	100.05
02 xtl 7 T	X lahar	77.56	37.78	-0.08	-0.03	40.30	0.02	0.16	0.28	20.79	0.19	0.00	-0.02	99.51
02 xtl 7 T	X lahar	78.10	37.93	-0.08	-0.05	40.88	0.01	0.15	0.27	20.44	0.16	0.00	-0.02	99.86
02 xtl 7 T	X lahar	79.11	38.42	-0.08	-0.03	41.23	0.00	0.14	0.23	19.40	0.22	0.02	-0.02	99.67
02 xtl 7 T	X lahar	79.51	38.20	-0.07	-0.02	41.61	0.00	0.15	0.24	19.11	0.22	0.01	0.03	99.58
02 xtl 7 T	X lahar	79.97	38.33	-0.07	-0.03	41.97	-0.01	0.14	0.24	18.74	0.25	0.02	-0.01	99.68
02 xtl 7 T	X lahar	79.74	38.30	-0.08	-0.02	41.68	0.01	0.14	0.24	18.88	0.23	0.03	0.01	99.51
02 xtl 7 T	X lahar	79.91	38.45	-0.08	-0.04	42.01	0.00	0.15	0.24	18.83	0.23	0.03	-0.03	99.94
02 xtl 7 T	X lahar	79.97	38.42	-0.08	-0.04	42.16	0.00	0.16	0.24	18.83	0.25	0.02	-0.02	100.08
02 xtl 7 T	X lahar	79.99	38.21	-0.06	-0.04	42.01	0.00	0.16	0.25	18.73	0.22	0.02	0.03	99.63
02 xtl 7 T	X lahar	79.85	38.04	-0.08	-0.04	42.05	-0.02	0.15	0.22	18.91	0.25	0.03	-0.04	99.66
02 xtl 7 T	X lahar	79.99	38.29	-0.07	-0.02	42.17	-0.02	0.15	0.24	18.80	0.22	0.01	-0.01	99.88

Table D.1 (Continued)

Sample	Lithology	Fo	SiO_2	Al_2O_3	Na_2O	MgO	K_2O	CaO	MnO	FeO	NiO	Cr_2O_3	TiO_2	Total
02 xtl 7 T	X lahar	80.05	38.17	-0.08	-0.04	42.19	-0.01	0.14	0.24	18.75	0.23	0.02	0.00	99.74
02 xtl 7 T	X lahar	80.04	38.18	-0.07	-0.03	41.91	0.01	0.15	0.24	18.63	0.23	0.03	0.01	99.39
02 xtl 7 T	X lahar	80.03	38.25	-0.08	-0.04	42.05	0.03	0.13	0.22	18.70	0.26	0.03	0.02	99.70
02 xtl 7 T	X lahar	80.15	38.34	-0.09	-0.04	42.22	0.01	0.15	0.24	18.63	0.22	0.04	0.02	99.86
02 xtl 7 T	X lahar	79.93	37.73	-0.07	-0.03	41.77	0.00	0.15	0.25	18.69	0.22	0.01	-0.04	98.83
02 xtl 7 T	X lahar	79.84	38.56	-0.07	-0.04	42.21	0.01	0.14	0.24	19.00	0.23	0.01	0.01	100.41
02 xtl 7 T	X lahar	79.90	38.15	-0.07	-0.04	42.11	-0.01	0.15	0.25	18.89	0.22	0.03	0.01	99.82
02 xtl 7 T	X lahar	79.86	38.09	-0.08	-0.04	42.12	0.00	0.14	0.24	18.93	0.26	0.02	0.04	99.83
02 xtl 7 T	X lahar	79.68	38.23	-0.07	-0.04	41.75	0.00	0.15	0.25	18.98	0.24	0.03	0.06	99.68
02 xtl 7 T	X lahar	79.73	38.36	-0.07	-0.03	42.07	0.00	0.14	0.23	19.07	0.24	0.02	-0.03	100.13
02 xtl 7 T	X lahar	79.58	38.09	-0.07	-0.02	41.58	0.01	0.15	0.26	19.01	0.21	0.02	-0.01	99.33
02 xtl 7 T	X lahar	79.53	38.39	-0.08	-0.03	41.96	-0.01	0.14	0.25	19.25	0.23	0.02	-0.04	100.24
02 xtl 7 T	X lahar	79.38	38.33	-0.07	-0.04	41.78	0.00	0.15	0.25	19.35	0.20	0.04	-0.01	100.10
02 xtl 7 T	X lahar	79.26	38.22	-0.07	-0.03	41.58	0.01	0.15	0.24	19.40	0.20	0.02	0.03	99.83
02 xtl 7 T	X lahar	79.08	38.23	-0.07	-0.04	41.54	0.02	0.15	0.24	19.59	0.20	0.01	-0.01	99.98
02 xtl 7 T	X lahar	78.99	38.26	-0.08	-0.03	41.37	0.00	0.16	0.24	19.62	0.19	0.02	0.00	99.86
02 xtl 7 T	X lahar	79.00	37.87	-0.07	-0.05	41.21	0.01	0.14	0.25	19.53	0.19	0.02	0.00	99.21
02 xtl 7 T	X lahar	78.62	38.05	-0.07	-0.02	41.46	0.01	0.14	0.26	20.10	0.19	0.02	-0.01	100.24
02 xtl 7 T	X lahar	78.87	38.29	-0.09	-0.03	41.37	0.01	0.14	0.25	19.75	0.21	0.04	-0.02	100.05
02 xtl 7 T	X lahar	78.73	38.17	-0.08	-0.04	41.21	0.01	0.16	0.28	19.85	0.17	0.02	0.01	99.88
02 xtl 7 T	X lahar	78.34	37.95	-0.07	-0.03	40.98	0.02	0.31	0.26	20.20	0.18	0.02	-0.02	99.93
02 xtl 7 T	X lahar	78.41	38.02	-0.08	-0.03	41.11	0.01	0.15	0.27	20.18	0.20	0.02	0.00	99.98
02 xtl 7 T	X lahar	78.09	38.10	-0.08	-0.03	40.86	0.00	0.14	0.28	20.44	0.19	0.01	-0.05	100.02
02 xtl 7 T	X lahar	77.83	37.78	-0.07	-0.04	40.71	0.00	0.16	0.26	20.67	0.18	0.02	0.00	99.78
02 xtl 7 T	X lahar	77.67	38.05	-0.08	-0.05	40.52	0.02	0.15	0.27	20.77	0.17	0.02	0.03	100.01
02 xtl 7 T	X lahar	77.26	38.11	-0.07	-0.05	40.40	0.00	0.15	0.28	21.20	0.18	0.02	0.00	100.37
02 xtl 7 T	X lahar	77.23	37.90	-0.08	-0.04	40.33	0.01	0.15	0.27	21.20	0.15	0.02	0.07	100.09
02 xtl 7 T	X lahar	77.06	38.03	-0.08	-0.03	39.99	0.00	0.16	0.29	21.22	0.16	0.02	0.00	99.86
02 xtl 7 T	X lahar	76.63	37.80	-0.07	-0.02	39.98	0.01	0.16	0.30	21.73	0.16	0.03	-0.01	100.16
02 xtl 7 T	X lahar	76.51	37.40	-0.08	-0.04	39.54	0.00	0.15	0.31	21.64	0.14	0.01	0.03	99.23
02 xtl 7 T	X lahar	75.29	37.17	-0.09	-0.05	38.81	0.01	0.16	0.29	22.71	0.15	0.03	-0.03	99.32
02 xtl 7 T	X lahar	75.34	37.63	-0.08	-0.03	38.68	0.00	0.19	0.34	22.57	0.13	0.01	-0.03	99.55

Table D.1 (Continued)

Sample	Lithology	Fo	SiO_2	Al_2O_3	Na_2O	MgO	K_2O	CaO	MnO	FeO	NiO	Cr_2O_3	TiO_2	Total
02 xtl 8 T	X lahar	74.08	37.38	-0.08	-0.03	37.93	0.01	0.17	0.32	23.66	0.13	0.01	0.00	99.62
02 xtl 8 T	X lahar	74.36	37.57	-0.08	-0.05	38.39	0.01	0.16	0.32	23.60	0.15	0.02	0.00	100.22
02 xtl 8 T	X lahar	74.35	37.23	-0.09	-0.05	38.15	-0.01	0.17	0.32	23.46	0.15	0.01	0.01	99.50
02 xtl 8 T	X lahar	74.72	37.51	-0.08	-0.05	38.57	0.00	0.16	0.34	23.26	0.14	0.01	0.05	100.03
02 xtl 8 T	X lahar	75.00	37.69	-0.08	-0.05	38.82	0.01	0.15	0.34	23.07	0.14	0.01	0.00	100.22
02 xtl 8 T	X lahar	75.21	37.66	-0.08	-0.03	39.00	0.00	0.15	0.29	22.92	0.13	0.03	0.03	100.21
02 xtl 8 T	X lahar	75.40	37.70	-0.09	-0.03	38.87	0.00	0.15	0.32	22.61	0.14	0.02	0.01	99.81
02 xtl 8 T	X lahar	75.79	37.90	-0.09	-0.04	39.32	0.02	0.15	0.32	22.38	0.13	0.02	0.03	100.26
02 xtl 8 T	X lahar	75.94	37.44	-0.07	-0.04	39.46	0.01	0.16	0.30	22.29	0.14	0.01	0.00	99.82
02 xtl 8 T	X lahar	76.09	37.75	-0.07	-0.03	39.33	0.00	0.17	0.30	22.03	0.17	0.03	0.06	99.84
02 xtl 8 T	X lahar	76.26	37.68	-0.09	-0.03	39.31	0.00	0.18	0.31	21.82	0.16	0.02	-0.03	99.47
02 xtl 8 T	X lahar	76.06	37.72	-0.09	-0.04	39.50	0.00	0.17	0.29	22.16	0.16	0.02	-0.01	100.01
02 xtl 8 T	X lahar	76.20	37.70	-0.09	-0.04	39.74	-0.01	0.16	0.29	22.12	0.15	0.01	0.03	100.19
02 xtl 8 T	X lahar	76.20	37.85	-0.09	-0.03	39.64	0.02	0.15	0.32	22.06	0.16	0.01	-0.01	100.21
02 xtl 8 T	X lahar	76.42	37.71	-0.05	-0.04	39.37	0.00	0.16	0.29	21.66	0.16	0.01	-0.02	99.37
02 xtl 8 T	X lahar	76.47	37.82	-0.09	-0.04	39.74	0.02	0.15	0.31	21.79	0.19	0.02	0.00	100.03
02 xtl 8 T	X lahar	76.39	37.95	-0.08	-0.04	39.71	-0.01	0.16	0.30	21.88	0.14	0.02	0.02	100.20
02 xtl 8 T	X lahar	76.43	37.87	-0.08	-0.03	39.55	0.01	0.15	0.33	21.75	0.15	0.01	0.04	99.85
02 xtl 8 T	X lahar	76.25	37.58	-0.07	-0.03	39.66	0.01	0.16	0.28	22.02	0.14	0.01	0.02	99.89
02 xtl 8 T	X lahar	76.21	37.88	-0.09	-0.04	39.74	0.00	0.15	0.30	22.11	0.15	0.03	-0.01	100.37
02 xtl 8 T	X lahar	76.56	37.79	-0.08	-0.03	39.78	-0.01	0.21	0.31	21.71	0.14	0.02	0.02	99.98
02 xtl 8 T	X lahar	76.52	37.73	-0.08	-0.04	39.80	0.00	0.15	0.32	21.77	0.14	0.03	0.01	99.95
02 xtl 8 T	X lahar	76.34	37.71	-0.08	-0.04	39.70	0.00	0.17	0.30	21.93	0.16	-0.01	0.06	100.04
02 xtl 8 T	X lahar	76.67	37.69	-0.09	-0.04	39.87	0.00	0.19	0.28	21.63	0.15	0.02	-0.03	99.84
02 xtl 8 T	X lahar	76.60	37.85	-0.08	-0.05	39.88	0.00	0.15	0.27	21.71	0.15	0.01	0.08	100.13
02 xtl 8 T	X lahar	76.69	37.77	-0.08	-0.03	39.88	0.01	0.16	0.30	21.61	0.13	0.00	0.02	99.87
02 xtl 8 T	X lahar	76.18	38.05	-0.09	-0.04	40.00	0.00	0.16	0.29	22.30	0.13	0.03	0.01	100.96
02 xtl 8 T	X lahar	76.61	37.73	-0.08	-0.05	39.93	0.02	0.15	0.31	21.73	0.14	0.01	0.01	100.03
02 xtl 8 T	X lahar	76.52	38.01	-0.08	-0.04	40.10	0.00	0.16	0.29	21.93	0.16	0.02	0.04	100.71
02 xtl 8 T	X lahar	76.90	36.95	0.15	0.00	40.23	0.01	0.17	0.30	21.54	0.16	0.03	0.02	99.58
02 xtl 8 T	X lahar	76.43	37.64	-0.09	-0.04	39.86	-0.01	0.15	0.30	21.91	0.16	0.03	0.01	100.05
02 xtl 8 T	X lahar	76.47	37.68	-0.08	-0.04	39.54	0.00	0.15	0.29	21.69	0.14	0.01	-0.02	99.50

Table D.1 (Continued)

Sample	Lithology	Fo	SiO_2	Al_2O_3	Na_2O	MgO	K_2O	CaO	MnO	FeO	NiO	Cr_2O_3	TiO_2	Total
02 xtl 8 T	X lahar	76.44	37.96	-0.08	-0.03	39.74	0.00	0.16	0.31	21.84	0.13	0.00	0.00	100.14
02 xtl 8 T	X lahar	76.21	37.74	-0.08	-0.04	39.74	0.01	0.15	0.29	22.11	0.14	0.02	-0.04	100.20
02 xtl 8 T	X lahar	76.39	37.91	-0.09	-0.03	39.70	0.00	0.14	0.28	21.87	0.15	0.02	0.01	100.07
02 xtl 8 T	X lahar	76.43	37.95	-0.08	-0.05	39.71	0.01	0.16	0.29	21.83	0.14	0.02	0.01	100.11
02 xtl 8 T	X lahar	76.33	37.67	-0.08	-0.03	39.76	0.01	0.16	0.30	21.98	0.15	0.00	0.02	100.05
02 xtl 8 T	X lahar	76.08	38.05	0.03	-0.04	39.64	0.01	0.14	0.31	22.21	0.15	0.02	0.01	100.57
02 xtl 8 T	X lahar	76.04	37.82	-0.08	-0.04	39.44	0.00	0.16	0.30	22.16	0.12	-0.01	0.01	100.01
02 xtl 8 T	X lahar	76.00	37.92	-0.08	-0.05	39.78	-0.01	0.15	0.32	22.39	0.13	0.00	-0.02	100.69
02 xtl 8 T	X lahar	76.08	37.34	-0.09	-0.03	39.35	0.00	0.59	0.31	22.06	0.14	0.01	0.00	99.80
02 xtl 8 T	X lahar	75.89	37.60	-0.08	-0.04	39.34	0.02	0.17	0.31	22.28	0.13	0.02	-0.03	99.86
02 xtl 8 T	X lahar	75.98	37.39	-0.08	-0.03	38.78	0.01	0.16	0.30	21.86	0.15	0.00	0.00	98.63
02 xtl 8 T	X lahar	75.90	37.65	-0.09	-0.04	39.31	0.01	0.15	0.31	22.25	0.15	0.02	-0.01	99.84
02 xtl 8 T	X lahar	75.19	37.77	-0.09	-0.04	39.26	0.01	0.15	0.31	23.09	0.15	0.01	-0.03	100.74
02 xtl 8 T	X lahar	75.37	37.51	-0.08	-0.02	38.69	0.01	0.14	0.28	22.53	0.13	0.02	-0.02	99.31
02 xtl 8 T	X lahar	75.24	37.42	-0.08	-0.02	38.60	0.02	0.16	0.33	22.64	0.16	0.02	0.01	99.35
02 xtl 8 T	X lahar	75.18	37.65	-0.08	-0.06	39.02	0.02	0.15	0.33	22.97	0.14	0.02	-0.01	100.29
02 xtl 8 T	X lahar	74.44	37.47	-0.09	-0.04	38.41	0.01	0.15	0.31	23.51	0.13	0.00	0.00	100.00
02 xtl 8 T	X lahar	74.43	37.40	-0.09	-0.05	38.63	0.00	0.16	0.34	23.66	0.11	0.02	0.00	100.33
02 xtl 8 T	X lahar	74.21	37.48	-0.08	-0.03	37.97	0.00	0.16	0.34	23.52	0.14	0.01	0.04	99.67
02 xtl 8 T	X lahar	73.85	37.44	-0.09	-0.05	38.27	0.01	0.15	0.33	24.15	0.13	0.02	-0.01	100.51
02 xtl 8, spl 10	X lahar	78.18	38.57	0.04	0.01	40.54	-0.01	0.16	0.36	20.16	0.19	0.10	0.01	100.13
02 xtl 8, spl 10	X lahar	78.46	38.34	0.02	0.01	40.41	-0.01	0.16	0.27	19.77	0.15	0.02	0.01	99.15
09 xtl 9, spl 11	X lahar	78.27	38.13	0.02	0.00	40.01	0.00	0.16	0.30	19.80	0.19	-0.02	0.01	98.62
09 xtl 9, spl 11	X lahar	77.98	38.07	0.01	-0.01	40.22	0.00	0.17	0.27	20.25	0.09	0.00	0.01	99.09
09 xtl 10, spl 12	X lahar	79.35	37.77	0.05	0.00	40.09	0.01	0.18	0.32	18.60	0.26	0.15	0.01	97.43
09 xtl 10, spl 12	X lahar	79.37	38.40	0.05	0.00	40.79	0.00	0.15	0.26	18.90	0.22	0.04	0.00	98.82
10 xtl 11, spl 13	MKLV-TF	63.45	36.01	-0.01	0.02	30.70	0.01	0.21	0.47	31.53	0.08	0.01	0.05	99.08
10 xtl 11, spl 13	MKLV-TF	63.64	35.71	0.01	0.01	30.84	0.01	0.21	0.56	31.41	0.07	0.01	0.05	98.89
10 xtl 12, spl 14	MKLV-TF	75.22	37.82	0.01	0.00	38.39	0.00	0.16	0.32	22.55	0.21	0.02	0.01	99.51
10 xtl 12, spl 15	MKLV-TF	75.88	38.18	0.03	0.02	38.73	-0.01	0.17	0.28	21.95	0.17	0.02	0.03	99.56
10 xtl 12, spl 16	MKLV-TF	74.23	37.80	0.04	0.00	37.58	0.00	0.16	0.27	23.25	0.18	-0.04	0.01	99.25
10 xtl 12, spl 17	MKLV-TF	74.13	37.91	0.03	0.01	37.60	-0.01	0.16	0.31	23.39	0.18	0.12	0.02	99.72

Table D.1 (Continued)

Sample	Lithology	Fo	SiO_2	Al_2O_3	Na_2O	MgO	K_2O	CaO	MnO	FeO	NiO	Cr_2O_3	TiO_2	Total
10 xtl 12, spl 17	MKLV-TF	74.19	37.72	0.03	0.00	37.72	-0.01	0.14	0.44	23.39	0.20	0.04	0.01	99.69
10 xtl 12, spl 18	MKLV-TF	74.97	37.87	0.04	-0.01	38.27	0.01	0.14	0.35	22.78	0.16	0.09	0.01	99.69
10 xtl 12, spl 18	MKLV-TF	75.01	37.60	0.02	0.01	38.26	0.01	0.14	0.42	22.72	0.16	0.07	0.01	99.41
10 xtl 3 glom	MKLV-TF	71.90	37.34	0.01	0.02	36.27	0.00	0.16	0.36	25.26	0.17	0.00	0.03	99.64
10 xtl 3 glom	MKLV-TF	71.83	37.23	0.17	0.05	35.73	0.02	0.19	0.33	24.98	0.18	0.02	0.04	98.93
10 xtl 3 glom	MKLV-TF	70.91	37.07	0.03	0.01	35.78	0.00	0.16	0.32	26.17	0.15	0.01	-0.01	99.70
10 xtl 3 glom	MKLV-TF	70.49	36.79	0.00	0.00	35.31	-0.01	0.18	0.33	26.35	0.13	0.02	0.07	99.17
10 xtl 4 glom	MKLV-TF	75.88	37.80	0.04	0.00	38.76	0.01	0.14	0.27	21.96	0.20	0.01	0.04	99.24
10 xtl 4 glom	MKLV-TF	78.17	38.12	0.04	0.00	40.45	0.00	0.15	0.24	20.14	0.23	0.02	-0.01	99.37
10 xtl 4 glom	MKLV-TF	70.32	36.89	0.03	0.03	35.10	0.01	0.19	0.36	26.41	0.11	0.01	0.01	99.16
10 xtl 4 glom	MKLV-TF	72.08	37.17	0.02	0.00	36.36	0.01	0.20	0.30	25.11	0.13	-0.01	0.03	99.31
10 xtl 7 tiny	MKLV-TF	63.31	35.84	0.01	0.02	30.73	0.00	0.23	0.44	31.75	0.08	0.01	-0.01	99.09
10 xtl 7 tiny	MKLV-TF	63.29	35.69	0.00	0.01	30.82	0.02	0.22	0.45	31.87	0.11	0.00	-0.03	99.16
10 xtl 7 tiny	MKLV-TF	67.66	36.62	0.01	0.01	33.49	0.01	0.18	0.40	28.53	0.07	-0.01	0.03	99.34
10 xtl 7 tiny	MKLV-TF	67.74	36.63	0.01	0.01	33.70	0.02	0.14	0.42	28.60	0.07	0.02	0.01	99.63
10 xtl 7 tiny	MKLV-TF	64.80	36.16	0.03	0.01	31.74	0.01	0.22	0.44	30.74	0.10	-0.01	0.04	99.49
10 xtl 7 tiny	MKLV-TF	69.98	36.86	0.01	0.00	34.96	0.02	0.14	0.35	26.74	0.10	0.02	0.03	99.23
10 xtl 7 tiny	MKLV-TF	70.02	36.86	0.03	0.00	35.09	0.00	0.13	0.36	26.79	0.09	0.00	0.04	99.39
10 xtl 10 lg	MKLV-TF	68.60	36.60	0.01	0.00	34.26	0.02	0.18	0.36	27.95	0.05	0.00	0.02	99.45
10 xtl 10 lg	MKLV-TF	67.60	36.24	0.02	0.00	33.58	0.01	0.16	0.39	28.69	0.10	-0.02	0.02	99.21
10 xtl 10 lg	MKLV-TF	65.95	36.32	0.01	0.02	32.55	0.02	0.19	0.42	29.96	0.11	-0.01	0.02	99.60
10 xtl 10 lg	MKLV-TF	63.75	35.82	0.02	0.00	30.90	0.01	0.24	0.42	31.32	0.09	0.00	0.07	98.89
03 xtl 1 T	MKPF	66.09	36.57	-0.07	-0.04	33.16	0.01	0.23	0.50	30.33	0.10	0.02	0.13	101.04
03 xtl 1 T	MKPF	66.03	36.31	-0.07	-0.04	32.86	0.00	0.21	0.50	30.13	0.12	0.01	0.06	100.21
03 xtl 1 T	MKPF	66.39	36.34	-0.09	-0.04	32.96	0.02	0.20	0.49	29.74	0.14	0.02	0.03	99.94
03 xtl 1 T	MKPF	66.17	36.41	-0.07	-0.05	33.05	0.01	0.18	0.49	30.12	0.13	0.01	-0.01	100.39
03 xtl 1 T	MKPF	66.33	36.45	-0.07	-0.04	33.13	-0.01	0.17	0.50	29.98	0.14	0.00	-0.02	100.37
03 xtl 1 T	MKPF	66.07	36.25	-0.06	-0.04	33.08	0.01	0.18	0.50	30.28	0.14	0.02	0.02	100.47
03 xtl 1 T	MKPF	66.29	36.13	-0.07	-0.05	33.24	0.02	0.17	0.53	30.14	0.12	0.02	0.07	100.45
03 xtl 1 T	MKPF	66.36	36.05	-0.06	-0.06	33.13	0.01	0.15	0.48	29.93	0.11	0.02	0.01	99.90
03 xtl 1 T	MKPF	66.37	35.99	-0.07	-0.03	33.31	0.01	0.17	0.47	30.09	0.14	0.01	-0.06	100.20
03 xtl 1 T	MKPF	66.44	36.12	-0.06	-0.03	33.35	0.02	0.16	0.51	30.02	0.15	0.02	0.02	100.36

Table D.1 (Continued)

Sample	Lithology	Fo	SiO_2	Al_2O_3	Na_2O	MgO	K_2O	CaO	MnO	FeO	NiO	Cr_2O_3	TiO_2	Total
03 xtl 1 T	MKPF	66.62	36.46	-0.08	-0.05	33.32	0.01	0.16	0.47	29.76	0.13	0.03	0.03	100.37
03 xtl 1 T	MKPF	66.63	36.47	-0.07	-0.04	33.45	0.00	0.15	0.45	29.87	0.13	0.02	0.04	100.58
03 xtl 1 T	MKPF	66.83	36.51	-0.07	-0.06	33.43	0.00	0.18	0.48	29.58	0.12	0.03	0.01	100.34
03 xtl 1 T	MKPF	66.75	36.04	-0.06	-0.04	33.48	-0.01	0.17	0.47	29.72	0.13	0.02	0.04	100.07
03 xtl 1 T	MKPF	66.81	36.37	-0.06	-0.04	33.52	0.00	0.17	0.48	29.68	0.12	0.01	0.03	100.37
03 xtl 1 T	MKPF	67.09	36.30	-0.07	-0.03	33.61	0.02	0.17	0.47	29.39	0.13	0.02	0.10	100.21
03 xtl 1 T	MKPF	67.16	36.31	-0.06	-0.04	33.67	0.01	0.17	0.48	29.34	0.14	0.02	0.07	100.20
03 xtl 1 T	MKPF	67.27	36.28	-0.07	-0.05	33.74	0.01	0.17	0.47	29.26	0.14	0.02	0.00	100.10
03 xtl 1 T	MKPF	67.24	36.46	-0.08	-0.03	33.65	0.01	0.18	0.47	29.23	0.15	0.00	0.07	100.21
03 xtl 1 T	MKPF	66.99	36.12	-0.03	-0.03	33.00	0.02	0.18	0.47	28.99	0.13	0.02	-0.01	98.93
03 xtl 1 T	MKPF	67.18	36.52	-0.07	-0.05	33.66	0.01	0.18	0.47	29.31	0.15	0.03	0.01	100.35
03 xtl 1 T	MKPF	67.14	36.51	-0.08	-0.04	33.68	0.00	0.19	0.49	29.39	0.12	0.02	0.02	100.42
03 xtl 1 T	MKPF	67.12	36.37	-0.08	-0.04	33.70	0.02	0.19	0.46	29.43	0.13	0.03	0.08	100.42
03 xtl 1 T	MKPF	67.24	36.28	-0.07	-0.04	33.67	0.01	0.19	0.46	29.24	0.15	0.02	-0.02	100.01
03 xtl 1 T	MKPF	66.81	36.71	-0.08	-0.06	33.57	0.02	0.20	0.49	29.72	0.14	0.02	0.04	100.91
03 xtl 1 T	MKPF	67.06	36.27	-0.07	-0.03	33.54	0.02	0.21	0.49	29.37	0.15	0.01	0.05	100.10
03 xtl 1 T	MKPF	67.07	36.47	-0.06	-0.02	33.50	0.01	0.26	0.48	29.32	0.12	0.01	0.02	100.19
03 xtl 2	MKPF	67.59	36.89	-0.07	-0.03	34.01	0.01	0.13	0.47	29.06	0.22	0.03	-0.01	100.82
03 xtl 2	MKPF	67.44	36.89	-0.08	-0.04	34.00	0.00	0.13	0.47	29.26	0.24	0.02	0.06	101.08
13 xtl 1 T	SDY	65.64	36.38	-0.08	-0.04	32.90	0.00	0.11	0.52	30.70	0.23	0.01	0.11	100.95
13 xtl 1 T	SDY	65.97	36.08	-0.08	0.00	32.44	0.01	0.16	0.55	29.83	0.21	0.02	0.00	99.30
13 xtl 1 T	SDY	65.87	36.68	-0.08	-0.05	33.04	0.00	0.11	0.53	30.52	0.21	0.02	0.00	101.12
13 xtl 1 T	SDY	65.95	36.47	-0.08	-0.05	32.94	0.02	0.11	0.56	30.31	0.25	0.02	0.04	100.72
13 xtl 1 T	SDY	65.73	35.43	-0.08	-0.04	32.34	0.01	0.10	0.54	30.06	0.22	0.02	0.02	98.74
13 xtl 1 T	SDY	65.56	36.70	-0.05	-0.05	32.15	0.03	0.10	0.54	30.11	0.21	0.02	0.04	99.89
13 xtl 1 T	SDY	65.79	36.47	-0.09	-0.05	32.94	0.02	0.10	0.56	30.53	0.23	0.02	0.00	100.87
13 xtl 1 T	SDY	65.86	36.33	-0.09	-0.05	32.90	0.00	0.10	0.54	30.40	0.21	0.02	-0.03	100.50
13 xtl 1 T	SDY	65.76	36.59	-0.08	-0.05	32.94	0.00	0.11	0.55	30.57	0.22	0.01	-0.05	100.97
13 xtl 1 T	SDY	65.80	36.62	-0.09	-0.03	32.88	0.02	0.10	0.56	30.46	0.22	0.01	0.02	100.90
13 xtl 1 T	SDY	66.01	36.46	-0.08	-0.05	33.01	0.02	0.10	0.52	30.30	0.25	0.02	0.01	100.69
13 xtl 1 T	SDY	65.86	36.35	-0.08	-0.04	33.06	0.02	0.09	0.56	30.54	0.21	0.00	-0.01	100.84
13 xtl 1 T	SDY	65.71	36.33	-0.07	-0.05	32.92	0.00	0.10	0.53	30.61	0.21	0.01	0.01	100.73

Table D.1 (Continued)

Sample	Lithology	Fo	SiO_2	Al_2O_3	Na_2O	MgO	K_2O	CaO	MnO	FeO	NiO	Cr_2O_3	TiO_2	Total
13 xtl 1 T	SDY	65.78	36.45	-0.08	-0.05	32.97	0.00	0.10	0.54	30.57	0.22	0.02	0.00	100.87
13 xtl 1 T	SDY	65.74	36.37	-0.08	-0.05	32.99	0.00	0.11	0.55	30.64	0.21	0.04	0.05	100.95
13 xtl 1 T	SDY	65.79	36.37	-0.09	-0.05	32.92	0.01	0.11	0.53	30.51	0.22	0.03	-0.01	100.71
13 xtl 1 T	SDY	65.98	36.53	-0.08	-0.05	33.01	0.02	0.12	0.53	30.35	0.21	0.03	0.05	100.84
13 xtl 1 T	SDY	66.14	36.49	-0.07	-0.04	33.13	0.01	0.11	0.54	30.24	0.24	0.03	0.00	100.79
13 xtl 1 T	SDY	65.97	36.59	-0.08	-0.04	33.09	0.01	0.10	0.54	30.43	0.19	0.00	0.00	100.95
13 xtl 1 T	SDY	66.08	36.41	-0.08	-0.05	33.17	0.01	0.11	0.56	30.35	0.24	0.02	-0.01	100.87
13 xtl 1 T	SDY	66.27	36.58	-0.09	-0.04	33.08	0.02	0.11	0.56	30.01	0.24	0.01	0.04	100.65
13 xtl 1 T	SDY	66.07	36.30	-0.08	-0.05	33.19	0.01	0.11	0.54	30.39	0.22	0.01	-0.02	100.76
13 xtl 1 T	SDY	66.07	36.42	-0.08	-0.05	33.00	0.02	0.12	0.53	30.21	0.22	0.00	0.06	100.58
19 xtl 1	QMI	82.38	38.88	0.03	0.00	43.39	-0.01	0.17	0.19	16.55	0.20	-0.01	-0.01	99.40
19 xtl 1	QMI	82.02	38.85	0.05	0.01	43.03	0.01	0.16	0.21	16.82	0.21	0.05	0.05	99.46
19 xtl 1	QMI	74.23	37.70	0.04	0.02	37.68	0.00	0.18	0.34	23.32	0.13	-0.01	0.00	99.40
19 xtl 2 lg	QMI	80.68	38.54	0.03	0.00	42.10	0.00	0.16	0.24	17.97	0.20	0.00	-0.03	99.20
19 xtl 2 lg	QMI	79.86	38.44	0.06	0.00	41.74	-0.01	0.16	0.24	18.76	0.21	0.00	0.01	99.61
19 xtl 3	QMI	85.24	39.03	0.03	0.01	45.44	0.00	0.17	0.17	14.03	0.25	0.04	-0.01	99.15
19 xtl 3	QMI	85.36	38.95	0.04	0.01	45.57	0.00	0.18	0.16	13.93	0.27	0.06	0.04	99.21
19 xtl 3	QMI	82.69	38.85	0.04	0.02	43.43	0.00	0.15	0.22	16.20	0.22	0.03	-0.01	99.15
19 xtl 3	QMI	82.85	39.08	0.03	0.01	43.80	0.00	0.14	0.20	16.16	0.27	0.04	0.05	99.78
19 xtl 4	QMI	83.23	39.22	0.03	0.00	43.80	0.00	0.15	0.19	15.74	0.29	0.05	0.02	99.49
19 xtl 4	QMI	83.39	39.21	0.02	0.01	43.88	0.00	0.15	0.20	15.58	0.27	0.04	0.02	99.37
19 xtl 4	QMI	77.26	37.58	0.50	0.03	39.66	0.00	0.18	0.27	20.81	0.16	0.41	0.09	99.68
19 xtl 4	QMI	75.08	37.66	0.03	0.00	38.23	0.00	0.15	0.30	22.62	0.16	-0.01	0.02	99.16
19 xtl 5 lg glom	QMI	85.18	39.52	0.04	0.01	45.21	-0.01	0.15	0.17	14.02	0.31	0.04	0.00	99.45
19 xtl 5 lg glom	QMI	85.35	39.61	0.03	0.00	45.28	-0.01	0.15	0.17	13.86	0.29	0.05	0.01	99.43
19 xtl 5 lg glom	QMI	76.42	37.79	0.02	0.01	39.00	0.00	0.14	0.29	21.45	0.15	0.00	0.00	98.85
19 xtl 5 lg glom	QMI	79.90	38.44	0.04	0.00	41.59	-0.01	0.15	0.24	18.65	0.21	-0.01	0.02	99.32
19 xtl 6 lg glom	QMI	85.68	39.57	0.05	0.01	45.66	0.01	0.15	0.16	13.60	0.30	0.04	0.01	99.56
19 xtl 6 lg glom	QMI	85.77	39.43	0.05	0.01	45.58	-0.01	0.16	0.16	13.48	0.30	0.03	0.02	99.22
19 xtl 6 lg glom	QMI	76.32	38.05	0.04	-0.01	39.06	0.01	0.17	0.31	21.60	0.18	-0.02	0.00	99.38
19 xtl 6 lg glom	QMI	78.98	38.29	0.04	0.00	40.78	-0.01	0.16	0.27	19.35	0.16	-0.01	0.01	99.04
19 xtl 7 lg glom	QMI	84.88	39.17	0.01	0.01	44.97	-0.01	0.15	0.17	14.28	0.23	0.04	0.01	99.03

Table D.1 (Continued)

Sample	Lithology	Fo	SiO_2	Al_2O_3	Na_2O	MgO	K_2O	CaO	MnO	FeO	NiO	Cr_2O_3	TiO_2	Total
19 xtl 7 lg glom	QMI	84.81	39.19	0.03	-0.01	44.95	-0.02	0.16	0.19	14.35	0.29	0.04	-0.05	99.13
19 xtl 7 lg glom	QMI	79.66	38.38	0.04	0.00	41.31	0.00	0.15	0.23	18.80	0.15	-0.02	0.02	99.07
19 xtl 7 lg glom	QMI	79.79	38.50	0.03	0.02	41.65	-0.01	0.15	0.28	18.81	0.16	0.01	0.02	99.62
19 xtl 8 lg glom	QMI	84.32	39.22	0.03	0.01	44.63	0.00	0.16	0.18	14.80	0.24	0.04	0.03	99.34
19 xtl 8 lg glom	QMI	84.28	39.46	0.02	0.02	44.62	0.00	0.15	0.17	14.84	0.24	0.04	0.01	99.56
19 xtl 8 lg glom	QMI	80.47	38.65	0.01	0.01	41.85	0.01	0.13	0.25	18.11	0.16	0.00	0.05	99.22
19 xtl 8 lg glom	QMI	64.86	51.01	2.22	0.02	22.04	0.00	0.88	0.74	21.28	0.06	0.02	0.17	98.44
19 xtl 9 lg glom	QMI	83.41	39.23	0.04	0.00	43.77	0.00	0.17	0.19	15.52	0.23	0.01	0.01	99.17
19 xtl 9 lg glom	QMI	82.69	39.10	0.05	0.00	43.29	0.00	0.16	0.19	16.15	0.24	0.01	0.04	99.24
19 xtl 9 lg glom	QMI	79.48	38.37	0.02	0.02	41.06	0.01	0.15	0.24	18.90	0.11	-0.02	0.09	98.95
19 xtl 9 lg glom	QMI	79.12	38.24	0.02	0.01	40.97	0.01	0.15	0.28	19.27	0.12	0.01	-0.04	99.05
19 xtl 10 lg glom	QMI	84.02	39.24	0.04	0.00	44.22	0.00	0.18	0.16	15.00	0.25	0.03	0.01	99.12
19 xtl 10 lg glom	QMI	83.21	39.15	0.03	0.00	43.68	0.01	0.18	0.20	15.71	0.23	0.03	0.03	99.24
19 xtl 10 lg glom	QMI	84.02	39.27	0.03	0.00	44.17	0.00	0.16	0.16	14.98	0.25	0.04	0.01	99.07
19 xtl 10 lg glom	QMI	78.84	38.44	0.02	0.01	40.72	0.01	0.17	0.24	19.48	0.11	0.02	0.00	99.23
19 xtl 10 lg glom	QMI	80.35	38.55	0.04	0.01	41.50	-0.01	0.15	0.24	18.09	0.17	0.01	0.02	98.76
19 xtl 11 lg glom	QMI	80.90	38.60	0.03	0.01	42.21	-0.01	0.15	0.21	17.77	0.23	0.03	0.02	99.24
19 xtl 11 lg glom	QMI	81.68	38.68	0.04	0.01	42.81	0.01	0.17	0.24	17.12	0.21	0.03	0.02	99.34
19 xtl 11 lg glom	QMI	79.22	38.19	0.04	0.01	41.15	0.00	0.15	0.25	19.24	0.15	0.00	0.00	99.17
19 xtl 11 lg glom	QMI	79.99	38.29	0.03	0.00	41.52	0.00	0.17	0.23	18.52	0.16	0.02	0.02	98.96
19 xtl 12 lg glom	QMI	82.55	38.52	0.03	0.01	43.21	-0.01	0.15	0.17	16.29	0.23	0.03	0.01	98.66
19 xtl 12 lg glom	QMI	81.56	38.59	0.03	0.01	42.69	0.00	0.15	0.20	17.20	0.20	0.03	0.00	99.11
19 xtl 12 lg glom	QMI	68.25	50.81	1.78	0.05	23.17	0.03	1.95	0.57	19.21	0.02	0.00	0.31	97.90
19 xtl 12 lg glom	QMI	75.06	37.66	0.02	0.00	38.29	-0.02	0.12	0.34	22.68	0.10	0.00	-0.01	99.17
19 xtl 13 lg glom	QMI	80.08	38.37	0.04	0.02	41.66	0.00	0.15	0.23	18.47	0.18	0.00	-0.01	99.11
19 xtl 13 lg glom	QMI	82.36	39.00	0.06	0.01	43.13	-0.01	0.17	0.21	16.47	0.20	0.02	0.03	99.29
19 xtl 13 lg glom	QMI	78.83	38.30	0.04	0.00	40.69	0.00	0.16	0.26	19.48	0.14	0.00	0.04	99.11
19 xtl 13 lg glom	QMI	79.14	38.30	0.04	0.00	41.16	0.00	0.17	0.23	19.33	0.16	0.01	-0.01	99.39
19 xtl 14 lg glom	QMI	79.96	38.35	0.05	0.01	41.47	0.01	0.16	0.22	18.53	0.17	0.03	0.02	99.02
19 xtl 14 lg glom	QMI	79.80	38.50	0.04	0.02	41.48	-0.01	0.16	0.22	18.72	0.13	0.01	0.02	99.28
19 xtl 14 lg glom	QMI	79.84	38.27	0.03	0.00	41.47	-0.01	0.15	0.25	18.66	0.16	0.02	0.01	99.01
19 xtl 14 lg glom	QMI	80.18	38.29	0.03	0.00	41.76	0.00	0.16	0.24	18.39	0.15	0.03	0.01	99.05

Table D.1 (Continued)

Sample	Lithology	Fo	SiO_2	Al_2O_3	Na_2O	MgO	K_2O	CaO	MnO	FeO	NiO	Cr_2O_3	TiO_2	Total
09 xtl1 lg	QMI	79.83	38.49	0.02	-0.01	41.53	-0.01	0.15	0.24	18.71	0.14	0.03	0.02	99.32
09 xtl1 lg	QMI	80.06	38.42	0.03	0.01	41.64	0.01	0.18	0.24	18.49	0.14	0.02	0.01	99.19
09 xtl1 lg	QMI	76.74	37.83	0.03	0.01	39.29	0.01	0.18	0.28	21.23	0.12	0.02	-0.01	99.00
09 xtl1 lg	QMI	77.17	37.80	0.01	0.01	39.59	0.00	0.18	0.27	20.87	0.14	0.00	-0.01	98.86
09 xtl 2	QMI	77.28	37.44	0.01	0.02	39.76	-0.01	0.16	0.26	20.84	0.13	0.00	0.00	98.61
09 xtl 2	QMI	77.14	38.41	0.05	0.01	39.41	-0.01	0.17	0.28	20.83	0.12	0.00	-0.02	99.25
24 xtl 1 core	PL INCL in EK	40.80	33.21	-0.06	-0.06	18.58	0.02	0.14	0.62	48.05	0.13	0.04	0.01	100.79
24 xtl 1 core	PL INCL in EK	41.01	33.04	-0.06	-0.06	18.63	0.04	0.14	0.62	47.78	0.13	0.03	0.04	100.46
24 xtl1	PL INCL in EK	44.78	33.56	-0.06	-0.05	20.59	0.02	0.13	0.67	45.26	0.13	0.03	0.05	100.45
24 xtl1 rim	PL INCL in EK	41.37	33.11	-0.06	-0.06	18.75	0.02	0.13	0.65	47.37	0.14	0.04	0.02	100.22
24 xtl 2 core	PL INCL in EK	43.81	33.40	-0.07	-0.07	20.17	0.02	0.13	0.60	46.13	0.11	0.05	0.04	100.66
24 xtl 2 core	PL INCL in EK	44.08	33.37	-0.07	-0.06	20.29	0.02	0.13	0.62	45.89	0.14	0.04	0.03	100.52
24 xtl 2	PL INCL in EK	43.83	33.42	-0.07	-0.05	20.11	0.01	0.13	0.61	45.94	0.11	0.04	0.04	100.43
24 xtl 2	PL INCL in EK	43.84	33.41	-0.07	-0.05	20.23	0.02	0.13	0.63	46.20	0.13	0.05	0.05	100.85
24 xtl 2	PL INCL in EK	43.63	33.47	-0.07	-0.05	20.02	0.02	0.14	0.62	46.10	0.14	0.04	0.04	100.57
24 xtl 2 rim	PL INCL in EK	43.91	33.28	-0.06	-0.04	20.11	0.02	0.23	0.59	45.79	0.14	0.02	0.10	100.28
24 xtl 3 core	PL INCL in EK	44.18	33.60	-0.07	-0.05	20.40	0.02	0.12	0.58	45.95	0.13	0.04	0.06	100.90
24 xtl 3 core	PL INCL in EK	44.17	33.52	-0.06	-0.04	20.33	0.03	0.12	0.59	45.80	0.13	0.04	0.13	100.69
24 xtl 3 rim	PL INCL in EK	44.00	33.42	-0.06	-0.06	20.19	0.03	0.14	0.60	45.82	0.14	0.05	0.04	100.42
24 xtl 3 rim	PL INCL in EK	44.25	33.38	-0.07	-0.04	20.23	0.02	0.15	0.56	45.44	0.12	0.05	0.02	99.99
24 xtl 4 T	PL INCL in EK	42.41	33.11	-0.07	-0.06	19.15	0.03	0.17	0.63	46.36	0.16	0.05	0.06	99.73
24 xtl 4 T	PL INCL in EK	42.25	33.17	-0.06	-0.05	19.18	0.04	0.15	0.63	46.74	0.17	0.05	0.04	100.16
24 xtl 4 T	PL INCL in EK	42.40	33.21	-0.08	-0.07	19.17	0.02	0.13	0.62	46.42	0.13	0.04	0.10	99.84
24 xtl 4 T	PL INCL in EK	42.16	33.08	-0.07	-0.06	19.11	0.02	0.13	0.60	46.73	0.14	0.04	0.09	99.94
24 xtl 4 T	PL INCL in EK	42.14	33.07	-0.07	-0.04	19.11	0.02	0.12	0.61	46.78	0.14	0.03	0.06	99.94
24 xtl 4 T	PL INCL in EK	42.27	33.16	-0.06	-0.05	19.21	0.03	0.14	0.61	46.76	0.12	0.03	0.05	100.09
24 xtl 4 T	PL INCL in EK	41.91	33.17	-0.06	-0.05	19.08	0.01	0.13	0.62	47.13	0.13	0.04	0.03	100.36
24 xtl 4 T	PL INCL in EK	42.24	33.17	-0.07	-0.05	19.09	0.03	0.13	0.63	46.53	0.12	0.05	0.03	99.78
24 xtl 4 T	PL INCL in EK	41.95	32.92	-0.06	-0.04	18.92	0.02	0.14	0.61	46.66	0.15	0.04	0.04	99.49
24 xtl 4 T	PL INCL in EK	41.97	33.21	-0.07	-0.06	19.09	0.01	0.14	0.59	47.06	0.13	0.05	0.05	100.34
24 xtl 4 T	PL INCL in EK	42.17	33.09	-0.06	-0.05	19.06	0.02	0.13	0.59	46.60	0.14	0.04	0.11	99.77
24 xtl 4 T	PL INCL in EK	42.13	33.19	-0.06	-0.05	19.09	0.01	0.13	0.59	46.74	0.13	0.03	0.04	99.94

Table D.1 (Continued)

Sample	Lithology	Fo	SiO_2	Al_2O_3	Na_2O	MgO	K_2O	CaO	MnO	FeO	NiO	Cr_2O_3	TiO_2	Total
24 xtl 4 T	PL INCL in EK	42.08	33.09	-0.06	-0.05	19.07	0.03	0.13	0.61	46.79	0.15	0.05	0.03	99.96
24 xtl 4 T	PL INCL in EK	42.16	33.09	-0.06	-0.04	18.99	0.02	0.15	0.61	46.45	0.14	0.03	0.07	99.56
24 xtl 4 T	PL INCL in EK	42.31	33.20	-0.07	-0.04	19.12	0.03	0.13	0.61	46.45	0.15	0.05	0.08	99.81
24 xtl 4 T	PL INCL in EK	42.30	33.20	-0.06	-0.05	19.13	0.01	0.14	0.59	46.53	0.13	0.05	0.06	99.83
24 xtl 4 T	PL INCL in EK	42.15	33.17	-0.06	-0.04	19.10	0.02	0.14	0.61	46.73	0.13	0.05	0.11	100.05
24 xtl 4 T	PL INCL in EK	41.90	33.17	-0.08	-0.07	19.12	0.02	0.14	0.60	47.24	0.17	0.03	0.04	100.53
24 xtl 4 T	PL INCL in EK	41.90	32.68	-0.06	-0.05	18.80	0.02	0.14	0.63	46.46	0.14	0.04	0.08	98.99
24 xtl 4 T	PL INCL in EK	41.95	32.97	-0.06	-0.05	19.00	0.03	0.14	0.62	46.86	0.13	0.04	0.02	99.83
24 xtl 4 T	PL INCL in EK	41.94	33.09	-0.08	-0.06	18.98	0.03	0.15	0.61	46.85	0.13	0.03	0.03	99.91
24 xtl 4 T	PL INCL in EK	42.06	33.12	-0.07	-0.06	19.04	0.03	0.14	0.62	46.73	0.15	0.05	0.04	99.92
24 xtl 4 T	PL INCL in EK	41.98	33.29	-0.08	-0.05	19.04	0.03	0.14	0.60	46.91	0.11	0.04	0.02	100.18
24 xtl 4 T	PL INCL in EK	42.13	32.92	-0.07	-0.06	19.07	0.03	0.14	0.61	46.69	0.13	0.05	0.07	99.70
24 xtl 4 T	PL INCL in EK	42.00	33.25	-0.07	-0.06	19.06	0.04	0.15	0.58	46.93	0.12	0.04	0.06	100.23
24 xtl 4 T	PL INCL in EK	42.04	33.12	-0.08	-0.06	19.05	0.01	0.14	0.64	46.82	0.13	0.05	0.10	100.07
24 xtl 4 T	PL INCL in EK	42.30	33.03	-0.06	-0.07	19.07	0.02	0.13	0.62	46.38	0.15	0.03	0.01	99.44
24 xtl 4 T	PL INCL in EK	42.17	33.23	-0.07	-0.05	19.08	0.01	0.14	0.60	46.64	0.13	0.04	0.05	99.91
24 xtl 4 T	PL INCL in EK	42.10	33.17	-0.06	-0.06	19.07	0.03	0.17	0.60	46.76	0.11	0.05	0.03	99.99
24 xtl 4 T	PL INCL in EK	41.98	33.12	-0.07	-0.05	19.14	0.01	0.12	0.60	47.16	0.15	0.04	0.04	100.38
24 xtl 4 T	PL INCL in EK	42.41	33.09	-0.07	-0.06	19.17	0.02	0.15	0.62	46.41	0.14	0.04	0.01	99.66
24 xtl 4 T	PL INCL in EK	42.18	33.15	-0.06	-0.06	19.06	0.02	0.15	0.62	46.58	0.14	0.03	0.04	99.78
24 xtl 4 T	PL INCL in EK	42.19	33.09	-0.07	-0.06	19.14	0.01	0.13	0.60	46.75	0.13	0.05	0.13	100.03
24 xtl 4 T	PL INCL in EK	42.02	33.17	-0.07	-0.05	19.10	0.02	0.14	0.65	46.98	0.14	0.05	0.05	100.29
24 xtl 4 T	PL INCL in EK	42.10	33.13	-0.05	-0.05	19.19	0.04	0.13	0.63	47.06	0.14	0.04	0.04	100.41
24 xtl 4 T	PL INCL in EK	42.17	33.14	-0.06	-0.05	19.11	0.03	0.15	0.61	46.70	0.17	0.04	0.01	99.95
24 xtl 4 T	PL INCL in EK	42.13	33.19	-0.07	-0.05	19.14	0.03	0.15	0.61	46.86	0.15	0.05	0.02	100.19
24 xtl 4 T	PL INCL in EK	42.25	33.16	-0.06	-0.05	19.05	0.04	0.14	0.62	46.43	0.15	0.04	0.05	99.66
24 xtl 4 T	PL INCL in EK	42.02	33.25	-0.06	-0.05	19.03	0.02	0.15	0.61	46.81	0.13	0.05	0.08	100.13
24 xtl 4 T	PL INCL in EK	42.13	32.89	-0.07	-0.05	19.06	0.01	0.15	0.60	46.66	0.15	0.04	0.07	99.63
24 xtl 4 T	PL INCL in EK	42.05	33.13	-0.08	-0.05	19.06	0.02	0.15	0.63	46.83	0.12	0.05	0.05	100.03
24 xtl 4 T	PL INCL in EK	42.11	32.95	-0.07	-0.06	19.11	0.01	0.13	0.61	46.82	0.13	0.04	0.05	99.85
24 xtl 4 T	PL INCL in EK	42.04	33.24	-0.06	-0.05	19.14	0.01	0.13	0.63	47.04	0.15	0.05	0.06	100.46
24 xtl 4 T	PL INCL in EK	42.08	33.23	-0.08	-0.05	19.07	0.03	0.13	0.62	46.79	0.14	0.05	0.09	100.15

Table D.1 (Continued)

Sample	Lithology	Fo	SiO_2	Al_2O_3	Na_2O	MgO	K_2O	CaO	MnO	FeO	NiO	Cr_2O_3	TiO_2	Total
24 xtl 4 T	PL INCL in EK	42.09	33.14	-0.07	-0.06	19.09	0.02	0.13	0.62	46.81	0.14	0.04	0.08	100.07
24 xtl 4 T	PL INCL in EK	42.23	33.30	-0.07	-0.05	19.17	0.02	0.12	0.59	46.75	0.16	0.04	0.06	100.20
24 xtl 4 T	PL INCL in EK	42.26	33.20	-0.06	-0.05	19.08	0.02	0.14	0.63	46.48	0.15	0.04	0.10	99.84
24 xtl 4 T	PL INCL in EK	42.17	33.16	-0.06	-0.04	19.14	0.02	0.13	0.59	46.80	0.12	0.03	0.04	100.04
24 xtl 4 T	PL INCL in EK	42.23	32.88	-0.06	-0.05	19.02	0.02	0.14	0.64	46.38	0.13	0.04	0.07	99.31
24 xtl 4 T	PL INCL in EK	42.12	33.10	-0.06	-0.07	19.04	0.01	0.13	0.62	46.65	0.13	0.03	0.08	99.79
24 xtl 4 T	PL INCL in EK	42.34	33.15	-0.07	-0.05	19.21	0.03	0.14	0.64	46.65	0.12	0.03	0.05	100.02
24 xtl 4 T	PL INCL in EK	42.11	33.22	-0.07	-0.05	19.11	0.02	0.12	0.59	46.83	0.11	0.02	0.03	100.06
24 xtl 4 T	PL INCL in EK	42.30	33.33	-0.06	-0.06	19.08	0.01	0.15	0.59	46.40	0.12	0.03	0.04	99.74
24 xtl 4 T	PL INCL in EK	42.32	33.22	-0.07	-0.06	19.18	0.02	0.15	0.59	46.59	0.13	0.05	0.03	99.98
24 xtl 4 T	PL INCL in EK	42.38	33.30	-0.06	-0.06	19.11	0.02	0.21	0.58	46.33	0.13	0.04	0.05	99.77

Table D.2 Olivine-hosted Spinel EMPA Spots in wt %. Sample label includes sample number and the olivine host to spinel. Cr#=molar 100*. Mg#= 100*Mg/(Mg+Fe). Fo is the average forsterite content of host olivine Fo=100*Mg/(Mg+Fe).

Sample	Lithology	SiO_2	Al_2O_3	FeO*	NiO	Na_2O	MgO	CaO	TiO_2	MnO	Cr_2O_3	V_2O_3	Total	Cr#	Mg#	Fo
01 Ol 1	X lahar	0.54	0.42	44.18	0.02	0.00	5.59	0.09	42.94	0.26	0.26	0.52	94.86	44.53	18.40	73.91
01 Ol 2	X lahar	0.08	5.09	60.39	0.16	0.00	5.32	0.01	10.83	0.34	12.60	0.66	95.67	76.20	58.75	63.74
01 Ol 3	X lahar	0.13	25.27	30.94	0.20	0.00	10.81	0.01	1.65	0.16	28.08	0.15	97.65	58.95	13.57	77.00
01 Ol 3	X lahar	0.04	25.03	32.53	0.23	0.01	9.45	0.00	1.51	0.25	27.54	0.14	96.94	58.72	38.39	81.75
01 Ol 4	X lahar	0.09	25.15	33.09	0.13	0.01	9.39	0.01	1.07	0.25	26.92	0.14	96.53	58.05	34.11	78.61
01 Ol 5	X lahar	0.05	0.20	44.18	-0.01	0.00	4.02	0.02	45.67	0.45	0.35	0.54	95.49	70.02	33.60	77.73
01 Ol 6	X lahar	0.10	23.67	38.02	0.07	0.02	8.47	0.01	1.15	0.24	23.94	0.19	96.20	56.66	13.96	76.10
02 Ol 08	X lahar	0.08	22.43	40.34	0.14	0.02	9.18	0.00	2.10	0.24	20.15	0.30	95.07	53.74	28.43	78.32
09 Ol 09	X lahar	0.05	23.93	39.21	0.12	-0.01	8.90	0.01	1.03	0.21	21.57	0.33	95.55	53.82	28.85	78.10
09 Ol 10	X lahar	0.09	28.07	33.20	0.16	0.01	10.48	0.01	0.95	0.19	22.86	0.11	96.36	51.28	28.80	79.36
10 Ol 11	MKLV-TF	0.11	1.98	69.94	0.09	0.01	2.34	0.05	17.80	0.43	0.83	0.81	94.47	35.26	36.01	63.50
10 Ol 12	MKLV-TF	0.05	19.89	39.34	0.14	0.00	8.03	0.00	1.14	0.25	25.97	0.36	95.29	62.80	38.93	75.11
10 Ol 12	MKLV-TF	0.56	22.54	37.58	0.11	0.01	8.91	0.00	1.03	0.28	24.48	0.20	95.97	58.41	26.68	75.11
10 Ol 12	MKLV-TF	0.10	17.91	43.64	0.18	0.01	7.30	0.00	1.32	0.27	24.54	0.28	95.63	63.91	29.72	74.16
10 Ol 12	MKLV-TF	0.09	21.28	39.38	0.20	0.02	7.99	0.01	1.08	0.19	25.09	0.29	95.84	60.39	22.97	74.90
19 Ol 1	QMI	0.05	32.75	27.53	0.20	0.01	11.81	0.01	1.02	0.24	22.93	0.23	96.78	31.96	43.33	84.12
19 Ol 1	QMI	0.40	33.52	26.33	0.21	0.07	12.19	0.07	1.04	0.19	22.98	0.27	97.27	31.50	45.21	84.12
19 Ol 1	QMI	0.06	34.37	26.50	0.16	0.00	12.10	0.01	0.95	0.20	22.80	0.24	97.39	30.80	44.87	83.63
19 Ol 1	QMI	0.06	33.47	27.62	0.21	0.01	12.08	0.01	0.94	0.22	22.51	0.24	97.37	31.09	43.80	84.12
19 Ol 2	QMI	0.08	32.46	28.24	0.21	0.02	11.60	0.00	0.98	0.22	23.01	0.26	97.08	32.23	42.28	82.89
19 Ol 3	QMI	0.07	32.66	29.93	0.18	0.00	10.99	0.01	1.05	0.25	21.59	0.21	96.95	30.73	39.55	82.11
19 Ol 3	QMI	0.06	33.08	28.46	0.24	0.01	11.44	0.01	0.95	0.21	22.35	0.15	96.94	31.19	41.74	82.11
19 Ol 3	QMI	0.06	33.45	28.02	0.14	0.01	11.65	0.00	0.91	0.16	22.21	0.15	96.78	30.82	42.57	82.11
19 Ol 3	QMI	0.08	33.80	27.29	0.18	0.00	11.90	0.00	1.03	0.21	22.07	0.15	96.73	30.46	43.74	83.76
19 Ol 3	QMI	0.09	34.11	26.34	0.26	0.00	12.29	0.01	0.98	0.18	22.41	0.25	96.93	30.59	45.42	83.76
19 Ol 3	QMI	0.06	33.99	26.09	0.20	0.01	12.53	0.02	0.95	0.20	22.71	0.22	96.98	30.95	46.12	83.76
19 Ol 3	QMI	0.07	33.93	26.42	0.24	0.00	12.36	0.00	1.09	0.15	22.48	0.19	96.94	30.77	45.48	84.07
19 Ol 3	QMI	0.05	33.94	25.86	0.24	0.01	12.61	0.01	0.97	0.19	22.78	0.19	96.84	31.05	46.50	84.07
19 Ol 3	QMI	0.06	33.39	26.69	0.19	0.01	12.06	0.01	1.02	0.17	22.87	0.14	96.60	31.49	44.61	84.07

Table D.2 (Continued)

Sample	Lithology	SiO_2	Al_2O_3	FeO*	NiO	Na_2O	MgO	CaO	TiO_2	MnO	Cr_2O_3	V_2O_3	Total	Cr#	Mg#	Fo
19 Ol 3	QMI	0.07	32.01	30.31	0.15	0.00	10.86	0.01	0.98	0.20	21.77	0.20	96.56	31.34	38.98	84.07
19 Ol 3	QMI	0.09	31.81	30.66	0.20	0.00	10.74	-0.01	1.02	0.22	21.75	0.24	96.71	31.44	38.43	81.00
19 Ol 4	QMI	0.06	29.63	26.96	0.15	0.00	11.96	0.02	1.35	0.20	26.72	0.29	97.33	37.69	44.16	84.72
19 Ol 4	QMI	0.09	29.64	27.25	0.21	0.00	11.96	0.02	1.20	0.23	26.55	0.34	97.49	37.53	43.90	84.72
19 Ol 4	QMI	0.04	29.55	27.12	0.16	0.01	12.14	-0.01	1.23	0.17	26.38	0.25	97.06	37.46	44.38	84.72
19 Ol 4	QMI	0.05	29.41	28.18	0.22	0.00	11.55	0.00	1.25	0.19	26.52	0.19	97.56	37.69	42.22	84.72
19 Ol 4	QMI	0.06	29.28	28.14	0.23	0.00	11.43	0.00	1.26	0.19	26.01	0.24	96.86	37.34	42.01	84.72
19 Ol 4	QMI	0.06	29.67	27.96	0.22	0.00	11.43	0.02	1.28	0.19	25.74	0.32	96.87	36.79	42.16	84.25
19 Ol 4	QMI	0.41	29.41	27.10	0.20	0.01	11.65	0.01	1.25	0.20	25.97	0.22	96.42	37.21	43.38	84.72
19 Ol 4	QMI	0.08	29.13	28.37	0.14	0.01	11.03	0.00	1.10	0.22	25.88	0.22	96.19	37.35	40.94	84.72
19 Ol 4	QMI	0.08	30.11	28.03	0.17	0.01	11.52	0.01	1.27	0.19	24.80	0.21	96.40	35.59	42.29	84.72
19 Ol 5	QMI	0.05	29.95	26.74	0.23	0.01	11.99	0.00	1.05	0.19	26.93	0.25	97.40	37.62	44.42	85.30
19 Ol 5	QMI	0.06	31.33	27.45	0.24	0.01	11.81	0.01	1.03	0.15	25.13	0.18	97.38	34.99	43.40	83.93
19 Ol 5	QMI	0.07	32.97	25.00	0.15	0.00	12.54	0.01	0.97	0.12	24.98	0.22	97.03	33.70	47.19	84.96
19 Ol 6	QMI	0.08	33.32	26.39	0.26	0.00	11.90	0.00	0.99	0.21	23.88	0.17	97.21	32.47	44.57	84.50
19 Ol 6	QMI	0.07	30.75	25.78	0.21	0.01	12.34	0.00	1.03	0.22	26.59	0.24	97.24	36.71	46.04	85.06
19 Ol 7	QMI	0.06	29.78	26.02	0.24	0.00	12.10	0.00	1.11	0.18	27.42	0.14	97.05	38.19	45.32	85.93
19 Ol 7	QMI	0.07	29.53	27.59	0.25	0.02	11.45	0.00	1.25	0.16	26.44	0.18	96.96	37.52	42.53	85.52
19 Ol 7	QMI	0.08	31.16	24.55	0.25	0.01	12.52	0.01	1.06	0.21	26.75	0.21	96.82	36.54	47.62	84.56
19 Ol 7	QMI	0.09	30.37	25.84	0.25	0.01	11.96	0.00	1.02	0.22	26.76	0.24	96.76	37.15	45.20	85.93
19 Ol 8	QMI	0.09	30.25	26.69	0.16	0.00	11.63	0.01	0.99	0.21	26.60	0.18	96.82	37.10	43.73	84.51
19 Ol 9	QMI	0.07	30.83	27.41	0.22	0.00	11.70	0.01	1.26	0.21	25.06	0.14	96.91	35.28	43.21	84.15
19 Ol 9	QMI	0.05	33.12	25.94	0.27	0.01	12.28	0.00	0.93	0.19	24.11	0.07	96.98	32.81	45.77	82.46
19 Ol 10	QMI	0.09	33.48	26.22	0.25	0.00	12.16	0.00	1.03	0.21	23.17	0.23	96.84	31.71	45.25	84.51
19 Ol 10	QMI	0.17	18.73	41.40	0.25	0.01	8.01	0.02	4.35	0.24	21.90	0.37	95.46	43.96	25.65	81.13
32 Ol 1	Xb	0.10	25.66	31.13	0.19	0.02	10.43	0.01	1.01	0.24	26.32	0.24	95.34	40.75	37.39	80.32
32 Ol 1	Xb	0.09	25.34	31.73	0.10	0.00	10.30	0.00	0.98	0.23	26.57	0.19	95.54	41.29	36.65	80.32
32 Ol 1	Xb	0.08	23.87	34.10	0.20	0.00	9.66	0.00	1.05	0.20	26.88	0.14	96.19	43.03	33.56	80.32
32 Ol 2	Xb	0.07	24.63	35.65	0.10	0.01	9.84	0.01	1.23	0.23	24.60	0.17	96.54	40.12	32.98	84.36
32 Ol 2	Xb	0.06	26.64	30.30	0.22	0.01	10.89	0.02	1.06	0.25	27.34	0.18	96.98	40.78	39.05	84.36
32 Ol 2	Xb	0.09	24.40	34.73	0.20	0.01	9.85	0.06	1.22	0.22	24.70	0.28	95.75	40.45	33.58	84.36

Table D.3 Groundmass Glass EMPA Spots in wt %.

Sample	Lithology	SiO_2	Al_2O_3	K_2O	CaO	MnO	FeO	Na_2O	MgO	TiO_2	Cr_2O_3	P_2O_5	NiO	Total
31	Wn	75.18	14.51	2.45	1.69	0.05	1.75	2.64	0.31	0.22	0.01	0.05	0.01	98.96
31	Wn	74.83	14.50	2.30	1.69	0.02	1.71	3.04	0.31	0.22	-0.02	0.04	0.01	98.76
31	Wn	75.49	14.71	2.41	1.70	0.03	1.67	2.94	0.31	0.20	-0.02	0.04	0.00	99.58
31	Wn	74.77	14.45	2.36	1.68	0.01	1.66	2.86	0.31	0.22	-0.01	0.05	0.00	98.44
31	Wn	75.79	14.68	2.28	1.64	0.04	1.68	3.59	0.32	0.21	-0.02	0.04	0.01	100.37
18B	EKPF	76.85	12.64	2.85	0.92	0.02	1.25	3.49	0.14	0.29	0.00	0.03	0.02	98.61
18B	EKPF	77.17	12.50	2.84	0.90	0.05	1.32	3.62	0.16	0.28	0.02	0.05	0.01	98.99
18B	EKPF	76.68	12.68	2.86	0.92	0.04	1.19	3.79	0.13	0.28	0.01	0.03	0.02	98.70
14	EKPF	74.28	16.49	1.75	1.25	0.02	0.72	5.61	0.04	0.17				100.39
14	EKPF	77.78	12.70	3.01	0.83	0.03	1.05	2.68	0.07	0.23				98.44
14	EKPF	77.48	12.37	2.98	0.81	0.05	2.17	2.79	0.53	0.26				99.51
14	EKPF	76.97	12.96	2.88	1.00	0.02	0.91	3.44	0.05	0.25				98.56
14	EKPF	76.82	13.37	2.84	1.00	-0.01	0.93	3.79	0.05	0.24				99.09
14	EKPF	74.86	14.26	2.39	1.40	0.01	1.15	4.83	0.17	0.22				99.34
14	EKPF	77.47	12.59	2.39	0.94	0.03	1.10	3.67	0.11	0.26				98.61
14	EKPF	77.28	12.95	3.10	0.90	0.02	1.13	2.89	0.08	0.26				98.70
14	EKPF	77.29	13.28	2.77	1.11	0.00	1.01	3.31	0.07	0.25				99.17
14	EKPF	78.15	12.84	3.10	0.86	0.04	1.04	2.91	0.07	0.27				99.38
14	EKPF	78.00	12.55	3.26	0.77	0.03	1.01	2.89	0.06	0.24				98.90
32	Xb	67.12	14.97	2.44	3.09	0.08	5.15	3.82	1.16	1.12	0.00	0.28	-0.02	99.35
32	Xb	67.54	15.00	2.49	2.84	0.07	4.98	4.07	1.10	1.14	-0.03	0.28	0.01	99.63
32	Xb	67.70	15.05	2.52	2.99	0.07	4.99	4.21	1.16	1.11	0.01	0.26	0.04	100.24
32	Xb	68.73	15.31	2.63	2.61	0.04	4.40	4.10	1.00	1.14	0.01	0.28	0.00	100.35
32	Xb	67.83	15.15	2.53	2.89	0.04	4.81	3.96	1.17	1.16	-0.01	0.28	0.01	99.92
32	Xb	67.75	15.03	2.59	3.02	0.06	4.99	4.20	1.11	1.15	0.01	0.24	0.00	100.28
02	X Lahar	65.15	14.34	3.42	3.22	0.11	5.68	4.71	1.32	1.80	-0.02	0.44	-0.01	100.36
02	X Lahar	68.48	15.04	4.20	2.17	0.05	4.28	4.40	0.92	1.02	-0.02	0.22	-0.02	100.91
02	X Lahar	68.27	15.04	4.15	2.01	0.07	4.69	4.29	1.04	1.04	0.00	0.25	0.02	101.00
02	X Lahar	65.32	14.96	3.10	3.37	0.08	5.60	4.86	0.67	2.38	-0.03	0.63	-0.01	101.18
02	X Lahar	69.56	15.05	3.79	2.17	0.07	4.40	2.59	0.95	1.03	-0.01	0.23	-0.01	99.94

Table D.3 (Continued)

Sample	Lithology	SiO_2	Al_2O_3	K_2O	CaO	MnO	FeO	Na_2O	MgO	TiO_2	Cr_2O_3	P_2O_5	NiO	Total
02	X Lahar	68.34	15.02	3.77	2.34	0.08	4.43	4.56	0.95	0.99	0.01	0.22	0.00	100.84
08A	MKLV-WC	73.20	11.85	4.51	0.50	0.04	2.66	4.69	0.11	1.39	-0.01	0.21	0.01	99.37
08A	MKLV-WC	72.74	12.63	5.40	0.38	0.04	2.75	4.05	0.09	1.37	0.03	0.21	-0.01	99.92
08A	MKLV-WC	73.33	13.03	5.60	0.37	0.04	2.16	4.49	0.14	0.93	0.01	0.17	0.01	100.51
08A	MKLV-WC	72.73	12.51	5.31	0.37	0.06	2.87	3.88	0.10	1.36	0.01	0.19	0.00	99.67
08A	MKLV-WC	71.77	13.17	4.88	0.63	0.03	2.26	4.65	0.08	1.23	0.00	0.18	0.03	99.12
11	SDO	77.75	11.21	4.66	0.31	0.06	2.16	3.11	0.13	0.53	0.00	0.04	0.01	100.10
11	SDO	77.30	11.29	4.37	0.32	0.04	2.13	3.33	0.13	0.52	0.00	0.02	0.02	99.62
11	SDO	76.99	11.50	4.37	0.31	0.04	2.14	3.42	0.14	0.54	0.01	0.03	0.02	99.61
11	SDO	76.45	11.55	4.52	0.32	0.03	2.30	3.62	0.15	0.56	0.01	0.04	0.00	99.70
11	SDO	77.43	11.30	4.49	0.35	0.05	1.97	3.69	0.13	0.52	-0.01	0.04	0.01	100.11
11	SDO	76.75	11.35	4.57	0.36	0.04	1.99	3.28	0.13	0.52	0.01	0.03	-0.01	99.16
11	SDO	76.53	11.66	4.39	0.46	0.03	2.01	2.69	0.13	0.47				98.52
11	SDO	74.97	12.53	4.37	0.61	-0.01	1.91	3.23	0.13	0.53				98.41
11	SDO	77.22	11.20	4.46	0.32	0.04	1.95	2.56	0.13	0.50				98.49
11	SDO	75.99	11.86	4.66	0.38	0.04	2.05	2.83	0.14	0.56				98.62
11	SDO	76.98	11.30	4.49	0.36	0.04	1.97	2.71	0.15	0.56				98.72
11	SDO	76.72	11.71	4.58	0.35	0.00	2.03	2.78	0.14	0.54				98.97
11	SDO	77.10	11.39	4.47	0.34	0.04	1.93	2.92	0.14	0.48				98.94
11	SDO	77.89	11.08	4.58	0.36	0.01	2.04	2.58	0.14	0.50				99.32
11	SDO	76.21	13.30	4.08	0.90	0.03	1.56	3.41	0.12	0.47				100.17
11	SDO	77.27	11.09	4.30	0.33	0.04	1.94	2.74	0.14	0.49				98.46
11	SDO	76.45	12.46	4.44	0.63	0.03	2.01	2.96	0.13	0.54				99.75
11	SDO	76.98	11.65	4.52	0.36	0.05	2.13	3.02	0.15	0.51				99.54
11	SDO	77.24	11.64	4.66	0.35	0.00	2.09	3.10	0.14	0.54				99.89
11	SDO	77.98	11.50	4.53	0.36	0.02	1.90	2.86	0.14	0.51				99.91
11	SDO	76.86	11.84	4.01	0.50	0.01	1.88	3.33	0.13	0.48				99.17
11	SDO	75.22	12.75	3.93	0.89	0.02	1.68	3.84	0.11	0.41				98.96
11	SDO	77.80	11.20	4.46	0.33	0.04	1.86	2.85	0.14	0.50				99.29
11	SDO	76.81	11.52	4.29	0.40	0.04	1.99	2.86	0.14	0.54				98.71

Table D.3 (Continued)

Sample	Lithology	SiO_2	Al_2O_3	K_2O	CaO	MnO	FeO	Na_2O	MgO	TiO_2	Cr_2O_3	P_2O_5	NiO	Total
11	SDO	77.45	11.54	4.29	0.34	0.01	1.99	2.92	0.13	0.53				99.31
13	SDY	77.67	11.40	4.83	0.30	0.01	2.01	3.38	0.14	0.48	-0.02	0.03	-0.02	100.42
13	SDY	77.10	11.36	4.80	0.31	0.04	1.95	3.20	0.14	0.49	0.01	0.05	-0.01	99.60
13	SDY	76.53	11.67	4.98	0.32	0.02	2.20	3.43	0.14	0.54	0.00	0.03	-0.01	100.05
13	SDY	75.54	11.97	4.89	0.36	0.03	2.14	3.67	0.15	0.53	0.01	0.04	-0.01	99.50
13	SDY	76.65	11.54	4.96	0.32	0.04	2.20	3.56	0.16	0.53	0.00	0.04	-0.01	100.15
19	QMI	73.65	14.41	3.94	0.69	0.05	1.55	4.64	0.14	0.25	0.01	0.03	0.01	99.55
19	QMI	73.85	14.22	4.07	0.67	-0.01	1.66	4.59	0.20	0.28	-0.01	0.05	0.01	99.79
19	QMI	73.75	14.21	4.00	0.58	0.04	1.66	4.25	0.17	0.27	0.00	0.04	-0.01	99.19
19	QMI	73.63	14.30	4.03	0.62	0.06	1.80	4.68	0.16	0.26	-0.03	0.02	-0.01	99.75
19	QMI	73.85	14.29	3.98	0.61	0.05	1.66	4.80	0.09	0.27	0.02	0.04	-0.01	99.85